HARNESSING LIGHT FOR NOVEL RADICAL CHEMISTRY FROM INTERMEDIATES WITH ESTABLISHED POLAR REACTIVITY

Thomas Hin-Fung Wong

UNIVERSITAT ROVIRA i VIRGILI

Harnessing Light for Novel Radical Chemistry from Intermediates with Established Polar Reactivity

Thomas Hin-Fung Wong

DOCTORAL THESIS
2024

UNIVERSITAT ROVIRA I VIRGILI
HARNESSING LIGHT FOR NOVEL RADICAL CHEMISTRY FROM INTERMEDIATES WITH ESTABLISHED POLAR REACTIVITY
Thomas Hin-Fung Wong

UNIVERSITAT ROVIRA I VIRGILI
HARNESSING LIGHT FOR NOVEL RADICAL CHEMISTRY FROM INTERMEDIATES WITH ESTABLISHED POLAR REACTIVITY
Thomas Hin-Fung Wong

Thomas Hin-Fung Wong

Harnessing Light for Novel Radical Chemistry from Intermediates with Established Polar Reactivity

Doctoral Thesis

Supervised by Prof. Paolo Melchiorre

ICIQ – Institut Català d'Investigació Química

Tarragona

2024

UNIVERSITAT ROVIRA I VIRGILI
HARNESSING LIGHT FOR NOVEL RADICAL CHEMISTRY FROM INTERMEDIATES WITH ESTABLISHED POLAR REACTIVITY
Thomas Hin-Fung Wong

UNIVERSITAT ROVIRA i VIRGILI

ICIQ Institut Català d'Investigació Química

Professor Paolo Melchiorre, Professor at the University of Bologna, Italy,
previously Group Leader at ICIQ

I STATE that the present study, entitled "Harnessing Light for Novel Radical Chemistry from Intermediates with Established Polar Reactivity", presented by THOMAS HIN-FUNG WONG for the award of the degree of Doctor of Philosophy, has been carried out under my supervision at the Institut Català d'Investigació Química (ICIQ).

Tarragona, 22th February, 2024

Doctoral Thesis Supervisor

Prof. Paolo Melchiorre

Acknowledgements

It was once said, "Getting a PhD is getting Permanent Head Damage." [1] Although being a major overstatement (I can confirm that I have not sustained any in the course of my study), this reflects the immense challenges one was put through for a PhD, and has resonated with generations of PhD students to come. In my case, this journey has been particularly challenging even before it had begun. I would like to acknowledge Prof. Chris Vanderwal (UC Irvine), Prof. Chi Ming Che, Prof. Ho Yu Au-Yeung and Prof. Don-Yan Jin (HKU) for the research opportunities, which led me to take on a professional scientific career. Thank you to Dr. Alex Karns (UC Irvine), Dr. Gareth Yu (HKU) as important mentors, your advice and support guided me to the lifelong journey I am in. Thank you to my parents for their unconditional support to my education. Thank you to Antony, Fai, Joson, Penny for being good friends and providing timely encouragement, especially when things were taking drastic turns and bumps. You all were the unsung heroes/heroines that helped me writing the chapters in life, much like what paper and ink is to this thesis.

First, I would like to express my sincere gratitude to my supervisor Prof. Paolo Melchiorre for giving me the chance to join his research group. Thank you for providing the freedom for me to be creative and explore different chemistry projects.

For three and a half years I have developed a broader view and deeper understanding of organic chemistry. This is the culmination of all the interactions with every co-worker, particularly those who collaborated with me. Thanks to Riccardo and Dengke for kickstarting my first project, and for training me with the survival research techniques. Thank you, Martin and Yann, for teaching me the importance of persistence, scientific vigor and attention to detail. Thank you Shuo, not only for what I have learned from you about radical chemistry, but also for being an off-peak hour lab companion. I will truly miss the extended chats we had about science and life.

Throughout the years, I was fortunate enough to be surrounded by a supportive gang that served as a great source of inspiration, motivation and joy. I want to thank Wei for the help in Barcelona, and being a lively fume hood neighbor while we were working in the same lab. Special thanks to Adrianna, Matteo, Laura, Florian, Igor and many more for being good company at times, when we share fruitful discussions on exciting chemistry, and memories of joy outside the lab. Also, from the bottom of my heart, I am expressing my deepest appreciation to Nuria, Laia and Miguel for keeping things in order, and volunteering to translate for the group of non-Spanish speakers. Most of the fascinating chemistry would not be possible without your effort behind the stage. I am also thankful for the technical support

[1] Anonymous, dated at the dawn of PhD program

from dedicated members of the research support area, especially the NMR, MS, spectroscopy, X-ray diffraction and chromatography units.

Finally, I am grateful for the Formació Investigadora Fellowship awarded by the Government of Catalonia and the European Social Fund (2021FI–B00304), and the financial support from the European Research Council (ERC-2015-CoG 681840- CATA-LUX)

List of Publications

Some of the results presented in this thesis have been published:

- Wong, T.H.-F.; Ma, D.; Di Sanza, R.; Melchiorre, P. "Photoredox Organocatalysis for the Enantioselective Synthesis of 1,7-Dicarbonyl Compounds." *Org. Lett.* **2022**, *24*, 8, 1695-1699.
- Berger, M.*; Ma, D.*; Baumgartner, Y.*; Wong, T.H.-F.; Melchiorre, P. "Stereoselective conjugate cyanation of enals by combining photoredox and organocatalysis." *Nat. Catal.* **2023**, 6, 332-338.
- Wu, S.; Wong, T.H.-F.; Righi, P.; Melchiorre, P. "Photochemical Organocatalytic Synthesis of Thioethers from Aryl Halides and alcohols*." J. Am. Chem. Soc.* **2024,** *146*, 5, 2907–2912.

Table of Contents

Chapter I

General Overview

The research work described in this doctoral thesis focuses on exploring novel, light-driven radical chemistry originating from intermediates with established polar reactivity. Specifically, the combination of photoredox catalysis with classical intermediates was studied as a method to achieve unconventional radical reactivity. The aim of this chapter is to introduce the basic concepts of photochemistry and different mechanisms for the photoactivation of organic molecules. Seminal examples are discussed to highlight how photochemical activation can enable the design of challenging radical-based transformations that are not feasible under thermal conditions, thus providing the context and the background that have motivated this research.

1.1 Photochemistry

All photochemical processes begin with an interaction between light and matter, through the absorption of a photon by a molecule to reach an electronically excited state.[1] This condition directly correlates to the principle of photochemical activation (the Grotthuss–Draper law) which articulates that *"only the light absorbed is effective in producing a photochemical change".* Although this statement may retrospectively sound trivial, the implication is that both photo-responsive motifs and light of appropriate energy has to be present for a photochemical event to occur. This statement is underpinned by the quantum mechanical description of matter, where molecules exhibit quantized energy levels ranging from their low energy 'ground states' to a number of higher-order states. The absorption of photons, packets of 'quantized' energy, can only take place if the photon is *exactly* of the same energy as the energy gap between an occupied energy state and an unoccupied energy state. Upon

[1] Balzani, V., Ceroni, P., Juris, A. "Photochemistry and Photophysics: Concept, Research and Applications" Weinheim, Wiley-VCH, 2014.

the absorption of light of adequate energy, a molecule can be electronically excited. This excited state comes from the transition of an electron from the highest occupied molecular orbital (HOMO, Figure 1.1.a) of the molecule, to its lowest unoccupied molecular orbital (LUMO). In this process, the molecule has gained a specific amount of energy (E, the energy of the photon), which is directly proportional to the frequency of the absorbed light ν (Planck's equation, with *h* being the Planck's constant).

$$E = h \cdot \nu = E_f - E_i$$

These excited states are described by the wave functions Ψ, with Ψ_i referring to the ground state and Ψ_f to the excited state (Figure 1.1.b).

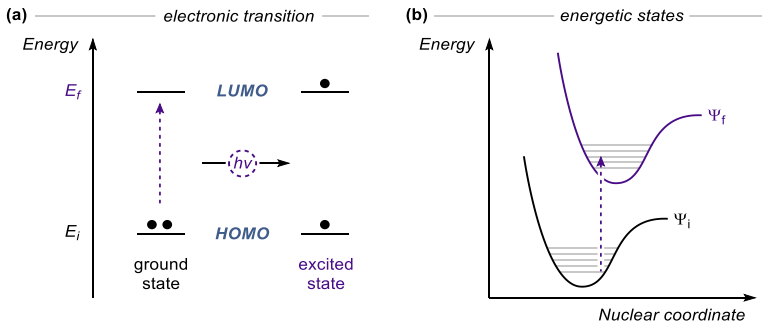

Figure 1.1. (**a**) Energy of the absorbed photon promotes the transition of an electron from the highest occupied molecular orbital (HOMO) to the lowest unoccupied molecular orbital (LUMO). (**b**) The electronic transition from the ground state Ψ_i to the excited state Ψ_f. Grey lines represent different rotation-vibrational levels.

This electronic transition changes the physical and chemical properties of a molecule; therefore, an excited molecule can be considered a different chemical entity from the ground state.[2] From the electronically excited state, various photophysical events can occur. First, the excited molecule can return to the ground state S_0 through thermal relaxation between vibrational levels ($S_1 \rightarrow S_0$, *non-radiative deactivation*, Figure 1.2). Alternatively, transitions

[2] Albini, A., Fagnoni, M. "Photochemically Generated Intermediates in Synthesis" John Wiley & Sons, 2013.

between different excited states ($S_1 \rightarrow S_0$, fluorescence; $T_1 \rightarrow S_0$, phosphorescence) can lead to re-emission of a photon, containing less energy than its incident counterpart.[3] Another possibility for the excited molecule is to engage in bimolecular photochemical processes, such as single-electron transfer (SET) or energy transfer (EnT), resulting in activated radical species that offer new-reactivity patterns unavailable under traditional thermal activation.

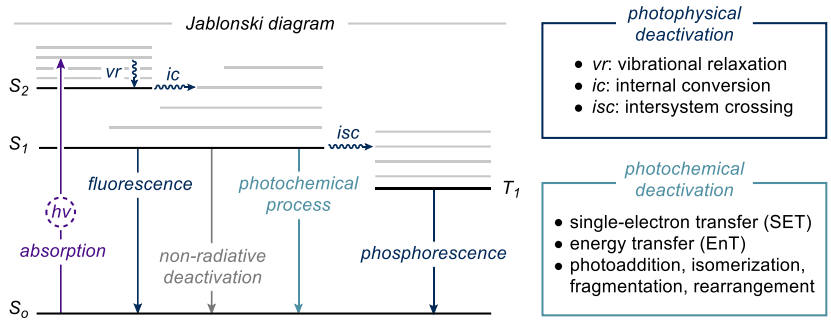

Figure 1.2. Photophysical and photochemical processes on a Jablonski diagram.

S: singlet state; *T*: triplet state.

The earliest reports of photochemical processes dated back to the 18th century.[4] However, organic photochemistry was only established as a field in the early 20th century, after Ciamician and Silber used sunlight to perform transformations of organic molecules in their pioneering studies.[5] From then until lately, only scattered and sporadic reports employed photochemistry for a limited array of organic transformations. This is partly due to the fact that most organic moieties do not interact with visible light, thus the photochemical activation of these colorless substrates required energetic UV-light. The high energy irradiation may affect a broad range of functionality, often leads to inefficient and unselective reactivity.

[3] Lakowicz, J. R. "Principles of Fluorescence Spectroscopy" Springer, 2006.

[4] (a) Roth, H. D. "The Beginnings of Organic Photochemistry." *Angew. Chem., Int. Ed.* **1989**, *28*, 1193; (b) König, B. "Chemical Photocatalysis", Berlin/Boston, Walter de Gruyter GmbH, 2013.

[5] (a) Ciamician, G.; Silber, P. "Chemische Lichtwirkungen" *Ber. Dtsch. Chem. Ges.* **1910**, *43*, 45; (b) Ciamician, G. "The Photochemistry of the Future." *Science*, **1912**, *926*, 385.

Furthermore, these processes required specialized equipment that limited a broad application of photochemistry.

These barriers were recently removed with the introduction of catalytic amount of colored metal complexes (*photoredox catalysts*) as intermediaries between visible light and colorless substrates. Independent reports from MacMillan,[6] Yoon,[7] and Stephenson[8] disclosed the use of tris(bipyridine)ruthenium(II) complex [$Ru(bpy)_3^{2+}$][9] as a photocatalyst to mediate SET processes triggered upon visible-light activation, thus generating radicals under mild conditions. This specific complex had already been used extensively in the context of artificial photosynthesis or water splitting,[10] but had found limited applications in organic chemistry.[11] With the seminal works beginning in 2008, the use of photoredox catalysts in organic synthesis initiated a renaissance of radical chemistry. Built on the research in asymmetric enamine-mediated catalysis,[12] the urge to uncover novel reactivity has provided a force for innovation in enantioselective radical chemistry[13] and photoredox catalysis.[6] The following section describes the polar chemistry of enamine and iminium ion intermediates,

---

[6] Nicewicz, D. A.; MacMillan, D. W. C. "Merging Photoredox Catalysis with Organocatalysis: The Direct Asymmetric Alkylation of Aldehydes." *Science* **2008**, *322*, 77.

[7] Ischay, M. A.; Anzovino, M. E.; Du, J.; Yoon, T. P. "Efficient Visible Light Photocatalysis of [2+2] Enone Cycloadditions." *J. Am. Chem. Soc.* **2008**, *130*, 12886.

[8] Narayanam, J. M. R.; Tucker, J. W.; Stephenson, C. R. J. "Electron-Transfer Photoredox Catalysis: Development of a Tin-Free Reductive Dehalogenation Reaction." *J. Am. Chem. Soc.* **2009**, *131*, 8756.

[9] Paris, J. P.; Brandt, W. W. "Charge Transfer Luminescence of a Ruthenium(II) Chelate." *J. Am. Chem. Soc*. **1959**, *81*, 5001.

[10] (a) Grätzel, M. "Artificial Photosynthesis: Water Cleavage Into Hydrogen and Oxygen by Visible Light." *Acc. Chem. Res*. **1981**, *14*, 376; (b) Meyer, T. J. "Chemical Approaches to Artificial Photosynthesis." *Acc. Chem. Res*. **1989**, *22*, 163.

[11] (a) Hedstrand, D. M.; Kruizinga, W. M.; Kellogg, R. M. "Light Induced and Dye Accelerated Reductions of Phenacyl Onium Salts by 1,4-Dihydropyridines." *Tetrahedron Lett*. **1978**, *19*, 1255; (b) Cano-Yelo, H.; Deronzier, A. "Photo-Oxidation of Some Carbinols by the Ru(II) Polypyridyl Complex-Aryl Diazonium Salt System." *Tetrahedron Lett*. **1984**, *25*, 5517; (c) Okada, K.; Okamoto, K.; Morita, N.; Okubo, K.; Oda, M. "Photosensitized Decarboxylative Michael Addition through *N*-(acyloxy)phthalimides *via* an Electron-Transfer Mechanism." *J. Am. Chem. Soc*. **1991**, *113*, 9401.

[12] (a) MacMillan, D.W.C. "The advent and development of organocatalysis." *Nature* **2008**, *455*, 304; (b) List, B. "Emil Knoevenagel and the roots of aminocatalysis." *Angew. Chem., Int. Ed.* **2010**, *49*, 1730.

[13] Beeson, T. D.; Mastracchio, A.; Hong, J.-B.; Ashton, K.; MacMillan, D. W. C. "Enantioselective Organocatalysis Using SOMO Activation." *Science* **2007**, *316*, 582.

and landmark approaches to harness light energy for their distinct radical chemistry, which also contributed to the development of photoredox catalysis.

1.2 Novel Reactivities from Traditional Enamine and Iminium Ion Intermediates

Enamines are formed upon the condensation of carbonyl compounds **1**, often a ketone or an aldehyde, with a primary or secondary amine (Figure 1.3a). The formation of enamine **I** results in the activation of the α-position of the original ketone, rendering it a good nucleophile.[14] Upon reaction with electrophiles and hydrolysis, the functionalized carbonyl product can be released while regenerating the amine, providing potential for catalysis. Indeed, this catalytic capability was realized by List, Lerner and Barbas[15], where enamine activation was recognized as a general mode of activation that enables diverse α-functionalizations to occur in enantioselective fashion.

MacMillan[16] reported a complementary strategy leveraging on the reversible formation of iminium ions **II** (Figure 1.3b). Condensation of the unsaturated carbonyl **2** with a catalytic amount of chiral amine, an electrophilic intermediate **II** was afforded. A broad panel of nucleophile have been intercepted by **II** to develop useful stereoselective β-functionalization of carbonyl compounds.

[14] Stork, G.; Terrell, R.; Szmuszkovicz, J. "A new synthesis of 2-alkyl and 2-acyl ketones." *J. Am. Chem. Soc.* **1954**, *76*, 2029.

[15] List, B.; Lerner, R. A. and Barbas, C. F. "Proline-Catalyzed Direct Asymmetric Aldol Reactions." *J. Am. Chem. Soc.* **2000**, *122*, 10, 2395.

[16] Ahrent, N. A.; Borths, C. J. and MacMillan D. W. C. "New Strategies for Organic Catalysis: The First Highly Enantioselective Organocatalytic Diels-Alder Reaction." *J. Am. Chem. Soc.* **2000**, *122*, 4243.

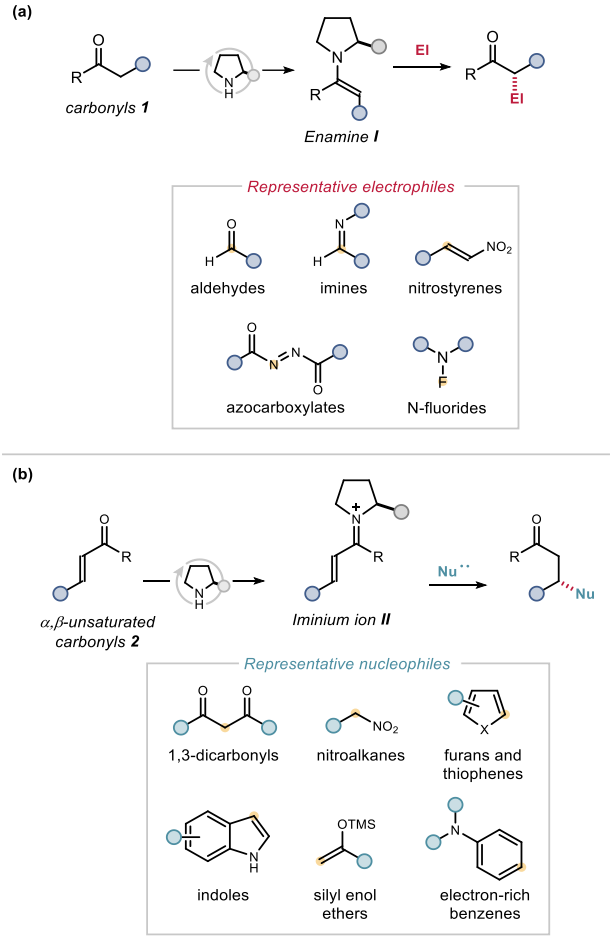

Figure 1.3. The polar reactivities of **(a)** enamine and **(b)** iminium ion intermediates.

Both enamine and iminium ion-mediated catalysis have been recognized as two generic modes of substrate activation. The power of a general mode of catalytic reactivity is that the intermediate formed upon activation of the substrate by the chiral catalyst can participate in many reaction types with consistently high stereoselectivity. On the other hand, the intrinsic limit of this approach is that it only allows the design of mechanistically related processes. Because of these constraints and the extraordinary levels of sophistication already reached, it was considered difficult to further broaden the reactivity boundaries of established modes of organocatalytic activation.

This situation changed dramatically when the tools of asymmetric catalysis were combined with photochemical reactivity. In their seminal report,[6] Nicewicz and MacMillan combined organo- and photocatalysis (Figure 1.4). Specifically, they used [Ru(bpy)$_3$Cl$_2$] (**PC**) to generate radicals **III** through reduction of bromomalonates **3**, which are otherwise inert toward polar substitution with enamines. Meanwhile, condensation of the chiral imidazolidinone catalyst with aldehydes **1** generated the nucleophilic chiral enamine intermediates **I**, which could intercept radicals **III** in a stereoselective fashion. The resulting α-amino radicals **IV** were then oxidized to iminium ions **II** by the excited Ru(II) complex. Eventually, hydrolysis of **II** delivered the enantioenriched α-alkylated aldehydes **4**, while turning the organocatalyst over.

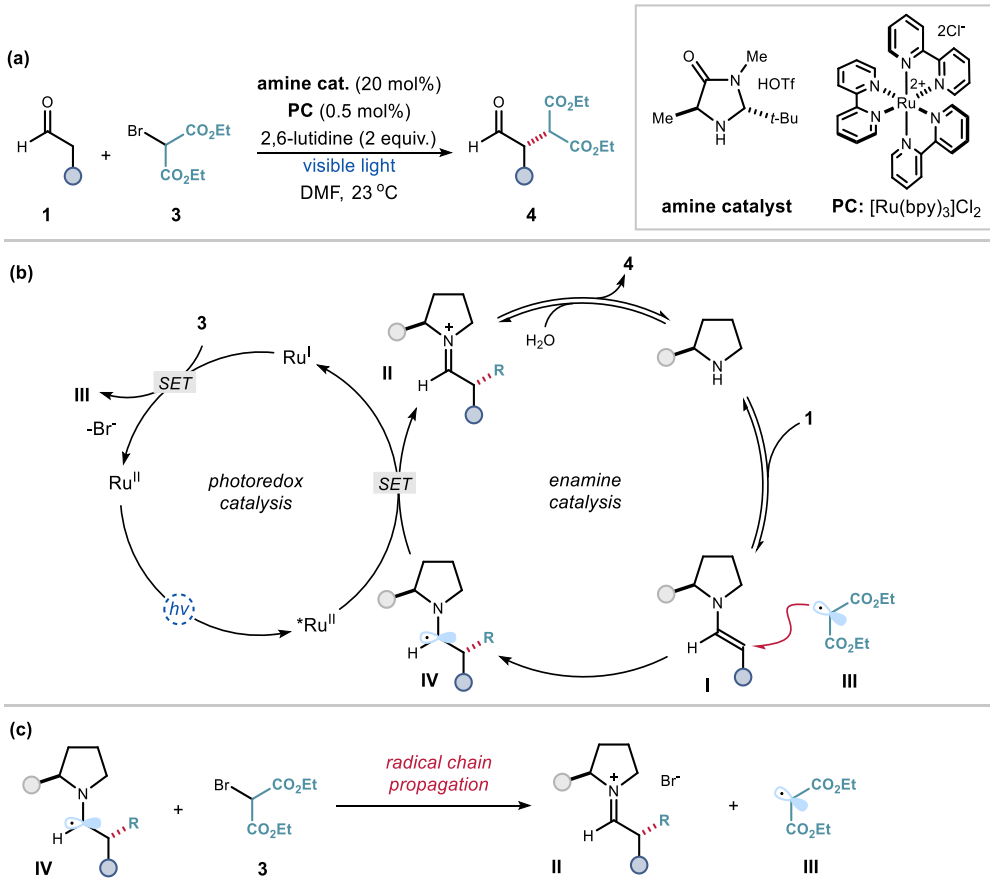

Figure 1.4. The merger of photoredox and organocatalysis for the enantioselective α-alkylation of aldehydes.

Later, Yoon and co-workers showed that, instead of the originally proposed two closed catalytic cycles, a chain propagation mechanism was responsible for product formation (Figure 1.4c). The photoexcited ruthenium catalyst acted as an initiator, and the chain process was propagated by the reductive properties of the α-amino radical **IV**.[17] The stereoselective intermolecular α-alkylation of aldehydes was a long-standing challenge in polar chemistry, which was finally extended leveraging on radical reactivity. Today, a large variety of photoredox catalysts are available and offer powerful tools to generate reactive intermediates through SET events.[18]

The use of a photocatalyst is not the only way to exploit the power of visible light in organocatalytic processes. Our research group found that enamines **I** can behave as a radical initiator upon direct absorption of the energy of photons. During a control experiment, we found that, for specific substrates **5**, the stereoselective reaction could proceed without the need for an external photoredox catalyst (Figure 1.5). While the individual components did not absorb visible light, specific non-covalent aggregations between the electron-rich enamine **I** and electron-poor **5** led to a new charge transfer absorption band in the visible light region.[19] This was because a colored aggregate can form in the ground state, which is known as "electron donor-acceptor" (*EDA)* complexes.[20] Upon irradiation with visible light, an intracomplex SET triggered the fragmentation of C-Br bond and formation of benzyl radicals **V**, which subsequently added stereoselectively to the ground-state enamines **I** to ultimately afford α-benzyl aldehydes **6** with high enantioselectivity. In general, this study established that the synthetic potential of enamine intermediates could be enhanced when

[17] Cismesia, M. A.; Yoon, T. P. "Characterizing Chain Processes in Visible Light Photoredox Catalysis." *Chem. Sci*. **2015**, *6*, 5426.

[18] Shaw, M. H.; Twilton, J.; MacMillan, D. W. C. "Photoredox Catalysis in Organic Chemistry." *J. Org. Chem*. **2016**, *81*, 6898.

[19] (a) Arceo, E.; Jurberg, I. D.; Álvarez-Fernández, A.; Melchiorre, P. "Photochemical Activity of a Key Donor-Acceptor Complex Can Drive Stereoselective Catalytic α-Alkylation of Aldehydes." *Nat. Chem.* **2013**, *5*, 750; (b) Bahamonde, A. and Melchiorre, P. "Mechanism of the Stereoselective α-Alkylation of Aldehydes Driven by the Photochemical Activity of Enamines." *J. Am. Chem. Soc.* **2016**, *138*, 25, 8019.

[20] Crisenza, G. E. M.; Mazzarella, D.; Melchiorre, P. "Synthetic Methods Driven by the Photoactivity of Electron Donor–Acceptor Complexes." *J. Am. Chem. Soc.* **2020**, *142*, 5461.

combined with their photochemical reactivity to unlock reaction pathways inaccessible with thermal activation.

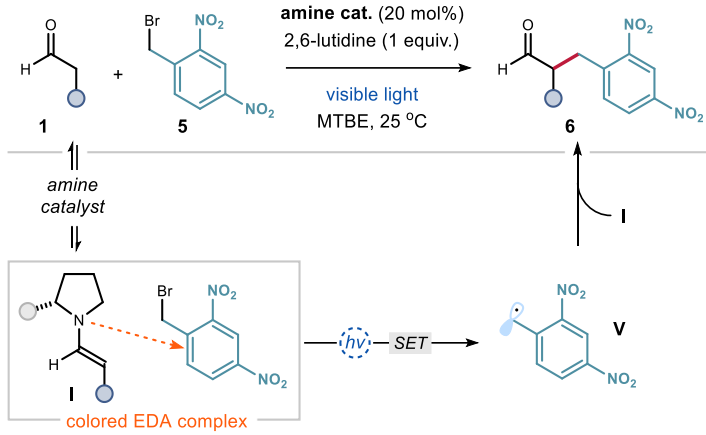

Figure 1.5. Photochemical stereoselective α-alkylation of aldehydes promoted by EDA complex formation. MTBE: methyl *tert*-butyl ether.

While studying enamines' ability to engage in the formation of photoactive EDA complexes, it was found that these chiral catalytic intermediates can engage in a different photochemical strategy for radical generation under mild conditions. Enamines **I** can absorb near UV light (from 365nm till 400 nm) to reach an electronically excited state, from where they can behave as good SET catalysts, mimicking the action of a photoredox catalyst (Figure 1.6). This is because light excitation turns a nucleophilic enamine intermediate [21] into a potent reductant.[22] This increased reducing power ($E^*(\mathbf{I}^{\bullet+}/\mathbf{I}^*)$ = -2.5 V vs Ag^+/Ag) was exploited to generate malonyl radicals **III** from bromomalonates **3**, which could not form EDA complexes with enamines. The ground-state nucleophilic chiral enamines **I** subsequently

[21] Mukherjee, S.; Yang, J. W.; Hoffmann, S.; List, B. "Asymmetric Enamine Catalysis." *Chem. Rev.* **2007**, *107*, 5471.

[22] Silvi, M.; Arceo, E.; Jurberg, I. D.; Cassani, C.; Melchiorre, P. "Enantioselective Organocatalytic Alkylation of Aldehydes and Enals Driven by the Direct Photoexcitation of Enamines." *J. Am. Chem. Soc.* **2015**, *137*, 6120.

intercepted **III** in an enantioselective fashion to afford the α-amino intermediates **IV**. These species then reduced another molecule of substrate **3** to sustain a radical chain process. The resulting iminium ions **II** were eventually hydrolyzed to product **4**, while releasing the aminocatalyst. This work highlighted how a well-established intermediate in ground-state polar chemistry could be repurposed using light to trigger new radical processes by employing its excited state reactivity.[23]

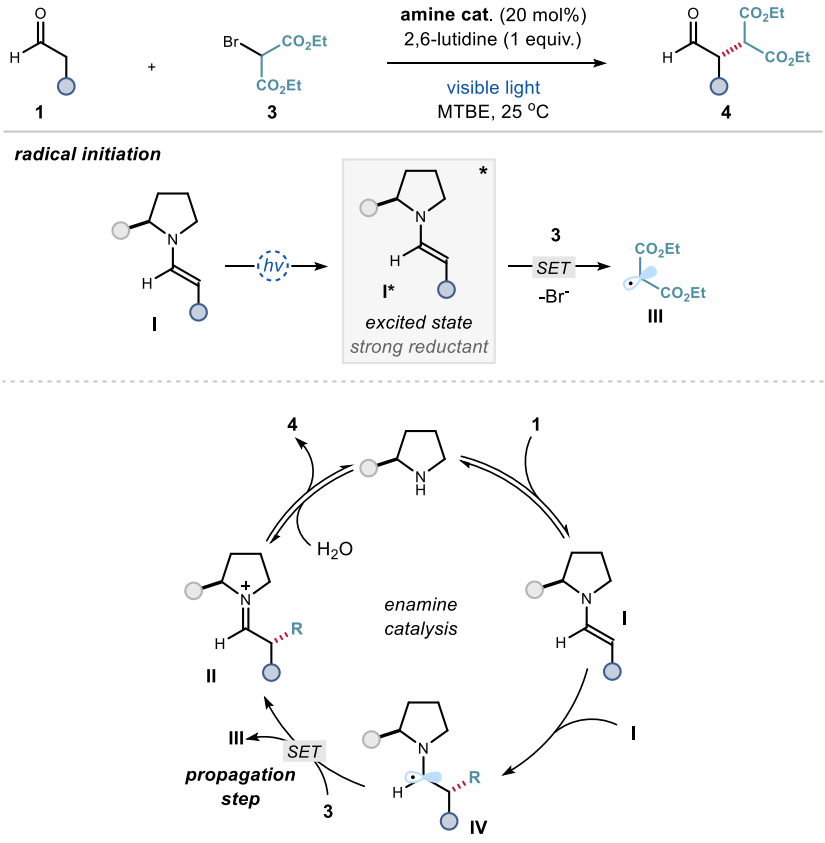

Figure 1.6. Direct photoexcitation of enamines **I** for the stereoselective α-alkylation of aldehydes.

[23] Silvi, M.; Melchiorre, P. "Enhancing the Potential of Enantioselective Organocatalysis with Light" *Nature* **2018**, *554*, 41.

While photochemical activation enabled novel enamine transformations, our group, by analogy, envisioned new radical synthetic avenues for iminium ion intermediates. As the electrophilic sibling of the enamine in organocatalysis, the iminium ion[24] also exhibited new reactivity upon photoexcitation. It was found that electrophilic chiral iminium ions **II** could absorb visible light to reach an electronically excited state (Figure 1.7).[25] These excited iminium ions **II*** acted as strong oxidants (E_{red}(**II***) = +2.40 V vs Ag^+/Ag) to generate radicals from organosilanes **7** through SET. The resulting chiral β-enaminyl and benzylic radicals (**VI** and **VII** respectively) coupled stereoselectively to afford enantioenriched β-functionalized aldehydes **8**. This new reactivity enabled the enantioselective functionalization of enals **2** with non-nucleophilic partners **7** that do not undergo conjugate addition under thermal conditions.

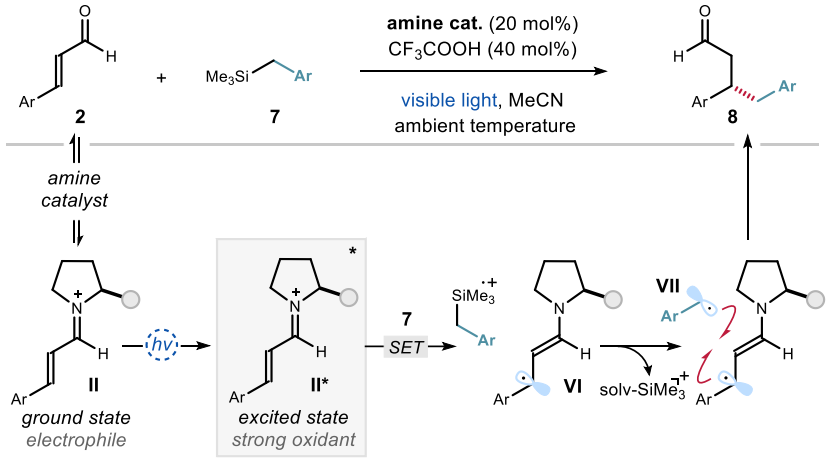

Figure 1.7. Photoexcitation of iminium ions for the enantioselective β-alkylation of enals.

[24] Erkkilä, A.; Majander, I.; Pihko, P. M. "Iminium Catalysis." *Chem. Rev.* **2007**, *107*, 5416.

[25] Silvi, M.; Verrier, C.; Rey, Y. P.; Buzzetti, L.; Melchiorre, P. "Visible-light excitation of iminium ions enables the enantioselective catalytic β-alkylation of enals." *Nat. Chem.* **2017**, *9*, 868.

These examples highlight how cornerstone intermediates of polar organocatalysis with well-known reactivity can be utilized in novel radical pathways upon exploring their photochemistry. In addition to using an external photocatalyst, some highly polarized intermediates can be activated directly with light, or form new visible-light-absorbing aggregates, which is useful for the formation of open-shell species.

Under these premises, this doctoral thesis has investigated the potential of polar organic intermediates with classical thermal reactivity to participate in new radical pathways through combination with photoredox catalysis. The following section details the general objectives of this research.

1.3 General Objectives and Summary

The principal objective of the research work to be described was to repurpose intermediates with established ionic chemistry for new radical processes. While their polar reactivities are well-understood, novel one-electron pathways become achievable through the use of appropriate photoredox catalysts. This enables distinct reactivity patterns, providing new synthetic avenues to overcome specific challenges in organic chemistry.

1.3.1 Enantioselective Conjugate Addition of Non-stabilized Radicals to Iminium Ions

In chapter II, an asymmetric organocatalytic method to synthesize 1,7-dicarbonyl compounds **10** containing a β-stereocenter is described.[26] While products **10** are useful synthetic targets and intermediates towards bioactive motifs, their enantioselective preparation is challenging. To overcome this drawback, we relied on ground-state chiral iminium ions **II** to trap open-shell species, generated by a visible-light-activated photoredox catalyst (Figure 1.8). The chemistry leveraged on the formation of γ-keto radicals **VIII**, generated upon oxidative ring opening of cyclobutanols **9**, mastered by an organic photoredox catalyst. This process

[26] Wong, T.H.-F.; Ma, D.; Di Sanza, R.; Melchiorre, P. "Photoredox Organocatalysis for the Enantioselective Synthesis of 1,7-Dicarbonyl Compounds." *Org. Lett.* **2022**, *24*, 8, 1695.

required the stereoselective interception of these non-stabilized primary radicals, a non-trivial task to be accomplished. This organocatalytic photoredox method served to prepare scaffolds found in natural products and drug molecules.

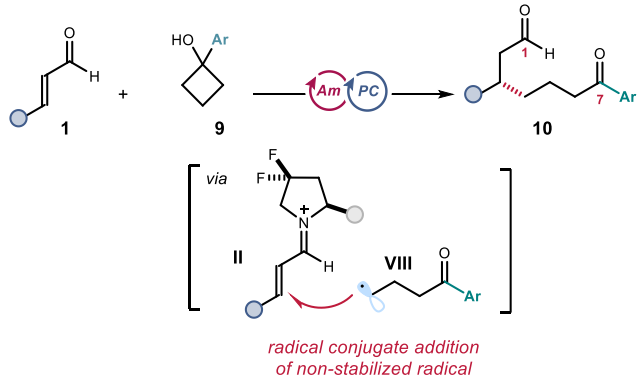

Figure 1.8. Photoredox organocatalysis for enantioselective conjugate additions of non-stabilized radical to enals. Ar: aryl substituent.

1.3.2 Radical Umpolung Strategy for the Stereoselective β-Functionalization of Enals

Chapter III details a distinct strategy to further expand the utility of iminium ion intermediates in asymmetric radical chemistry.[27] The synergistic action of a chiral organocatalyst with a visible-light-activated photoredox catalyst promoted the SET reduction of iminium ions (Figure 1.9), inducing a formal inversion of polarity.[28] The is because the resultant chiral radical **VI**, being nucleophilic in character, could be intercepted by an electrophile, such as an acrylate ester **11** to provide 1,6-dicarbonyl compounds **12** with good enantioselectivity and perfect β-site selectivity.

---

[27] Berger, M.; Ma, D.; Baumgartner, Y.; Wong, T. H.-F.; Melchiorre, P. "Stereoselective conjugate cyanation of enals by combining photoredox and organocatalysis." *Nat. Catal.* **2023**, 6, 332.

[28] Seebach, D. "Methods of reactivity umpolung." *Angew. Chem., Int. Ed.* **1979**, *18*, 239.

This approach further enabled the conjugate cyanation of linear enals, a long-standing challenge in asymmetric catalysis. The key feature was the use of an electrophilic cyanide source **13** for stereogenic radical group transfer, which provided β-cyanoaldehyde **14** with exclusive chemoselectivity and good enantiocontrol.

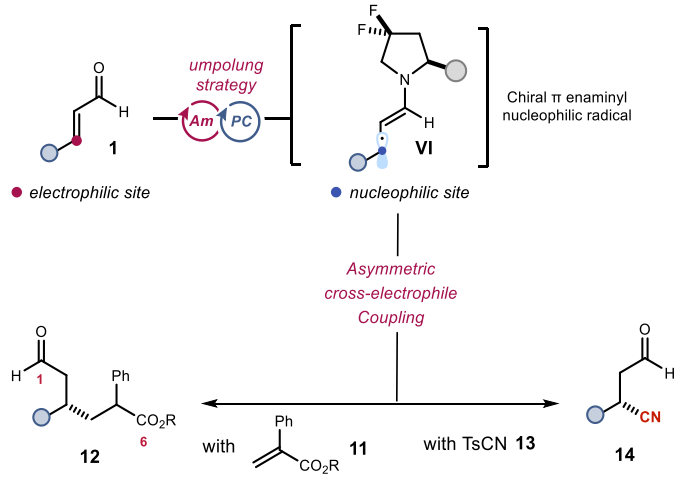

Figure 1.9. Radical *umpolung* strategy for the stereoselective β-functionalization of enals. Ts: tosyl.

1.3.3 Photochemical Synthesis of Thioethers from Aryl Chlorides and Alcohols

Chapter IV discusses a photochemical, organocatalytic method to synthesize thioethers, by combining novel radical chemistry and traditional ionic reactivity of thiourea.[29] While much progress was made in radical activation of aryl chlorides by photoreductants, types of transformation unlocked by the resulting aryl radicals **IX** remained limited. Recognizing *N*-tetramethylthiourea **15** as a simple sulfur source for intercepting aryl radicals, we have

[29] Wu, S.; Wong, T. H.-F.; Righi, P.; Melchiorre, P. "Photochemical Organocatalytic Synthesis of Thioethers from Aryl Chlorides and Alcohols". *J. Am. Chem. Soc.* **2024**, *146*, 2907.

developed a thiol-free organocatalytic protocol that stitches aryl chlorides **16** and alkyl alcohols **17** together under mild conditions, yielding a diverse array of aryl alkyl thioethers **18** (Figure 1.10). Central to this approach was the discovery that radicals **IX** would add to thiourea **15**, which can then be oxidized to form aryl isothiouronium ions **X**. This is a known class of polar intermediate for metal and thiol-free synthesis of thioethers. Formation of **X** under photochemical conditions would permit an intersection with the established polar deoxythiolation pathway with nucleophilic alcohols, delivering thioethers in a mild, selective fashion.

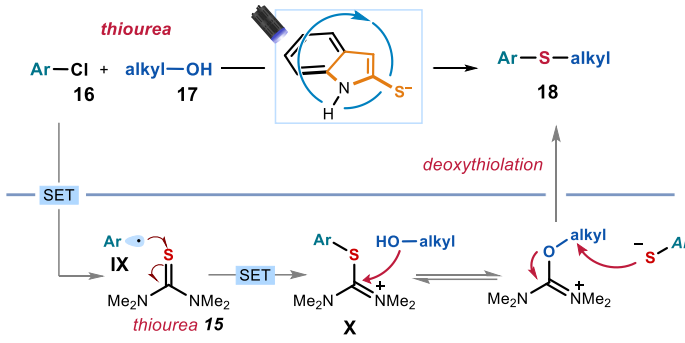

Figure 1.10. Photochemical organocatalytic synthesis of thioethers from aryl chlorides and alcohols

Chapter II

Enantioselective Catalytic Conjugate Addition of Non-stabilized Primary Radicals to Enals

Target

To develop a catalytic system for the enantioselective conjugate addition of non-stabilized, primary radicals to β-substituted aliphatic and aromatic enals, leading to chiral 1,7-dicarbonyl compounds.

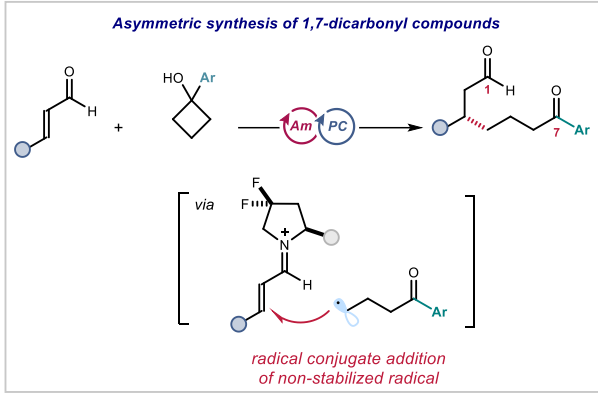

Tool

The synergistic use of a photoredox catalyst, which promotes the generation of non-stabilized radicals from strained-ring precursors, and a chiral secondary amine catalyst, which generates ground-state chiral iminium ions that trap open-shell intermediates and controls stereogenic bond formation with high enantioselectivity.[1]

[1] The project discussed in this chapter has been conducted in collaboration with Dr. Dengke Ma and Dr. Riccardo Di Sanza. I have contributed to exploring the substrate scope of the reaction, synthetic applications and conducted the mechanistic investigations.

This study has been published: Wong, T.H.-F.; Ma, D.; Di Sanza, R.; Melchiorre, P. "Photoredox Organocatalysis for the Enantioselective Synthesis of 1,7-Dicarbonyl Compounds". *Org. Lett.* **2022**, *24*, 8, 1695.

2.1 Introduction

Iminium ion-based catalysis is a powerful method to activate α,β-unsaturated carbonyl compounds.[2] This mode of activation relies on the reversible condensation of chiral amine catalysts with α,β-unsaturated carbonyl substrates to afford a conjugated iminium ion **I** (Figure 2.1a). This intermediate exhibits enhanced electrophilicity with respect to the parent enal due to a decrease in the energy of its lowest unoccupied molecular orbital (LUMO). Consequently, iminium ions react readily with electron-rich partners.[3] Asymmetric iminium ion-based catalysis is commonly used for two types of reactions: cycloadditions and conjugate additions of soft nucleophiles. Although a number of nucleophiles are amenable to this second type of transformation, they are restricted by intrinsic electronic requirements.

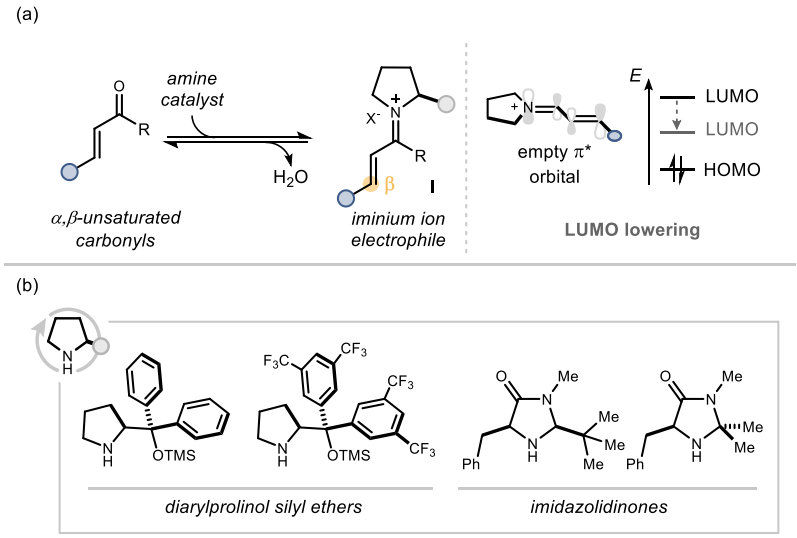

Figure 2.1. (a) General concept of iminium ion activation **(b)** Selected secondary amine catalysts commonly used in iminium-ion activation.

Over the years, various chiral amines derived from natural sources were developed as organocatalysts. Notably, diarylprolinol silyl ethers developed independently by Jørgensen

[2] Erkkilä, A.; Majander, I.; Pihko, P. M. "Iminium Catalysis." *Chem. Rev.* **2007**, *107*, 12, 5416.

[3] (a) Lelais, G.; MacMillan, D.W.C. "Modern strategies in organic catalysis: the advent and development of iminium activation." *Aldrichimica Acta*. **2006**, *39*, 3, 79. (b) Dalko, P. I. "Comprehensive Enantioselective Organocatalysis." Wiley-VCH Verlag, 2013.

and Hayashi,[4] and imidazolidinones developed by MacMillan[5] (Figure 2.1b), both derived from proteinogenic amino acids, are the most commonly employed. They were later found to engage in multiple modes of reactivity, in addition to iminium ion catalysis, in enantioselective fashion. For effective asymmetric induction, these "privileged catalysts"[6] have to fulfill three requirements: (*i*) efficient condensation with the unsaturated carbonyl substrate in a reversible manner, (*ii*) control over the geometry and conformation of the resulting iminium ion, and (*iii*) selective shielding of one of the prochiral faces of the intermediate to provide enantiofacial discrimination.

While iminium ion has prevailed as a generic mode of action for polar chemistry, it is yet difficult to intercept open-shell radical species. For asymmetric iminium ion catalysis to be efficiently applied in the radical regime, a key obstacle had to be overcome: the racemic background reaction known as the *Giese reaction*, that arises from the addition of reactive nucleophilic radicals to electron-poor olefins, including enals.[7] Since this reactivity occurs without the need of catalyst activation, stereogenic bond formation without conformational organization leads to poor stereocontrol. It was theorized that a generally effective approach for enantiocontrol in radical reaction would require "(1) the substrate (to) be placed in a well-defined chiral microenvironment upon binding to the (chiral) template and (2) the substrate-template binding conferring a kinetic advantage to the transformation of interest."[8]

---

[4] (a) Franzén, J.; Marigo, M.; Fielenbach, D.; Wabnitz. T. C.; Kjærsgaard, A.; Jørgensen, K. A. "A General Organocatalyst for Direct α-Functionalization of Aldehydes: Stereoselective C−C, C−N, C−F, C−Br, and C−S Bond-Forming Reactions. Scope and Mechanistic Insights." *J. Am. Chem. Soc.* **2005**, *127*, 18296; (b) Hayashi, Y.; Gotoh, H.; Hayashi, T.; Shoji, M. "Diphenylprolinol Silyl Ethers as Efficient Organocatalysts for the Asymmetric Michael Reaction of Aldehydes and Nitroalkenes." *Angew. Chem., Int. Ed.* **2005**, *44*, 4212.

[5] Ahrendt, K.A.; Borths, C.J.; MacMillan, D.W.C. "New strategies for organic catalysis: the first highly enantioselective organocatalytic Diels− Alder reaction." *J. Am. Chem. Soc.* **2000**, *122*,17, 4243.

[6] Yoon, T.P.; Jacobsen, E.N. "Privileged Chiral Catalysts." *Science* **2003**, *299*, 5613, 1691.

[7] Giese, B. "Formation of C-C Bonds by Addition of Free Radicals to Alkenes." *Angew. Chem., Int. Ed.* **1983**, *22*, 10, 753.

[8] Cauble, D. F.; Lynch, V.; Krische, M. J. "Studies on the Enantioselective Catalysis of Photochemically Promoted Transformations: "Sensitizing Receptors" as Chiral Catalysts." *J. Org. Chem.* **2003**, *68*, 15.

In 2017, our group uncovered the ability of chiral iminium ions **I**, derived from aromatic enals **1**, to become strong oxidants upon absorption of visible light.[9] This new mode of activation paved the way for a new method to alkylate enals at the β-position stereoselectively (Figure 2.2). Specifically, the oxidative power of the excited iminium ion was harnessed to generate carbon-centered radicals upon single-electron transfer (SET) oxidation of stable non-nucleophilic precursors. Only in presence of chiral amine catalyst and formation of iminium ion, excitation and radical generation could occur. This chemistry was proposed to proceed via a radical coupling event between the chiral β-enaminyl radical **IIIa**, arising from the iminium ion, and the open-shell intermediate **II** generated from benzyl silanes **2**. Since radicals were generated in proximity, the radical coupling with vicinal benzylic radical could efficiently occur, preventing the racemic background process.[10] The overall reaction delivered enantioenriched aldehydes **3** with β-functionalization.

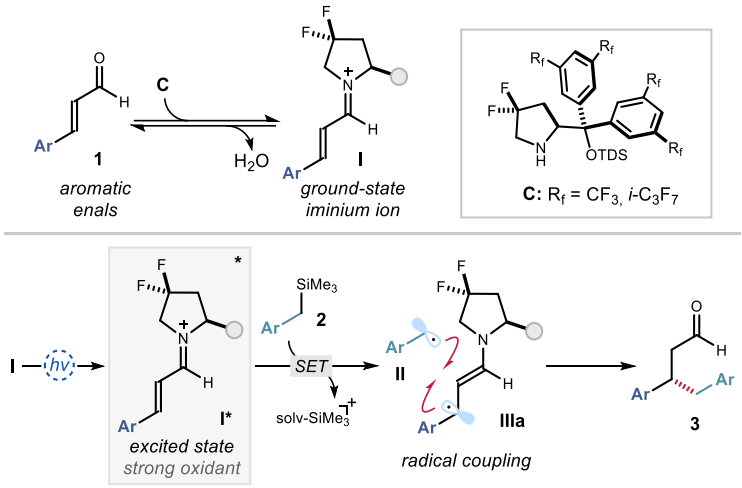

Figure 2.2. Excited-state iminium ion reactivity of aromatic enals. TDS: *tert*-hexyldimethylsilyl.

Despite previously reported aminocatalysts were ill-suited for this transformation, a difluorinated prolinol catalyst **C** was rationally designed for the photoexcitation of chiral

[9] Silvi, M.; Verrier, C.; Rey, Y. P.; Buzzetti, L.; Melchiorre, P. "Visible-light excitation of iminium ions enables the enantioselective catalytic β-alkylation of enals." *Nat. Chem.* **2017**, *9*, 868.

[10] Leifert, D.; Studer, A. "The Persistent Radical Effect in Organic Synthesis." *Angew. Chem., Int. Ed.* **2020**, *59*, 74.

iminium ions. The *gem*-difluorine moiety was essential to increase stability towards oxidation of the amine catalyst, therefore preventing its decomposition under the highly oxidizing conditions.

In subsequent studies, the scope of radical precursors amenable to this chemistry was greatly expanded. However, non-stabilized primary radicals remained recalcitrant to participate in intermolecular stereogenic bond formation, mainly associated with the difficulty for radical generation upon iminium ion photoexcitation, and their poor tendency towards productive radical coupling. Another limitation was related to the need of an aromatic substituent at the β-position of enal **1**, since an aliphatic group completely hampered the excited-state reactivity the iminium ion. One possibility for this lack of reactivity is ascribable to the inability of aliphatic iminium ions to absorb light in the visible region. Other contributing factors might be related to the formation of photo- and redox-active dienamines[11] that interfere with SET events (Figure 2.3a), or an inefficient radical coupling with the transient β-enaminyl radicals **IIIb**, which are less stabilized and more short-lived than the phenyl substituted counterparts **IIIa** (Figure 2.3b).

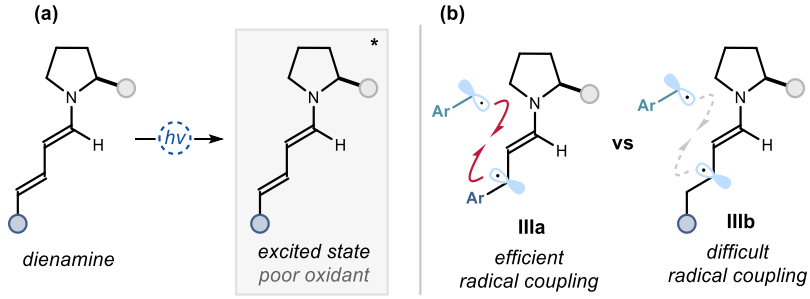

Figure 2.3. Rationalization for the lack of photoreactivity in aliphatic iminium ions based on (**a**) the electronic properties of photoexcited dienamines and (**b**) the stability of the β-enaminyl radical for radical coupling.

[11] (a) Silvi, M.; Arceo, E.; Jurberg, I. D.; Cassani, C.; Melchiorre, P. "Enantioselective Organocatalytic Alkylation of Aldehydes and Enals Driven by the Direct Photoexcitation of Enamines." *J. Am. Chem. Soc.* **2015**, *137*, 6120; (b) Bamahonde, A.; Melchiorre, P. "Mechanism of the Stereoselective α-Alkylation of Aldehydes Driven by the Photochemical Activity of Enamines." *J. Am. Chem. Soc.* **2016**, *138*, 8019. (c) Balletti, M.; Wachsmuth, T.; Di Sabato, A.; Hartley, W. C.; Melchiorre, P. "Enantioselective catalytic remote perfluoroalkylation of α-branched enals driven by light." *Chem. Sci.* **2023**, *14*, 4923.

To overcome these challenges, we surmised that decoupling the radical generation strategy from the stereo-determining C-C bond-forming event would be critical. When a light-activated photoredox catalyst generates radicals form redox-active substrates, the ground-state electrophilic iminium ion **I** would intercept the ensuing radicals, imparting enantioselectivity by out-competing racemic background reactions. In particular, we hoped that this approach could realize the stereoselective interception of non-stabilized primary radical, which had remained challenging due to their transient nature.

This chapter discusses the development of a dual-catalytic strategy that combined ground-state iminium ion catalysis with the action of an external photoredox catalyst, which secured the generation of non-stabilized radicals **IV** from strained-ring alcohols, and their stereocontrolled interception. The net reaction is an enantioselective radical conjugate addition to *both linear aliphatic* and *aromatic* enals **1**, affording 1,7-dicarbonyl compound **5** with a β-stereocenter (Figure 2.4), which served to prepare useful scaffolds found in natural products and drug molecules.

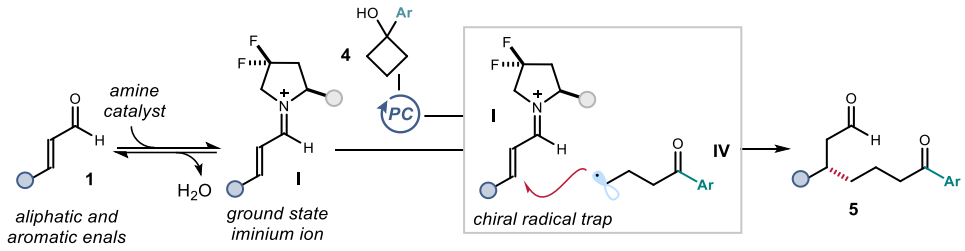

Figure 2.4. Proposed strategy for developing an enantioselective conjugate addition of non-stabilized radicals to aromatic and aliphatic enals.

In the following sections, literature precedence for catalytic asymmetric radical conjugate addition reactions will be discussed. The scientific background and previous studies that were essential to the development of the present research project will also be detailed.

2.2 Background

2.2.1 Enantioselective Radical Conjugate Additions with Chiral Lewis acids catalysts

Nucleophilic carbon-centered radicals are prone to attack electron-deficient olefins.[12] Their conjugate addition to α,β-unsaturated carbonyl substrates represents an important class of C-C bond-forming process. This approach has gained further prominence with the development of mild and tunable radical generation by means of photoredox catalysis.[13] Nonetheless, development of an enantioselective variant has been challenging, as the chiral catalyst-activated substrate would need to out-compete the racemic background reactions to achieve good stereocontorl.

The initial solutions to control the stereochemical outcome of a radical conjugate addition relied on chiral auxiliaries.[14] The first example describing an asymmetric catalytic strategy was published in 1996 by Sibi and Porter, who reported a Lewis acid-assisted enantioselective radical conjugate addition.[15] They disclosed that a metal complex, generated upon coordination of a chiral ligand $\mathbf{L_1}$* to a Zn^{2+} or Mg^{2+} cation, could activate acyclic amides **6**, adorned with an oxazolidinone moiety, while shielding one of the prochiral faces of the alkene (Figure 2.5a). Stereocontrolled radical addition to the β-position delivered products **8** with moderate to good enantioselectivity. The key to achieving high enantioenrichment rested on the strong binding and conformational control by the metal complex (Figure 2.5b). In addition, activation of acrylamides **6** increased the rate of radical conjugate addition, outcompeting racemic background reactions.

Importantly, as metal-ligand coordination is reversible, ligand exchange would release the product, thus unlocking the opportunity for catalysis. Lowering the loading of the Lewis

---

[12] (a) Giese, B. "The Stereoselectivity of Intermolecular Free Radical Reactions." *Angew. Chem., Int. Ed.* **1989**, *28*, 969; (b) Srikanth, G. S. C.; Castle, S. L. "Advances in radical conjugate additions." *Tetrahedron* **2005**, *61*, 10377.

[13] Kanegusuku, A. L. G.; Roizen, J. L. "Recent Advances in Photoredox-Mediated Radical Conjugate Addition Reactions: An Expanding Toolkit for the Giese Reaction."*Angew. Chem., Int. Ed.* **2021**, *60*, 39, 21116.

[14] Porter, N. A.; Giese, B.; Curran, D. P. "Acyclic Stereochemical Control in Free-Radical Reactions." *Acc. Chem. Res.* **1991**, *24*, 296.

[15] Sibi, M. P.; Ji, J.; Wu, J. H.; Gürtler, S.; Porter, N. A. "Chiral Lewis Acid Catalysis in Radical Reactions: Enantioselective Conjugate Radical Additions." *J. Am. Chem. Soc.* **1996**, *118*, 9200.

acid from 1 equivalent to 20 mol% retained the reactivity with diminished yet significant level of enantioinduction (67-70%). This indicated that catalyst turnover was feasible in this reaction, which therefore could be considered as the first example of catalytic enantioselective radical conjugate addition. Nonetheless, the main drawback of this system was the need for cryogenic temperatures (–78 °C), highlighting the difficulty to minimize the rate of a strong background racemic process. Modifying the chiral bisoxazoline ligand **L₁*** to a more rigid scaffold **L₂*** secured the level of enantioinduction at ambient temperature and allowed a low catalyst loading (Figure 2.5c).[16]

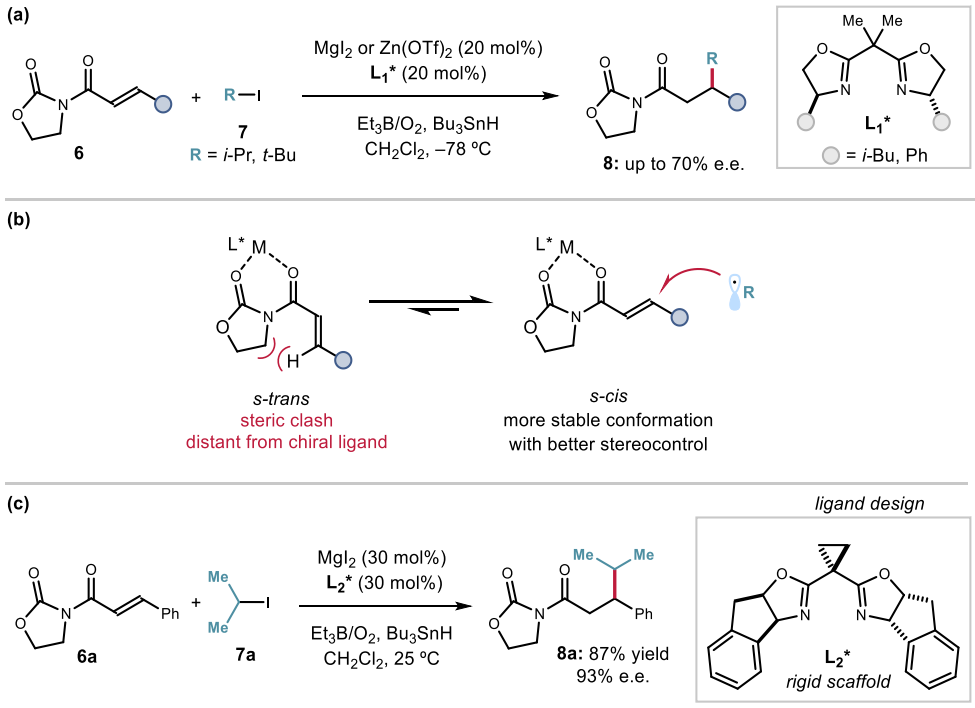

Figure 2.5. (**a**) The first catalytic enantioselective chiral Lewis acid-mediated radical conjugate addition. (**b**) An improved protocol enabled by ligand design. (**c**) Stereochemical model for stereoinduction.

[16] Sibi, M. P.; Ji, J. "Practical and Efficient Enantioselective Conjugate Radical Additions." *J. Org. Chem.* **1997**, *62*, 3800.

This Lewis acid-based catalytic system was later extended to a variety of conjugated carbonyl substrates, including β-acyloxy acrylates,[17] imides,[18] acyloxy pyrones,[19] and α′-phosphoric enones.[20] There are two main disadvantages to this strategy: (*i*) the substrates ought to be judiciously designed and prepared, since a preinstalled moiety (e.g. oxazolidinone) was essential as the anchoring point for binding to Lewis acid catalyst; (*ii*) stoichiometric, hazardous stannane and borane reagents were needed for radical generation.

Subsequently, the Sibi group also reported a radical conjugate addition to benzoate derivatives **9** (Figure 2.6). Even though enones offer a monodentate handle for binding to the chiral Lewis acid metal complex, inclusion of a sterically demanding benzoate moiety enabled stereo-discrimination between the prochiral faces of the exocyclic double bond, permitting high stereoselectivity.[21] Specifically, the lone-pair electrons on the carbonyl oxygen of substrate **9** coordinated to the chiral aluminum(salen) complex **[Al]**. The most stable transition state **TS-I** left the *si*-face of the alkene more exposed for radical addition, and delivered the enantioenriched products **10** (Figure 2.6). In addition to secondary and tertiary alkyl iodides, *n*-propyl iodide and 1-iodopent-4-ene were also suitable to this reactivity. This served as a proof of concept that non-stabilized, primary radicals can be captured asymmetrically.

[17] Sibi, M. P.; Zimmerman, J.; Rheault, T. "Enantioselective Conjugate Radical Addition to β-Acyloxy Acrylate Acceptors: An Approach to Acetate Aldol-Type Products." *Angew. Chem., Int. Ed.* **2003**, *42*, 4521.

[18] Sibi, M. P.; Petrovic, G.; Zimmerman, J. "Enantioselective Radical Addition/Trapping Reactions with α,β-Disubstituted Unsaturated Imides. Synthesis of anti-Propionate Aldols." *J. Am. Chem. Soc.* **2005**, *127*, 2390.

[19] Sibi, M. P.; Zimmerman, J. "Pyrones to Pyrans: Enantioselective Radical Additions to Acyloxy Pyrones." *J. Am. Chem. Soc.* **2006**, *128*, 13346.

[20] Lee, S.; Kim, S. "Enantioselective Radical Conjugate Addition to α′-Phosphoric Enones." *Org. Lett.* **2008**, *10*, 4255.

[21] Sibi, M. P.; Nad, S. "Enantioselective Radical Reactions: Stereoselective Aldol Synthesis from Cyclic Ketones." *Angew. Chem., Int. Ed.* **2007**, *46*, 9231.

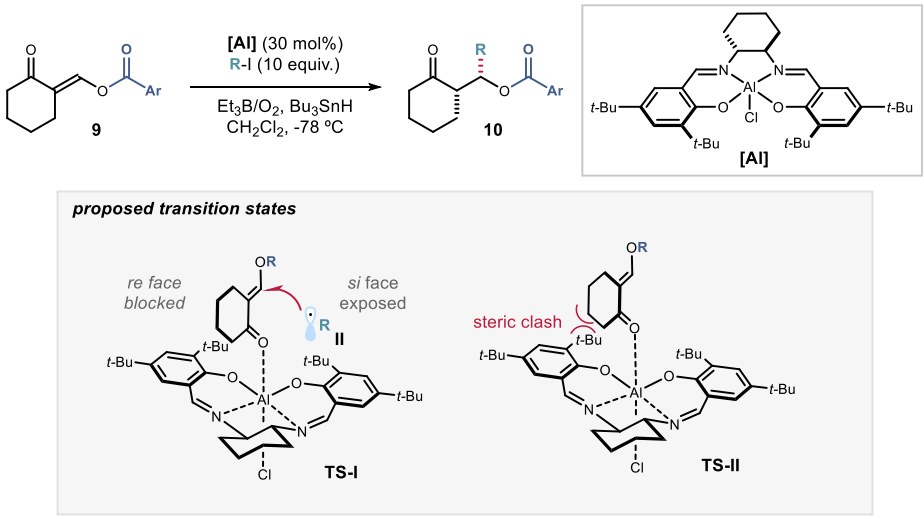

Figure 2.6. Radical conjugate addition to cyclic ketones bearing an exocyclic alkene and a benzoate ester.

With the advent of photoredox catalysis,[22] some drawbacks associated with Sibi's strategy could be overcome by using a catalyst activated by light to generate radicals under mild conditions.[13] In 2015, Yoon and co-workers realized a dual catalytic strategy for enantioselective β-functionalization. A ruthenium-based photoredox catalyst was utilized to generate nucleophilic radicals **VI** from α-aminosilanes **12**[23] and α-phenoxysilanes[24] (Figure 2.7). A scandium(III) Lewis acid, coordinated by PyBox ligand **L*** could bind and activate a crotonate substrate bearing a pyrazolidinone moiety (**11**) to form an electrophilic chiral intermediate **V**. The radical **VI**, produced upon SET oxidation of **12** by the photoredox catalyst and fragmentation of the trimethylsilyl group, could undergo radical conjugate addition to **V** to deliver α-carbonyl radical **VII**. SET, protonation and ligand exchange released the enantioenriched, β-functionalized product **13**. This system established the

[22] Shaw, M. H.; Twilton, J.; MacMillan, D. W. C. "Photoredox Catalysis in Organic Chemistry." *J. Org. Chem.* **2016**, *81*, 6898.

[23] Ruiz Espelt, L.; McPherson, I. S.; Wiensch, E. M.; Yoon, T. P. "Enantioselective Conjugate Additions of α-Amino Radicals via Cooperative Photoredox and Lewis Acid Catalysis." *J. Am. Chem. Soc.* **2015**, *137*, 2452.

[24] Dong, X.; Li, Q. Y.; Yoon, T. P. "Enantioselective Synthesis of γ-Oxycarbonyl Motifs by Conjugate Addition of Photogenerated α-Alkoxy Radicals." *Org. Lett.* **2021**, *23*, 5703.

feasibility of combining a chiral Lewis acid with photocatalytically generated radicals to perform asymmetric radical conjugate additions.

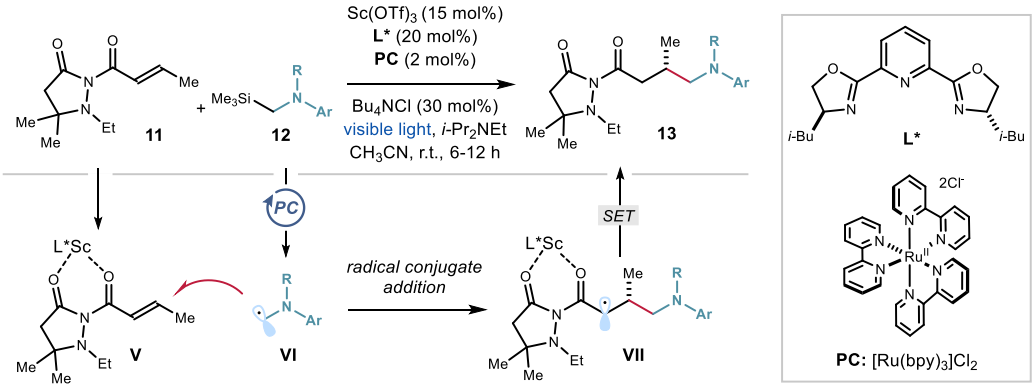

Figure 2.7. Asymmetric radical conjugate addition using photocatalytically generated α-amino radicals.

r.t.: room temperature

In 2016, Meggers *et al.* disclosed a similar reaction, where they used a chiral-at-metal Lewis acid in concert with an organic photoredox catalyst (Figure 2.8).[25] Using potassium trifluoroborate salts **15** as precursor, benzylic, secondary and tertiary alkyl, and α-oxy radicals could be generated and captured in a stereocontrolled fashion. Compared to the previous work where only α-heteroatomic radicals could be used, this report demonstrated a broader scope of substrates with a lower catalyst loading.

The C2-symmetrical Rh(III) catalyst **Λ-[Rh]** poised conformational constraints on substrates **14** by coordination to the imidazole template, while drastically increasing reaction rate of radical addition to acrylamide (> 3 x 10^4 fold) when compared to racemic background reaction. Oxidation of potassium trifluoroborate salts **15** by the excited organic photocatalyst **PC*** delivered an alkyl radical **II** that was captured enantioselectively by **VIII** to afford intermediates **IX**. SET from **PC**$^{\bullet-}$ to resultant radical **IX** released the enantioenriched products **16** in high yield, while ligand exchange restored **VIII** for the next cycle of catalysis. The versatility of this system was demonstrated in subsequent reports by the use of various radical

[25] Huo, H.; Harms, K.; Meggers, E. "Catalytic, Enantioselective Addition of Alkyl Radicals to Alkenes via Visible-Light-Activated Photoredox Catalysis with a Chiral Rhodium Complex." *J. Am. Chem. Soc.* **2016**, *138*, 6936.

precursors, such as dihydropyridines (DHPs)[26] and *N*-(acyloxy)phthalimides,[27] which reacted smoothly to afford β-functionalized products **16**.

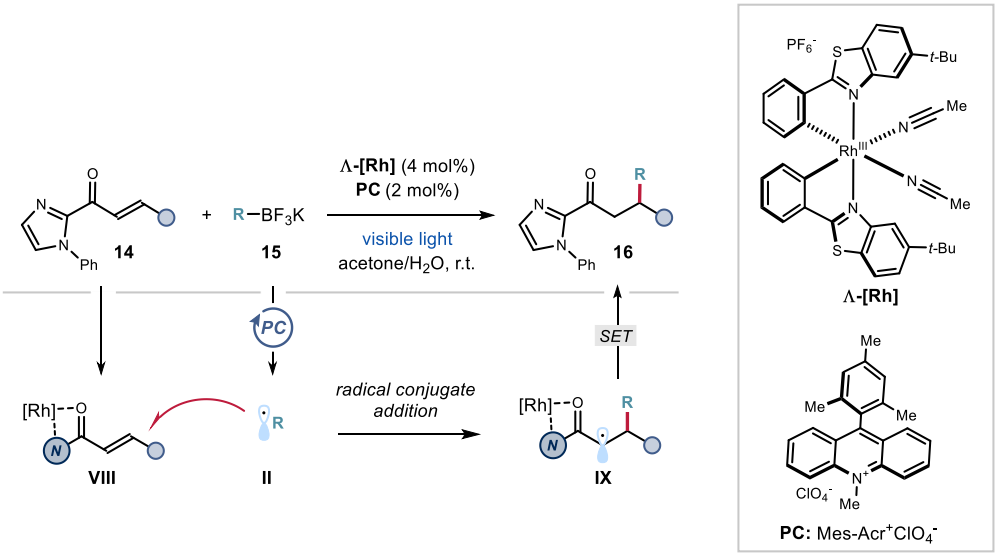

Figure 2.8. Photocatalytic asymmetric radical conjugate addition reaction using trifluoroborates as source of alkyl radicals.

A new system for asymmetric conjugate additions was recently reported based on the use of a chiral Ni(II) complex **[Ni]**, generated in situ by coordination of a nickel salt with a dibenzofurandiyl-2,2′-bis(4-phenyloxazoline) chiral ligand **L*** (Figure 2.9).[28] However, this work diverged mechanistically from Meggers and Yoon's systems, since no external photocatalyst was employed. Instead, it was proposed that the nickel complex acted both as a chiral Lewis acid and a photoredox catalyst for the enantioselective radical conjugate addition of α-amino radicals to *N*-acyl pyrazole-templated Michael acceptors **17**.

[26] de Assis, F. F.; Huang, X.; Akiyama, M.; Pilli, R. A.; Meggers, E. "Visible-Light-Activated Catalytic Enantioselective β-Alkylation of α,β-Unsaturated 2-Acyl Imidazoles Using Hantzsch Esters as Radical Reservoirs." *J. Org. Chem.* **2018**, *83*, 10922.

[27] Ma, J.; Lin, J.; Zhao, L.; Harms, K.; Marsch, M.; Xie, X.; Meggers, E. "Synthesis of β-Substituted γ-Aminobutyric Acid Derivatives through Enantioselective Photoredox Catalysis." *Angew. Chem., Int. Ed.* **2018**, *57*, 11193.

[28] Shen, X.; Li, Y.; Wen, Z.; Cao, S.; Hou, X.; Gong, L. "A Chiral Nickel DBFOX Complex as a Bifunctional Catalyst for Visible-Light-Promoted Asymmetric Photoredox Reactions." *Chem. Sci.* **2018**, *9*, 4562.

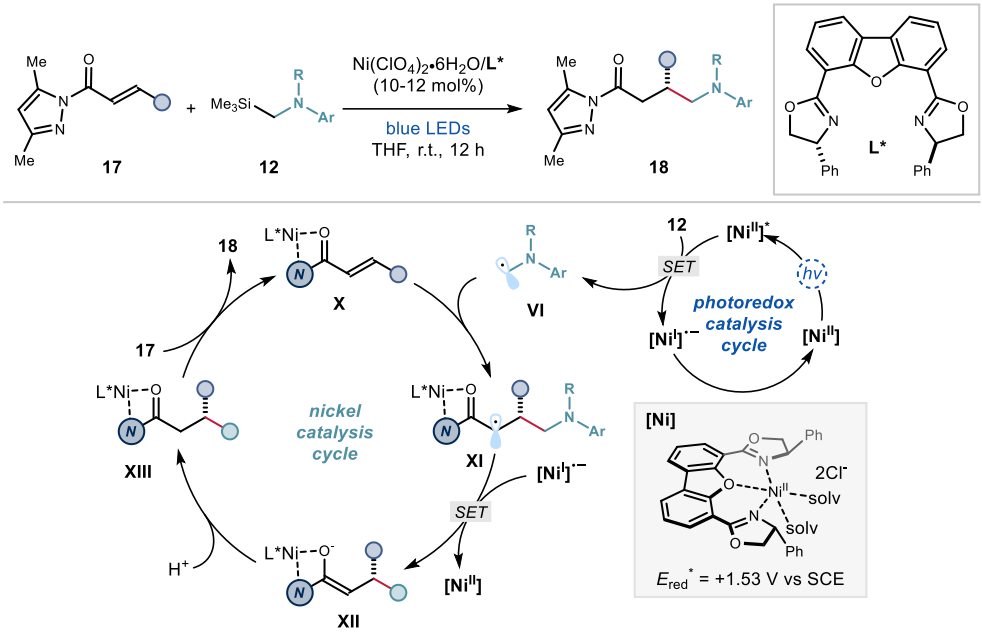

Figure 2.9. A nickel complex acting as bifunctional photoredox and chiral Lewis acid catalyst. THF: tetrahydrofuran, LED: light-emitting diode.

In the proposed mechanism, the colored Ni complex (**[Ni]**) reached an excited state **[Ni]*** upon absorption of visible light. **[Ni]*** (E^*_{red}= +1.53V vs SCE, standard calomel electrode**)** is a good oxidant able to generate α-amino radicals **VI** through SET oxidation of the corresponding trimethylsilyl precursors **12**. Concomitantly, coordination of substrate **17** to another molecule of **[Ni]** enhanced its electrophilicity and promoted the radical 1,4-addition to **X**. SET from the **[Ni]**$^{\bullet-}$ to α-carbonyl radicals **XI** provided metal-enolate complexes **XII** while regenerating **[Ni]**. Subsequent protonation and ligand dissociation eventually delivered products **18** in high yield and enantioselectivity while restarting the catalytic cycle.

The Xiao group reported an alternative method to bypass the use of precious metals as catalysts, employing a novel octahedral Co(II)-complex based on a chiral N_4-ligand (**[Co]**) (Figure 2.10).[29] DHPs **19** were selected as a source of carbon-centered radicals for their conjugate addition to imidazole-bound enoates **14**.

[29] Zhang, K.; Lu, L.-Q.; Jia, Y.; Wang, Y.; Lu, F.-D.; Pan, F.; Xiao, W.-J. "Exploration of Novel Chiral Cobalt Catalyst for Visible-Light-Induced Enantioselective Radical Conjugate Addition." *Angew. Chem., Int. Ed.* **2019**, *58*, 13375.

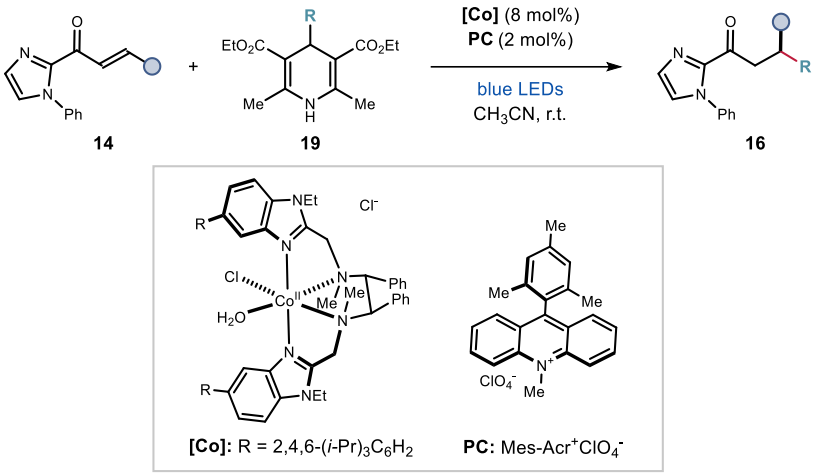

Figure 2.10. Asymmetric photochemical Giese reactions catalyzed by an octahedral chiral cobalt catalyst.

These recent examples showcase how the power of modern photoredox catalysis has been harnessed to facilitate the development of catalytic enantioselective radical conjugate additions. However, the discussed systems are restricted by the need to preinstall a specific anchoring group (e.g. oxazolidinone, acyl pyrazoles and imidazoles) within the unsaturated carbonyl substrates, to facilitate chelation to a chiral Lewis acid catalyst.

2.2.2 Organocatalytic and Biocatalytic Asymmetric Radical Conjugate Additions

In addition to transition metal-based systems, some metal-free methods have been developed for asymmetric catalytic radical conjugate addition processes. In 2005, Bach and co-workers described an intramolecular radical addition of pyrrolidines **20** to afford spirocyclic compounds **21** (Figure 2.11).[30] The chiral benzophenone-containing catalyst **BP** coordinated with substrate **20** through hydrogen-bonding interactions, effectively shielding one prochiral faces of the substrate. UV-light irradiation of the benzophenone moiety within intermediate **XIV** promoted SET oxidation of the pyrrolidine unit that, upon proton loss, generated the α-

[30] Bauer, A.; Westkämper, F.; Grimme, S.; Bach, T. "Catalytic enantioselective reactions driven by photoinduced electron transfer." *Nature* **2005**, *436*, 1139.

amino radical intermediate (**XV**). A stereocontrolled cyclization and followed by protonation delivered the chiral products **21**.

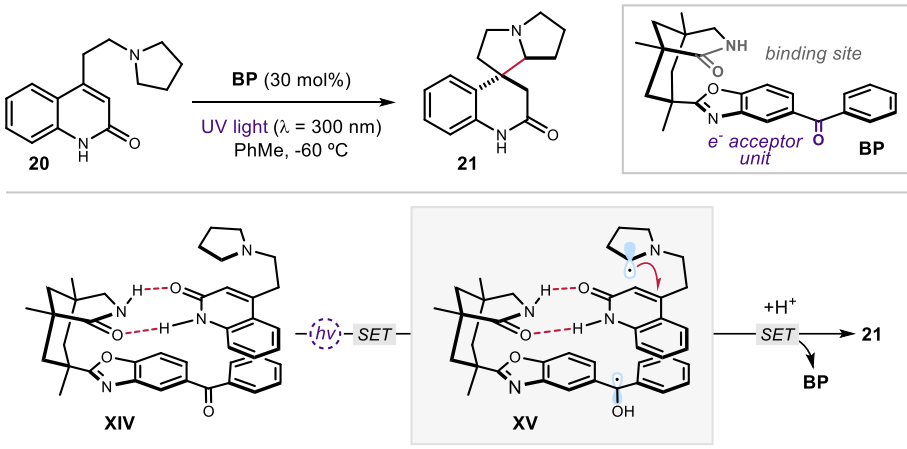

Figure 2.11. Enantioselective photoinduced-electron-transfer (PET)-mediated cyclization.

A strategy to functionalize cyclic enones was reported by our research group. In particular, the combination of a chiral primary amine catalyst **A1** and a photoredox catalyst (**PC**) could promote an intermolecular radical conjugate addition to β-substituted cyclic enones **22** to forge quaternary carbon stereocenters in an enantioselective fashion (Figure 2.12).[31] The key to success of the reaction was to achieve in situ formation of the electrophilic iminium ion **XVI**, through condensation of chiral primary amine catalyst **A1** with enones. Upon addition of radicals **II** to the chiral iminium ions **XVI**, the 3π-radical cations **XVII** underwent intramolecular SET from an electron-rich carbazole moiety, strategically placed within the chiral organocatalyst **A1**. This afforded more stable carbazole radical cations, therefore preventing the unproductive β-scission that could revert back to **XVI** and **II**. The subsequent fast tautomerization from the enamines to the imines **XVIII** avoided a back-electron transfer. [32] Finally, reduction of the carbazole radical cations **XIX** from the reduced

[31] Murphy, J. J.; Bastida, D.; Paria, S.; Fagnoni, M.; Melchiorre, P. "Asymmetric Catalytic Formation of Quaternary Carbons by Iminium Ion Trapping of Radicals." *Nature* **2016**, *532*, 218.

[32] Rappaport, Z., Ed. The Chemistry of Enamines; John Wiley and Sons: Chichester, 1994.

photocatalyst and hydrolysis regenerated the aminocatalyst **A1**.[33] The presence of a β-substituent in the enone substrate helped to slow down the rate of the racemic background reaction, which was essential to achieve cyclic ketone products **24** with a high level of chirality induction.[34]

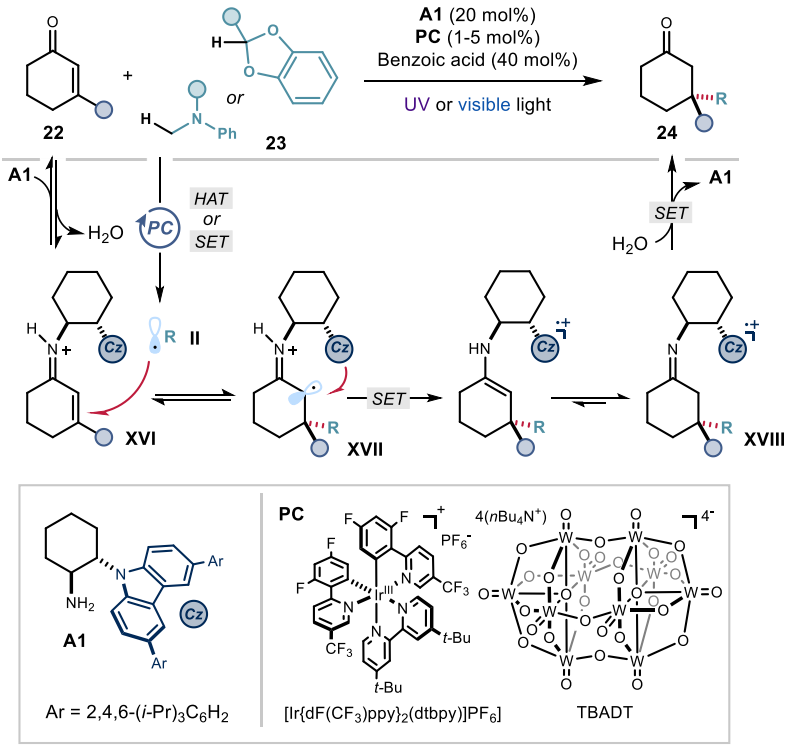

Figure 2.12. Photochemical organocatalytic strategy for the formation of quaternary stereocenters by radical conjugate addition to iminium ions. TBADT: tetrabutylammonium decatungstate.

In this study, chiral iminium ions **XVI** was isolated as bright-yellow crystals. X-ray crystallographic analyses[35] established a short distance (3.10 Å) between the electron-rich

[33] Bahamonde, A.; Murphy, J. J.; Savarese, M.; Brémond, E.; Cavalli, A.; Melchiorre, P. "Studies on the enantioselective iminium ion trapping of radicals triggered by an electron-relay mechanism." *J. Am. Chem. Soc.* **2017**, *139*, 4559.

[34] Bastida, D. "Novel Enantioselective Aminocatalytic Processes by means of Vinylogous Reactivity and Photoredox Catalysis". Ph.D. Thesis, Universitat Rovira i Virgili, Tarragona, Spain, 2015.

[35] Crystallographic data for compound **XV** has been deposited with the Cambridge Crystallographic Data Centre, accession number CCDC 1437991.

carbazole unit and the electron-deficient iminium ion, suggesting the formation of an intramolecular electron donor-acceptor (EDA) complex[36] (Figure 2.13). Capitalizing upon this observation, the photoactivity of the intermediate EDA complex was used to trigger radical conjugate addition to β-substituted cyclic enones **22** without using an external photocatalyst.[37] Condensation of the modified carbazole catalyst **A2** with a cyclic enone **22** generated an intramolecular EDA complex **XVI**. Upon irradiation with visible light, an intramolecular SET was induced to give intermediate **XIX**, bearing a persistent carbazole radical cation moiety. This functionality could act as a SET oxidant (E (**A1**$^{\bullet+}$/**A1**) = +1.09 V vs. Ag^+/Ag in CH_3CN) to generate radicals **II** from suitable precursors such as **2** (E_{red} < +1.09 V). These two SET events constituted the initiation of a radical chain process. Interception of **II** by the ground-state iminium ion **XVI** through Giese addition and subsequent intramolecular SET afforded intermediate **XVIII**, which propagated the radical-chain process through oxidation of **2**.

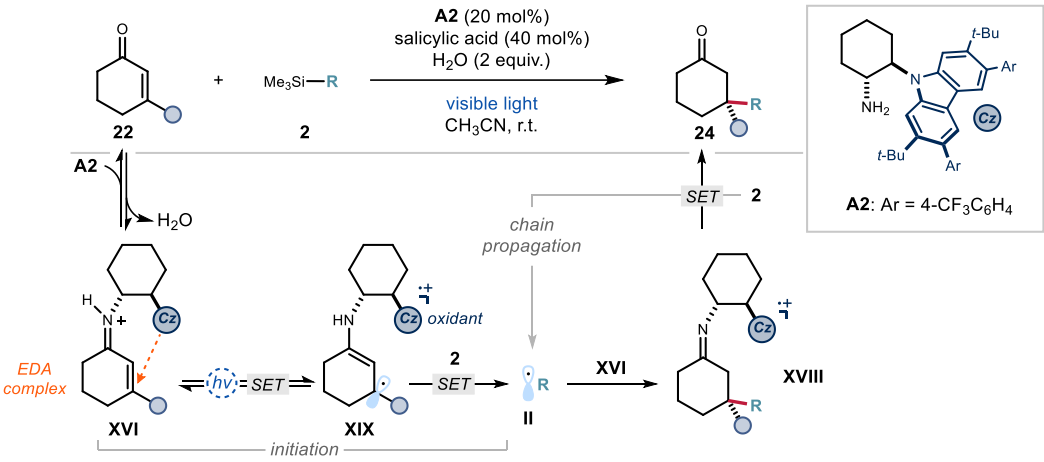

Figure 2.13. Intramolecular iminium ion-based EDA complex that triggers a photochemical asymmetric conjugate addition reaction.

[36] Crisenza, G. E. M.; Mazzarella, D.; Melchiorre, P. "Synthetic Methods Driven by the Photoactivity of Electron Donor–Acceptor Complexes." *J. Am. Chem. Soc.* **2020**, *142*, 12, 5461

[37] Cao, Z.-Y.; Ghosh, T.; Melchiorre, P. "Enantioselective radical conjugate additions driven by a photoactive intramolecular iminium-ion-based EDA complex." *Nat. Commun.* **2018**, *9*, 3274.

It was later demonstrated that ground-state iminium ions derived from α,β-unsaturated aldehydes were also amenable to stereoselectively trap photochemically generated radicals, including by an external photoredox catalyst. Specifically, difluorinated secondary aminocatalyst **C**, which was purposely designed to promote the excited-state reactivity of iminium ions, could enhance reactivity of enals as carbon-centered radicals acceptors while promoting stereogenic bond formation (Figure 2.14a).[38] The reactivity was initially disclosed by our research group in 2019, where nucleophilic acyl radicals **XX** generated from direct photolysis of 4-substituted 1,4-DHPs were intercepted by the ground-state iminium ion, yielding 1,4-dicarbonyl compounds with a β stereocenter. Selective excitation of 1,4-DHP was realized upon 460 nm illumination, a region of visible spectrum that iminium ions of type **I** do not absorb. Since this reactivity did not rely on the excitation of iminium ions, enals with aliphatic substituents, unsuitable for direct excitation, unsuitable for direct excitation, could be reacted. However, the presence of uncatalyzed racemic processes somewhat plagued the stereoselectivity (Figure 2.14b, product **26** formed with 52- 73% e.e.).

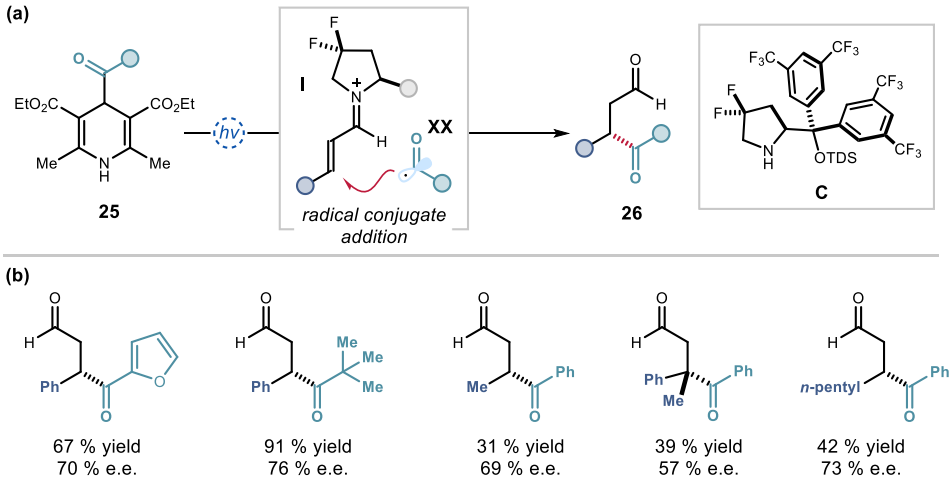

Figure 2.14. (a) Stereocontrolled conjugate addition of acyl radicals mediated by ground-state iminium ion reactivity. **(b)** Selected examples.

[38] Goti, G.; Bieszczad, B.; Vega-Peñaloza, A.; Melchiorre, P. "Stereocontrolled Synthesis of 1,4-Dicarbonyl Compounds by Photochemical Organocatalytic Acyl Radical Addition to Enals." *Angew. Chem., Int. Ed.* **2019**, *58*, 1213.

A more general strategy was disclosed in 2021. In this study, a strongly oxidizing acridinium photocatalyst was used to form nucleophilic radicals from stable precursors, in combination with highly electrophilic ground-state iminium ions, which stereoselectively intercept these open-shell species (Figure 2.15).[39] The system delivered highly enantioenriched chiral β-functionalized aldehydes **3** from benzyl and α-aminosilanes, 1,4-DHPs, silicates and trifluoroborate salts as radical precursors. In a separate study, α-ketocarboxylates were also competent reaction partners, delivering 1,4-dicarbonyl after decarboxylation and conjugate addition of acyl radical.[40] When a cyclopropyl substituted enal was subjected to reaction conditions, direct β-functionalized product was observed without ring-opening, showing that a reduced 5π radical **IIIb** was not generated. This was consistent with the asymmetric conjugate addition mechanism, and the reported reactivity was therefore distinct from the previous studies that involved radical coupling.

[39] Le Saux, E.; Ma, M.; Bonilla, P.; Holden, C.M.; Lustosa, D.; Melchiorre, P. "A General Organocatalytic System for Enantioselective Radical Conjugate Additions to Enals." *Angew. Chem., Int. Ed.* **2021**, *60*, 5357.

[40] Zhao, J.-J.; Zhang, H.-H.; Shen, X.; Yu, S. "Enantioselective Radical Hydroacylation of Enals with α-Ketoacids Enabled by Photoredox/Amine Cocatalysis." *Org. Lett.* **2019**, *21*, 913.

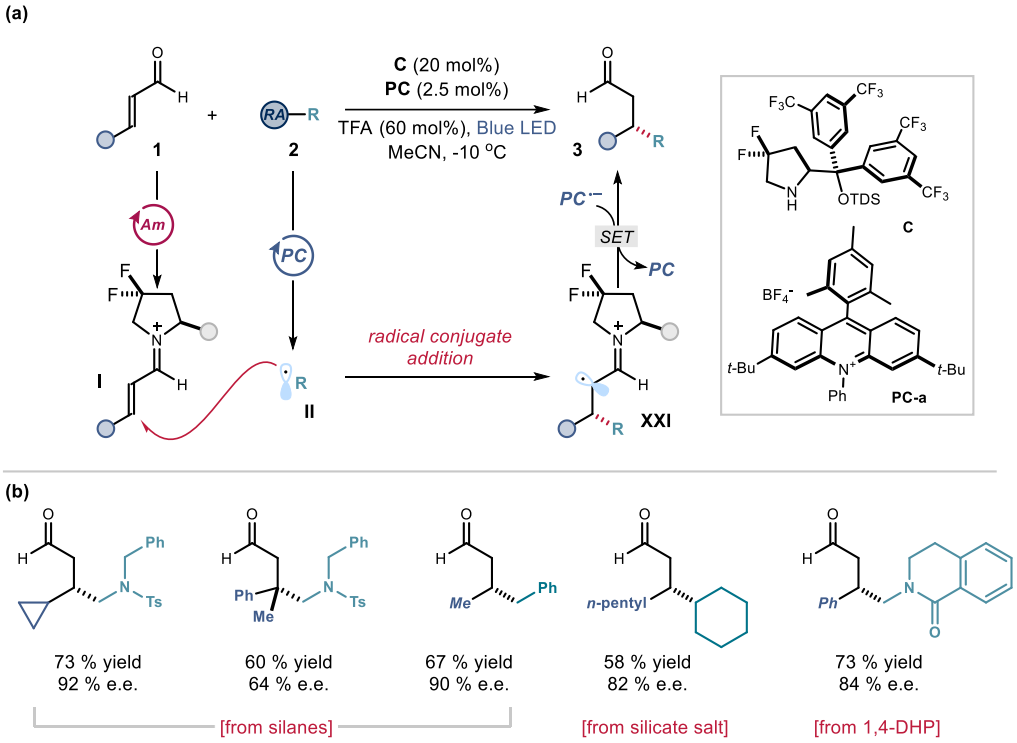

Figure 2.15. **(a)** Stereocontrolled conjugate addition of acyl radicals mediated by ground-state iminium ion reactivity. RA: redox auxiliary, TFA: trifluoroacetic acid. **(b)** Selected examples from the reaction scope.

The discussed examples described the asymmetric interception of radicals stabilized by hyperconjugation (i.e. secondary and tertiary), in direct vicinity with unsaturated π system (i.e. allylic and benzylic) or heteroatoms. On the other hand, non-stabilized primary radicals, due to their reactive nature, are more challenging partner for enantioselective bond formation. A general method to realize such transformation was reported by Hyster lately in an intramolecular fashion (Figure 2.16).[41]

[41] Clayman, P. D.; Hyster, T.D. "Photoenzymatic Generation of Unstabilized Alkyl Radicals: An Asymmetric Reductive Cyclization." *J. Am. Chem. Soc.* **2020**, *142*, 15673.

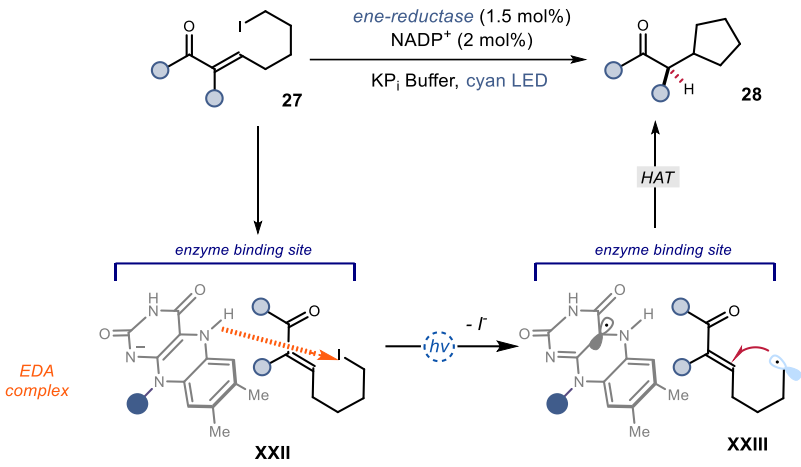

Figure 2.16. Stereocontrolled, intramolecular conjugate addition of primary radicals by a photoenzymatic approach. $NADP^+$: Nicotinamide adenine dinucleotide phosphate, KP_i: Potassium phosphate.

Upon binding of acrylate substrates **27** to the active site of an ene-reductase enzyme, mainly through hydrogen bonding with His-191 and Asn-194 residues,[42] a new absorption band (λ_{max}= 485 nm) was detected by UV-visible spectroscopic analysis. This observation suggested the formation of aggregate **XXII** via charge transfer interaction between flavin cofactor and the σ^*_{C-I} orbital of the substrate. Photoirradiation resulted in the reduction of alkyl iodide, substrate forming a primary radical **XXIII** that readily underwent 5-exo-trig cyclization with the unsaturated carbonyl moiety. The resultant α radical was then quenched through a stereo-defining hydrogen atom transfer (HAT) step, affording products **28** with an α-stereocenter.

Overall, the reported organocatalytic strategies for asymmetric radical conjugate additions are mostly limited to cyclic enones and unsaturated lactam. Recent studies have extended the chemistry to include synthetically more versatile enals. Yet further studies to demonstrate the utility of the methodology are desirable, in particular when it comes to the trap of primary radicals.

[42] Sandoval, B.A.; Meichan, A.J.; Hyster, T.K. "Enantioselective Hydrogen Atom Transfer: Discovery of Catalytic Promiscuity in Flavin-Dependent 'Ene'-Reductases." *J. Am. Chem. Soc.* **2017**, *139*, 33, 11313.

2.3 Design and Target of the Project

The present study was motivated by our interest in developing a catalytic method for enantioselective radical conjugate additions to unmodified, acyclic α,β-unsaturated aldehydes. While significant advancements were made in both fields of asymmetric radical conjugate addition and mild generation of primary radicals, a general platform to combine both strategies for engaging non-stabilized primary radicals in stereoselective bond formation remained elusive. This is not a trivial target since non-stabilized primary radicals are generally recalcitrant to asymmetric bond-forming processes, due to their high reactivity and fleeting nature.[43]

We aimed at filling this gap in synthetic methodology by using a dual catalytic system, in which the radical formation and the stereo-determining step were decoupled. (Figure 2.17a) Specifically, we envisioned the use of an external photoredox catalyst as a reliable method to generate non-stabilized primary radicals, in combination with a chiral amine catalyst for iminium ion formation. The main challenge was to avoid racemic product formation derived from the background addition of radical to enals, and possible alternative pathways (e.g., hydrogen atom abstraction and fragmentation) of non-stabilized radicals. We believed that both problems could be avoided by efficient trapping of radicals by means of a highly reactive chiral iminium ion **I**. If successful, our protocol would enable direct access to 1,7-dicarbonyl compounds **5** with a β-stereogenic center.

[43] For rare examples of asymmetric addition of primary radicals to unsaturated carbonyls, see Ref 21, 39, 41.

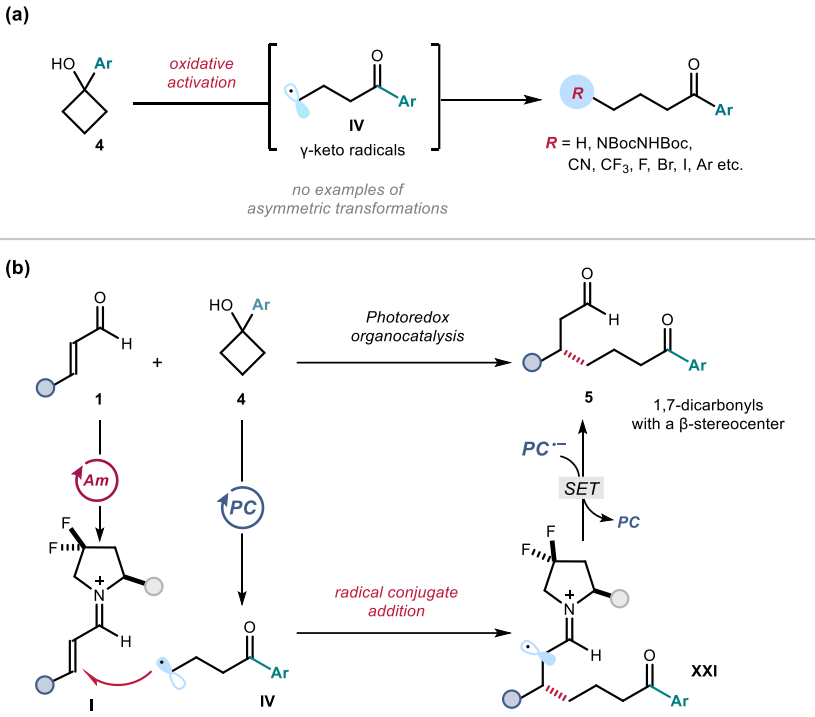

Figure 2.17. (a) Design plan for the enantioselective catalytic synthesis of 1,7-dicarbonyl compounds via stereocontrolled iminium ion trap of primary radicals **IV (b)** Oxidative ring-opening of cyclobutanols **4** to afford γ-keto radicals **IV** and the ensuing functionalization.

Specifically, we sought to use cyclobutanols **4** as suitable radical precursors for the desired transformation. Cyclobutanols have recently found wide synthetic application as versatile radical precursors.[44] Upon oxidative activation and strain-promoted ring opening, they offer access to γ-keto radicals **IV**, which can be intercepted to realize the formal remote

[44] For selected reviews: (a) Ren, R.; Zhu, C. "Radical-Mediated Ring-Opening Functionalization of Cyclobutanols: A Shortcut to γ- Substituted Ketones." *Synlett* **2016**, *27*, 1139; (b) Wu, X.; Zhu, C. "Recent Advances in Ring-Opening Functionalization of Cycloalkanols by C−C σ-Bond Cleavage." *Chem. Rec.* **2018**, *18*, 587; (c) Morcillo, S.P. "Radical-Promoted C−C Bond Cleavage: A Deconstructive Approach for Selective Functionalization." *Angew. Chem., Int. Ed.* **2019**, *58*, 14044; (d) Murakami, M.; Ishida, N. "Cleavage of Carbon−Carbon σ-Bonds of Four-Membered Rings." *Chem. Rev.* **2021**, *121*, 264; (e) Yu, X.-Y.; Chen, J.-R.; Xiao, W.-J. "Visible Light-Driven Radical-Mediated C−C Bond Cleavage/Functionalization in Organic Synthesis." *Chem. Rev.* **2021**, *121*, 506.

functionalization of carbonyl compounds (Figure 2.17b).[45, 46, 47] The activation of cyclobutanols was achieved using catalytic transition metals, stoichiometric oxidants, and photoredox catalysts. The resulting γ-keto radicals **IV** have been used in a wide range of functionalization (i.e. amination[46a,b], halogenation[46c], and trifluoromethylation[46d]) and C-C bond forming processes (including C(sp^3)-C(sp)[47a], C(sp^3)-C(sp^3)[47b], and C(sp^3)-C(sp^2) [47c]). Yet, to the best of our knowledge, enantioselective methods for the stereocontrolled interception of γ-keto primary radicals **IV** derived from cyclobutanols **4** have not been reported.

1,7-Dicarbonyls compounds are found in natural products and pharmaceutically relevant molecules, and could be useful intermediates to prepare bioactive compounds.[48] While some

---

[45] Yayla, H. G.; Wang, H.; Tarantino, K. T.; Orbe, H. S.; Knowles, R. R. "Catalytic Ring-Opening of Cyclic Alcohols Enabled by PCET Activation of Strong O–H Bonds." *J. Am. Chem. Soc.* **2016**, *138*, 10794.

[46] (a) Ren, R.; Zhao, H.; Huan, L.; Zhu, C. "Manganese-Catalyzed Oxidative Azidation of Cyclobutanols: Regiospecific Synthesis of Alkyl Azides by C-C Bond Cleavage". *Angew. Chem., Int. Ed.* **2015**, *54*, 12692; (b) Guo, J.; Hu, A.; Chen, Y.; Sun, J.; Tang, H.; Zuo, Z. "Photocatalytic C-C Bond Cleavage and Amination of Cycloalkanols by Cerium(III) Chloride Complex". *Angew. Chem., Int. Ed.* **2016**, *55*, 15319; (c) Zhao, H.; Fan, X.; Yu, J.; Zhu, C. "Silver-Catalyzed Ring-Opening Strategy for the Synthesis of β- and γ-Fluorinated Ketones." *J. Am. Chem. Soc.* **2015**, *137*, 10, 3490; (d) Wu, S.; Li, J.; He, R.; Jia, K.; Chen, Y. "Terminal Trifluoro-methylation of Ketones via Selective C–C Cleavage of Cycloalkanols Enabled by Hypervalent Iodine Reagents.' *Org. Lett.* **2021**, *23*, 9204.

[47] (a) Ren, R.; Wu, Z.; Xu, Y.; Zhu, C. "C–C Bond-Forming Strategy by Manganese-Catalyzed Oxidative Ring-Opening Cyanation and Ethynylation of Cyclobutanol Derivatives." *Angew. Chem., Int. Ed.* **2016**, *55*, 2866; (b) Hu, A.; Chen, Y.; Guo, J.; Yu, N.; An, Q.; Zuo, Z. "Cerium-Catalyzed Formal Cycloaddition of Cycloalkanols with Alkenes through Dual Photoexcitation". *J. Am. Chem. Soc.* **2018**, *140*, 13580; (c) Huang, L.; Ji, T.; Rueping, M. "Remote Nickel-Catalyzed Cross-Coupling Arylation via Proton-Coupled Electron Transfer-Enabled C–C Bond Cleavage." *J. Am. Chem. Soc.* **2020**, *142*, 3532

[48] (a) Paquette, L. A.; Collado, I.; Purdie, M. "Total Synthesis of Spinosyn A. 2. Degradation Studies Involving the Pure Factor and Its Complete Reconstitution." *J. Am. Chem. Soc.* **1998**, *120*, 2553; (b) Vanhaecke, T.; Papeleu, P.; Elaut, G.; Rogiers, V. "Trichostatin A-like hydroxamate histone deacetylase inhibitors as therapeutic agents: toxicological point of view." *Curr. Med. Chem.* **2004**, *11*, 1629; (c) de Figueiredo, R. M.; Berner, R.; Julis, J.; Liu, T.; Türp, D.; Christmann, C. "Bidirectional, organocatalytic synthesis of lepidopteran sex pheromones." *J. Org. Chem.* **2007,** *72*, 640; (d) Lecerf-Schmidt, F.; Haudecoeur, R.; Peres, B.; Ferreira Queiroz, M. M.; Marcourt, L.; Challal, S.; Ferreira Queiroz, E.; Sotoing Taiwe, G.; Lomberget, T.; Le Borgne, M.; Wolfender, J.-L.; De Waard, M.; Robins, R. J.; Boumendjel, A. "Biomimetic synthesis of Tramadol." *Chem. Commun.* **2015**, *51*, 14451.

methods involving polar cascade, [49] organometallic addition[50] and radical migration[51] are available for the synthesis of 1,7-dicarbonyls (Figure 2.18), they require tailored substrates. Importantly, the vast majority of these methods do not provide stereocontrolled entries into chiral 1,7-dicarbonyl compounds. Rare examples were first disclosed by Schneider, where chiral 1,7-dicarbonyls were prepared iminium ion catalyzed, vinylogous Mukaiyama Michael reaction between cinnamaldehyde and dienol silyl ether[49a], followed by Ooi through a chiral Brønsted base controlled, asymmetric 1,6-addition of enolate to dienyl carbonyl compounds[49b]. In both cases, structure of substrates were carefully designed for good stereocontorl. Our proposed strategy, which combines photoredox catalysis and organocatalysis, can offer a direct asymmetric route to chiral 1,7-dicarbonyls.

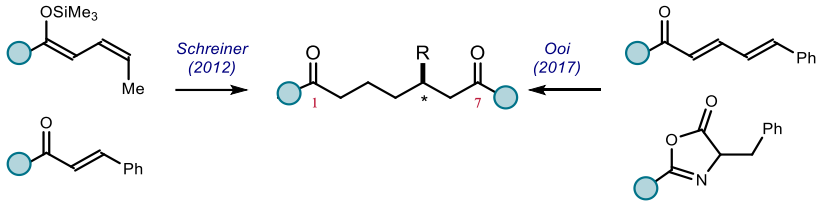

Figure 2.18. Previous strategies in synthesizing chiral 1,7-dicarbonyl compounds.

[49] (a) Chetia, A.; Saikia, C. J.; Lekhok, K. C.; Boruah, R. C. "A facile synthesis of 1,7-dicarbonyl compounds via three-component Michael addition reactions." *Tetrahedron Lett.* **2004**, 45, 2649; (b) Gupta, G.; Sudhir, S.; Mandal, T.; Schneider, C. "Organocatalytic, Highly Enantioselective Vinylogous Mukaiyama–Michael Reaction of Acyclic Dienol Silyl Ethers." *Angew Chem, Int. Ed.* **2012**, *51*, 50, 12609; (c) Uraguchi, D.; Yoshioka, K.; Ooi, T. "Complete diastereodivergence in asymmetric 1,6-addition reactions enabled by minimal modification of a chiral catalyst." *Nat. Comm.* **2017**, 8, 14793.

[50] Xu, C.-M.; Yang, L.; Huang, D.-F.; Niu, T.; Fu, Y.; Hu, Y.-L. "Preparation of Diketones via the Reaction of Bisorganozinc Iodides and Benzoyl Chlorides." *Chin. J. Org. Chem*. **2010**, 30, 1240.

[51] (a) Huang, Z.; Xu, J. "One-pot synthesis of symmetric 1,7-dicarbonyl compounds via a tandem radical addition–elimination–addition reaction." *RSC Adv.* **2013**, *3*, 15114; (b) Ren, R.; Wu, Z.; Huan, L. Chen, Z. "Synergistic Strategies of Cyano Migration and Photocatalysis for Difunctionalization of Unactivated Alkenes: Synthesis of Di- and Mono-Fluorinated Alkyl Nitriles." *Adv. Synth. Catal.* **2017**, *359*, 3052; (c) Sarkar, S.; Banerjee, A.; Yao, W.; Patterson, E. V.; Ngai, M.-Y. "Photocatalytic Radical Aroylation of Unactivated Alkenes: Pathway to β-Functionalized 1,4-, 1,6-, and 1,7-Diketones." *ACS Catal.* **2019**, *9*, 10358.

2.4 Results and Discussion

2.4.1 Optimization of the Reaction Conditions and Substrate Scope for Aliphatic Enals

We started our investigation using cyclobutanol **4a** (E(**IV/4**) = +1.48 V vs SCE) with a *p*-methoxyphenyl substituent (PMP) and pentenal **2a** as the model substrates (Table 2.1). 3,6-Di-*tert*-butyl-9-mesityl-10-phenylacridinium tetrafluoroborate **PC-a** was selected as the organic photocatalyst (E*= +2.10 V vs SCE),[52] since it has the required redox potential to effectively activate **4a** via an SET oxidation. The experiments were conducted at –10 ºC in CH_3CN under irradiation by a single high-power light-emitting diode (HP LED, λ_{max} = 460 nm) with an irradiance at 45 mW/cm^2, as controlled by an external power supply (reactor setup detailed in Figure 2.26 of the experimental section). Trifluoroacetic acid (TFA, 1 equiv.) was used to secure the effective formation of the chiral iminium ion of type **I**.

The *gem*-difluorinated diarylprolinol silylether organocatalyst **C**, which we previously designed for the photoactivation of iminium ions[9], afforded the expected product **5a** with high enantioselectivity and good yield (Table 2.1, entry 1, 54% yield and 95.5:4.5 e.r.). Other amine catalysts (such as diphenylpyrrolidinol catalyst **A** and imidazolidinone catalyst **B**) with an established ability to promote asymmetric iminium-ion-mediated polar processes offered reduced catalytic activity and stereoselectivity (entries 2 and 3, respectively). Other photoredox catalysts (**PC-b** and **c**) were ill-suited to efficiently promote the model reaction (entries 5-6). Control experiments were also performed, showing that photocatalyst **PC-a** (entry 7) and light (entry 8) were essential for reactivity. Complete decomposition of cyclobutanol **4a** was observed in both cases, which can be justified by its sensitivity to TFA.

[52] Joshi-Pangu, A.; Lévesque, F.; Roth, H. G.; Oliver, S. F.; Campeau, L.-C.; Nicewicz, D.; DiRocco, D. A. "Acridinium-Based Photocatalysts: A Sustainable Option in Photoredox Catalysis." *J. Org. Chem.* **2016**, *81*, 7244.

Table 2.1. Optimization studies with aliphatic enals.[a]

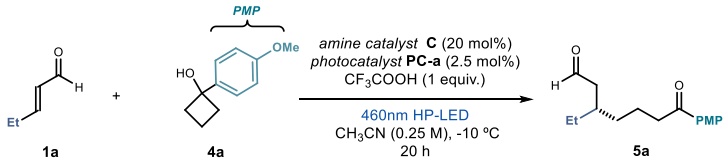

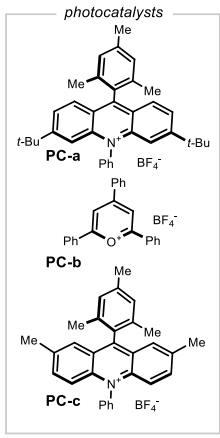

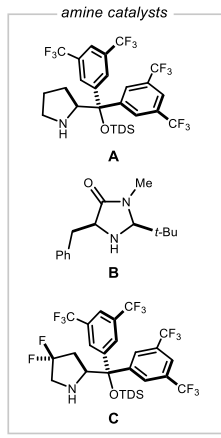

entry	Deviation from Standard Conditions	yield (%)[b]	e.r.[c]
1	amine **C** (standard)	65 (54)	95.5:4.5
2	amine **A**	30	52.5:47.5
3	amine **B**	53	54:46
4	No amine catalyst	12	50:50
5	**PC-b**	37	91:9
6	**PC-c**	17	N.D.
7	No photocatalyst	0	-
8	reaction in dark	0	-
9	at ambient temperature	15	78.5:21.5
10	with 80% TFA	60	92:8

[a] Reactions performed on a 0.1 mmol scale for 20 h using 3 equiv. of **1a**, 20 mol% of aminocatalyst, 2.5 mol% of photocatalyst, and 100 mol% of TFA in 0.2 mL of CH_3CN under illumination by a single high-power LED (λ_{max} = 460 nm, 45 mW/cm^2) at -10 ºC. [b] Yield determined by ^{1}H NMR analysis of the crude mixture using benzyl chloride as the internal standard; yield of the isolated product **5a** is reported in brackets. [c]Enantiomeric ratio of **5a**. N.D.: not determined.

In the absence of catalyst **C** (entry 4), a low reactivity was also observed. This hints to the presence of a background racemic radical addition to enals. Accordingly, reducing the amount of acid co-catalyst, which helped accelerating iminium ion formation, led to a drastic decrease in level of stereoselectivity (entry 10). Temperature was also important in securing efficiency: when performing the model reaction at ambient temperature, both yield and enantioselectivity of product **5a** dropped drastically (entry 9).

Using the optimized conditions, we next explored the generality of the method for the asymmetric synthesis of chiral 1,7-dicarbonyl compounds **5** (Figure 2.19). We found that enals bearing a variety of saturated aliphatic substituents at the β position, including ethyl (product **5a**), methyl (**5b**), *n*-pentyl (**5c**), and isopropyl (**5d**) moieties, were suitable substrates. In all cases, the corresponding products were obtained in high enantioselectivity (e.r. ranging from 93:7 to 95.5:4.5), while the yields decreased with increasing steric hindrance of the β-substituent. Enals with a cyclohexyl or tert-butyl substituent were poorly reacting, whereas those bearing a homobenzyl group (adduct **5e**), a terminal olefin (**5f**), and an ether functionality (**5g**) were compatible with the reaction conditions.
In addition to cyclobutanol **4a**, the less electron-rich analog bearing a phenyl substituent (E_{ox} = +1.78 V vs SCE) offered a similar reactivity, effectively leading to product **5h** in 57% yield and 97.5:2.5 e.r. Nonetheless, cyclobutanols with more electron-rich aryl rings are not compatible for the reactivity. Substitution at C2 or heteroatom at C3 of four-membered ring led to deleterious effects on the reaction outcome.

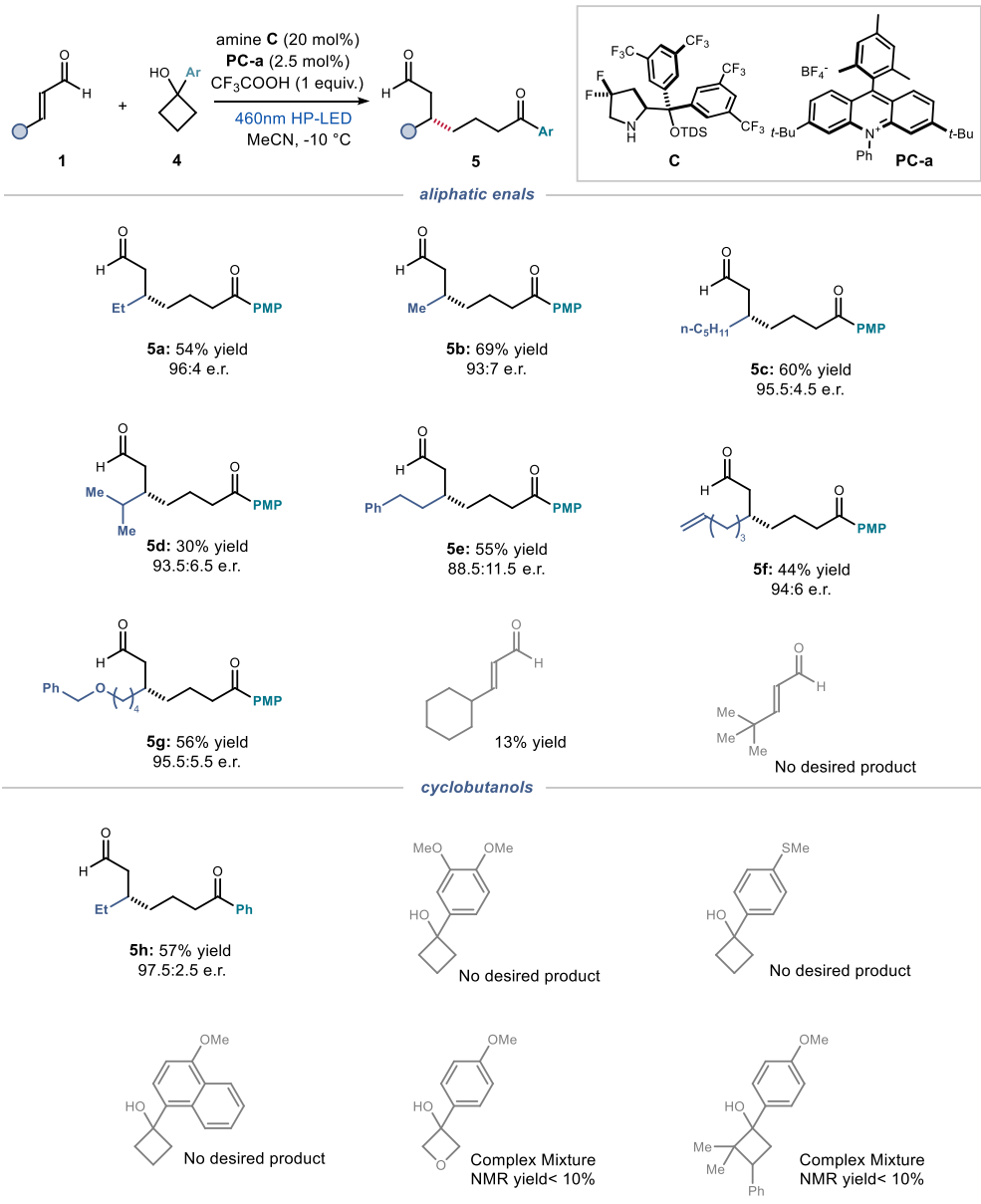

Figure 2.19. Substrate scope for the asymmetric synthesis of 1,7-dicarbonyl compounds. Reactions performed on a 0.1 mmol scale using 3 equiv. of enal **1** in 0.2 mL of CH_3CN under illumination at 460 nm for 20-22 h. Yields and enantiomeric excesses of the isolated products **5** are reported below each entry (average of two runs per substrate).

2.4.2 Reaction Optimization for Aromatic Enals and Substrate Scope

To examine the reactivity of aromatic enals for this transformation, we then attempted the same reaction with cinnamaldehyde **1h**, which has a β-phenyl substituent. Adopting the optimal conditions for aliphatic enals (Table 2.2, entry 1), the reaction did provide the desired product with mediocre yield and good stereochemical outcome (61% yield and 91:9 e.r.). Using 30 mol% of aminocatalyst **C** while reducing the amount of TFA (entry 2) delivered product **5i** in higher yield while maintaining the enantioselectivity. Organocatalyst **A** afforded product in moderate stereoinduction and low level of product formation (entry 3), whereas catalyst **B** provided racemic product with diminished yield (entry 4). Exclusion of aminocatalyst **C** or light (entry 5 and 6, respectively) completely shut down the reactivity. Nonetheless, exclusion of photocatalyst (entry 7) provided a small amount of product with the same enantiomeric excess as the optimal conditions. This suggests that the direct excitation of the iminium ion (see Figure 2.28) plays a comparatively minor role in the observed reactivity. Instead, the SET events are more effectively facilitated by the acridinium catalyst.

Table 2.2. Optimization studies with aromatic enals.[a]

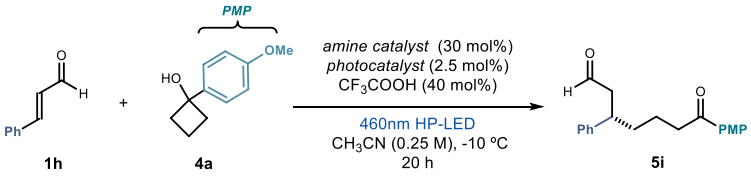

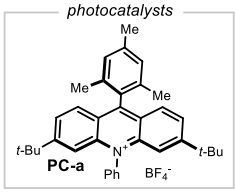

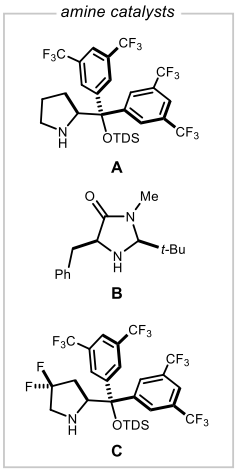

entry	Deviation from Standard Conditions	yield (%)[b]	e.r.[c]
1	with 20 % **C**,100% TFA	61	91:9
2	amine **C** (standard)	74 (86)	91:9
3	amine **A**	10	77.5:22.5
4	amine **B**	46	50:50
5	No amine catalyst	0	-
6	reaction in dark	0	-
7	No photocatalyst	19	91:9

[a] Reactions performed on a 0.1 mmol scale for 20 h using 3 equiv. of **1h**, 30 mol% of aminocatalyst **A**, 2.5 mol% of photocatalyst, and 40 mol% of TFA in 0.2 mL of CH_3CN under illumination by a single high-power LED (λ_{max} = 460 nm, 45 mW/cm^2) under -10 °C. [b] Yield determined by ^{1}H NMR analysis of the crude mixture using benzyl chloride as the internal standard; yield of the isolated **5i** is reported in brackets. [c]Enantiomeric ratio of **5i**.

We then investigated the effects of substituents on the aromatic ring (Figure 2.20). Electron-donating methyl (adduct **5j**) and electron-withdrawing fluorine (**5l**) groups had little effects on enantioselectivity. *Para*- and *meta*-trifluoromethyl-phenyl enals offered similar results (**5n** and **5o**), showing that the reaction system tolerated substituents at different positions of the aromatic ring. Aromatic enals bearing a trimethyl silyl (**5k**) and a chloro group(**5m**), which can serve as synthetic handles for further modifications, could also be used. In addition to the basic phenyl ring, other aromatic systems, including thiophene (**5p**) and naphthalene (**5q**), were compatible with the protocol. On the other hand, electron-rich enals, such as those with a *para*-methoxyphenyl or 2-furyl substituent are unreactive.

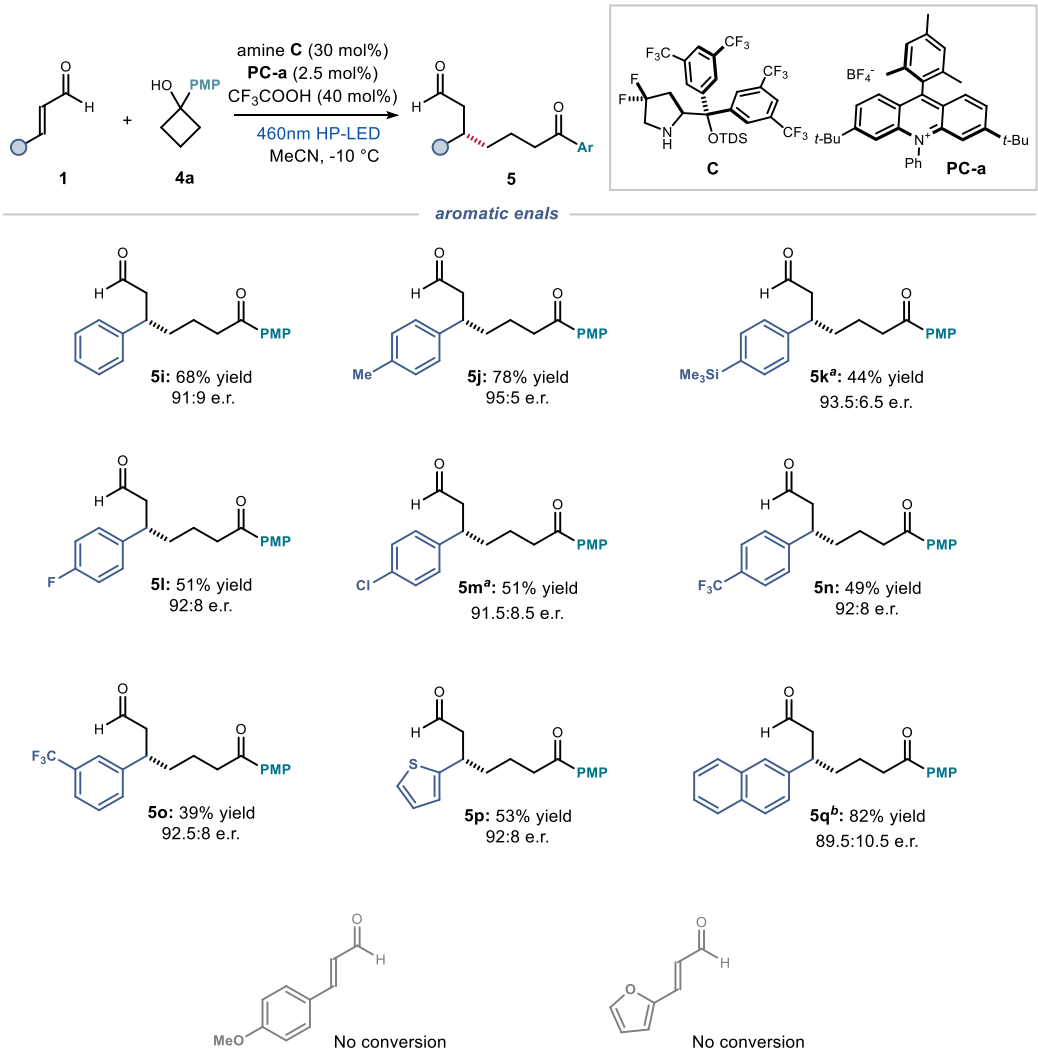

Figure 2.20. Substrate scope for the asymmetric synthesis of 1,7-dicarbonyl compounds. Reactions performed on a 0.1 mmol scale using 3 equiv. of enal **1** in 0.2 mL of CH_3CN under illumination at 460 nm, for 18-20 h. Yields and enantiomeric excesses of the isolated products **5** are reported below each entry (average of two runs per substrate). [a] Reaction for 40 h. [b]Using 5 mol% of photocatalyst **PC-a** in a CH_3CN:CH_2Cl_2 mixture (4:1) as solvent.

2.4.3 Synthetic Applications

To examine the utility of the method, we performed the model reaction on a 1 mmol scale using a different photoreactor (see section 2.6.4 for details of the reaction setup), which offered product **5a** in synthetically useful amount (Figure 2.21a, **5a** formed in 66% yield and 95:5 e.r., 173 mg). We then sought to convert adduct **5a** into analogs of straight-chain pharmacophores through functional group interconversion (Figure 2.21b). Firstly, a reductive amination with 1-(4-piperidinyl)-1,3-dihydro-2H-benzimidazol-2-one smoothly afforded the chiral adduct **29** bearing an (*S*)-2-ethyl-7-oxoheptamine skeleton without erosion of enantiopurity or reduction of the ketone group (path *i*). Product **29** is an analog of *Benperidol*, a neuroleptic used as selective ligand for dopaminergic D2-receptors.[53] In addition, after redox manipulation (path *ii*), the two carbonyl groups within **5a** could be selectively altered to achieve a 7-hydroxylheptanoic acid **30**, an intermediate in the preparation of asthma medication *Seratrodust*.[54] These operations demonstrated that the two carbonyl groups in the product can be selectively transformed into various functionalities.

The dicarbonyl skeleton in **5a** could also be diversified through a Wittig-olefination (path *iii*), which afforded the 1,9-dicarbonyl product **31** with a δ-stereogenic center, predominantly as an *(E)*-olefin (>10:1). This structure resembled the backbone of the queen substance, a honeybee pheromone.[55] Lastly (path *iv*), a Lewis base-catalyzed intramolecular aldol reaction[56] led to the cyclohexanol scaffold **32**, decorated with three stereogenic centers, with good yield and diastereoselectivity. The relative configuration of the major diastereoisomer of **32** was assigned by means of NMR studies (detailed in section 2.6.10), while the absolute

[53] Moerlein, S. M.; Banks, W. R.; Parkinson, D. "Production of fluorine-18 labeled (3-N-methyl) benperidol for PET investigation of cerebral dopaminergic receptor binding." *Int. J. Rad. Appl. Instrum. A* **1992**, *43*, 913.

[54] (a) Shiraishi, M.; Kato, K.; Terao, S.; Ashida, Y.; Terashita, Z.; Kito, G. "Quinones. 4. Novel eicosanoid antagonists: synthesis and pharmacological evaluation." *J. Med. Chem.* **1989**, *32*, 2214; b) Wouters, J.; Durant, F.; Masereel, B. "Antagonism of the TXA2 receptor by seratrodast: a structural approach." *Bioorg. Med. Chem. Lett.* **1999**, *9*, 2867.

[55] Butler, C. G.; Callow, R. K.; Johnston, N. C. "The isolation and synthesis of queen substance, 9-oxodec-trans-2-enoic acid, a honeybee pheromone." *Proc. Royal Soc. B* **1962**, *155*, 417.

[56] Ghobril, C.; Sabot, C.; Mioskowski, C.; Baati, R. "TBD-Catalyzed Direct 5-and 6-enolexo Aldolization of Ketoaldehydes." *Eur. J. Org. Chem.* **2008**, 4104.

configuration of the minor isomer of **32** was unambiguously assigned by X-ray crystallographic analysis. [57]

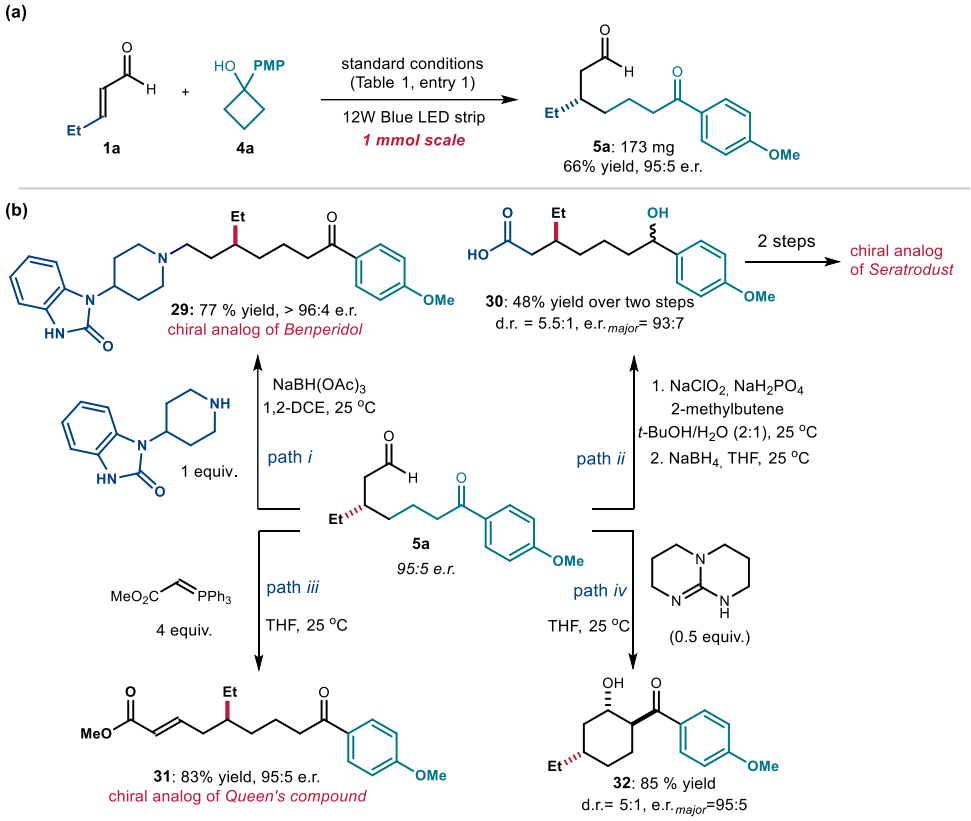

Figure 2.21. Synthetic Applications of 1,7-Dicarbonyl Compound **(a)** Scale up reaction conducted at 1 mmol scale **(b)** Product modifications by established reactions.1,2-DCE: 1,2-dichloroethane.

2.4.4 Mechanistic Investigations

To glean insight into the reaction mechanism, we conducted Stern-Volmer fluorescence quenching experiments (Figure 2.22a). We found that cyclobutanol **4a** efficiently quenched the fluorescence of the excited photocatalyst **PC-a** (K_{SV} = 70.3 M^{-1}). Cyclic voltammetry

[57] Crystallographic data for compound $\mathbf{32_{minor}}$ has been deposited with the Cambridge Crystallographic Data Centre, accession number CCDC 2144951. The experimental results are detailed in section 2.6.9

(Figure 2.22b) established the thermodynamic feasibility of a SET oxidation of cyclobutanol **4a** (E(**IV**/**4**)= +1.48 V vs SCE) by the excited **PC-a** (E^*_{red}= + 2.10 V vs SCE).[61]

Based on these findings, we propose the mechanism detailed in Figure 2.22c. The light-activated photocatalyst Mes-Acr$^+$Ph* would activate cyclobutanol **4** through SET oxidation to afford the γ-keto radical **IV** upon radical ring opening. This non-stabilized primary radical **IV** is then captured by the chiral iminium ion **I** in a stereocontrolled fashion. The emerging α-iminyl radical cation **XXI** (E_{red} ~ +0.8 V vs Ag/AgCl)[9] is then quenched by the reduced photocatalyst (Mes-Acr•Ph, $E_{1/2}$ = -0.56 V vs SCE),[61] thus closing the photoredox catalytic cycle. Hydrolysis of the ensuing enamine **XXIV** leads to the desired chiral 1,7-dicarbonyl compound **5** while turning the chiral amine catalyst **C** over.

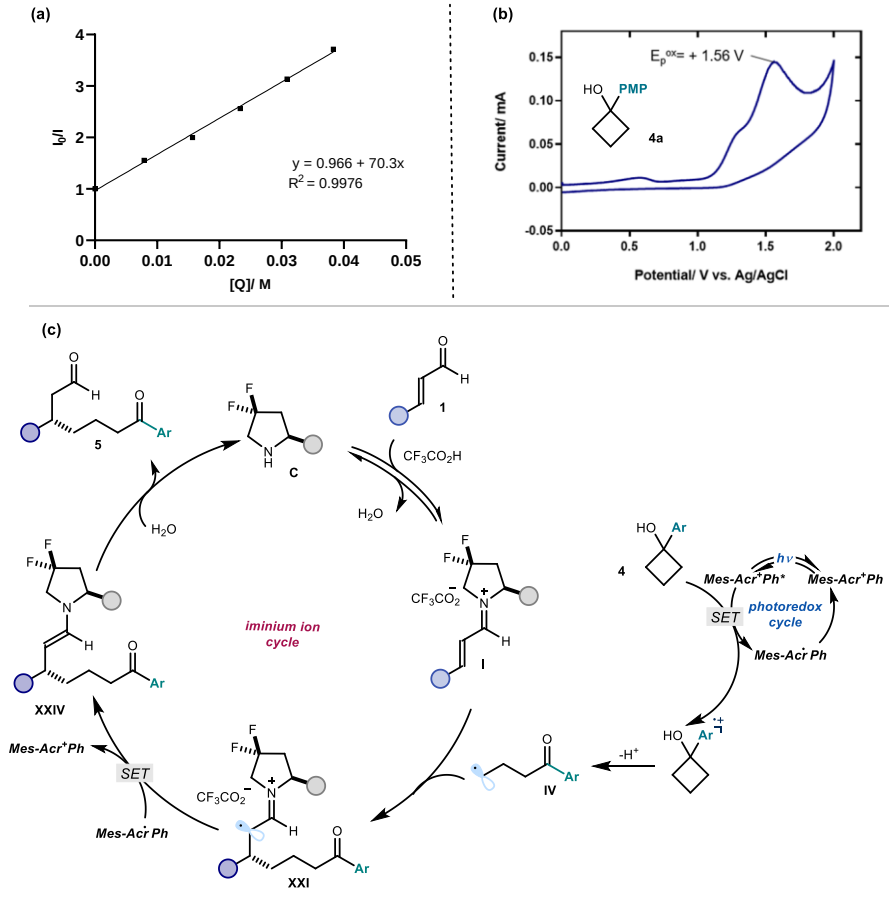

Figure 2.22. Mechanistic studies **(a)** Stern-Volmer quenching of PC-a fluorescence by cyclobutanol **4a** **(b)** Cyclic voltammogram of **4a** **(c)** Proposed reaction mechanism.

Another plausible mechanism to activate cyclobutanol is by proton-coupled electron transfer (PCET),[45] potentially with the concerted action of acridinium ion and trifluoroacetate anion in this system. To probe whether such process was involved, the corresponding cyclobutyl methyl ether **33** was subjected to reaction conditions for a control reaction (Figure 2.23a). Product **5a** can still be obtained in comparable amount. This is in agreement with the proposal that the excited photocatalyst is activating cyclobutanol via SET oxidation of the PMP motif. An alternative chain propagation mechanism, in which cyclobutanol would be oxidized by the intermediate α-iminyl radical cation **XXV** to form the enamine **XXVI** and another equivalent of non-stabilized radical, was also considered. Previous studies estimated the oxidation potential of the 3π-intermediates of type **XXV**[9] from the corresponding enamine **XXVI** to be ~+0.8 V vs Ag^+/Ag in CH_3CN. As shown in Figure 2.23b, the SET from **4a**, which has a high redox potential (E (**IV**/**4a**) = +1.56 V), to α-iminyl radical cation **XXV** would be an endergonic and thermodynamically disfavored process, therefore precluding a possible step for radical chain propagation. We also measured a quantum yield (Φ) for the model reaction as low as 0.04 (calibrated by potassium ferrioxalate actinometer in water, see experimental details in section 2.6.7). This value is consistent with our mechanistic proposal for a closed catalytic cycle, suggesting that a chain propagation mechanism, if present, is not a dominant path.[58]

[58] (a) Buzzetti, L.; Crisenza, G. E. M.; Melchiorre, P. "Mechanistic Studies in Photocatalysis." *Angew. Chem., Int. Ed.* **2019**, 58, 3730; (b) Cismesia, M. A.; Yoon, T. P. "Characterizing Chain Processes in Visible Light Photoredox Catalysis." *Chem. Sci.* **2015**, *6*, 5426.

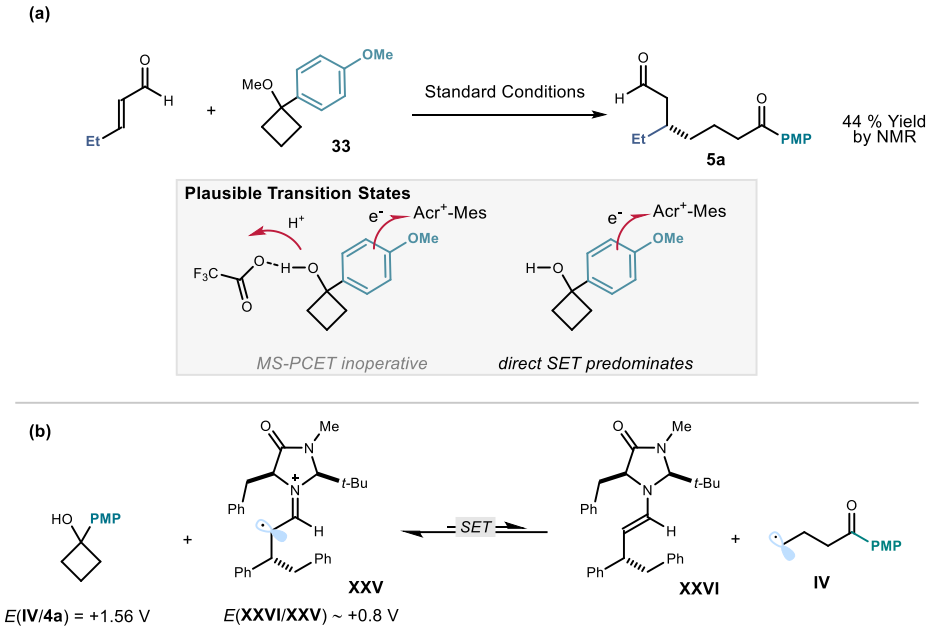

Figure 2.23. Mechanistic experiments to probe alternative reaction pathways **(a)** A control experiment with **4a-Me** as the radical precursor **(b)** a hypothetical SET between 4a and intermediate to propagate a radical chain.

2.5 Conclusions

In summary, we have developed a catalytic enantioselective method that offers a rare entry into chiral 1,7-dicarbonyl compounds. The chemistry relies on the formation of γ-keto radicals, generated upon oxidative ring opening of cyclobutanols mastered by a photoredox catalyst. The key for success was the stereocontrolled interception of non-stabilized primary radicals by a chiral iminium ion intermediate. In addition, trivial synthetic elaborations of the 1,7-dicarbonyl products served to prepare novel, chiral analogues of known natural products and drug molecules.[59]

[59] (a) Lovering, F.; Bikker, J.; Humblet, J. "Escape from Flatland: Increasing Saturation as an Approach to Improving Clinical Success." *J. Med. Chem.* **2009**, *52*, 6752; (b) Lovering, F. "Escape from Flatland 2: complexity and promiscuity." *Med. Chem. Commun.* **2013**, *4*, 515.

2.6 Experimental Section

General Information. The ^{1}H NMR, $^{19}F\{^{1}H\}$ NMR, $^{13}C\{^{1}H\}$ NMR spectra, HPLC and UPC^2 traces are available in the literature[1] and are not reported in the present dissertation.

The NMR spectra were recorded at 300 MHz, 400 MHz and 500 MHz for ^{1}H, 101 MHz and 126 MHz for $^{13}C\{^{1}H\}$, 471 MHz for $^{19}F\{^{1}H\}$, respectively. The chemical shifts (δ) for ^{1}H and $^{13}C\{^{1}H\}$ are given in ppm relative to residual signals of the solvents ($CHCl_3$ at 7.26 ppm for ^{1}H NMR, 77.00 ppm for $^{13}C\{^{1}H\}$NMR). Coupling constants are given in Hz. The following abbreviations are used to indicate the multiplicity: s, singlet; d, doublet; t, triplet; q, quartet; quint, quintet; sept, septet; m, multiplet; br s, broad signal.

High-resolution mass spectra (HRMS) were obtained from the ICIQ High-Resolution Mass Spectrometry Unit on MicroTOF Focus and Maxis Impact (Bruker Daltonics) with electrospray ionization. X-ray data were obtained from the ICIQ X-Ray Unit using a Bruker-Nonius diffractometer equipped with an APPEX 2 4K CCD area detector. Optical rotations were measured on a Polarimeter Jasco P-1030 and are reported as follows: $[\alpha]_D$ ambient temperature (c in g per 100 mL of solvent). Cyclic voltammetry studies were carried out on a Princeton Applied Research PARSTAT 2273 potentiostat offering compliance voltage up to ± 100 V (available at the counter electrode), ± 10 V scan range and ± 2 A current range. UV-vis measurements were carried out on an Agilent Cary 60 spectrophotometer equipped with silicon diode detector, double beam optics and 80 Hz Xenon Flash Lamp as light source. The emission spectra were recorded using a Fluorolog Horiba Jobin Yvon spectrofluorimeter equipped with a photomultiplier detector, a double monochromator, and a 450W xenon light source.

General Procedures. All reactions were set up under an argon atmosphere in oven-dried glassware using standard Schlenk techniques, unless otherwise stated. Synthesis grade solvents were used as purchased. Anhydrous solvents were taken from a commercial SPS solvent dispenser. Chromatographic purification of products was accomplished using flash column chromatography (FC) on silica gel (Merck, 230-400 mesh). For thin layer chromatography (TLC) analysis throughout this work, Merck precoated TLC plates (silica gel 60 GF_{254}, 0.25 mm) were used, using UV light as the visualizing method and either phosphomolybdic acid in EtOH, dinitrophenylhydrazine in EtOH/H_2O, *p*-anisaldehyde or

basic aqueous potassium permanganate ($KMnO_4$), and heat as developing agents. Organic solutions were concentrated under reduced pressure on a Büchi rotary evaporator (*in vacuo* at 40 ºC, ~5 mbar).

Determination of Enantiomeric Purity: HPLC analysis on chiral stationary phase was performed on an Agilient 1200 series HPLC, using Daicel Chiralpak IA-3, IC-3 and ID-3 columns with hexanes:*i*PrOH as the eluent. UPC^2 analysis on chiral stationary phase was performed on a Waters Acquity instrument using IC-3, ID-3, IE-3 and IG-3 chiral columns. The exact conditions for the analyses are specified within the characterization section. HPLC and UPC^2 traces were compared to racemic samples prepared by running the reaction in the presence of a catalytic amount (20 mol%) of an approximately 1:1 mixture of (2*R*, 5*R*)- and (2*S*, 5*S*)-2-*tert*-butyl-3-methyl-5-benzyl-4-imidazolidinone, which are commercially available form Sigma Aldrich.

Materials: Commercial grade reagents and solvents were purchased at the highest commercial quality from Sigma Aldrich, Fluka, Acros Organics, Fluorochem, Tokyo Chemical Industry or Alfa Aesar and used as received, unless otherwise stated. The aminocatalysts **A**[60]and **C**[9] was prepared according to the reported literature. Photocatalyst **PC-a** was prepared according to the reported literature.[61] Some of the enal substrates **1**, including (*E*)-pent-2-enal **1a**, crotonaldehyde **1b**, (*E*)-oct-2-enal **1c**, (*E*)-4-methylpent-2-enal **1d**, cinnamaldehyde **1h**, (*E*)-3-(p-tolyl)acrylaldehyde **1i**, (*E*)-3-(4-fluorophenyl)acrylaldehyde **1k**, and (*E*)-3-(4-chlorophenyl)acrylaldehyde **1l** are commercially available, if liquid they were distilled prior to use. Other enals and radical precursors were prepared according to the literature procedure, as detailed in Section 2.6.1.

[60] Hörmann, F.M.; Kerzig, C.; Chung, T.S.; Bauer, A.; Wenger, O.S.; Bach, T. "Triplet Energy Transfer from Ruthenium Complexes to Chiral Eniminium Ions: Enantioselective Synthesis of Cyclobutane-carbaldehydes by [2+2] Photocycloaddition." *Angew. Chem., Int. Ed.* **2020**, *59*, 24, 9659.

[61] White, A. R.; Wang, L.; Nicewicz, D. A. "Synthesis and Characterization of Acridinium Dyes for Photoredox Catalysis." *Synlett* **2019**, 827.

2.6.1 Synthesis of the Substrates

Synthesis of cyclobutanol 4a and 4b

Cyclubutanols **4a** and **4b** were synthesized using procedures reported in the literature.[62]

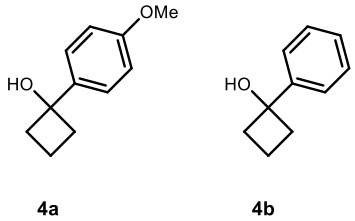

Figure 2.24. Cyclobutanols prepared according to procedures reported in the literature

Synthesis of enals 2

Some of the enals **2** were synthesized using procedures reported in the literature. Figure 2.25 depicts the enals that have been synthesized and the corresponding references.[63,64,65,66,67]

---

[62] Croft, R. A.; Dubois, M. A. J.; Boddy, A. J.; Denis, C.; Lazaridou, A.; Voisin-Chiret, A. S.; Bureau, R.; Choi, C.; Mousseau, J. J.; Bull, J. A. "Catalytic Friedel-Crafts Reactions on Saturated Heterocycles and Small Rings for sp^3-sp^2 Coupling of Medicinally Relevant Fragments." *Eur. J. Org. Chem.* **2019**, 5385.

[63]Franzoni, I.; Guénée, L.; Mazet, C. "Access to congested quaternary centers by Pd-catalyzed intermolecular γ-arylation of unactivated α,β-unsaturated aldehydes." *Chem. Sci.* **2013**, *4*,2619.

[64] Diedrich, M. K.; Klärner, F.-G.; Beno, B. R.; Houk, K. N.; Senderowitz, H.; Still, C. W. "Experimental Determination of the Activation Parameters and Stereoselectivities of the Intramolecular Diels−Alder Reactions of 1,3,8-Nonatriene, 1,3,9-Decatriene, and 1,3,10-Undecatriene and Transition State Modeling with the Monte Carlo-Jumping Between Wells/Molecular Dynamics Method." *J. Am. Chem. Soc.* **1997**, *119*, 10255.

[65] Mazzarella, D.; Crisenza, G. E. M.; Melchiorre, P. "Asymmetric Photocatalytic C−H Functionalization of Toluene and Derivatives." *J. Am. Chem. Soc.* **2018**, *140*, 8439.

[66] Jiang, L.; Li, H.; Zhou, J.-F.; Yuan, M.-W.; Li, H.-L.; Chuan, Y.-M.; Yuan, M.-L. "Secondary amine-catalyzed [3 + 3] benzannulation to access polysubstituted benzenes through iminium activation." *Synth. Commun.* **2018**, *48*, 336.

[67] Battistuzzi, G.; Cacchi, S.; Fabrizi, G. "An Efficient Palladium-Catalyzed Synthesis of Cinnamaldehydes from Acrolein Diethyl Acetal and Aryl Iodides and Bromides." *Org. Lett.* **2003**, *5*, 777.

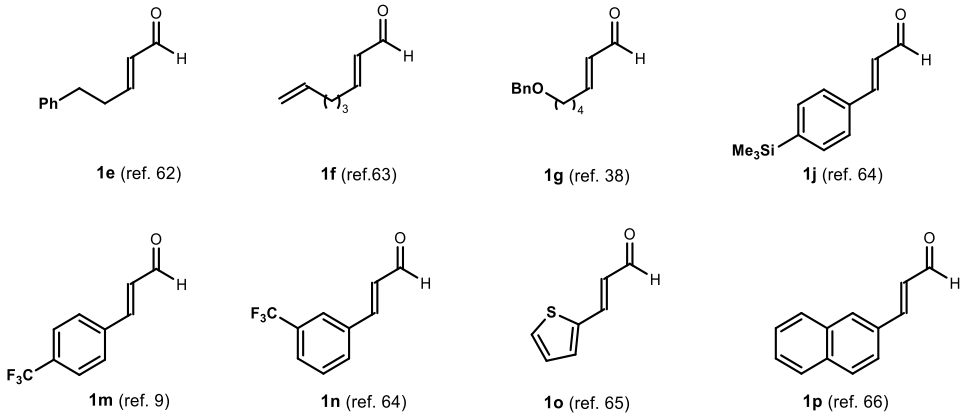

Figure 2.25. Enals synthesized according to procedures reported in the literature

2.6.2 General Procedure for the Asymmetric Synthesis of 1,7-Dicarbonyl Compounds

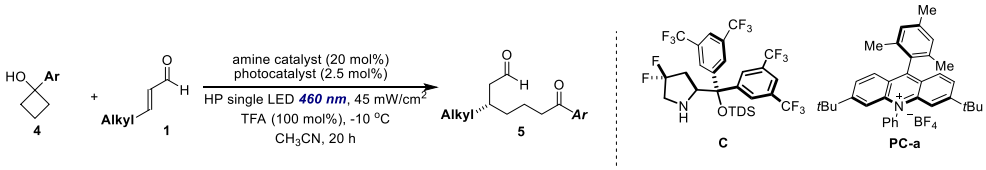

General Procedure A for *Aliphatic Enals*: To a 5 mL argon-purged glass vial were added cyclobutanol **4** (0.1 mmol, 1 equiv.), the amine catalyst **C** (14.1 mg, 0.02 mmol, 0.2 equiv.), enal **1** (*if solid*, 0.3 mmol, 3 equiv.), and the photocatalyst **PC-a** (1.4 mg, 2.5 μmol, 2.5 mol%). The reaction mixture was degassed through vacuum pumping and backfilling with argon for 4 times. Then, enal **1** (*if liquid*, 0.3 mmol, 3 equiv.) followed by 200 μL of an argon-sparged 0.5 M acetonitrile solution of trifluoroacetic acid (7.4 μL, 0.1 mmol, 100 mol%) were added. The vial was sealed with Parafilm, and then placed into an aluminum block on a 3D-printed holder, fitted with a 460 nm high-power single LED. The irradiance was fixed at 45 ± 2 mW/cm^2, as controlled by an external power supply and measured using a photodiode light detector. This setup secured a reliable irradiation while keeping a distance of 1 cm between the reaction vessel and the light source. The temperature was kept at -10 °C with a chiller connected to the irradiation plate (the setup is detailed in Figure 2.26)

The reaction was stirred for the indicated time, then the solvent was evaporated and the crude mixture was purified by flash column chromatography on silica gel to furnish the product **5**.

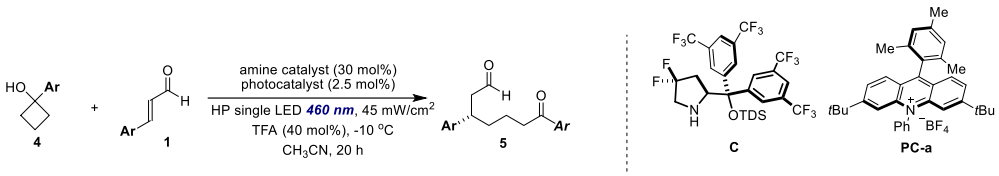

General Procedure B for *Aromatic Enals*: To a 5 mL argon-purged glass vial were added the cyclobutanol **4** (0.1 mmol, 1 equiv), amine catalyst **C** (21.1 mg, 0.03 mmol, 0.3 equiv.), the enal **1** (if solid, 0.3 mmol, 3 equiv.), and the photocatalyst 4a (1.4 mg, 2.5 μmol, 2.5 mol%). The reaction mixture was then degassed by vacuum pumping and backfilling with argon for 4 times. Then, enal **1** (if liquid, 0.3 mmol, 3 equiv.) followed by 200 μL of an argon-sparged 0.2 M acetonitrile solution of trifluoroacetic acid (3.0 μL, 0.04 mmol, 40 mol%) were added. The vial was sealed with Parafilm, and then placed into an aluminum block on a 3D-printed holder, fitted with a 460 nm high-power single LED. The irradiance was fixed at 45 ± 2 mW/cm^2, as controlled by an external power supply and measured using a photodiode light detector. This setup secured a reliable irradiation while keeping a distance of 1 cm between the reaction vessel and the light source. The temperature was kept at -10 °C with a chiller connected to the irradiation plate (the setup is detailed in Figure 2.26)

The reaction was stirred for the indicated time, then the solvent was evaporated and the crude mixture was purified by flash column chromatography on silica gel to furnish the product **5**.

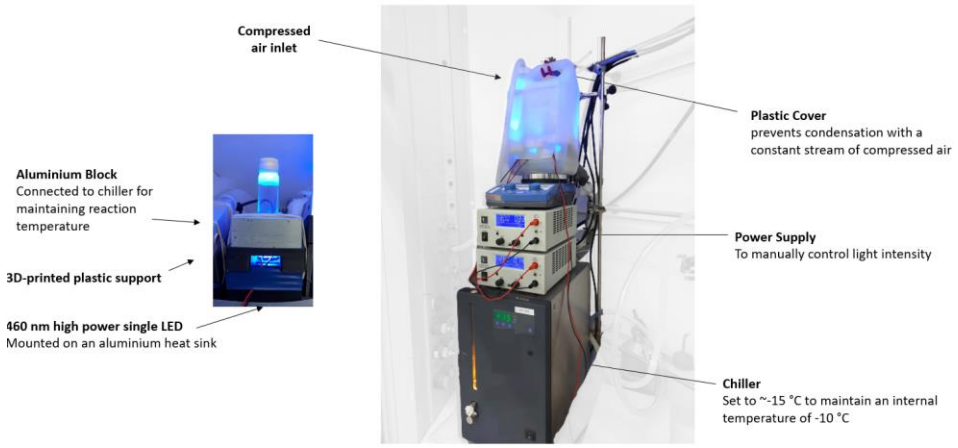

Figure 2.26. Detailed set-up and illumination system. The light source for illuminating the reaction vessel consisted of a single 460 nm high-power LED (LZ1-00DB00) purchased from ledengin.

2.6.3 Characterization of Products

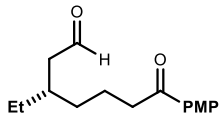

(*S*)-3-ethyl-7-(4-methoxyphenyl)-7-oxoheptanal (**5a**). Prepared according to general procedure **A** using (*E*)-pent-2-enal **1a** (29 μL, 0.3 mmol) and cyclobutanol **4a** (17.8 mg, 0.1 mmol) for 20 h. The crude mixture was purified by column chromatography (SiO_2, 12:1 n-hexanes: EtOAc) to afford product **5a** as a colorless oil (14.5 mg, 54% yield, average of two runs, 91% ee). The enantiomeric excess was determined by HPLC analysis on a Daicel Chiralpak ID-3 column (90:10 hexanes:*i*PrOH, flow rate 1.0 mL/min, 20 °C, λ = 215 nm: τ_{major} = 31.20 min, τ_{minor} = 36.21 min). $[\alpha]_D^{23.5}$ = -1.9 (c = 0.62, $CHCl_3$, 91% ee).

^{1}H NMR (500 MHz, $CDCl_3$): δ = 9.77 (t, *J* = 2.3 Hz, 1H), 7.95 – 7.90 (m, 2H), 6.95 – 6.90 (m, 2H), 3.86 (s, 3H), 2.91 (t, *J* = 7.3 Hz, 2H), 2.38 (dd, *J* = 6.6, 2.3 Hz, 2H), 1.96 (quint, *J* = 6.5 Hz, 1H), 1.76 – 1.69 (m, 2H), 1.48 – 1.39 (m, 2H), 1.39 – 1.30 (m, 2H), 0.88 (t, *J* = 7.4 Hz, 3H) ppm.

^{13}C{^{1}H} NMR (126 MHz, $CDCl_3$): δ = 203.0, 198.6, 163.4, 130.2, 130.1, 113.7, 55.4, 48.0, 38.2, 34.3, 33.3, 26.4, 21.5, 10.8 ppm.

HRMS (ESI): Calculated for $C_{16}H_{23}O_3$ $[M+H]^+$: 263.1642, found: 263.1645.

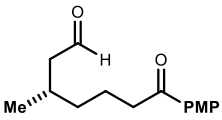

(*S*)-7-(4-methoxyphenyl)-3-methyl-7-oxoheptanal (**5b**). Prepared according to general procedure **A** using crotonaldehyde **1b** (25 μL, 0.3 mmol) and cyclobutanol **4a** (18.0 mg, 0.1 mmol) for 21 h. The crude mixture was purified by column chromatography (SiO_2, 12:1 n-hexanes: EtOAc) to afford product **5b** as a colorless oil (17.0 mg, 69% yield, average of two runs, 86% ee). The enantiomeric excess was determined by HPLC analysis on a Daicel Chiralpak ID-3 column (90:10 hexanes:*i*PrOH, flow rate 1.0 mL/min, 20 °C, λ = 215 nm: τ_{major} = 33.85 min, τ_{minor} = 38.22 min). $[\alpha]_D^{24}$ = -8.6 (c = 0.78, $CHCl_3$, 86% ee).

^{1}H NMR (400 MHz, $CDCl_3$): δ = 9.76 (t, *J* = 2.5 Hz, 1H), 7.96 – 7.90 (m, 2H), 6.95 – 6.89 (m, 2H), 3.86 (s, 3H), 2.91 (ddd, *J* = 7.6, 6.9, 1.6 Hz, 2H), 2.43 (ddd, *J* = 16.2, 5.7, 1.9 Hz, 1H), 2.26 (ddd, *J* = 16.2, 7.8, 2.5 Hz, 1H), 2.17 – 2.04 (m, 1H), 1.85 – 1.65 (m, 2H), 1.46 – 1.35 (m, 1H), 1.35 – 1.27 (m, 1H), 0.99 (d, *J* = 6.7 Hz, 3H) ppm.

$^{13}C\{^{1}H\}$ NMR (101 MHz, $CDCl_3$): δ = 202.8, 198.6, 163.4, 130.2, 130.1, 113.7, 55.4, 50.9, 38.1, 36.4, 28.0, 21.7, 19.8 ppm.

HRMS (ESI): Calculated for $C_{15}H_{21}O_3$ $[M+H]^+$: 249.1485, found: 249.1489.

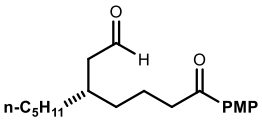

(*S*)-3-(4-(4-methoxyphenyl)-4-oxobutyl)octanal (**5c**). Prepared according to general procedure **A** using (*E*)-oct-2-enal **1c** (45 μL, 0.3 mmol) and cyclobutanol **4a** (17.8 mg, 0.1 mmol) for 22 h. The crude mixture was purified by column chromatography (SiO_2, 15:1 hexanes: EtOAc) to afford product **5c** as a colorless oil (18.5 mg, 60% yield, average of two runs, 91% ee). The enantiomeric excess was determined by HPLC analysis on a Daicel Chiralpak ID-3 column (90:10 hexanes:*i*PrOH, flow rate 1.0 mL/min, 20 °C, λ = 215 nm: τ_{major} = 22.94 min, τ_{minor} = 27.23 min). $[\alpha]_D^{24}$ = -0.5 (c = 0.91, $CHCl_3$, 91% ee).

^{1}H NMR (300 MHz, $CDCl_3$): δ = 9.77 (t, *J* = 2.3 Hz, 1H), 7.96 – 7.89 (m, 2H), 6.96 – 6.89 (m, 2H), 3.87 (s, 3H), 2.91 (t, *J* = 7.3 Hz, 2H), 2.38 (dd, *J* = 6.6, 2.3 Hz, 2H), 2.06-1.95 (m, 1H), 1.79 – 1.67 (m, 2H), 1.43 – 1.22 (m, 10H), 0.87 (t, *J* = 6.8 Hz, 3H) ppm.

$^{13}C\{^{1}H\}$ NMR (101 MHz, $CDCl_3$): δ = 203.1, 198.7, 163.4, 130.2, 130.1, 113.7, 55.4, 48.5, 38.2, 33.9, 33.8, 32.9, 32.0, 26.3, 22.6, 21.5, 14.0 ppm.

HRMS (ESI): Calculated for $C_{19}H_{29}O_3$ $[M+H]^+$: 305.2111, found: 305.2113.

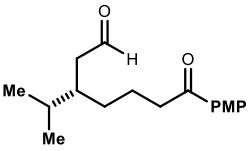

(*S*)-3-isopropyl-7-(4-methoxyphenyl)-7-oxoheptanal (**5d**). Prepared according to general procedure **A** using (*E*)-4-methylpent-2-enal **1d** (34.9 μL, 0.3 mmol) and cyclobutanol **4a** (17.8 mg, 0.1 mmol) for 22 h. The crude mixture was purified by column chromatography (SiO_2, 12:1 hexanes: EtOAc) to afford product **5d** as a colorless oil (8.5 mg, 30% yield, average of two runs, 86% ee). The enantiomeric excess was determined by HPLC analysis on a Daicel Chiralpak ID-3 column (85:15 hexanes :*i*PrOH, flow rate 1.0 mL/min, 20 °C, λ = 215 nm: τ_{major} = 20.41 min, τ_{minor} = 25.56 min). $[\alpha]_D^{24}$ = +5.3 (c = 0.30, $CHCl_3$, 86% ee).

^{1}H NMR (300 MHz, $CDCl_3$): δ = 9.78 (t, *J* = 2.2 Hz, 1H), 7.97 – 7.90 (m, 2H), 6.96 – 6.89 (m, 2H), 3.87 (s, 3H), 2.91 (t, *J* = 7.2 Hz, 2H), 2.42 (ddd, *J* = 16.5, 5.8, 2.1 Hz, 1H), 2.28 (ddd, *J* = 16.5, 7.1, 2.4 Hz, 1H), 1.98 – 1.87 (m, 1H), 1.83 – 1.65 (m, 3H), 1.51 – 1.37 (m, 1H), 1.34 – 1.26 (m, 1H), 0.88 (d, *J* = 6.8 Hz, 3H), 0.85 (d, *J* = 6.8 Hz, 3H) ppm.

^{13}C{^{1}H} NMR (101 MHz, $CDCl_3$): δ = 203.3, 198.6, 163.4, 130.3, 130.1, 113.7, 55.4, 45.4, 38.5, 38.2, 31.3, 29.8, 22.1, 19.7, 18.4 ppm.

HRMS (ESI): Calculated for $C_{17}H_{25}O_3$ [M+H]$^+$: 277.1798, found: 277.1798.

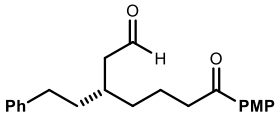

(*R*)-7-(4-methoxyphenyl)-7-oxo-3-phenethylheptanalal (**5e**). Prepared according to general procedure **A** using (*E*)-5-phenylpent-2-enal **1e** (48.0 mg, 0.3 mmol) and cyclobutanol **4a** (17.8 mg, 0.1 mmol) for 20 h. The crude mixture was purified by column chromatography (SiO_2, 10:1 hexanes: EtOAc) to afford product **5e** as a colorless oil (18.7 mg, 55% yield, average of two runs, 78% ee). The enantiomeric excess was determined by HPLC analysis on a Daicel Chiralpak ID-3 column (85:15 hexanes:*i*PrOH, flow rate 1.0 mL/min, 20 °C, λ = 215 nm: τ_{major} = 28.76 min, τ_{minor} = 30.67 min). $[\alpha]_D^{24}$ = +5.3 (c = 0.77, $CHCl_3$, 78% ee).

^{1}H NMR (400 MHz, $CDCl_3$): δ = 9.77 (t, *J* = 2.2 Hz, 1H), 7.97 – 7.90 (m, 2H), 7.29 – 7.24 (m, 2H), 7.20 – 7.14 (m, 3H), 6.97 – 6.90 (m, 2H), 3.87 (s, 3H), 2.91 (t, *J* = 7.2 Hz, 2H), 2.62 (t, *J* = 8.1 Hz, 2H), 2.45 (dd, *J* = 6.6, 2.2 Hz, 2H), 2.08 (sept, *J* = 6.4 Hz, 1H), 1.79 – 1.62 (m, 4H), 1.55 – 1.38 (m, 2H) ppm.

^{13}C{^{1}H} NMR (101 MHz, $CDCl_3$): δ = 202.7, 198.5, 163.4, 142.0, 130.2, 130.1, 128.4, 128.3, 125.8, 113.7, 55.4, 48.3, 38.1, 35.7, 33.5, 33.0, 32.4, 21.2 ppm.

HRMS (ESI): Calculated for $C_{22}H_{27}O_3$ [M+H]$^+$: 339.1955, found: 339.1955.

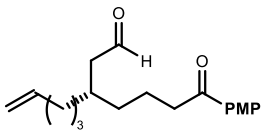

(*S*)-3-(4-(4-methoxyphenyl)-4-oxobutyl)oct-7-enal (**5f**). Prepared according to general procedure **A** using *(E)*-octa-2,7-dienal **1f** (35 μL, 0.3 mmol) and the cyclobutanol **4a** (17.8 mg, 0.1 mmol). The crude mixture was purified by column chromatography (SiO_2, 12:1 hexanes: EtOAc) to afford product **5f** as a colorless oil (13.0 mg, 44% yield, average of two runs, 87% purity by mole, 88% ee).

For obtaining pure NMR spectra, the product was further purified by preparative TLC (10% Et_2O in CH_2Cl_2).The enantiomeric excess was determined by UPC[2] analysis on a Daicel Chiralpak IC-3 column (gradient: 1 min 100% CO_2; 5 min 100% CO_2 to 60% CO_2 – 40% *i*PrOH; flow rate 2.0 mL/min; diode array: τ_{major} =4.50 min, τ_{minor} = 4.75 min) $[\alpha]_D^{24}$ = +7.3 (c = 1.00, $CHCl_3$, 88% ee).

^{1}H NMR (500 MHz, $CDCl_3$): δ = 9.77 (t, *J* = 2.2 Hz, 1H), 7.95 – 7.92 (m, 2H), 6.95 – 6.92 (m, 2H), 5.78 (ddt, *J* = 16.9, 10.2, 6.7 Hz, 1H), 5.01 – 4.92 (m, 2H), 3.87 (s, 3H), 2.91 (t, *J* = 7.3 Hz, 2H), 2.39 (dt, *J* = 6.5, 2.2 Hz, 2H), 2.10 – 1.88 (m, 3H), 1.73 (quint, *J* = 7.4 Hz, 2H), 1.63 – 1.29 (m, 6H) ppm.

^{13}C{^{1}H} NMR (126 MHz, $CDCl_3$): δ = 202.9, 198.6, 163.4, 138.6, 130.3, 130.1, 114.6, 113.7, 55.5, 53.4, 48.4, 38.2, 33.8, 33.7, 33.4, 32.7, 25.9, 21.4 ppm.

HRMS (ESI): Calculated for $C_{19}H_{26}O_3Na$ $[M+Na]^+$: 325.1774, found: 325.1780.

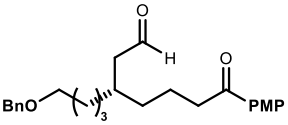

(*S*)-3-(4-(benzyloxy)butyl)-7-(4-methoxyphenyl)-7-oxoheptanal (**5g**). Prepared according to general procedure **A** using (*E*)-7-(benzyloxy)hept-2-enal **1g** (70.2 mg, 0.3 mmol) and cyclobutanol **4a** (17.8 mg, 0.1 mmol). The crude mixture was purified by column chromatography (SiO_2, 10:1 hexanes: EtOAc) to afford product **3g** as a colorless oil (22.3 mg, 56% yield, average of two runs, 81% ee). The enantiomeric excess was determined by UPC[2] analysis on a Daicel Chiralpak IC-3 column (gradient: 1 min 100% CO_2; 5 min 100% CO_2 to 60% CO_2 – 40% *i*PrOH; flow rate 2.0 mL/min; diode array: τ_{major} =5.31 min, τ_{minor} = 4.97 min). $[\alpha]_D^{24}$ = +1.2 (c = 0.11, $CHCl_3$, 81% ee).

^{1}H NMR (500 MHz, $CDCl_3$): δ = 9.76 (t, J = 2.2 Hz, 1H), 7.94 – 7.91 (m, 2H), 7.35 – 7.31 (m, 5H), 6.94 – 6.91 (m, 2H), 4.49 (s, 2H), 3.87 (s, 3H), 3.46 (t, *J* = 6.5 Hz, 2H), 2.90 (t, *J* = 7.3 Hz, 2H), 2.38 (ddd, *J* = 6.4, 2.2, 0.9 Hz, 2H), 2.06 – 1.96 (sept, *J* = 6.3 Hz, 1H), 1.78 – 1.66 (quint, *J* = 7.5 Hz, 2H), 1.60 (quint, *J* = 6.9 Hz, 2H), 1.48 – 1.23 (m, 6H) ppm.

^{13}C{^{1}H} NMR (126 MHz, $CDCl_3$): δ = 203.0, 198.7, 163.4, 138.6, 130.3, 130.1, 128.4, 127.7, 127.5, 113.7, 72.9, 70.2, 55.5, 53.5, 48.4, 38.2, 33.8, 32.8, 29.9, 23.3, 21.4 ppm.

HRMS (ESI): Calculated for $C_{25}H_{32}O_4Na$ $[M+Na]^+$: 419.2193, found: 419.2189.

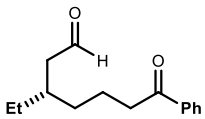

(*S*)-3-ethyl-7-oxo-7-phenylheptanal (**5h**)/ Prepared according to general procedure **A** using (*E*)-pent-2-enal **1a** (29 μL, 0.3 mmol) and cyclobutanol **4b** (14.8 mg, 0.1 mmol). The crude mixture was purified by column chromatography (SiO_2, 12:1 n-hexanes: EtOAc), followed by preparative TLC (33% Et_2O in hexanes) to afford product **5h** as a colorless oil (14.0 mg, 57% yield, average of two runs, 95% ee). The enantiomeric excess was determined by UPC^2 analysis on a Daicel Chiralpak IC-3 column (gradient: 1 min 100% CO_2; 5 min 100% CO_2 to 60% CO_2 – 40% *i*PrOH; flow rate 2.0 mL/min; diode array: τ_{major} = 4.59 min, τ_{minor} = 4.46 min). $[\alpha]_D^{24}$ = +2.0 (c = 0.15, $CHCl_3$, 95% ee).

^{1}H NMR (400 MHz, $CDCl_3$): δ = 9.79 (t, *J* = 2.3 Hz, 1H), 7.96 – 7.94 (m, 2H), 7.58 – 7.54 (m, 1H), 7.48 – 7.44 (m, 2H), 2.97 (t, *J* = 7.2 Hz, 2H), 2.39 (dd, *J* = 6.6, 2.2 Hz, 2H), 1.97 (sept, *J* = 6.6, 2.3 Hz, 1H), 1.75 (quint, *J* = 7.5 Hz, 2H), 1.49 – 1.46 (m, 2H), 1.40 – 1.33 (m, 2H), 0.89 (t, *J* = 7.4 Hz, 3H) ppm.

^{13}C{^{1}H} NMR (126 MHz, $CDCl_3$): δ = 203.0, 200.0, 137.0, 133.0, 128.6, 128.0, 48.0, 38.5, 34.2, 33.2, 26.4, 21.2, 10.9 ppm.

HRMS (ESI): Calculated for $C_{15}H_{20}O_3Na$ $[M+Na]^+$: 271.1305, found: 271.1300.

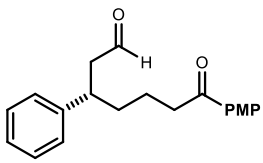

(*S*)-7-(4-methoxyphenyl)-7-oxo-3-phenylheptanal (5i). Prepared according to the general procedure **B** using (*E*)-cinnamaldehyde **1h** (38 μL, 0.3 mmol) and cyclobutanol **4a** (18.0 mg, 0.1 mmol). The crude mixture was purified by column chromatography (SiO_2, 10% EtOAc in hexanes) to afford the product **5i** as a yellow oil (21.1 mg, 68% yield, average of 2 runs, 82% ee). The enantiomeric excess was determined by UPC^2 analysis on a Daiacel Chiralpak IE-3 column (gradient: 1 min 100% CO_2; 5 min 100% CO_2 to 60% CO_2 – 40% MeCN; 8 min 60% CO_2 – 40% MeCN; flow rate 2.0 mL/min; diode array: τ_{major} = 6.55 min, τ_{minor} = 7.10 min). $[\alpha]_D^{24}$ = –2.0 (c = 0.10, $CHCl_3$, 82% ee).

^{1}H NMR (500 MHz, $CDCl_3$): δ = 9.66 (t, *J* = 2.0 Hz, 1H), 7.92 – 7.86 (m, 2H), 7.30 (t, *J* = 7.6 Hz, 2H), 7.21 (dd, *J* = 7.4, 5.3 Hz, 3H), 6.93 – 6.85 (m, 2H), 3.86 (s, 3H), 3.24 (quint, *J* = 7.14 Hz, 1H), 2.95 – 2.77 (m, 2H), 2.74 (dd, *J* = 7.3, 2.0 Hz, 2H), 1.84 – 1.50 (m, 5H). 2.88 (ddt, *J* = 9.5, 7.2, 2.8 Hz, 2H), 2.76 (dd, *J* = 7.3, 2.0 Hz, 2H), 1.80 – 1.52 (m, 4H) ppm.

$^{13}C\{^{1}H\}$ NMR (101 MHz, $CDCl_3$): δ =201.8, 198.5, 163.4, 143.4, 130.3, 130.0, 128.7, 127.5, 126.7, 113.7, 55.5, 50.6, 40.0, 37.9, 36.0, 22.2 ppm.

HRMS (ESI): Calculated for $C_{20}H_{22}O_3Na$ $[M+Na]^+$: 333.1461, found: 333.1462.

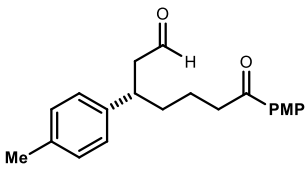

(*S*)-7-(4-methoxyphenyl)-7-oxo-3-(p-tolyl)heptanal (5j). Prepared according to the general procedure **B** using (*E*)-3-(*p*-tolyl)acrylaldehyde **1i** (43.9 mg, 0.3 mmol) and cyclobutanol **4a** (17.8 mg, 0.1 mmol). The crude mixture was purified by column chromatography (SiO_2, gradient from 5% to 30 % EtOAc in hexanes) to afford the product **5j** as a yellow oil (25.0 mg, 78% yield, average of 2 runs, 90% ee). The enantiomeric excess was determined by UPC[2] analysis on a Daiacel Chiralpak IE-3 column, gradient: 1 min 100% CO_2; 10 min 100% CO_2 to 60% CO_2 – 40% MeCN; 13 min 60% CO_2 – 40% MeCN; 15 min 60% CO_2 – 40% MeCN to 100% CO_2; flow rate 2.0 mL/min; diode array: τ_{major} = 12.59 min, τ_{minor} = 14.34 min). $[\alpha]_D^{24}$ = –10.2 (c = 0.20, $CHCl_3$, 90% ee)

^{1}H NMR (500 MHz, $CDCl_3$): δ = 9.66 (t, *J* = 2.1 Hz, 1H), 7.88 – 7.86 (m, 2H), 7.12 – 7.07 (m, 4H), 6.92 – 6.89 (m, 2H), 3.86 (s, 3H), 3.21 – 3.16 (m, 1H), 2.91 – 2.81 (m, 2H), 2.71 (dd, *J* = 7.3, 2.1 Hz, 2H), 2.31 (s, 3H), 1.76 – 1.57 (m, 4H) ppm.

$^{13}C\{^{1}H\}$ NMR (126 MHz, $CDCl_3$): δ = 202.0, 198.5, 163.3, 140.3, 136.2, 130.2, 130.0, 129.4, 127.3, 113.7, 55.4, 50.6, 39.6, 37.9, 36.1, 22.2, 21.0 ppm.

HRMS (ESI): Calculated for $C_{21}H_{24}NaO_3$ $[M+Na]^+$: 347.1618, found: 347.1610.

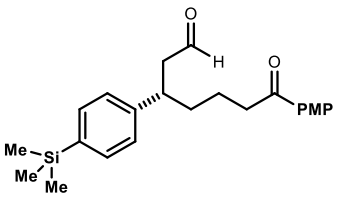

(S)-7-(4-methoxyphenyl)-7-oxo-3-(4-(trimethylsilyl)phenyl)-heptanal (5k). Prepared according to the general procedure **B** using (*E*)-3-(4-(trimethylsilyl)phenyl)acrylaldehyde **1j** (61.3 mg, 0.3 mmol) and cyclobutanol **4a** (17.8 mg, 0.1 mmol) for 40 hours of reaction time. The crude mixture was purified by column chromatography (SiO_2, gradient from 5% to 30 % EtOAc in hexanes) to afford the product **5k** as a yellow oil (16.9 mg, 44% yield, average of 2 runs, 88% ee). The enantiomeric excess was determined by UPC[2]

analysis on a Daiacel Chiralpak ID-3 column (gradient: 1 min 100% CO_2; 5 min 100% CO_2 to 60% CO_2 – 40% MeCN; flow rate 2.0 mL/min; diode array: τ_{major} = 4.90 min, τ_{minor} = 5.24 min). $[\alpha]_D^{24}$ = +3.6 (c = 0.20, $CHCl_3$, 88% ee)

^{1}H NMR (400 MHz, $CDCl_3$): δ = 9.67 (t, *J* = 2.0 Hz, 1H), 7.90 – 7.85 (m, 2H), 7.48 – 7.42 (m, 2H), 7.21 – 7.16 (m, 2H), 6.93 – 6.88 (m, 2H), 3.86 (s, 3H), 3.22 (m, 1H), 2.95 – 2.78 (m, 2H), 2.74 (dd, *J* = 7.4, 2.0 Hz, 2H), 1.80 – 1.70 (m, 2H), 1.69 – 1.50 (m, 2H), 0.25 (s, 9H) ppm.

^{13}C{^{1}H} NMR (101 MHz, $CDCl_3$): δ = 201.8, 198.5, 163.4, 143.9, 138.6, 133.8, 130.2, 130.0, 126.9, 113.7, 55.4, 50.5, 39.9, 37.9, 35.9, 22.2, -1.1 ppm.

HRMS (ESI): Calculated for $C_{23}H_{30}NaO_3Si$ $[M+Na]^+$: 405.1856, found: 405.1839.

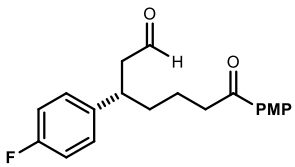

(*S*)-3-(4-fluorophenyl)-7-(4-methoxyphenyl)-7-oxoheptanal (5l). Prepared according to the general procedure **B** using *E*)-3-(4-fluorophenyl)acrylaldehyde **1k** (45.0 mg, 39.3 µL, 0.3 mmol) and cyclobutanol **4a** (17.8 mg, 0.1 mmol). The crude mixture was purified by column chromatography (SiO_2, gradient from 5% to 20 % EtOAc in hexanes) to afford the product **5l** as a yellow oil (16.2 mg, 51% yield, average of 2 runs, 84% ee). The enantiomeric excess was determined by UPC^2 analysis on a Daiacel Chiralpak IC-3 column (gradient: 1 min 100% CO_2; 5 min 100% CO_2 to 60% CO_2 – 40% MeCN; flow rate 2.0 mL/min; diode array: τ_{major} = 4.95 min, τ_{minor} = 4.63 min). $[\alpha]_D^{25}$ = +2.9 (c = 0.20, $CHCl_3$, 84% ee)

^{1}H NMR (500 MHz, $CDCl_3$): δ = 9.66 (t, *J* = 1.9 Hz, 1H), 7.89 – 7.86 (m, 2H), 7.17 – 7.14 (m, 2H), 7.00 – 6.93 (m, 2H), 6.92 – 6.89 (m, 2H), 3.86 (s, 3H), 3.22 (quint, *J* = 7.5 Hz, 1H), 2.92 – 2.81 (m, 2H), 2.73 (t, *J* = 1.9 Hz, 1H), 2.72 (dd, *J* = 3.0, 1.9 Hz, 1H), 1.78 – 1.57 (m, 3H) ppm.**^{19}F{^{1}H} NMR (471MHz, $CDCl_3$):** δ = -116.3 ppm.

^{13}C{^{1}H} NMR (126 MHz, $CDCl_3$): δ = 201.4, 198.4, 163.4, 161.6 (d, $J_{C\text{-}F}$ = 244.9 Hz), 139.1 (d, $J_{C\text{-}F}$ = 3.2 Hz), 130.2, 130.0, 128.9 (d, $J_{C\text{-}F}$ = 7.8 Hz), 115.5 (d, $J_{C\text{-}F}$ = 21.2 Hz), 113.7, 55.5, 50.7, 39.2, 37.8, 36.1, 22.1 ppm.

HRMS (ESI): Calculated for $C_{20}H_{21}FO_3Na$ $[M+Na]^+$: 351.1367, found: 351.1364.

(*S*)-3-(4-chlorophenyl)-7-(4-methoxyphenyl)-7-oxoheptanal (5m).

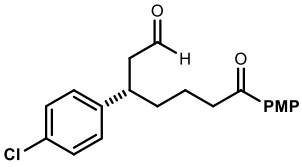

Prepared according to the general procedure **B** using (*E*)-3-(4-chlorophenyl)acrylaldehyde **1l** (50.0 mg, 0.3 mmol) and cyclobutanol **4a** (17.8 mg, 0.1 mmol) for 38 hours of reaction time. The crude mixture was purified by column chromatography (SiO_2, gradient from 5% to 30 % EtOAc in hexanes) to afford the product **5m** as a yellow oil (17.5 mg, 51% yield, average of 2 runs, 84% ee). The enantiomeric excess was determined by UPC^2 analysis on a Daiacel Chiralpak IG-3 column (gradient: 1 min 100% CO_2; 5 min 100% CO_2 to 60% CO_2 – 40% MeCN; flow rate 2.0 mL/min; diode array: τ_{major} = 4.88 min, τ_{minor} = 4.72 min). $[\alpha]_D^{24}$ = +0.7 (c = 0.20, $CHCl_3$, 84% ee)

^{1}H NMR (500 MHz, $CDCl_3$): δ = 9.66 (t, J = 1.8 Hz, 1H), 7.88 – 7.86 (m, 2H), 7.28 – 7.26 (m, 2H), 7.15 – 7.12 (m, 2H), 6.92– 6.89 (m, 2H), 3.86 (s, 3H), 3.21 (quint, *J* = 7.5 Hz, 1H), 2.92 – 2.82 (m, 2H), 2.73 (t, *J* = 2.1 Hz, 1H), 2.72 (dd, *J* = 3.4, 1.8 Hz, 1H), 1.77 – 1.56 (m, 4H) ppm.

^{13}C{^{1}H} NMR (126 MHz, $CDCl_3$): δ = 201.1, 198.3, 163.4, 142.0, 132.4, 130.2, 130.0, 128.9 (2C), 113.7, 55.5, 50.5, 39.3, 37.8, 35.9, 22.1 ppm.

HRMS (ESI): Calculated for $C_{20}H_{21}ClO_3Na$ $[M+Na]^+$: 367.1071, found: 367.1066.

(*S*)-7-(4-methoxyphenyl)-7-oxo-3-(4-(trifluoromethyl)phenyl)heptanal (5n). Prepared according to the general procedure **B** using (*E*)-3-(4-(trifluoromethyl)phenyl)acrylaldehyde

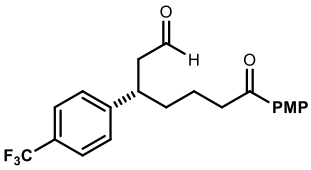

1m (60.0 mg, 0.3 mmol) and cyclobutanol **4a** (17.8 mg, 0.1 mmol). The crude mixture was purified by column chromatography (SiO_2, gradient from 5% to 20 % EtOAc in hexanes) to afford the product **5n** as a yellow oil (18.5 mg, 49% yield, average of 2 runs, 84% ee). The enantiomeric excess was determined by UPC^2 analysis on a Daiacel Chiralpak IG-3 column (gradient: 1 min 100% CO_2; 5 min 100% CO_2 to 60% CO_2 – 40% MeCN; flow rate 2.0 mL/min; diode array: τ_{major} = 3.76 min, τ_{minor} = 3.63 min). $[\alpha]_D^{25}$ = +10.6 (c = 0.20, $CHCl_3$, 84% ee)

^{1}H NMR (500 MHz, $CDCl_3$): δ = 9.68 (t, J = 1.7 Hz, 1H), 7.88 – 7.85 (m, 2H), 7.56 (d, *J* = 7.6 Hz, 2H), 7.33 (d, *J* = 8.0 Hz, 2H), 6.92 – 6.89 (m, 2H), 3.86 (s, 3H), 3.31 (quint, *J* = 7.0 Hz, 1H), 2.93 – 2.81 (m, 2H), 2.78 (ddd, *J* = 7.7, 3.3, 1.7 Hz, 2H), 1.81 – 1.57 (m, 4H) ppm.

^{19}F {^{1}H} NMR (471 MHz, $CDCl_3$): δ = -62.4 ppm.

^{13}C{^{1}H} NMR (126 MHz, $CDCl_3$): δ = 200.7, 198.3, 163.5, 147.8, 130.2, 129.9, 129.1 (q, J_{C-F} = 32.2 Hz), 127.9, 125.70 (q, J_{C-F} = 3.8 Hz), 124.1 (q, J_{C-F} = 272.0 Hz), 113.7, 55.5, 50.4, 39.7, 37.7, 35.7, 22.1 ppm.

HRMS (ESI): Calculated for $C_{21}H_{22}F_3O_3$ [M+H]$^+$: 379.1516, found: 379.1515.

(*S*)-7-(4-methoxyphenyl)-7-oxo-3-(3-(trifluoromethyl)phenyl)-heptanal (5o). Prepared

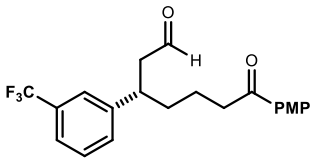

according to the general procedure **B** using (E)-3-(3-(trifluoromethyl)phenyl)acrylaldehyde **1n** (60.0 mg, 0.3 mmol) and cyclobutanol **4a** (17.8 mg, 0.1 mmol). The crude mixture was purified by column chromatography (SiO_2, gradient from 5% to 20 % EtOAc in hexanes) to afford the product **5o** as a yellow oil (14.5 mg, 39% yield, average of 2 runs, 84% ee). The enantiomeric excess was determined by UPC^2 analysis on a Daiacel Chiralpak IG-3 column (gradient: 1 min 100% CO_2; 5 min 100% CO_2 to 60% CO_2 – 40% MeCN; flow rate 2.0 mL/min; diode array: τ_{major} = 3.49 min, τ_{minor} = 4.00 min). $[\alpha]_D^{25}$ = +4.9 (c = 0.20, $CHCl_3$, 84% ee)

^{1}H NMR (500 MHz, $CDCl_3$): δ = 9.69 (t, *J* = 1.6 Hz, 1H), 7.89 – 7.86 (m, 2H), 7.49 – 7.39 (m, 4H), 6.92 – 6.89 (m, 2H), 3.86 (s, 3H), 3.36 – 3.27 (m, 1H), 2.94 – 2.82 (m, 2H), 2.82 – 2.76 (m, 2H), 1.84 – 1.57 (m, 4H) ppm.

^{19}F {^{1}H} NMR (471 MHz, $CDCl_3$): δ = -62.5 ppm.

^{13}C{^{1}H} NMR (126 MHz, $CDCl_3$): δ = 200.7, 198.3, 163.5, 144.7, 131.1 (m), 130.3, 130.0, 129.2, 124.1 (q, J_{C-F} = 3.7 Hz), 124.1 (q, J_{C-F} =272.2 Hz), 123.7 (q, J_{C-F} = 3.8 Hz), 113.74, 55.5, 50.4, 39.7, 37.7, 35.8, 22.1 ppm.

HRMS (ESI): Calculated for $C_{21}H_{22}F_3O_3$ [M+H]$^+$: 379.1516, found: 379.1507.

(*S*)-7-(4-methoxyphenyl)-7-oxo-3-(thiophen-2-yl)heptanal (5p). Prepared according to the general procedure **B** using (*E*)-3-(thiophen-2-yl)acrylaldehyde **1o** (41.5 mg, 0.3 mmol) and cyclobutanol **4a** (17.8 mg, 0.1 mmol). The crude mixture was purified by column chromatography (SiO_2, 10% EtOAc in hexanes) to afford the product **5p** as a yellow oil (16.7 mg, 53% yield, average of 2 runs, 84% ee). The enantiomeric excess was determined by UPC^2 analysis on a Daiacel Chiralpak IG-3 column (gradient: 1 min 100% CO_2; 5 min 100% CO_2 to 60% CO_2 – 40% MeCN; flow rate 2.0 mL/min; diode array: τ_{major} = 4.71 min, τ_{minor} = 5.04 min). $[\alpha]_D^{24}$ = +8.8 (c = 0.15, $CHCl_3$, 84% ee)

^{1}H NMR (500 MHz, $CDCl_3$): δ = 9.71 (t, *J* = 1.8 Hz, 1H), 7.95 – 7.81 (m, 2H), 6.94 – 6.89 (m, 3H), 6.86 (ddd, J = 3.5, 1.2, 0.6 Hz, 1H), 3.86 (s, 3H), 3.57 (quint, J = 7.4, 6.7 Hz, 1H), 2.96 – 2.83 (m, 2H), 2.78 (t, J = 1.8 Hz, 1H), 2.77 (dd, J = 1.9, 1.1 Hz, 1H), 1.83 – 1.76 (m, 1H), 1.76 – 1.68 (m, 3H) ppm.

^{13}C{^{1}H} NMR (126 MHz, $CDCl_3$): δ = 201.2, 198.4, 163.4, 147.3, 130.3, 130.0, 126.8, 124.3, 123.5, 113.7, 55.5, 51.2, 37.7, 37.0, 35.4, 22.0 ppm.

HRMS (ESI): Calculated for $C_{18}H_{20}O_3SNa$ $[M+Na]^+$: 339.1025, found: 339.1038.

(*S*)-7-(4-methoxyphenyl)-3-(naphthalen-2-yl)-7-oxoheptanal (5q). Prepared with modified conditions to the general procedure **B** using *(E)*-3-(naphthalen-2-yl)acrylaldehyde **2p** (54.7 mg, 0.3 mmol), cyclobutanol **4a** (17.8 mg, 0.1 mmol), photocatalyst **PC-a** (2.9 mg, 5.0 µmol, 5.0 mol%), and MeCN/CH_2Cl_2 (4:1) as solvent. The crude mixture was purified by column chromatography (SiO_2, gradient from 10% to 15% EtOAc in hexanes) to afford the product **5q** as a brown oil (30.3 mg, 82% yield, average of 2 runs, 80% ee). The enantiomeric excess was determined by UPC^2 analysis on a Daiacel Chiralpak IC-3 column (gradient: 1 min 100% CO_2; 5 min 100% CO_2 to 60% CO_2 – 40% *i*PrOH; 8 min 60% CO_2 – 40% *i*PrOH; flow rate 2.0 mL/min; diode array: τ_{major} = 6.43 min, τ_{minor} = 6.08 min). $[\alpha]_D^{24}$ = - 7.3 (c = 0.10, $CHCl_3$, 80% ee)

^{1}H NMR (300 MHz, $CDCl_3$): δ = 9.71 (t, J = 2.0 Hz, 1H), 7.89 – 7.77 (m, 5H), 7.69 – 7.64 (m, 1H), 7.52 – 7.41 (m, 2H), 7.37 (dd, *J* = 8.5, 1.8 Hz, 1H), 6.91 – 6.83 (m, 2H), 3.86 (s, 3H),

3.43 (quint, *J* = 7.3 Hz, 1H), 2.99 – 2.77 (m, 3H), 1.89 – 1.79 (m, 2H), 1.71 – 1.55 (m, 2H) ppm.

$^{13}C\{^{1}H\}$ NMR (101 MHz, $CDCl_3$): δ = 201.7, 198.5, 163.4, 158.8, 140.8, 133.5, 132.5, 130.3, 128.6, 127.7, 127.6, 126.6, 126.2, 125.6, 125.5, 113.7, 55.4, 50.5, 40.1, 37.9, 35.9, 22.3 ppm.

HRMS (ESI): Calculated for $C_{24}H_{24}O_3Na$ $[M+Na]^+$: 383.1618, found: 383.1621.

2.6.4 Scale-up Procedure for the Synthesis of 5a

A different setup was used for the scale-up reaction. It consists of a 4 cm diameter jar fitted with a standard 29 sized ground glass joint. A commercial 1-meter blue LED strip (λ = 465 nm) was wrapped around the jar, followed by a layer of aluminium foil and cotton for insulation. An inlet and outlet allow the circulation of liquid from a Huber Minichiller 300 inside the jar (Figure S5).

To a 10 mL oven-dried Schlenk tube, cyclobutanol **4a** (178.2 mg, 1.0 mmol, 1 equiv.), catalyst **C** (141.0 mg, 0.2 mmol, 0.2 equiv.) and photocatalyst **PC-a** (14.4 mg, 25 μmol, 2.5 mol%) were sequentially added. The Schlenk tube was degased with freeze-pump-thaw cycle for four times. Then, *(E)*-pent-2-enal **1a** (290 μL, 3.0 mmol, 3 equiv.) were added, followed by 2 mL of an argon-sparged acetonitrile solution of trifluoroacetic acid (77 μL, 1.0 mmol, 1 equiv.). The Schlenk tube was sealed with Parafilm, and placed into the reactor described above, with the temperature set at -15 °C. The reaction was stirred for 20 hours, then the solvent was evaporated and the crude mixture was purified by flash column chromatography(SiO_2, 1:12 EtOAc: hexanes) to furnish the product **5a** (173 mg, 0.66 mmol, 66% yield, 90% ee) as a yellow oil.

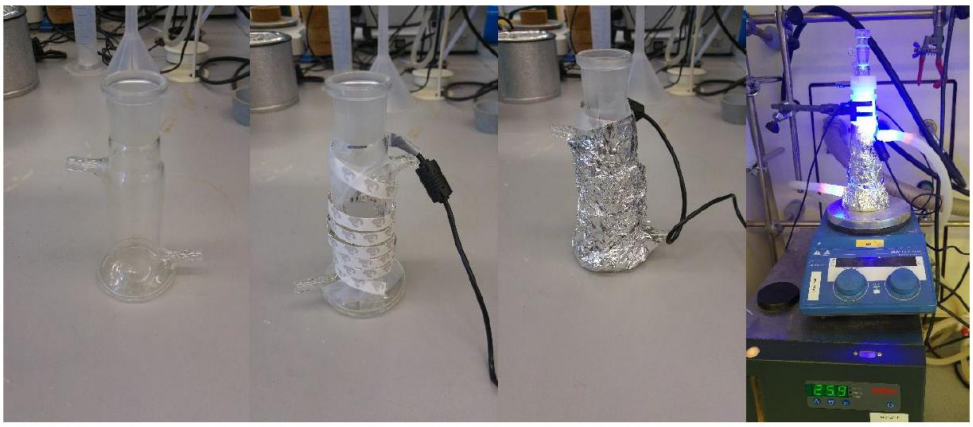

Figure 2.27. Fully assembled photoreactor for the 1 mmol scale photochemical radical conjugate addition

2.6.5 Procedure for Product Transformation

Reductive Amination

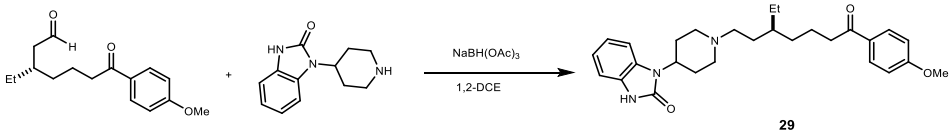

29

5a (7.0 mg, 0.027 mmol, 1.0 equiv.) and 4-(2-keto-1-benzimidazolinyl)piperidine (5.8 mg, 0.027 mmol, 1.0 equiv.) was stirred in 1,2-dichloroethane (1,2-DCE, 2 mL). $NaBH(OAc)_3$ (22 mg, 0.108 mmol, 4.0 equiv.) was then added and the mixture was stirred for 5 hours.

The reaction was quenched with $NaHCO_3$ (aq) and the aqueous layer was extracted by CH_2Cl_2. The organic layers were combined, dried by $MgSO_4$ and concentrated *in vacuo*. The residue was then purified on a column (SiO_2, CH_2Cl_2 to 85% EtOAc in CH_2Cl_2) to afford *(S)*-1-(1-(3-ethyl-7-(4-methoxyphenyl)-7-oxoheptyl)piperidin-4-yl)-1,3-dihydro-2H-benzo[d]imidazol-2-one (**29**) as a colorless oil (9.6 mg, 77 %). The enantiomeric excess was determined by HPLC analysis on a Daiacel Chiralpak IA-3 column (85:15 hexanes:*i*PrOH, flow rate 1.0 mL/min, 25 °C, λ = 215 nm: τ_{major} = 16.82 min, τ_{minor} = 19.00 min). $[\alpha]_D^{24}$ = -4.7 (c = 0.10, $CHCl_3$, >90% ee).

^{1}H NMR (500 MHz, $CDCl_3$): δ = 7.96 – 7.93 (m, 2H), 7.29 – 7.26 (m, 1H), 7.12 – 7.09 (m, 1H), 7.04 (m, 2H), 6.94 – 6.91 (m, 2H), 4.44 (tt, *J* = 12.5, 4.3 Hz, 1H), 3.87 (s, 3H), 3.68 (td, *J* = 6.9, 0.9 Hz, 2H), 3.27 (dt, *J* = 13.1, 2.8 Hz, 2H), 2.91 (td, *J* = 7.1, 1.3 Hz, 2H), 2.81 (td, *J* = 12.4, 2.5 Hz, 2H), 2.35 (qd, *J* = 12.5, 4.2 Hz, 2H), 1.85 (ddd, *J* = 11.9, 4.3, 2.0 Hz, 2H),

1.76 – 1.69 (m, 2H), 1.60 – 1.30 (m, 2H), 1.45 (quint, *J* = 5.9 Hz, 1H), 1.39 – 1.30 (m, 4H), 0.86 (t, J = 7.4 Hz, 3H) ppm.

$^{13}C\{^1H\}$ NMR (101 MHz, $CDCl_3$): δ = 199.1, 163.4, 154.9, 130.3, 130.2, 129.3, 127.9, 121.1, 121.0, 113.7, 109.6 (2C), 61.1, 55.4, 51.1, 46.4, 38.5, 36.3, 35.6, 32.8, 30.6, 25.9, 21.5, 10.7 ppm.

HRMS (ESI): Calculated for $C_{28}H_{38}N_3O_3$ $[M+H]^+$:464.2908, found: 464.2908.

Reduction-Oxidation Sequence

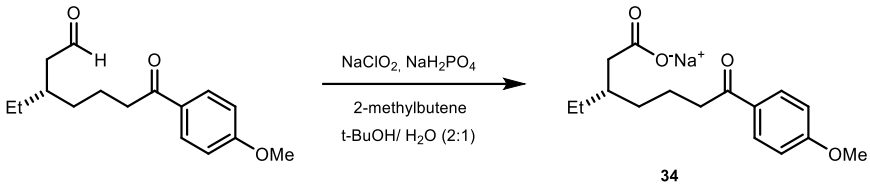

34

5a (50 mg, 0.19 mmol, 1.0 equiv.) and 2-methylbutene (0.48 mL, 3.8 mmol, 20 equiv.) was stirred in *tert*-butanol (2 mL). $NaClO_2$ (35 mg, 0.38 mmol, 2.0 equiv.) and NaH_2PO_4 (93 mg, 0.75 mmol, 4.0 equiv.) was dissolved in water (1 mL) and was added dropwise to the aforementioned organic solution. The mixture was stirred vigorously for 2 hours. After which, it was diluted with water and was extracted with CH_2Cl_2. The organic layers were combined, dried by $MgSO_4$ and concentrated in vacuo to afford (*S*)-3-ethyl-7-(4-methoxyphenyl)-7-oxoheptanoate, sodium salt (**34**) as a colorless oil. (42.5 mg, 75 %) The product can be used directly for the next step without further purification.

^1H NMR (500 MHz, $CDCl_3$): δ = 7.95 – 7.92 (m, 2H), 6.93 – 6.91 (m, 2H), 3.86 (s, 3H), 2.92 (t, *J* = 7.4 Hz, 2H), 2.32 (dd, *J* = 6.9, 0.7 Hz, 2H), 1.85 (quint, *J* = 6.6 Hz, 1H), 1.78 – 1.70 (m, 2H), 1.46 – 1.36 (m, 4H), 0.89 (t, *J* = 7.4 Hz, 3H) ppm.

$^{13}C\{^1H\}$ NMR (126 MHz, $CDCl_3$): δ =199.0, 179.0, 163.4, 130.3, 130.1, 113.7, 55.5, 38.3, 36.2, 33.0, 26.1, 24.8, 21.4, 10.7 ppm.

HRMS (ESI): Calculated for $C_{16}H_{21}O_4$ $[M-Na]^-$:277.1445, found: 277.1446.

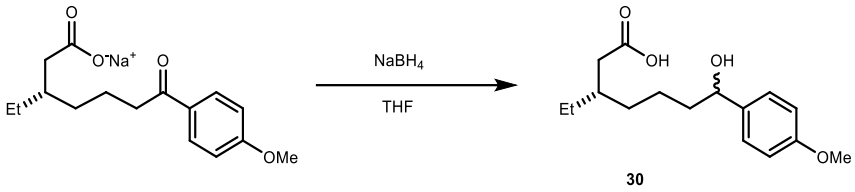

30

To a stirred solution of **34** (42.5 mg, 0.15 mmol, 1.0 equiv.) in dry THF (5 mL) was added $NaBH_4$ (11.4 mg, 0.30 mmol, 2.0 equiv.). The reaction mixture was stirred 14 hours and was quenched with 1.0 M HCl. The aqueous layer was extracted by CH_2Cl_2. The organic layers were combined, dried by $MgSO_4$ and concentrated in vacuo. The residue was then purified by flash column chromatography (SiO_2, 25 to 50 % EtOAc in hexanes) to afford (*S*)-3-ethyl-7-hydroxy-7-(4-methoxyphenyl)heptanoic acid (**30**) as an oil. (26.4 mg, 64 %, 48% over two steps).

$[\alpha]_D^{24}$ = +2.6 (c = 0.10, $CHCl_3$, d.r.= 5.5:1, 85% ee).

^{1}H NMR (500 MHz, $CDCl_3$, mixture of diastereomers): δ = 7.27 – 7.24 (m, 2H), 6.89 – 6.86 (m, 2H), 4.62 (t, *J* = 6.5 Hz, 1H), 3.80 (s, 3H), 2.26 (td, *J* = 6.7, 2.2 Hz, 2H), 1.79 (m, 3H), 1.71 – 1.61 (m, 2H), 1.41 – 1.31 (m, 4H), 0.86 (t, *J* = 7.4 Hz, 3H) ppm.

^{13}C{^{1}H} NMR (126 MHz, $CDCl_3$, mixture of diastereomers): δ = 178.5, 159.0, 136.9, 127.1, 113.9, 74.1, 55.3, 39.0, 38.3, 36.2, 33.1, 26.2, 22.8, 10.8 ppm.

HRMS (ESI): Calculated for $C_{16}H_{23}O_4$ [M-H]$^-$: 279.1601, found: 279.1602.

30 (1 mg) was derivatized by stirring with Me_3SiCHN_2 (3 drops, 2.0 M in n-hexanes) in methanol (2 mL) for 30 minutes. The enantiomeric excess was determined after by UPC^2 analysis on a Daiacel Chiralpak IG-3 column (gradient: 1 min 100% CO_2; 5 min 100% CO_2 to 60% CO_2 – 40% *i*PrOH; flow rate 2.0 mL/min; diode array). Diastereoisomer A: τ_{Major} = 5.02 min, τ_{Minor} = 2.97 min. Diastereoisomer B: τ_{Major} = 6.03 min, τ_{Minor} =2.67 min.

Mono-olefination

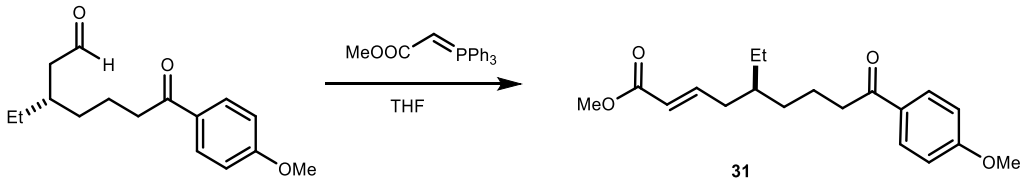

31

5a (5.5 mg, 0.02 mmol, 1.0 equiv.) was dissolved in dry THF (5 mL) and was stirred with methyl (triphenylphosphoranylidene)acetate (36 mg, 0.08 mmol, 4.0 equiv.) at room temperature for 15 hours. Organic solvents were removed in vacuo. The residue was re-dissolved in 20% Et_2O in hexanes (10 mL), filtered through a silica plug and then purified through preparative TLC (CH_2Cl_2: Et_2O: hexanes= 2:1:3) to afford (*S*)-methyl *(E)*-5-ethyl-9-(4-methoxyphenyl)-9-oxonon-2-enoate (**31**) as a colorless oil. (5.8 mg, 83 %, E:Z> 10:1) The enantiomeric excess was determined by UPC[2] analysis on a Daiacel Chiralpak ID-3 column (gradient: 1 min 100% CO_2; 5 min 100% CO_2 to 60% CO_2 – 40% *i*-PrOH; flow rate 2.0 mL/min; diode array: τ_{major} = 4.80 min, τ_{minor} = 4.91 min).

$[\alpha]_D^{24}$ = -3.4 (c = 0.10, $CHCl_3$, 90% ee).

^{1}H NMR (500 MHz, $CDCl_3$): δ = 7.95 – 7.92 (m, 2H), 6.98-6.90 (m, 3H), 5.83 (dt, *J* = 15.6, 1.4 Hz, 1H), 3.87 (s, 3H), 3.73 (s, 3H), 2.90 (t, *J* = 7.2 Hz, 2H), 2.23 – 2.18 (m, 2H), 1.70 (quint, *J* =7.5 Hz, 2H), 1.53 – 1.46 (dt, *J* = 12.7, 6.5 Hz, 1H), 1.41 – 1.28 (m, 4H), 0.87 (t, *J* = 7.4 Hz, 3H) ppm.

^{13}C{^{1}H} NMR (126 MHz, $CDCl_3$): δ = 206.9, 198.8, 167.0, 163.4, 148.4, 130.3, 130.1, 122.1, 113.7, 55.5, 51.4, 38.7, 36.0, 32.8, 30.9, 25.7, 21.6, 10.8 ppm.

HRMS (ESI): Calculated for $C_{19}H_{26}O_4Na$ $[M+Na]^+$: 341.1723, found: 341.1716.

Aldol Cyclization

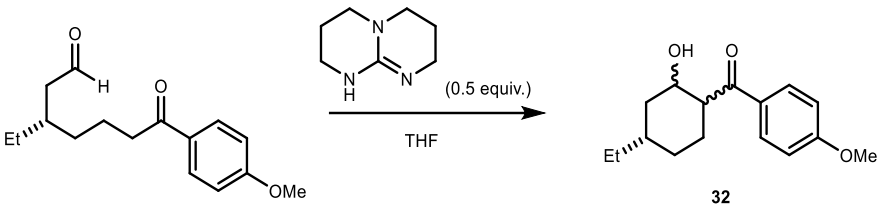

32

The procedure was adapted from previous report[56]. 1,5,7-triazabicyclo[4.4.0]dec-5-ene (TBD, 5.3 mg, 0.04 mmol, 0.5 equiv.) was dissolved in dry THF (0.1 mL) and was added to a stirred solution of **3a** (20 mg, 0.08 mmol, 1.0 equiv.) in dry THF (0.2 mL). The reaction mixture was stirred at room temperature for 1 hour and quenched with saturated NH_4Cl (aq). The aqueous layer was extracted with Et_2O, which was dried and concentrated. The crude product was purified by column chromatography (SiO_2, 10 to 20 % EtOAc in hexanes) to afford (*S*)- (4-ethyl-2-hydroxycyclohexyl)(4-methoxyphenyl)methanone (**32**, 85% combined, d.r.=5:1). The relative configurations were assigned based on X-ray crystallography and 2D-NMRs (See section 2.6.9-2.6.10 for details)

(1S,2S,4S)-4-ethyl-2-hydroxycyclohexyl)(4-methoxyphenyl)methanone (32_{major}).

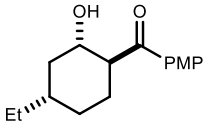

The product was obtained as a colorless oil (14.4 mg, 72%). The relative configuration was confirmed by 2D-NMRs (see section 2.6.10). The enantiomeric excess was determined by UPC^2 analysis on a Daiacel Chiralpak ID-3 column (gradient: 1 min 100% CO_2; 5 min 100% CO_2 to 60% CO_2 – 40% MeCN; 8 min 60% CO_2 – 40% MeCN; flow rate 2.0 mL/min; diode array: τ_{major} = 7.62 min, τ_{minor} = 6.27 min). $[\alpha]_D^{24}$ = -5.6 (c = 0.10, $CHCl_3$, 90% ee).

^{1}H NMR (500 MHz, $CDCl_3$): δ = 7.94 – 7.91 (m, 2H), 6.96 – 6.93 (m, 2H), 4.32 (br s, 1H), 4.26 (dd, *J* = 2.3, 1.2 Hz, 1H), 3.88 (s, 3H), 3.24 (ddd, *J* = 12.7, 3.5, 1.8 Hz, 1H), 2.02 (dtd, *J* = 13.8, 3.6, 1.9 Hz, 1H), 1.95 (dd, *J* = 13.0, 3.5 Hz, 1H), 1.93 – 1.86 (m, 1H), 1.76 (dt, *J* = 12.0, 3.5 Hz, 2H), 1.59 (s, 1H), 1.29 – 1.21 (m, 2H), 1.13 – 1.03 (m, 2H), 0.91 (t, *J* = 7.5 Hz, 3H) ppm. **^{13}C{^{1}H} NMR (126 MHz, $CDCl_3$):** δ = 204.8, 163.9, 130.8, 128.7, 114.0, 66.9, 55.6, 47.8, 38.5, 32.2, 32.0, 29.7, 24.8, 11.3 ppm.

HRMS (ESI): Calculated for $C_{16}H_{22}O_3Na$ $[M+Na]^+$: 285.1461, found: 285.1458.

(1R,2R,4S)-4-ethyl-2-hydroxycyclohexyl)(4-methoxyphenyl)methanone (32$_{minor}$).

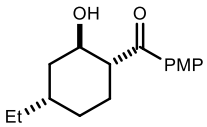

The product was obtained as a colorless oil (2.6 mg, 13%). The absolute configuration was confirmed by X-ray crystallography (see section 2.6.9). The enantiomeric excess was determined by UPC^2 analysis on a Daiacel Chiralpak IE-3 column (gradient: 1 min 100% CO_2; 5 min 100% CO_2 to 60% CO_2 – 40% *i*-PrOH; flow rate 2.0 mL/min; diode array: τ_{major} = 5.97 min, τ_{minor} = 6.05 min). $[\alpha]_D^{24}$= -19.7 (c = 0.10, $CHCl_3$, 91% ee).

^{1}H NMR (500 MHz, $CDCl_3$): δ = 7.97 – 7.93 (m, 2H), 6.96 – 6.93 (m, 2H), 4.26 (t, *J* = 9.8 Hz, 1H), 3.87 (s, 3H), 3.28 – 3.19 (m, 1H), 2.18 (d, *J* = 3.6 Hz, 1H), 1.99 (dt, *J* = 13.0, 3.9 Hz, 1H), 1.81 (tt, *J* = 11.6, 3.8 Hz, 2H), 1.64 – 1.57 (m, 3H), 1.46 – 1.31 (m, 3H), 0.91 (t, *J* = 7.4 Hz, 3H) ppm.**^{13}C{^{1}H} NMR (126 MHz, $CDCl_3$):** δ = 202.0, 163.6, 130.8, 129.5, 113.8, 66.8, 55.5, 53.3, 36.9, 35.2, 28.7, 25.2, 24.9, 12.3 ppm.

HRMS (ESI): Calculated for $C_{16}H_{22}O_3Na$ $[M+Na]^+$: 285.1461, found: 285.1462.

2.6.6 UV-Visible and Fluorescence Spectroscopies

Absorption Spectrum of Iminium ion I and Emission spectrum of light source

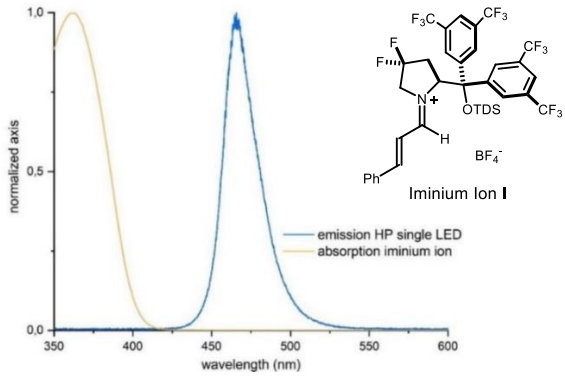

Figure 2.28. Normalized absorption of iminium ion **I** and emission of the blue HP LED used in this study.

The emission spectra were recorded in a Fluorolog Horiba Jobin Yvon spectrofluorimeter equipped with a photomultiplier detector, a double monochromator, and a 450W xenon light source. The tail of absorption of the iminium ion **I** obtained by condensation of cinnamaldehyde with **C** is around 420 nm while the HP single LED used in this study has an emission centered at 465 nm. By plotting these absorption and emission spectra together (Figure 2.28), we observed a slight overlap which may explain the excited iminium ion-based reactivity with aromatic enals.

Absorption and Emission Spectra of Acridinium Photocatalyst PC-a

2.5 mL of HPLC grade MeCN, thoroughly degassed by freeze-pump-thaw, were placed in a 10 x 10 mm light path quartz fluorescence cuvette equipped with Silicone/PTFE 3.2 mm septum under an argon atmosphere. Then, 10 µL of a 1 mM solution of photocatalyst **PC-a** in MeCN was added to give a final concentration of 4 µM. To measure the emission spectrum, the excitation wavelength was fixed at 444 nm (incident light slit regulated to 3 nm)

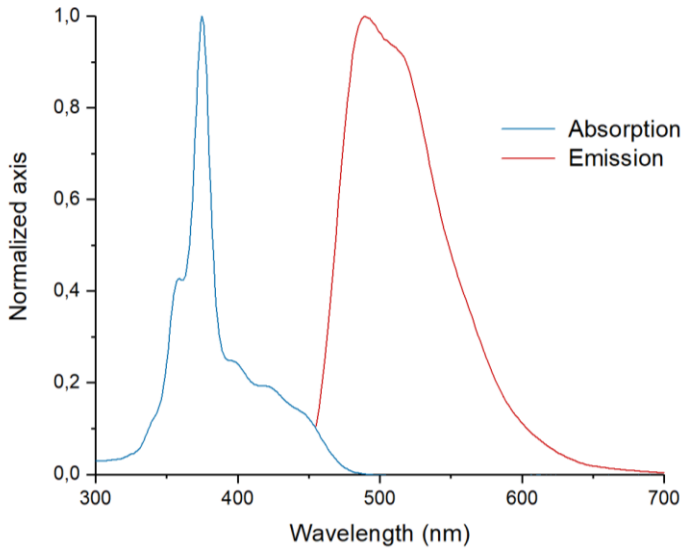

Figure 2.29. Absorption and emission spectra of photocatalyst **PC-a**

Stern-Volmer quenching studies with Cyclobutanol 4a

A 1.0 M solution of Cyclobutanol **4a** in MeCN was prepared, and 20 µL of this stock solution were added to the solution of photocatalyst **PC-a**, prepared as described above. The addition of **4a** solution was repeated for five consecutive times. After each addition, the solution was mixed by sparging with argon for 20 s. An absorption spectrum and an emission spectrum of the solution were then recorded. The excitation wavelength was fixed at 444 nm (incident light slit regulated to 3 nm); the emission light was acquired from 455 nm to 700 nm (emission light slit regulated to 3 nm). A solvent blank was subtracted from all the measurements. The excitation wavelength was chosen in order to avoid saturation of the emission detector. The results shown in Figure 2.30 indicate that **4a** quenches the excited state of **PC-a** and its emission. No change in the absorption spectra of the solution was observed during the addition of **4a** (Figure 2.31).

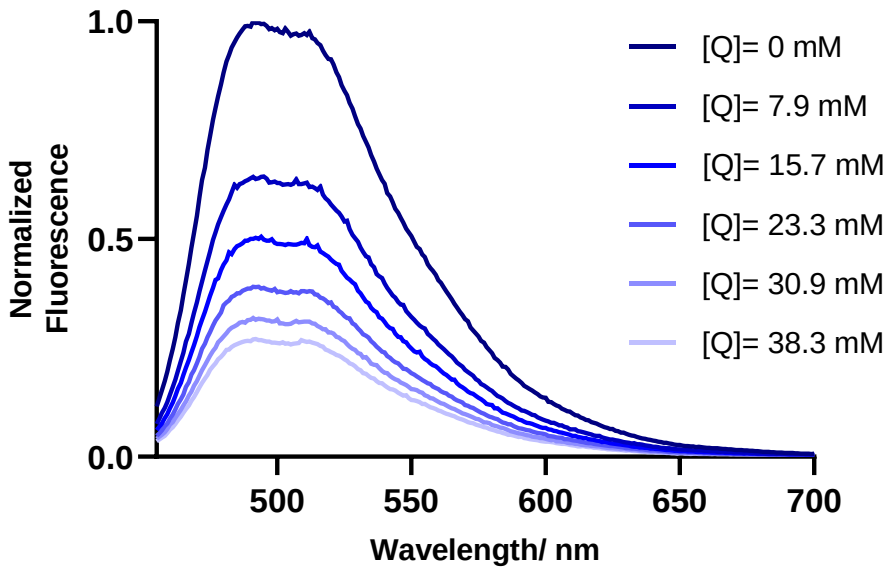

Figure 2.30. Emission spectra of the photocatalyst **PC-a** emission (4 µM in MeCN) in the presence of increasing amounts of cyclobutanol **4a** [Q].

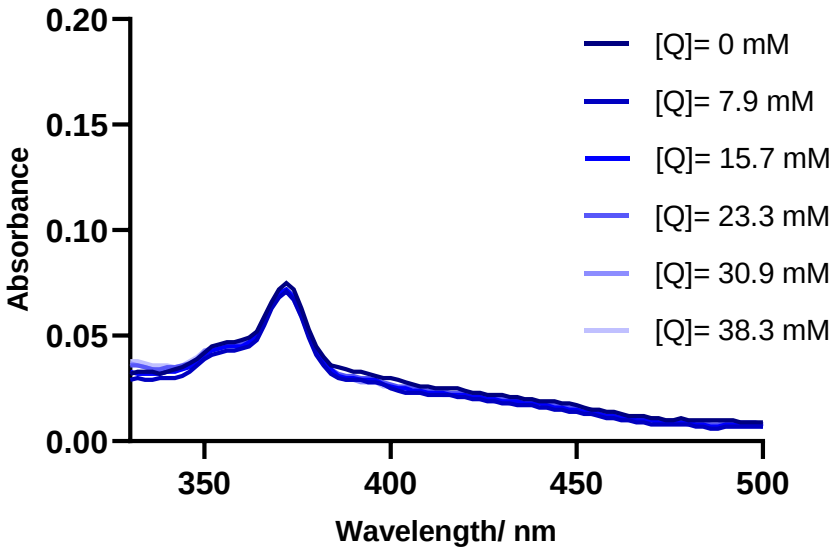

Figure 2.31. UV-vis absorption spectra of the photocatalyst **PC-a** (4 μM in MeCN) in the presence of increasing amounts of cyclobutanol **4a** [Q].

The Stern-Volmer plot (Figure 2.32), derived from the normalized emission intensity at 491 nm, shows a linear correlation between the amounts of **4a** and the ratio I^0/I. On the basis of the following Equation 1, we calculated the Stern-Volmer constant K_{SV} [68] as **70.3 M^{-1}**.

$$\frac{I^0}{I} = 1 + K_{SV}[Q] \cdots\cdots\cdots\cdots\cdots\cdots\cdots \boldsymbol{Eq.1}$$

[68] J. R. Lakowicz, Ed. *Principles of Fluorescence Spectroscopy*, Plenum Press, **1983**, 52.

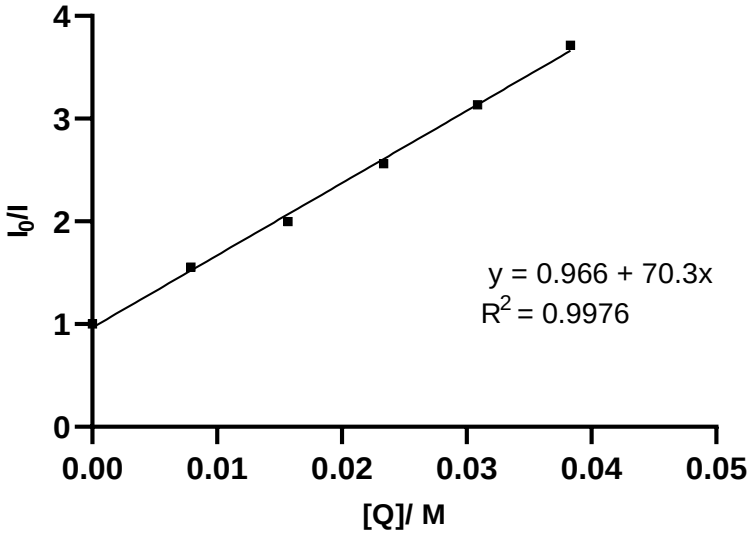

Figure 2.32. Stern-Volmer quenching plot using **4a** as a quencher.

2.6.7 Quantum Yield Determination

A ferrioxalate actinometer solution was prepared by following the Hammond variation of the Hatchard and Parker procedure[69] outlined in the *Handbook of Photochemistry*.[70] Ferrioxalate actinometer solution measures the decomposition of Fe(III) to Fe(II) ions, which are complexed by 1,10-phenanthroline and monitored by UV/Vis absorbance at 510 nm. The number of moles of Fe(II)-phenanthroline complex formed are directly proportional to moles of photons absorbed. The values of the quantum yield of potassium ferrioxalate are related to concentration and wavelength.

[69] Hatchard, C. G., Parker, C. A. "A new sensitive chemical actinometer II. Potassium ferrioxalate as a standard chemical actinometer." *Proc. R. Soc. (London)*, **1956**, *235*, 518.

[70] Montalti, M., Credi, A., Prodi, L., Gandolfi, M.T. *Handbook of photochemistry*, Taylor & Francis, **2006**, 601.

The solutions were prepared and stored in the dark (red light):

0.012M Potassium ferrioxalate solution: 147.4 mg of potassium ferrioxalate (commercially available from Alfa Aesar) and 69.5 μL of sulfuric acid (96%) were added to a 25 mL volumetric flask, and filled to the mark with HPLC grade water.

Phenanthroline solution: 100 mg of 1,10-phenanthroline in a 50 mL volumetric flask, filled to the mark with HPLC grade water (0.2% by weight).

Buffer solution: to a 100 mL volumetric flask 4.94 g of NaOAc and 1.0 mL of sulfuric acid (96%) were added and filled to the mark with HPLC grade water.

Internal standard solution: 1.261 g of 1,3,5-trimethoxybenzene was added to a 5 mL volumetric flask which was filled up with HPLC grade acetonitrile (1.50 M).

Reaction setup:

Reaction solution: A Schlenk flask was charged with amine catalyst **C** (14.1 mg, 0.02 mmol), cyclobutanol **4a** (17.8 mg, 0.1 mmol), photocatalyst **PC-a** (1.4 mg, 2.5 μmol), acetonitrile (0.2 mL). After four cycles of freeze-pump-thaw (with septum), trifluoroacetic acid (7.7 μL, 0.1 mmol) and *(E)*-pent-2-enal **1a** (29.3 μL, 0.30 mmol) were added and the tube was sealed with parafilm and put in the HP-LED 460 nm at 1 cm distance at -10 ºC with irradiance of 22 mW/cm^2. Three different reactions were set up and irradiated for different times: 15 min, 30 min and 45 min. After each reaction was finished, internal standard solution (66 μL, 0.1 mmol) was added. This solution was diluted with 3 mL of acetone, from the solution was taken 1 mL to be analyzed by GC-FID.

Actinometer solutions: A Schlenk flask of the same dimensions as used for the reaction mixtures was loaded with 0.2 mL of actinometer solution and placed on the HP-LED the same light intensity as the reaction (without freeze-pump-thaw). Three different actinometer solutions were irradiated in sequence for 20 s, 40 s and 80 s. To irradiate the Schlenk tube, it was placed on the holder with the light off and the light was turned on for the desired time. After each irradiation the actinometer solutions were carefully transferred into a 10 mL volumetric flask, then 0.5 mL of phenanthroline solution and 2.0 mL of buffer solution were

added and the flask was filled up with water. The mixture was then analyzed by UV-Vis spectroscopy (Figure 2.33).

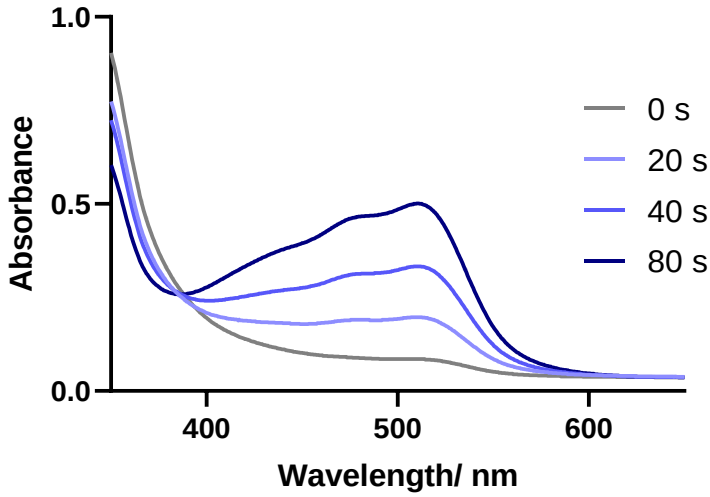

Figure 2.33. UV-Vis recorded spectra of the actinometer solutions irradiated for different periods of times.

The moles of Fe(II) formed for each sample are determined using Beers' Law (Eq. 2):

$$Moles\ of\ Fe(II) = \frac{V_1 V_3 \cdot \Delta A\ (510\ \text{nm})}{10^3 V_2 l \cdot \varepsilon(510\ nm)} \cdots\cdots\cdots\cdots\cdots\cdots\cdots \boldsymbol{Eq.2}$$

where V_1 is the irradiated volume (0.2 mL), V_2 is the aliquot of the irradiated solution taken for the quantification of the Fe(II) complex (0.2 mL), V_3 is the final volume after complexation with phenanthroline (10 mL), l is the optical path-length of the irradiation cell (1 cm), Δ A(510 nm) is the optical difference in absorbance between the irradiated solution and the one stored in the dark, $\varepsilon_{510\ nm}$ is the extinction coefficient the complex $[Fe(phen)_3]^{2+}$ at 510 nm (11100 L mol^{-1} cm^1).[12]

The moles of Fe(II) formed (x) are plotted as a function of time (t) (Figure 2.34). The slope of this line was correlated to the moles of incident photons by unit of time ($q^0_{n,p}$) by the use of the following Equation 3:

$$\Phi(\lambda) = \frac{dx/dt}{q^0_{n,p}[1 - 10^{-A(\lambda)}]} \quad \ldots\ldots\ldots\ldots\ldots\ldots \boldsymbol{Eq.3}$$

where the quantum yield (Φ) for formation of Fe(II) at 458 nm is 1.11[71], dx/dt is the rate of change of a measurable quantity (spectral or any other property), $[1\text{-}10^{-A(\lambda)}]$ is the ratio of absorbed photons by the solution, and A(λ) is the absorbance of the actinometer at the wavelength used to carry out the experiments (460 nm). The absorbance at 460 nm (A(460)) was 0.18.

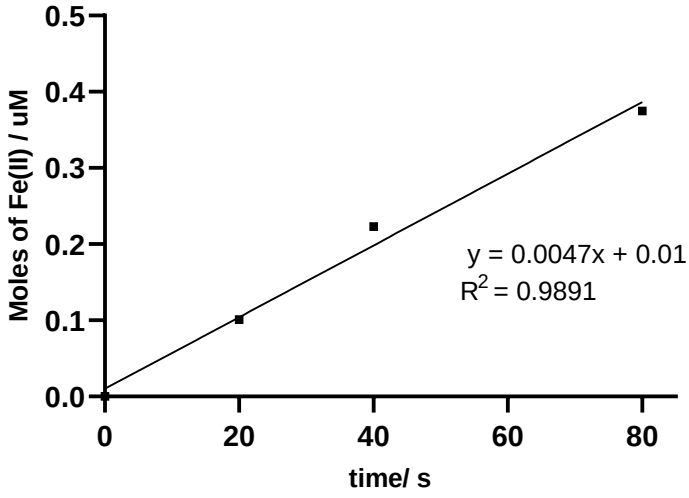

Figure 2.34. Plot of the moles of Fe(II) generated from the irradiation of the actinometer solutions, against time.

The photon flux, which is $q^0_{n,p}$, was determined to **1.19×10^{-8} einstein s^{-1}**.

The moles of product per unit of time are plotted against the number of photons absorbed (Figure 2.35). The photons absorbed are correlated to the number of incident photons by the

[71] Holubov, C. A.; Langford, C. H. "Wavelength and Temperature Dependence in the Photolysis of the Chemical Actinometer, Potassium trisoxalatoferrate(III), at Longer Wavelengths." *Inorganica Chim. Acta* **1981**, *53*, 59.

use of Equation 4. According to this, if we plot the moles of product (y-axis) versus the moles of incident photons ($q^0_{n,p}dt$, x-axis), the slope is equal to:

$$\text{slope} = \Phi[1 - 10^{-A(460\ nm)}] \ldots\ldots\ldots\ldots\ldots\ldots\ldots \boldsymbol{Eq.4}$$

where Φ is the quantum yield to be determined and $A_{460\ nm}$ is the absorption of the reaction under study. $A_{460\ nm}$ was measured to be of 0.68 for the model reaction mixture after 50-fold dilution.

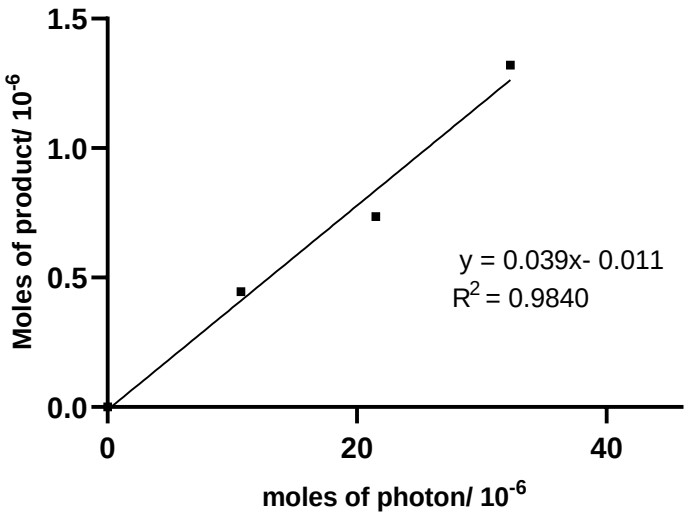

Figure 2.35. Plot of the moles of products generated from the irradiation of the reaction solutions, against the moles of photons absorbed by each reaction solution.

The quantum yield of the conjugate radical addition of cyclobutanol **4a** to (*E*)-pent-2-enal was calculated to be **0.04**.

2.6.8 Cyclic Voltammetry

Cyclic voltammetry (CV) measurements were carried out on a Princeton Applied Research PARSTAT 2273 instrument with a glassy carbon disk electrode (diameter: 3 mm) as working electrode. A silver wire coated with AgCl immersed in a saturated aqueous solution

of KCl and separated from the analyte by a fritted glass disk was employed as the reference electrode and a Pt wire auxiliary electrode completed the electrochemical setup. The scan rate was 100 mV/s. The substrates were measured at concentration of 5.0 mM in acetonitrile with 0.1M NBu_4PF_6 as electrolyte. Potentials are quoted with E_p^A (E_{Ox}) refers to the anodic peak potential.

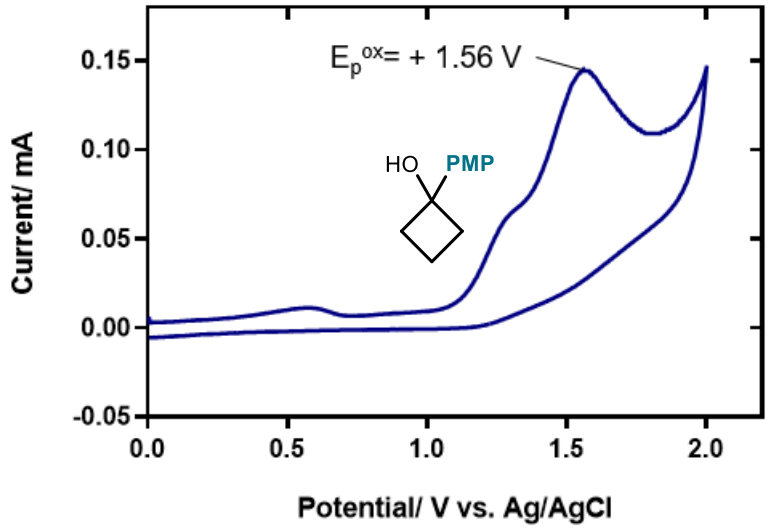

Figure 2.36. Cyclic voltammogram of **[4a]** in MeCN. Irreversible oxidation. $E_p^A = E_p^{ox}$ (**4a**$^{\bullet+}$/**4a**) = +1.56 V.

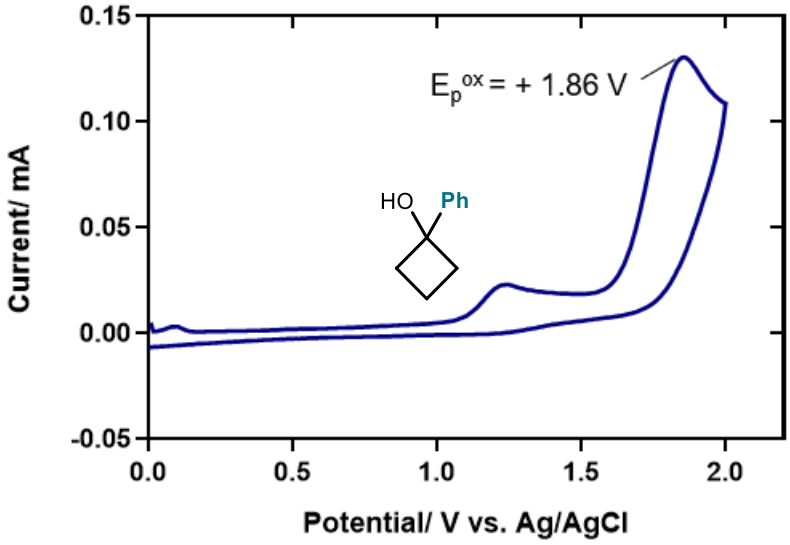

Figure 2.37. Cyclic voltammogram of **[4b]** in MeCN. Irreversible oxidation. $E_p^A = E_p^{ox}$ (**4b**$^{\bullet+}$/**4b**) = +1.86 V.

The conversion of the redox potential from Ag/AgCl to Saturated Calomel Electrode (SCE) was done according to the literature by measuring the redox potential of ferrocene as reference in MeCN.[72]

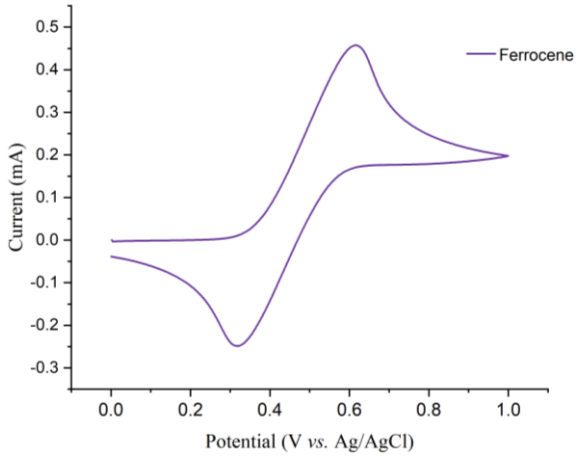

Figure 2.38. CV of ferrocene in CH_3CN, reversible reduction and oxidation $E_{1/2}$ = +0.46 V.

With the reference CV, the redox potential *vs.* SCE in MeCN was calculated using the following equations:

$$E_p^{ox}$$ (**4a**$^{\bullet+}$/**4a**, Ag/AgCl to Fc/Fc$^+$) = 1.56 - 0.46 = +1.10 V *vs.* Fc$^+$/Fc

$$E_p^{ox}$$ (**4a**$^{\bullet+}$/**4a**, Fc/Fc$^+$ to SCE) = 1.10+ 0.38= +1.48 V *vs.* SCE

Similarly,

$$E_p^{ox}$$ (**4b**$^{\bullet+}$/**4b**, Ag/AgCl to Fc/Fc$^+$) = 1.86 - 0.46 = +1.40 V *vs.* Fc$^+$/Fc

$$E_p^{ox}$$ (**4b**$^{\bullet+}$/**4b**, Fc/Fc$^+$ to SCE) = 1.40+ 0.38= +1.78 V *vs.* SCE

[72] Pavlishchuk, V. V.; Addison, A. W. "Conversion constants for redox potentials measured versus different reference electrodes in acetonitrile solutions at 25°C." *Inorganica Chim. Acta.* **2000**, *298*, 97.

2.6.9 X-ray Crystallographic Data of 32_{minor}

Crystals of the compound **32_{minor}** were obtained by slow evaporation of its solution in nitromethane.

Full sphere single crystal data collection of **32_{minor}** where performed at 100 K on a Bruker Kappa Apex II DUO diffractometer equipped with a Cryostream 700 plus low temperature device, a microsource anode with Mo Kα (λ= 0.71073 Å)

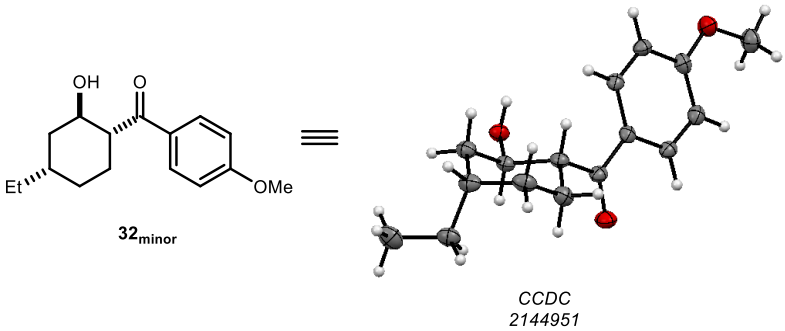

Figure 2.39. Structure of **32_{minor}**. Thermal ellipsoids represent 50% probability surfaces.

Table 2.3. Crystal data and structure refinement for *CCDC 2144951*.

Empirical formula	C16H22O3
Formula weight	262.33
Temperature	100(2)K
Wavelength	1.54178 Å
Crystal system	orthorhombic
Space group	P 21 21 21
Unit cell dimensions	a = 5.3830(2)Å a= 90°.
	b = 11.3439(5)Å b = 90°.
	c = 23.0341(9)Å g = 90°.

Volume 1406.56(10) $Å^3$

Z 4

Density (calculated) 1.239 Mg/m^3

Absorption coefficient 0.673 mm^{-1}

F(000) 568

Crystal size 0.080 x 0.050 x 0.020 mm^3

Theta range for data collection 3.838 to 63.053°.

Index ranges -4<=h<=6,-13<=k<=10,-26<=l<=24

Reflections collected 6086

Independent reflections 2188[R(int) = 0.0215]

Completeness to theta =63.053° 98.7%

Absorption correction Multi-scan

Max. and min. transmission 0.75 and 0.64

Refinement method Full-matrix least-squares on F^2

Data / restraints / parameters 2188/ 0/ 174

Goodness-of-fit on F^2 1.019

Final R indices [I>2sigma(I)] R1 = 0.0289, wR2 = 0.0744

Flack parameter x =0.03(10)

Largest diff. peak and hole 0.133 and -0.168 $e.Å^{-3}$

Table 2.4. Bond lengths [Å] and angles [°] for *CCDC 2144951*.

Bond lengths----

O2 C3 1.428(2)

O2	H2O	0.8499
O3	C13	1.364(3)
O3	C16	1.434(3)
O1	C1	1.228(3)
C1	C10	1.483(3)
C1	C2	1.518(3)
C5	C6	1.531(3)
C5	C8	1.533(3)
C5	C4	1.537(3)
C5	H5	1.0000
C6	C7	1.516(3)
C6	H6A	0.9900
C6	H6B	0.9900
C7	C2	1.535(3)
C7	H7A	0.9900
C7	H7B	0.9900
C8	C9	1.529(4)
C8	H8A	0.9900
C8	H8B	0.9900
C9	H9A	0.9800
C9	H9B	0.9800
C9	H9C	0.9800
C10	C11	1.393(3)
C10	C15	1.405(3)

C11 C12 1.380(3)

C11 H11 0.9500

C12 C13 1.390(3)

C12 H12 0.9500

C13 C14 1.391(3)

C14 C15 1.375(3)

C14 H14 0.9500

C15 H15 0.9500

C16 H16A 0.9800

C16 H16B 0.9800

C16 H16C 0.9800

C2 C3 1.537(3)

C2 H2 1.0000

C3 C4 1.518(3)

C3 H3 1.0000

C4 H4A 0.9900

C4 H4B 0.9900

Angles----------

C3 O2 H2O 111.6

C13 O3 C16 117.71(17)

O1 C1 C10 119.81(19)

O1 C1 C2 118.58(19)

C10 C1 C2 121.62(17)

C6 C5 C8 113.5(2)

C6 C5 C4 109.22(19)

C8 C5 C4 111.68(19)

C6 C5 H5 107.4

C8 C5 H5 107.4

C4 C5 H5 107.4

C7 C6 C5 113.16(19)

C7 C6 H6A 108.9

C5 C6 H6A 108.9

C7 C6 H6B 108.9

C5 C6 H6B 108.9

H6A C6 H6B 107.8

C6 C7 C2 111.49(19)

C6 C7 H7A 109.3

C2 C7 H7A 109.3

C6 C7 H7B 109.3

C2 C7 H7B 109.3

H7A C7 H7B 108.0

C9 C8 C5 112.1(2)

C9 C8 H8A 109.2

C5 C8 H8A 109.2

C9 C8 H8B 109.2

C5 C8 H8B 109.2

H8A C8 H8B 107.9

C8 C9 H9A 109.5

C8 C9 H9B 109.5

H9A C9 H9B 109.5

C8 C9 H9C 109.5

H9A C9 H9C 109.5

H9B C9 H9C 109.5

C11 C10 C15 117.8(2)

C11 C10 C1 118.72(18)

C15 C10 C1 123.50(19)

C12 C11 C10 122.3(2)

C12 C11 H11 118.9

C10 C11 H11 118.9

C11 C12 C13 119.1(2)

C11 C12 H12 120.5

C13 C12 H12 120.5

O3 C13 C14 115.87(19)

O3 C13 C12 124.53(19)

C14 C13 C12 119.60(19)

C15 C14 C13 120.94(19)

C15 C14 H14 119.5

C13 C14 H14 119.5

C14 C15 C10 120.3(2)

C14 C15 H15 119.8

C10 C15 H15 119.8

O3 C16 H16A 109.5

O3 C16 H16B 109.5

H16A C16 H16B 109.5

O3 C16 H16C 109.5

H16A C16 H16C 109.5

H16B C16 H16C 109.5

C1 C2 C7 110.99(18)

C1 C2 C3 110.60(17)

C7 C2 C3 108.13(17)

C1 C2 H2 109.0

C7 C2 H2 109.0

C3 C2 H2 109.0

O2 C3 C4 110.80(17)

O2 C3 C2 111.86(16)

C4 C3 C2 110.85(17)

O2 C3 H3 107.7

C4 C3 H3 107.7

C2 C3 H3 107.7

C3 C4 C5 113.36(19)

C3 C4 H4A 108.9

C5 C4 H4A 108.9

C3 C4 H4B 108.9

C5 C4 H4B 108.9

H4A C4 H4B 107.7

Table 2.5. Torsion angles [°] for *CCDC 2144951*.

C8	C5	C6	C7	73.5(2)
C4	C5	C6	C7	-51.9(2)
C5	C6	C7	C2	57.0(2)
C6	C5	C8	C9	160.88(19)
C4	C5	C8	C9	-75.1(2)
O1	C1	C10	C11	-10.1(3)
C2	C1	C10	C11	169.83(19)
O1	C1	C10	C15	167.9(2)
C2	C1	C10	C15	-12.1(3)
C15	C10	C11	C12	0.1(3)
C1	C10	C11	C12	178.30(19)
C10	C11	C12	C13	-1.4(3)
C16	O3	C13	C14	177.97(19)
C16	O3	C13	C12	-1.3(3)
C11	C12	C13	O3	-179.62(19)
C11	C12	C13	C14	1.2(3)
O3	C13	C14	C15	-178.99(19)
C12	C13	C14	C15	0.3(3)
C13	C14	C15	C10	-1.6(3)
C11	C10	C15	C14	1.3(3)
C1	C10	C15	C14	-176.72(19)

O1 C1 C2 C7 41.1(3)

C10 C1 C2 C7 -138.9(2)

O1 C1 C2 C3 -79.0(2)

C10 C1 C2 C3 101.1(2)

C6 C7 C2 C1 -179.79(18)

C6 C7 C2 C3 -58.3(2)

C1 C2 C3 O2 -55.8(2)

C7 C2 C3 O2 -177.52(16)

C1 C2 C3 C4 180.00(16)

C7 C2 C3 C4 58.3(2)

O2 C3 C4 C5 177.84(18)

C2 C3 C4 C5 -57.4(2)

C6 C5 C4 C3 52.4(2)

C8 C5 C4 C3 -74.0(3)

Symmetry operations

---

1 'x, y, z'

2 '-x+1/2, -y, z+1/2'

3 '-x, y+1/2, -z+1/2'

3 'x+1/2, -y+1/2, -z'

2.6.10 Determination of the Stereochemistry of 32_{major}

2D NMR experiments allowed us to determine the relative stereochemistry of the aldol product **32**$_{major}$. Inversion of both C1 and C2 stereocenters is responsible for the formation of these two stereoisomers.

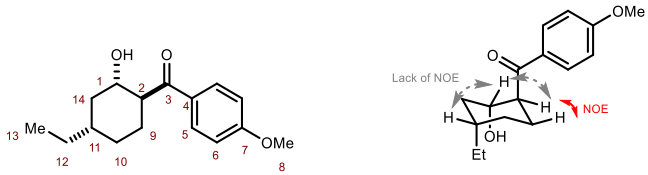

Figure 2.40. Atom numbering (*left*) and NOE correlations (*right*) within product 32_{major}.

Table 2.6. ^{1}H, $^{13}C\{^{1}H\}$ chemical shift and COSY correlations in **32**$_{major}$

Atom	^{1}H δ (ppm)	COSY Correlation	^{13}C δ (ppm)
1	4.26	2, 14	66.9
2	4.32	1, 9 (equatorial), 14	47.8
3	-	-	204.8
4	-	-	163.9
5	7.94 – 7.91	6	130.8
6	6.96 – 6.93	5	128.7
7	-	-	114.0
8	3.88	-	55.6
9	3.24 (equatorial) 2.02 (axial)	9 (axial), 10 (both) 1, 9 (equatorial), 10 (axial),11	32.2
10	1.76 (equatorial) 1.95 (axial)	9 (both), 10 (axial), 11, 12 9 (equatorial), 10 (equatorial), 11	32.0
11	1.13–1.03	9, 10 (both),12	29.7
12	1.29 – 1.21	10, 13	24.8
13	0.91	12	11.3
14	1.93 – 1.86	11	38.5

^{1}H-^{1}H COSY of **32$_{major}$** (500 MHz, $CDCl_3$)

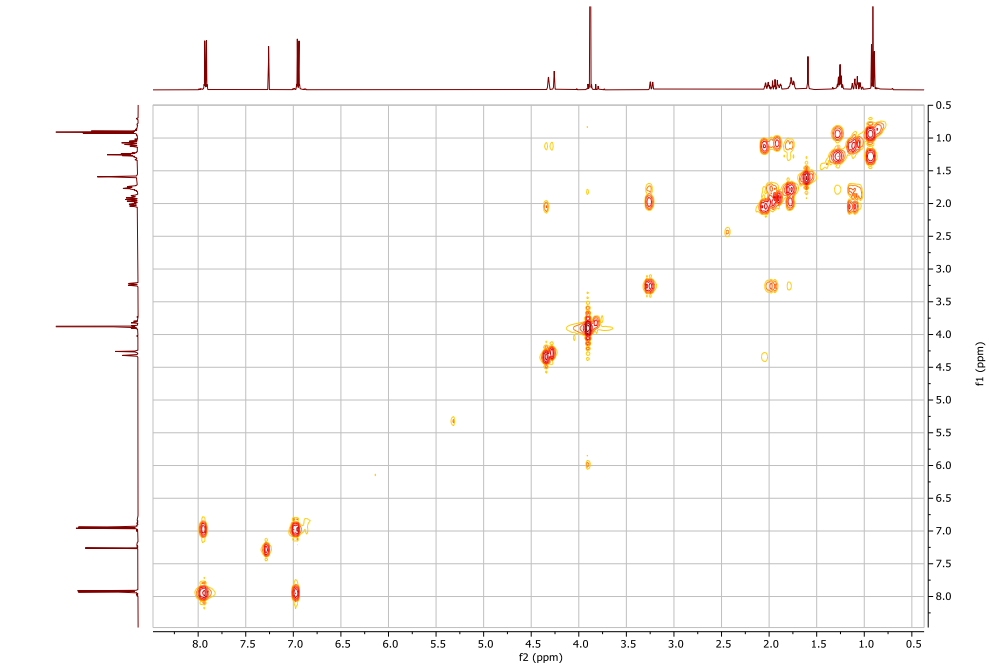

^{1}H-^{1}H NOESY of **32$_{major}$** (500 MHz, $CDCl_3$)

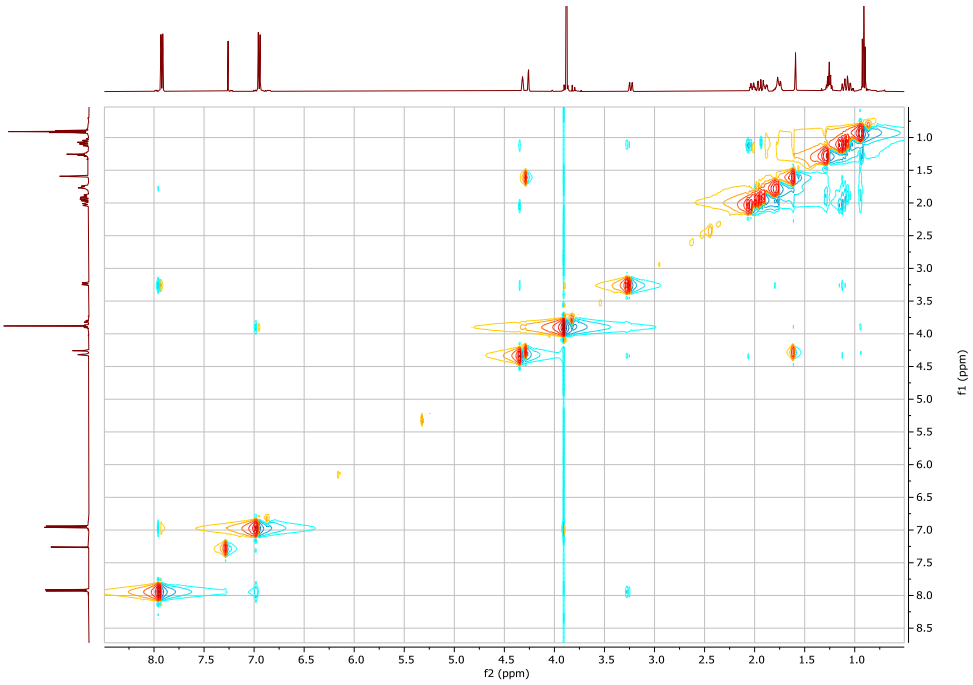

Chapter III

Radical *Umpolung* Strategy for the Stereoselective β-Functionalization of Enals

Target

To develop a radical *umpolung* platform for the asymmetric coupling of two electrophiles, allowing the regio- and enantio-selective synthesis of 1,6-dicarbonyl compound and β-cyanoaldehyde.

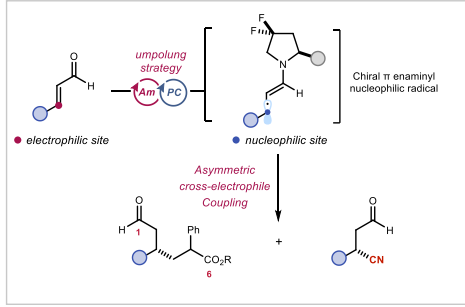

Tool

Cooperative use of a chiral secondary amine catalyst, for the electrophilic iminium ion activation of enals, and a photoredox catalyst, which promotes the reduction of iminium ion to generate a nucleophilic chiral radical.[1]

[1] The project discussed in this chapter has been conducted in collaboration with Dr. Martin Berger, Dr. Dengke Ma, and Dr. Yann Baumgartner. I was involved in the investigation of the scope of the Giese reaction, and contributed to mechanistic investigations.

This study has been published: Berger, M.; Ma, D.; Baumgartner, Y.; Wong, T.H.-F.; Melchiorre, P. "Stereoselective conjugate cyanation of enals by combining photoredox and organocatalysis." *Nat. Catal.* **2023**, 6, 332.

3.1 Introduction

Understanding the polarity of functional groups is the foundation stone of modern organic chemistry. [2] The collected insight empowers chemists to explain properties and transformations of molecules and guide synthetic logic for methodology development and molecular assemble. As a versatile strategy, organocatalysis is known to modulate polarity of α,β-unsaturated carbonyl compounds, enabling a diverse array of chemical transformations:

In the polar domain, aminocatalysts condense with enals and enones, forming charged iminium ions **I**. This causes the intrinsically electrophilic β-position to be further polarized, enabling more facile addition of nucleophiles. (Figure 3.1a) Another important approach involves catalysts that can invert the native polarity of functional groups, known as *umpolung* reactivity.[3] For instance, *N*-heterocyclic carbene (NHC) catalysts[4] can condense with enals to form a Breslow intermediate of type **II** that is nucleophilic at the carbonyl carbon and the β-position (Figure 3.1b).[5] Since this approach switches the natural polarity of the substrate, it can offer valuable synthetic opportunities that is otherwise unusual, if not impossible.

Analogous trends are emerging in the radical domain: unsaturated carbonyls compounds can serve as *acceptors of nucleophilic radicals*. Aminocatalysts form electronically activated iminium ion adducts with enals and enones, enhancing the rate of polarity-matched[6] addition of nucleophilic radicals (Figure 3.2a).

---

[2] (a) Kermack, W. O. and Robinson, R. "LI.—An explanation of the property of induced polarity of atoms and an interpretation of the theory of partial valencies on an electronic basis." *J. Chem. Soc. Trans.* **1922,** *121*, 427; (b) Corey, E. J.; Cheng, X. -M. *The Logic of Chemical Synthesis.* Wiley, **1995**. (c) Clayden, J.; Greeves, N.; Warren, S.; Wothers, P. *Organic Chemistry.* 1st ed.; Oxford University Press., **2001**; pp 123-133.

[3] Seebach, D. "Methods of reactivity umpolung." *Angew. Chem., Int. Ed.* **1979**, *18*, 239.

[4] (a) Hopkinson, M.; Richter, C.; Schedler, M. and Glorius, F. "An overview of N-heterocyclic carbenes." *Nature* **2014**, *510*, 485; (b) Flanigan, D. M.; Romanov-Michailidis, F.; White, N. A. and Rovis, T. "Organocatalytic Reactions Enabled by N-Heterocyclic Carbenes." *Chem. Rev.* **2015**, *115*, 17, 9307.

[5] Breslow, R. "On the Mechanism of Thiamine Action. IV.1 Evidence from Studies on Model Systems." *J. Am. Chem. Soc.* **1958**, *80*, 3719.

[6] Parsaee, F.; Senarathna, M. C.; Kannangara, P. B.; Alexander, S. N.; Arche, P. D. E.; Welin, E. R. "Radical philicity and its role in selective organic transformations." *Nat. Rev. Chem.* **2021**, *5*,486.

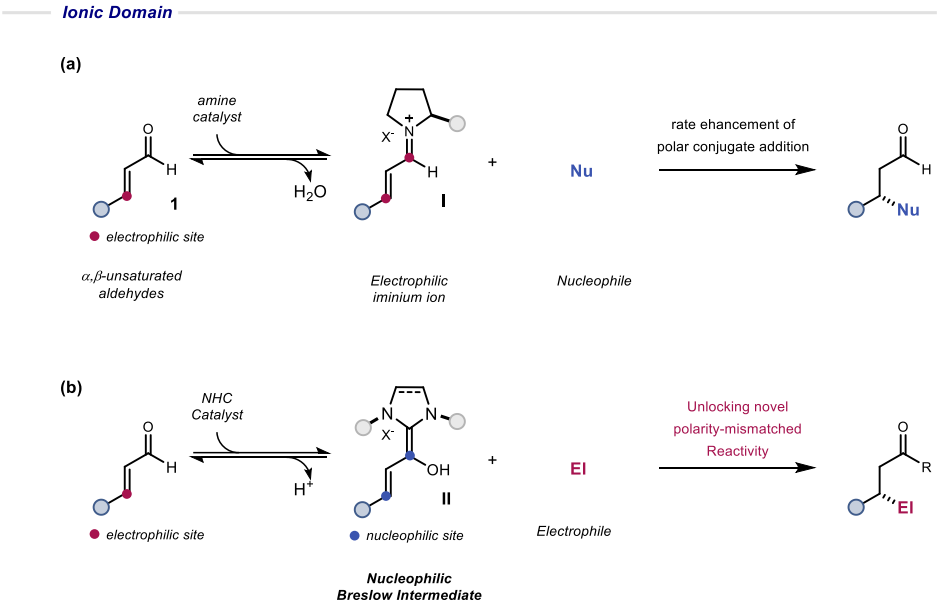

Figure 3.1. β-Functionalization of unsaturated carbonyl compounds through innate and inverted polarity (*umpolung*). Established polar chemistry through **(a)** electrophilic activation with innate polarity, which enhances rate of nucleophile attack; **(b)** N-heterocyclic carbene (NHC) catalyst inverts the polarity to enable coupling with an electrophile.

The main target of this research endeavor was to expand novel radical chemistry of iminium ion intermediates with orthogonal logic (Figure 3.2b). Specifically, we envisaged that these electrophilic intermediates **I**, formed between amine catalysts and enals, could be readily reduced via single electron transfer (SET) mediated by a visible light activated photoredox catalyst. This is because the iminium ion has increased tendency to undergo SET reduction when compared to the parent enal. This SET reduction would lead to the 5π-electron radical **III**, which is nucleophilic in nature, therefore leading to an inversion of the native polarity of the iminium ion. Radical **III** might in principle react with electrophilic traps, allowing a formal cross-electrophile coupling. This mode of reaction would fundamentally switch the role of unsaturated carbonyls compounds, which would behave as *radical precursors*.

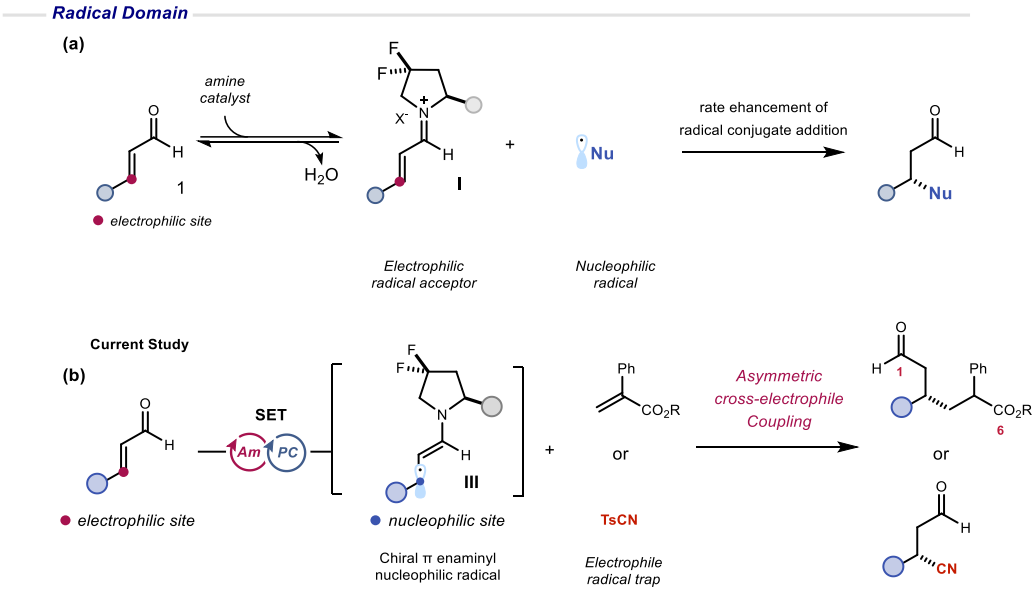

Figure 3.2. Radical chemistry by formation of iminium ion intermediate, that **(a)** serves as electrophilic radical acceptors; **(b)** undergo single electron transfer (SET) reduction to form a nucleophilic radical, which react with electrophilic radical traps.

This chapter describes the conception and realization of this radical *umpolung* strategy for chiral iminium ions (Figure 3.2b). In addition to devising tactics to achieve this polarity inverted reactivity, efforts were also dedicated to the precise control over these chemical transformations[7], specifically distinguished manipulation of functional groups within a substrate[7a] (chemoselectivity), differentiation of positions of similar polarity (regioselectivity), and, ultimately, the discerning bond formation at pro-chiral faces[7b] (enantioselectivity).

In the following sections, landmark works for exploring the chemistry of 5π-electron radical intermediate, generated from electrophilic adducts not only from iminium ions **I**, are discussed, with specific attention paid to their potential application in enantioselective transformations.

---

[7] (a) Shenvi, R. A.; O'Malley, D. P. and Baran, P. S. "Chemoselectivity: the mother of invention in total synthesis." *Acc. Chem. Res.* **2009**, *42*, 530; (b) Seebach, D. "Organic synthesis—where now?" *Angew. Chem., Int. Ed.* **1990**, *29*, 1320.

3.2 Background

3.2.1 Organocatalytic Strategy to Generate 5π-electron Intermediates

In 2013, the MacMillan group disclosed a redox-neutral coupling between saturated ketones **2** or aldehydes **6** with cyanoarenes **3** (Figure 3.3a),[8] made possible by combining photoredox catalysis and enamine catalysis. In their proposed mechanism, it was suggested that $Ir(ppy)_3$ photocatalyst, upon visible light excitation, enabled the SET reduction of electron-deficient arenes **3** (i.e. 1,4-dicyanobenzene and 4-cyanopyridine), providing a long-lived radical anion **IV**. Meanwhile ketone **2**, activated via in situ formation of enamine **V**, was readily oxidized by $PC^{\bullet+}$ to afford the amine 3π-electron radical intermediate **VI**. The latter intermediate had a substantially increased acidity of the β-C−H bond. Upon deprotonation, the 5π-electron β-enaminyl radical **VII** was generated, which then participated in a radical coupling with the persistent radical **IV**. Extrusion of cyanide then regenerated aromaticity, yielding product **4**. The overall process was the formal C-H functionalization of otherwise unreactive β-position of saturated ketones with exclusive site-selectivity. As a stand-alone example, using cinchona alkaloid **5** as the chiral amine catalyst yielded the chiral product with moderate level of enantioenrichment. Further efforts to improve the enantioinduction were complicated by the fact that the stereocenter is not configurationally stable under the applied photoredox conditions.[9] Follow-up work demonstrated that radical coupling of **VII** could also occur with ketyl radicals and α-amino radicals.[10]

As the unpaired electron is in conjugation with π electrons of electron rich enamine, the 5π-electron radical generated from aldehydes (**III**) or ketones (**VII)** was predicted to be nucleophilic in nature. Subsequent study has extended this reactivity to the interception of an electron-deficient olefin **7** through radical conjugate addition, or Giese reaction, providing

---

[8] Pirnot, M. T.; Rankic, D. A.; Martin, D. B. C; MacMillan, D. W. C. "Photoredox activation for the direct β-arylation of ketones and aldehydes" *Science* **2013**, *339*, 6127, 1593.

[9] DeHovitz, J. S.; Loh, Y. Y.; Kautzky, J. A.; Nagao, K.; Meichan, A. J.; Yamauchi, M.; MacMillan, D. W. C.; Hyster, T. K. "Static to inducibly dynamic stereocontrol: The convergent use of racemic β-substituted ketones" *Science* **2020**, *369*, 6507, 1113.

[10] (a) Petronijević, F. R.; Nappi, M.; MacMillan, D. W. C."Direct β-functionalization of cyclic ketones with aryl ketones via the merger of photoredox and organocatalysis." J. Am. Chem. Soc. **2013**, *135*, 18323; (b) Jeffreym J. L.; Petronijević, F. R.; MacMillan, D. W. C. "Selective Radical–Radical Cross-Couplings: Design of a Formal β-Mannich Reaction." *J. Am. Chem. Soc.* **2015**, *137*, 26, 8404.

1,6-dicarbonyl compound **8** from saturated aliphatic aldehydes **6** (Figure 3.3b).[11] However, products **8** were always isolated as a mixture of diastereomers in almost equal amount and in racemic form.

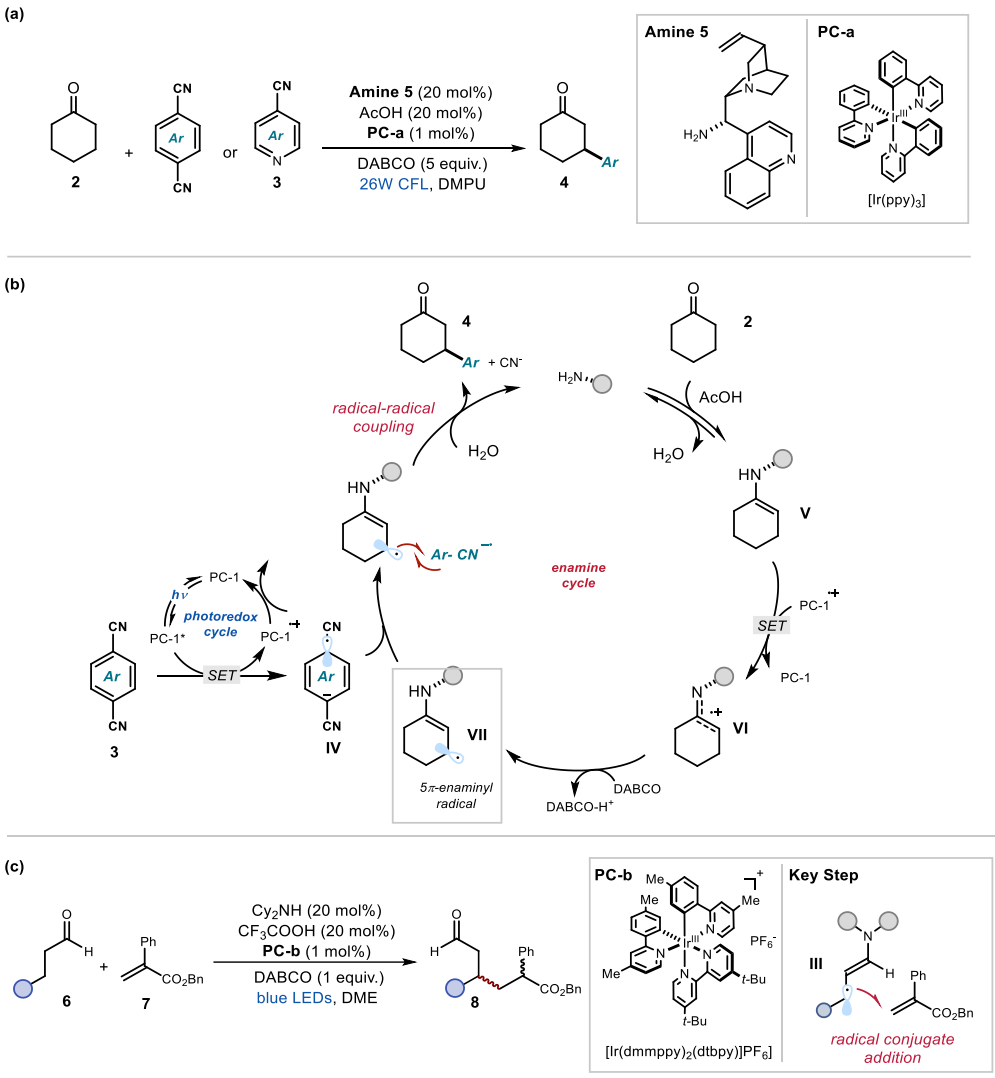

Figure 3.3. Combining photoredox and enamine catalysis to form 5π-electron Intermediates. **(a)** Photoredox organocatalytic procedure for asymmetric β-C−H arylation of saturated carbonyls and **(b)** its reaction mechanism, **(c)** Extension of the reaction system to radical conjugate addition. AcOH: Acetic acid; DABCO:

[11] Terrett, J. A.; Clift, M. D. and MacMillan, D. W. C. "Direct β-Alkylation of Aldehydes via Photoredox Organocatalysis" *J. Am. Chem. Soc.* **2014**, *136*, 19, 6858.

1,4-diazobicyclo[2.2.2]nonane; PC: photocatalyst; CFL: compact fluorescent lamp; DMPU: 1,3-dimethyltetrahydropyrimidin-2(1H)-one; LED: light emitting diode; DME: 1,2-dimethoxyethyane; Bn: benzyl; Cy: cyclohexyl.

Our research group found that, in addition to enamines, chiral iminium ions are also suitable intermediate to access 5π-electron radical species (Figure 3.4). This photo-organocatalytic chemistry rested on the direct excitation of the colored iminium ion **III**,[12] which displayed strongly oxidizing properties (E_{red}^* ~ +2.45 V vs Ag/Ag^+) upon irradiation by 420 nm light. When benzyl silane **9a** was used as reaction partner,[12a] a photoinduced SET event triggered the formation of the chiral β-enaminyl intermediate **III** along with a neutral benzyl radical arising fromirreversible fragmentation of the C-Si bond. A radical coupling then forged the stereogenic center, with selectivity secured by the sterically demanding moiety within the chiral amine **D**. The overall sequence afforded an asymmetric β-benzylation without the need of an external photocatalyst.

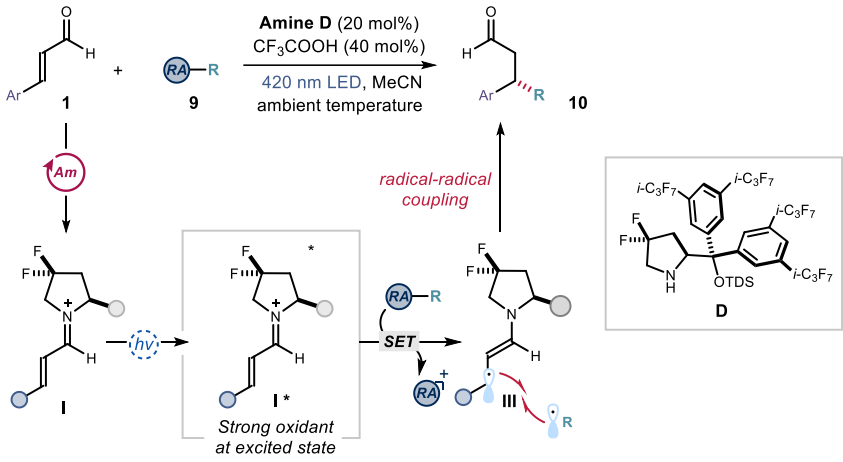

Figure 3.4. Enantioselective β-benzylation of enals **1** by Photo-oganocatalysis.

TDS: *tert*-hexyldimethylsilyl; RA: redox auxiliary.

[12] (a) Silvi, M.; Verrier, C.; Rey, Y. P.; Buzzetti, L.; Melchiorre, P. "Visible-light excitation of iminium ions enables the enantioselective catalytic β-alkylation of enals" *Nat. Chem.* **2017**, *9*, 868; (b) Verrier, C.; Alandini, N.; Pezzetta, C.; Moliterno, M.; Buzzetti, L.; Hepburn, H. B.; Vega-Peñaloza, A.; Silvi, M; Melchiorre, P. "Direct Stereoselective Installation of Alkyl Fragments at the β-Carbon of Enals via Excited Iminium Ion Catalysis" *ACS Catal.* **2018**, *8*, 1062; (c) Berger, M.; Carboni, D.; Melchiorre, P. "Photochemical Organocatalytic Regio- and Enantioselective Conjugate Addition of Allyl Groups to Enals" *Angew. Chem., Int. Ed.* **2021**, *60*, 26373.

Other radical precursors adorned with a redox auxiliary (Figure 3.5), such as 4-alkyl substituted dihydropyridines (DHP **9b**)[12b] and allyl silane **9a**, [12c] were also amenable to this excited-state reactivity of chiral iminium ions, affording chiral β-alkylation and allylation products respectively. Selected substrates such as cyclopropanol **9c**, alkenoic and allenic acid **9d**, which contained polarized functionalities for ionic reactivity, could engage in radical polar cross-over sequences,[13] leading to cyclic products with multiple stereocenters. This platform was also compatible with alternative processes for photoactivation, including multi-site proton-coupled electron transfer (MS-PCET)[14a] or the excitation of electron donor-acceptor (EDA) complexes,[14b] proving the generality of this mode of reactivity. The key to these stereocontrolled radical transformations was to combine enantioselective iminium ion catalysis with light-driven radical formation through SET processes. However, only aromatic enals could participate in the direct excitation of iminium ions, mainly due to their better visible light absorption compared to their aliphatic counterparts.

[13] (a) Woźniak, Ł.; Magagnano, G.; Melchiorre, P. "Enantioselective Photochemical Organocascade Catalysis" *Angew. Chem. Int. Ed*. **2018**, *57*, 1068; (b) Bonilla, P.; Rey, Y. P.; Holden, C. M.; Melchiorre, P. "Photo-Organocatalytic Enantioselective Radical Cascade Reactions of Unactivated Olefins" *Angew. Chem., Int. Ed*. **2018**, *57*, 12819; (c) Perego, L. A.; Bonilla, P.; Melchiorre, P. "Photo-Organocatalytic Enantioselective Radical Cascade Enabled by Single-Electron Transfer Activation of Allenes" *Adv. Synth. Catal*. **2020**, *362*, 302.

[14] (a) Mazzarella, D.; Crisenza, G.; Melchiorre, P. "Asymmetric Photocatalytic C–H Functionalization of Toluene and Derivatives" *J. Am. Chem. Soc*. **2018**, *140*, 8439; (b) Rodríguez, R.; Sicignano, M.; Alemán, J. "Fluorinated sulfinates as source of alkyl radicals in the photo-enantiocontrolled β-functionalization of enals" *Angew. Chem., Int. Ed*. **2022**, e20211263.

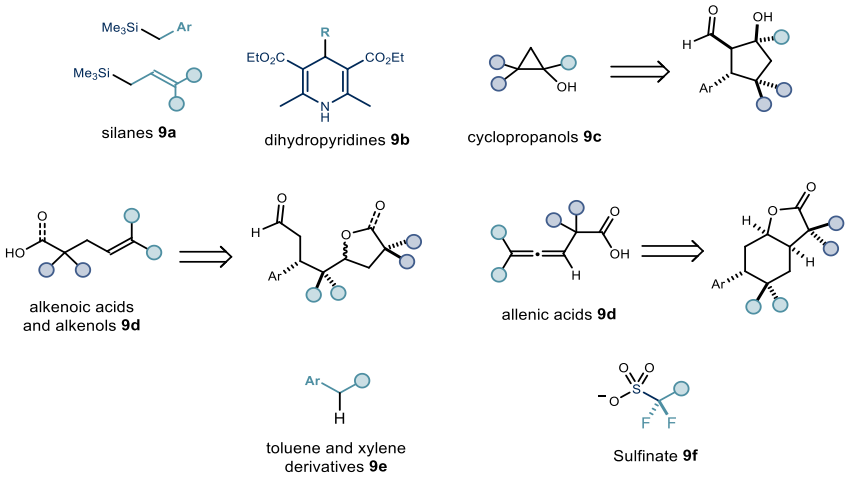

Figure 3.5. Radical precursors compatible with excited-state iminium ion chemistry.

Apart from chiral amines, chiral phosphoric acid catalysis was also found to activate α,β-unsaturated ketones for generating 5π-electron intermediate (Figure 3.6).[15] In 2022, Jiang and co-workers have shown that chiral phosphoric acids can facilitate the net-reductive coupling between enones **11** and 2-vinyl azines **12**, enabled by DHPs as the terminal reductants (Figure 3.6a).[15a] Upon activation by chiral Brønsted acid **CPA-a**, an electrophilic adduct was formed from enone **11**, rendering it a better electron acceptor. Reduction by photoredox catalyst **PC** using reductant **R-4** provided β-enolate radical **VIII.** Concurrently, the vinyl pyridine **12** was protonated by **CPA-a,** which positioned it in proximity to intermediate **VIII** while activating it towards radical acceptance. In this ternary complex, the stereochemical information was provided by the chiral catalyst, which enabled radical conjugate addition to occur in asymmetric fashion. Notably, this cross-coupling between two olefins involved the stereoselective formation of two non-adjacent stereogenic centers in product **13**, with excellent diastereomeric and enantiomeric ratio (d.r. up to 12:1, e.e. up to 99%). A pertinent discovery was that tailoring the structure of the DHP reductant had drastic effects on both product formation and stereocontrol. This could be explained by changes in reductant

[15] (a) Kong, M.; Tan, Y.; Zhao, X.; Qiao, B.; Tan, C.-H.; Cao, C. and Jiang, Z. "Catalytic Reductive Cross Coupling and Enantioselective Protonation of Olefins to Construct Remote Stereocenters for Azaarenes." *J. Am. Chem. Soc.* **2021**, *143*, 10, 4024; (b) Li, Y.; Han, C.; Wang, Y.; Huang, X.; Zhao, X.; Qiao, B.; Jiang, Z. "Catalytic Asymmetric Reductive Azaarylation of Olefins via Enantioselective Radical Coupling." *J. Am. Chem. Soc.* **2022**, *144*, 17, 7805.

structure modulating occurrence of undesired side reactions, such as uncatalyzed racemic reduction and over-reduction of enone **11** leading to saturated ketone by-products.

In addition to radical conjugate addition mechanisms, a different procedure that permitted the 5π-electron intermediate to take part in stereoselective radical coupling was also disclosed[15b] (Figure 3.6b). Light-assisted SET mediated by a photocatalyst furnished the intermediate **VIII** and a persistent pyridinyl radical. In a ternary complex held together by hydrogen bonding between **CPA-b** and the two radical intermediates, stereocontrolled radical coupling ultimately provided β-azaarylation of enone with good level of stereoinduction. Other chiral organocatalysts, such as thiourea and primary amine, were also employed. The aryl substituent at the ketone substrate was essential, restricting the utility of this synthetic method.

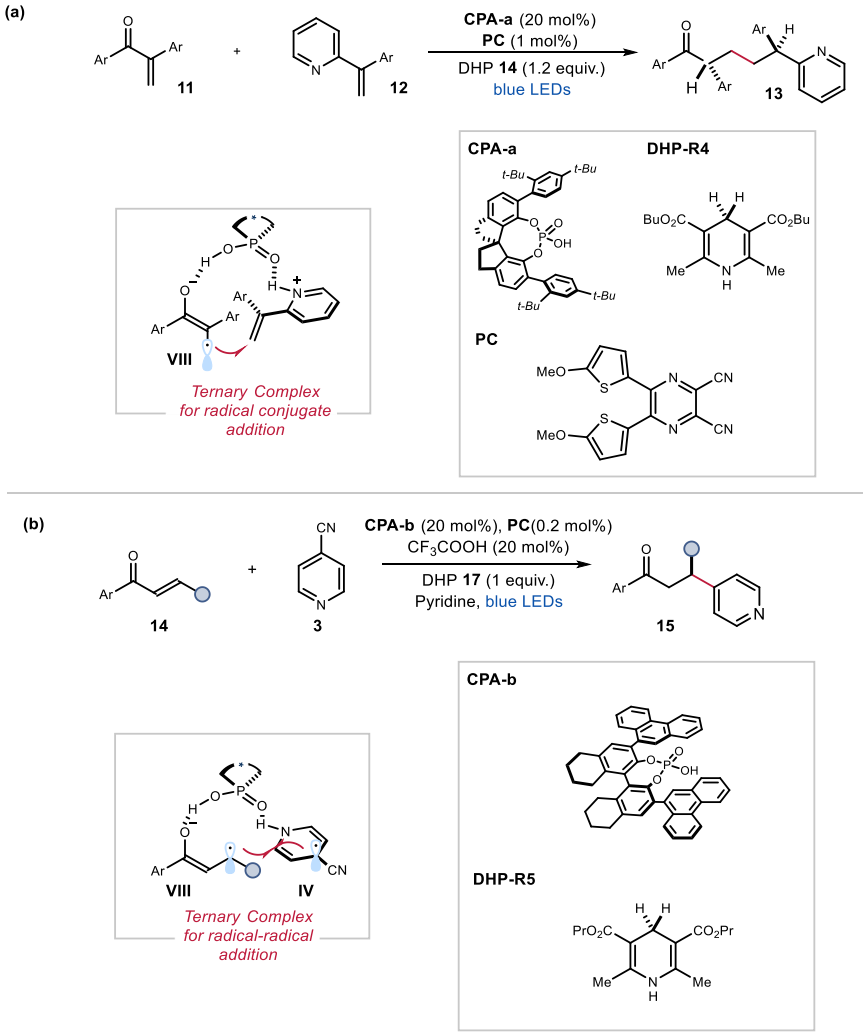

Figure 3.6. Formation of 5π-electron intermediates enabled by hydrogen bonding catalysis. **(a)** reductive coupling between two activated olefins. **(b)** Asymmetric β-azaarylation of enones **15**.

3.2.2 Metal-catalyzed Conditions to Generate Chiral 5π-Electron Intermediate

In addition to chiral organic catalysts, transition metal-based systems were also found useful to catalyze asymmetric reactions involving a 5π-electron intermediate.

As a leading example, the [2+2] cycloaddition between two olefins is an important reaction only made possible by photochemistry. Since the reaction is thermally disallowed, reactivity can be triggered only when one substrate is excited to a triplet diradical state.[16] While the cyclobutane product containing multiple stereocenters is of good synthetic value, stereochemical control is problematic because of racemic background reactions through free substrate activation by direct light irradiation. While initial successes were achieved by inclusion of chiral hydrogen-bonding motifs,[17] the contribution of uncatalyzed background reaction in these systems remained noticeable. Consequently, high catalyst loading (typically >50 mol%) and cryogenic reaction temperature (< -25 °C) were necessary for securing high level of stereoinduction.

A complementary mode of activation was developed by Yoon,[18] who reported a photoredox approach for initiating this reactivity (Figure 3.7): by coordination to Lewis acid catalysts, enones **14** were rendered more electrophilic, permitting reductive activation by a photoredox

---

[16] Woodward, R. B.; Hoffmann, R. "The Conservation of Orbital Symmetry." *Angew. Chem., Int. Ed.* **1969**, *8*, 11, 781.

[17] (a) Cauble, D. F.; Lynch, V.; Krische, M. J. "Studies on the Enantioselective Catalysis of Photochemically Promoted Transformations: 'Sensitizing Receptors' as Chiral Catalysts." *J. Org. Chem.* **2003**, *68*, 15; (b) Müller, C.; Bauer, A. and Bach, T. "Light-Driven Enantioselective Organocatalysis." *Angew. Chem., Int. Ed.* **2009**, *48*, 6640.

[18] (a) Ischay, M. A.; Anzovino, M. E.; Du, J.; Yoon, T. P. "Efficient Visible Light Photocatalysis of [2+2] Enone Cycloadditions." *J. Am. Chem. Soc.* **2008,** *130*, 12886; (b) Du, J.; Yoon, T. P. "Crossed Intermolecular [2+2] Cycloadditions of Acyclic Enones via Visible Light Photocatalysis." *J. Am. Chem. Soc.* **2009,** *131*, 14604; (c) Du, J.; Espelt, L. R.; Guzei, I. A.; Yoon, T. P. "Photocatalytic reductive cyclizations of enones: Divergent reactivity of photogenerated radical and radical anion intermediates." *Chem. Sci.* **2011**, *2*, 2115.

catalyst **PC**. This SET process provided a 5π-electron β-enolate radical **VIII** that intercepted another electron-deficient olefin **16**. Subsequent cyclization-reoxidation resulted in cycloadduct **17**, while regenerating the photocatalyst. Leveraging on these findings, a general strategy for efficient intermolecular enantioselective [2+2] cycloadditions was reported (Figure 3.7).[19] Specifically, enone **14** formed a Lewis acid-base adduct where stereocontrol was inferred by the Schiff-base ligand **L***/europium complex. No effective radical generation was found in absence of the chiral catalyst, therefore the system was not affected by an uncatalyzed racemic reaction. 1,2-Trans cycloadducts **17** were obtained in a high enantiomeric excess (85% e.e.) at ambient temperature. A curious discovery was made when the reduced salicylamine ligand **L*-H$_2$** was employed, since the other 1,2-cis diastereomer **17'** was preferentially formed while maintaining high level of enantiocontrol (up to 95% e.e.).

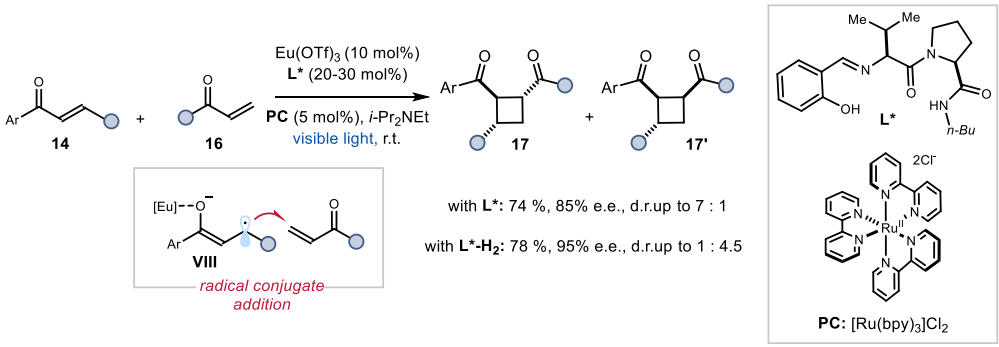

Figure 3.7. Stereoselective [2+2] intermolecular cycloaddition catalysed by chiral Lewis acid.

Another privileged catalytic system for asymmetric photochemistry is the bis-cyclometalated chiral-at-metal complexes Δ-**[Rh]**. These propeller-type C2-symmetrical catalysts, which are coordinated to two achiral 5-(*tert*-butyl)-2-phenyl benzoxazole or benzothiazole ligands and two labile acetonitrile ligands, can be further coordinated with carbonyl substrates with dual coordination ability. In 2017, Meggers have realized an unusual asymmetric β-

[19] (a) Du, J.; Skubi, K.L.; Schultz, D.M. and Yoon, T.P. "A Dual-Catalysis Approach to Enantioselective [2 + 2] Photocycloadditions Using Visible Light" *Science* **2014**, *344*, 6182, 392; (b) Daub, M. E.; Jung, H.; Lee, B. J.; Won, J.; Baik, M. -Y. and Yoon, T. P. "Enantioselective [2+2] Cycloadditions of Cinnamate Esters: Generalizing Lewis Acid Catalysis of Triplet Energy Transfer." *J. Am. Chem. Soc.* **2019**, *141*, 9543.

functionalization of saturated acyl imidazoles **18** (Figure 3.8).[20] This transformation was achieved based on the insightful observation that chiral rhodium enolate complex **IX**, formed in situ by coordination of **18** to Δ-**[Rh]-a** and deprotonation, can behave as a strong reductant upon photoexcitation ($E^* \sim -1.74$ V vs Ag/AgCl)[21]. Visible light promoted reduction of ketone **19** by **IX**, which was accompanied by a proton transfer, affording radical **X** and the corresponding 5π-electron β-enolate radical **VIII** coordinated to the chiral rhodium complex. This sequence was favored by the low bond-dissociation energy (BDE) of the C-H bond at the β-carbon within the enolate intermediate **IX**, allowing regioselective C-H functionalization. A radical coupling forged the new C-C bond, followed by protonation and ligand exchange, yielding products **20** with two neighboring stereogenic centers in good diasteroselectivity. Since photoactivity and radical generation was contingent to the coordination of the enolate substrate to the chiral metal complex, racemic background reaction was absent and a high stereoselectivity was achieved for this direct β-C-H functionalization. However, as a limitation, an aryl substituent in **18** was indispensable for reactivity.

Other concurrent reports also demonstrated that radical **VIII** can participate in enantioselective radical coupling with *N*-centered and carbon-centered radicals generated through PCET processes,[22] showcasing the versatility of this methodology.

---

[20] Ma, J.; Rosales, A. R.; Huang, X.; Harms, K.; Riedel, R.; Wiest, O.; Meggers, E. "Visible-Light-Activated Asymmetric β-C–H Functionalization of Acceptor-Substituted Ketones with 1,2-Dicarbonyl Compounds." *J. Am. Chem. Soc.* **2017**, *139*, 17245.

[21] Huo, H.; Shen, X.; Wang, C.; Zhang, L.; Röse, P.; Chen, L. -A.; Harms, K.; Marsch, M.; Hilt, G. and Meggers, E. "Asymmetric photoredox transition-metal catalysis activated by visible light." *Nature* **2014**, *515*, 100.

[22] Zhou, Z.; Li, Y.; Han, B.; Gong, L. and Meggers, E. "Enantioselective catalytic β-amination through proton-coupled electron transfer followed by stereocontrolled radical–radical coupling." *Chem. Sci.* **2017**, *8*, 5757; (b) Yuan, W.; Zhou, Z.; Gong, L. and Meggers, E. "Asymmetric alkylation of remote C(sp^3)–H bonds by combining proton-coupled electron transfer with chiral Lewis acid catalysis" *Chem. Comm.* **2017**, *53*, 8964.

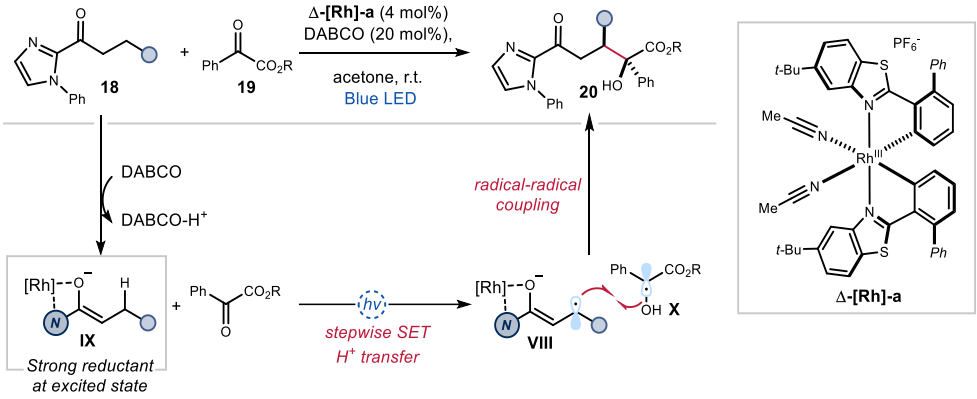

Figure 3.8. β-C-H Functionalization of saturated acylimidazole **18** through radical coupling with ketone **19**, enabled by direct photoexcitation of chiral-at-metal catalyst **Δ-[Rh]**. r.t.:room temperature.

This catalytic photochemical platform also served to activate α,β-unsaturated acrylamides via net-reductive conditions (Figure 3.9).[23] Specifically, coordination of substrate **14** to **Δ-[Rh]-b** provided a chiral, electrophilic metal complex intermediate **XII**. Upon excitation, the DHP reductant **R-2** could drive a SET event (E^* = -2.23 V vs. ferrocene redox couple, Fc^+/Fc) to reduce **XII** (E_{red} = -1.62 V vs. Fc^+/Fc), yielding the β-enolate radical **VIII** bound to the chiral metal complex that intercepted the electron-poor allylic sulfone **21** in an asymmetric fashion. The resultant α-carbonyl radical **XI** then underwent homolytic C-S bond cleavage to provide the formal allylation product **22** with a β-stereocenter. Product **22'**, containing a β-sulfonyl group, was also obtained with good steroinduction (up to 89% e.e.). Its formation can be justified by the enantioselective trap of the sulfonyl radical **XIII** generated during the β-scission event, through radical conjugate addition to **XII**. The possibility of polar sulfa-Michael addition by sulfinate anion to derive **22'** yet cannot be excluded.

[23] Huang, X.; Luo, S.; Burghaus, O.; Webster, R.D.; Harms, K. and Meggers, E. "Combining the catalytic enantioselective reaction of visible-light-generated radicals with a by-product utilization system." *Chem. Sci.* **2017**, *8*, 7126.

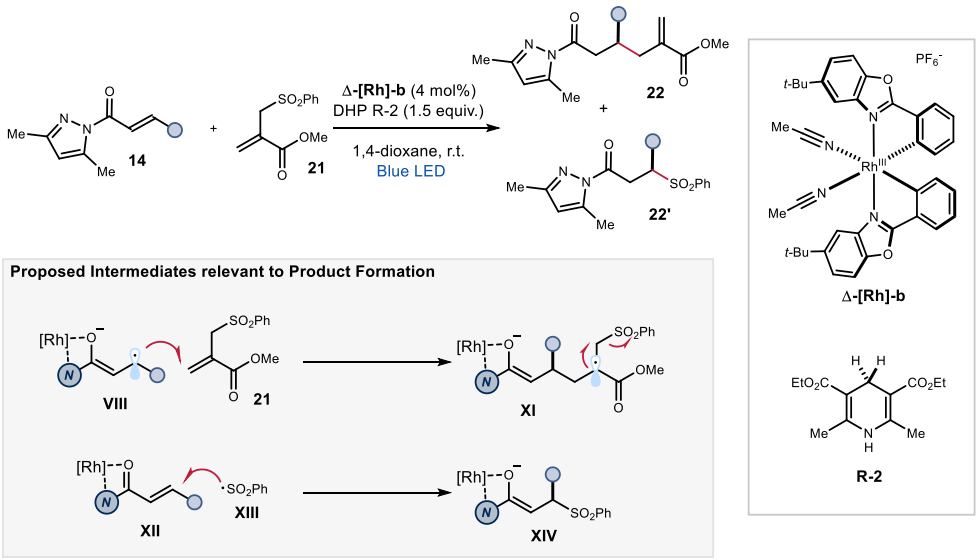

Figure 3.9. Reductive coupling of acrylamides **14** and acrylates **21** by combining photoredox catalysis and Lewis acid catalysis.

3.3 Design and Target of the Project

The target of this research project was to implement a dual catalytic strategy to activate enals towards the formation of a chiral 5π-electron radical with a nucleophilic character (*umpolung* reactivity, Figure 3.10). Through LUMO lowering, iminium ion **I**, generated upon condensation of a chiral amine catalyst and enal **1**, has enhanced electrophilic properties. As a crucial aspect of our strategy, we reasoned that the electron-poor nature of iminium ion **I** (E_{red} ~ -0.7 V vs Ag/Ag^+) could be leveraged to facilitate SET reduction, mastered by a photoredox catalyst. This SET event would lead to the formation of chiral 5π-electron radical **III**. In different studies, this intermediate **III**, accessed from saturated aldehydes, was shown to possess nucleophilic character,[11] guiding us to design polarity-matched transformations.

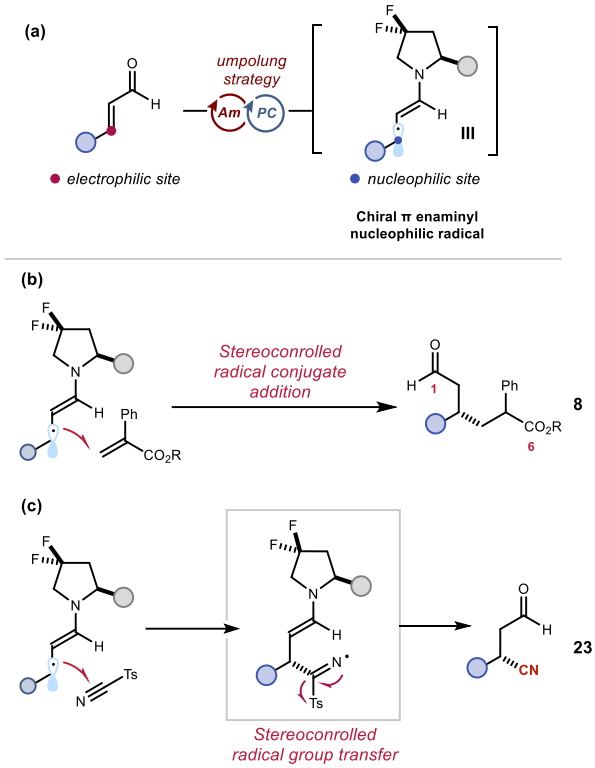

Figure 3.10. Our proposed radical *umpolung* strategy involves **(a)** generation of the chiral radical intermediate **III** by combining photoredox and asymmetric iminium ion catalysis, and its stereocontrolled interception through (**b**) radical conjugate addition or (**c**) radical group transfer. Ts: Tosyl.

The ability to generate radical **III** directly from enals **1** would offer a protocol to formally reverse the substrate polarity, since the originally electrophilic β-carbon in **1** would become nucleophilic in **III**. The facile formation of chiral β-enaminyl radical intermediates served as the main feature of this strategy, which may open up novel opportunities to engage different electrophilic radical traps in stereocontrolled fashion. The success of this tactic depends on the ability of the chiral amine catalyst to (i) selectively activate enals through condensation, permitting the selective SET reduction over the other electrophile; (ii) intertwine radical generation with chiral catalyst iminium ion formation, thus hampering uncatalyzed racemic reactivity.[24]

[24] Nagib, D. A. "Asymmetric Catalysis in Radical Chemistry." *Chem. Rev.* **2022**, *122*, 15989.

The photochemistry of chiral 5π-electron radicals was first studied in a cross-electrophile coupling between two α,β-unsaturated carbonyl compounds (Figure 3.10b), which would provide synthetic entry into 1,6-dicarbonyl compounds **8** that are otherwise difficult to access via polar reactions. Furthermore, we postulated that this *umpolung* activation mode could be general, so attempt was made to develop novel radical asymmetric processes. Bearing that in mind, we developed a chemo- and enantioselective conjugate cyanation of enals (Figure 3.10c) based on a radical group transfer transformation to deliver β-cyanoaldehyde **23**.

3.4 Results and Discussions

3.4.1 Development of Radical *Umpolung* Giese Addition for the Synthesis of 1,6-dicarbonyl Compound

1,6-Dicarbonyl compounds have been long recognized as a challenging synthetic target.[25] The most straightforward disconnection is to bisect the molecule, but this leads to two α,β-unsaturated carbonyl compounds, with a C-C bond formation disfavored by their natural polarities, between two electrophilic β-positions. Although ionic tactics were developed to invert the innate electronic properties (*umpolung*)[3] of carbonyl compounds, unsaturated carbonyl dimerization based on NHC catalysis[4] would lead to intermediate **II** that undergoes cyclization [26], thus losing the dicarbonyl connectivity (Figure 3.11, polar chemistry). Therefore, existing methods to access this desired motif resorted to synthetic detours, utilizing sigmatropic rearrangements of specialized precursors.[27]

---

[25] Organic Synthesis: The Disconnection Approach; Warren, S. and Wyatt, P. eds.,Wiley, **2008**, p.199.

[26] (a) Chiang, P. -C.; Kaeobamrung, J. and Bode, J. W. "Enantioselective, Cyclopentene-Forming Annulations via NHC-Catalyzed Benzoin−Oxy-Cope Reactions." *J. Am. Chem. Soc.* **2007**, *129*, 3520; (b) Cardinal-David, B.; Raup, D. E. A. and Scheidt, K. A. "Cooperative N-Heterocyclic Carbene/Lewis Acid Catalysis for Highly Stereoselective Annulation Reactions with Homoenolates." *J. Am. Chem. Soc.* **2010**, *132*, 5345; (c) White, N. A. and Rovis, T. "Oxidatively Initiated NHC-Catalyzed Enantioselective Synthesis of 3,4-Disubstituted Cyclopentanones from Enals" *J. Am. Chem. Soc.* **2015**, *137*, 10112.

[27] (a) Evans, D. A.; Baillargeon, D. J. and Nelson J. V. "A general approach to the synthesis of 1,6-dicarbonyl substrates. New applications of base-accelerated oxy-Cope rearrangements" *J. Am. Chem. Soc.*, **1978**, *100*, 2242; (b) Suresh, R.; Massad, I. and Marek, I. "Stereoselective tandem iridium-catalyzed alkene isomerization-cope rearrangement of ω-diene epoxides: efficient access to acyclic 1,6-dicarbonyl compounds." *Chem. Sci.* **2021**, *12*, 9328.

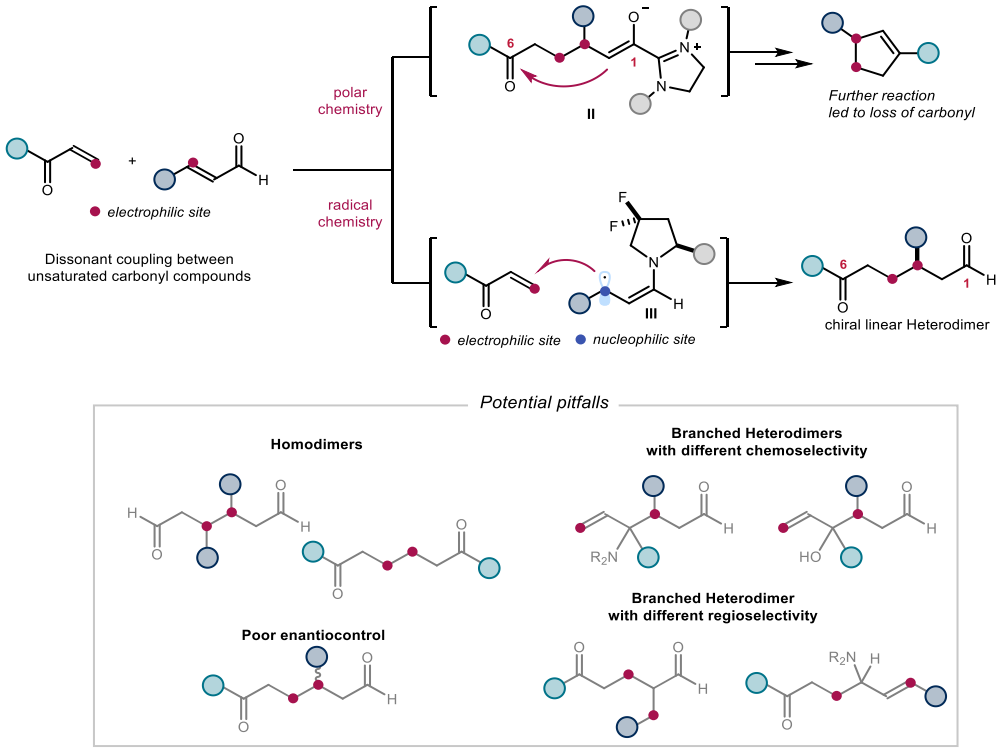

Figure 3.11. Synthesis of 1,6-dicarbonyl compounds. **(a)** polar chemistry leads to further reaction, losing dicarbonyl connectivity, **(b)** radical chemistry allows the desired reactivity, yet it is challenging to achieve stereoselectivity.

On the other hand, facile formation of the C-C bond of interest can be achieved by switching to radical reactivity (Figure 3.11, radical chemistry). Precedence in electrochemical[28] studies have illustrated the feasibility of this transformation through SET reduction of electron-deficient alkenes, while relying on radical conjugate additions to afford 1,6-dicarbonyl moiety. Yet these systems were limited to homodimerization, since the use of two different alkenes resulted in a mixture of products (Figure 3.11, potential pitfalls), such as homo- versus heterodimers, and products with different connectivities (linear vs branched).

[28] (a) Hirofumi, M.; Kazuharu, N.; Tsuneaki, H.; Ikuzo, N. "Selective Dimerization by Paired Electrolysis of Enol Acetate." *Chem. Lett.* **1991**, 20, 9, 1661; (b) Fussing, I.; Hammerich, O.; Hussain, A.; Nielsen, M. F. and Utley, J. H. "The Influence of Solvent on the Mechanism and Stereochemistry of Electrohydrodimerization. The Reduction of Cinnamic Acid Esters in Methanol." *Acta Chem. Scand.* **1998**, *52*, 328.

Most importantly, asymmetric version of this electrochemical transformation is yet to be realized. Recent work that combined modern visible-light photocatalysis with chiral Lewis acid catalysts[19] showed initial promise in tackling this problem.

We sought to address this synthetic conundrum by capitalizing on the selective condensation between a chiral amine catalyst and enals, which would allow its preferential activation for SET reduction. This radical **III** in turn engages acrylate **7** through Giese addition, realizing a cross-electrophile coupling to obtain 1,6-dicarbonyl compounds. Although previous method using saturated aldehydes as substrates delivered the same product scaffold,[11] *asymmetric catalytic* variant of this process has yet to be realized.

3.4.1.1 Reaction Optimization and Substrate Scope

Our radical *umpolung* strategy is reliant on the cooperative action of a chiral organocatalyst and a photoredox catalyst. Therefore, the first target would be to identify suitable aminocatalyst, photocatalyst and reducing agent to access the desired chiral 5π-electron radical. Building on previous knowledge that difluorinated pyrrolidinols **C** and **D** are robust catalysts for iminium ion activation compatible with light-driven radical chemistry, we tested its potential in this *umpolung* strategy. The combination of 4-CzIPN photocatalyst[29] and 1,4-DHP as a terminal reductant[15,23,30] was a promising starting point to unlock this novel mode of reactivity.

---

[29] Shang, T.-Y.; Lu, L.-H.; Cao, Z.; Liu, Y.; He, W.-M. and Yu, B. "Recent advances of 1,2,3,5-tetrakis(carbazol9-yl)-4,6-dicyanobenzene (4-CzIPN) in photocatalytic transformations." *Chem. Commun.* **2019**, *55*, 5408.

[30] (a) Stradins, J.; Baumane, L.; Kalnins, A.; Uldrikis, J.; Bisenieks, E.; Poikans, J. and Duburs, G. "Special features of the electrochemical oxidation of substituted 4-carboxy-1,4-dihydropyridines." *Chem. Heterocycl. Compd.* **2000**, *36*, 1177; (b)Wang, P.-Z.; Chen, J.-R. and Xiao, W.-J. "Hantzsch esters: an emerging versatile class of reagents in photoredox catalyzed organic synthesis." *Org. Biomol. Chem.* **2019**, *17*, 6936.

Table 3.1. Optimization Studies for asymmetric 1,6-dicarbonyl compound synthesis.[a]

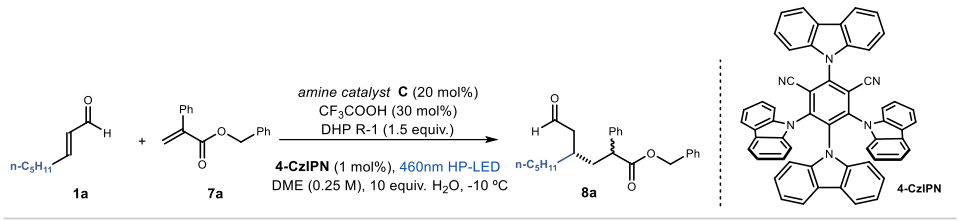

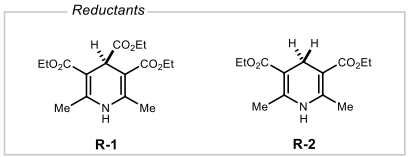

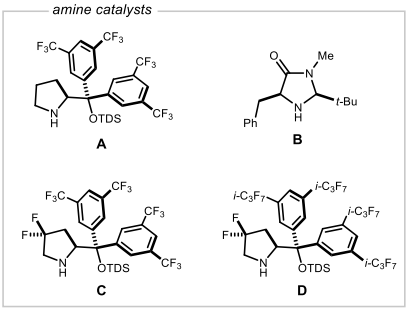

entry	Deviation from Standard Conditions	yield (%, d.r.)[b]	e.r.$_1$,e.r.$_2$[c]
1	amine **C** (standard)	88 (1.1:1)	94:6 , 88:12
2	amine **A**	29 (2:1)	78:22 , 64:32
3	amine **B**	90 (1.2:1)	77.5:22.5 , 60:40
4	amine **D**	90 (1.1:1)	94:6 , 88:12
5	No amine catalyst	<15 (1.5:1)	-
6	No photocatalyst	0	-
7	Reaction in dark	0	-
8	1.5 eq. DHP **R-2**	0	-
9	with 3 eq. H_2O	21 (1:1)	94:6 , 82.5:17.5
10	with 21 eq. H_2O	19 (1.1:1)	-

[a] Reactions performed on a 0.1 mmol scale for 20 h using 3 equiv. of **1a**, 20 mol% of aminocatalyst, 1 mol% of 4-CzIPN photocatalyst, and 30 mol% of TFA in 0.2 mL of DME under illumination by a single high-power LED (λ_{max} = 460 nm, 60 mW/cm^2) at -10 °C. [b] Yield determined by ^{1}H NMR analysis of the crude mixture using trichloroethylene as the internal standard; yield of the isolated product **8a** is reported in brackets. [c]Enantiomeric ratio of **8a**.

Initial experiments of cross-electrophile coupling were conducted in dimethoxy ethane (DME) as solvent under irradiation by a blue LED (light emitting diode, λ_{max} = 460 nm), using the organic photocatalyst 4-CzIPN (1 mol%) and dihydropyridine **R-1** as the terminal reductant (Table 3.1). In order to guarantee a high concentration of iminium ion intermediate, *trans*-oct-2-enal **1a** was used in excess (3 equiv.) together with 30 mol% of trifluoroacetic acid (TFA) co-catalyst. Upon light irradiation, amine **C** provided high yield of 1,6-dicarbonyl compound **8a** as a linear heterodimer (88% yield, entry 1) as a single product. Nonetheless, there was no relative control over the nonadjacent stereocenters and a mixture of diastereomers in almost equal amount was obtained. The two diastereomeric diols **24a** and

24b could be separated and characterized after reduction of product **8a** by $LiAlH_4$ (path *i*, Figure 3.12). Further esterification by *p*-nitrobenzoyl chloride (path *ii*) led to diesters **25** that facilitated enantiomeric ratio determination (e.r. of diastereomer 1=94:6, e.r., of diastereomer 2 = 88:12).

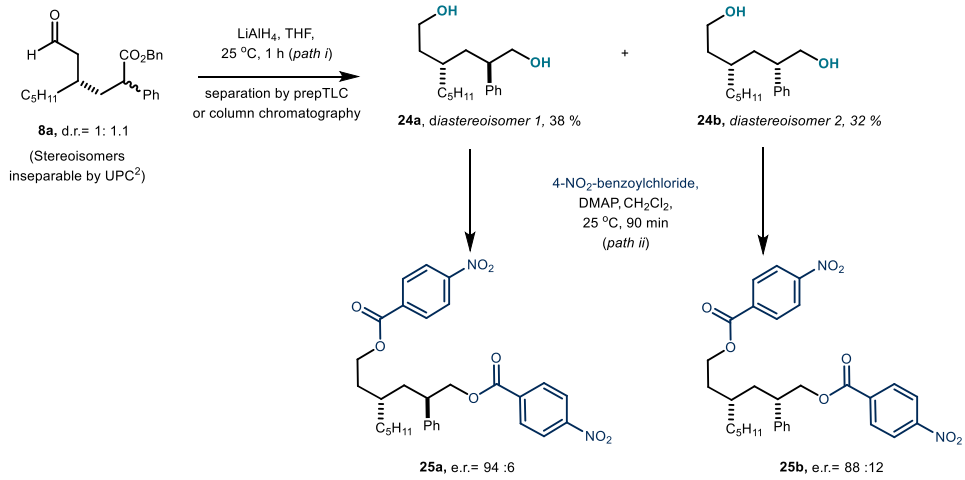

Figure 3.12. Derivitization sequence to separate diastereoisomers and determine e.r. of **8.** DMAP: 4-dimethylaminopyridine.

Chiral secondary amine catalysts **A** and **B**, which have an established profile to promote iminium-ion-based polar processes, afforded the target product **8a** with moderate enantioselectivity (entries 2 and 3). A related difluorinated catalyst **D**, which possesses sterically more demanding perfluoro-isopropyl groups on the arene scaffold, provided comparable results to **C** (entry 4). Exclusion of aminocatalyst provided small yet non-negligible degree of product formation (entry 5), hinting that a racemic background pathway could be operative, plausibly upon activation towards SET reduction of the enal substrates by TFA.

In the absence of photocatalyst or light, the reactivity was fully inhibited (entries 6-7), suggesting the cross-electrophile coupling is possible only by synchronous action of both the photoredox and the amine catalyst. The nature of the reductant was also important, since Hantzsch ester **R-2**, bearing two hydrogens at the C4 position, did not provide the target 1,6-

dicarbonyl product (entry 8), due to competitive polar reduction of enal via hydride delivery.[31] Interestingly, the reaction provided optimal results with 10 equivalents of water, while deviation from this amount had deleterious effects on product yield (entries 9 and 10).

We then used the optimized conditions (entry 3) to explore the substrate scope with respect to enals. *p*-Methoxybenzyl (PMB) 2-phenyl acrylate **7b** was used as the model substrate to facilitate product isolation. Adopting the optimized conditions on a synthetically meaningful scale (0.25 mmol), a diverse array of enal substrates could be transformed (Figure 3.13). Various aliphatic substituents at the β-position of enals (products **8b**-**8e**) were tested to study the sensitivity to steric encumberment: product yield was reduced with increased congestion (adduct **8c** to **8d**), while the stereoinduction remained high (e.r.> 93:7 for most adducts). Terminal and internal alkenes and alkyne moieties with different degrees of substitution (adducts **8f**-**8i**) were well-tolerated.

Owing to the mild reaction conditions, a variety of reactive functional groups within the enal substrate were preserved, including alkyl chloride (**8j**), unprotected alcohol (**8k**), benzyl ether (**8l**), methyl ester (**8m**) and phthalimide moiety (**8n**). Unsaturated aldehydes bearing arenes with different electronic demands were also converted, providing adducts **8o** to **8r** with consistent yield and enantiomeric ratio. On the other hand, enals with β-aromatic substituents, e.g. cinnamaldehyde, were not reactive. Besides, an α-substituted enal did not deliver the desired product. This might be due to its reduced propensity to condense with weakly nucleophilic catalyst **C** and form an iminium ion**.**

[31] Yang, Y. W.; Hechavarria Fonseca, M. T. H. and List, B. "A metal-free transfer hydrogenation: organocatalytic conjugate reduction of α,β-unsaturated aldehydes." *Angew. Chem., Int. Ed.* **2004**, *43*, 6660.

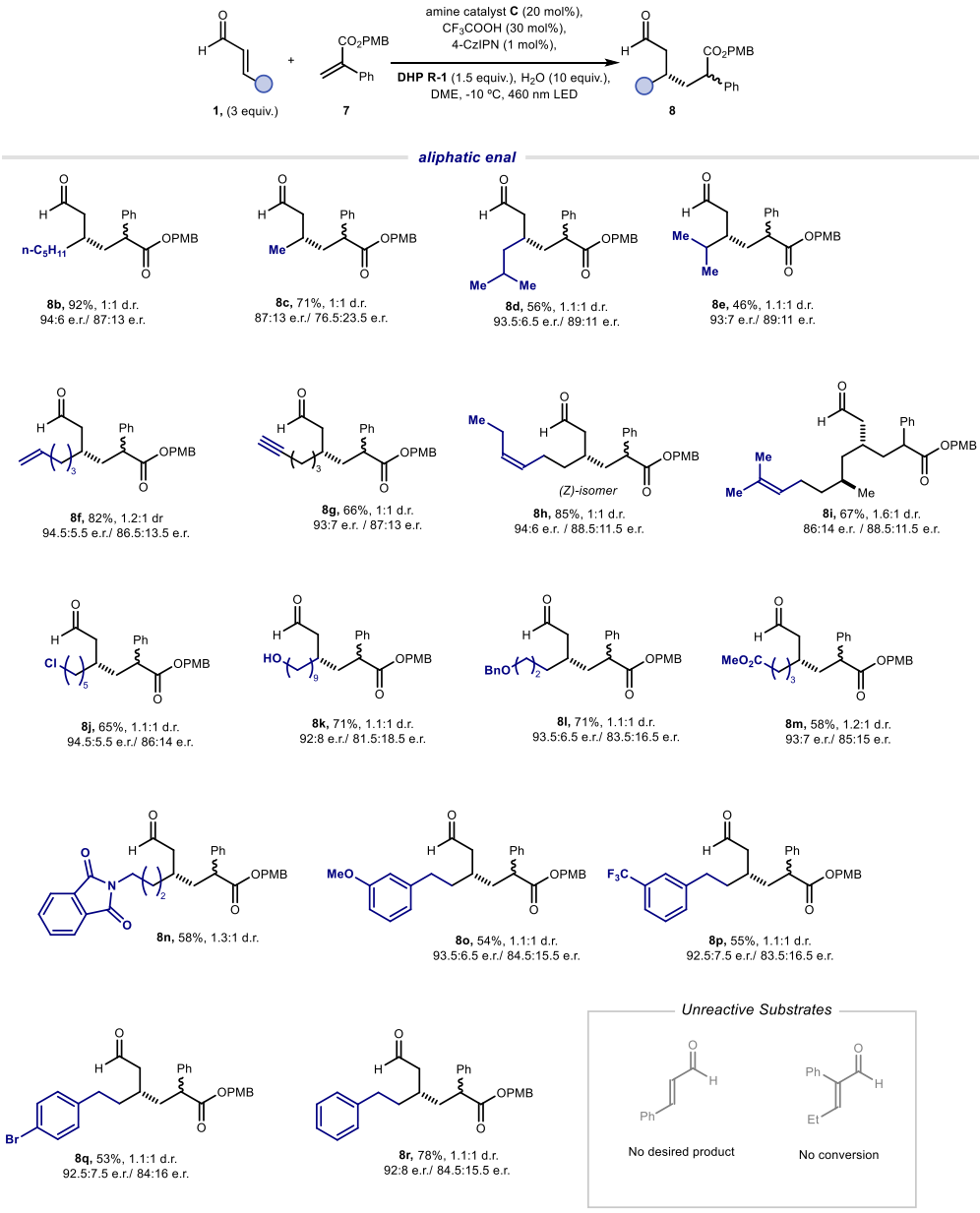

Figure 3.13. Substrate scope of enals **1** for the asymmetric cross-electrophile coupling between two Michael acceptors, leading to 1,6-dicarbonyl compounds. Reactions performed on a 0.25 mmol scale using 3 equiv. of enal **1** and acrylate **7b** in 0.5 mL of DME under illumination at 460 nm for 18-22 h. The e.r. values for both diastereomers of **8** are reported. PMB: *para*-methoxybenzyl.

The stereochemistry of compound **25r**, the fully reduced descendant of product **8r**, was unambiguously established by X-ray crystallographic analysis of the derivative obtained after acylation (Figure 3.14 the experimental details described in section 3.6.12).[32]

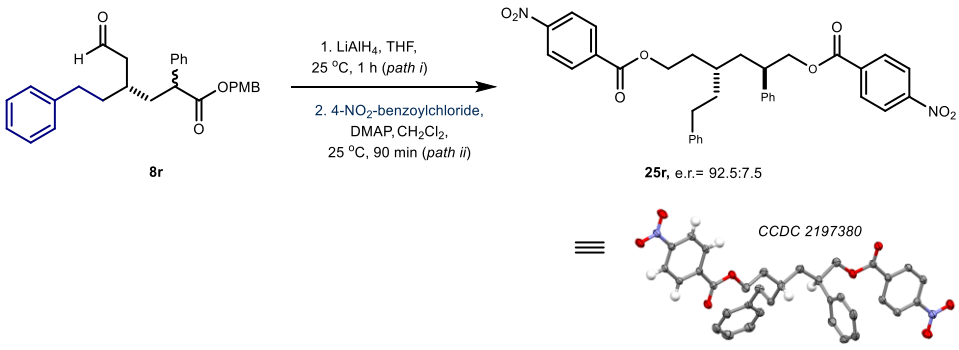

Figure 3.14. Derivitization of product **8r** for absolute configuration determination via X-ray single crystal analyses.

The scope of acrylate esters amenable to this strategy was also examined with *trans*-2-octenal as reaction partner[33] (Figure 3.15). Phenyl acrylates **7** decorated with various aromatic substituents were suitable coupling partners, leading to the corresponding aldehyde products **8s** to **8z** with high yields and enantiocontrol. The α-phenyl group bearing halides (**8s, 8t, 8x, 8y**), electronically donating (**8u, 8w**) or withdrawing groups (**8v, 8y**) of various substitution pattern all provided products in moderate to good yield. In addition to benzyl ester, switching to methyl ester still afforded product (adduct **8z**). In all entries, the chiral catalyst could not exert any significant level of control over the relative stereochemistry of products (d.r.<1.5:1 for most adducts).

[32] Crystallographic data for compound **25r** has been deposited with the Cambridge Crystallographic Data Centre, accession number CCDC 2197380.

[33] Enantiomeric excess measurement was unsuccessful for some of the products, as the four stereoisomers were not separable on chiral HPLC. They have also decomposed upon $LiAlH_4$ reduction for derivatization

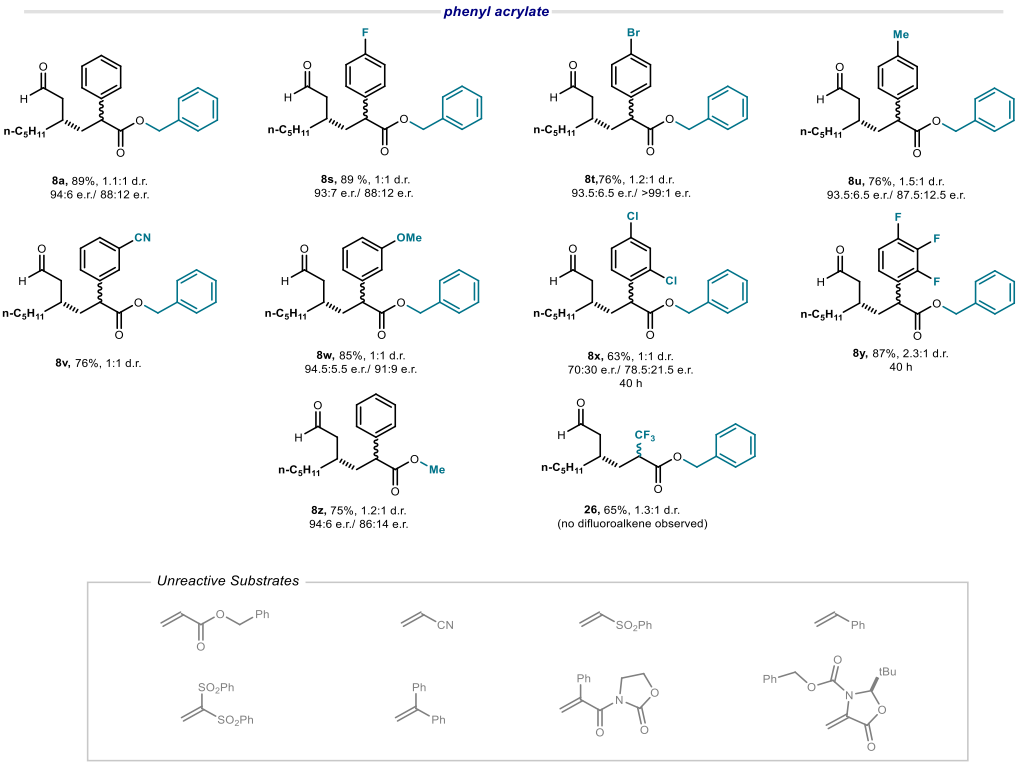

Figure 3.15. Substrate scope of acrylate **7** for the asymmetric cross-electrophile coupling between two Michael acceptors, leading to 1,6-dicarbonyl compounds. Reactions performed on a 0.25 mmol scale using 3 equiv. of enal **1a** in 0.5 mL of DME under illumination at 460 nm for 18-22 h. The e.r. values for both diastereomers of **8** are reported.

On the other hand, removal of the phenyl group (benzyl acrylate) or the ester functionality (styrene) rendered the substrate unreactive. The only reactive trap was found when the phenyl group was replaced by trifluoromethyl group, affording the Giese addition product **26** in moderate yield (65 %). In an attempt to mitigate the poor diastereocontrol (Figure 3.15, grey box), Michael acceptors with mono- and bi-substitution were used, yet they were not engaged under the reaction conditions. Acryloyl oxazolidinones were also not converted, thus dismissing the possibility to control the α-ester stereocenter with chiral auxiliaries[34] or chiral

[34] (a) Evans, D. A. and Shaw, J. T. "Recent advances in asymmetric synthesis with chiral imide auxiliaries" Actualité Chimique **2003**, *11*, 4, 35; (b) Aycock, R. A.; Vogt, D. B. and Jui, N. T. "A practical and scalable system for heteroaryl amino acid synthesis" *Chem. Sci*. **2017**, *8*, 7998.

Lewis acid catalysts[35]. Alternative approach to control the formation of this stereocenter by a chiral Brønsted acid only offered mediocre results, highlighting the difficulties in controlling diastereoselectivity.

3.4.1.2 Extension of the Reactivity to an Asymmetric Formal β-Allylation

To expand the applicability of this radical *umpolung* platform, allyl sulfone **21** was used as a different radical trap for to achieve an allylation reaction. Upon radical conjugate addition, β-scission of the α-carbonyl radical intermediate **XV** would readily occur. This led to desulfonylation, restoring the α,β-unsaturated ester functionality.[23] This overall transformation would offer a rare example of asymmetric catalytic conjugate allylation of enals.

Employing catalyst **C** under similar conditions developed for the Giese addition, the formal allylation product **27** could be isolated with moderate yield (60%, Table 3.2, entry 1) and stereocontrol (e.r. = 87:13). Yet an appreciable amount of the β-sulfonyl ester side-product **27'** was detected (14%), which derived from reduction before β-fragmentation and desulfonylation could occur. Amines **A** and **B** provided inferior results (entries 2 and 3), whereas the fluorinated catalyst **D** exhibited comparable performance to catalyst **C** (entry 4). Exclusion of the amine catalyst, photoredox catalyst or light completely shut down the reactivity (entries 5-7), showcasing that all reaction components are essential.

Further optimization revealed that trichloroacetic acid (TCA) as a co-catalyst, along with an additional equivalent of enal, improved the stereoinduction, probably by favoring iminium ion formation (e.r. = 90:10, entry 8). It was found that higher temperature could help the desulfonylation process, affording the allylation product with higher yields, albeit at the expense of enantioselectivity (entries 9-10).

---

[35] (a) Sibi, M. P.; Ji, J.; Wu, J. H.; Gürtler, S.; Porter, N. A. "Chiral Lewis Acid Catalysis in Radical Reactions: Enantioselective Conjugate Radical Additions" *J. Am. Chem. Soc.* **1996**, *118*, 9200; (b) Song, S. and Wang, P.-S. "Asymmetric Photocatalytic C(sp^3)–H Bond Addition to α-Substituted Acrylates" *Org. Lett.* **2021**, *23*, 8, 3157.

Table 3.2. Optimization studies.[a]

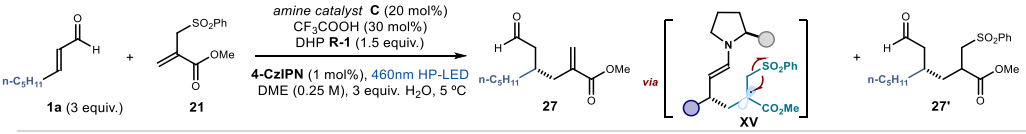

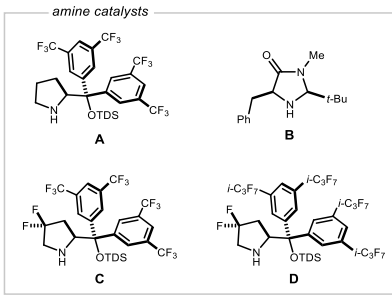

entry	Deviation from Standard Conditions	yield (%,a:a')[b]	e.r. of a[c]
1	amine **C**	74 (60:14)	87:13
2	amine **A**	15 (10:5)	-
3	amine **B**	50 (40:10)	83.5:16.5
4	amine **D**	80 (60:20)	87:13
5	No amine catalyst	0	-
6	No photocatalyst	0	-
7	Reaction in dark	0	-
8	30 mol% TCA, 4 eq. Enal	80 (60:20)	90:10
9	at -10 °C	66 (46:20)	87.5:12.5
10	at ambient temperature	54 (50:4)	80:20

[a] Reactions performed on a 0.1 mmol scale for 20 h using 3 equiv. of **1a**, 20 mol% of aminocatalyst, 1 mol% of 4-CzIPN photocatalyst, and 30 mol% of TFA in 0.2 mL of DME under illumination by a single high-power LED (λ_{max} = 460 nm, 60 mW/cm^2) at -10 °C. [b] Yield determined by ^{1}H NMR analysis of the crude mixture using trichloroethylene as the internal standard; yield of the isolated product **27** is reported in brackets. [c]Enantiomeric ratio of **27**.

In attempt to convert the side product **27'** into the target adduct **27** by polar elimination, the crude mixture after reaction completion was stirred with a base for 30 minutes. Weak bases (pK_a of conjugate acid <10, e.g. $NaHCO_3$, NEt_3, iPr_2NEt) had not effects on product distribution, while stronger bases (pK_a of conjugate acid ~14, DBU and TMG) led to complete decomposition.

These results have hinted at the generality of this radical *umpolung* strategy. With the appropriate choice of radical acceptors, different chiral products could be prepared through different reaction pathways. It can be envisioned that utilization of other reaction partners may unlock novel synthetic methodologies.

3.4.1.3 Mechanistic Studies

To better understand the radical generation processes, a series of mechanistic experiments were conducted.

Radical Generation and Intermediacy of 5π-Electron Radicals

In order to examine the potential photoactivity of the reaction partners, UV-visible spectra of acrylates were measured (section 3.6.8): none of them showed appreciable absorption in the visible region, both alone or in presence of equimolar amount of DHP **R-1**. A control experiment was also conducted by excluding the photocatalyst from the reaction, and no conversion of the starting materials was observed. This suggested that direct excitation of substrates or electron donor-acceptor (EDA) complex[36] could not occur under reaction conditions, and the photocatalyst 4-CzIPN is the only species that can be excited by the 460 nm light source.

Upon portion-wise addition of **R-1**, fluorescence of 4-CzIPN, arising from 460nm laser excitation, was quenched (K_{SV} = 30.5 M^{-1}) in a ratiometric manner, following the Stern Volmer equation. In contrast, increasing concentration of acrylate **7a** did not lead to diminished fluorescence. Voltammetric studies confirmed that oxidation potential of DHP ($E(\mathbf{R}^{\bullet+}/\mathbf{R})$ ~ +1.3 V vs SCE, standard calomel electrode) matched that of the excited photocatalyst, whereas SET from 4-CzIPN* to acrylate **7a** (E_{red} = -2.09 V vs SCE) was endergonic and therefore implausible.

This led us to propose that the excited photocatalyst would oxidize the DHP reductant (Figure 3.16, left). The reduced photocatalyst could then undergo SET to the iminium ion **I** (E_{red} ~ -0.7 V vs Ag/Ag^{+}), forming the 5π-electron radical **III**. Another possibility is that the excited photocatalyst could first reduce the iminium ion intermediate, while the 4-CzIPN$^{\bullet+}$ will be reduced by 1,4-DHP to regenerate the photocatalyst (Figure 3.16, right). Although iminium

[36] (a) Crisenza, G. E. M.; Mazzarella, D.; Melchiorre, P. "Synthetic Methods Driven by the Photoactivity of Electron Donor–Acceptor Complexes." *J. Am. Chem. Soc.* **2020**, *142*, 12, 5461; (b) Ma, D.; Wong, T.H.-F.; Melchiorre, P. "Asymmetric Photoredox Reactions without Photocatalysts." In *Catalytic Asymmetric Synthesis*, 4th ed.; Akiyama, T.; Ojima, K. Eds; John Wiley & Sons, Inc., 2022; pp. 329.

ions formed from cinnamaldehydes could be crystallized[12a] (CCDC1494741), we encountered challenges associated with isolation of the counterpart from octenal. As a result, Stern-Volmer quenching studies with iminium ion **I** could not be conducted, and the two proposed photocatalytic cycles could not be distinguished.

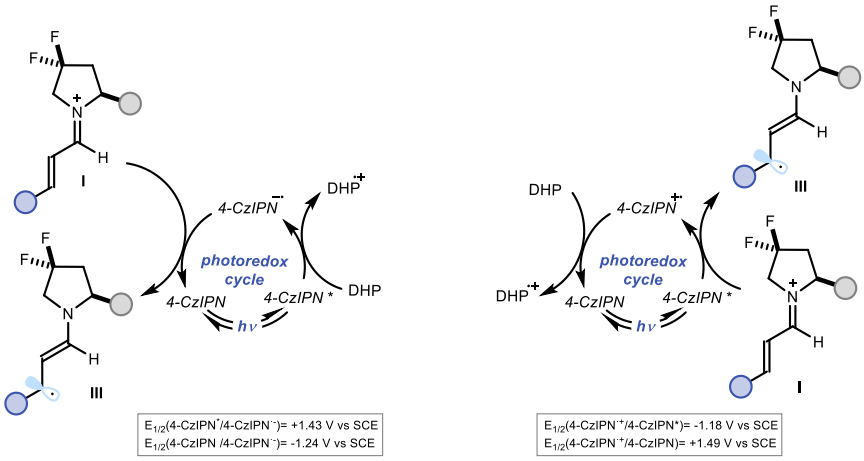

Figure 3.16. Proposed photoredox catalytic cycles. *(left)* SET sequence initiated by oxidation of DHP reductant; *(right)* SET sequence initiated by reduction of the iminium ions.

Performing the reaction under air atmosphere or in the presence of a radical scavenger (TEMPO, 3 equiv.) completely suppressed the reactivity. Although TEMPO adduct could not be detected, the results were consistent with the radical nature of the reaction. To probe the formation of 5π-electron radical in our reaction conditions, a radical clock experiment was conducted with enal bearing a β-cyclopropyl substituent. (Figure 3.17, experimental details in section 3.6.11). A cyclopentane product **29** could be isolated and characterized. This result is consonant with the formation of the 5π-electron radical **XVI** that underwent facile ring-opening to furnish a more stable benzylic radical **XVII**. Unexpectedly, after conjugate addition to acrylate **7b**, the electrophilic radical **XVIII** would then attack the electron-rich dienamine for a 5-exo-trig cyclization, regenerating 5π-electron radical that could be oxidized by the photocatalyst. The overall process provided a redox-neutral, formal [3+2] ring expansion, in agreement with the proposal that 5π-electron radical is a reaction intermediate.

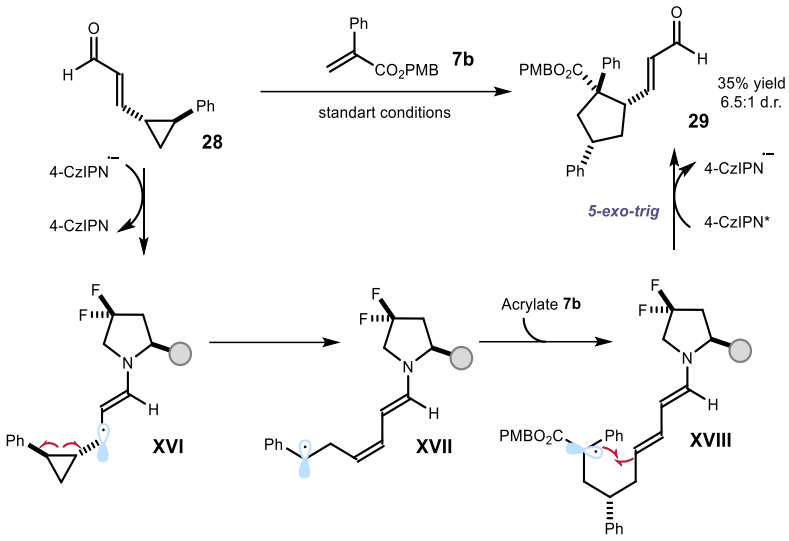

Figure 3.17. Radical clock experiment confirming the transient formation of the 5π-electron-enaminyl radical intermediate

Giese Addition and Formation of α-Stereocenter

Once the 5π-electron radical was generated, it would be intercepted by the acrylate trap, the resultant α-radical **XIX** could be quenched reductively, either through stepwise reduction-protonation[34b,37] (E(**XIX**/**XX**) ~ -0.8 V vs Fc^+/Fc)[38] or a concerted HAT step from radical cation of DHP reductant[39] (Figure 3.18). These steps were proposed to occur with poor

[37] Yin, Y.; Dai, Y.; Jia, H.; Li, J.; Bu, L.; Qiao, B.; Zhao, X. and Jiang, Z. "Conjugate Addition–Enantioselective Protonation of N-Aryl Glycines to α-Branched 2-Vinylazaarenes via Cooperative Photoredox and Asymmetric Catalysis." *J. Am. Chem. Soc.* **2018**, *140*, 19, 6083.

[38] Schmittel, M.; Lal, M.; Lal, R.; Röck, M.; Langels, A.; Rappoport, Z.; Basheer, A.; Schlirf, J.; Deiseroth, H.-J.; Flörke, U.; Gescheidt, G. "A comprehensive picture of the one-electron oxidation chemistry of enols, enolates and α-carbonyl radicals: oxidation potentials and characterization of radical intermediates." *Tetrahedron* **2009**, *65*, 10842.

[39] (a) Sumino, S. and Ryu, I. "Hydroalkylation of Alkenes Using Alkyl Iodides and Hantzsch Ester under Palladium/Light System" *Org. Lett.* **2016**, *18*, 52; (b) Trowbridge, A.; Reich, D. and Gaunt, M. J. "Multicomponent synthesis of tertiary alkylamines by photocatalytic olefin-hydroaminoalkylation." *Nature* **2018**, *561*, 522; (c) Rossolini, T.; Leitch, J. A.; Grainger, R. and Dixon, D. J. "Photocatalytic Three-Component Umpolung Synthesis of 1,3-Diamines." *Org. Lett.* **2018**, *20*, 21, 6794; (d) Lahdenperä, A. S. K.; Bacoş, P. D. and Phipps, R. J. "Enantioselective Giese Additions of Prochiral α-Amino Radicals." *J. Am. Chem. Soc.* **2022**, *144*, 49, 22451.

stereocontrol, as 1,6-dicarbonyl products are always obtained as mixture of diastereomers with apparent substrate-controlled selectivity.

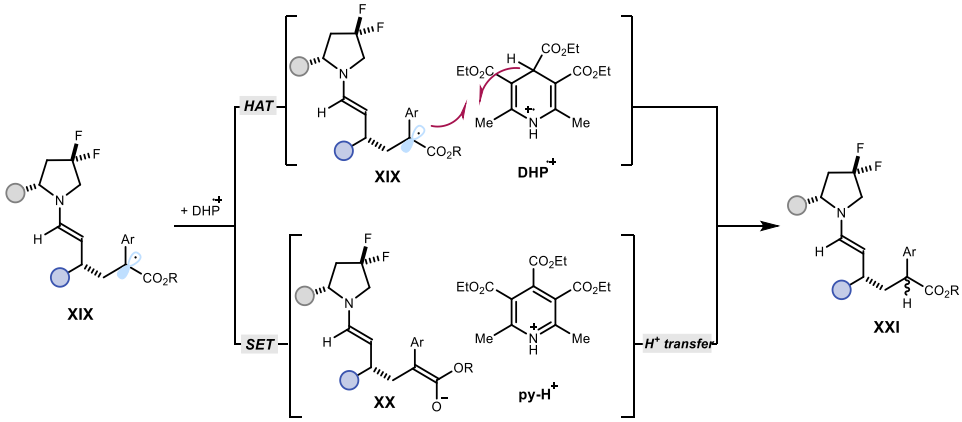

Figure 3.18. Proposed mechanisms for stereogenic C-H bond formation through a concerted HAT step (*upper*) or a reduction-protonation sequence (*lower*).

A deuterium labelling experiment was conducted, in attempt to disentangle the two plausible pathways (section 3.6.11). Using deuterium oxide in place of water as additive (Figure 3.19), deuterium incorporation was observed at the α-position of the ester (78% yield for **8a-d**, d.r.=1.2:1, 45% labelling). This result may suggest that DHP can act as the source of hydrogen for the reduction of α-radical **XIX** through a concerted HAT event. The SET followed by deuteriation of **XX** from D_2O is also operative.

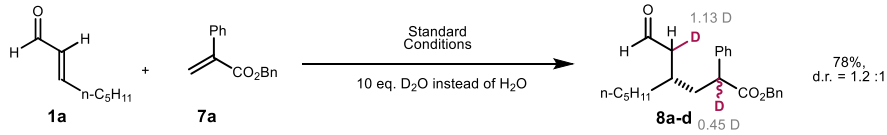

Figure 3.19. Deuterium-labelling experiment

The isolated product **8a** from standard reaction conditions was stirred in a buffered solution mimicking acidity of the standard reaction (20% pyrrolidine, 30% CF_3COOH, 10 eq. D_2O). No detectable isotope scrambling occurred to positions adjacent to both carbonyl groups and the diastereomeric ratios remained unchanged, suggesting that epimerization through

reversible enolization does not occur under the reaction conditions. While it can be proposed that failure to improve the diastereocontrol at the α-stereocenter is partly due to its formation through multiple pathways, explanation for these results remains at a speculative level.

Alternative Reaction Mechanisms

It could be suggested that the α-radical could abstract an hydrogen atom from DHP (E(**R**$^{\bullet+}$/**R**) = +0.9 V vs Fc^{+}/Fc), providing radical cation that could reduce another equivalent of iminium ion **I**, either through direct SET or mediation by ground state photocatalyst, for a radical chain propagation (Figure 3.20). This process is, however, not feasible as the events are thermodynamically disfavored. A small quantum yield (Φ = 0.04) indicated that the said chain mechanism, if exists, had minute contribution to the observed reactivity.

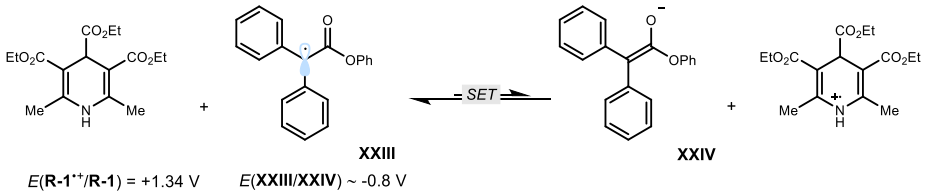

Figure 3.20. a hypothetical SET event to sustain a radical chain.

Taken together, we propose the reaction mechanism depicted in Figure 3.21. Upon excitation, photocatalyst 4-CzIPN ($E_{1/2}$(**4-CzIPN*/4-CzIPN**$^{\bullet-}$) = +1.43 V vs SCE)[40] oxidizes **R-1** reductant, forming 4-CzIPN$^{\bullet-}$ ($E_{1/2}$(**4-CzIPN /4-CzIPN**$^{\bullet-}$) = -1.24 V vs SCE) that is potent to reduce the electron-poor iminium ion **I**, generated upon condensation of aminocatalyst **C** and enal **1**. This SET affords the chiral β-enaminyl radical **III**. The chiral fragment within **III** could then govern the stereo-determining bond formation with acrylate **7**, inferring a high degree of enantioselectivity. The ensuing α-radical **XIX** is then susceptible to concerted/step-wise HAT from DHP$^{\bullet-}$, providing closed-shell enamine intermediate **XXI**. Hydrolysis of **XXI** provides the target chiral 1,6-dicarbonyl compound **8** while regenerating the organo-catalyst **C**, restarting the catalytic cycle.

---

[40] Speckmeier, E.; Fischer, T. G.; Zeitler, K. "A Toolbox Approach To Construct Broadly Applicable Metal-Free Catalysts for Photoredox Chemistry: Deliberate Tuning of Redox Potentials and Importance of Halogens in Donor–Acceptor Cyanoarenes." *J. Am. Chem. Soc.* **2018**, *140*, 45, 15353.

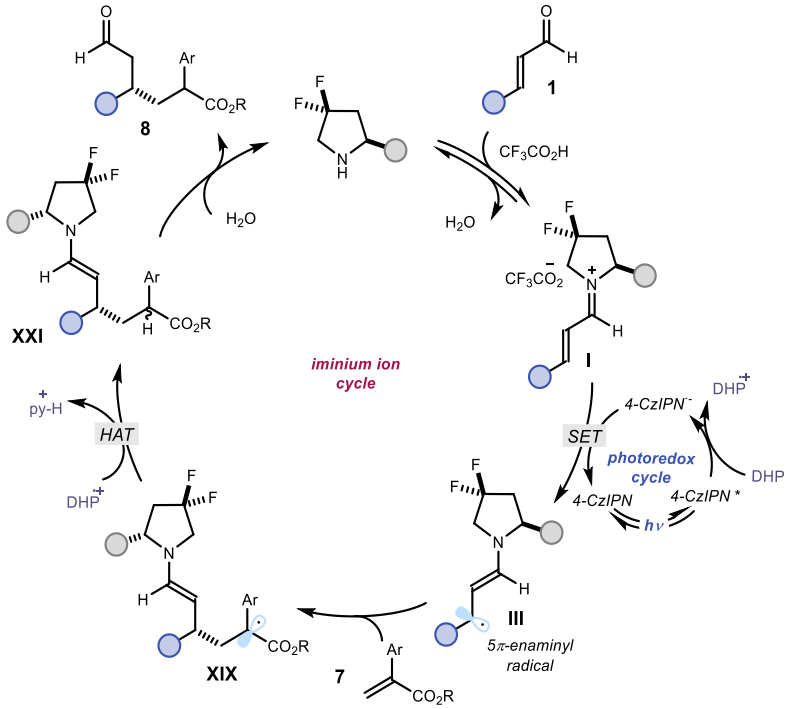

Figure 3.21. Proposed reaction mechanism for cross-electrophile coupling.

3.4.2 Development of an Enantioselective Conjugate Cyanation of Enals

The cyanation of carbonyl compounds is a reaction with historical significance. As early as 1912, Bredig and Fiske[41] used a cinchona natural product catalyst to promote the addition of HCN to benzaldehyde (Figure 3.22a, upper panel). Despite its low stereoselectivity (e.r. < 55:45) in product **30**, this process offered the first example of non-enzymatic asymmetric catalysis developed by chemists.[42c] After a century of development, this catalytic asymmetric reaction [42] is regarded as a classical transformation that has reached high level of

[41] Bredig, G. and Fiske, P. S. "Beiträge zur chemischen Physiologie und Pathologie." *Biochem. Z.* **1912**, *46*, 7.

[42] (a) Kurono, N. and Ohkuma, T. "Catalytic asymmetric cyanation reactions." *ACS Catal.* **2016**, *6*, 989. (b) Reetz, M. T.; Kunisch, F. and Heitmann, P. "Chiral Lewis acids for enantioselective C–C bond formation." *Tetrahedron Lett.* **1986**, *27*, 4721. (c) Zuend, S. J.; Coughlin, M. P.; Lalonde, M. P. and Jacobsen, E. N. "Scalable catalytic asymmetric Strecker syntheses of unnaturalα-amino acids." *Nature* **2009**, *461*, 968. (d) Zhou, H.; Zhou, Y.; Bae, H. Y.; Leutzsch, M.; Li Y.; De, C. K.; Cheng, G.-J. and List, B. "Organocatalytic stereoselective cyanosilylation of small ketones." *Nature* **2022**, *605*, 84.

sophistication (Figure 3.22a, middle panel) and found wide application for the preparation of valuable chiral cyanohydrins.[43]

The versatility of the cyanation chemistry was later expanded to the asymmetric conjugate addition to α,β-unsaturated carbonyl compounds, including imides[44] and ketones[45] These processes relied on chiral catalysts and steric hinderance at the carbonyl carbon of substrate that could secure complete chemoselectivity for the cyanide 1,4-addition. However, to date, the stereoselective preparation of β-cyanoaldehydes **23** had remained elusive (Figure 3.22b). Racemic examples for conjugate cyanation of α,β-unsaturated aldehydes **1** are also rare and restricted to purposely tailored cyclic substrates.[46] The intrinsic overwhelming preference, i.e. *chemoselectivity*, of enals **1** for reacting with the nucleophilic cyanide at the aldehydic functionality (1,2-addition) instead of the β-carbon (1,4-addition) is a consequence of combined electronic, steric factors with hard-soft-acid-base polarizability match,[47] and was observed at a very early stage. In 1954, Prelog and Wilhelm[48] reinvestigated the pioneering

---

[43] (a) Gregory, R. J. "Cyanohydrins in nature and the laboratory: biology, preparations, and synthetic applications." *Chem. Rev.*, **1999**, *99*, 3649. (b) Zeng, X.-P., Sun, J.-C.; Liu, C.; Ji, C.-B. and Peng, Y.-Y. "Catalytic asymmetric cyanation reactions of aldehydes and ketones in total synthesis." *Adv. Synth. Catal.* **2019**, *361*, 3281.

[44] (a) Sammis, G. M. and Jacobsen, E. N. "Highly enantioselective, catalytic conjugate addition of cyanide to α,β-unsaturated imides." *J. Am. Chem. Soc.* **2003**, *125*, 4442; (b) Sammis, G. M.; Danjo, H. and Jacobsen, E. N. "Cooperative dual catalysis: application to the highly enantioselective conjugate cyanation of unsaturated imides." *J. Am. Chem. Soc.* **2004**, *126*, 9928.

[45] Tanaka, Y.; Kanai, M. and Shibasaki, M. "A catalytic enantioselective conjugate addition of cyanide to enones." *J. Am. Chem. Soc.* **2008**, *130*, 6072; (b) Tanaka, Y.; Kanai, M. and Shibasaki, M. "Catalytic enantioselective construction of β-quaternary carbons via a conjugate addition of cyanide to β,β-disubstituted α,β-unsaturated carbonyl compounds." *J. Am. Chem. Soc.* **2010**, *132*, 8862; (c) Provencher, B. A.; Bartelson, K. J.; Liu, Y.; Foxman, B. M. and Deng, L. "Structural study-guided development of versatile phase-transfer catalysts for asymmetric conjugate additions of cyanide." *Angew. Chem., Int. Ed.*, **2011**, *50*, 10565.

[46] (a) Ito, Y.; Kato, H.; Imai, H. and Saegusa, T. "A novel conjugate hydro- cyanation with $TiCl_4$-tert-butyl isocyanide." *J. Am. Chem. Soc.* **1982**, *104*, 6449; (b) Jansen, B. J. M.; Sengers, H. H. W. J. M.; Bos, H. J. Y. and de Groot, A. "A new stereoselective approach for the total synthesis of (±)-isotadeonal, (±)-polygodial, (±)-warburganal, and (±)-muzigadial." *J. Org. Chem.* **1988**, *53*, 855.

[47] Nagata, W. and Yoshioka, M. in *Organic Reactions*, Vol. 25; Dauben, W. G., Ed., Wiley-Interscience, **1978**, pp 255–476.

[48] Prelog, V. and Wilhelm, M. "Untersuchungen über asymmetrische Synthesen VI). Der Reaktionsmechanismus und der sterische Verlauf der asymmetrischen Cyanhydrin-synthese." *Helv. Chim. Acta*. **1954**, *37*, 1634.

organocatalytic system of Bredig and Fiske.[41] They realized that cinnamaldehyde (Figure 3.20b) reacted with HCN with exclusive 1,2-chemoselectivity. All the methodologies reported so far confirmed that linear enals undergo preferential addition at the carbonyl moiety to provide cyanohydrin **31**. [43b,49] As a consequence, there is no general 1,4-cyanation procedure that can override the intrinsic selectivity for enals through ionic pathways.

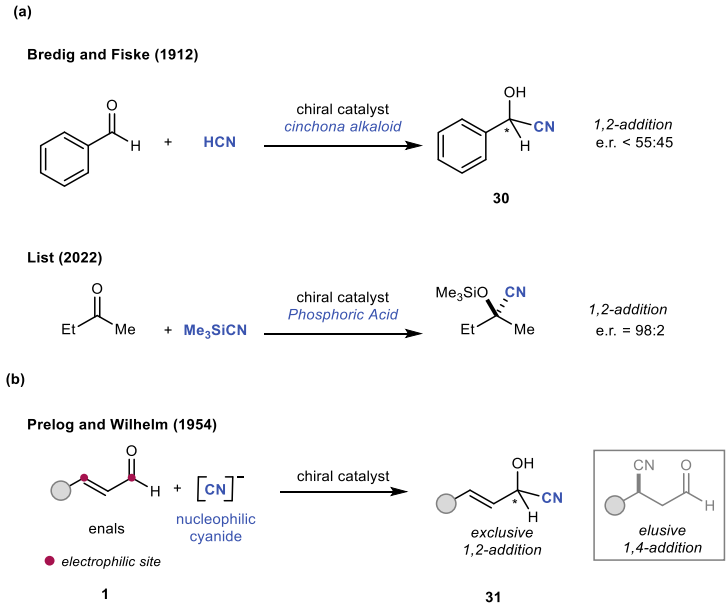

Figure 3.22. State of the art of asymmetric catalytic polar cyanation of carbonyl compounds. **(a)** Pioneering studies using the classic polar nucleophilic reactivity of cyanide with carbonyl compounds. **(b)** Efforts on cyanation of enals leading to exclusive 1,2-addition products.

Informed by the notion that classic ionic processes are not suitable for the conjugate cyanation of enals, we pondered the question whether the developed one-electron reductive procedure of iminium ions, based on radical mechanisms, can achieve the target. This umpolung strategy would involve the use of an electrophilic nitrile source, which could react exclusively with

[49] (a) Hayashi, M.; Miyamoto, Y.; Inoue, T. and Oguni, N. "Enantioselective trimethylsilylcyanation of some aldehydes catalyzed by chiral Schiff base-titanium alkoxide complexes." *J. Org. Chem.* **1993**, *58*, 1515; (b) Hamashima, Y.; Sawada, D.; Kanai, M. and Shibasaki, M. "A new bifunctional asymmetric catalysis: an efficient catalytic asymmetric cyanosilylation of aldehydes." *J. Am. Chem. Soc.* **1999**, *121*, 2641.

chiral β-enaminyl radical **III** while leaving the electrophilic carbonyl carbon site in enal **1** intact.

Identification of a suitable electrophilic nitrile source would be crucial to realize our design plan. In 1992, Barton and co-workers established the ability of the stable and readily available tosyl cyanide (TsCN) to intercept nucleophilic, carbon-centered radicals,[50] affording iminyl radical **XXV** that undergo facile β-fragmentation to extrude sulfinate radical $SO_2Ar^{\bullet}$ **XIII** while delivering the cyanation product **33** (Figure 3.23a). The resulting nitrile transfer strategy has found broad synthetic application since then,[51] but an asymmetric catalytic variant has remained unknown.

We considered that it is possible for the nucleophilic, chiral radical **III** to attack TsCN, while the β-scission event could restore nitrile functionality to deliver the cyanation product. Therefore, we set out to use TsCN in an enantioselective framework to develop a photoredox organocatalytic conjugate cyanation of enals (Figure 3.23b). If successfully combined with a stereocontrolled radical-based C-C bond forming step, this strategy would offer the first example of asymmetric catalytic conjugate cyanation of enals. Herein, an initial solution to this longstanding problem is reported, detailing the β-cyanation of aliphatic enals proceeding with exclusive chemoselectivity and good enantioselecivity by the synergy of photoredox and organocatalysis.

---

[50] Barton, D. H. R.; Jaszberenyl, J. C. and Theodorakis, E. A. "The invention of radical reactions. Part XXIII new reactions: nitrile and thiocyanate transfer to carbon radicals from sulfonyl cyanides and sulfonyl isothiocyanates." *Tetrahedron* **1992**, *48*, 2613.

[51] Patel, R. I.; Sharma, S. and Sharma, A. "Cyanation: a photochemical approach and applications in organic synthesis." *Org. Chem. Front.*, **2021**, *8*, 3166. For selected examples: (b) Gaspar, B. and Carreira, E. M. "Mild cobalt-catalyzed hydrocyanation of olefins with tosyl cyanide." *Angew. Chem., Int. Ed.* **2007**, *46*, 4519; (c) Ren, R.; Wu, Z.; Xu, Y. and Zhu, C. "C–C bond-forming strategy by manganese-catalyzed oxidative ring-opening cyanation and ethynylation of cyclobutanol derivatives." *Angew. Chem., Int. Ed.* **2016**, *55*, 2866; (d) Ramirez, N. P.; König, B.; Gonzalez-Gomez, J. C. "Decarboxylative Cyanation of Aliphatic Carboxylic Acids via Visible-Light Flavin Photocatalysis." *Org. Lett.* **2019**, *21*, 1368.

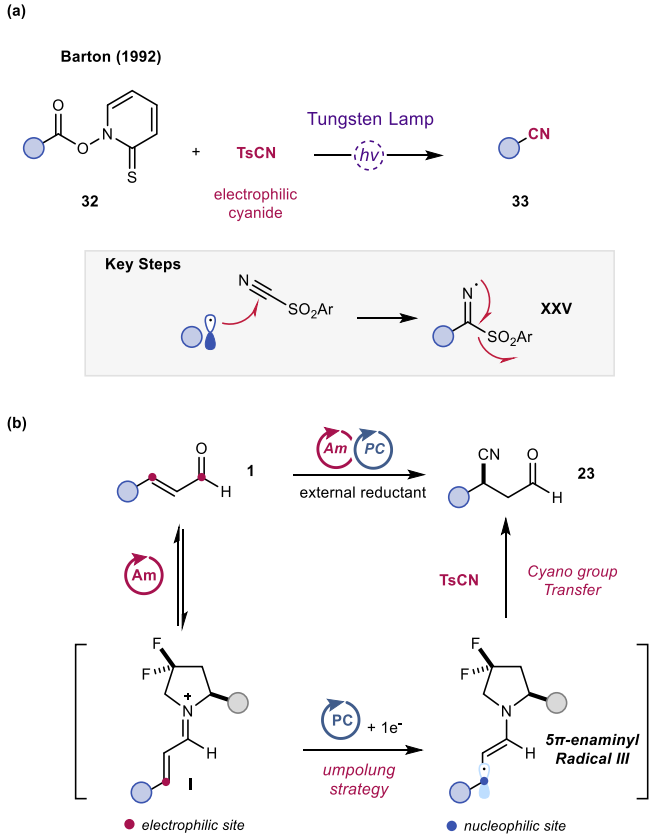

Figure 3.23. Past and present work on radical cyanation **(a)** Seminal work by Barton reporting TsCN as a nitrile source for radical cyanation **(b)** Design plan for the stereoselective conjugate cyanation of enals via radical *umpolung* strategy. Ts: Tosyl; Ar: aromatic group.

3.4.2.1 Optimization Studies and Substrate Scope

Adapting the conditions developed for the 1,6-dicarbonyl synthesis, β-cyanooctanal **23a** was obtained in good yield (67%, Table 3.3, entry 1) and complete β-selectivity, albeit moderate enantioenrichment (e.r. = 71:29). Nonetheless, a significant amount of β-sulfonylaldehyde **23'** was obtained (76%) with poorly reproducible level of stereoinduction (e.r.~ 57.5:42.5 to 75.5:25.5). This by-product arose from the competitive addition of the tosyl radical **XIII** (or sulfinate upon reduction) to enal **1a**, similar to previous disclosure.[23]

Other chiral catalysts, such as amines **A** and **B** afforded the desired cyanation product with poor yield and no stereocontrol (entries 2 and 3). The use of ethyl acetate as solvent secured a significant increase in stereocontrol (e.r. = 81:19, entry 4). A final cycle of catalyst optimization established amine **D** as suitable for improving enantiocontrol while preserving the catalytic activity (e.r. = 88:12, entry 5), yet a higher reaction temperature was needed for good conversion. Increasing the catalyst loading to 30 mol% offered the optimal results (entry 6, **23a** isolated in 75% yield and e.r. = 91:9, single regioisomer), yet by-product **23a'** was still formed in a significant amount (88%).

Control experiments confirmed that the presence of amine catalyst, photocatalyst and light were essential for appreciable reactivity (entries 7-9). Control experiments using Hanszch ester **R-2** as the reducing agent (entry 10) led to a significantly diminished yield of **23a**, as enal substrates were converted to saturated aldehyde via polar reduction. Nucleophilic nitrile sources used previously for the cyanation of carbonyl compounds only provided 1,2-addition product (entries 11-12, cyanohydrin **31**). These control experiments established the importance to tailor the structure of the nitrile source and the reductant.

Table 3.3. Optimization Study for an enantioselective conjugate cyanation .[a]

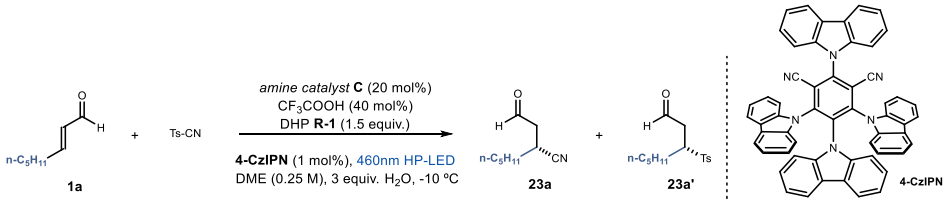

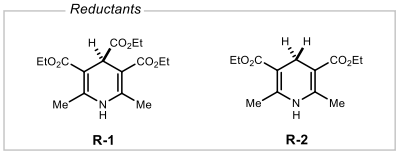

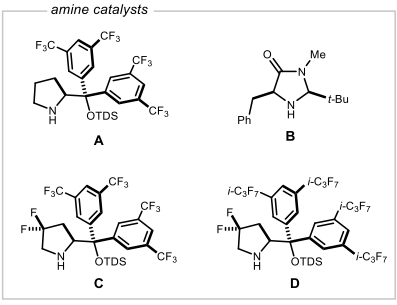

entry	Deviation from Standard Conditions	yield (%)[b]	e.r.[c]
1	amine **C**	67	71:29
2	amine **A**	21	52:48
3	amine **B**	20	50:50
4	amine **C** in EtOAc	63	81:19
5	amine **D** in EtOAc, 5 °C	56	88:12
6	30 mol% amine **D** in EtOAc, 5 °C	77(75)	91:9
7	No amine catalyst	<10	-
8	No photocatalyst	0	-
9	Reaction in dark	0	-
10	1.5 eq. DHP **R-2**	15	-
11	Me_3SiCN as CN source	<5	-
12	n-$Bu_4N^+CN^-$ as CN source	<5	-

[a] Reactions performed on a 0.1 mmol scale for 20 h using 3 equiv. of **1a**, 20 mol% of aminocatalyst, 1 mol% of 4-CzIPN photocatalyst, and 40 mol% of TFA in 0.2 mL of DME under illumination by a single high-power LED (λ_{max} = 460 nm, 60 mW/cm^2). [b] Yield determined by ^{1}H NMR analysis of the crude mixture using trichloroethylene as the internal standard; yield of the isolated product **23a** is reported in brackets. [c]Enantiomeric ratio of **23a**.

Examining the substrate scope with the optimal conditions (entry 6), a broad panel of enals was subjected to the conjugate cyanation (Figure 3.24). To prevent product loss due to volatility and enable separation from by-product **23'**, the corresponding cyano-alcohols **34**, formed upon $NaBH_4$ reduction of the crude products, were isolated. For products of higher polarity, direct isolation as cyanoaldehyde **23** was feasible.

A wide range of structurally diverse aliphatic substituents at the β position of enals was well-tolerated, with the corresponding β-cyanoaldehydes formed with high stereoselectivity (e.r. consistently in the range of 90:10), whereas no 1,2-addition product was detected. The lowest level of stereocontrol was achieved with crotonaldehyde (product **34b**, 85:15 e.r.), which is a consequence of the small size of the methyl fragment challenging the chiral catalyst's ability to infer stereoselectivity. Branched substituents at the β-carbon of enals (products **34c**-**d**) were transformed in fair yield.

Both terminal (adduct **34e**) and internal olefins (**34g** and **34h**), as well as alkyne (**34f**) could be retained, showing that the presence of unsaturation did not lead to undesired side reactions. A panel of reactive functional groups were compatible with the cyanation conditions, including an unprotected alcohol (**23i**), a phthlamide (product **23k**), and an amide (**23l**), demonstrating the good chemoselectivity of this procedure. As a result of their increased polarity, the products were isolated as cyanoaldehdyes without reductive derivatization. Precursor bearing other sensitive moieties including a benzyl ether functionality (**34j**), a preinstalled nitrile (**34m**), arenes decorated with different functional groups of varying electronic demands (**34o** to **34r**) were well converted to products.

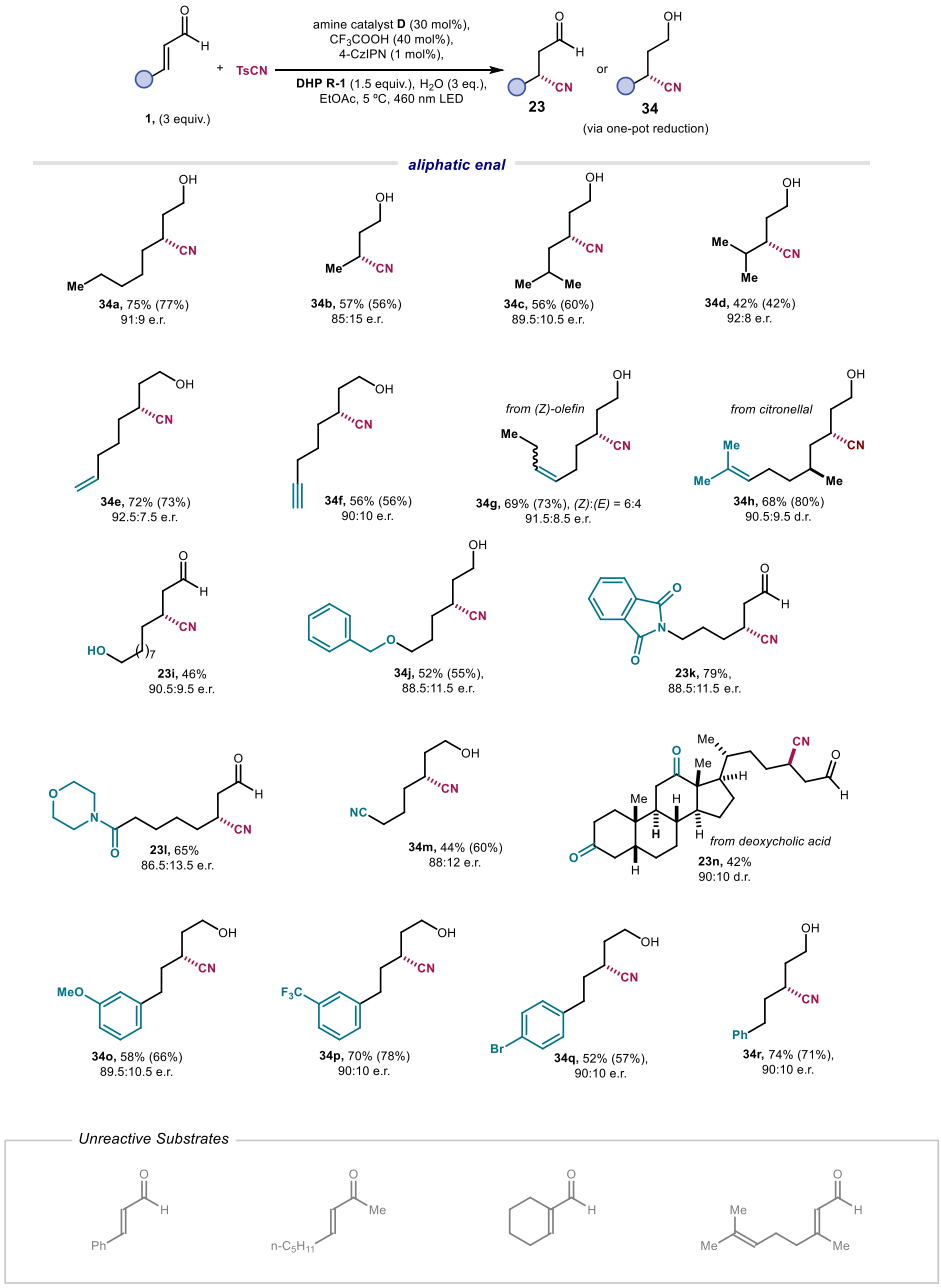

Figure 3.24. Substrate scope of enals for the asymmetric conjugate cyanation. Reactions performed on a 0.25 mmol scale using 3 equiv. of enal **1** in 0.5 mL of EtOAc under illumination at 460 nm for 18-22 h. Products were isolated as cyanoaldehydes **23** or cyanoalcohols **34** upon one-pot $NaBH_4$ reduction of crude mixture ($NaBH_4$ in THF/water 4:1, 0 °C, 1.5 h). For cyanoalcohols **34,** yields are given over two steps (analytical yields of cyanoaldehydes **23** are given in parentheses)

The method was also suitable for the cyanation of natural product-derived scaffolds, such as a chiral terpene (**34h**, from *citronellal*) and a complex steroid derivative adorned with reactive ketone functionalities (**23n**, from *deoxycholic acid*). The corresponding cyanation products were obtained with good stereoselectivity (e.r. ~ 90:10), establishing that catalyst control is the dictating factor for stereoinduction, while pre-existing chiral centers had no observable effect on the stereogenic bond formation.

As a limitation of the system, linear methyl enones, α-substituted and 2,2-disubstuted enals did not yield the desired products, possibly because of their low tendency to form iminium ion with the weakly nucleophilic amine catalyst **D**. Cinnamaldehyde also remained unreactive under this set of reaction conditions.

3.4.2.2 Synthetic Applications

To investigate the synthetic utility of this methodology, the conjugate cyanation of **1a** was scaled up to 1 mmol scale with negligible effects on reaction efficiency (Figure 3.25a, product **34a** isolated in 55% yield and e.r. = 90.5:9.5).

The conjugate cyanation granted access to difunctional β-cyanoaldehyde adducts **23** that are readily converted to a variety of useful chiral building blocks (Figure 3.25b). After borohydride reduction and isolation (path *iii*), cyanoalcohol **34d** was acylated (path *iv*). Diffractable crystals were obtained by vapor diffusion from a solution of the benzoate ester **35**, which enabled the assignment of the absolute configuration by single-crystal X-ray crystallographic analysis (section 3.6.12).[52]

[52] Crystallographic data for compound **38** has been deposited with the Cambridge Crystallographic Data Centre, accession number CCDC 2197381.

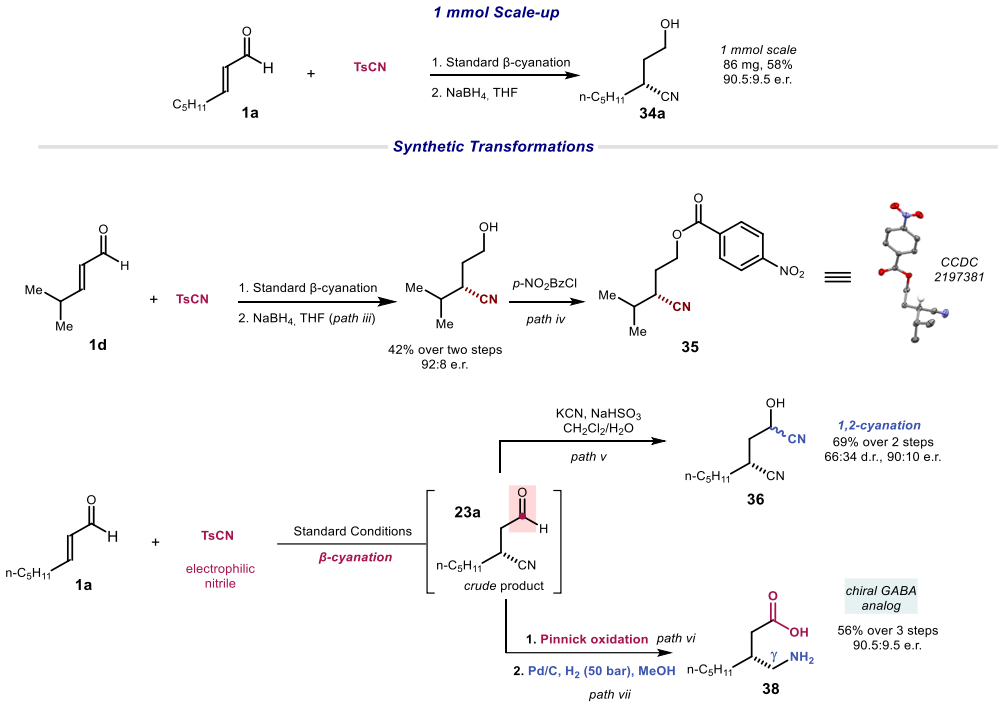

Figure 3.25. Synthetic manipulations of β-cyanoaldehydes. **(a)** 1 mmol scale-up stereoselective conjugate cyanation, **(b)** Synthetic modifications *en route* to useful organic scaffolds. Conditions for Pinnick oxidation: $NaClO_2$, NaH_2PO_4, *t*-BuOH:water (2:1).

Leveraging on the synthetic versatility of the aldehyde moiety, the crude reaction mixture was further reacted with a traditional nucleophilic cyanide (path *v*). This telescoped double cyanation, which sequentially combined a radical and a polar process with orthogonal chemoselectivity, directly led to cyanohydrin **36** in high yield and enantiopurity, despite a poor diastereocontrol (d.r. = 66:34). Alternatively, the crude product **23a** could undergo Pinnick oxidation to β-cyano-carboxylic acid **37** (path *vi*). Subsequent heterogeneous hydrogenation of the nitrile functionality (path *vii*) offered a straightforward entry into biologically valuable γ-aminobutyric acid (GABA) derivative **38** in moderate yield without erosion of enantioenrichment.

3.4.2.3 Mechanistic Discussions

Figure 3.26a details our proposed mechanism for this stereoselective conjugate cyanation of enals **1**. Upon excitation, photocatalyst 4-CzIPN is quenched by dihydropyridine **R-1** (E (**R**$^{\bullet+}$**/R**) = +1.28 V vs SCE) to form 4-CzIPN$^{\bullet-}$ ($E_{1/2}$(**4-CzIPN/4-CzIPN**$^{\bullet-}$) = –1.24 V vs SCE). The 4-CzIPN$^{\bullet-}$ would undergo an SET to the electron-poor iminium ion **I**, generated upon condensation of aminocatalyst **D** and enal **1**, to afford the chiral β-enaminyl radical **III**. The steric fragment within **III** could then master the interception of TsCN, inferring a high degree of stereoselectivity and β-site selectivity. Upon stereocontrolled nitrile transfer, the ensuing radical **XXV** undergoes β-fragmentation, leading to enamine **XXVI** while releasing the tosyl radical **XIII**, responsible for the formation of by-product **23'**. Hydrolysis of **XXVI** will then afford the target chiral β-cyanoaldehyde **23** while regenerating the organocatalyst **D**.

Precedent literature has demonstrated that TsCN can be reductively activated, yielding tosyl radical and cyanide anion.[53] To investigate whether this was a relevant pathway in our system, CV measurements showcased that TsCN (E_{red} = -1.32V vs Ag/AgCl) has a higher reduction potential than iminium ion (E_{red} ~ -0.7 V VS Ag/AgCl), which suggested that iminium ion can be favorably reduced in the presence of TsCN. In Stern-Volmer quenching studies, TsCN had marginal effects (K_{SV} < 5 M^{-1}) on the emission intensity from the excited photocatalyst. These results are consistent with our proposed mechanism.

[53] Sun, J.; Li, P.; Guo, L.; Yu, F.; He, Y.-P. and Chu, L. "Catalytic, metal-free sulfonylcyanation of alkenes via visible light organophotoredox catalysis." *Chem. Commun.* **2018**, *54*, 3162.

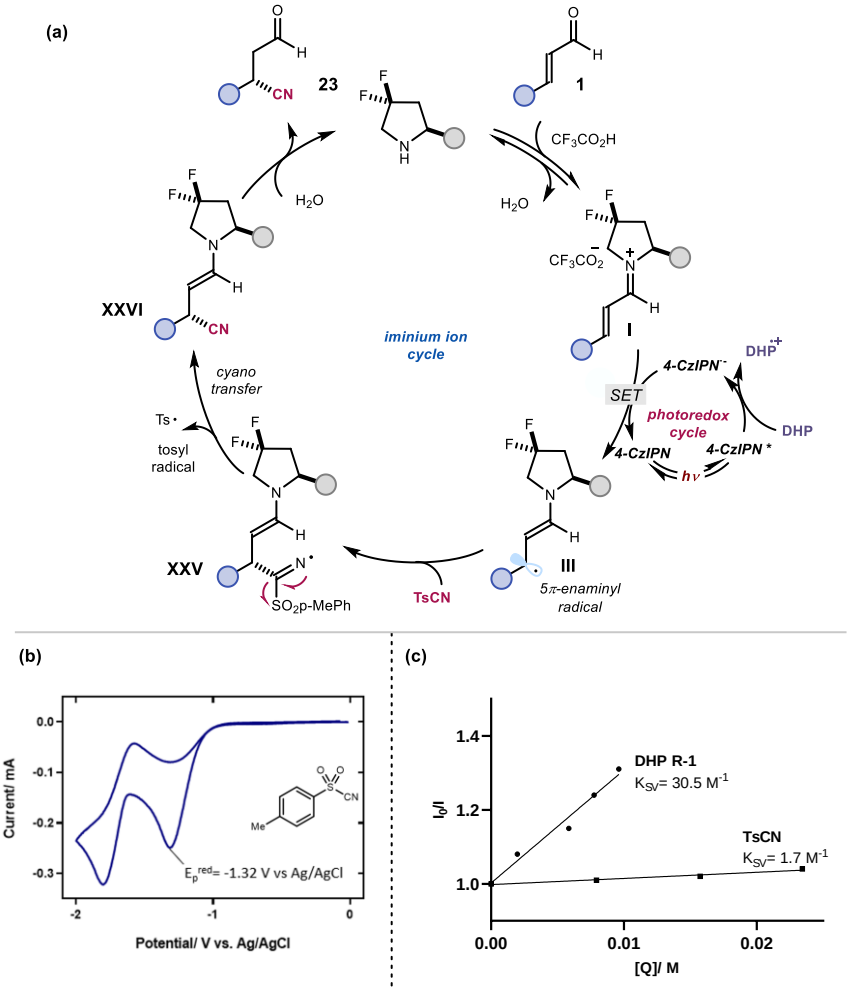

Figure 3.26. Mechanistic studies for stereoselective conjugate cyanation of enals. **(a)** Proposed reaction mechanism. **(b)** Stern-Volmer quenching of 4-CzIPN **(c)** Cyclic voltammogram of TsCN.

3.5 Conclusions

To summarize, this chapter has shown how the synergistic action of photoredox catalysis and asymmetric organocatalysis can provide a versatile strategy to address longstanding problems in the asymmetric synthesis of valuable chiral molecules. Through a reductive radical *umpolung* logic, chiral 1,6-dicarbonyl compounds were synthesized through coupling of two different electron-deficient olefins. Realization of this tactic further enabled discovery of the first enantioselective conjugate cyanation of α,β-unsaturated aldehydes. Good functional group compatibility, exclusive regioselectivity and good enantioselectivity could be obtained for both transformations.

3.6 Experimental Section

General Information. The ^{1}H NMR, ^{19}F NMR, ^{13}C NMR spectra, HPLC and UPC^{2} traces are available in the literature[1] and are not reported in the present dissertation.

The NMR spectra were recorded at 300 MHz, 400 MHz and 500 MHz for ^{1}H, 101 MHz and 126 MHz for $^{13}C\{^{1}H\}$ and $^{13}C\{^{1}H, ^{19}F\}$, 471 MHz for ^{19}F and $^{19}F\{^{1}H\}$, respectively. The chemical shifts (δ) for ^{1}H and $^{13}C\{^{1}H\}$ are given in ppm relative to residual signals of the solvents ($CHCl_3$ at 7.26 ppm for ^{1}H NMR, 77.16 ppm for $^{13}C\{^{1}H\}$NMR). Coupling constants are given in Hz. The following abbreviations are used to indicate the multiplicity: s, singlet; d, doublet; t, triplet; q, quartet; quint, quintet; sept, septet; m, multiplet; br s, broad signal. High-resolution mass spectra (HRMS) were obtained from the ICIQ High-Resolution Mass Spectrometry Unit on MicroTOF Focus and Maxis Impact (Bruker Daltonics) with electrospray ionization (ESI) or or atmospheric pressure chemical ionization (APCI). X-ray data were obtained from the ICIQ X-Ray Unit using a Bruker-Nonius diffractometer equipped with an APPEX 2 4K CCD area detector. Optical rotations were measured on a Polarimeter Jasco P-1030 and are reported as follows: $[\alpha]_D$ ambient temperature (c in g per 100 mL of solvent). Cyclic voltammetry studies were carried out on a Princeton Applied Research PARSTAT 2273 potentiostat offering compliance voltage up to ± 100 V (available at the counter electrode), ± 10 V scan range and ± 2 A current range. UV-vis measurements were carried out on an Agilent Cary 60 spectrophotometer equipped with silicon diode detector, double beam optics and 80 Hz Xenon Flash Lamp as light source. The emission spectra were recorded using a Fluorolog Horiba Jobin Yvon spectrofluorimeter equipped with a photomultiplier detector, a double monochromator, and a 450W xenon light source. Ozonolysis was carried out using a CMG 5-5 Ozone Generator and the OMG 200-2 Ozone Analyzer. Hydrogenation was carried out using a H-Cube Pro system using disposible CatCarts cartridges (30 mm, 10% Pd/C).

General Procedures. All reactions were set up under an argon atmosphere in dry glassware using standard Schlenk techniques, unless otherwise stated. Synthesis grade solvents were used as purchased. Anhydrous solvents were taken from a commercial SPS solvent dispenser. Chromatographic purification of products was accomplished using flash column chromatography (FC) on silica gel (Merck, 230-400 mesh). For thin layer chromatography

(TLC) analysis throughout this work, Merck precoated TLC plates (silica gel 60 GF254, 0.25 mm) were used, using UV light as the visualizing agent and common laboratory stains (potassium permanganate ($KMnO_4$), vanillin, phosphomolybdic acid (PMA), bromocresol) as developing agents. For preparative thin layer chromatography (prepTLC) purification throughout this work, Uniplate precoated TLC plates (silica gel GF254, 1000 micron) were used, using UV light as the visualizing agent. Organic solvents were removed under reduced pressure on a Büchi rotary evaporator.

Determination of Enantiomeric Purity: UPC^2 analysis on chiral stationary phase was performed on a Waters ACQUITY® instrument using IA-3, IB-3, ID-3, IE-3, IG-3 and OJ-3 chiral columns. HPLC analysis on chiral stationary phase was performed on an Agilient 1200 series HPLC, using Daicel Chiralpak IC-3 column with hexane:iPrOH as the eluent. The exact conditions for the analyses are specified in the experimental section of the individual compounds. UPC^2 traces were compared to racemic samples prepared by running the reaction either in the presence of a catalytic amount (20 mol%) of racemic catalyst **C** (for the conjugate cyanation) or racemic catalyst **B** (for the cross electrophile coupling), the latter being commercially available from Sigma Aldrich.

Materials: Commercial grade reagents and solvents were purchased at the highest commercial quality from Sigma Aldrich, Fluka, Acros Organics, Fluorochem or Alfa Aesar and used as received unless otherwise stated. The photocatalyst 4-CzIPN is commercially available and was used as obtained. The chiral secondary amine catalysts **A** and **B** are commercially available, while amine catalysts **C** and **D** were prepared according to reported procedures[12]. Some of the enal substrates 1, including octenal **1a**, crotonaldehyde **1c**, (E)-4-methylpent-2-enal **1e**, and enal **1h** are commercially available and were distilled prior to use. Other enals or acrylates were prepared according to literature procedures or as detailed in Section 3.6.1.

3.6.1 Synthesis of the Substrates and reagents

Preparation of Enals 1

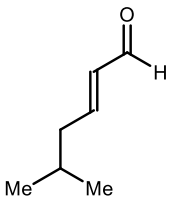

(*E*)-5-methylhex-2-enal (**1d**): prepared as reported in the literature, spectroscopic data are consistent with those previously reported[54].

^{1}H NMR (400 MHz, $CDCl_3$): δ = 9.52 (d, *J* = 7.9 Hz, 1H), 6.83 (dt, *J* = 15.5, 7.4 Hz, 1H), 6.12 (ddt, *J* = 15.6, 7.9, 1.4 Hz, 1H), 2.23 (td, *J* = 7.1, 1.4 Hz, 2H), 1.83 (sept, *J* = 6.6 Hz, 1H), 0.96 (d, *J* = 6.7 Hz, 6H) ppm.

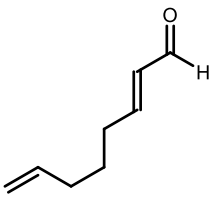

(E)-octa-2,7-dienal (**1f**). prepared as reported, spectroscopic data are consistent with those previously reported [55].

^{1}H NMR (300 MHz, $CDCl_3$): δ 9.51 (d, *J* = 7.9 Hz, 1H), 6.85 (dt, *J* = 15.6, 6.8 Hz, 1H), 6.12 (ddt, *J* = 15.6, 7.9, 1.5 Hz, 1H), 5.79 (ddt, *J* = 16.9, 10.2, 6.7 Hz, 1H), 5.09 – 4.96 (m, 2H), 2.35 (dtd, *J* = 8.1, 6.9, 1.5 Hz, 2H), 2.11 (dtt, *J* = 8.0, 6.8, 1.4 Hz, 2H), 1.62 (tt, *J* = 8.1, 6.9 Hz, 2H) ppm.

(*E*)-Oct-2-en-7-ynal (**1g**). The product was synthesized by stirring hex-5-ynal (0.800 g, 8.32 mmol, 1.0 equiv.), which was synthesized from 5-hexyn-1-ol using reported procedure [56], with (triphenylphosphoranylidene)-acetaldehyde (5.07 g, 2.0 equiv.) in dry CH_2Cl_2. The reaction was stirred at room temperature for 48 hours. The reaction mixture was carefully concentrated *in vacuo*, re-dissolved in 10% Et_2O in *n*-pentane and filtered through a pad of celite. The crude product was then purified by flash column chromatography (SiO_2, 5% Et_2O in n-pentane) to

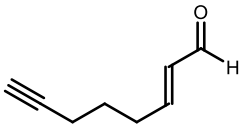

[54] Guo, C.; Saifuddin, M; Saravanan, T.; Sharifi, M. and Poelarends, G. J. "Biocatalytic Asymmetric Michael Additions of Nitromethane to α,β-Unsaturated Aldehydes via Enzyme-bound Iminium Ion Intermediates." *ACS Catal.* **2019,** *9*, 4369–4373.

[55] Singh, O. V.; Han, H. "Tandem Overman Rearrangement and Intramolecular Amidomercuration Reactions. Stereocontrolled Synthesis of cis- and trans-2,6-Dialkylpiperidines." *Org. Lett.* **2004,** *6*, 3067.

[56] Amoroso, J. W.; Borketey, L. S.; Prasad, G. and Schnarr, N. A. "Direct Acylation of Carrier Proteins with Functionalized β-Lactones." *Org. Lett.* **2010,** *12*, 2330.

afford **1l** as a colorless oil (562 mg, 55% yield). *Remarks: Product is highly volatile and would oxidise readily.*

^{1}H NMR (400 MHz, $CDCl_3$): δ = 9.51 (d, *J* = 7.8 Hz, 1H), 6.84 (dt, *J* = 15.6, 6.7 Hz, 1H), 6.15 (ddt, *J* = 15.6, 7.8, 1.5 Hz, 1H), 2.48 (dtd, *J* = 7.6, 6.8, 1.5 Hz, 2H), 2.26 (td, *J* = 6.9, 2.6 Hz, 2H), 1.99 (t, *J* = 2.6 Hz, 1H), 1.75 (p, *J* = 7.2 Hz, 2H) ppm.

^{13}C{^{1}H} NMR (101 MHz, $CDCl_3$): δ = 194.0, 157.3, 133.6, 83.3, 69.5, 31.6, 26.6, 18.0 ppm.

HRMS (APCI): Calculated for $[C_8H_{11}O]^+$ $[M+H]^+$: 123.0804, found: 123.0799.

(*S*,*E*)-5,9-Dimethyldeca-2,8-dienal (**1i**). (S)-3,7-dimethyloct-6-enal (1.00 g, 6.48 mmol, 1.0 equiv.) was dissolved in THF (anhydrous, 13.0 mL) under an Argon atmosphere. (Triphenylphosphoranylidene)-acetaldehyde (2.37 g, 7.78 mmol, 1.2 equiv.) was added and the mixture was refluxed for 2 days. Upon concentration, the product was filtered through a pad of silica gel (eluting with CH_2Cl_2). The filtrate was concentrated and purified by column chromatography (SiO_2, 1% EtOAc in hexanes) to afford afford 300 mg (26%) of **1j** as colorless oil. Analytical data is in agreement with the literature[57].

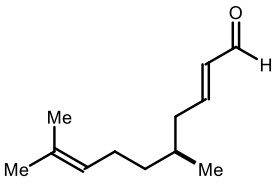

^{1}H NMR (500 MHz, $CDCl_3$): δ = 9.51 (d, *J* = 7.9 Hz, 1H), 6.83 (dt, *J* = 15.0, 7.3 Hz, 1H), 6.12 (ddd, *J* = 15.5, 7.9, 1.4 Hz, 1H), 2.39 – 2.32 (m, 1H), 2.22 – 2.15 (m, 1H), 2.06 – 1.94 (m, 2H), 1.74 – 1.66 (m, 1H), 1,69 (s, 3H), 1.60 (s, 3H), 1.43 – 1.32 (m, 1H), 1.29 – 1.17 (m, 2H), 0.94 (d, *J* = 6.7 Hz, 3H) ppm.

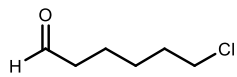

6-Chlorohexanal. Dess-martin periodinane (9.01 mmol, 3.82 g, 1.2 equiv.) was added portionwise to a mixture of 6-chlorohexan-1-ol (7.51 mmol, 1.0 mL, 1.0 equiv.) and water (8.26 mmol, 149 µL, 1.1 equiv.) in CH_2Cl_2 (37 mL) previously cooled to 0 °C. The reaction mixture was let to warm to room temperature and further stirred for 2 h until completion of the reaction. The reaction

[57] Landa, A.; Puente, Á.; Santos, J. I.; Vera, S.; Oiarbide, M. and Palomo, C. "Catalytic Conjugate Additions of Geminal Bis(sulfone)s: Expanding the Chemistry of Sulfones as Simple Alkyl Anion Equivalents." *Chem. Eur. J.* **2009,** 15, 11954.

mixture was then cooled to 0 °C and carefully quenched by a 1:1 mixture of 10% aq. $Na_2S_2O_3$ and sat. aq. $NaHCO_3$ (50 mL) and let to stir until complete dissolution of the reaction mixture. The organic layer was further washed with a 1:1 mixture of 10% aq. $Na_2S_2O_3$ and sat. aq. $NaHCO_3$ (3x 25 mL) and dried over $MgSO_4$. The volatiles were removed under reduced pressure and the crude was purified by flash column chromatography (SiO_2, 25% Et_2O in hexanes) to obtain 6-chlorohexanal (1.01 g, quant.) as a colorless oil. Spectroscopic data are consistent with those previously reported.[58]

^{1}H NMR (400 MHz, $CDCl_3$): δ = 9.78 (t, *J* = 1.6 Hz, 1H), 3.54 (t, *J* = 6.6 Hz, 2H), 2.47 (td, *J* = 7.3, 1.6 Hz, 2H), 1.88 – 1.75 (m, 2H), 1.71 – 1.60 (m, 2H), 1.53 – 1.39 (m, 2H) ppm.

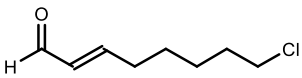

(*E*)-8-Chlorooct-2-enal (**1j**). Under an atmosphere of argon, a solution of (triphenylphosphoranylidene)acetaldehyde (10.9 mmol, 3.32 g, 1.4 equiv.) and 6-chlorohexanal (7.80 mmol, 1.01 g, 1.0 equiv.) in anhydrous THF (16 mL) was stirred under reflux for 16 h. The reaction mixture was allowed to cool to room temperature and carefully concentrated under reduced pressure. The crude was purified by flash column chromatography (SiO_2, 20% Et_2O in hexanes) to obtain **1s** (324 mg, 26%, *E*/*Z* = 9:1) as a colorless oil. (NMR spectra contain solvent peaks due to low boiling point of product).

^{1}H NMR (300 MHz, $CDCl_3$, mixture of isomers): δ = 9.51 (d, *J* = 7.9 Hz, 1H), 7.16 – 7.00 (m, 1H, *Z*-isomer), 6.84 (dt, *J* = 15.6, 6.8 Hz, 1H, *E*-isomer), 6.34 – 6.25 (m, 1H, *Z*-isomer), 6.12 (ddt, *J* = 15.6, 7.9, 1.5 Hz, 1H, *E*-isomer), 3.54 (t, *J* = 6.6 Hz, 3H) 2.43 – 2.31 (m, 2H), 1.93 – 1.72 (m, 2H), 1.63 – 1.45 (m, 4H) ppm.

^{13}C{^{1}H} NMR (101 MHz, $CDCl_3$, major isomer): δ = 194.1, 158.2, 133.4, 44.9, 32.6, 32.4, 27.3, 26.5 ppm.

HRMS (ESI): Calculated for $[C_8H_{13}ClONa]^+$ $[M+Na]^+$: 183.0547; found: 183.0543.

[58] Fox, R. J.; Lalic, G. and Bergman, R. G. "Regio- and Stereospecific Formation of Protected Allylic Alcohols via Zirconium-Mediated S_N2' Substitution of Allylic Chlorides." *J. Am. Chem. Soc.* **2007,** 129, 14144.

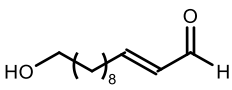

(*E*)-12-Hydroxydodec-2-enal (**1k**). Under an atmosphere of argon, a solution of undec-10-en-1-ol (5.12 mmol, 1.0 mL, 1.0 equiv.), acrolein (15.4 mmol, 1.0 mL, 3.0 equiv.) and Hoveyda-Grubbs Catalyst 2nd Generation (51.2 μmol, 32.2 mg, 1 mol%) in anhydrous CH_2Cl_2 (10 mL) was stirred under reflux for 16 h. The volatiles were removed under reduced pressure and the crude purified by flash column chromatography (SiO_2, 5-10% Et_2O in hexanes) to obtain **1q** (433 mg, 43%) as a colorless oil. Spectroscopic data are consistent with those previously reported[59].

^{1}H NMR (500 MHz, $CDCl_3$): δ = 9.50 (d, *J* = 7.9 Hz, 1H), 6.85 (dt, *J* = 15.6, 6.8 Hz, 1H), 6.11 (ddt, *J* = 15.6, 7.9, 1.5 Hz, 1H), 3.64 (t, *J* = 6.6 Hz, 2H), 2.36 – 2.29 (m, 2H), 1.60 – 1.54 (m, 2H), 1.53 – 1.48 (m, 2H), 1.35 – 1.29 (m, 10H).

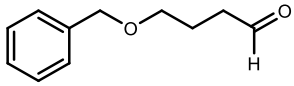

4-(Benzyloxy)butanal. Dess-martin periodinane (9.43 mmol, 4.00 g, 1.1 equiv.) was added portionwise to a mixture of 4-(benzyloxy)butan-1-ol (8.50 mmol, 1.5 mL, 1.0 equiv.) and water (8.93 mmol, 161 μL, 1.05 equiv.) in CH_2Cl_2 (42 mL) previously cooled to 0 °C. The reaction mixture was allowed to warm to room temperature and further stirred for 2 h until completion of the reaction. The reaction mixture was then cooled to 0 °C and carefully quenched by a 1:1 mixture of 10% aq. $Na_2S_2O_3$ and sat. aq. $NaHCO_3$ (75 mL) and let to stir until complete dissolution of the reaction mixture. The organic layer was further washed with a 1:1 mixture of 10% aq. $Na_2S_2O_3$ and sat. aq. $NaHCO_3$ (3x 50 mL) and dried over $MgSO_4$. The volatiles were removed under reduced pressure and the crude was purified by flash column chromatography (SiO_2, 5-10% EtOAc in hexanes) to obtain 4-(benzyloxy)butanal (1.35 g, 89%) as a colorless oil. Spectroscopic data are consistent with those previously reported[60].

^{1}H NMR (400 MHz, $CDCl_3$): δ = 9.78 (t, *J* = 1.6 Hz, 1H), 7.40 – 7.24 (m, 5H), 4.49 (s, 2H), 3.51 (t, *J* = 6.1 Hz, 2H), 2.55 (td, *J* = 7.1, 1.6 Hz, 2H), 1.95 (tt, *J* = 7.1, 6.0 Hz, 2H) ppm.

---

[59] Nishimura, T.; Sawano, T. and Hayashi, T. "Asymmetric Synthesis of β-Alkynyl Aldehydes by Rhodium-Catalyzed Conjugate Alkynylation." *Angew. Chem., Int. Ed.* **2009,** *48*, 8057.

[60] Packard, G. K.; Hu, Y.; Vescovi, A. and Rychnovsky, S. D. "Synthesis of Rimocidinolide Methyl Ester, the Aglycone of (+)-Rimocidin." *Angew. Chem., Int. Ed.* **2004,** 43, 2822.

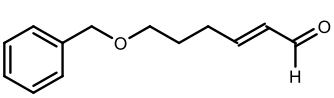

(*E*)-6-(Benzyloxy)hex-2-enal (**1l**). Under an argon atmosphere a solution of (triphenylphosphoranylidene)acetaldehyde (9.09 mmol, 2.77 g, 1.2 equiv.) and 4-(benzyloxy)butanal (7.57 mmol, 1.35 g, 1.0 equiv.) in anhydrous THF (15 mL) was stirred under reflux for 16 h. The reaction mixture was allowed to cool to room temperature and concentrated under reduced pressure. The crude was purified by flash column chromatography (SiO_2, 10-15% EtOAc in hexanes) to obtain **1n** (654 mg, 42 %, *E*/*Z* = 9:1) as a colorless oil.

^{1}H NMR (500 MHz, $CDCl_3$, mixture of isomers): δ = 9.53 (d, *J* = 8.0 Hz, 1H, *Z*-isomer), 9.49 (d, *J* = 7.9 Hz, 1H, *E*-isomer), 7.37 – 7.29 (m, 5H), 7.10 – 7.02 (m, 1H, *Z*-isomer), 6.85 (dt, *J* = 15.7, 6.8 Hz, 1H, *E*-isomer), 6.31 – 6.25 (m, 1H, *Z*-isomer), 6.12 (ddt, *J* = 15.6, 7.9, 1.5 Hz, 1H, *E*-isomer), 4.50 (s, 2H), 3.51 (t, *J* = 6.1 Hz, 2H), 2.55 (td, *J* = 7.1, 1.6 Hz, 1H, *Z*-isomer), 2.49 – 2.42 (m, 2H, *E*-isomer), 1.98 – 1.93 (m, 1H, *Z*-isomer), 1.83 (tt, *J* = 7.4, 6.2 Hz, 2H, *E*-isomer) ppm.

^{13}C{^{1}H} NMR (126 MHz, $CDCl_3$, major isomer): δ = 194.2, 158.3, 138.4, 133.3, 128.6, 127.8, 127.8, 73.2, 69.2, 29.7, 28.2 ppm.

HRMS (ESI): Calculated for $[C_{13}H_{16}O_2Na]^+$ $[M+Na]^+$: 227.1043; found: 227.1038.

Methyl 5-oxopentanoate. A few drops of conc. sulfuric acid were added to a solution of δ-

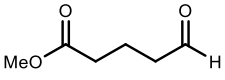

valerolactone (25.0 mmol, 2.50 g, 1.0 equiv.) in methanol (50 mL) and the reaction mixture was stirred under reflux for 2 h. The solvent was then removed under reduced pressure and the obtained crude was then dissolved in CH_2Cl_2 (150 mL) and cooled to 0 °C. Dess-martin periodinane (30.0 mmol, 12.7 g, 1.2 equiv.) was added portionswise to the reaction mixture, followed by water (28.7 mmol, 518 μL, 1.15 equiv.). The reaction mixture was then let to warm to room temperature and further stirred for 2 h until completion of the reaction. The reaction mixture was then cooled to 0 °C and carefully quenched by a 1:1 mixture of 10% aq. $Na_2S_2O_3$ and sat. aq. $NaHCO_3$ (150 mL) and let to stir until complete dissolution of the reaction mixture. The organic layer was further washed with a 1:1 mixture of 10% aq. $Na_2S_2O_3$ and sat. aq. $NaHCO_3$ (3x 100 mL) and dried

over $MgSO_4$. The volatiles were removed under reduced pressure and the crude was purified by flash column chromatography (SiO_2, 20% EtOAc in hexanes) to obtain methyl 5-oxopentanoate (2.00 g, 62%) as a colorless oil. Spectroscopic data are consistent with those previously reported[61].

^{1}H NMR (400 MHz, $CDCl_3$): δ = 9.74 (t, *J* = 1.3 Hz, 1H), 3.64 (s, 3H), 2.50 (td, *J* = 7.2, 1.3 Hz, 2H), 2.35 (t, *J* = 7.3 Hz, 2H), 1.93 (qq, *J* = 7.1 Hz, 2H) ppm.

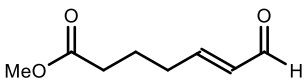

Methyl (*E*)-7-oxohept-5-enoate (**1m**). Under an atmosphere of argon, a solution of (triphenylphosphoranylidene)acetaldehyde (18.4 mmol, 5.61 g, 1.2 equiv.) and methyl 5-oxopentanoate (15.4 mmol, 2.00 g, 1.0 equiv.) in anhydrous THF (31 mL) was stirred under reflux for 16 h. The reaction mixture was allowed to cool to room temperature and concentrated under reduced pressure. The crude was purified by flash column chromatography (SiO_2, 5-20% EtOAc in hexanes) to obtain **1u** as a colorless oil. Spectroscopic data are consistent with those previously reported[62].

^{1}H NMR (400 MHz, $CDCl_3$): δ = 9.50 (d, *J* = 7.8 Hz, 1H), 6.81 (dt, *J* = 15.7, 6.7 Hz, 1H), 6.12 (ddt, *J* = 15.7, 7.8, 1.5 Hz, 1H), 3.66 (s, 3H), 2.41 – 2.33 (m, 4H), 1.85 (qq, *J* = 7.4 Hz, 2H) ppm.

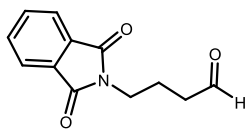

4-(1,3-Dioxoisoindolin-2-yl)butanal. The product was synthesized by stirring 2-(4-hydroxybutyl)isoindoline-1,3 dione (2.51 g, 11.4 mmol, 1.00 equiv.), which was prepared according to previous report[63], with pyridinium chlorochromate (PCC, 2.95 g, 1.20 equiv.) in dry CH_2Cl_2 (15 mL) overnight. The crude product was filtered through a pad of celite, concentrated *in vacuo* and purified by flash column chromatography (SiO_2, 25%

[61] Gannett, P. M.; Nagel, D. L.; Reilly, P. J.; Lawson, T.; Sharpe, J. and Toth, B. "Capsaicinoids: their separation, synthesis, and mutagenicity." *J. Org. Chem.* **1988**, 53, 1064.

[62] Egger, J.; Bretscher, P.; Freigang, S.; Kopf, M. and Carreira, E. M. "Discovery of a highly potent anti-inflammatory epoxyisoprostane-derived lactone." *J. Am. Chem. Soc.* **2014,** 136, 17382.

[63] Wappes, E. A.; Nakafuku, K. M. and Nagib, D. A. "Directed β C–H Amination of Alcohols via Radical Relay Chaperones." *J. Am. Chem. Soc.* **2017,** 139, 10204.

EtOAc in hexanes) to afford the aldehyde as white solid (1.40 g, 56% yield). The spectroscopic data is consistent with previous report.[64]

^{1}H NMR (300 MHz, $CDCl_3$): δ = 9.67 (t, *J* = 1.2 Hz, 1H), 7.75 – 7.65 (m, 2H), 7.65 – 7.58 (m, 2H), 3.60 (t, *J* = 6.9 Hz, 2H), 2.46 (td, *J* = 7.2, 1.2 Hz, 2H), 1.89 (p, *J* = 7.0 Hz, 2H) ppm.

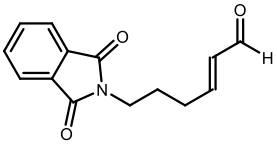

(*E*)-6-(1,3-Dioxoisoindolin-2-yl)hex-2-enal (**1n**). The product was synthesized by stirring 4-(1,3-dioxoisoindolin-2-yl)butanal (2.10 g, 9.67 mmol, 1.0 equiv.) with (triphenylphosphoranylidene)-acetaldehyde (3.53 g, 1.2 equiv.) in dry THF (21.0 mL). The reaction was heated under reflux for 24 hours. The reaction mixture was concentrated *in vacuo* and purified by flash column chromatography (SiO_2, 25% EtOAc in hexanes). The crude product was then recrystallized from CH_2Cl_2/ hexanes to afford **3m** as white solid. (582 mg, 25% yield).

^{1}H NMR (500 MHz, $CDCl_3$): δ = 9.38 (d, *J* = 7.8 Hz, 1H), 7.74 (dd, *J* = 5.5, 3.0 Hz, 2H), 7.64 (dd, *J* = 5.5, 3.1 Hz, 2H), 6.77 (dt, *J* = 15.6, 6.7 Hz, 1H), 6.05 (ddt, *J* = 15.7, 7.8, 1.6 Hz, 1H), 3.65 (t, *J* = 7.0 Hz, 2H), 2.38 – 2.29 (m, 2H), 1.84 (p, *J* = 7.4 Hz, 2H) ppm.

^{13}C{^{1}H} NMR (126 MHz, $CDCl_3$): δ = 193.9, 168.5, 156.7, 134.2, 133.6, 132.1, 123.5, 37.4, 30.1, 26.9 ppm.

HRMS (ESI): Calculated for $[C_{14}H_{13}NO_3Na]^+$ $[M+Na]^+$: 266.0788, found: 266.0788.

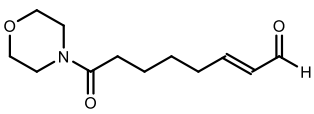

(*E*)-8-Morpholino-8-oxooct-2-enal (**1o**). A solution of 1-morpholinohept-6-en-1-one (7.00 mol, 1.38 g, 1.0 equiv. previously prepared following a reported procedure [65] in anhydrous CH_2Cl_2 (28 mL) was cooled to -78 °C and degassed with a stream of oxygen. Ozone was then bubbled through the reaction mixture until it turned light blue. The reaction

[64] Spallarossa, M.; Wang, Q.; Riva, R. and Zhu, J. "Synthesis of Vinyl Isocyanides and Development of a Convertible Isonitrile." *Org. Lett.* **2016,** 18, 1622.

[65] Bigi, M. A. and White, M. C. "Terminal Olefins to Linear α,β-Unsaturated Ketones: Pd(II)/Hypervalent Iodine Co-catalyzed Wacker Oxidation–Dehydrogenation." *J. Am. Chem. Soc.* **2013,** 135, 7831.

was then purged with oxygen to remove excess of ozone and quenched with excess dimethyl sulfide. The reaction mixture was then let to warm to room temperature, the organic layer was washed with brine (3 x 30 mL) and dried over $MgSO_4$. The volatiles were removed under reduced pressure to obtain crude 6-morpholino-6-oxohexanal (950 mg, 68%) which was engaged in the next step without further purification.

Under an atmosphere of argon, a solution of (triphenylphosphoranylidene)acetaldehyde (5.72 mmol, 1.74 g, 1.2 equiv.) and 6-Morpholino-6-oxohexanal (4.77 mmol, 950 mg, 1.0 equiv.) in anhydrous THF (10 mL) was stirred under reflux for 16 h. The reaction mixture was allowed to cool to room temperature and concentrated under reduced pressure. The crude was purified by flash column chromatography (SiO2, 2% MeOH in CH_2Cl_2) to obtain **1p** (219 mg, 20%) as a gum.

^{1}H NMR (500 MHz, $CDCl_3$): δ = 9.50 (d, *J* = 7.8 Hz, 1H), 6.85 (dt, *J* = 15.6, 6.7 Hz, 1H), 6.12 (ddt, *J* = 15.6, 7.9, 1.5 Hz, 1H), 3.69 – 3.65 (m, 4H), 3.65 – 3.59 (m, 2H), 3.49 – 3.42 (m, 2H), 2.41 – 2.35 (m, 2H), 2.34 (t, *J* = 7.3 Hz, 2H), 1.74 – 1.67 (m, 2H), 1.60 – 1.53 (m, 2H) ppm.

^{13}C{^{1}H} NMR (126 MHz, $CDCl_3$): δ = 194.1, 171.2, 158.2, 133.3, 67.1 (rotamer), 66.8 (rotamer), 46.1, 42.1, 32.7 (rotamer), 32.7 (rotamer), 27.8, 24.7 ppm.

HRMS (ESI): Calculated for $[C_{12}H_{19}NO_3Na]^+$ $[M+Na]^+$: 248.1257; found: 248.1261.

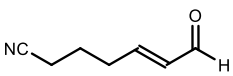

(*E*)-7-Oxohept-5-enenitrile (**1p**). Under an atmosphere of argon, a solution of hex-5-enenitrile (9.30 mmol, 1.0 mL, 1.0 equiv.), acrolein (45.0 mmol, 3.0 mL, 4.8 equiv.) and Hoveyda-Grubbs Catalyst 2nd Generation (186 μmol, 117 mg, 2 mol%) in anhydrous CH_2Cl_2 (19 mL) was stirred under reflux for 16 h. The volatiles were removed under reduced pressure and the crude purified by flash column chromatography (SiO_2, 50% EtOAc in hexanes) to obtain **1o** (340 mg, 30%) as colorless oil. Spectroscopic data are consistent with those previously reported[66].

[66] Shiomi, S.; Sugahara, E. and Ishikawa, H. "Efficient Organocatalytic Construction of C4-Alkyl Substituted Piperidines and Their Application to the Synthesis of (+)-α-Skytanthine." *Chem. Eur. J.* **2015,** 21, 14758.

^{1}H NMR (400 MHz, $CDCl_3$): δ = 9.53 (d, *J* = 7.7 Hz, 1H), 6.80 (dt, *J* = 15.7, 6.7 Hz, 1H), 6.17 (ddt, *J* = 15.7, 7.7, 1.5 Hz, 1H), 2.57 – 2.48 (m, 2H), 2.46 – 2.36 (m, 2H), 1.95 – 1.86 (m, 2H).

(*R*,*E*)-6-((*5R,8R,9S,10S,13R,14S,17R*)-10,13-Dimethyl-3,12-dioxohexadecahydro-1H-cyclopenta[a]phenanthren-17-yl)hept-2-enal (**1q**).

(*R*)-4-((5R,8R,9S,10S,13R,14S,17R)-10,13-dimethyl-3,12-dioxohexadecahydro-1H-cyclopenta[a]phenanthren-17-yl)pentanal (600 mg, 1.61 mmol, 1.0 equiv., prepared according to a previous report[67]) was dissolved in THF (anhydrous, 10.0 mL) under an argon atmosphere. (triphenylphosphoranylidene)-acetaldehyde (784 mg, 2.58 mmol, 1.6 equiv.) were added and the mixture was refluxed for 6 days. In order to achieve full conversion, another 0.4 equiv. of (triphenylphosphoranylidene)-acetaldehyde were added and the mixture was refluxed for 1 day. Upon concentration, the mixture was purified by column chromatography (SiO2, 15-20% EtOAc in hexanes). Fractions with minor impurities (< 20% by NMR) were combined, concentrated and purified again by column chromatography (SiO_2, 1% MeOH in CH_2Cl_2) to afford 84.0 mg (13%) of **1r** as colorless foam. $[\alpha]_D^{25}$ = +76.4 (c = 1.0, $CHCl_3$)

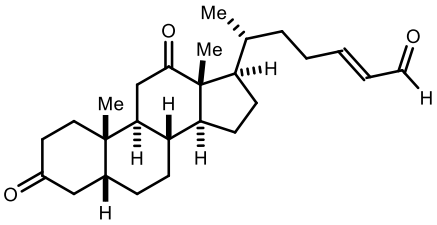

^{1}H NMR (400 MHz, $CDCl_3$): δ = 9.49 (d, *J* = 7.9 Hz, 1H), 6.84 (ddd, *J* = 15.6, 7.2, 6.3 Hz, 1H), 6.11 (ddt, *J* = 15.6, 7.9, 1.5 Hz, 1H), 2.66 – 2.52 (m, 2H), 2.49 – 2.22 (m, 3H), 2.22 – 2.14 (m, 1H), 2.13 – 1.98 (m, 3H), 1.92 (dddd, *J* = 15.9, 8.3, 6.3, 3.4 Hz, 6H), 1.76 (ddt, *J* = 11.9, 7.1, 4.1 Hz, 2H), 1.67 – 1.56 (m, 2H), 1.50 – 1.38 (m, 2H), 1.37 – 1.26 (m, 4H), 1.18 – 1.07 (m, 1H), 1.10 (s, 3H), 1.05 (s, 3H), 0.88 (d, *J* = 6.2 Hz, 3H) ppm.

^{13}C{^{1}H} NMR (101 MHz, $CDCl_3$): δ = 214.2, 212.2, 194.3, 159.4, 133.0, 58.7, 57.7, 46.7, 44.4, 43.8, 42.2, 38.5, 37.0, 36.9, 35.9, 35.7, 35.6, 33.7, 30.0, 27.8, 26.7, 25.6, 24.4, 22.3, 18.8, 11.8 ppm.

[67] Edelsztein, V. C.; Di Chenna, P. H. and Gerardo, B. "Synthesis of C-C bonded dimeric steroids by olefin metathesis." *Tetrahedron* **2009,** 65, 3615.

HRMS (ESI): Calculated for $[C_{27}H_{42}NaO_4]^+$ [M+MeOH+Na]$^+$: 453.2975; found: 453.2970.

6-Oxohexanoic acid. A solution of 6-heptenoic acid (7.21 mol, 977 µL, 1.0 equiv.) in anhydrous CH_2Cl_2 (29 mL) was cooled to -78 °C and degassed with a stream of oxygen. Ozone was then bubbled through the reaction mixture until it turned blue. The reaction was then purged with oxygen to remove excess of ozone and quenched with excess dimethyl sulfide. The reaction mixture was then lallowed to warm to room temperature, the organic layer was washed with sat. aq. NH_4Cl (3x 30 mL) and dried over $MgSO_4$. The volatiles were removed under reduced pressure to obtain crude 6-oxohexanoic acid (969 mg, quant.) which was engaged in the next step without further purification.

(*E*)-8-Oxooct-6-enoic enal (**1r**). 6-Oxohexanoic acid (937 mg, 7.20 mmol, 1.0 equiv.) was dissolved in THF (anhydrous, 14.4 mL) under an Argon atmosphere. (Triphenylphosphoranylidene)-acetaldehyde (2.894 g, 9.36 mmol, 1.3 equiv.) was added and the mixture was stirred for 6 days at room temperature. Upon concentration, the residue was purified by column chromatography (SiO_2, EtOAc/hexanes/AcOH = 20:79:1) to afford 289 mg (26%) of **1t** as bright yellow solid.

^{1}H NMR (500 MHz, $CDCl_3$): δ = 9.51 (d, *J* = 7.9 Hz, 1H), 6.84 (dt, *J* = 15.6, 6.8 Hz, 1H), 6.14 (ddt, *J* = 15.6, 7.8, 1.5 Hz, 1H), 2.43 – 2.34 (m, 4H), 1.75 – 1.66 (m, 2H), 1.64 – 1.55 (m, 2H) ppm.

^{13}C{^{1}H} NMR (126 MHz, $CDCl_3$): δ = 194.2, 178.5, 157.9, 133.4, 33.6, 32.4, 27.3, 24.2 ppm.

HRMS (ESI): Calculated for $[C_8H_{11}O_3]^-$ [M-H]$^-$: 155.0714; found: 155.0714.

3-(3-Methoxyphenyl)propanal. 3-(3-methoxyphenyl)propan-1-ol (1.66 g, 10.0 mmol, 1.0 equiv.) was dissolved in CH_2Cl_2 (50 mL). The mixture was cooled to 0 °C and Dess-Martin periodinane (5.09 g, 12.0 mmol, 1.2 equiv.) was added in portions over 10 minutes. The mixture

was stirred for 16 h and quenched carefully with a mixture of aqueous $NaHCO_3$ (saturated, 100 mL) and aqueous NaS_2O_3 (10%, 100 mL) and stirred vigorously for 1 hour. The layers were separated and the aqueous layer was extracted with CH_2Cl_2 (2 x 100 mL). The combined organic layers were dried with $MgSO_4$, concentrated and purified by column chromatography (SiO_2, 10% EtOAc in hexanes) to afford 1.56 g (95%) of aldehyde. Analytical data is in agreement with the literature[68].

^{1}H NMR (500 MHz, $CDCl_3$): δ = 9.82 (t, *J* = 1.4 Hz, 1H), 7.21 (td, *J* = 7.7, 0.8 Hz, 1H), 6.80 – 6.73 (m, 3H), 3.80 (s, 3H), 2.94 (t, *J* = 7.6 Hz, 2H), 2.78 (t, *J* = 7.7 Hz, 2H) ppm.

(*E*)-5-(3-Methoxyphenyl)pent-2-enal (**1s**). 3-(3-methoxyphenyl)propanal (1.56 g, 9.53 mmol, 1.0 equiv.) was dissolved in THF (anhydrous, 19 mL) under an argon atmosphere. (Triphenylphosphoranylidene)-acetaldehyde (3.48 g, 11.4 mmol, 1.2 equiv.) was added and the mixture was refluxed for 1 day. Upon concentration, the product was purified by column chromatography (SiO_2, 5-10% EtOAc in hexanes). Clean fractions were combined to afford 751 mg (41%) of **1f** as yellow oil.

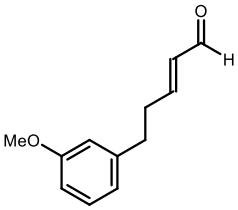

^{1}H NMR (400 MHz, $CDCl_3$): δ = 9.50 (d, *J* = 7.8 Hz, 1H), 7.23 (dd, *J* = 8.2, 7.5 Hz, 1H), 6.85 (dt, *J* = 15.6, 6.7 Hz, 1H), 6.80 – 6.73 (m, 3H), 6.14 (ddt, *J* = 15.7, 7.9, 1.5 Hz, 1H), 3.80 (s, 3H), 2.81 (t, *J* = 7.6 Hz, 2H), 2.71 – 2.63 (m, 2H) ppm.

^{13}C{^{1}H} NMR (101 MHz, $CDCl_3$): δ = 194.1, 159.9, 157.4, 142.0, 133.6, 129.7, 120.8, 114.4, 111.6, 55.3, 34.2 (2C) ppm.

HRMS (ESI): Calculated for $[C_{12}H_{14}NaO_2]^+$ $[M+Na]^+$: 213.0886; found: 213.0889.

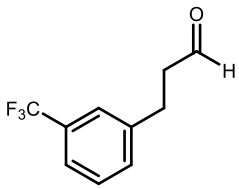

3-(3-(Trifluoromethyl)phenyl)propanal. 3-(3-(trifluoromethyl)phenyl)-propan-1-ol (2.04 g, 10.0 mmol, 1.0 equiv.) was dissolved in CH_2Cl_2 (50 mL). The mixture was cooled to 0 °C and Dess-Martin periodinane (5.09 g, 12.0 mmol, 1.2 equiv.)

[68] Ren, W.; Chang, W.; Dai, J.; Li, J. and Shi, Y. "An Effective Pd-Catalyzed Regioselective Hydroformylation of Olefins with Formic Acid." *J. Am. Chem. Soc.* **2016,** 138, 14864.

was added in portions over 10 minutes. The mixture was stirred for 16 h and quenched carefully with a mixture of aqueous $NaHCO_3$ (saturated, 100 mL) and aqueous NaS_2O_3 (10%, 100 mL) and stirred vigorously for 1 hour. The layers were separated and the aqueous layer was extracted with CH_2Cl_2 (2 x 100 mL). The combined organic layers were dried with $MgSO_4$, concentrated and purified by column chromatography (SiO_2, 10% EtOAc in n-hexanes) to afford 1.47 g (73%) of aldehyde. Analytical data is in agreement with the literature.[69]

^{1}H NMR (500 MHz, $CDCl_3$): δ = 9.83 (t, *J* = 1.2 Hz, 1H), 7.50 – 7.36 (m, 4H), 3.02 (t, *J* = 7.5 Hz, 2H), 2.83 (td, *J* = 7.5, 0.9 Hz, 2H) ppm.

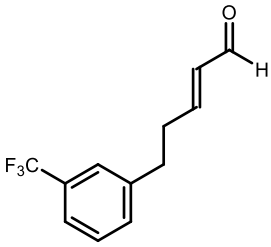

(*E*)-5-(3-(trifluoromethyl)phenyl)pent-2-enal (**1t**). 3-(3-(trifluoromethyl)phenyl)propanal (1.47 g, 7.28 mmol, 1.0 equiv.) was dissolved in THF (anhydrous, 15 mL) under an Argon atmosphere. (Triphenylphosphoranylidene)-acetaldehyde (2.22 g, 7.28 mmol, 1.0 equiv.) was added and the mixture was refluxed for 1 day. Upon concentration, the product was purified by column chromatography (SiO_2, 5-10% EtOAc in hexanes). Clean fractions were combined to afford 545 mg (33%) of **1g** as yellow oil.

^{1}H NMR (400 MHz, $CDCl_3$): δ = 9.51 (d, *J* = 7.8 Hz, 1H), 7.57 – 7.34 (m, 4H), 6.84 (dt, *J* = 15.7, 6.7 Hz, 1H), 6.14 (ddt, *J* = 15.7, 7.8, 1.5 Hz, 1H), 2.90 (d, *J* = 7.4 Hz, 2H), 2.74 – 2.64 (m, 2H) ppm.

^{13}C{^{1}H} NMR (126 MHz, $CDCl_3$): δ = 193.8, 156.3, 141.3, 133.8, 131.9, 131.1 (q, *J* = 32.0 Hz), 129.2, 125.2 (q, *J* = 3.9 Hz) 124.2 (q, *J* = 271.8 Hz), 123.5 (q, *J* = 3.8 Hz), 34.1, 34.0 ppm.

^{19}F{^{1}H} NMR (471 MHz, $CDCl_3$): δ = -62.64 ppm.

---

[69] Uto, Y.; Ogata, T., Harada, J.; Kiyotsuka, Y.; Ueno, Y.; Miyazawa, Y.; Kurata, H.; Deguchi, T.; Watanabe, N.; Takagi, T.; Wakimoto S.; Okuyama, R.; Abe, M.; Kurikawa, N.; Kawamura, S.; Yamato, M. and Osumi, J. "Novel and potent inhibitors of stearoyl-CoA desaturase-1. Part I: Discovery of 3-(2-hydroxyethoxy)-4-methoxy-N-[5-(3-trifluoromethylbenzyl)thiazol-2yl]benzamide." *Bio. Med. Chem. Lett.* **2009,** 19, 4151.

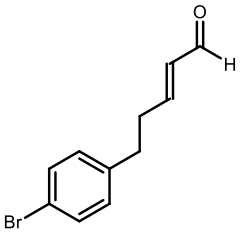

HRMS (ESI): Calculated for $[C_{12}H_{11}F_3NaO]^+$ $[M+Na]^+$: 251.0654; found: 251.0653.

3-(4-Bromophenyl)propanal. 3-(4-bromophenyl)propan-1-ol (2.15 g, 10.0 mmol, 1.0 equiv.) was dissolved in CH_2Cl_2 (50 mL). The mixture was cooled to 0 °C and Dess-Martin periodinane (5.09 g, 12.0 mmol, 1.2 equiv.) was added in portions over 10 minutes. The mixture was stirred for 16 h and quenched carefully with a mixture of aqueous $NaHCO_3$ (saturated, 100 mL) and aqueous NaS_2O_3 (10%, 100 mL) and stirred vigorously for 1 hour. The layers were separated and the aqueous layer was extracted with CH_2Cl_2 (2 x 100 mL). The combined organic layers were dried with $MgSO_4$, concentrated and purified by column chromatography (SiO_2, 10% EtOAc in hexanes) to afford 1.40 g (66%) of aldehyde as bright-yellow solid. Analytical data is in agreement with the literature[70].

^{1}H NMR (500 MHz, $CDCl_3$): δ = 9.81 (s, 1H), 7.41 (d, *J* = 8.3 Hz, 1H), 7.07 (d, *J* = 8.4 Hz, 2H), 2.91 (t, *J* = 7.4 Hz, 2H), 2.77 (td, *J* = 7.5, 1.1 Hz, 3H) ppm.

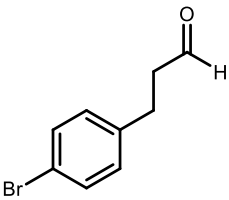

(*E*)-5-(4-Bromophenyl)pent-2-enal (**1u**). 3-(4-bromophenyl)propanal (1.40 g, 6.58 mmol, 1.0 equiv.) was dissolved in THF (anhydrous, 15 mL) under an Argon atmosphere. (Triphenylphosphoranylidene)-acetaldehyde (3.21 g, 10.5 mmol, 1.6 equiv.) was added and the mixture was refluxed for 1 day. Upon concentration, the product was purified by column chromatography (SiO_2, 5-10% EtOAc in hexanes) to afford 970 mg (62%) of **1h**. Analytical data is in agreement with the literature[71].

[70] Frost, C. G. and Hartley, B. C. "Lewis Base-Promoted Hydrosilylation of Cyclic Malonates: Synthesis of β-Substituted Aldehydes and γ-Substituted Amines." *J. Org. Chem.* **2009,** 74, 3599.

[71] Liu, Y.; Izzo, J. A.; McLeod, D.; Ričko, S.; Svenningsen, E. B.; Poulsen, T. B. and Jørgensen, K. A. "Organocatalytic Asymmetric Multicomponent Cascade Reaction for the Synthesis of Contiguously Substituted Tetrahydronaphthols." *J. Am. Chem. Soc.* **2021**, 143, 8208.

^{1}H NMR (500 MHz, $CDCl_3$): δ = 9.49 (d, *J* = 7.8 Hz, 1H), 7.43 (d, *J* = 8.4 Hz, 2H), 7.06 (d, *J* = 8.6 Hz, 2H), 6.82 (dt, *J* = 15.7, 6.7 Hz, 1H), 6.13 (ddt, *J* = 15.7, 7.8, 1.5 Hz, 1H), 2.79 (t, *J* = 7.6 Hz, 2H), 2.68 – 2.60 (m, 2H) ppm.

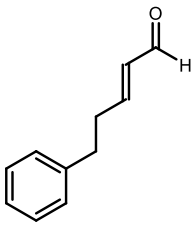

(*E*)-5-Phenylpent-2-enal (**1v**): prepared as reported literature, spectroscopic data are consistent with those previously reported[72].

^{1}H NMR (500 MHz, $CDCl_3$): δ = 9.50 (dd, *J* = 7.9, 0.8 Hz, 1H), 7.33 – 7.29 (m, 2H), 7.25 – 7.16 (m, 3H), 6.86 (dt, *J* = 15.7, 6.7 Hz, 1H), 6.14 (ddt, *J* = 15.6, 7.9, 1.5 Hz, 1H), 2.84 (t, *J* = 7.6 Hz, 2H), 2.70 – 2.65 (m, 2H) ppm.

(*E*)-3-(*trans*-2-Phenylcyclopropyl)acrylaldehyde (**28**). Under an atmosphere of argon, a solution of (triphenylphosphoranylidene)-acetaldehyde (8.28 mmol, 2.52 g, 1.4 equiv.) and (*trans*)-2-phenylcyclopropane-1-carbaldehyde (5.92 mmol, 865 mg, 1.0 equiv. prepared following a reported procedure[73]) in anhydrous THF (12 mL) was stirred under reflux for 16 h. The reaction mixture was allowed to cool to room temperature and concentrated under reduced pressure. The crude was purified by flash column chromatography (SiO_2, 5-10% Et_2O in hexanes) to obtain **10** (621 mg, 61%) as an orange solid. Spectroscopic data are consistent with those previously reported[74].

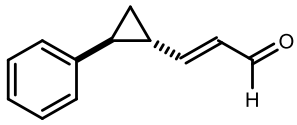

^{1}H NMR (400 MHz, $CDCl_3$): δ = 9.47 (d, *J* = 7.8 Hz, 1H), 7.34 – 7.26 (m, 2H), 7.25 – 7.19 (m, 1H), 7.14 – 7.07 (m, 2H), 6.46 (dd, *J* = 15.4, 9.7 Hz, 1H), 6.21 (dd, *J* = 15.4, 7.8 Hz, 1H), 2.33 – 2.26 (m, 1H), 1.96 (dddd, *J* = 9.5, 8.3, 5.4, 4.0 Hz, 1H), 1.64 – 1.56 (m, 1H), 1.41 (ddd, *J* = 9.0, 5.3 Hz, 1H) ppm.

---

[72] Bouisseau, A.; Gao, M. and Willis, M. C. "Traceless Rhodium-Catalyzed Hydroacylation Using Alkyl Aldehydes: The Enantioselective Synthesis of β-Aryl Ketones." *Chem. Eur. J.* **2016,** 22, 15624.

[73] Schmittel, M.; Mahajan, A. A.; Bucher, G. and Bats J. W. "Thermal C2−C6 Cyclization of Enyne−Allenes. Experimental Evidence for a Stepwise Mechanism and for an Unusual Thermal Silyl Shift." *J. Org. Chem.* **2007**, 72, 2166.

[74] Li, Z.; Huang, M.; Zhang, X.; Chen, J. and Huang, Y. "N-Heterocyclic Carbene-Catalyzed Four-Component Reaction: Chemoselective $C_{radical}$-$C_{radical}$ Relay Coupling Involving the Homoenolate Intermediate." *ACS Catal.* **2011,** 11, 10123.

Synthesis of Acrylates 7

General procedure **A** for the synthesis of benzyl phenylacetate esters: To a 25 mL round bottom flask was added phenylacetic acid (1.05 equiv.), potassium carbonate (0.6 equiv.) and benzyl bromide (1.0 equiv.). DMF (5.0 mL) was added and the reaction stirred at room temperature for 6 hours. Then, water (10 mL) and Et_2O (10 mL) were added. The layers were separated and the organic layer was washed with water (5 x 10 mL), dried with $MgSO_4$, and concentrated *in vacuo* to afford desired ester product. The ester was used directly in the next step without further purification.

General procedure **B** for synthesis of benzyl acrylate esters: the procedure was adopted from a previous report.[23] To a 50 mL round bottom flask was added benzyl phenylacetate ester (1.0 equiv.), potassium carbonate (1.0 equiv.), paraformaldehyde (10.0 equiv.) and tetrabutylammonium iodide (1.0 equiv.). Toluene (30 mL) was added and the reaction was heated at 80 °C and stirred for 4 hours in the dark. The reaction mixture was then washed with water, the layers were separated, and the organic layer was dried with $MgSO_4$. The crude product was then concentrated, re-dissolved in 10% Et_2O in hexanes and purified by passing through a pad of silica.

Benzyl 2-phenylacrylate (7a). Prepared according to reported procedure [25] using 2-phenylacrylic acid (500 mg, 3.37 mmol, 1.05 equiv.). The product was obtained as a colorless oil which solidifies upon storage at -20 °C (785 mg, 98% yield). The spectroscopic data is consistent with previous report[75].

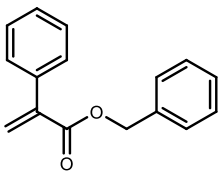

^{1}H NMR (400 MHz, $CDCl_3$): δ = 7.40-7.29 (m, 10H), 6.39 (d, *J* = 1.0 Hz, 1H), 5.93 (d, *J* = 1.0 Hz, 1H), 5.29 (s, 2H) ppm.

[75] Buxton, C. S.; Blakemore, D. C. and Bower, J. F. "Reductive Coupling of Acrylates with Ketones and Ketimines by a Nickel-Catalyzed Transfer-Hydrogenative Strategy." *Angew. Chem., Int. Ed.* **2017,** 56, 13824.

4-Methoxybenzyl 2-phenylacrylate (7b). Oxalyl chloride (11.4 mmol, 1.0 mL, 1.15 equiv.) was added to a solution of 2-phenylacrylic acid (10.0 mmol, 1.48 g, 1.0 equiv.) in anhydrous CH_2Cl_2 (25 mL) under inert atmosphere at 0 °C, followed by a few drops of DMF. The reaction mixture was let to warm to room temperature and stirred until the bubbling ceased. The reaction mixture was concentrated under reduced pressure and placed under an inert atmosphere. The crude residue was dissolved in anhydrous CH_2Cl_2 (25 mL) and (4-methoxyphenyl)methanol (11.4 mmol, 1.4 mL, 1.15 equiv.), pyridine (11.4 mmol, 922 μL, 1.15 equiv.) and *N*,*N*-dimethylpyridin-4-amine (1.00 mmol, 122 mg, 0.1 equiv.) were added to the reaction mixture, which was let to stir for 3 h. The reaction mixture was then quenched and washed with 1M HCl (3x 20 mL) and brine (20 mL) and the organic layer was dried over $MgSO_4$. The volatiles were removed under reduced pressure and the crude was purified by flash column chromatography (SiO_2, 10% EtOAc in hexanes) to obtain **5a** (2.15 g, 80%) as a colorless oil. Spectroscopic data are consistent with those previously reported.[76]

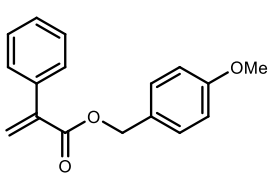

^{1}H NMR (400 MHz, $CDCl_3$): δ = 7.42 (dtd, *J* = 5.4, 3.1, 1.6 Hz, 2H), 7.38 – 7.33 (m, 5H), 6.94 – 6.88 (m, 2H), 6.37 (d, *J* = 1.2 Hz, 1H), 5.91 (d, *J* = 1.2 Hz, 1H), 5.23 (s, 2H), 3.82 (s, 3H) ppm.

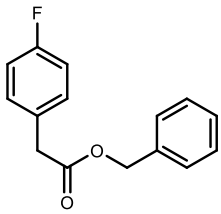

Benzyl 2-(4-fluorophenyl)acetate. Prepared according to the general procedure **A** using 4-fluorophenyl acetic acid (510 mg, 3.31 mmol). The product was obtained as a colorless oil, which solidifies upon storage at -20 °C (725 mg, 94% yield). The spectroscopic data is consistent with previous report[77].

[76] Kawashima, S., Aikawa, K. & Mikami, K. "Rhodium-Catalyzed Hydrocarboxylation of Olefins with Carbon Dioxide." *Eur. J. Org. Chem.* **2016,** 3166.

[77] Yu, W.; Yang, S., Xiong, F.; Fan, T.; Feng, Y.; Huang Y.; Fu J. and Wang T. "Palladium-catalyzed carbonylation of benzylic ammonium salts to amides and esters via C–N bond activation." *Org. Biomol. Chem*. **2018,** 16, 3099–3103

^{1}H NMR (400 MHz, $CDCl_3$): δ = 7.37 –7.28 (m, 5H), 7.36 – 7.21 (m, 2H), 6.99 (t, *J* = 8.7 Hz, 2H), 5.13 (s, 2H), 3.63 (s, 2H) ppm.

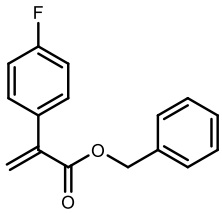

Benzyl 2-(4-fluorophenyl)acrylate (7c). Prepared according to general procedure **B** using benzyl 2-(4-fluororophenyl)acetate (770 mg, 3.15 mmol). The product was obtained as a light-yellow oil which solidifies upon storage at -20 °C (561 mg, 69% yield).

^{1}H NMR (500 MHz, $CDCl_3$): δ = 7.45 – 7.30 (m, 7H), 7.09 – 7.00 (m, 2H), 6.40 (d, *J* = 1.1 Hz, 1H), 5.90 (d, *J* = 1.1 Hz, 1H), 5.27 (s, 2H) ppm.

^{13}C{^{1}H} NMR (126 MHz, $CDCl_3$): δ = 166.5, 162.9 (d, J_{C-F} = 247.7 Hz), 140.3, 136.0, 132.8 (d, J_{C-F} = 3.3 Hz), 130.2 (d, J_{C-F} = 8.1 Hz), 128.7, 128.4, 128.3, 127.3, 115.2 (d, J_{C-F} = 21.6 Hz), 67.0 ppm.

^{19}F{^{1}H} NMR (471 MHz, $CDCl_3$): δ = -113.79 ppm.

HRMS (ESI): Calculated $C_{16}H_{13}FO_2Na$ $[M+Na]^+$: 279.0792, found: 279.0787.

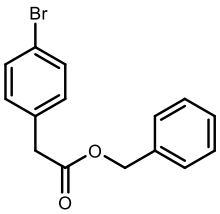

Benzyl 2-(4-bromophenyl)acetate. Prepared according to general procedure **A** using 4-bromophenyl acetic acid (510 mg, 2.37 mmol). The product was obtained 3d as a colorless oil which solidifies upon storage at -20 °C (677 mg, 98% yield). The spectroscopic data is consistent with previous report[54].

^{1}H NMR (400 MHz, $CDCl_3$): δ = 7.45 (d, *J* = 8.4 Hz, 2H), 7.37 – 7.27 (m, 5H), 7.16 (d, *J* = 8.7 Hz, 2H), 5.13 (s, 2H), 3.62 (s, 2H) ppm.

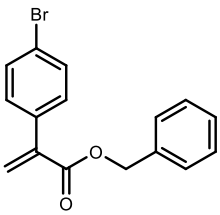

Benzyl 2-(4-bromophenyl)acrylate (7d). Prepared according to general procedure **B** using Benzyl 2-(4-bromorophenyl)acetate (677 mg, 2.22 mmol). The product was obtained 3d as a colorless oil which solidifies upon standing (567 mg, 81% yield). The spectroscopic data is consistent with previous report[72].

^{1}H NMR (400 MHz, $CDCl_3$): δ = 7.48 (d, *J* = 8.5 Hz, 2H), 7.43 – 7.33 (m, 5H), 7.30 (d, *J* = 8.5 Hz, 2H), 6.42 (d, *J* = 1.1 Hz, 1H), 5.93 (d, *J* = 1.1 Hz, 1H), 5.27 (s, 2H) ppm.

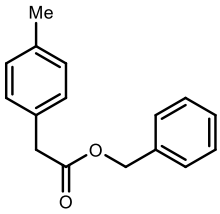

Benzyl 2-(p-tolyl)acetate. Prepared according to general procedure **A** using p-tolyl acetic acid (510 mg, 3.40 mmol). The product was obtained as a colorless oil (707 mg, 91% yield). The spectroscopic data is consistent with previous report[35b].

^{1}H NMR (400 MHz, $CDCl_3$): δ = 7.44 – 7.24 (m, 5H), 7.18 (d, *J* = 8.1 Hz, 2H), 7.14 (d, *J* = 8.0 Hz, 2H), 5.13 (s, 2H), 3.64 (s, 2H), 2.34 (s, 3H) ppm.

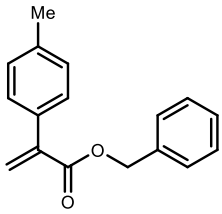

Benzyl 2-(p-tolyl)acrylate (7e). Prepared according to general procedure **B** using benzyl 2-(p-tolyl)acetate (707 mg, 2.94 mmol). The product was obtained as a colorless oil (390 mg, 55% yield). The spectroscopic data is consistent with previous report. [35b]

^{1}H NMR (500 MHz, $CDCl_3$): δ = 7.46 – 7.29 (m, 7H), 7.21 – 7.07 (m, 2H), 6.35 (d, *J* = 1.2 Hz, 1H), 5.89 (d, *J* = 1.2 Hz, 1H), 5.29 (s, 2H), 2.34 (s, 3H) ppm.

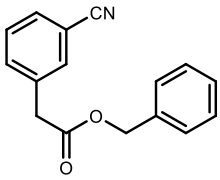

Benzyl 2-(3-cyanophenyl)acetate. Prepared according to general procedure **A** using 3-cyanophenyl acetic acid (510 mg, 3.16 mmol). The product was obtained as a brown oil (718 mg, 95% yield).

^{1}H NMR (500 MHz, $CDCl_3$): δ = 7.63 – 7.55 (m, 2H), 7.55 – 7.49 (m, 1H), 7.43 (td, *J* = 7.6, 0.9 Hz, 1H), 7.40 – 7.33 (m, 2H), 7.33 – 7.29 (m, 1H), 5.15 (s, 2H), 3.70 (s, 2H) ppm.

^{13}C{^{1}H} NMR (126 MHz, $CDCl_3$): δ = 170.4, 135.5, 135.4, 134.1, 133.1, 131.1, 129.5, 128.8, 128.6, 128.5, 118.7, 112.9, 67.23, 40.8. ppm

HRMS (ESI): Calculated for $C_{16}H_{13}NO_2Na$ $[M+Na]^+$: 274.0837, found: 274.0838.

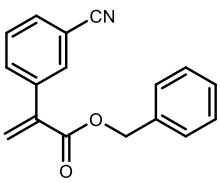

Benzyl 2-(3-cyanophenyl)acrylate (7f). Prepared according to general procedure **B** using Benzyl 2-(3-cyanophenyl)acetate (1210 mg, 4.82 mmol) with 4Å molecular sieves (10% by weight, 120 mg). The product was purified by column chromatography (SiO_2, 10% Et_2O in hexanes) to obtain 3d as a yellow oil (202 mg, 16% yield) which solidifies upon storage at -10 ºC.

^{1}H NMR (500 MHz, $CDCl_3$): δ = 7.77 (td, *J* = 1.7, 0.6 Hz, 1H), 7.69 (ddd, *J* = 7.9, 1.9, 1.2 Hz, 1H), 7.63 (dt, *J* = 7.8, 1.4 Hz, 1H), 7.48 (td, *J* = 7.8, 0.6 Hz, 1H), 7.45 – 7.41 (m, 4H), 7.41 – 7.29 (m, 1H), 6.56 (d, *J* = 0.8 Hz, 1H), 6.02 (d, *J* = 0.8 Hz, 1H), 5.32 (s, 2H) ppm.

^{13}C{^{1}H} NMR (126 MHz, $CDCl_3$): δ = 165.5, 139.3, 137.8, 135.5, 132.8, 132.1, 131.6, 129.1, 129.0, 128.7, 128.5, 128.2, 118.6, 112.4, 67.16 ppm.

HRMS (ESI): Calculated for $C_{17}H_{13}NO_2Na$ $[M+Na]^+$: 286.0838, found: 286.0837.

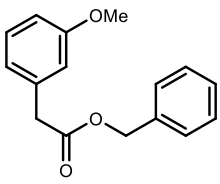

Benzyl 2-(3-methoxyphenyl)acetate. Prepared according to general procedure **A** using 3-methoxyphenyl acetic acid (500 mg, 3.01 mmol). The product was obtained as a colorless oil (713 mg, 96% yield).

^{1}H NMR (500 MHz, $CDCl_3$): δ = 7.43 – 7.28 (m, 5H), 7.24 (t, *J* = 7.8 Hz, 1H), 6.90 – 6.79 (m, 3H), 5.14 (s, 2H), 3.78 (s, 3H), 3.65 (s, 2H) ppm.

^{13}C{^{1}H} NMR (126 MHz, $CDCl_3$): δ = 171.4, 159.9, 136.0, 135.4, 129.7, 128.7, 128.4, 128.3, 121.8, 114.9, 113.0, 66.8, 55.3, 41.5 ppm.

HRMS (ESI): Calculated for $C_{16}H_{16}O_3Na$ $[M+Na]^+$: 279.0992, found: 279.0982.

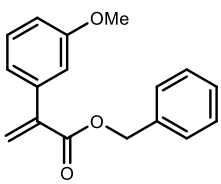

Benzyl 2-(3-methoxyphenyl)acrylate (7g). Prepared according to the general procedure **B** using benzyl 2-(3-methoxyphenyl)acetate (384 mg, 1.50 mmol). The product was obtained as a light yellow oil (150 mg, 37% yield).

^{1}H NMR (500 MHz, $CDCl_3$): δ = 7.49 – 7.33 (m, 5H), 7.30 (dd, *J* = 8.2, 7.7 Hz, 1H), 7.05 (ddd, *J* = 7.6, 1.6, 1.0 Hz, 1H), 7.01 (dd, *J* = 2.6, 1.6 Hz, 1H), 6.92 (ddd, *J* = 8.3, 2.6, 0.9 Hz, 1H), 6.42 (d, *J* = 1.2 Hz, 1H), 5.95 (d, *J* = 1.2 Hz, 1H), 5.31 (s, 2H), 3.81 (s, 3H) ppm.

^{13}C{^{1}H} NMR (126 MHz, $CDCl_3$): δ = 166.5, 159.4, 141.2, 138.0, 136.0, 129.2, 128.7, 128.3, 128.3, 127.2, 120.9, 114.0 (2C), 66.9, 55.3 ppm.

HRMS (ESI): Calculated for $C_{17}H_{16}O_3Na$ $[M+Na]^+$: 291.0992, found: 291.0978.

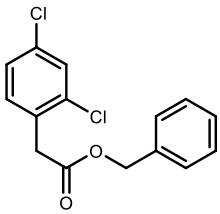

Benzyl 2-(2,4-dichlorophenyl)acetate. Prepared according to general procedure **A** using 2,4-dichlorophenyl acetic acid (615 mg, 3.00 mmol). The product was obtained 3d as a colorless, translucent solid (823 mg, 97% yield).

^{1}H NMR (500 MHz, $CDCl_3$): δ = 7.44 – 7.30 (m, 6H), 7.25 – 7.18 (m, 2H), 5.16 (s, 2H), 3.81 (s, 2H) ppm.

^{13}C{^{1}H} NMR (126 MHz, $CDCl_3$): δ = 170.2, 135.8, 134.0, 132.4, 131.0, 129.5, 128.7, 128.5, 128.4, 127.4, 67.1, 38.7 ppm.

HRMS (ESI): Calculated for $C_{15}H_{12}Cl_2O_2Na$ $[M+Na]^+$: 317.0107, found: 317.0105.

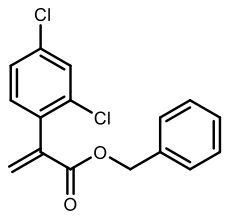

Benzyl 2-(2,4-dichlorophenyl)acrylate (7h). Prepared according to general procedure **B** using benzyl 2-(2,4-dichlorophenyl)acetate (830 mg, 2.81 mmol). The product was obtained 3d as a colorless oil which solidifies upon standing (560 mg, 65% yield).

^{1}H NMR (500 MHz, $CDCl_3$): δ = 7.41 (d, *J* = 2.1 Hz, 1H), 7.38 – 7.28 (m, 5H), 7.24 (d, *J* = 2.1 Hz, 1H), 7.19 (d, *J* = 8.2 Hz, 1H), 6.58 (d, *J* = 1.2 Hz, 1H), 5.81 (d, *J* = 1.1 Hz, 1H), 5.23 (s, 2H) ppm.

^{13}C{^{1}H} NMR (126 MHz, $CDCl_3$): δ = 165.5, 139.4, 135.8, 135.2, 134.9, 134.3, 131.8, 130.1, 129.4, 128.7, 128.4, 128.3, 127.2, 67.2 ppm.

HRMS (ESI): Calculated for $C_{16}H_{12}Cl_2O_2Na$ $[M+Na]^+$: 329.0107, found: 329.0095.

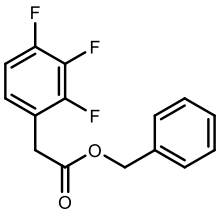

Benzyl 2-(2,3,4-trifluorophenyl)acetate. Prepared according to general procedure **A** using 2,4-dichlorophenyl acetic acid (615 mg, 3.00 mmol). The product was obtained 3d as a colorless, translucent solid (823 mg, 97% yield).

^{1}H NMR (500 MHz, $CDCl_3$): δ = 7.43 – 7.27 (m, 5H), 7.09 (qd, *J* = 9.2, 5.1 Hz, 1H), 6.85 (dddd, *J* = 9.2, 8.4, 3.7, 2.2 Hz, 1H), 5.18 (s, 2H), 3.79 (br s, 2H) ppm.

^{19}F{^{1}H} NMR (471 MHz, $CDCl_3$): δ = -119.5 (dd, *J* = 14.6, 2.8 Hz), -137.0 (dd, *J* = 20.8, 3.1 Hz), -142.41 (dd, *J* = 21.3, 15.4 Hz) ppm.

^{13}C{^{1}H} NMR (126 MHz, $CDCl_3$): δ = 169.1, 156.8 (d, J_{C-F} = 239.3 Hz), 152.87 – 143.9 (m), 135.6, 129.8 (q, J_{C-F} = 29.3 Hz), 128.7, 128.5, 128.3, 116.4 (dd, J_{C-F} = 19.4, 9.4 Hz), 112.6 (dd, J_{C-F} = 22.2, 16.4 Hz), 110.6 (ddd, J_{C-F} = 24.4, 6.5, 4.0 Hz), 67.3, 28.4 (q, J_{C-F} = 2.6 Hz) ppm.

HRMS (ESI): Calculated for $C_{16}H_{11}F_3O_2Na$ $[M+Na]^+$: 303.0603, found: 303.0602.

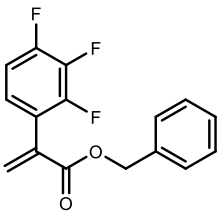

Benzyl 2-(2,3,4-trifluorophenyl)acrylate (7i). Prepared according to general procedure **B** using Benzyl 2-(2,3,4-trifluorophenyl)acetate (693 mg, 2.47 mmol). The product was obtained 3d as a colorless oil which solidifies upon storage at
-20 ºC (178 mg, 25% yield).

^{1}H NMR (400 MHz, $CDCl_3$): δ = 7.43 – 7.29 (m, 4H), 7.12 (qd, *J* = 9.2, 5.0 Hz, 1H), 6.86 (tdd, *J* = 7.0, 3.8, 1.9 Hz, 1H), 6.83 (d, *J* = 0.9 Hz, 1H), 6.03 (d, *J* = 0.8 Hz, 1H), 5.26 (s, 2H) ppm.

^{19}F {^{1}H} NMR (376 MHz, $CDCl_3$): δ = -117.22 (dd, *J* = 15.0, 2.1 Hz), -135.03 (dd, *J* = 21.6, 2.1 Hz),
-142.39 (dd, *J* = 21.3, 15.0 Hz) ppm.

^{13}C{^{1}H} NMR (101 MHz, $CDCl_3$): δ = 164.7, 155.7 (d, *J* = 247.6 Hz), 150.0 – 147.7 (m), 147.6 – 144.9 (m), 135.6, 133.5, 129.0 (2C), 128.6, 128.4, 128.1, 116.8 (ddd, *J* = 19.4, 9.9, 1.7 Hz), 116.1 (dd, *J* = 21.7, 16.1 Hz), 110.7 (ddd, *J* = 24.8, 6.7, 4.1 Hz), 67.4 ppm.

HRMS (ESI): Calculated for $C_{16}H_{11}F_3O_2Na$ $[M+Na]^+$: 315.0603, found: 315.0605.

Methyl 2-phenylacrylate (7j). Procedure adapted from previous report.[78] To a 25 mL round bottom flask was added 2-phenylacrylic acid (500 mg, 3.37 mmol, 1.05 equiv.), potassium carbonate (267 mg, 0.6 equiv.) and methyl iodide (190 μL, 1.0 equiv.). DMF (5.0 mL) was added and reaction was stirred at room temperature for 6 hours. Upon completion of reaction water (10 mL) and Et_2O (10 mL) was added. The layers were separated in a separatory funnel. The organic layer was washed with water (5 x 10 mL), dried with $MgSO_4$ and concentrated *in vacuo* to afford desired **5b** as a light-yellow oil (497 mg, 95% yield). The spectroscopic data is consistent with previous report.[26]

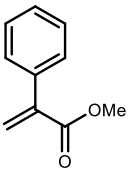

^{1}H NMR (300 MHz, $CDCl_3$): δ = 7.62 – 7.39 (m, 2H), 7.37 – 7.28 (m, 3H), 6.36 (d, *J* = 1.2 Hz, 1H), 5.89 (d, *J* = 1.2 Hz, 1H), 3.82 (s, 3H) ppm.

Benzyl 2-(trifluoromethyl)acrylate (7k). The product was synthesized by stirring of 2-(trifluoromethyl)acrylic acid (98.0 mg, 0.70 mmol, 1.0 eq.), 4-dimethylaminopyridine (86.2 mg, 1.0 eq.), and benzyl alcohol (42.7 mg, 1.00 eq.) in dry CH_2Cl_2 (15 mL). Upon cooling to 0 ºC, 1-ethyl-3-carbodiimide hydrochloride (EDC-HCl, 161 mg, 1.20 eq.) was added for reaction to proceed overnight. The reaction mixture was washed with saturated NH_4Cl solution (15 mL) and water (15 mL). The organic layer was separated, dried with $MgSO_4$ and concentrated in vacuo. The crude product was then purified by flash column chromatography(SiO_2, 10% Et_2O in hexanes) to afford a colorless oil (159 mg, 99 % yield). The spectroscopic data is consistent with previous report.[70]

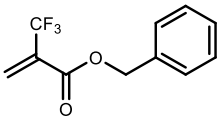

^{1}H NMR (300 MHz, $CDCl_3$): δ = 7.72 – 7.32 (m, 5H), 6.76 (d, *J* = 1.4 Hz, 1H), 6.44 (d, *J* = 1.3 Hz, 1H), 5.32 (s, 2H) ppm.

^{19}F NMR (282 MHz, $CDCl_3$): δ = -65.79 ppm.

[78] Zhu, Q. and Nocera, D. G. "Photocatalytic Hydromethylation and Hydroalkylation of Olefins Enabled by Titanium Dioxide Mediated Decarboxylation." *J. Am. Chem. Soc.* **2020,** 142, 17913.

Preparation of Dihydropyridines

Triethyl 2,6-dimethyl-1,4-dihydropyridine-3,4,5-tricarboxylate (R-1). 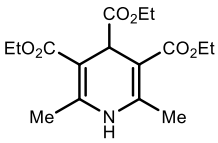

Ethyl glyoxylate (50 % by weight in PhMe, 11.0 mL, 1.0 equiv., 55.5 mmol) and ethyl (*Z*)-3-aminobut-2-enoate (14.0 mL, 2.0 equiv., 111 mmol) was stirred in glacial acetic acid (25 mL) for 16 hours. After removal of volatiles, the residue was transferred to a separation funnel containing aqueous $NaHCO_3$ (saturated, 100 mL) and the product was extracted with EtOAc (3 x 200 mL). After concentration of the combined organic layers, the product was purified by flash column chromatography (SiO_2, 25% EtOAc in hexanes) to afford a bright yellow solid, which was then recrystallized from CH_2Cl_2/hexanes to afford R-1 as a white crystalline solid. (7.27 g, 40% yield)

^{1}H NMR (500 MHz, $CDCl_3$): δ = 6.18 (br s, 1H), 4.82 (s, 1H), 4.28 – 4.11 (m, 4H), 4.07 (q, *J* = 7.1 Hz, 2H), 2.28 (s, 6H), 1.28 (t, *J* = 7.1 Hz, 6H), 1.20 (t, *J* = 7.1 Hz, 3H) ppm.

^{13}C{^{1}H} NMR (126 MHz, $CDCl_3$): δ = 174.4, 167.4, 145.6, 98.8, 60.8, 60.1, 40.7, 19.3, 14.5, 14.3 ppm.

HRMS (ESI): Calculated for $[C_{16}H_{23}NO_6Na]^+$ [M+Na]$^+$: 348.1418, found: 348.1412.

3,5-diethyl 4-(5-phenylpentyl) 2,6-dimethyl-1,4-dihydropyridine-3,4,5-tricarboxylate (R-3).

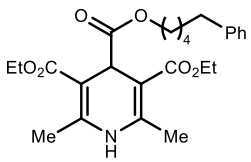

The product was synthesized by stirring 5-phenylpentan-1-ol (458 uL, 1.00 eq.) and the corresponding carboxylic acid (996 mg, 1.10 eq, synthesized based on previous report[6]) with 4-dimethylaminopyridine (DMAP, 36.7 mg, 1.00 eq.), 1-ethyl-3-carbodiimide hydrochloride (EDC-HCl, 690 mg, 1.00 eq.), in dry CH_2Cl_2 (15 mL) at 0 °C for 30 minutes, which was then stirred at room temperature for 15 hours. After removal of volatiles, the mixture was washed with sat NH_4Cl and purified through a silica column (25 % EtOAc in hexanes) to afford a white solid (1010 mg, 77 % yield)

^{1}H NMR (500 MHz, $CDCl_3$): δ= 7.30 – 7.26 (m, 2H), 7.21 – 7.14 (m, 3H), 5.68 (br s, 1H), 4.85 (s, 1H), 4.25 – 4.15 (m, 4H), 4.02 (t, *J* = 6.6 Hz, 2H), 2.59 (t, *J* = 7.4 Hz, 2H), 2.30 (s, 6H), 1.73 – 1.58 (m, 4H), 1.39 – 1.33 (m, 2H), 1.28 (t, *J* = 7.1 Hz, 6H) ppm.

$^{13}C\{^{1}H\}$ NMR (126 MHz, $CDCl_3$): δ= 173.9, 167.4, 145.3, 142.6, 128.5, 128.4, 125.8, 99.1, 64.8, 60.1, 40.4, 36.0, 31.2, 28.7, 25.7, 19.5, 14.5 ppm.

HRMS (ESI): Calculated for $C_{25}H_{33}NO_6Na$ $[M+Na]^+$: 466.2200, found: 466.2201.

3.6.2 General Procedure for Radical Umpolung Giese Addition

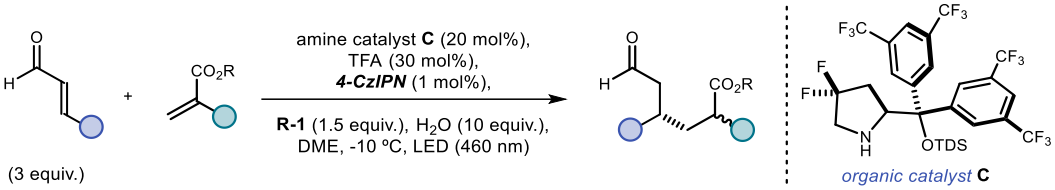

General Procedure C (*for 0.25 mmol scale*): To a 8.0 mL argon-purged glass vial, containing the acrylate **7** (1.0 equiv.), enal **1** (3.0 equiv.), DHP **R-1** (375 µmol, 1.5 equiv.), 4-CzIPN (2.50 µmol, 1 mol%) and amine catalyst **C** (50.0 µmol, 20 mol%), was added 500 µL of dimethoxyethane, H_2O (2.50 mmol, 10 equiv.) and CF_3COOH (75.0 µmol, 30 mol%). The vial was sealed with Parafilm, and then placed into a cooled aluminium support mounted on an aluminium block fitted with a 460 nm high-power single LED (λ = 460 nm, irradiance = 60 mW/cm^2, as controlled by an external power supply; the set-up is detailed in Figure 3.27). This set-up secured a reliable irradiation while keeping a constant distance of 1 cm between the reaction vessel and the light source. The reaction was stirred under visible light irradiation at -10 °C internal temperature for 16 hours. Then the solvent was evaporated, and the crude mixture was purified by column chromatography on SiO_2 to furnish product **8** in the stated yield and enantiomeric purity. Diastereomeric ratio was determined by ^1H NMR analysis of the crude mixture.

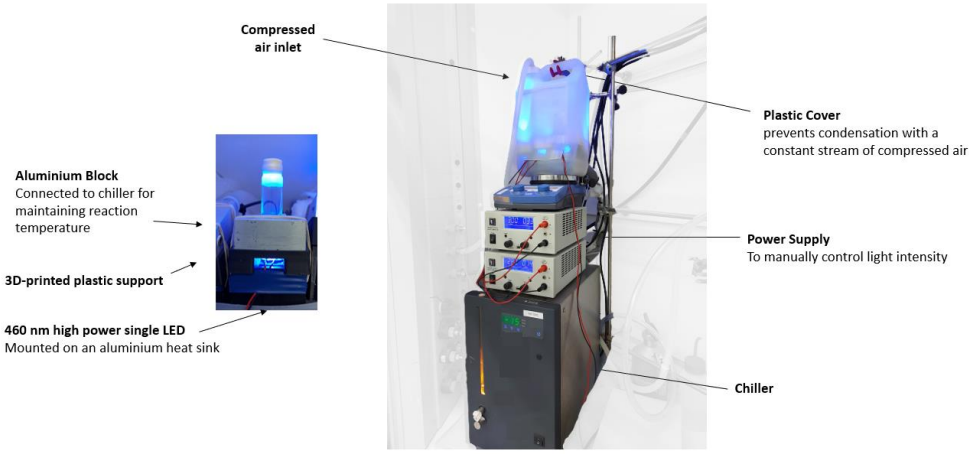

Figure 3.27. Detailed set-up and illumination system used in these studies. The light source consisted of a single 460 nm high-power LED (LZ1-00DB00) purchased from LedEngin; distance between LED and reaction vessel = 1 cm.

Derivatization of 6 for determination of enantiomeric ratio by UPC^2 analysis

Direct measurement of enantiomeric ratios of the individual diastereoisomers of 1,6-dicarbonyls **6** failed in our hands due to inseparability of the four stereoisomers. Therefore, the following reaction sequence was performed for e.r. determination of the individual diastereoisomers (as outlined in Figure 3.28). Upon global reduction of **8**, the diastereoisomeric mixture of the obtained diols **24** could be separated by preparative TLC. Then, the individual diastereomeric diols were converted to their 4-nitrobenzoic esters **25** by global acylation which could then be used for determination of the e.r. values by UPC^2 analysis.

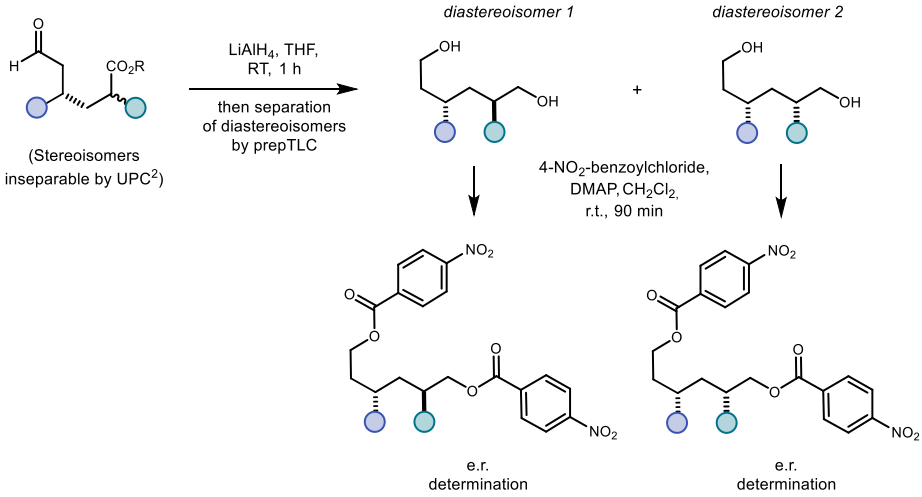

Figure 3.28. Reaction sequence to separate diastereoisomers and determine e.r. of **8**

Procedure:

An analytical sample of 1,6-dicarbonyl product **8** (5.00 mg) was dissolved in 500 µL of THF. $LiAlH_4$ (5 equiv.) were added and the mixture was stirred for 1 h. The reaction mixture was diluted with Et_2O (2.0 mL), quenched with Glauber's salt ($NaSO_4 \cdot 10\ H_2O$) and then filtered over a pad of SiO_2, which was subsequently rinsed with EtOAc. The volatiles were removed under reduced pressure and the two diastereomeric diols **24** were separated by preparative TLC using EtOAc in hexanes (generally 75% EtOAc in hexanes).

The obtained diols were then further functionalized to the 4-nitrobenzoates **25** as follows: The diol **24** together with a slight excess of both *p*-NO_2-benzoyl chloride and 4-dimethylaminopyridine (DMAP) were suspended in CH_2Cl_2 (0.5 mL) and the solution was allowed to stir for 90 minutes. The ester **25** was separated by preparative TLC from unreacted starting material (generally 25% EtOAc in hexanes) and analyzed by UPC^2 analysis with conditions specified in the experimental section of the individual compounds.

Radical Umpolung Giese Addition at 1 mmol Scale

To a 8.0 mL argon-purged glass vial, containing the acrylate **7b** (1.00 mmol, 268 mg, 1 equiv.), octenal **1a** (3.00 mmol, 379 mg, 448 μL), DHP **R-3*** (1.20 mmol, 532 mg 1.2 equiv.), 4-CzIPN (10.0 μmol, 7.9 mg, 1 mol%) and amine catalyst **C** (2.00 mmol, 141 mg, 20 mol%), was added 2.0 mL of dimethoxyethane, H_2O (10.0 mmol, 180 μL, 10 equiv.) and TFA (300 μmol, 23 μL, 30 mol%). The vial was sealed with Parafilm, and then placed into a cooled alluminium support mounted on an aluminium block fitted with a 460 nm high-power single LED (λ = 460 nm, irradiance = 90 mW/cm^2, as controlled by an external power supply; the set-up is detailed in Supplementary Figure 3.27). This set-up secured a reliable irradiation while keeping a constant distance of 1 cm between the reaction vessel and the light source. The reaction was stirred under visible light irradiation at -10 °C internal temperature for 72 hours. Then the solvent was evaporated, and the crude mixture was purified by flash column chromatography (SiO_2, 5-10% EtOAc in hexanes) to afford product **8b** as a pale yellow oil (258 mg, 65% yield) in a 1:1 diastereomeric ratio. The enantiomeric ratio of the corresponding 4-nitrobenzoate derivative, prepared following the general procedure, was determined to be 93:7 for *diastereomer 1* by UPC^2 analysis on a Daicel Chiralpak OJ-3 column (eluent: 100% CO_2 for 1 min, gradient 100% - 85% CO_2 in CH_3CN for 5 min, 85% CO_2 in CH_3CN for 2 min, gradient 85% - 100% CO_2 in CH_3CN for 1 min; flow rate 2.0 mL/min, λ = 256 nm; τ_{Major} = 4.65 min, τ_{Minor} = 4.40 min), and 84:16 for *diastereomer 2* by UPC^2 analysis on a Daicel Chiralpak ID-3 column (eluent: 100% CO_2 for 1 min, gradient 100% - 80% CO_2 in CH_3CN for 5 min, 80% CO_2 in CH_3CN for 2 min, gradient 80% - 100% CO_2 in CH_3CN for 1 min; flow rate 2.0 mL/min, λ = 256 nm; τ_{Major} = 8.00 min, τ_{Minor} = 7.55 min).

Spectroscopic data are consistent with those of the smaller scale reaction.

* Reductant **R-3** was used for its improved solubility

3.6.3 Characterization Data for 1,6-dicarbonyl products

Benzyl (*4S*)-phenyl-4-(2-oxoethyl)nonanoate (8a)

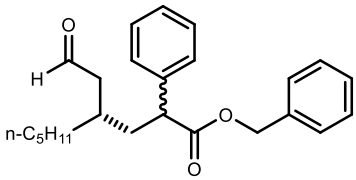

Prepared according to the general procedure **C** using octenal **1a** (46.0 μL, 300 μmol) and acrylate **7a** (23.8 mg, 100 μmol), the crude product was purified by flash column chromatography (silica, 5% EtOAc in hexanes) to obtain product **8a** as a colorless oil (33.0 mg, 89% yield) in a 1.1:1 diastereomeric ratio. Analytical data is in agreement with the literature[11]. The enantiomeric ratio of the corresponding 4-nitrobenzoate derivative, prepared following the general procedure, was determined to be 94:6 for *diastereomer 1* by UPC^2 analysis on a Daicel Chiralpak OJ-3 column (eluent: 100% CO_2 for 1 min, gradient 100% - 93% CO_2 in CH_3CN for 11 min, 93% CO_2 in CH_3CN for 2 min, gradient 93% - 100% CO_2 in CH_3CN for 1 min; flow rate 2.0 mL/min, λ = 254 nm; τ_{Major} = 9.40 min, τ_{Minor} = 8.60 min.), and 88:12 for *diastereomer 2* by UPC^2 analysis on a Daicel Chiralpak ID-3 column (eluent: 100% CO_2 for 1 min, gradient 100% - 60% CO_2 in CH_3CN for 5 min, 60% CO_2 in CH_3CN for 2 min, gradient 60% - 100% CO_2 in CH_3CN for 1 min; flow rate 2.0 mL/min, λ = 254 nm; τ_{Major} = 5.40 min, τ_{Minor} = 5.25 min.) $[\alpha]_D^{24}$ = -118.3 (c = 0.5, $CHCl_3$, 1.1:1 d.r., 94:6 e.r.[1], 88:12 e.r.[2]).

^{1}H NMR (500 MHz, $CDCl_3$, mixture of diastereoisomers): δ = 9.66 (t, *J* = 2.3 Hz, 1H), 9.64 (t, *J* = 2.2 Hz, 1H), 7.35 – 7.29 (m, 14H), 7.27 – 7.24 (m, 6H), 5.16 (d, *J* = 12.4 Hz, 2H), 5.08 (dd, *J* = 12.4, 2.4 Hz, 2H), 3.74 – 3.70 (m, 2H), 2.36 – 2.33 (m, 4H), 2.22 – 2.16 (m, 2H), 2.13 – 2.02 (m, 1H), 1.86 – 1.73 (m, 1H), 1.50 – 1.13 (m, 18H), 0.91 – 0.87 (m, 6H) ppm.

4-Methoxybenzyl (4*S*)-4-(2-oxoethyl)-2-phenylnonanoate (8b).

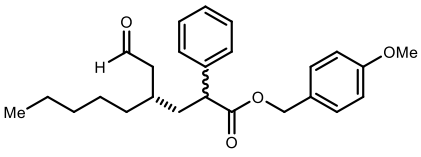

Following the general procedure **C** using acrylate **7b** (250 μmol, 67.0 mg) and octenal **1a** (750 μmol, 94.5 mg, 112 μL), purification of the crude product by flash column chromatography (SiO_2, 5-10% EtOAc in hexanes) afforded product **8b** as a pale yellow oil (91.0 mg, 92% yield) in a 1:1

diastereomeric ratio. The enantiomeric ratio of the corresponding 4-nitrobenzoate derivative, prepared following the general procedure, was determined to be 94:6 for *diastereomer 1* by UPC^2 analysis on a Daicel Chiralpak OJ-3 column (eluent: 100% CO_2 for 1 min, gradient 100% - 85% CO_2 in CH_3CN for 5 min, 85% CO_2 in CH_3CN for 2 min, gradient 85% - 100% CO_2 in CH_3CN for 1 min; flow rate 2.0 mL/min, λ = 256 nm; τ_{Major} = 4.60 min, τ_{Minor} = 4.35 min), and 87:13 for *diastereomer 2* by UPC^2 analysis on a Daicel Chiralpak ID-3 column (eluent: 100% CO_2 for 1 min, gradient 100% - 80% CO_2 in CH_3CN for 5 min, 80% CO_2 in CH_3CN for 2 min, gradient 80% - 100% CO_2 in CH_3CN for 1 min; flow rate 2.0 mL/min, λ = 256 nm; τ_{Major} = 7.80 min, τ_{Minor} = 7.45 min). $[\alpha]_D^{26}$ = -6.5 (c = 1.0, $CHCl_3$, 1:1 d.r., 94:6 e.r.[1], 87:13 e.r.[2]).

^{1}H NMR (400 MHz, $CDCl_3$, mixture of diastereoisomers): δ = 9.63 (t, *J* = 2.4 Hz, 1H), 9.60 (t, *J* = 2.2 Hz, 1H), 7.34 – 7.25 (m, 10H), 7.21 – 7.15 (m, 4H), 6.87 – 6.80 (m, 4H), 5.08 (d, *J* = 12.0 Hz, 2H), 4.98 (d, *J* = 12.1 Hz, 1H), 4.97 (d, *J* = 12.1 Hz, 1H), 3.80 (s, 6H), 3.66 (td, *J* = 7.8, 3.6 Hz, 2H), 2.30 (ddt, *J* = 4.5, 2.2, 1.0 Hz, 4H), 2.17 – 2.10 (m, 1H), 2.06 – 1.99 (m, 1H), 1.88 – 1.80 (m, 3H), 1.75 (dd, *J* = 13.7, 7.0 Hz, 1H), 1.30 – 1.15 (m, 16H), 0.88 – 0.82 (m, 6H) ppm.

^{13}C{^{1}H} NMR (101 MHz, $CDCl_3$, mixture of diastereoisomers): δ = 202.7, 202.5, 173.7, 173.7, 159.7 (2C), 138.8, 138.8, 130.0, 130.02, 128.8, 128.8, 128.1, 128.1 (2C), 128.0, 127.5 (2C), 114.0 (2C), 66.6 (2C), 55.4 (2C), 49.4, 49.4, 48.3, 48.2, 38.0, 38.0, 34.0, 33.9, 32.0, 32.0, 31.1, 31.0, 26.1, 26.0, 22.6 (2C), 14.1, 14.1 ppm.

HRMS (ESI): Calculated for $C_{25}H_{32}O_4Na$ $[M+Na]^+$: 419.2193; found: 419.2193.

4-Methoxybenzyl (*S*)-4-methyl-6-oxo-2-phenylhexanoate (**8c**).

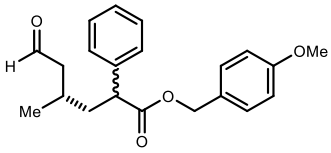

Following the general procedure **C** using acrylate **7b** (250 µmol, 67.0 mg) and enal **1c** (750 µmol, 52.5 mg, 61.6 µL), purification of the crude product by flash column chromatography (SiO_2, 5-10% EtOAc in hexanes) afforded product **8c** as a pale yellow oil (60.0 mg, 71% yield) in a 1:1 diastereomeric ratio. The enantiomeric ratio of the corresponding 4-nitrobenzoate derivative, prepared following the general procedure, was determined to be 87:13 for *diastereomer 1* by UPC^2 analysis on a

Daicel Chiralpak IA-3 column (eluent: 100% CO_2 for 1 min, gradient 100% - 70% CO_2 in MeOH for 8 min, 70% CO_2 in MeOH for 4 min, gradient 70% - 100% CO_2 in MeOH for 2 min; flow rate 2.0 mL/min, λ = 256 nm; τ_{Major} = 10.65 min, τ_{Minor} = 10.95 min), and 76.5:23.5 for *diastereomer 2* by UPC^2 analysis on a Daicel Chiralpak ID-3 column (eluent: 100% CO_2 for 1 min, gradient 100% - 60% CO_2 in CH_3CN for 5 min, 60% CO_2 in CH_3CN for 2 min, gradient 60% - 100% CO_2 in CH_3CN for 1 min; flow rate 2.0 mL/min, λ = 256 nm; τ_{Major} = 6.10 min, τ_{Minor} = 5.65 min). $[\alpha]_D^{26}$ =-11.2 (c = 1.0, $CHCl_3$, 1:1 d.r., 87:13 e.r.[1], 76.5:23.5 e.r.[2]).

^{1}H NMR (500 MHz, $CDCl_3$, mixture of diastereoisomers): δ = 9.66 – 9.63 (m, 1H), 9.63 – 9.61 (m, 1H), 7.35 – 7.25 (m, 10H), 7.22 – 7.16 (m, 4H), 6.87 – 6.82 (m, 4H), 5.08 (d, *J* = 12.1 Hz, 2H), 5.00 (d, *J* = 12.0 Hz, 1H), 4.97 (d, *J* = 12.1 Hz, 1H), 3.79 (s, 6H), 3.73 – 3.65 (m, 2H), 2.42 – 2.34 (m, 2H), 2.24 – 2.13 (m, 3H), 2.02 – 1.87 (m, 4H), 1.68 – 1.63 (m, 1H), 0.98 (d, *J* = 6.7 Hz, 3H), 0.95 (d, *J* = 6.2 Hz, 3H) ppm.

^{13}C{^{1}H} NMR (126 MHz, $CDCl_3$, mixture of diastereoisomers): δ = 202.3, 202.2, 173.8, 173.6, 159.7 (2C), 139.0, 138.4, 130.0, 130.0, 128.8 (2C), 128.2, 128.0 (2C), 128.0, 127.6, 127.5, 114.0 (2C), 66.6 (2C), 55.4 (2C), 51.0, 50.8, 49.4, 49.3, 40.7, 40.0, 26.5, 26.0, 19.9, 19.5 ppm.

HRMS (ESI): Calculated for $C_{21}H_{24}O_4Na$ $[M+Na]^+$: 363.1567; found: 363.1566.

4-Methoxybenzyl (*S*)-6-methyl-4-(2-oxoethyl)-2-phenylheptanoate (**8d**).

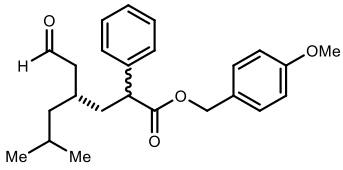

Following the general procedure **C** using acrylate **7b** (250 μmol, 67.0 mg) and a solution of enal **1d** (750 μmol, 187 mg, 45 wt% in n-hexanes), purification of the crude product by flash column chromatography (SiO_2, 5-10% EtOAc in hexanes) afforded product **8d** as a pale yellow oil (54.0 mg, 56% yield) in a 1.1:1 diastereomeric ratio. The enantiomeric ratio of the corresponding 4-nitrobenzoate derivative, prepared following the general procedure, was determined to be 93.5:6.5 for *diastereomer 1* by UPC^2 analysis on a Daicel Chiralpak OJ-3 column (eluent: 100% CO_2 for 1 min, gradient 100% - 95% CO_2 in CH_3CN for 5 min, 95% CO_2 in CH_3CN for 2 min, gradient 95% - 100% CO_2 in CH_3CN for 1 min; flow rate 2.0 mL/min, λ = 256 nm; τ_{Major} = 6.50 min, τ_{Minor} = 5.95 min), and 89:11 for *diastereomer 2* by

UPC^2 analysis on a Daicel Chiralpak ID-3 column (eluent: 100% CO_2 for 1 min, gradient 100% - 60% CO_2 in CH_3CN for 5 min, 60% CO_2 in CH_3CN for 2 min, gradient 60% - 100% CO_2 in CH_3CN for 1 min; flow rate 2.0 mL/min, λ = 256 nm; τ_{Major} = 5.40 min, τ_{Minor} = 5.20 min). $[\alpha]_D^{26}$ = -1.1 (c = 1.0, $CHCl_3$, 1.1:1 d.r., 93.5:6.5 e.r.[1], 89:11 e.r.[2]).

^{1}H NMR (400 MHz, $CDCl_3$, mixture of diastereoisomers): δ = 9.62 (t, *J* = 2.4 Hz, 1H), 9.60 (t, *J* = 2.3 Hz, 1H), 7.33 – 7.24 (m, 10H), 7.19 (dd, *J* = 8.7, 2.2 Hz, 4H), 6.86 – 6.81 (m, 4H), 5.10 (d, *J* = 12.0 Hz, 1H), 5.08 (d, *J* = 12.0 Hz, 2H), 4.98 (d, *J* = 12.0 Hz, 1H), 4.96 (d, *J* = 12.0 Hz, 2H), 3.79 (s, 6H), 3.67 (t, *J* = 7.7 Hz, 2H), 2.37 – 2.23 (m, 4H), 2.18 – 2.10 (m, 1H), 2.07 – 1.98 (m, 1H), 1.92 – 1.79 (m, 3H), 1.75 – 1.68 (m, 1H), 1.62 – 1.54 (m, 2H), 1.22 – 1.05 (m, 6H), 0.85 (d, *J* = 6.6 Hz, 3H), 0.78 (d, *J* = 6.6 Hz, 3H), 0.76 (d, *J* = 6.6 Hz, 3H), 0.75 (d, *J* = 6.6 Hz, 3H) ppm.

^{13}C{^{1}H} NMR (101 MHz, $CDCl_3$, mixture of diastereoisomers): δ = 202.7, 202.6, 173.7, 173.7, 159.7 (2C), 138.8, 138.7, 130.1, 130.1, 128.9, 128.8, 128.1, 128.1 (2C), 128.1, 127.6, 127.5, 114.0, 114.0, 66.6 (2C), 55.4 (2C), 49.4, 49.3, 48.6, 48.5, 44.0, 43.9, 38.4, 38.3, 29.0, 29.0, 25.2 (2C), 23.0, 22.7, 22.6, 22.6 ppm.

HRMS (ESI): Calculated for $C_{24}H_{30}O_4Na$ $[M+Na]^+$: 405.2036; found: 405.2038.

4-Methoxybenzyl (*S*)-4-isopropyl-6-oxo-2-phenylhexanoate (**8e**).

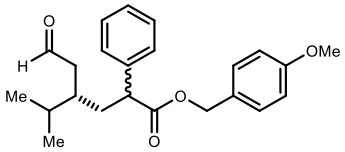

Following the general procedure **C** using acrylate **7b** (250 μmol, 67.0 mg) and enal **1e** (750 μmol, 73.5 mg, 87.0 μL), purification of the crude product by flash column chromatography (SiO_2, 5-10% EtOAc in hexanes) afforded product **8e** as a pale yellow oil (42.0 mg, 46% yield) in a 1.1:1 diastereomeric ratio. The enantiomeric ratio of the corresponding 4-nitrobenzoate derivative, prepared following the general procedure, was determined to be 93:7 for *diastereomer 1* by UPC^2 analysis on a Daicel Chiralpak OJ-3 column (eluent: 99% CO_2 in CH_3CN for 20 min; flow rate 2.0 mL/min, λ = 256 nm; τ_{Major} = 14.0 min, τ_{Minor} = 12.15 min), and 89:11 for *diastereomer 2* by UPC^2 analysis on a Daicel Chiralpak ID-3 column (eluent: 100% CO_2 for 1 min, gradient 100% - 60% CO_2 in CH_3CN for 5 min, 60% CO_2 in CH_3CN for 2 min, gradient 60% - 100% CO_2 in

CH_3CN for 1 min; flow rate 2.0 mL/min, λ = 258 nm; τ_{Major} = 5.60 min, τ_{Minor} = 5.35 min). $[\alpha]_D^{26}$ = +2.4 (c = 0.5, $CHCl_3$, 1.1:1 d.r., 93:7 e.r.[1], 89:11 e.r.[2]).

^{1}H NMR (400 MHz, $CDCl_3$, mixture of diastereoisomers): δ = 9.61 (t, *J* = 2.4 Hz, 1H), 9.58 (t, *J* = 2.2 Hz, 1H), 7.34 – 7.24 (m, 10H), 7.22 – 7.15 (m, 4H), 6.88 – 6.81 (m, 4H), 5.09 (d, *J* = 12.0 Hz, 1H), 5.08 (d, *J* = 12.0 Hz, 1H), 4.98 (d, *J* = 12.0 Hz, 1H), 4.97 (d, *J* = 12.1 Hz, 1H), 3.79 (s, 6H), 3.65 – 3.59 (m, 2H), 2.39 – 2.29 (m, 2H), 2.26 – 2.15 (m, 3H), 1.95 – 1.90 (m, 1H), 1.85 – 1.70 (m, 4H), 1.69 – 1.58 (m, 2H), 0.84 (d, *J* = 6.8 Hz, 3H), 0.83 – 0.79 (m, 6H), 0.78 (d, *J* = 6.8 Hz, 3H) ppm.

^{13}C{^{1}H} NMR (101 MHz, $CDCl_3$, mixture of diastereoisomers): δ = 203.0, 202.8, 173.8, 173.7, 159.7 (2C), 138.9, 138.7, 130.1, 130.1, 128.9, 128.9, 128.2, 128.1, 128.1 (2C), 127.6, 127.6, 114.0 (2C), 66.6 (2C), 55.4 (2C), 49.7, 49.6, 45.3, 45.2, 36.4, 36.2, 35.6, 35.2, 30.1, 30.1, 19.5, 19.4, 18.4, 18.2 ppm.

HRMS (ESI): Calculated for $C_{23}H_{28}O_4Na$ $[M+Na]^+$: 391.1880; found: 391.1872.

4-Methoxybenzyl (*S*)-4-(2-oxoethyl)-2-phenylnon-8-enoate (8f)

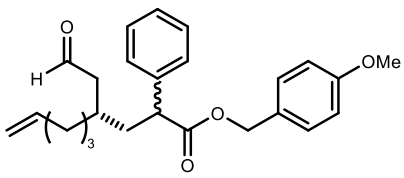

Following the general procedure **C** using acrylate **7b** (250 μmol, 67.0 mg) and enal **1f** (750 μmol, 93.0 mg), purification of the crude product by flash column chromatography (SiO_2, 5-10% EtOAc in hexanes) afforded product **8f** as a pale yellow oil (81.0 mg, 82% yield) in a 1.2:1 diastereomeric ratio. The enantiomeric ratio of the corresponding 4-nitrobenzoate derivative, prepared following the general procedure, was determined to be 94.5:5.5 for *diastereomer 1* by UPC[2] analysis on a Daicel Chiralpak OJ-3 column (eluent: 100% CO_2 for 1 min, gradient 100% - 85% CO_2 in CH_3CN for 8 min, 85% CO_2 in CH_3CN for 4 min, gradient 85% - 100% CO_2 in CH_3CN for 2 min; flow rate 2.0 mL/min, λ = 300 nm; τ_{Major} = 4.85 min, τ_{Minor} = 4.55 min), and 86.5:13.5 for *diastereomer 2* by UPC[2] analysis on a Daicel Chiralpak ID-3 column (eluent: 100% CO_2 for 1 min, gradient 100% - 60% CO_2 in CH_3CN for 5 min, 60% CO_2 in CH_3CN for 2 min, gradient 60% - 100% CO_2 in CH_3CN for 1 min; flow rate 2.0 mL/min, λ = 256 nm; τ_{Major} = 5.65 min, τ_{Minor} = 5.45 min).$[\alpha]_D^{26}$ = -7.4 (c = 1.0, $CHCl_3$, 1.2:1 d.r., 94.5:5.5 e.r.[1], 86.5:13.5 e.r.[2]).

^{1}H NMR (500 MHz, $CDCl_3$, mixture of diastereoisomers): δ = 9.63 (t, *J* = 2.3 Hz, 1H), 9.61 (t, *J* = 2.2 Hz, 1H), 7.34 – 7.25 (m, 10H), 7.22 – 7.16 (m, 4H), 6.88 – 6.82 (m, 4H), 5.80 – 5.69 (m, 2H), 5.08 (d, *J* = 12.0 Hz, 1H), 5.08 (d, *J* = 12.0 Hz, 1H), 5.00 – 4.92 (m, 6H), 3.79 (s, 6H), 3.69 – 3.63 (m, 2H), 2.38 – 2.27 (m, 4H), 2.18 – 2.12 (m, 1H), 2.07 – 2.03 (m, 1H), 2.01 – 1.93 (m, 4H), 1.90 – 1.80 (m, 3H), 1.76 (dd, *J* = 13.9, 7.0 Hz, 1H), 1.37 – 1.27 (m, 8H) ppm.

^{13}C{^{1}H} NMR (126 MHz, $CDCl_3$, mixture of diastereoisomers): δ = 202.5, 202.4, 173.7, 173.7, 159.7 (2C), 138.8, 138.7, 138.5, 138.5, 130.1, 130.1, 128.9, 128.8, 128.1 (2C), 128.0 (2C), 127.6, 114.9, 114.0, 114.0, 66.6, 55.4, 49.4, 49.4, 48.2, 48.2, 37.9, 33.8, 33.8, 33.5, 33.3, 30.9, 30.9, 25.7, 25.6 ppm.

HRMS (ESI): Calculated for $C_{25}H_{30}O_4Na$ $[M+Na]^+$: 417.2036; found: 417.2034.

4-Methoxybenzyl (*4S*)-4-(2-oxoethyl)-2-phenylnon-8-ynoate (8g)

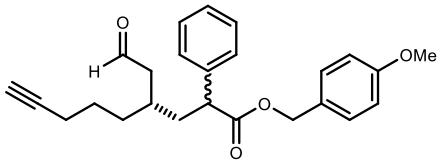

Prepared according to general procedure **C** using acrylate **7b** (250 μmol, 67.0 mg) and enal **1g** (91.6 mg, 750 μmol). The product was purified by flash column chromatography (SiO_2, 20-33% EtOAc in hexanes) to obtain **8g** as a colourless oil (62.3 mg, 66% yield) in a 1:1 diastereomeric ratio.

The enantiomeric ratio of *diastereomer 1* the corresponding 4-nitrobenzoate was determined to be 93.0:7.8 by UPC^2 analysis on a Daicel Chiralpak OJ-3 column (eluent: 100% CO_2 for 1 min, gradient 100% - 85% CO_2 in CH_3CN for 5 min, 85% CO_2 in CH_3CN for 2 min, gradient 85% - 100% CO_2 in CH_3CN for 1 min; flow rate 2.0 mL/min, λ = 256 nm, τ_{Major} = 5.57 min, τ_{Minor} = 5.14 min.), and 87.2:12.8 for *diastereomer 2* by UPC^2 analysis on a Daicel Chiralpak ID-3 column (eluent: 100% CO_2 for 1 min, gradient 100% - 82% CO_2 in CH_3CN for 11 min, 82% CO_2 in CH_3CN for 4 min, gradient 82% - 100% CO_2 in CH_3CN for 1 min; flow rate 2.0 mL/min, λ = 256 nm, τ_{Major} = 12.0 min, τ_{Minor} = 11.53 min.)

$[\alpha]_D^{25.5}$ = +0.73 (c = 0.5, $CHCl_3$, 1:1 d.r., 93.0:7.0 e.r.[1], 87.2:12.8 e.r.[2]).

^{1}H NMR (500 MHz, $CDCl_3$, mixture of diastereoisomers): δ= 9.66 (t, *J* = 2.2 Hz, 1H), 9.64 (t, *J* = 2.1 Hz, 1H), 7.39 – 7.26 (m, 10H), 7.24 – 7.16 (m, 4H), 6.92 – 6.83 (m, 4H), 5.11 (dd, *J* = 12.0, 1.9 Hz, 2H), 5.00 (d, *J* = 12.0 Hz, 2H), 3.82 (s, 6H), 3.75 – 3.66 (m, 2H), 2.42 – 2.29 (m, 3H), 2.26 – 2.06 (m, 6H), 1.98 (t, *J* = 2.6 Hz, 1H), 1.95 (d, *J* = 2.7 Hz, 1H), 1.89 (ddd, *J* = 11.8, 8.4, 5.9 Hz, 4H), 1.78 (dt, *J* = 14.1, 7.1 Hz, 1H), 1.56 – 1.38 (m, 8H) ppm.

^{13}C NMR (126 MHz, $CDCl_3$, mixture of diastereoisomers): δ= 202.3, 202.1, 173.6 (2C), 159.7 (2C), 138.7, 138.6, 130.1, 130.1, 128.9, 128.8, 128.1 (2C), 128.0 (2C), 127.6, 127.6, 114.0, 114.0, 84.1, 84.0, 68.8, 68.8, 66.6 (2C), 55.4 (2C), 49.3, 49.3, 48.2 (2C), 37.8, 37.8, 33.1, 32.8, 30.6, 30.5, 25.3, 25.3, 18.5, 18.5 ppm.

HRMS (ESI): Calculated for $C_{25}H_{28}O_4Na$ $[M+Na]^+$: 415.1880, found: 415.1882.

4-Methoxybenzyl (*S*,*Z*)-4-(2-oxoethyl)-2-phenyldec-7-enoate (**8h**)

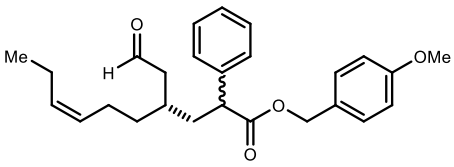

Following the general procedure **C** using acrylate **7b** (250 μmol, 67.0 mg) and enal **1h** (750 μmol, 109 mg, 126 μL), purification of the crude product by flash column chromatography (SiO_2, 5-10% EtOAc in hexanes) afforded product **8h** as a pale yellow oil (87.0 mg, 85% yield) in a 1:1 diastereomeric ratio. The enantiomeric ratio of the corresponding 4-nitrobenzoate derivative, prepared following the general procedure, was determined to be 94:6 for *diastereomer 1* by UPC^2 analysis on a Daicel Chiralpak OJ-3 column (eluent: 100% CO_2 for 1 min, gradient 100% - 85% CO_2 in CH_3CN for 8 min, 85% CO_2 in CH_3CN for 4 min, gradient 85% - 100% CO_2 in CH_3CN for 2 min; flow rate 2.0 mL/min, λ = 256 nm; τ_{Major} = 4.75 min, τ_{Minor} = 4.40 min), and 88.5:11.5 for *diastereomer 2* by UPC^2 analysis on a Daicel Chiralpak ID-3 column (eluent: 100% CO_2 for 1 min, gradient 100% - 80% CO_2 in CH_3CN for 5 min, 80% CO_2 in CH_3CN for 2 min, gradient 80% - 100% CO_2 in CH_3CN for 1 min; flow rate 2.0 mL/min, λ = 256 nm; τ_{Major} = 8.15 min, τ_{Minor} = 7.80 min). $[\alpha]_D^{26}$ = -5.6 (c = 1.0, $CHCl_3$, 1:1 d.r., 94:6 e.r.[1], 88.5:11.5 e.r.[2]).

^{1}H NMR (500 MHz, $CDCl_3$, mixture of diastereoisomers): δ = 9.63 (t, *J* = 2.3 Hz, 1H), 9.60 (t, *J* = 2.2 Hz, 1H), 7.34 – 7.25 (m, 10H), 7.22 – 7.17 (m, 4H), 6.86 – 6.82 (m, 4H), 5.40 – 5.30 (m, 2H), 5.27 – 5.15 (m, 2H), 5.09 (d, *J* = 12.0 Hz, 1H), 5.08 (d, *J* = 12.0 Hz, 1H),

4.98 (d, *J* = 12.0 Hz, 1H), 4.97 (d, *J* = 12.0 Hz, 1H), 3.79 (s, 6H), 3.70 – 3.64 (m, 2H), 2.37 – 2.27 (m, 4H), 2.20 – 2.14 (m, 1H), 2.09 – 2.05 (m, 1H), 2.01 – 1.93 (m, 8H), 1.90 – 1.84 (m, 3H), 1.81 – 1.75 (m, 1H), 1.45 – 1.38 (m, 2H), 1.37 – 1.30 (m, 2H), 0.94 (td, *J* = 7.5, 1.7 Hz, 6H) ppm. **$^{13}C\{^1H\}$ NMR (126 MHz, $CDCl_3$, mixture of diastereoisomers):** δ = 202.5, 202.3, 173.7 (2C), 159.7 (2C), 138.8, 138.7, 132.4 (2C), 130.0, 130.0, 128.9, 128.8, 128.2, 128.2, 128.1 (2C), 128.0 (2C), 127.5 (2C), 114.0 (2C), 66.6 (2C), 55.4 (2C), 49.4, 49.3, 48.1, 48.1, 37.9, 37.9, 34.1, 33.9, 30.8, 30.7, 24.1, 24.0, 20.6 (2C), 14.4 (2C) ppm.

HRMS (ESI): Calculated for $C_{26}H_{32}O_4Na$ $[M+Na]^+$: 431.2193; found: 431.2192.

4-Methoxybenzyl (4*S*,6*S*)-6,10-dimethyl-4-(2-oxoethyl)-2-phenylundec-9-enoate (**8i**)

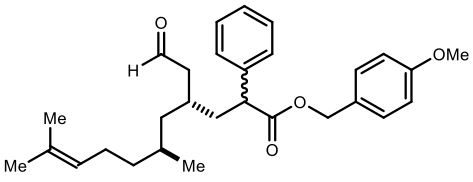

Following the general procedure **C** using acrylate **7b** (250 μmol, 67.0 mg) and enal **1i** (750 μmol, 135 mg), purification of the crude product by flash column chromatography (SiO_2, 5-10% EtOAc in hexanes) afforded product **8i** as a pale yellow oil (75.0 mg, 67% yield) in a 1.6:1 diastereomeric ratio. The enantiomeric ratio of the corresponding 4-nitrobenzoate derivative, prepared following the general procedure, was determined to be 86:14 for *diastereomer 1* by UPC^2 analysis on a Daicel Chiralpak OJ-3 column (eluent: 100% CO_2 for 1 min, gradient 100% - 80% CO_2 in iPrOH for 8 min, 80% CO_2 in iPrOH for 4 min, gradient 80% - 100% CO_2 in iPrOH for 2 min; flow rate 2.0 mL/min, λ = 256 nm; τ_{Major} = 4.60 min, τ_{Minor} = 4.20 min), and 88.5:11.5 for *diastereomer 2* by UPC^2 analysis on a Daicel Chiralpak IB-3 column (eluent: 100% CO_2 for 1 min, gradient 100% - 80% CO_2 in iPrOH for 8 min, 80% CO_2 in iPrOH for 4 min, gradient 80% - 100% CO_2 in iPrOH for 2 min; flow rate 2.0 mL/min, λ = 256 nm; τ_{Major} = 7.05 min, τ_{Minor} = 7.20 min). $[\alpha]_D^{26}$ = -2.3 (c = 1.0, $CHCl_3$, 1.6:1 d.r., 86:14 e.r.[1], 88.5:11.5 e.r.[2]).

^1H NMR (400 MHz, $CDCl_3$, mixture of diastereoisomers): δ = 9.65 – 9.57 (m, 2H), 7.34 – 7.24 (m, 10H), 7.24 – 7.16 (m, 4H), 6.87 – 6.80 (m, 4H), 5.14 – 4.93 (m, 6H), 3.79 (s, 6H), 3.70 – 3.63 (m, 2H), 2.41 – 2.29 (m, 2H), 2.29 – 2.18 (m, 3H), 1.99 – 1.86 (m, 7H), 1.68 (dt, *J* = 4.3, 1.3 Hz, 6H), 1.67 – 1.61 (m, 2H), 1.59 (dd, *J* = 8.0, 1.3 Hz, 6H), 1.44 (dt, *J* = 9.5,

7.1 Hz, 2H), 1.36 – 1.28 (m, 2H), 1.22 – 1.16 (m, 2H), 1.11 – 0.97 (m, 4H), 0.85 (d, *J* = 6.5 Hz, 3H), 0.71 (d, *J* = 6.5 Hz, 3H) ppm.

$^{13}C\{^{1}H\}$ NMR (101 MHz, $CDCl_3$, mixture of diastereoisomers): δ = 202.6, 202.5, 173.8, 173.6, 159.7, 159.7, 139.0, 138.6, 131.4, 131.4, 130.1, 130.0, 128.9, 128.8, 128.1, 128.0, 128.0 (2C), 127.6, 127.5, 124.8, 124.7, 114.0, 114.0, 66.6 (2C), 55.4, 55.4, 49.4, 49.3, 48.8, 48.7, 42.4, 42.3, 38.2, 37.8, 37.2, 37.2, 29.8, 29.7, 28.9, 28.6, 25.8, 25.8, 25.5, 25.5, 19.8, 19.6, 17.8, 17.8 ppm.

HRMS (ESI): Calculated for $C_{29}H_{38}O_4Na$ $[M+Na]^+$: 473.2662; found: 473.2660.

4-Methoxybenzyl (*S*)-10-chloro-4-(2-oxoethyl)-2-phenyldecanoate (**8j**)

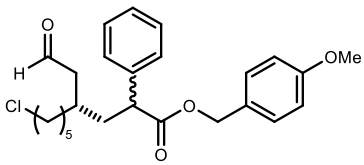

Following the general procedure **C** using acrylate **7b** (250 μmol, 67.0 mg) and enal **1j** (750 μmol, 52.5 mg, 61.6 μL), purification of the crude product by flash column chromatography (SiO_2, 10-20% EtOAc in hexanes) afforded product **8j** as a pale yellow oil (70.5 mg, 65% yield) in a 1:1 diastereomeric ratio. The enantiomeric ratio of the corresponding
4-nitrobenzoate drivative, prepared following the general procedure, was determined to be 94.5:5.5 for *diastereomer 1* by UPC[2] analysis on a Daicel Chiralpak IA-3 column (eluent: 100% CO_2 for 1 min, gradient 100% - 80% CO_2 in MeOH for 20 min, 80% CO_2 in MeOH for 8 min, gradient 85% - 100% CO_2 in MeOH for 1 min; flow rate 2.0 mL/min, λ = 256 nm; τ_{Major} = 20.65 min, τ_{Minor} = 21.10 min), and 86:14 for *diastereomer 2* by UPC[2] analysis on a Daicel Chiralpak OJ-3 column (eluent: 100% CO_2 for 1 min, gradient 100% - 90% CO_2 in CH_3CN for 5 min, 90% CO_2 in CH_3CN for 2 min, gradient 90% - 100% CO_2 in CH_3CN for 1 min; flow rate 2.0 mL/min, λ = 256 nm; τ_{Major} = 6.80 min, τ_{Minor} = 6.50 min). $[\alpha]_D^{26}$ = -3.6 (c = 1.0, $CHCl_3$, 1:1 d.r., 94.5:5.5 e.r.[1], 86:14 e.r.[2]).

^{1}H NMR (400 MHz, $CDCl_3$, mixture of diastereoisomers): δ = 9.63 (t, *J* = 2.3 Hz, 1H), 9.61 (t, *J* = 2.1 Hz, 1H), 7.34 – 7.24 (m, 10H), 7.22 – 7.16 (m, 4H), 6.87 – 6.80 (m, 4H), 5.09 (d, *J* = 12.0 Hz, 1H), 5.08 (d, *J* = 12.0 Hz, 1H), 4.98 (d, *J* = 12.1 Hz, 2H), 3.79 (s, 6H), 3.69 – 3.61 (m, 2H), 3.50 (t, *J* = 6.7 Hz, 2H), 3.48 (t, *J* = 6.7 Hz, 2H), 2.38 – 2.26 (m, 4H), 2.16

(ddd, *J* = 13.7, 8.4, 6.4 Hz, 1H), 2.07 – 1.99 (m, 1H), 1.90 – 1.81 (m, 3H), 1.76 – 1.67 (m, 5H), 1.37 – 1.23 (m, 12H) ppm.

$^{13}C\{^{1}H\}$ NMR (101 MHz, $CDCl_3$, mixture of diastereoisomers): δ = 202.4, 202.3, 173.7, 173.6, 159.7 (2C), 138.7, 138.7, 130.1 (2C), 128.9, 128.9, 128.1, 128.0, 128.0 (2C), 127.6, 127.6, 114.0 (2C), 66.6 (2C), 55.4 (2C), 49.4, 49.4, 48.3, 48.2, 45.1, 45.0, 37.9 (2C), 33.9, 33.8, 32.5 (2C), 30.9 (2C), 27.1, 27.0, 25.7, 25.7 ppm.

HRMS (ESI): Calculated for $C_{26}H_{31}ClO_4Na$ $[M+Na]^+$: 453.1803; found: 453.1796.

4-Methoxybenzyl (*S*)-13-hydroxy-4-(2-oxoethyl)-2-phenyltridecanoate (**8k**)

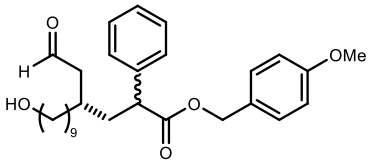

Following the general procedure **C** using acrylate **7b** (250 μmol, 67.0 mg) and enal **1k** (750 μmol, 153 mg), purification of the crude product by flash column chromatography (SiO_2, 5-10% EtOAc in hexanes) afforded product **8k** as a pale yellow oil (84.0 mg, 71% yield) in a 1.1:1 diastereomeric ratio. The enantiomeric ratio of the corresponding 4-nitrobenzoate derivative, prepared following the general procedure, was determined to be 92:8 for *diastereomer 1* by UPC^2 analysis on a Daicel Chiralpak OJ-3 column (eluent: 100% CO_2 for 1 min, gradient 100% - 10% CO_2 in CH_3CN for 19 min, 10% CO_2 in CH_3CN for 6 min, gradient 10% - 100% CO_2 in CH_3CN for 1 min; flow rate 2.0 mL/min, λ = 256 nm; τ_{Major} = 23.90 min, τ_{Minor} = 22.75 min), and 81.5:18.5 for *diastereomer 2* by UPC^2 analysis on a Daicel Chiralpak OJ-3 column eluent: 100% CO_2 for 1 min, gradient 100% - 10% CO_2 in CH_3CN for 19 min, 10% CO_2 in CH_3CN for 6 min, gradient 10% - 100% CO_2 in CH_3CN for 1 min; flow rate 2.0 mL/min, λ = 256 nm; τ_{Major} = 25.60 min, τ_{Minor} = 23.80 min). $[\alpha]_D^{26}$ = -4.8 (c = 1.0, $CHCl_3$, 1,1:1 d.r., 92:8 e.r.[1], 81.5:18.5 e.r.[2])

^{1}H NMR (500 MHz, $CDCl_3$, mixture of diastereoisomers): δ = 9.62 (t, *J* = 2.4 Hz, 1H), 9.60 (t, *J* = 2.2 Hz, 1H), 7.34 – 7.24 (m, 10H), 7.21 – 7.15 (m, 4H), 6.87 – 6.80 (m, 4H), 5.08 (d, *J* = 12.0 Hz, 2H), 4.98 (d, *J* = 12.1 Hz, 1H), 4.97 (d, *J* = 12.1 Hz, 1H), 3.79 (s, 6H), 3.69 – 3.63 (m, 2H), 3.63 (td, *J* = 6.7, 1.2 Hz, 4H), 2.35 – 2.26 (m, 4H), 2.19 – 2.10 (m, 1H), 2.06 – 2.01 (m, 1H), 1.89 – 1.80 (m, 3H), 1.77 – 1.71 (m, 1H), 1.60 (bs, 2H), 1.63 – 1.52 (m, 4H), 1.34 – 1.17 (m, 28H) ppm.

$^{13}C\{^{1}H\}$ NMR (126 MHz, $CDCl_3$, mixture of diastereoisomers): δ = 202.8, 202.6, 173.8, 173.7, 159.7 (2C), 138.8, 138.8, 130.0, 130.0, 128.9, 128.8, 128.1 (2C), 128.1 (2C), 127.5 (2C), 114.0, 113.9, 66.6 (2C), 63.2 (2C), 55.4 (2C), 49.4, 49.4, 48.3, 48.3, 38.0 (2C), 34.1, 33.9, 32.9 (2C), 31.1, 31.0, 29.8, 29.7, 29.6 (2C), 29.5 (2C), 29.5 (2C), 26.4, 26.3, 25.8 (2C) ppm.

HRMS (ESI): Calculated for $C_{29}H_{40}O_5Na$ $[M+Na]^+$: 491.2768; found: 491.2768.

4-Methoxybenzyl (*S*)-7-(benzyloxy)-4-(2-oxoethyl)-2-phenylheptanoate (8l)

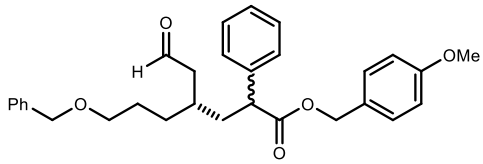

Following the general procedure **C** using acrylate **7b** (250 μmol, 67.0 mg) and enal **1l** (750 μmol, 153 mg), purification of the crude product by flash column chromatography (SiO_2, 5-10% EtOAc in hexanes) afforded product **8l** as a pale yellow oil (84.0 mg, 71% yield) in a 1.1:1 diastereomeric ratio. The enantiomeric ratio of the corresponding 4-nitrobenzoate derivative, prepared following the general procedure, was determined to be 93.5:6.5 for *diastereomer 1* by UPC^2 analysis on a Daicel Chiralpak OJ-3 column (eluent: 100% CO_2 for 1 min, gradient 100% - 75% CO_2 in CH_3CN for 8 min, 75% CO_2 in CH_3CN for 4 min, gradient 75% - 100% CO_2 in CH_3CN for 2 min; flow rate 2.0 mL/min, λ = 256 nm; τ_{Major} = 6.15 min, τ_{Minor} = 5.75 min), and 83.5:16.5 for *diastereomer 2* by UPC^2 analysis on a Daicel Chiralpak ID-3 column (eluent: 100% CO_2 for 1 min, gradient 100% - 60% CO_2 in CH_3CN for 5 min, 60% CO_2 in CH_3CN for 2 min, gradient 60% - 100% CO_2 in CH_3CN for 1 min; flow rate 2.0 mL/min, λ = 256 nm; τ_{Major} = 6.95 min, τ_{Minor} = 6.70 min). $[\alpha]_D^{26}$ = -3.2 (c = 1.0, $CHCl_3$, 1.1:1 d.r., 93.5:6.5 e.r.[1], 83.5:16.5 e.r.[2]).

^{1}H NMR (400 MHz, $CDCl_3$, mixture of diastereoisomers): δ = 9.63 (t, *J* = 2.3 Hz, 1H), 9.61 (t, *J* = 2.1 Hz, 1H), 7.40 – 7.22 (m, 20H), 7.22 – 7.15 (m, 4H), 6.90 – 6.80 (m, 4H), 5.08 (d, *J* = 12.1 Hz, 1H), 5.08 (d, *J* = 12.1 Hz, 1H), 4.98 (d, *J* = 12.0 Hz, 1H), 4.98 (d, *J* = 12.0 Hz, 1H), 4.48 (s, 2H), 4.45 (s, 2H), 3.79 (s, 3H), 3.79 (s, 3H), 3.71 – 3.64 (m, 2H), 3.42 (t, *J* = 6.3 Hz, 2H), 3.38 (t, *J* = 6.3 Hz, 2H), 2.39 – 2.28 (m, 4H), 2.20 – 2.01 (m, 2H), 1.94 – 1.82 (m, 3H), 1.81 – 1.74 (m, 1H), 1.59 – 1.37 (m, 8H) ppm.

$^{13}C\{^{1}H\}$ NMR (101 MHz, $CDCl_3$, mixture of diastereoisomers): δ = 202.4, 202.3, 173.7, 173.7, 159.7 (2C), 138.7, 138.7, 138.6, 138.6, 130.0 (2C), 128.7, 128.8, 128.5 (2C), 128.1 (2C), 128.1 (2C), 127.8, 127.7, 127.7 (2C), 127.6 (2C), 114.0 (2C), 73.1, 73.0, 70.3, 70.3, 66.6 (2C), 55.4 (2C), 49.4, 49.3, 48.2 (2C), 37.8, 37.8, 30.9, 30.7, 30.6, 30.4, 26.7, 26.6 ppm.

HRMS (ESI): Calculated for $C_{30}H_{34}O_5Na$ $[M+Na]^+$: 497.2298; found: 497.2295.

1-(4-Methoxybenzyl) 8-methyl (*S*)-4-(2-oxoethyl)-2-phenyloctanedioate (**8m**)

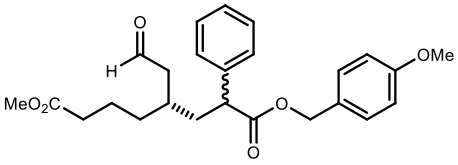

Following the general procedure **C** using acrylate **7b** (250 μmol, 67.0 mg) and enal **1m** (750 μmol, 117 mg), purification of the crude product by flash column chromatography (SiO2, 5-10% EtOAc in hexanes) afforded product **8m** as a pale yellow oil (62.0 mg, 58% yield) in a 1.2:1 diastereomeric ratio. The enantiomeric ratio was determined to be 93:7 for *diastereomer 1* and 85:15 for *diastereomer 2* by UPC[2] analysis on a Daicel Chiralpak IA-3 column (eluent: 100% CO_2 for 1 min, gradient 100% - 75% CO_2 in iPrOH for 49 min, 75% CO_2 in iPrOH for 10 min, gradient 75% - 100% CO_2 in iPrOH for 1 min; flow rate 2.0 mL/min, λ = 256 nm; τ_{Major} = 45.35 min, τ_{Minor} = 46.25 min for *diastereomer 1*, and τ_{Major} = 47.80 min, τ_{Minor} = 47.05 min for *diastereomer 2)*. $[\alpha]_D^{26}$ = -4.8 (c = 1.0, $CHCl_3$, 1.2:1 d.r., 93:7 e.r.[1], 85:15 e.r.[2]).

^{1}H NMR (500 MHz, $CDCl_3$, mixture of diastereoisomers): δ = 9.63 (t, J = 2.2 Hz, 1H), 9.61 (t, J = 2.0 Hz, 1H), 7.34 – 7.22 (m, 10H), 7.21 – 7.16 (m, 4H), 6.87 – 6.79 (m, 4H), 5.08 (d, J = 12.1 Hz, 2H), 4.97 (d, J = 12.0 Hz, 1H), 4.97 (d, J = 12.0 Hz, 1H), 3.79 (s, 6H), 3.67 – 3.62 (m, 8H), 2.37 – 2.30 (m, 4H), 2.27 – 2.18 (m, 4H), 2.16 – 2.11 (m, 1H), 2.07 – 2.03 (m, 1H), 1.90 – 1.82 (m, 3H), 1.79 – 1.73 (m, 1H), 1.60 – 1.50 (m, 4H), 1.37 – 1.27 (m, 4H) ppm.

$^{13}C\{^{1}H\}$ NMR (126 MHz, $CDCl_3$, mixture of diastereoisomers): δ = 202.2, 202.0, 173.8, 173.8, 173.6 (2C), 159.7 (2C), 138.7, 138.6, 130.1 (2C), 128.9, 128.9, 128.1, 128.0, 128.0 (2C), 127.6 (2C), 114.0 (2C), 66.6 (2C), 55.4 (2C), 51.6 (2C), 49.4, 49.3, 48.0 (2C), 37.7, 37.7, 34.0, 34.0, 33.4, 33.2, 30.8, 30.6, 21.7, 21.7 ppm.

HRMS (ESI): Calculated for $C_{25}H_{30}O_6Na$ $[M+Na]^+$: 449.1935; found: 449.1936.

4-Methoxybenzyl (S)-7-(1,3-dioxoisoindolin-2-yl)-4-(2-oxoethyl)-2-phenylheptanoate (8n)

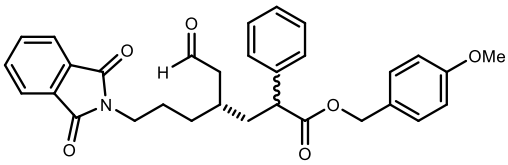

Prepared according to general procedure **C** using acrylate **7b** (250 μmol, 67.1 mg) and enal **1n** (750 μmol, 182 mg). The product was purified by flash column chromatography (SiO_2, 10-25% EtOAc in hexanes) to obtain **3d** as a pale yellow oil (72.3 mg, 56% yield) in a 1.3:1 diastereomeric ratio.

$[\alpha]_D^{25.5}$ = +0.73 (c = 0.5, $CHCl_3$, 1.3:1 d.r.).

^{1}H NMR (400 MHz, $CDCl_3$, mixture of diastereoisomers): δ= 9.61 (t, *J* = 2.1 Hz, 1H), 9.60 (t, *J* = 2.0 Hz, 1H), 7.87 – 7.79 (m, 4H), 7.75 – 7.68 (m, 4H), 7.33 – 7.21 (m, 10H), 7.20 – 7.14 (m, 4H), 6.86 – 6.79 (m, 4H), 5.06 (d, *J* = 12.0 Hz, 2H), 4.96 (d, *J* = 12.0 Hz, 1H), 4.96 (d, *J* = 12.0 Hz, 1H), 3.78 (s, 3H), 3.77 (s, 3H), 3.66 – 3.53 (m, 4H), 2.39 – 2.26 (m, 4H), 2.21 – 2.11 (m, 1H), 2.06 – 2.00 (m, 1H), 1.93 – 1.82 (m, 3H), 1.76 – 1.69 (m, 1H), 1.66 – 1.55 (m, 4H), 1.45 – 1.27 (m, 6H) ppm.

^{13}C NMR (101 MHz, $CDCl_3$, mixture of diastereoisomers): δ= 202.0, 201.9, 173.6, 173.5, 168.5, 168.4, 159.7 (2C), 138.7, 138.6, 134.1 (2C), 132.2, 132.2, 130.1, 130.1, 128.9, 128.9, 128.0 (2C), 128.0 (2C), 127.6, 127.6, 123.3 (2C), 114.0 (2C), 66.6 (2C), 55.4 (2C), 49.4, 49.3, 48.1 (2C), 38.0, 37.9, 37.8, 37.7, 31.3, 31.2, 30.7, 30.6, 25.7, 25.6 ppm.

HRMS (ESI): Calculated for $C_{31}H_{31}NO_6Na$ $[M+Na]^+$: 536.2044; found: 536.2040.

4-Methoxybenzyl (*S*)-4-(3-methoxyphenethyl)-6-oxo-2-phenylhexanoate (**8o**).

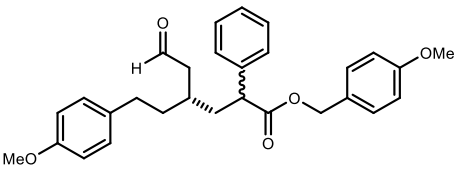

Following the general procedure **C** using acrylate **7b** (250 μmol, 67.0 mg) and enal **1s** (750 μmol, 143 mg), purification of the crude product by flash column chromatography (SiO_2, 5-10% EtOAc in hexanes) and preparative thin layer chromatography (SiO_2, CH_2Cl_2) afforded product **8o** as a pale yellow oil (62.0 mg, 54%

yield) in a 1.1:1 diastereomeric ratio. The enantiomeric ratio of the corresponding 4-nitrobenzoate derivative, prepared following the general procedure, was determined to be 93.5:6.5 for *diastereomer 1* by UPC^2 analysis on a Daicel Chiralpak OJ-3 column (eluent: 100% CO_2 for 1 min, gradient 100% - 60% CO_2 in CH_3CN for 5 min, 60% CO_2 in CH_3CN for 2 min, gradient 60% - 100% CO_2 in CH_3CN for 1 min; flow rate 2.0 mL/min, λ = 256 nm; τ_{Major} = 4.65 min, τ_{Minor} = 4.35 min), and 84.5:15.5 for *diastereomer 2* by UPC^2 analysis on a Daicel Chiralpak IC-3 column (eluent: 100% CO_2 for 1 min, gradient 100% - 65% CO_2 in CH_3CN for 5 min, 65% CO_2 in CH_3CN for 2 min, gradient 65% - 100% CO_2 in CH_3CN for 1 min; flow rate 2.0 mL/min, λ = 256 nm; τ_{Major} = 6.85 min, τ_{Minor} = 7.10 min). **$[\alpha]_D^{26}$** = -6.0 (c = 1.0, $CHCl_3$, 1.1:1 d.r., 93.5:6.5 e.r.[1], 84.5:15.5 e.r.[2]).

^{1}H NMR (500 MHz, $CDCl_3$, mixture of diastereoisomers): δ = 9.63 (t, *J* = 2.3 Hz, 1H), 9.60 (t, *J* = 2.1 Hz, 1H), 7.36 – 7.25 (m, 10H), 7.22 – 7.15 (m, 6H), 6.88 – 6.81 (m, 4H), 6.76 – 6.64 (m, 6H), 5.08 (d, *J* = 12.0 Hz, 1H), 5.08 (d, *J* = 12.0 Hz, 1H), 4.99 (d, *J* = 12.0 Hz, 1H), 4.98 (d, *J* = 12.0 Hz, 1H), 3.80 (s, 6H), 3.79 (s, 3H), 3.78 (s, 3H), 3.72 – 3.63 (m, 2H), 2.61 – 2.48 (m, 4H), 2.42 – 2.33 (m, 4H), 2.28 – 2.19 (m, 1H), 2.16 – 2.08 (m, 1H), 1.99 – 1.89 (m, 3H), 1.85 – 1.76 (m, 1H), 1.73 – 1.58 (m, 4H) ppm.

^{13}C{^{1}H} NMR (126 MHz, $CDCl_3$, mixture of diastereoisomers): δ = 202.3, 202.1, 173.6, 173.6, 159.8 (2C), 159.7 (2C), 143.5, 143.4, 138.7 (2C), 130.1, 130.0, 129.5, 129.5, 128.9, 128.8, 128.1, 128.0, 128.0, 128.0, 127.6, 127.6, 120.8, 120.8, 114.2, 114.1, 114.0 (2C), 111.4, 111.3, 66.6 (2C), 55.4 (2C), 55.2 (2C), 49.4, 49.3, 48.1, 48.1, 37.9, 37.8, 35.8, 35.7, 32.9, 32.9, 30.9, 30.7 ppm.

HRMS (ESI): Calculated for $C_{29}H_{32}O_5Na$ $[M+Na]^+$: 483.2142; found: 483.2153.

4-Methoxybenzyl (*S*)-6-oxo-2-phenyl-4-(3-(trifluoromethyl)phenethyl)hexanoate (8p)

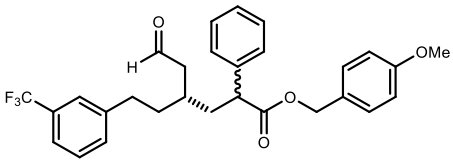

Following the general procedure **C** using acrylate **7b** (250 μmol, 67.0 mg) and enal **1t** (750 μmol, 171 mg), purification of the crude product by flash column chromatography (SiO_2, 5-10% EtOAc in hexanes) and preparative thin layer chromatography (SiO_2, CH_2Cl_2) afforded product **8p** as a pale yellow oil (68.0 mg, 55% yield) in a 1.1:1 diastereomeric ratio.

The enantiomeric ratio of the corresponding 4-nitrobenzoate derivative, prepared following the general procedure, was determined to be 92.5:7.5 for *diastereomer 1* by UPC^2 analysis on a Daicel Chiralpak OJ-3 column (eluent: 100% CO_2 for 1 min, gradient 100% - 60% CO_2 in CH_3CN for 5 min, 60% CO_2 in CH_3CN for 2 min, gradient 60% - 100% CO_2 in CH_3CN for 1 min; flow rate 2.0 mL/min, λ = 256 nm; τ_{Major} = 3.55 min, τ_{Minor} = 3.25 min), and 83.5:16.5 for *diastereomer 2* by UPC^2 analysis on a Daicel Chiralpak IE-3 column (eluent: 100% CO_2 for 1 min, gradient 100% - 80% CO_2 in MeOH for 38 min, 80% CO_2 in MeOH for 5 min, gradient 80% - 100% CO_2 in MeOH for 1 min; flow rate 2.0 mL/min, λ = 256 nm; τ_{Major} = 31.35 min, τ_{Minor} = 30.75 min). $[\alpha]_D^{26}$ = -4.6 (c = 1.0, $CHCl_3$, 1.1:1 d.r., 92.5:7.5 e.r.[1], 83.5:16.5 e.r.[2]).

^{1}H NMR (400 MHz, $CDCl_3$, mixture of diastereoisomers): δ = 9.65 (t, *J* = 2.1 Hz, 1H), 9.63 (t, *J* = 2.0 Hz, 1H), 7.48 – 7.40 (m, 2H), 7.41 – 7.22 (m, 16H), 7.22 – 7.15 (m, 4H), 6.87 – 6.80 (m, 4H), 5.09 (d, *J* = 12.0 Hz, 1H), 5.08 (d, *J* = 12.0 Hz, 1H), 4.99 (d, *J* = 12.0 Hz, 1H), 4.98 (d, *J* = 12.0 Hz, 1H), 3.79 (s, 3H), 3.78 (s, 3H), 3.70 – 3.63 (m, 2H), 2.67 – 2.51 (m, 4H), 2.48 – 2.34 (m, 4H), 2.31 – 2.22 (m, 1H), 2.16 – 2.07 (m, 1H), 2.02 – 1.87 (m, 3H), 1.85 – 1.77 (m, 1H), 1.70 – 1.57 (m, 4H) ppm.

^{13}C{^{1}H} NMR (101 MHz, $CDCl_3$, mixture of diastereoisomers): δ = 201.9, 201.8, 173.6, 173.5, 159.8 (2C), 142.8, 142.7, 138.6, 138.5, 131.8 (q, *J* = 1.1 Hz), 131.8 (q, *J* = 1.1 Hz), 130.8 (q, *J* = 31.9 Hz), 130.8 (q, *J* = 32.0 Hz), 130.1, 130.1, 129.0, 128.9, 128.9, 128.9, 128.0, 128.0, 128.0, 128.0, 127.7, 127.6, 125.1 (q, *J* = 3.7 Hz), 125.0 (q, *J* = 3.7 Hz), 124.3 (q, *J* = 272.4 Hz, 2C), 123.0 (q, *J* = 3.9 Hz, 2C), 114.0 (2C), 66.7 (2C), 55.4, 55.4, 49.4, 49.4, 48.1 (2C), 37.8, 37.69, 35.8, 35.7, 32.7, 32.7, 30.8, 30.8 ppm.

^{19}F NMR (376 MHz, $CDCl_3$, mixture of diastereoisomers): δ = -62.59 ppm.

HRMS (ESI): Calculated for $C_{29}H_{29}F_3O_4Na$ $[M+Na]^+$: 521.1910; found: 521.1908.

4-Methoxybenzyl (*S*)-4-(4-bromophenethyl)-6-oxo-2-phenylhexanoate (**8q**)

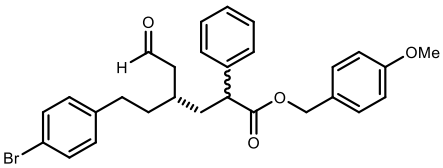

Following the general procedure **C** using acrylate **7b** (250 μmol, 67.0 mg) and enal **1u** (750 μmol, 179 mg), purification of the crude product by flash column chromatography (SiO_2, 5-10% EtOAc in hexanes) and preparative thin layer chromatography (SiO_2, CH_2Cl_2) afforded product **8q** as a pale yellow oil (68.0 mg, 53% yield) in a 1.1:1 diastereomeric ratio. The enantiomeric ratio of the corresponding 4-nitrobenzoate derivative, prepared following the general procedure, was determined to be 92.5:7.5 for *diastereomer 1* by UPC^2 analysis on a Daicel Chiralpak OJ-3 column (eluent: 100% CO_2 for 1 min, gradient 100% - 60% CO_2 in CH_3CN for 5 min, 60% CO_2 in CH_3CN for 2 min, gradient 60% - 100% CO_2 in CH_3CN for 1 min; flow rate 2.0 mL/min, λ = 256 nm; τ_{Major} = 4.70 min, τ_{Minor} = 4.40 min), and 84:16 for *diastereomer 2* by UPC^2 analysis on a Daicel Chiralpak IC-3 column (eluent: 100% CO_2 for 1 min, gradient 100% -70% CO_2 in CH_3CN for 5 min, 70% CO_2 in CH_3CN for 2 min, gradient 70% - 100% CO_2 in CH_3CN for 1 min; flow rate 2.0 mL/min, λ = 256 nm; τ_{Major} = 7.05 min, τ_{Minor} = 7.30 min).$[\alpha]_D^{26}$ = -9.0 (c = 1.0, $CHCl_3$, 1.1:1 d.r., 92.5:7.5 e.r.[1], 84:16 e.r.[2]).

^{1}H NMR (500 MHz, $CDCl_3$, mixture of diastereoisomers): δ = 9.62 (t, *J* = 2.2 Hz, 1H), 9.59 (t, *J* = 2.1 Hz, 1H), 7.40 – 7.36 (m, 2H), 7.36 – 7.34 (m, 2H), 7.33 – 7.23 (m, 10H), 7.20 – 7.15 (m, 4H), 7.00 – 6.96 (m, 2H), 6.94 – 6.89 (m, 2H), 6.86 – 6.82 (m, 4H), 5.08 (d, *J* = 12.0 Hz, 1H), 5.07 (d, *J* = 12.0 Hz, 1H), 4.98 (d, *J* = 12.0 Hz, 1H), 4.97 (d, *J* = 12.0 Hz, 1H), 3.79 (s, 3H), 3.79 (s, 3H), 3.68 – 3.60 (m, 2H), 2.56 – 2.43 (m, 4H), 2.42 – 2.33 (m, 4H), 2.26 – 2.18 (m, 1H), 2.13 – 2.05 (m, 1H), 1.98 – 1.92 (m, 1H), 1.92 – 1.85 (m, 2H), 1.82 – 1.76 (m, 1H), 1.66 – 1.54 (m, 4H) ppm.

^{13}C{^{1}H} NMR (126 MHz, $CDCl_3$, mixture of diastereoisomers): δ = 202.1, 202.0, 173.6, 173.6, 159.7 (2C), 140.8, 140.7, 138.6 (2C), 131.6, 131.5, 130.2, 130.1, 130.1, 130.1, 128.9, 128.9, 128.0, 128.0, 128.0, 127.9, 127.6, 127.6, 119.8, 119.7, 114.0 (2C), 66.7 (2C), 55.4 (2C), 49.4, 49.3, 48.1, 48.1, 37.8, 37.7, 35.7, 35.6, 32.2, 32.2, 30.6, 30.5 ppm.

HRMS (ESI): Calculated for $C_{28}H_{29}BrO_4Na$ $[M+Na]^+$: 531.1141; found: 531.1141.

4-Methoxybenzyl (*S*)-6-oxo-4-phenethyl-2-phenylhexanoate (**8r**).

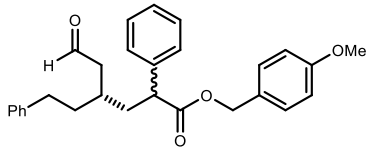

Following the general procedure **C** using acrylate **7b** (250 μmol, 67.0 mg) and enal **1v** (750 μmol, 120 mg), purification of the crude product by flash column chromatography (SiO_2, 5-10% EtOAc in hexanes) and preparative thin layer chromatography (SiO_2, CH_2Cl_2) afforded product **8r** as a pale yellow oil (84.0 mg, 78% yield) in a 1.1:1 diastereomeric ratio. The enantiomeric ratio of the corresponding 4-nitrobenzoate derivative, prepared following the general procedure, was determined to be 92:8 for *diastereomer 1* by UPC^2 analysis on a Daicel Chiralpak OJ-3 column (eluent: 100% CO_2 for 1 min, gradient 100% - 75% CO_2 in CH_3CN for 8 min, 75% CO_2 in CH_3CN for 4 min, gradient 75% - 100% CO_2 in CH_3CN for 2 min; flow rate 2.0 mL/min, λ = 256 nm; τ_{Major} = 6.10 min, τ_{Minor} = 5.65 min), and 84.5:15.5 for *diastereomer 2* by UPC^2 analysis on a Daicel Chiralpak ID-3 column (eluent: 85% CO_2 in CH_3CN for 20 min; flow rate 2.0 mL/min, λ = 256 nm; τ_{Major} = 12.75 min, τ_{Minor} = 11.60 min).

$[\alpha]_D^{26}$ = -4.6 (c =1.0 , $CHCl_3$, 1.1:1 d.r., 92:8 e.r.[1], 84.5:15.5 e.r.[2]).

^{1}H NMR (500 MHz, $CDCl_3$, mixture of diastereoisomers): δ = 9.65 (t, *J* = 2.3 Hz, 1H), 9.62 (t, *J* = 2.1 Hz, 1H), 7.38 – 7.25 (m, 14H), 7.24 – 7.18 (m, 6H), 7.17 – 7.12 (m, 2H), 7.12 – 7.07 (m, 2H), 6.90 – 6.83 (m, 4H), 5.10 (d, *J* = 12.0 Hz, 1H), 5.10 (d, *J* = 12.0 Hz, 1H), 5.01 (d, *J* = 12.0 Hz, 1H), 5.00 (d, *J* = 12.0 Hz, 1H), 3.83 (s, 3H), 3.82 (s, 3H), 3.74 – 3.65 (m, 2H), 2.62 – 2.52 (m, 4H), 2.44 – 2.37 (m, 4H), 2.29 – 2.23 (m, 1H), 2.17 – 2.11 (m, 1H), 2.01 – 1.92 (m, 3H), 1.86 – 1.81 (m, 1H), 1.76 – 1.68 (m, 2H), 1.68 – 1.60 (m, 2H) ppm.

^{13}C{^{1}H} NMR (126 MHz, $CDCl_3$, mixture of diastereoisomers): δ = 202.3, 202.2, 173.7, 173.7, 159.8 (2C), 141.9, 141.8, 138.7, 138.7, 130.1, 130.1, 128.9, 128.9, 128.6, 128.6, 128.4, 128.4, 128.1, 128.1, 128.0, 128.0, 127.6, 127.6, 126.1 (2C), 114.0 (2C), 66.7 (2C), 55.4 (2C), 49.4, 49.4, 48.2, 48.2, 37.9, 37.9, 36.0, 35.8, 32.9, 32.8, 30.9, 30.8 ppm.

HRMS (ESI): Calculated for $C_{28}H_{30}O_4Na$ $[M+Na]^+$: 453.2036; found: 453.2041.

Benzyl (*4S*)-(4-fluorophenyl)-4-(2-oxoethyl)nonanoate (8s)

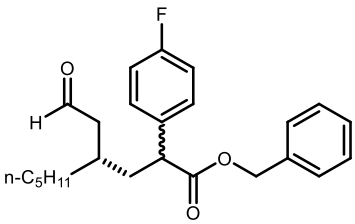

Prepared according to the general procedure **C** using octenal **1a** (112 μL, 750 μmol) and acrylate **7c** (64.0 mg, 250 μmol), the crude product was purified by flash column chromatography (silica, 5% EtOAc in hexanes) to obtain **8s** as a colorless oil (85.0 mg, 89% yield) in a 1:1 diastereomeric ratio. The enantiomeric ratio of the corresponding 4-nitrobenzoate derivative, prepared following the general procedure, was determined to be 93:7 for *diastereomer 1* by UPC^2 analysis on a Daicel Chiralpak OJ-3 column (eluent: 100% CO_2 for 1 min, gradient 100% - 93% CO_2 in CH_3CN for 5 min, 93% CO_2 in CH_3CN for 2 min, gradient 93% - 100% CO_2 in CH_3CN for 1 min; flow rate 2.0 mL/min, λ = 255 nm; τ_{Major} = 6.25 min, τ_{Minor} = 5.80 min.), and 88:12 for *diastereomer 2* by UPC^2 analysis on a Daicel Chiralpak ID-3 column (eluent: 100% CO_2 for 1 min, gradient 100% - 80% CO_2 in CH_3CN for 5 min, 80% CO_2 in CH_3CN for 2 min, gradient 80% - 100% CO_2 in CH_3CN for 1 min; flow rate 2.0 mL/min, λ = 256 nm; τ_{Major} = 7.15 min, τ_{Minor} = 6.95 min). $[\alpha]_D^{24}$ = -87.9 (c = 1.0, $CHCl_3$, 1:1 d.r., 93:7 e.r.[1], 88:12 e.r.[2]).

^{1}H NMR (500 MHz, $CDCl_3$, mixture of diastereoisomers): δ = 9.67 (t, *J* = 2.3 Hz, 1H), 9.65 (t, *J* = 2.1 Hz, 1H), 7.35 – 7.21 (m, 14H), 7.03 (m, 4H), 5.16 (d, *J* = 12.3 Hz, 2H), 5.09 (dd, *J* = 12.3, 2.7 Hz, 2H), 3.76 – 3.69 (m, 2H), 2.37 – 2.28 (m, 4H), 2.20 – 2.09 (m, 1H), 2.10 – 2.00 (m, 1H), 1.89 – 1.82 (m, 3H), 1.77 (dt, *J*= 14.1, 7.1 Hz, 1H), 1.44 – 1.21 (m, 16H), 0.91 – 0.86 (m, 6H) ppm.

^{13}C{^{1}H} NMR (126 MHz, $CDCl_3$, mixture of diastereoisomers): δ = 202.5, 202.4, 173.7, 173.5, 162.3 (d, J_{C-F} = 246.0 Hz, 2C), 135.8 (2C) 134.5 (d, J_{C-F} = 3.3 Hz), 134.4 (d, J_{C-F} = 3.2 Hz), 129.7 (d, J_{C-F} = 7.8 Hz), 129.6 (d, J_{C-F} = 7.8 Hz), 128.6 (2C), 128.4 (2C), 128.2, 128.2, 115.7 (d, J_{C-F} = 21.5 Hz), 115.7 (d, J_{C-F} = 21.3 Hz) 66.8 (2C), 48.6, 48.6, 48.3, 48.2, 38.1, 38.0, 34.1, 33.8, 32.0, 31.9, 31.0, 30.8, 26.1, 26.0, 22.6 (2C), 14.1, 14.1 ppm.

^{19}F{^{1}H} NMR (471 MHz, $CDCl_3$, mixture of diastereoisomers): δ = -115.04, -115.07 ppm.

HRMS (ESI): Calculated for $[C_{24}H_{29}FO_3Na]^+$ $[M+Na]^+$: 407.1993, found: 407.1997.

Benzyl (*4S*)-(4-bromophenyl)-4-(2-oxoethyl)nonanoate (8t)

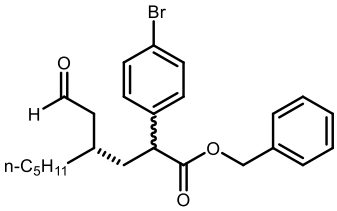

Prepared according to the general procedure **C** using octenal **1a** (112 μL, 750 μmol) and acrylate **7d** (63.0 mg, 250 μmol). The product was purified by flash column chromatography (SiO_2, 5% EtOAc in hexanes) to obtain **8t** as a colourless oil (76.4 mg, 76% yield) in a 1.2:1 diastereomeric ratio.

The enantiomeric ratio of *diastereomer 1* the corresponding 4-nitrobenzoate was determined to be 93.7:6.3 by UPC^2 analysis on a Daicel Chiralpak OJ-3 column (eluent: 100% CO_2 for 1 min, gradient 100% - 80% CO_2 in CH_3CN for 5 min, 80% CO_2 in CH_3CN for 2 min, gradient 80% - 100% CO_2 in CH_3CN for 1 min; flow rate 2.0 mL/min, λ = 256 nm, τ_{Major} = 4.86 min, τ_{Mjnor} = 4.55 min.), and >99.0:1.0 for *diastereomer 2* by UPC^2 analysis on a Daicel Chiralpak ID-3 column (eluent: 100% CO_2 for 1 min, gradient 100% - 60% CO_2 in CH_3CN for 5 min, 60% CO_2 in CH_3CN for 2 min, gradient 60% - 100% CO_2 in CH_3CN for 1 min; flow rate 2.0 mL/min, λ = 256 nm, τ_{Major} = 5.59 min, τ_{Minor} = 5.79 min.)

$[\alpha]_D^{25}$ = -136.0 (c = 0.5, $CHCl_3$, 1.2:1 d.r., 93.7:6.3 e.r.[1], >99.0:1.0 e.r.[2]).

^{1}H NMR (500 MHz, CDCl3, mixture of diastereoisomers): δ= 9.67 (t, *J* = 2.3 Hz, 1H), 9.65 (t, *J* = 2.0 Hz, 1H), 7.47 (dq, *J* = 9.1, 2.6 Hz, 4H), 7.36 – 7.32 (m, 6H), 7.30 – 7.24 (m, 4H), 7.23 – 7.14 (m, 4H), 5.15 (dd, *J* = 12.3, 1.3 Hz, 2H), 5.08 (dd, *J* = 12.3, 2.4 Hz, 2H), 3.68 (td, *J* = 7.5, 2.4 Hz, 2H), 2.41 – 2.27 (m, 4H), 2.14 (ddd, *J* = 13.6, 8.0, 6.9 Hz, 1H), 2.08 – 2.01 (m, 1H), 1.85 (dq, *J* = 12.1, 7.0, 5.6 Hz, 3H), 1.83 – 1.73 (m, 1H), 1.46 – 1.14 (m, 16H), 0.89 (td, *J* = 7.2, 5.3 Hz, 6H) ppm.

^{13}C{^{1}H} NMR (126 MHz, CDCl3, mixture of diastereoisomers): δ= 202.5, 202.3, 173.2 (2C), 137.8, 137.7, 135.8 (2C), 132.0, 132.0, 129.9, 129.8, 128.7 (2C), 128.5 (2C), 128.3, 128.3, 121.6 (2C), 67.0 (2C), 48.9, 48.8, 48.3, 48.3, 37.9, 37.8, 34.1, 33.7, 32.0, 32.0, 31.0, 30.9, 26.1, 26.0, 22.7 (2C), 14.2 (2C) ppm.

HRMS (ESI): Calculated for $C_{24}H_{29}BrO_3Na$ $[M+Na]^+$: 467.1192, found: 467.1194.

Benzyl (*4S*)-(4-methylphenyl)-4-(2-oxoethyl)nonanoate (**8u**)

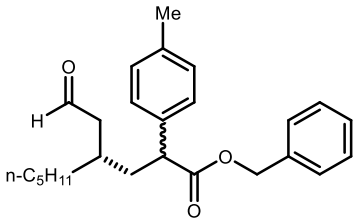

Prepared according to the general procedure **C** using octenal **1a** (112 μL, 750 μmol) and acrylate **7e** (63.0 mg, 250 μmol), the crude product was purified by flash column chromatography (silica, 5% EtOAc in hexanes) to obtain product **8u** as a colorless oil (72.0 mg, 76% yield) in a 1.5:1 diastereomeric ratio. The enantiomeric ratio was determined to be 93.5:6.5 and 87.5:12.5 by HPLC analysis on a Daicel Chiralpak IC-3 column, isocratic 96:4 n-hexane: iPrOH, flow rate = 0.45 mL/min, 15 °C; λ = 215 nm; Diastereoisomer 1: τ_{Major} = 36.70 min, τ_{Minor} = 51.65 min. Diastereoisomer 2: τ_{Major} = 34.55 min, τ_{Minor} = 44.55 min). $[\alpha]_D^{25}$ = -4.5 (c = 0.5, $CHCl_3$, 1.5:1 d.r., 93.5:6.5 e.r.[1], 87.5:12.5 e.r.[2]).

^{1}H NMR (500 MHz, $CDCl_3$, mixture of diastereoisomers): δ = 9.66 (t, *J* = 2.4 Hz, 1H), 9.63 (t, *J* = 2.2 Hz, 1H), 7.37 – 7.31 (m, 6H), 7.29 – 7.26 (m, 4H), 7.23 – 7.19 (m, 4H), 7.17 – 7.13 (m, 4H), 5.17 (d, *J* = 12.4 Hz, 2H), 5.07 (dd, *J* = 12.4, 2.0 Hz, 2H), 3.73 – 3.67 (m, 2H), 2.36 (s, 6H), 2.34 – 2.32 (m, 4H), 2.24 – 2.13 (m, 1H), 2.11 – 2.02 (m, 1H), 1.89 (m, 3H), 1.78 (dt, *J*=14.1, 7.1 Hz, 1H), 1.44 – 1.14 (m, 16H), 0.91 – 0.87 (m, 6H) ppm.

^{13}C{^{1}H} NMR (126 MHz, $CDCl_3$, mixture of diastereoisomers): δ = 202.8, 202.7, 173.9, 173.8, 137.3 (2C), 136.0 (2C), 135.7 (2C), 129.6, 129.5, 128.6 (2C), 128.3, 128.2 (2C) 128.2, 128.0, 127.9, 66.7 (2C), 49.0 (2C), 48.3, 48.3, 37.9, 37.9, 34.1, 33.8, 32.1, 32.0, 31.1, 31.0, 26.1, 26.0, 22.87 (2C), 21.2 (2C), 14.2, 14.1 ppm.

HRMS (ESI): Calculated for $C_{25}H_{32}O_3Na$ $[M+Na]^+$: 403.2244, found: 403.2250.

Benzyl (*4S*)-(3-cyanophenyl)-4-(2-oxoethyl)nonanoate (**8v**)

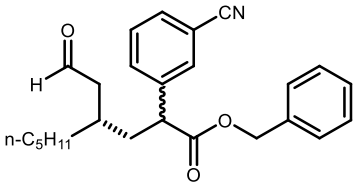

Prepared according to general procedure **C** using (*E*)-oct-2-enal **1a** (112 µL, 0.75 mmol) and acrylate **7f** (63.1 mg, 0.25 mmol). The product purified by flash column chromatography (SiO_2,7 % EtOAc in hexanes) to obtain was obtained **8v** as a light yellow oil (72.4 mg, 76 % yield) in a 1:1 diastereomeric ratio.

$[\alpha]_D^{26}$ = -4.52 (c = 0.5, $CHCl_3$, 1:1 d.r.).

^{1}H NMR (500 MHz, CDCl3, mixture of diastereoisomers): δ= 9.65 (t, *J* = 2.1 Hz, 1H), 9.64 (t, *J* = 1.9 Hz, 1H), 7.63 – 7.59 (m, 2H), 7.58 – 7.52 (m, 4H), 7.51 – 7.39 (m, 2H), 7.36 – 7.29 (m, 6H), 7.26 – 7.22 (m, 4H), 5.14 (dd, *J* = 12.2, 2.5 Hz, 2H), 5.07 (dd, *J* = 12.2, 2.7 Hz, 2H), 3.72 (ddd, *J* = 8.3, 7.0, 4.2 Hz, 2H), 2.42 – 2.29 (m, 4H), 2.23 – 2.02 (m, 4H), 1.79 (dddt, *J* = 27.7, 25.0, 13.9, 6.7 Hz, 4H), 1.47 – 1.25 (m, 14H), 0.86 (m, 6H) ppm.

^{13}C{^{1}H} NMR (126 MHz, CDCl3, mixture of diastereoisomers): δ=202.1, 202.0, 172.7, 172.6, 140.3, 140.2, 135.5 (2C), 132.6, 132.6, 131.8, 131.7, 131.3 (2C), 129.7, 129.7, 128.7 (2C), 128.6 (2C), 128.4 (2C), 118.6, 118.6, 113.0, 113.0, 67.2 (2C), 49.1, 48.9, 48.3, 48.1, 38.1, 37.8, 33.9, 33.7, 32.0, 31.9, 31.0, 30.8, 29.8, 26.1, 26.0, 22.6, 14.1, 14.1 ppm.

HRMS (ESI): Calculated for $C_{25}H_{29}NO_3Na$ $[M+Na]^+$: 415.1882, found: 415.1882.

Benzyl (*4S*)-(3-methoxyphenyl)-4-(2-oxoethyl)nonanoate (8w)

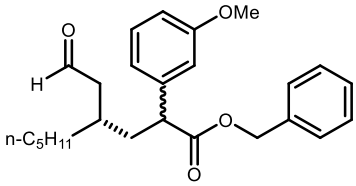

Prepared according to the general procedure E using octenal **1a** (112 µL, 750 µmol) and acrylate **7g** (67.0 mg, 250 µmol), the crude product was purified by flash column chromatography (SiO_2, 5% EtOAc in hexanes) to obtain product **8w** as a colorless oil (83.5 mg, 85% yield) in a 1:1 diastereomeric ratio. The enantiomeric ratio of the corresponding 4-nitrobenzoate derivative, prepared following the general procedure, was determined to be 94.5:5.5 for *diastereomer 1* by UPC^2 analysis on a Daicel Chiralpak OJ-3 column (eluent: 100% CO_2 for 1 min, gradient 100% - 93% CO_2 in CH_3CN for 11 min, 93% CO_2 in CH_3CN for 2 min,

gradient 93% - 100% CO_2 in CH_3CN for 1 min; flow rate 2.0 mL/min, λ = 256 nm; τ_{Major} = 8.35 min, τ_{Minor} = 7.75 min.), and 91:9 for *diastereomer 2* by UPC[2] analysis on a Daicel Chiralpak ID-3 column (eluent: 100% CO_2 for 1 min, gradient 100% - 80% CO_2 in CH_3CN for 5 min, 80% CO_2 in CH_3CN for 2 min, gradient 80% - 100% CO_2 in CH_3CN for 1 min; flow rate 2.0 mL/min, λ = 256 nm; τ_{Major} = 8.20 min, τ_{Minor} = 7.85 min.)

$[\alpha]_D^{24}$ = -83.1 (c = 1.0, $CHCl_3$, 1:1 d.r., 94.5:5.5 e.r.[1], 91:9 e.r.[2]).

^{1}H NMR (500 MHz, $CDCl_3$, mixture of diastereoisomers): δ = 9.67 (t, *J* = 2.3 Hz, 1H), 9.64 (t, *J* = 2.2 Hz, 1H), 7.35 – 7.31 (m, 6H), 7.31 – 7.19 (m, 6H), 6.93 – 6.88 (m, 3H), 6.88 – 6.80 (m, 3H), 5.17 (d, *J* = 12.3 Hz, 2H), 5.09 (dd, *J* = 12.3, 2.3 Hz, 2H), 3.80 (s, 3H), 3.79 (s, 3H), 3.75 – 3.65 (m, 2H), 2.39 – 2.30 (m, 4H), 2.17 (ddd, *J* = 13.7, 8.1, 6.7 Hz, 1H), 2.13 – 2.03 (m, 1H), 1.95 – 1.84 (m, 3H), 1.80 (dt, *J* = 14.0, 7.1 Hz, 1H), 1.47 – 1.15 (m, 16H), 0.92 – 0.86 (m, 6H) ppm.

^{13}C{^{1}H} NMR (126 MHz, $CDCl_3$, mixture of diastereoisomers): δ = 202.7, 202.5, 173.5 (2C), 156.0, 159.9, 140.2, 140.2, 135.9 (2C), 129.8, 129.8, 128.6 (2C), 128.3 (2C), 128.2, 128.2, 120.5, 120.4, 113.6, 113.6, 113.1, 113.1, 66.7 (2C), 55.3 (2C), 49.4, 49.4, 48.3, 48.3, 37.9, 37.8, 34.0, 33.9, 32.0, 32.0, 31.1, 31.0, 26.1, 26.0, 22.6 (2C), 14.1, 14.1 ppm.

HRMS (ESI): Calculated for $C_{25}H_{32}O_4Na$ $[M+Na]^+$: 419.2193, found: 419.2181.

Benzyl (*4S*)-(2,4-dichlorophenyl)-4-(2-oxoethyl)nonanoate (8x)

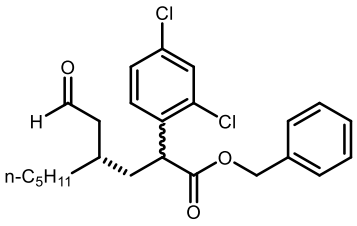

Prepared according to general procedure **C** using (*E*)-oct-2-enal **1a** (112 μL, 0.75 mmol) and acrylate **7h** (67.1 mg, 0.25 mmol). The product was purified through flash column chromatography(SiO_2, 5% EtOAc in hexanes) to obtain **8x** as a colourless oil (68.3 mg, 63% yield) in a 1:1 diastereomeric ratio. (*determined by the ^{1}H NMR integrals of benzylic positions of esters*)

The enantiomeric ratio of *diastereomer 1* the corresponding 4-nitrobenzoate was determined to be 70.2:29.8 by UPC[2] analysis on a Daicel Chiralpak OJ-3 column (eluent: 100% CO_2 for 1 min, gradient 100% - 80% CO_2 in CH_3CN for 5 min, 80% CO_2 in CH_3CN for 2 min, gradient 80% - 100% CO_2 in CH_3CN for 1 min; flow rate 2.0 mL/min, λ = 255 nm, τ_{Major} = 4.42 min,

τ_{Minor} = 4.11 min.), and 78.3.2:21.7 for *diastereomer 2* by UPC^2 analysis on a Daicel Chiralpak ID-3 column (eluent: 100% CO_2 for 1 min, gradient 100% - 90% CO_2 in CH_3CN for 11 min, 90% CO_2 in CH_3CN for 2 min, gradient 90% - 100% CO_2 in CH_3CN for 1 min; flow rate 2.0 mL/min, λ = 256 nm, τ_{Major} = 14.15 min, τ_{Minor} = 13.34 min.)

$[\alpha]_D^{24}$ = -116.7 (c = 0.5, $CHCl_3$, 1:1 d.r., 70.2:29.8 e.r., 78.3:21.7 e.r.).

^{1}H NMR (500 MHz, $CDCl_3$, mixture of diastereoisomers): δ= 9.66 (m, 2H), 7.40 (d, *J* = 2.2 Hz, 2H), 7.35 – 7.28 (m, 6H), 7.29 – 7.23 (m, 6H), 7.21 (td, *J* = 8.8, 2.2 Hz, 2H), 5.15 (d, *J* = 12.3 Hz, 2H), 5.14 – 5.05 (m, 2H), 4.29 – 4.21 (m, 2H), 2.38 (dt, *J* = 6.3, 2.3 Hz, 2H), 2.34 (dd, *J* = 6.4, 2.3 Hz, 2H), 2.09 (ddd, *J* = 14.4, 8.0, 6.8 Hz, 1H), 2.01 (ddd, *J* = 14.3, 8.1, 6.5 Hz, 1H), 1.86 (hept, *J* = 6.4 Hz, 2H), 1.78 (dt, *J* = 13.8, 6.9 Hz, 1H), 1.71 (dt, *J* = 14.0, 7.0 Hz, 1H), 1.40 – 1.17 (m, 16H), 0.86 (td, *J* = 7.1, 4.4 Hz, 6H) ppm.

^{13}C{^{1}H} NMR (126 MHz, $CDCl_3$, mixture of diastereoisomers): δ= 202.4, 202.2, 172.8 (2C), 135.7 (2C), 135.4, 135.2, 134.7, 134.7, 133.8 (2C), 129.8, 129.7 (2C), 129.6, 128.7 (2C), 128.4 (2C), 128.2 (2C), 127.7 (2C), 67.1. 67.0, 48.4, 48.2, 44.8, 44.7, 37.5, 37.4, 33.9, 33.9, 32.0, 32.0, 31.1, 30.9, 26.1, 26.0, 22.7, 22.6, 14.2 (2C) ppm.

HRMS (ESI): Calculated for $C_{24}H_{28}Cl_2O_3Na$ $[M+Na]^+$: 457.1308, found: 457.1317.

Benzyl (*4S*)-(2,3,4-trifluorophenyl)-4-(2-oxoethyl)nonanoate (**8y**)

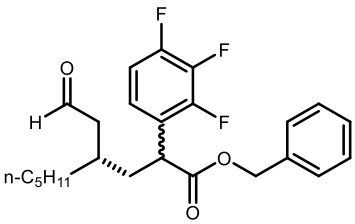

Prepared according to general procedure A using (*E*)-oct-2-enal **1a** (112 μL, 0.75 mmol) and acrylate **7i** (67.1 mg, 0.25 mmol). The product was purified by flash column chromatography (SiO_2,5% EtOAc in hexanes) to obtain **8y** as a colourless oil (82.7 mg, 87% yield) in a 2.3:1 diastereomeric ratio.

$[\alpha]_D^{24}$ = +5.10 (c = 1.0, $CHCl_3$, 2.3:1 d.r.).

^{1}H NMR (500 MHz, $CDCl_3$, mixture of diastereoisomers): δ= 9.72 (dd, *J* = 2.6, 1.7 Hz, 1H), 9.68 (t, *J* = 2.0 Hz, 1H), 7.39 – 7.30 (m, 6H), 7.34 – 7.23 (m, 4H), 7.15 – 7.05 (m, 2H), 6.86 (tdd, *J* = 9.1, 3.8, 2.3 Hz, 2H), 5.17 (t, *J* = 2.0 Hz, 4H), 4.12 (td, *J* = 9.0, 5.8 Hz, 2H), 2.43 (tdd, *J* = 14.0, 5.5, 1.9 Hz, 2H), 2.40 – 2.32 (m, 2H), 2.34 – 2.25 (m, 1H), 2.21 (ddd, *J* =

14.4, 8.5, 6.1 Hz, 2H), 1.97 (ddd, *J* = 14.3, 9.2, 5.1 Hz, 1H), 1.92 – 1.79 (m, 2H), 1.45 – 1.12 (m, 16H), 0.87 (dt, *J* = 15.5, 7.2 Hz, 6H) ppm.

$^{19}F\{^{1}H\}$ NMR (471 MHz, $CDCl_3$, mixture of diastereoisomers): δ= -118.62 (d, *J* = 15.0 Hz, 1F), -118.81 (d, *J* = 15.0 Hz, 1F), -136.65 (d, *J* = 21.2 Hz, 1F), -136.68 (d, *J* = 20.8 Hz, 1F), -141.75 (dd, *J* = 20.8, 15.1 Hz, 1F), -141.86 (dd, *J* = 20.8, 15.0 Hz, 1F) ppm.

$^{13}C\{^{1}H, ^{19}F\}$ NMR (126 MHz, $CDCl_3$, mixture of diastereoisomers): δ= 202.3, 202.1, 171.4, 171.4, 156.5, 156.4, 149.0, 148.9, 147.3 (2C), 135.7, 135.6, 128.6 (2C), 128.4, 128.4, 128.1, 128.1, 117.6, 117.5, 116.1, 116.1, 111.0, 111.0, 67.3, 67.3, 48.4, 48.0, 38.7, 38.6, 35.0, 34.6, 34.4, 33.1, 32.0, 31.9, 31.1, 30.9, 26.1, 25.9, 22.6, 22.6, 14.1, 14.1 ppm.

HRMS (ESI): Calculated for $C_{24}H_{27}F_3O_3Na$ $[M+Na]^+$: 443.1805, found: 443.1800.

Methyl (*4S*)-phenyl-4-(2-oxoethyl)nonanoate (8z)

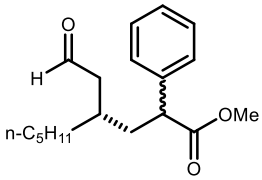

Prepared according to the general procedure **C** using octenal **1a** (112 μL, 750 μmol) and acrylate **7j** (40.5 mg, 250 μmol), the crude product was purified by flash column chromatography (silica, 5% EtOAc in hexanes) to obtain product **8z** as a colorless oil (54.0 mg, 75% yield) in a 1.2:1 diastereomeric ratio. Analytical data is in agreement with the literature.[11] The enantiomeric ratio of the corresponding 4-nitrobenzoate derivative, prepared following the general procedure, was determined to be 94:6 for *diastereomer 1* by UPC^2 analysis on a Daicel Chiralpak OJ-3 column (eluent: 100% CO_2 for 1 min, gradient 100% - 85% CO_2 in CH_3CN for 11 min, 85% CO_2 in CH_3CN for 2 min, gradient 85% - 100% CO_2 in CH_3CN for 1 min; flow rate 2.0 mL/min, λ = 258 nm; τ_{Major} = 4.60 min, τ_{Minor} = 4.35 min.), and 86.0:14.0 for *diastereomer 2* by UPC^2 analysis on a Daicel Chiralpak ID-3 column (eluent: 100% CO_2 for 1 min, gradient 100% - 60% CO_2 in CH_3CN for 5 min, 60% CO_2 in CH_3CN for 2 min, gradient 60% - 100% CO_2 in CH_3CN for 1 min; flow rate 2.0 mL/min, λ = 256 nm; τ_{Major} = 5.65 min, τ_{Minor} = 5.40 min). $[\alpha]_D^{24}$ = -148.1 (c = 0.5, $CHCl_3$, 1.2:1 d.r., 94:6 e.r.[1], 86:14 e.r.[2]).

^{1}H NMR (500 MHz, $CDCl_3$, mixture of diastereoisomers): δ = 9.72 (t, *J* = 2.3 Hz, 1H), 9.69 (t, *J* = 2.2 Hz, 1H), 7.47 – 7.18 (m, 10H), 3.68 (s, 6H), 2.40 – 2.34 (m, 4H), 2.19 – 2.14 (m, 2H), 2.07 – 2.02 (m, 2H), 1.94 – 1.84 (m, 4H), 1.81 – 1.75 (m, 2H), 1.47 – 1.09 (m, 14H), 0.98 – 0.76 (m, 6H) ppm.

Benzyl (*4S*)- (2-oxoethyl)-2-(trifluoromethyl)nonanoate (**26**)

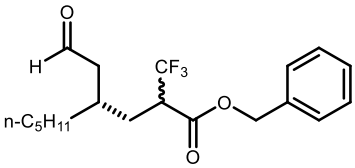

Prepared according to general procedure **C** using (*E*)-oct-2-enal **1a** (112 µL, 0.75 mmol) and acrylate **7k** (57.5 mg, 0.25 mmol). The product was purified by flash column chromatography (SiO_2,5% EtOAc in n-hexanes) to obtain **26** as a light yellow oil (58.6 mg, 65% yield) in a 1.3:1 diastereomeric ratio.

$[\alpha]_D^{24}$ = -128.1 (c = 0.5, $CHCl_3$, 1.3:1 d.r.).

^{1}H NMR (500 MHz, $CDCl_3$, mixture of diastereoisomers): δ= 9.63 (t, *J* = 1.9 Hz, 1H), 9.61 (t, *J* = 1.9 Hz, 1H), 7.42 – 7.30 (m, 10H), 5.25 (dd, *J* = 12.1, 6.7 Hz, 2H), 5.20 (dd, *J* = 12.2, 6.1 Hz, 2H), 3.29 – 3.14 (m, 2H), 2.51 – 2.36 (m, 1H), 2.37 – 2.31 (m, 2H), 2.31 – 2.21 (m, 1H), 2.06 (ddd, *J* = 14.0, 10.9, 4.7 Hz, 2H), 1.99 – 1.85 (m, 2H), 1.80 – 1.64 (m, 2H), 1.36 – 1.12 (m, 16H), 0.87 (t, *J* = 7.2 Hz, 6H) ppm.

^{19}F NMR (471 MHz, $CDCl_3$, mixture of diastereoisomers): δ= -68.29 (d, *J* = 8.7 Hz), -68.34 (d, *J* = 8.6 Hz) ppm.

^{13}C{^{1}H} NMR (126 MHz, $CDCl_3$, mixture of diastereoisomers): δ= 201.5 (2C), 167.4 (m, 2C), 135.1, 135.0, 128.8, 128.8, 128.7 (2C), 128.6 (2C), 124.8 (q, *J* = 280.1 Hz, 2C), 67.8 (2C), 48.9 – 48.1 (m), 48.2, 47.6 (2C), 34.5 (2C), 32.9 (2C), 31.9, 31.9, 30.7 (dd, *J* = 41.0, 1.8 Hz), 30.5 (d, *J* = 33.1 Hz), 26.2, 25.8, 22.6 (2C), 14.1, 14.1 ppm.

HRMS (ESI): Calculated for $C_{19}H_{25}F_3O_3Na$ $[M+Na]^+$: 381.1648, found: 381.1645.

Methyl (*S*)-2-methylene-4-(2-oxoethyl)nonanoate (**27**)

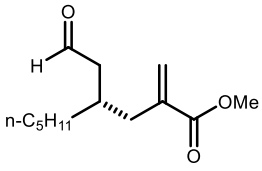

To a 8.0 mL argon-purged glass vial, containing allylic sulfone **21** (24.0 mg, 100 µmol), octenal **1a** (59.6 µL, 400 µmol, 4.0 equiv.), DHP **R-1** (48.5 mg, 150 µmol, 1.5 equiv.), 4-CzIPN (1.0 mg, 1.0 µmol, 1 mol%) and amine catalyst **C** (14.0 mg, 20.0 µmol, 20 mol%), was added 200 µL of dimethoxyethane, H_2O (5.5 µL, 300 µmol, 3 equiv.) and trichloroacetic acid (3.0 µL 30.0 µmol, 30 mol%). The vial was sealed with Parafilm, and then placed into a cooled aluminium support mounted on an aluminium block fitted with a 460 nm high-power single LED (λ = 460 nm, irradiance = 60 mW/cm^2). The reaction was stirred under

visible light irradiation at 5 °C internal temperature for 16 hours. The product was purified by flash column chromatography (SiO_2,5% EtOAc in hexanes) to obtain **27** as a colorless oil (13.5 mg, 60% yield). The enantiomeric ratio of the corresponding 2,4-dinitrophenylhydrazone derivative (prepared following the general procedure of β-cyanoaldehydes **23**), was determined to be 90.0:10.0 by UPC^2 analysis on a Daicel Chiralpak IE-3 column (eluent: 100% CO_2 for 1 min, gradient 100% - 60% CO_2 in EtOH for 5 min, 60% CO_2 in CH_3CN for 2 min, gradient 60% - 100% CO_2 in EtOH for 1 min; flow rate 2.0 mL/min, λ = 348 nm; τ_{Major} = 6.60 min, τ_{Minor} = 6.25 min). $[\alpha]_D^{25}$ = -0.9 (c = 0.1, $CHCl_3$, 90:10 e.r.).

^{1}H NMR (500 MHz, $CDCl_3$): δ = 9.74 (t, *J* = 2.2 Hz, 1H), 6.22 (d, *J* = 1.5 Hz, 1H), 5.55 (d, *J* = 1.3 Hz, 1H), 3.76 (s, 3H), 2.50 – 2.42 (m, 1H), 2.40 – 2.27 (m, 2H), 2.25 – 2.20 (m, 1H), 2.18 – 2.16 (m, 1H), 1.39 – 1.23 (m, 8H), 0.88 (t, *J* = 7.1 Hz, 3H) ppm.

^{13}C{^{1}H} NMR (126 MHz, $CDCl_3$): δ = 203.0, 167.6, 138.9, 127.2, 52.1, 48.1, 37.2, 34.3, 32.3, 32.1, 26.4, 22.7, 14.2 ppm.

HRMS (ESI): Calculated for $C_{13}H_{22}O_3Na$ $[M+Na]^+$: 249.1461, found: 249.1452.

Derivatization of 1,6-Dicarbonyl Products

Separation of diastereomers

Lithium aluminium hydride (500 μmol, 19.0 mg, 2.0 equiv.) was added portion wise to a solution of **8b** (250 μmol, 99.0 mg, 1.0 equiv.) in anhydrous THF (1.0 mL) at 0 °C under an argon atmosphere. The reaction mixture was allowed to warm to room temperature and was stirred for 3 h. The reaction mixture was then diluted with Et_2O (20 mL), cooled to 0 °C and carefully quenched by addition of Glauber's salt ($NaSO_4 \cdot 10\ H_2O$). After 10 min the solids were removed by filtration over a silica pad, which was thoroughly rinsed with EtOAc. The volatiles were removed under reduce pressure and the crude was purified by flash column chromatography (SiO_2, 25-50% EtOAc in n-hexanes) to afford (2*R*,4*S*)-4-pentyl-2-phenylhexane-1,6-diol (**24a**, 25.0 mg, 38% yield, see x-ray analysis) and (2*S*,4*S*)-4-pentyl-2-phenylhexane-1,6-diol (**24b**, 21.0 mg, 32% yield) as colorless oils.

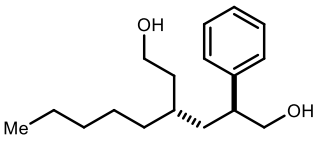

24a:$[\alpha]_D^{26}$ = -34.1 (c = 1.0, $CHCl_3$, 93:7 e.r.).

^{1}H NMR (400 MHz, $CDCl_3$): δ = 7.36 – 7.28 (m, 2H), 7.25 – 7.17 (m, 3H), 3.75 – 3.64 (m, 2H), 3.59 – 3.51 (m, 2H), 2.93 – 2.84 (m, 1H), 1.62 – 1.56 (m, 2H), 1.56 – 1.47 (m, 2H), 1.47 – 1.37 (m, 2H), 1.32 – 1.15 (m, 7H), 0.87 (t, *J*=7.1 Hz, 3H) ppm.

^{13}C{^{1}H} NMR (101 MHz, $CDCl_3$): δ = 142.6, 128.9, 128.2, 126.9, 68.1, 61.1, 46.4, 37.3, 36.5, 33.4, 32.4, 31.7, 25.7, 22.8, 14.2 ppm.

HRMS (ESI): Calculated for $[C_{17}H_{28}O_2Na]^+$ $[M+Na]^+$: 287.1982; found: 287.1972.

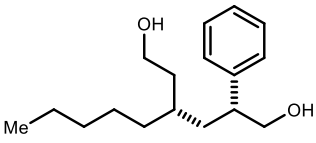

24b:$[\alpha]_D^{26}$ = +6.6 (c = 1.0, $CHCl_3$, 84:16 e.r.).

^{1}H NMR (400 MHz, $CDCl_3$): δ = 7.36 – 7.28 (m, 2H), 7.27 – 7.17 (m, 3H), 3.71 (d, *J* = 6.6 Hz, 2H), 3.69 – 3.51 (m, 2H), 2.95 – 2.84 (m, 1H), 1.61 (t, *J* = 7.0 Hz, 2H), 1.59 – 1.45 (m, 2H), 1.39 – 1.09 (m, 9H), 0.85 (t, *J* = 7.2 Hz, 3H).

^{13}C{^{1}H} NMR (101 MHz, $CDCl_3$): δ = 142.8, 128.8, 128.2, 126.9, 68.0, 60.9, 46.2, 36.5, 36.3, 34.6, 32.2, 32.0, 26.2, 22.8, 14.2.

HRMS (ESI): Calculated for $[C_{17}H_{28}O_2Na]^+$ $[M+Na]^+$: 287.1982; found: 287.1973.

3.6.4 General Procedure for the Conjugate Cyanation of Enals

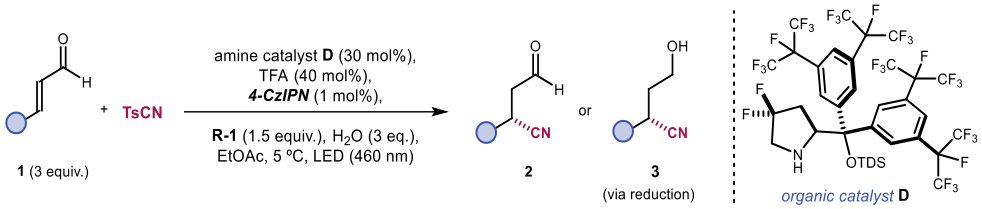

General procedure D (*for 0.25 mmol scale*): An 8.0 mL vial equipped with a stirring bar was charged with tosyl cyanide (48 mg, 250 µmol, 95% purity, 1.0 equiv.), the chiral amine catalyst **D** (83 mg, 75.0 µmol, 0.3 equiv.), **R-1** (122 mg, 375 µmol, 1.5 equiv.), 4-CzIPN (2 mg, 2.50 µmol, 1 mol%) and enal **1** (3.0 equiv.). The vial was sealed with a septum and purged with argon. The reactants were suspended in EtOAc (500 µL, ensure that all compounds are suspended) and deionized water (13.5 µL, 3.0 equiv.) was added. Then, CF_3COOH (7.5 µL, 100 µmol, 0.4 eq) was added and the vial was instantly placed in a pre-cooled metal support (set for an internal temperature of 5 °C) mounted on an aluminum block fitted with a high-power single blue LED (λ_{max} = 460 nm, irradiance set at 60 mW/cm^2 as controlled by an external power supply). The set-up secured a reliable irradiation while keeping a distance of 1 cm between the reaction vessel and the light source (set-up detailed in Figure 3.27). After 16 hours (unless otherwise stated), the mixture was concentrated under reduced pressure.

β-cyanation with Kessil Lamp setup

The reaction mixture (0.25 mmol standard scale) was prepared as describedin general procedure **D** and the vial containing all reactants was instantly placed in a cooling bath (set to 5 °C) using a cryostat. The mixture was irradiated with a Kessil lamp (PR160L-456 nm, 40 W) for 18 hours. After 40 hours, the mixture was concentrated under reduced pressure. A mixture containing the β-cyanoaldehyde **23a** (67% NMR yield) and the sulfone by-product **23a'** (73% NMR yield) was obtained. The crude target product **23a** was reduced according to the general procedure **E** and the desired alcohol was purified by flash column chromatography (SiO_2, 15-20% EtOAc in hexanes) to afford product **34a** as a pale-yellow oil (25.0 mg, 65% yield). Analytical data was in agreement with the product obtained from the single LED experiment as described above. The enantiomeric ratio was determined as described above to be 90:10 by UPC^2 analysis.

Figure 3.29. Set-up for the conjugate cyanation of octenal **1a** using a Kessil lamp (456 nm, maximal intensity). The vial was placed in a toluene bath which was externally cooled to 5 °C by a cryostat (Thermo Fisher Scientific - EK90 Immersion Cooler). Distance from the Kessil lamp to the bottom of the vial was approximately 5 cm.

β-cyanation at 1 mmol scale

An 8 mL vial equipped with a stirring bar was charged with tosyl cyanide (191 mg, 1.00 mmol, 95% purity, 1.0 equiv.), Amine **D** (331 mg, 300 µmol, 0.3 equiv.), **R-1** (390 mg, 1.20 mmol, 1.2 equiv.), 4-CzIPN (8 mg, 10.0 µmol, 1 mol%) and **1a** (450 µL, 3.00 mmol, 3.0 equiv.). The vial was sealed with a septum and purged with Argon. The reactants were suspended in EtOAc (2.00 mL, ensure that all compounds are suspended) and deionized water (54.1 µL, 3.0 equiv.) was added. Then, TFA (30.0 µL, 400 µmol, 400 µmol) was added and the vial was instantly placed in a pre-cooled metal block (setup detailed in Figure 3.27, set for

an internal temperature of 5 °C) and irradiated with a high-power single LED (460 nm, irradiance 60 mW/cm^2). After 40 hours, the mixture was concentrated under reduced pressure.

The crude reaction mixture containing the β-cyanoaldehyde **23a** (58% NMR yield) and the sulfone by-product **23a'** (68% NMR yield) was dissolved in THF (8.00 mL) and then water (2.00 mL) was added. After cooling 0 °C with an ice bath, $NaBH_4$ (380 mg, 10.0 mmol, 10 equiv.) was added in a few portions while rigorous stirring. After 10 minutes, the ice bath was removed and the mixture was stirred for 90 minutes at ambient temperature. After cooling to 0 °C with an ice bath, the slurry was quenched dropwise with 1 N HCl until gas evolution ceased. The mixture was transferred to a separation funnel and extracted with CH_2Cl_2 (3 x 50 mL). The combined organic layers were dried with $MgSO_4$ and concentrated. A mixture containing the β-cyanoaldehyde with 58% NMR yield was obtained. The crude mixture was purified by flash column chromatography (SiO_2, 15-20% EtOAc in hexanes) to afford product **34a** as a pale-yellow oil (86.0 mg, 55% yield). Analytical data was in agreement with the product obtained from the 0.25 mmol scale experiment as described above. The enantiomeric ratio of the corresponding 4-nitrobenzoate derivative was determined to be 90.5:9.5 by UPC^2 analysis on a Daicel Chiralpak IA-3 column as described for the 0.25 mmol scale experiment.

Determination of analytical yields for the conjugate cyanation of enals. Analytical yields were determined by ^{1}H NMR analysis (400 MHz) of the crude reaction mixtures using trichloroethylene (TCE, 22.5 uL, 250 µmol, 1.0 equiv.) as the internal standard. For integration, aldehydic peaks have been used (d_1 = 6 seconds). This analysis allowed to infer the analytic yields of both the target cyanation product **23** and the by-product **23'** (arising from the competitive addition of tosyl radical to enal **1**), which was typically formed in a similar amount as the target adduct **23**. *For each specific entry (see below), we report the analytical yields of products **23** and **23'**.* The aldehydic peaks typically appear in the following order from low to high field, as shown in Figure 3.30 (case example using octenal **1a**).

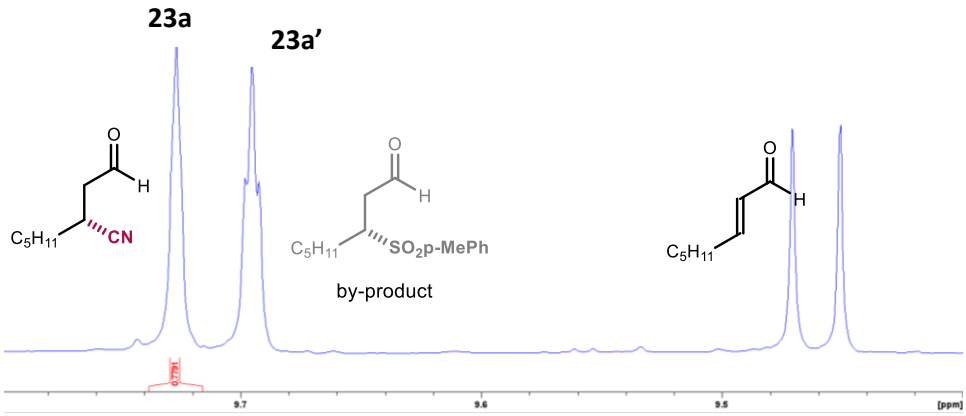

Figure 3.30. Crude reaction mixture using **1a** (400 MHz), showing aldehydic products: β-cyanoaldehyde **23a** (br s, left); β-sulfone aldehyde **23a'** (t, *J* = 1.00 Hz), and octenal starting material **1a** (d, *J* = 8.0 Hz, right)

It was not always possible to isolate the cyanoaldehydes **23** because of a difficult separation from the β-sulfone aldehyde by-product **23'**. When the direct isolation of pure cyanoaldehydes was not feasible, they were isolated as cyano-alcohols **34** upon reduction of the crude reaction mixture according to Figure 3.31. *Conversion to alcohols **34** allowed a simple separation from the sulfone by-product **23'***

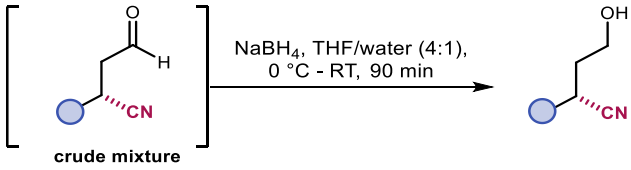

Figure 3.31. Reduction of cyanoaldehydes **23** (crude mixture) to their corresponding cyanoalcohols **34**

Reduction to β-cyanoalcohols 34 (*one-pot*) - General procedure E: Upon completion of the organocatalytic conjugate cyanation, the solvent was evaporated and the crude reaction mixture containing **23** was dissolved in THF (2.0 mL); then water (0.5 mL) was added. After cooling to 0 °C with an ice bath, $NaBH_4$ (94.6 mg, 2.50 mmol, 10 equiv.) was added in a few portions under vigorous stirring. After 10 minutes, the ice bath was removed and the mixture was stirred for 90 minutes at ambient temperature. After cooling to 0 °C with an ice bath, the slurry was quenched dropwise with 1 N HCl until gas evolution ceased. The mixture was transferred to a separation funnel and extracted with CH_2Cl_2 (3 x 20 mL). The combined organic layers were dried with $MgSO_4$ and concentrated. The β-cyano-alcohols **34** were isolated under conditions stated at the individual compounds below.

Derivatization of products 23 or 34 for determination of the enantiomeric ratio by UPC^2 analysis

In order to determine the enantiomeric ratio of the products, β-cyanoaldehydes **23** were converted into the corresponding 2,4-dinitrophenylhydrazones (see Figure 3.32), while β-cyanoalcohols **34** were best analysed upon derivatisation into the corresponding nitrobenzoic esters (Figure 3.33).

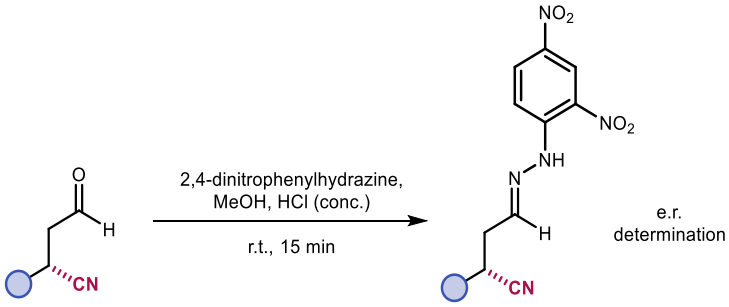

Figure 3.32. Preparation of an analytical sample of 2,4-dinitrophenylhydrazones from β-cyanoaldehydes **23**

Procedure: A analytical sample of cyanoaldehyde **23** (1.00 mg) and 1 equiv. of 2,4-dinitrophenylhydrazine were dissolved in MeOH (0.3 mL). 1 drop of concentrated HCl was added and the solution was allowed to stand for 15 minutes and then concentrated under reduced pressure. The hydrazone was separated from unreacted hydrazine by preparative TLC

and the enantiomeric ratio of the hydrazones was determined by UPC^2 analysis with conditions specified in the experimental section of the individual compounds.

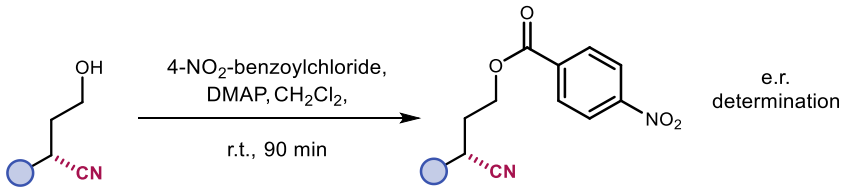

Figure 3.33. Preparation of an analytical sample of 4-nitrobenzoic esters from β-cyanoalcohols **34**.

Procedure: An analytical sample of cyanoalcohol **34** (1.00 mg) and 1 equiv. of *p*-NO_2-benzoyl chloride were suspended in CH_2Cl_2 (0.3 mL). 1 equiv. of 4-dimethylaminopyridine (DMAP) was added and the solution was allowed to stir for 90 minutes. The ester was separated from unreacted reactands by preparative TLC and the enantiomeric ratio of the benzoic ester was determined by UPC^2 analysis with conditions specified in the experimental section of the individual compounds.

3.6.5 Characterization of cyanation products

(*R*)-2-(2-Hydroxyethyl)heptanenitrile (34a).

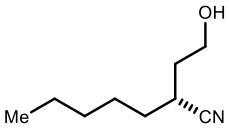

Following the general procedure **D** using enal **1a** (750 μmol, 94.5 mg), a mixture containing the β-cyanoaldehyde **23a** (77% NMR yield) and the sulfone by-product **23a'** (45% NMR yield) was obtained. The crude target product was reduced according to the general procedure **E** and the desired alcohol was purified by flash column chromatography (SiO_2, 15-20% EtOAc in hexanes) to afford product **34a** as a pale-yellow oil (29.0 mg, 75% yield). The enantiomeric ratio of the corresponding 4-nitrobenzoate derivative was determined to be 90.5:9.5 by UPC^2 analysis on a Daicel Chiralpak IA-3 column (eluent: 100% CO_2 for 1 min, gradient 100% - 60% CO_2 in CH_3CN for 5 min, 60% CO_2 in CH_3CN for 2 min, gradient 60% - 100% CO_2 in CH_3CN for 1 min; flow rate 2.0 mL/min, λ = 256 nm; τ_{Major} = 4.25 min, τ_{Minor} = 4.55 min). $[\alpha]_D^{25}$ = -2.0 (c = 1.0, $CHCl_3$, 90.5:9.5 e.r.).

^{1}H NMR (400 MHz, $CDCl_3$): δ = 3.86-3.79 (m, 2H), 2.85-2.76 (m, 1H), 1.88-1.78 (m, 2H), 1.69-1.39 (m, 4H), 1.38-1.27 (m, 4H), 0.93-0.87 (t, *J* = 6.9 Hz, 3H) ppm.

^{13}C{^{1}H} NMR (126 MHz, $CDCl_3$): δ = 122.2, 59.9, 35.0, 32.3, 31.4, 28.3, 26.9, 22.5, 14.1 ppm.

HRMS (APCI): Calculated for $C_9H_{18}NO$ $[M+H]^+$: 156.1383; found: 156.1386.

(*R*)-4-Hydroxy-2-methylbutanenitrile (**34b**).

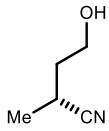

Following the general procedure **D** using enal **1c** (750 μmol, 52.5 mg), a mixture containing the β-cyanoaldehyde **23b** (56% NMR yield) and the sulfone by-product **23b'** (45% NMR yield) was obtained. The crude target product was reduced according to the general procedure **E** and the desired alcohol was purified by flash column chromatography (SiO_2, 15-20% EtOAc in hexanes) to afford product **34b** as a pale-yellow oil (14.0 mg, 57% yield). During all operations, low pressure was avoided due to the high volatility of the compound. The enantiomeric ratio of the corresponding 4-nitrobenzoate derivative was determined to be 85:15 by UPC^2 analysis on a Daicel Chiralpak IA-3 column (eluent: 100% CO_2 for 1 min, gradient 100% - 90% CO_2 in CH_3CN for 5 min, 90% CO2 in

CH_3CN for 2 min, gradient 90% - 100% CO_2 in CH_3CN for 1 min; flow rate 2.0 mL/min, λ = 255 nm; τ_{Major} = 6.15 min, τ_{Minor} = 6.30 min). $[\alpha]_D^{25}$ = -43.7 (c = 0.5, $CHCl_3$, 85:15 e.r.).

^{1}H NMR (400 MHz, $CDCl_3$): δ = 3.81 (dd, *J* = 6.6, 5.4 Hz, 2H), 2.94-2.84 (m, 1H), 1.90-1.74 (m, 2H), 1.35 (d, *J* = 7.1 Hz, 3H) ppm.

^{13}C{^{1}H} NMR (101 MHz, $CDCl_3$): δ = 123.0, 59.6, 36.6, 22.2, 18.0 ppm.

HRMS: not obtained due to volatility

(*R*)-2-(2-Hydroxyethyl)-4-methylpentanenitrile (**34c**).

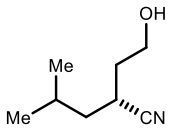

Following the general procedure **D** using enal **1d** (750 μmol, 187 mg, 45 w% in hexanes), a mixture containing the β-cyanoaldehyde **23c** (60% NMR yield) and the sulfone by-product **23c'** (85% NMR yield) was obtained. The crude target product was reduced according to the general procedure **E** and the desired alcohol was purified by flash column chromatography (SiO_2, 15-20% EtOAc in hexanes) to afford product **34c** as a colorless oil (19.5 mg, 56% yield). The enantiomeric ratio of the corresponding 4-nitrobenzoate derivative was determined to be 89.5:10.5 by UPC^2 analysis on a Daicel Chiralpak IA-3 column (eluent: 100% CO_2 for 1 min, gradient 100% - 60% CO_2 in CH_3CN for 5 min, 60% CO_2 in CH_3CN for 2 min, gradient 60% - 100% CO_2 in CH_3CN for 1 min; flow rate 2.0 mL/min, λ = 256 nm; τ_{Major} = 3.90 min, τ_{Minor} = 4.15 min). $[\alpha]_D^{25}$ = -1.2 (c = 0.5, $CHCl_3$, 89.5:10.5 e.r.).

^{1}H NMR (400 MHz, $CDCl_3$): δ = 3.83 (t, *J* = 5.7 Hz, 2H), 2.92 – 2.78 (m, 1H), 1.94 – 1.74 (m, 3H), 1.72 (br s, OH), 1.63 (ddd, *J* = 13.5, 10.4, 5.0 Hz, 1H), 1.33 (ddd, *J* = 13.5, 9.3, 5.4 Hz, 1H), 0.97 (d, *J* = 6.6 Hz, 3H), 0.94 (d, *J* = 6.6 Hz, 3H) ppm.

^{13}C{^{1}H} NMR (126 MHz, $CDCl_3$): δ = 122.2, 59.8, 41.3, 35.3, 26.4, 26.3, 23.0, 21.6 ppm.

HRMS (APCI): Calculated for $C_8H_{16}NO$ $[M+H]^+$: 142.1226; found: 142.1231.

***(S)*-4-Hydroxy-2-isopropylbutanenitrile** (**34d**).

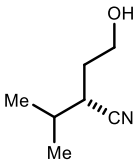

Following the general procedure **D** using enal **1e** (750 μmol, 73.5 mg), a mixture containing the β-cyanoaldehyde **23d** (42% NMR yield) and the sulfone by-product **23d'** (> 95% NMR yield) was obtained. The crude target product was reduced according to the general procedure **E** and the desired alcohol was purified by flash column chromatography (SiO_2, 15-20% EtOAc in hexanes) to afford product **34d** as a pale-yellow oil (13.0 mg, 42% yield). *During all operations, low pressure was avoided due to potential volatility.* The enantiomeric ratio of the corresponding 4-nitrobenzoate derivative was determined to be 92:8 by UPC^2 analysis on a Daicel Chiralpak IA-3 column (eluent: 100% CO_2 for 1 min, gradient 100% - 60% CO_2 in CH_3CN for 5 min, 60% CO_2 in CH_3CN for 2 min, gradient 60% - 100% CO_2 in CH_3CN for 1 min; flow rate 2.0 mL/min, λ = 256 nm; τ_{Major} = 3.95 min, τ_{Minor} = 4.05 min). $[\alpha]_D^{25}$ = -20.9 (c = 0.5, $CHCl_3$, 92:8 e.r.).

^{1}H NMR (400 MHz, $CDCl_3$): δ = 3.92-3.76 (m, 2H), 2.79-2.69 (m, 1H), 1.96-1.74 (m, 3H), 1.08 (dd, *J* = 7.9, 6.7 Hz, 6H) ppm.

^{13}C{^{1}H} NMR (126 MHz, $CDCl_3$): δ = 121.0, 60.2, 35.5, 32.8, 30.2, 21.1, 18.7 ppm.

HRMS (APCI): Calculated for $C_7H_{14}NO$ $[M+H]^+$: 128.1070; found: 128.1071.

***(R)*-2-(2-Hydroxyethyl)hept-6-enenitrile** (**34e**).

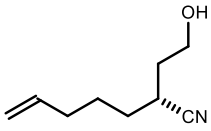

Following the general procedure **D** using enal **1f** (750 μmol, 93.0 mg), a mixture containing the β-cyanoaldehyde **23e** (73% NMR yield) and the sulfone by-product **23e'** (< 10% NMR yield) was obtained. The crude target product was reduced according to the general procedure **E** and the desired alcohol was purified by flash column chromatography (SiO_2, 15-20% EtOAc in hexanes) to afford product **34e** as a pale yellow oil (27.5 mg, 72% yield). The enantiomeric ratio of the corresponding 4-nitrobenzoate derivative was determined to be 92.5:7.5 by UPC^2 analysis on a Daicel Chiralpak IA-3 column (eluent: 100% CO_2 for 1 min, gradient 100% - 60% CO_2 in CH_3CN for 5 min, 60% CO_2 in CH_3CN for 2 min, gradient 60% - 100% CO_2 in CH_3CN for 1

min; flow rate 2.0 mL/min, λ = 256 nm; τ_{Major} = 4.20 min, τ_{Minor} = 4.60 min). $[\alpha]_D^{25}$ = -4.9 (c = 1.0, $CHCl_3$, 92.5:7.5 e.r.).

^{1}H NMR (500 MHz, $CDCl_3$): δ = 5.78 (ddt, *J* = 17.0, 10.2, 6.7 Hz, 1H), 5.06 – 5.00 (m, 1H), 5.00 – 4.96 (m, 1H), 3.89 – 3.72 (m, 2H), 2.88 – 2.75 (m, 1H), 2.18 – 2.03 (m, 2H), 1.86 – 1.80 (m, 2H), 1.71 – 1.50 (m, 4H) ppm.

^{13}C{^{1}H} NMR (126 MHz, $CDCl_3$): δ = 137.8, 122.1, 115.5, 59.7, 34.9, 33.2, 31.6, 28.1, 26.4 ppm.

HRMS (APCI): Calculated for $C_9H_{16}NO$ $[M+H]^+$: 154.1226; found: 154.1230.

(*R*)-2-(2-Hydroxyethyl)hept-6-ynenitrile (**34f**).

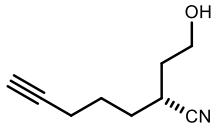

Following the general procedure **D** using enal **1g** (750 μmol, 91.5 mg), a mixture containing the β-cyanoaldehyde **23g** (56% NMR yield) and the sulfone by-product **23g'** (41% NMR yield) was obtained. The crude target product was reduced according to the general procedure **E** and the desired alcohol was purified by flash column chromatography (SiO_2, 15-20% EtOAc in hexanes) to afford product **34f** as a pale yellow oil (21.0 mg, 56% yield). The enantiomeric ratio of the corresponding 4-nitrobenzoate derivative was determined to be 90:10 by UPC^2 analysis on a Daicel Chiralpak ID-3 column (eluent: 100% CO_2 for 1 min, gradient 100% - 60% CO_2 in i-PrOH for 5 min, 60% CO_2 in i-PrOH for 2 min, gradient 60% - 100% CO_2 in i-PrOH for 1 min; flow rate 2.0 mL/min, λ = 256 nm; τ_{Major} = 4.40 min, τ_{Minor} = 4.55 min). $[\alpha]_D^{25}$ = -51.3 (c = 1.0, $CHCl_3$, 90:10 e.r.).

^{1}H NMR (400 MHz, $CDCl_3$): δ = 3.89 – 3.76 (m, 2H), 2.92 – 2.78 (m, 1H), 2.30 – 2.23 (m, 2H), 1.98 (t, *J* = 2.7 Hz, 1H), 1.89 – 1.63 (m, 6H) ppm.

^{13}C{^{1}H} NMR (101 MHz, $CDCl_3$): δ = 121.8, 83.3, 69.4, 59.7, 34.9, 31.2, 27.9, 25.9, 18.1 ppm.

HRMS (APCI): Calculated for $C_9H_{14}NO$ $[M+H]^+$: 152.1070; found: 152.1069.

(*2R,4S*)-2-(2-Hydroxyethyl)-4,8-dimethylnon-7-enenitrile (**34g**).

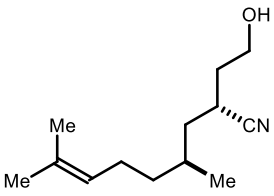

Following the general procedure **D** using enal **1h** (750 μmol, 135 mg), a mixture containing the β-cyanoaldehyde **23g** (80% NMR yield) and the sulfone by-product **23g'** (> 95% NMR yield) was obtained. The crude target product was reduced according to the general procedure **E** and the desired alcohol was purified by flash column chromatography (SiO_2, 15-20% EtOAc in hexanes) to afford product **34g** as a pale yellow oil (35.5 mg, 68% yield). Since determination of the d.r. by NMR was not successful due to overlapping signals, the diastereomeric ratio of the corresponding 4-nitrobenzoate derivative was determined to be 90.5:9.5 by UPC^2 analysis on a Daicel Chiralpak ID-3 column (eluent: 100% CO_2 for 1 min, gradient 100% - 60% CO_2 in CH_3CN for 5 min, 60% CO_2 in CH_3CN for 2 min, gradient 60% - 100% CO_2 in CH_3CN for 1 min; flow rate 2.0 mL/min, λ = 257 nm; τ_{Major} = 4.95 min, τ_{Minor} = 6.05 min). $[\alpha]_D^{25}$ = -4.7 (c = 1.0, $CHCl_3$, 90.5:9.5 d.r.).

^{1}H NMR (400 MHz, $CDCl_3$, major diastereomer): δ = 5.12 – 5.05 (m, 1H), 3.83 (dd, *J* = 6.6, 5.4 Hz, 2H), 2.96 – 2.82 (m, 1H), 2.07-1.93 (m, 2H), 1.85-1.77 (m, 2H), 1.76 – 1.65 (m, 6H), 1.60 (s, 3H), 1.38 – 1.17 (m, 3H), 0.94 (d, *J* = 6.5 Hz, 3H) ppm.

^{13}C{^{1}H} NMR (101 MHz, $CDCl_3$, major diastereomer): δ = 131.8, 124.3, 122.1, 59.8, 39.6, 37.5, 35.6, 30.8, 26.3, 25.8, 25.5, 18.9, 17.8 ppm.

HRMS (APCI): Calculated for $C_{13}H_{24}NO$ $[M+H]^+$: 210.1852; found: 210.1858.

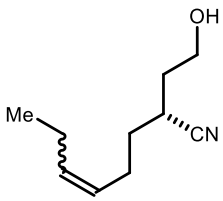

(*R*)-2-(2-Hydroxyethyl)oct-5-enenitrile (**34h**).

Following the general procedure **D** using enal **1i** (750 μmol, 104 mg), a mixture containing the β-cyanoaldehyde **23h** (73% NMR yield) and the sulfone by-product **23h'** (32% NMR yield) was obtained. The crude target product was reduced according to the general procedure **E** and the desired alcohol was purified by flash column chromatography (SiO_2, 15-20% EtOAc in hexanes) to afford product **23h** as a pale yellow oil (21.0 mg, 69% yield, *Z:E* = 6:4). The enantiomeric ratio of the corresponding 4-nitrobenzoate derivative was determined to be 91.5:8.5 for both double bond isomers by UPC^2 analysis on a Daicel Chiralpak IE-3 column (eluent: 100% CO_2 for 1 min, gradient 100% - 60% CO_2 in MeOH for 14 min, 60% CO_2 in

MeOH for 2 min, gradient 60% - 100% CO_2 in MeOH for 1 min; flow rate 2.0 mL/min, λ = 254 nm; (*Z*)-isomer: τ_{Major} = 11.45 min, τ_{Minor} = 12.00 min; (*E*)-isomer: τ_{Major} = 12.25 min, τ_{Minor} = 12.50 min). $[\alpha]_D^{25}$ = +6.2 (c = 1.0, $CHCl_3$, *E:Z* = 60:40, 91.5:8.5 e.r.).

^{1}H NMR (500 MHz, $CDCl_3$, mixture of *E/Z*-isomers): δ = 5.60 – 5.50 (m, 1H, minor), 5.50 – 5.41 (m, 1H, major), 5.35 (td, *J* = 7.7, 6.1 Hz, 1H, minor), 5.30 – 5.22 (m, 1H, major), 3.87 – 3.77 (m, 4H, major & minor), 2.88 – 2.78 (m, 2H, major & minor), 2.32 – 1.93 (m, 8H, major & minor), 1.90-1.80 (m, 4H, major & minor), 1.78 – 1.58 (m, 6H, major and minor), 0.97 (t, *J* = 7.5, 3H, major), 0.96 (t, *J* = 7.5, 3H, minor).

^{13}C{^{1}H} NMR (126 MHz, $CDCl_3$, mixture of *E/Z*-isomers): δ = 134.3, 133.9, 126.7, 126.5, 122.1, 122.0, 59.8, 59.8, 34.9, 34.9, 32.3, 32.2, 30.1, 27.7, 27.6, 25.7, 24.8, 20.7, 14.4, 13.9 ppm.

HRMS (APCI): Calculated for $C_{10}H_{18}NO$ $[M+H]^+$: 168.1383; found: 168.1385.

***(R)*-11-Hydroxy-2-(2-oxoethyl)undecanenitrile** (**34i**).

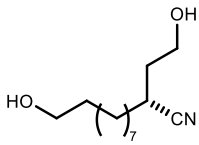

Following the general procedure **D** using enal **1k** (750 μmol, 149 mg), a mixture containing the β-cyanoaldehyde **23i** (47% NMR yield) and the sulfone by-product **23i'** (75% NMR yield) was obtained. The crude target product was loaded on column chromatography (SiO_2, 20% EtOAc in hexanes). After 3 days, the product was eluted (20-30% EtOAc in hexanes). Product-containing fractions were combined, concentrated and purification by chromatography was repeated as described above to afford the aldehyde product **34i** as a pale yellow oil (25.5 mg, 46% yield). The enantiomeric ratio of the corresponding dinitrophenylhydrazone derivative (see Figure S4) was determined to be 90.5:9.5 by UPC^2 analysis on a Daicel Chiralpak IE-3 column (eluent: 100% CO_2 for 1 min, gradient 100% - 60% CO_2 in EtOH for 5 min, 60% CO_2 in EtOH for 10 min, gradient 60% - 100% CO_2 in EtOH for 1 min; flow rate 2.0 mL/min, λ = 345 nm; τ_{Major} = 10.55 min, τ_{Minor} = 11.45 min). $[\alpha]_D^{25}$ = -32.4 (c = 0.5, $CHCl_3$, 90.5:9.5 e.r.).

Note: This compound was found unstable and decomposed upon storage at -20 °C for several months.

^{1}H NMR (400 MHz, $CDCl_3$): δ = 9.77 (s, 1H), 3.63 (t, *J* = 6.6 Hz, 2H), 3.13 – 3.02 (m, 1H), 2.90 (dd, *J* = 18.5, 6.9 Hz, 1H), 2.73 (dd, *J* = 18.5, 6.5 Hz, 1H), 1.67 – 1.19 (m, 17H).

^{13}C{^{1}H} NMR (101 MHz, $CDCl_3$): δ = 197.3, 121.2, 63.2, 45.7, 32.9, 31.9, 29.5, 29.4, 29.3, 29.0, 27.1, 25.8, 24.9 ppm.

HRMS (ESI): Calculated for $C_{13}H_{23}NNaO_2$ $[M+Na]^+$: 248.1621; found: 248.1624.

(*R*)-5-(Benzyloxy)-2-(2-hydroxyethyl)pentanenitrile (**34j**).

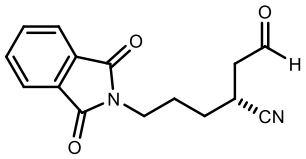

Following the general procedure **D** using enal **1l** (750 μmol, 153 mg), a mixture containing the β-cyanoaldehyde **23j** (55% NMR yield) and the sulfone by-product **23j'** (72% NMR yield) was obtained. The crude target product was reduced according to the general procedure **E** and the desired alcohol was purified by flash column chromatography (SiO_2, 15-20% EtOAc in hexanes) to afford product **34j** as a pale-yellow oil (30.0 mg, 52% yield). The enantiomeric ratio of the corresponding 4-nitrobenzoate derivative was determined to be 88.5:11.5 by UPC^2 analysis on a Daicel Chiralpak IA-3 column (eluent: 100% CO_2 for 1 min, gradient 100% - 60% CO_2 in CH_3CN for 5 min, 60% CO_2 in CH_3CN for 2 min, gradient 60% - 100% CO_2 in CH_3CN for 1 min; flow rate 2.0 mL/min, λ = 257 nm; τ_{Major} = 5.50 min, τ_{Minor} = 6.40 min). $[\alpha]_D^{25}$ = +0.1 (c = 1.0, $CHCl_3$, 88.5:11.5 e.r.).

^{1}H NMR (400 MHz, $CDCl_3$): δ = 7.40 – 7.23 (m, 5H), 4.50 (s, 2H), 3.85 – 3.75 (m, 2H), 3.57 – 3.47 (m, 2H), 2.89 – 2.78 (m, 1H), 1.97 – 1.60 (m, 6H), 1.52 (t, *J* = 4.9 Hz, OH) ppm.

^{13}C{^{1}H} NMR (126 MHz, $CDCl_3$): δ = 138.4, 128.6 (2C), 127.8 (2C), 127.8, 122.1, 73.1, 69.3, 59.7, 34.9, 29.3, 28.0, 27.4 ppm.

HRMS (APCI): Calculated for $C_{14}H_{20}NO_2$ $[M+H]^+$: 234.1489; found: 234.1493.

(*R*)-5-(1,3-dioxoisoindolin-2-yl)-2-(2-oxoethyl)pentanenitrile (**23k**).

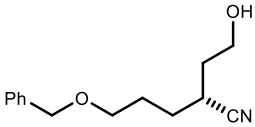

Following the general procedure **D** using enal **1n** (750 μmol, 182 mg), a mixture containing the β-cyanoaldehyde **23k** (71% NMR

yield) and the sulfone by-product **23k'** (78% NMR yield) was obtained. The crude target product was purified by flash column chromatography (SiO_2, 20-30% EtOAc in hexanes). Product containing fractions were loaded on a pad of SiO_2, kept to open air and eluted after 16 h with EtOAc. The filtrate was concentrated and purified by preparative TLC (SiO_2, 70% EtOAc in hexanes) to afford the aldehyde product **23k** as a pale-yellow wax (53.5 mg, 79% yield). The enantiomeric ratio of the corresponding dinitrophenylhydrazone derivative (see Figure S4) was determined to be 88.5:11.5 by UPC^2 analysis on a Daicel Chiralpak OJ-3 column (eluent: 100% CO_2 for 1 min, gradient 100% - 60% CO_2 in i-PrOH for 5 min, 60% CO_2 in i-PrOH for 2 min, gradient 60% - 100% CO_2 in i-PrOH for 1 min; flow rate 2.0 mL/min, λ = 345 nm; τ_{Major} = 5.65 min, τ_{Minor} = 6.00 min). $[\alpha]_D^{25}$ = +3.3 (c = 1.0, $CHCl_3$, 88.5:11.5 e.r.).

^{1}H NMR (400 MHz, $CDCl_3$): δ = 9.74 (s, 1H), 7.84 (dd, *J* = 5.5, 3.0 Hz, 2H), 7.72 (dd, *J* = 5.4, 3.1 Hz, 2H), 3.74 (t, *J* = 6.8 Hz, 2H), 3.22 – 3.12 (m, 1H), 2.90 (ddd, *J* = 18.6, 7.0, 0.7 Hz, 1H), 2.74 (ddd, *J* = 18.6, 6.4, 0.7 Hz, 1H), 2.03 – 1.90 (m, 1H), 1.90 – 1.79 (m, 1H), 1.76 – 1.58 (m, 2H) ppm.

^{13}C{^{1}H} NMR (101 MHz, $CDCl_3$): δ = 196.9, 168.5 (2C), 134.2 (2C), 132.1 (2C), 123.5 (2C), 120.6, 45.5, 36.9, 29.2, 26.4, 24.5 ppm.

HRMS (ESI): Calculated for $C_{15}H_{14}N_2NaO_3$ $[M+Na]^+$: 293.0897; found: 293.0895.

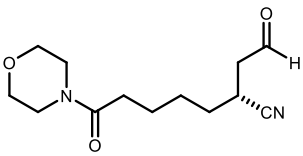

(*R*)-7-Morpholino-7-oxo-2-(2-oxoethyl)heptanenitrile (**23l**). Following the general procedure **D** using enal **1o** (750 μmol, 169 mg), a mixture containing the β-cyanoaldehyde **23l** (64% NMR yield) and the sulfone by-product **23l'** (86% NMR yield) was obtained. The crude target product was purified by flash column chromatography (SiO_2, 1% MeOH in CH_2Cl_2). The product-containing fractions were combined and loaded on another column chromatography (SiO_2, 100% EtOAc). After 16 h, the product was eluted with EtOAc to afford the aldehyde product **23l** as a pale yellow oil (41.0 mg, 65% yield). The enantiomeric ratio of the corresponding dinitrophenylhydrazone derivative (see Figure S4) was determined to be 86.5:13.5 by UPC^2 analysis on a Daicel Chiralpak IB-3 column (eluent: 100% CO_2 for 1 min, gradient 100% - 70% CO_2 in EtOH for 34 min, 70% CO_2 in EtOH for

2 min, gradient 70% - 100% CO_2 in EtOH for 1 min; flow rate 2.0 mL/min, λ = 345 nm; τ_{Major} = 27.70 min, τ_{Minor} = 28.05 min). $[\alpha]_D^{25}$ = +2.4 (c = 1.0, $CHCl_3$, 86.5:13.5 e.r.).

^{1}H NMR (400 MHz, $CDCl_3$): δ = 9.75 (s, 1H), 3.70 – 3.63 (m, 4H), 3.63 – 3.57 (m, 2H), 3.45 (t, *J* = 4.9 Hz, 2H), 3.14 – 3.04 (m, 1H), 2.90 (ddd, *J* = 18.6, 6.9, 0.7 Hz, 1H), 2.75 (ddd, *J* = 18.6, 6.5, 0.7 Hz, 1H), 2.33 (t, *J* = 7.2 Hz, 2H), 1.76 – 1.45 (m, 6H) ppm.

^{13}C{^{1}H} NMR (101 MHz, $CDCl_3$): δ = 197.2, 171.1, 121.0, 67.0, 66.7, 46.0, 45.6, 42.1, 32.6, 31.7, 26.9, 24.7, 24.4 ppm.

HRMS (ESI): Calculated for $C_{13}H_{20}N_2NaO_3$ $[M+Na]^+$: 275.1366; found: 275.1365.

(*R*)-2-(2-Hydroxyethyl)hexanedinitrile (**34m**).

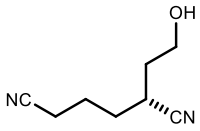

Following the general procedure **D** using enal **1p** (750 μmol, 92.5 mg), a mixture containing the β-cyanoaldehyde **23m** (60% NMR yield) and the sulfone by-product **23m'** (75% NMR yield) was obtained. The crude target product was reduced according to the general procedure **E** and the desired alcohol was purified by flash column chromatography (SiO_2, 40-50% EtOAc in hexanes). Product-containing fractions were combined and purified by preparative TLC (SiO_2, 100% EtOAc) to afford product **34m** as a pale yellow oil (17.0 mg, 44% yield). The enantiomeric ratio of the corresponding 4-nitrobenzoate derivative was determined to be 88:12 by UPC^2 analysis on a Daicel Chiralpak ID-3 column (eluent: 100% CO_2 for 1 min, gradient 100% - 60% CO_2 in i-PrOH for 5 min, 60% CO_2 in i-PrOH for 2 min, gradient 60% - 100% CO_2 in i-PrOH for 1 min; flow rate 2.0 mL/min, λ = 256 nm; τ_{Major} = 5.35 min, τ_{Minor} = 5.60 min). $[\alpha]_D^{25}$ = -55.8 (c = 0.5, $CHCl_3$, 88:12 e.r.).

^{1}H NMR (400 MHz, $CDCl_3$): δ = 3.91 – 3.76 (m, 2H), 2.96 – 2.84 (m, 1H), 2.51 – 2.41 (m, 2H), 1.97 – 1.74 (m, 6H) ppm.

^{13}C{^{1}H} NMR (101 MHz, $CDCl_3$): δ = 121.3, 118.9, 59.4, 34.7, 31.1, 27.8, 23.2, 17.0 ppm.

HRMS (APCI): Calculated for $C_8H_{13}N_2O$ $[M+H]^+$: 153.1022; found: 153.1022.

(*2R,5R*)-5-((*5R,8R,9S,10S,13R,14S,17R*)-10,13-dimethyl-3,12-dioxohexadecahydro-1H-cyclopenta[a]phenanthren-17-yl)-2-(2-oxoethyl)hexanenitrile (**23n**).

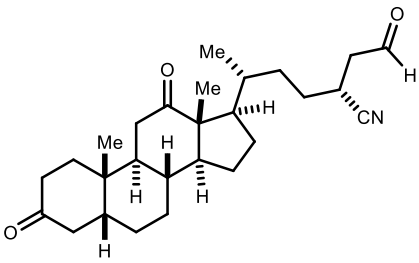

Tosyl cyanide (1.0 equiv., 19.0 mg, 100 μmol, 95%), enal **1q** (2.0 equiv., 79.5 mg, 200 μmol), dihydropyridine **R-1** (1.2 eq, 39.0 mg, 120 μmol), aminocatalyst **D** (0.3 equiv., 31.1 mg, 30.0 μmol) and 4-CzlPN (1 mol%, 790 μg, 1.00 μmol) were loaded in a reaction vial and the vessel was sealed with a septum and flushed with argon. Then, EtOAc (200 μL), water (3.0 equiv., 5.41 μL) and TFA (0.4 equiv., 2.97 μL, 40.0 μmol) was added and the vial was immediately placed in a cooling block (set to 5 °C internal temperature) and irradiated with 460 nm (90 mW/cm^2) for 16 hours. The crude mixture, containing β-cyanoaldehyde **23n** (44% NMRy) and sulfone by-product **23n'** (83% NMRy) was concentrated and loaded on column chromatography (SiO_2, 15% EtOAc in hexanes). After 16 h being absorbed on the SiO_2 (in order to decompose unstable and inseparable sulfone by-product **23n'**), the product was eluted (15-30% EtOAc in hexanes). The product-containing fractions were combined, concentrated and column chromatography was repeated as described above to afford the aldehyde product **23n** as a white solid (42.5 mg, 42% yield). Although no minor diaseteroisomer could be observed by NMR analysis, we conducted chiral chromatographic analysis of the the corresponding dinitrophenylhydrazone derivative to reveal a d.r. of 90:10 by UPC^2 analysis on a Daicel Chiralpak ID-3 column (eluent: 100% CO_2 for 1 min, gradient 100% - 60% CO_2 in MeOH for 5 min, 60% CO_2 in MeOH for 2 min, gradient 60% - 100% CO_2 in MeOH for 1 min; flow rate 2.0 mL/min, λ = 343 nm; τ_{Major} = 6.00 min, τ_{Minor} = 4.95 min). $[\alpha]_D^{25}$ = +56.1 (c = 0.5, $CHCl_3$, 90:10 d.r.).

^{1}H NMR (400 MHz, $CDCl_3$, major diastereoisomer): δ = 9.77 (s, 1H), 3.13 – 3.01 (m, 1H), 2.92 (ddd, *J* = 18.6, 6.9, 0.7 Hz, 1H), 2.74 (ddd, *J* = 18.6, 6.6, 0.8 Hz, 1H), 2.67 – 2.52 (m, 2H), 2.34 (td, *J* = 14.6, 5.3 Hz, 1H), 2.23 – 2.14 (m, 1H), 2.13-1.27 (m, 21H), 1.19-1.07 (m, 1H), 1.11 (s, 3H), 1.06 (s, 3H), 0.86 (d, *J* = 7.3 Hz, 3H) ppm.

^{13}C{^{1}H} NMR (101 MHz, $CDCl_3$, major diastereoisomer): δ = 214.3, 212.2, 197.3, 121.1, 58.7, 57.7, 46.4, 45.9, 44.4, 43.8, 42.3, 38.5, 37.1, 36.9, 35.8, 35.6, 35.3, 32.6, 28.7, 27.7, 26.7, 25.6, 24.9, 24.4, 22.3, 18.8, 11.9. ppm.

HRMS (ESI): Calculated for $C_{28}H_{43}NNaO_4$ $[M+ Na+MeOH]^+$: 480.3084; found: 480.3093.

(*R*)-4-Hydroxy-2-(3-methoxyphenethyl)butanenitrile (**34o**).

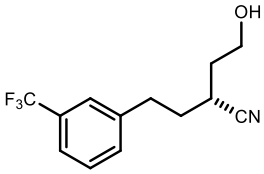

Following the general procedure **D** using enal **1s** (750 μmol, 143 mg), a mixture containing the β-cyanoaldehyde **23o** (66% NMR yield) and the sulfone by-product **23o'** (64% NMR yield) was obtained. The crude target product was reduced according to the general procedure **E** and the desired alcohol was purified by flash column chromatography (SiO_2, 15-20% EtOAc in hexanes) followed by preparative TLC (SiO2, 60% EtOAc in hexane) to afford product **34o** as a pale-yellow oil (32.0 mg, 58% yield). The enantiomeric ratio of the corresponding 4-nitrobenzoate derivative was determined to be 89.5:10.5 by UPC^2 analysis on a Daicel Chiralpak IE-3 column (eluent: 100% CO_2 for 1 min, gradient 100% - 70% CO_2 in CH_3CN for 12 min, 70% CO_2 in CH_3CN for 2 min, gradient 70% - 100% CO_2 in CH_3CN for 1 min; flow rate 2.0 mL/min, λ = 259 nm; τ_{Major} = 11.95 min, τ_{Minor} = 12.30 min). $[\alpha]_D^{25}$ = +31.6 (c = 1.0, $CHCl_3$, 89.5:10.5 e.r.).

^{1}H NMR (500 MHz, $CDCl_3$): δ = 7.22 (t, *J* = 7.7 Hz, 1H), 6.82 – 6.72 (m, 3H), 3.86 – 3.77 (m, 5H), 2.93 – 2.84 (m, 1H), 2.84 – 2.69 (m, 2H), 2.01 – 1.81 (m, 4H) ppm.

^{13}C{^{1}H} NMR (126 MHz, $CDCl_3$): δ = 159.9, 141.8, 129.8, 121.9, 120.9, 114.3, 111.8, 59.8, 55.3, 34.9, 33.9, 33.5, 27.8 ppm.

HRMS (ESI): Calculated for $C_{13}H_{17}NNaO_2$ $[M+Na]^+$: 242.1151; found: 242.1146.

(*R*)-4-Hydroxy-2-(3-(trifluoromethyl)phenethyl)butanenitrile (**34p**).

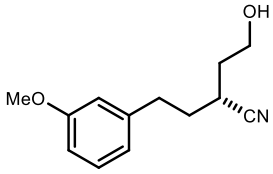

Following the general procedure **D** using enal **1t** (750 μmol, 171 mg), a mixture containing the β-cyanoaldehyde **23p** (78% NMR yield) and the sulfone by-product **23p'** (79% NMR yield) was obtained. The crude target product was reduced according to the general procedure **E** and the desired alcohol was purified by flash column chromatography (SiO_2, 15-20% EtOAc in hexanes) to afford product **34p** as a colorless oil (44.5 mg, 70% yield). The enantiomeric ratio of the corresponding 4-nitrobenzoate derivative was

determined to be 90:10 by UPC^2 analysis on a Daicel Chiralpak ID-3 column (eluent: 100% CO_2 for 1 min, gradient 100% - 60% CO_2 in CH_3CN for 5 min, 60% CO_2 in CH_3CN for 2 min, gradient 60% - 100% CO_2 in CH_3CN for 1 min; flow rate 2.0 mL/min, λ = 256 nm; τ_{Major} = 4.15 min, τ_{Minor} = 4.35 min). $[\alpha]_D^{25}$ = +14.4 (c = 1.0, $CHCl_3$, 90:10 e.r.).

^{1}H NMR (400 MHz, $CDCl_3$): δ = 7.38 – 7.21 (m, 4H), 3.75 – 3.60 (m, 2H), 2.83 (ddd, *J* = 14.7, 9.6, 5.5 Hz, 1H), 2.75 – 2.61 (m, 2H), 1.91 – 1.65 (m, 4H) ppm.

^{13}C{^{1}H} NMR (101 MHz, $CDCl_3$): δ = 141.2, 132.0 (q, *J* = 1.5 Hz), 131.1 (q, *J* = 32.2 Hz), 129.2, 125.2 (q, *J* = 3.6 Hz), 124.20 (q, *J* = 272.3 Hz), 123.5 (q, *J* = 3.9 Hz), 121.6, 59.6, 34.8, 33.8, 33.3, 27.9 ppm.

^{19}F NMR (376 MHz, $CDCl_3$): δ = -62.7 ppm.

HRMS (ESI): Calculated for $C_{13}H_{14}F_3NNaO$ $[M+Na]^+$: 280.0920; found: 280.0919.

(*R*)-2-(4-Bromophenethyl)-4-hydroxybutanenitrile (**34q**).

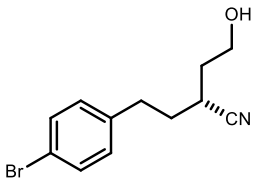

Following the general procedure **D** using enal **1u** (750 μmol, 179 mg), a mixture containing the β-cyanoaldehyde **23u** (57% NMR yield) and the sulfone by-product **23u'** (61% NMR yield) was obtained. The crude target product was reduced according to the general procedure **E** and the desired alcohol was purified by flash column chromatography (SiO_2, 15-20% EtOAc in hexanes) to afford product **34q** as a pale yellow oil (34.5 mg, 52% yield). The enantiomeric ratio of the corresponding 4-nitrobenzoate derivative was determined to be 90:10 by UPC^2 analysis on a Daicel Chiralpak IA-3 column (eluent: 100% CO_2 for 1 min, gradient 100% - 60% CO_2 in CH_3CN for 5 min, 60% CO_2 in CH_3CN for 2 min, gradient 60% - 100% CO_2 in CH_3CN for 1 min; flow rate 2.0 mL/min, λ = 257 nm; τ_{Major} = 5.70 min, τ_{Minor} = 6.00 min). $[\alpha]_D^{25}$ = +26.1 (c = 1.0, $CHCl_3$, 90:10 e.r.).

^{1}H NMR (400 MHz, $CDCl_3$): δ = 7.41 (d, *J* = 8.4 Hz, 2H), 7.08 (d, *J* = 8.6 Hz, 2H), 3.82 (br t, *J* = 5.5 Hz, 2H), 2.92 – 2.66 (m, 3H), 2.01 – 1.76 (m, 4H) ppm.

^{13}C{^{1}H} NMR (101 MHz, $CDCl_3$): δ = 139.2, 131.9 (2C), 130.3 (2C), 121.7, 120.4, 59.7, 34.9, 33.8, 32.9, 27.7 ppm.

HRMS (ESI): Calculated for $C_{12}H_{14}BrNNaO$ $[M+Na]^+$: 290.0151 found: 290.0155.

(*R*)-4-Hydroxy-2-phenethylbutanenitrile (**34r**).

Following the general procedure **D** using enal **1v** (750 μmol, 120 mg), a mixture containing the β-cyanoaldehyde **23r** (71% NMR yield) and the sulfone by-product **23r'** (73% NMR yield) was obtained. The crude target product was reduced according to the general procedure **E** and the desired alcohol was purified by flash column chromatography (SiO_2, 15-20% EtOAc in hexanes) to afford product **34r** as a colorless oil (35.0 mg, 74% yield). The enantiomeric ratio of the corresponding 4-nitrobenzoate derivative was determined to be 90:10 by UPC^2 analysis on a Daicel Chiralpak IA-3 column (eluent: 100% CO_2 for 1 min, gradient 100% - 60% CO_2 in CH_3CN for 5 min, 60% CO_2 in CH_3CN for 2 min, gradient 60% - 100% CO_2 in CH_3CN for 1 min; flow rate 2.0 mL/min, λ = 257 nm; τ_{Major} = 4.95 min, τ_{Minor} = 5.10 min). $[\alpha]_D^{25}$ = +30.1 (c = 1.0, $CHCl_3$, 90:10 e.r.).

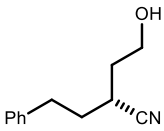

^{1}H NMR (400 MHz, $CDCl_3$): δ = 7.34 – 7.28 (m, 2H), 7.25 – 7.18 (m, 3H), 3.86 – 3.75 (m, 2H), 2.91 (ddd, *J* = 14.1, 9.0, 4.6 Hz, 1H), 2.86 – 2.71 (m, 2H), 2.04 – 1.80 (m, 4H) ppm.

^{13}C{^{1}H} NMR (126 MHz, $CDCl_3$): δ = 140.2, 128.8 (2C), 128.5 (2C), 126.5, 121.9, 59.7, 34.9, 34.0, 33.4, 27.8 ppm.

HRMS (APCI): Calculated for $C_{12}H_{16}NO$ $[M+H]^+$: 190.1226; found: 190.1235.

3.6.6 Derivatization of β-Cyanoaldehyde

(*4R*)-2-Hydroxy-4-pentylpentanedinitrile (**35**).

Following the general procedure **D** using enal **1a** (750 μmol, 94.5 mg), the crude mixture containing cyanoaldehyde **23a** was used without purification (evaporation of the solvent, *one-pot approach*). A solution of $NaHSO_3$ (104 mg, 1.00 mmol, 4.0 equiv.) in water (0.5 mL) was added to the crude product and the mixture was cooled to 0 °C. Then, a solution of KCN (130 mg, 2.00 mmol, 8.0 equiv.) in water (1.0 mL) was added dropwise and stirred for 10 minutes at 0 °C. CH_2Cl_2 (1.5 mL) was added and the mixture was stirred vigorously at room temperature under open air. The mixture was transferred to a separation

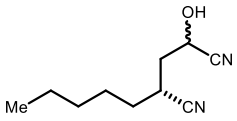

funnel and extracted with CH_2Cl_2 (3 x 20 mL). The combined layers were dried with $MgSO_4$ and concentrated. Column chromatography (SiO_2, 5-8% EtOAc in hexanes) afforded 31.0 mg (69% yield over 2 steps) of cyanohydrine **35** as a diastereomeric mixture of 66:34. The enantiomeric ratios of the corresponding 4-nitrobenzoate derivatives were determined to be 90:10 (for both diastereoisomers) by UPC^2 analysis on a Daicel Chiralpak IA-3 column (eluent: 100% CO_2 for 1 min, gradient 100% - 60% CO_2 in MeOH for 5 min, 60% CO_2 in MeOH for 2 min, gradient 60% - 100% CO_2 in MeOH for 1 min; flow rate 2.0 mL/min, λ = 254 nm) Major diastereoisomer: τ_{Major} = 4.80 min, τ_{Minor} = 4.35 min, Minor diastereoisomer: τ_{Major} = 4.50 min, τ_{Minor} = 5.20 min. $[\alpha]_D^{25}$ = -143.2 (c = 0.5, $CHCl_3$, 66:34 d.r., 90:10 e.r.).

^{1}H NMR (400 MHz, $CDCl_3$, mixture of diastereoisomers): δ = 4.78 – 4.64 (m, 2H, major & minor), 3.24 – 2.98 (br m, 2 OH, major & minor), 2.93 (ddt, *J* = 10.3, 8.9, 5.4 Hz, 1H, major), 2.86 – 2.70 (m, 1H, minor), 2.29 – 2.04 (m, 4H, major & minor), 1.75 – 1.28 (m, 16H, major & minor), 0.91 (t, *J* = 6.9 Hz, 6H, major & minor).

^{13}C{^{1}H} NMR (101 MHz, $CDCl_3$, mixture of diastereoisomers): δ = 120.8 (2C), 119.0, 118.8, 59.5, 58.5, 37.4, 37.4, 32.1, 32.1, 31.2 (2C), 27.9, 27.7, 26.8, 26.7, 22.5 (2C), 14.0 (2C) ppm.

HRMS (APCI): Calculated for $C_{10}H_{17}N_2O$ $[M+H]^+$: 181.1335; found: 181.1331.

(*R*)-3-Cyanooctanoic acid (**36**).

Following the general procedure **D** using enal **1a** (750 μmol, 94.5 mg), the crude mixture

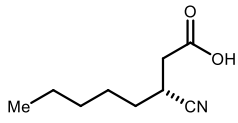

containing cyanoaldehyde **23a** was used without purification (evaporation of the solvent, *one-pot approach*). The crude mixture was redissolved in t-BuOH (8.0 mL) and 2-methylbut-1-ene (808 μL, 7.50 mmol, 30 equiv.) was added. Then, a solution of $NaClO_2$ (271 mg, 3.00 mmol, 12 equiv.) and NaH_2PO_4 (300 mg, 2.50 mmol, 10 equiv.) in water (4.0 mL) was added dropwise and the mixture was stirred for 2 hours at room temperature. The mixture was diluted with water (30 mL), acidified to pH = 3 by use of aqueous HCl (1.0 M) and extracted with CH_2Cl_2 (3 x 30 mL). The combined organic layers were dried with $MgSO_4$, concentrated and the product was purified by column chromatography (SiO_2, 8-15% EtOAc in hexanes with 1% AcOH). The crude product was then repurified by column chromatography (SiO_2, 10-15%

EtOAc in hexanes for elution of pyridine followed by 1% AcOH in EtOAc for elution of product) to obtain 26.0 mg (62%) of the desired cyanoacid **36** as bright yellow oil. NMR data was found to be in agreement with the literature[79].

^{1}H NMR (400 MHz, $CDCl_3$) δ = 3.06 – 2.94 (m, 1H), 2.77 (dd, *J* = 17.1, 7.7 Hz, 1H), 2.62 (dd, *J* = 17.1, 6.6 Hz, 1H), 1.73 – 1.21 (m, 8H), 0.91 (t, *J* = 6.8 Hz, 3H) ppm.

(*R*)-3-(Aminomethyl)octanoic acid (**37**).

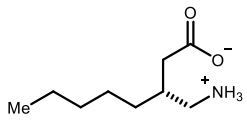

Cyanoacid **36** (26.1 mg, 154 μmol) was dissolved in MeOH (100 mL, HPLC grade and the solution was subjected to hydrogenation using a H-Cube pro apparatus (conditions: new Pd/C cartridge, 70 °C, 50 bar H_2, 1.0 mL/min). The apparatus was flushed with MeOH (3 x 20 mL) and the combined fractions were concentrated to afford 24.5 mg (91%) of aminoacid **37** as off-white semi-solid without need for further purification.

Determination of e.r.: 1.00 mg of **37** was dissolved in MeOH (1 mL) and Me_3SiCHN_2 (2M in diethylether, 0.3 mL) was added. After 5 minutes, the mixture was dried under reduced pressure, and the methylester was re-dissolved in $CHCl_3$ (0.2 mL) and 4-NO_2-benzoyl chloride (5.0 equiv.) and 4-dimethylaminopyridine (DMAP, 5.0 equiv.) were added. After stirring for 1 h, the amide was isolated by preparative TLC (20% EtOAc in n-hexanes) and the enantiomeric ratio was determined to be 90.5:9.5 by UPC^2 analysis on a Daicel Chiralpak ID-3 column (eluent: 100% CO_2 for 1 min, gradient 100% - 60% CO_2 in CH_3CN for 5 min, 60% CO_2 in CH_3CN for 2 min, gradient 60% - 100% CO_2 in CH_3CN for 1 min; flow rate 2.0 mL/min, λ = 262 nm; τ_{Major} = 5.15 min, τ_{Minor} = 5.40 min). $[\alpha]_D^{25}$ = -97.6 (c = 0.5, MeOH, 90.5:9.5 e.r.).

^{1}H NMR (400 MHz, CD_3OD) δ = 2.98 (dd, *J* = 12.8, 4.7 Hz, 1H), 2.90 (dd, *J* = 12.8, 7.5 Hz, 1H), 2.45 (dd, *J* = 16.0, 4.4 Hz, 1H), 2.33 (dd, *J* = 16.0, 8.0 Hz, 1H), 2.08 – 1.98 (m, 1H), 1.43 – 1.26 (m, 8H), 0.92 (t, *J* = 6.8 Hz, 3H).

---

[79] Monge, D.; Martín-Zamora, E.; Vázquez, J.; Alcarazo, M.; Álvarez, E.; Fernández, R. and Lassaletta, J. M. "Enantioselective Conjugate Addition of *N,N*-Dialkylhydrazones to α-Hydroxy Enones." *Org. Lett.* **2007**, 9, 2867–2870.

$^{13}C\{^{1}H\}$ NMR (101 MHz, CD_3OD) δ = 179.0, 45.1, 41.0, 35.3, 33.4, 33.0, 27.4, 23.6, 14.4 ppm.

HRMS (ESI): Calculated for $[C_9H_{20}NO_2]^+$ $[M+H]^+$: 174.1489; found: 174.1496.

3.6.7 Characterization of β-Sulfone Aldehyde by-product

Due to the inseparability of the aldehydic reaction products **23a** and **23a'**, a clean mixture was obtained upon reduction to alchools **3** and column chromatography purification, as described below.

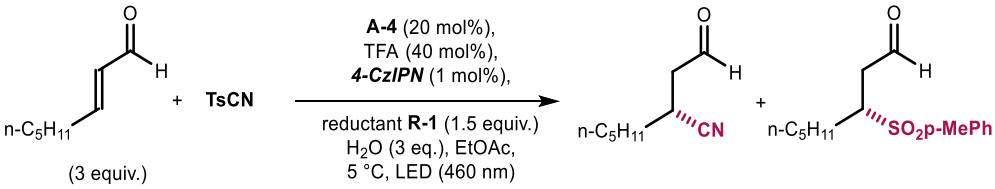

Following the general procedure **D** using enal **1a** (750 μmol, 94.5 mg), the crude product was purified by flash column chromatography (SiO_2, $CHCl_3$) to afford 38.0 mg of an inseparable mixture of **23a** and **23a'** (and traces of pyridine byproduct).

Upon reduction of the crude mixture obtained with enal **1a**, the alcohol derivatives of **23a** and **23a'** could be separated readily by column chromatography. This allowed us to isolate and characterise the sulfonyl-alcohol by-product **34a'**:

3-Tosyloctan-1-ol (**34a'**).

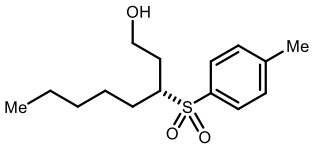

A 8.0 mL vial equipped with a stirring bar was charged with tosyl cyanide (19.1 mg, 100 µmol, 95% purity, 1.0 equiv.), amine **C** (14.0 mg, 20.0 µmol, 0.2 equiv.), **R-1** (49.0 mg, 150 µmol, 1.5 equiv.), 4-CzIPN (1.00 mg, 1.00 µmol, 1 mol%) and octenal **1a** (44.8 µL, 300 µmol, 3.0 equiv.). The vial was sealed with a septum and purged with Argon. The reactants were suspended in EtOAc (200 µL, ensure that all compounds are suspended) and deionized water (5.4 µL, 3.0 equiv.) was added. Then, TFA (2.23 µL, 30 µmol, 0.3 equiv.) was added and the vial was instantly placed in a pre-cooled metal block (set for an internal temperature of -10 °C) and irradiated with a high-power single LED (460 nm, irradiance 90 mW/cm^2). After 16 hours the mixture was concentrated under reduced pressure. The residue was dissolved in THF (0.40 mL) and then water (0.10 mL) was added. After cooling to 0 °C with an ice bath, $NaBH_4$ (37.8 mg, 1.00 mmol, 10 equiv.) was added in a few portions while rigorous stirring. After 10 minutes, the ice bath was removed and the mixture was stirred for 90 minutes at ambient temperature. After cooling to 0 °C with an ice bath, the slurry was quenched dropwise with 1 N HCl until gas evolution ceased. The mixture was transferred to a separation funnel and extracted with CH_2Cl_2 (3 x 20 mL). The desired alcohol were purified by flash column chromatography (SiO_2, 15-20% EtOAc in hexanes) to afford 20.0 mg (70%) of sulfone alcohol **34a'** as a pale-yellow oil. The enantiomeric ratio of the corresponding 4-nitrobenzoate (prepared in anaolgy to the general procedure for derivatization of β-cyanoalcohols) was determined to be 86:14 by UPC^2 analysis on a Daicel Chiralpak IE-3 column (eluent: 100% CO_2 for 1 min, gradient 100% - 60% CO_2 in CH_3CN for 5 min, 60% CO_2 in CH_3CN for 2 min, gradient 60% - 100% CO_2 in CH_3CN for 1 min; flow rate 2.0 mL/min, λ = 224 nm; τ_{Major} = 6.20 min, τ_{Minor} = 6.40 min). $[\alpha]_D^{25}$ = -3.2 (c = 1.0, $CHCl_3$, 86:14 e.r.).

^{1}H NMR (400 MHz, $CDCl_3$) δ = 7.76 (d, *J* = 8.2 Hz, 2H), 7.36 (d, *J* = 8.1 Hz, 2H), 3.90 – 3.80 (m, 1H), 3.75 – 3.65 (m, 1H), 3.19 – 3.08 (m, 1H), 2.45 (s, 3H), 2.15 – 2.02 (m, 2H), 1.92 – 1.73 (m, 2H), 1.54 – 1.35 (m, 2H), 1.32 – 1.13 (m, 4H), 0.83 (t, *J* = 6.9 Hz, 3H) ppm.

^{13}C{^{1}H} NMR (126 MHz, $CDCl_3$) δ = 144.8, 134.7 (2C), 129.9 (2C), 129.1, 62.0, 60.0, 31.6, 31.0, 28.7, 26.4, 22.4, 21.8, 14.0 ppm.

HRMS (ESI): Calculated for $C_{15}H_{25}O_3S$ $[M+H]^+$: 285.1519; found: 285.1523.

3.6.8 UV-Visible and Fluorescence studies

The following section reports the UV/Vis spectra of substrates and reductant **R-1** used in this study. None of the substrates (alone or as mixture) can absorb significantly at 460 nm. The best absorbing species is the photoredox catalyst 4-CzIPN.

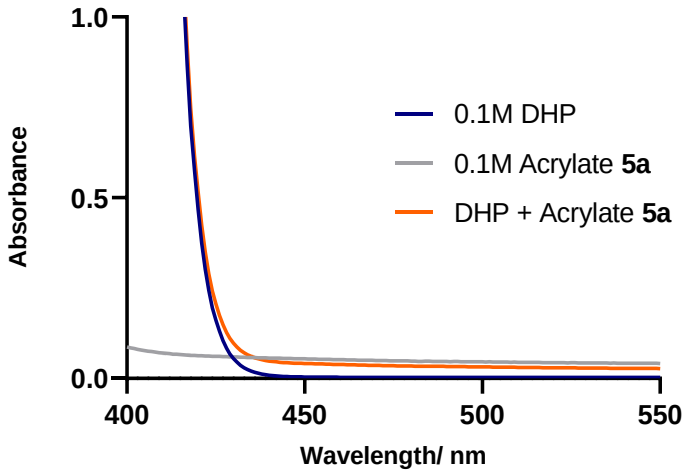

Figure 3.34. UV-Vis absorption spectra, recorded in DME in 1 cm path quartz cuvettes using an Agilent Cary 60 spectrophotometer. DHP [**R-1**] = 0.10 M, [**7a**] = 0.10 M.

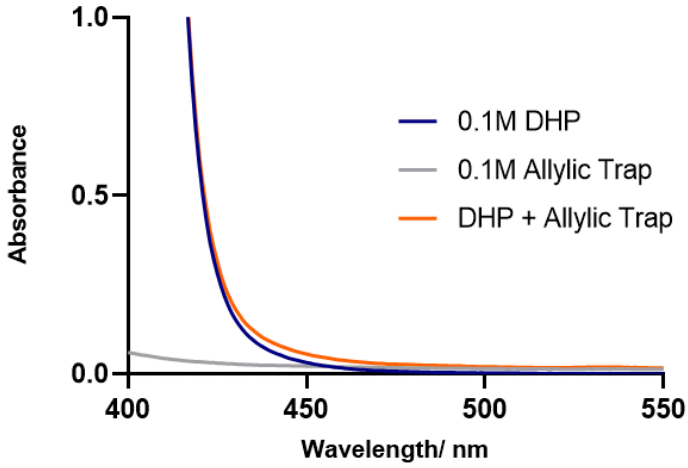

Figure 3.35. UV-Vis absorption spectra, recorded in DME in 1 cm path quartz cuvettes using an Agilent Cary 60 spectrophotometer. DHP [**R-1**] = 0.10 M, Allylic Trap **[21]** = 0.10 M.

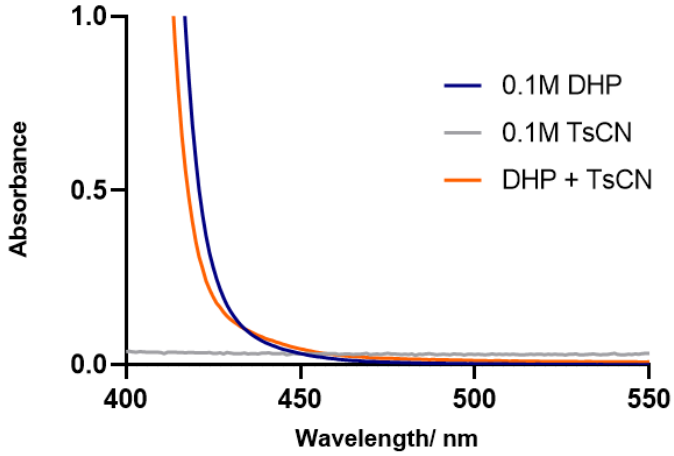

Figure 3.36. UV-Vis absorption spectra, recorded in DME in 1 cm path quartz cuvettes using an Agilent Cary 60 spectrophotometer. DHP [**R-1**] = 0.10 M, [**TsCN**] = 0.10 M.

Stern-Volmer Quenching Studies

To evaluate the feasibility of the proposed reductive quenching of the excited photocatalyst **4-CzPIN** ($E_{1/2}(PC^*/PC^{\bullet-})$ = +1.35 V vs SCE) by dihydropyridine **R-1** (E_{ox} = +1.36 V vs. Ag/AgCl), we conducted Stern Volmer studies, which confirmed this mechanistic scenario. The emission spectra were recorded in a Fluorolog Horiba Jobin Yvon spectrofluorimeter equipped with a photomultiplier detector, a double monochromator, and a 450W xenon light source. 2.5 mL of HPLC grade DME, thoroughly degassed by freeze-pump-thaw, were placed in a 10 x 10 mm light path quartz fluorescence cuvette equipped with Silicone/PTFE 3.2 mm septum under an argon atmosphere. Then, 25 µL of a 1.5 mM solution of photocatalyst 4-CzIPN in DME was added to give a final concentration of 15 µM. To measure the emission spectrum, the excitation wavelength was fixed at 460 nm (incident light slit regulated to 3 nm).

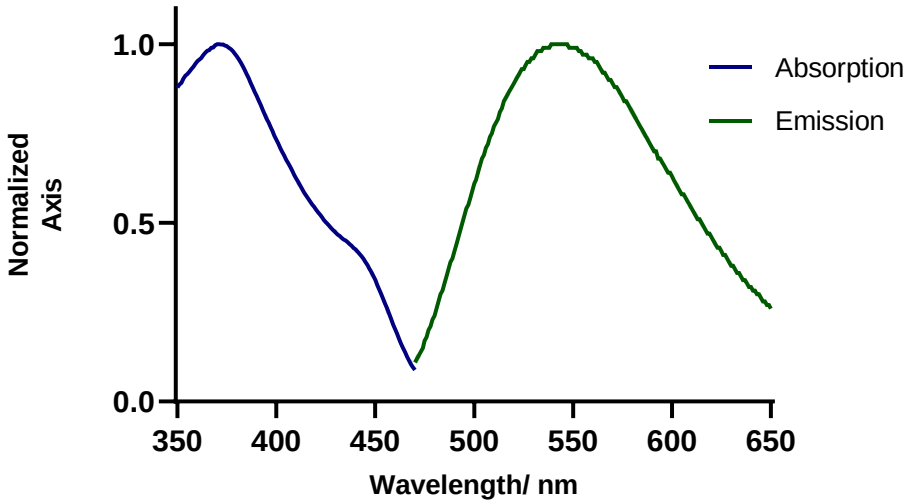

Figure 3.37. Absorption and emission spectra of photocatalyst 4-CzIPN

Stern-Volmer quenching studies with dihydropyridine R-1

A 0.25 M solution of dihydropyridine **R-1** in DME was prepared, and 20 μL of this stock solution was added to the solution of photocatalyst 4-CzIPN, prepared as described above. The addition of **R-1** solution was repeated four consecutive times. After each addition, the solution was sparged with argon for 20 s. An absorption spectrum and an emission spectrum of the solution were then recorded. The excitation wavelength was fixed at 460 nm (incident light slit regulated to 3 nm); the emission light was acquired from 470 nm to 650 nm (emission light slit regulated to 3 nm). A solvent blank was subtracted from all the measurements. The excitation wavelength was chosen in order to avoid saturation of the emission detector. The results shown in Figure 3.38 indicate that **R-1** quenches the excited state of 4-CzIPN and its emission. No change in the relevant region of absorption spectra were observed during the addition of **R-1** (Figure 3.39).

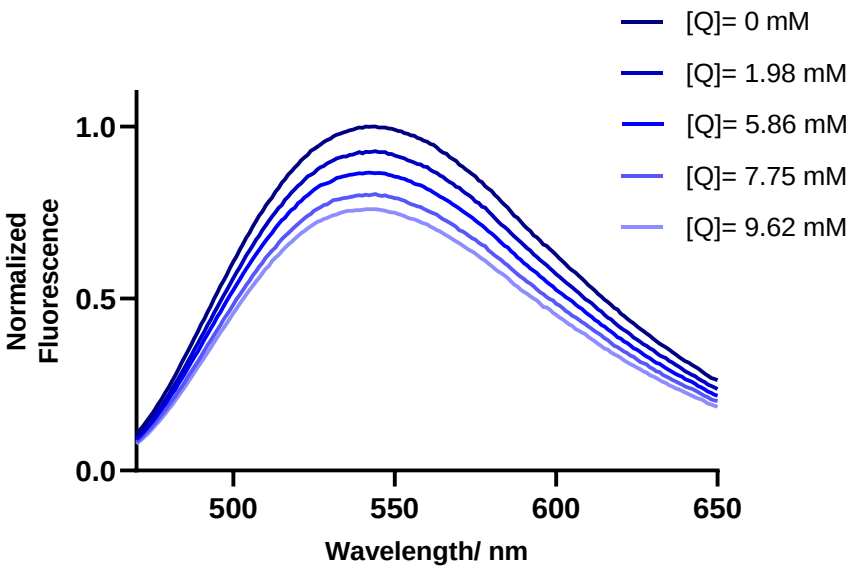

Figure 3.38. Emission of the photocatalyst 4-CzIPN (15 µM in DME) in the presence of increasing amounts of dihydropyridine **R-1** [Q].

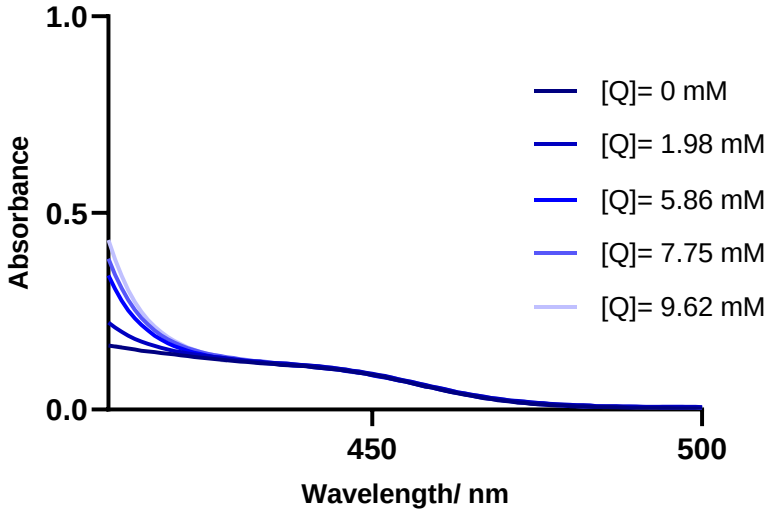

Figure 3.39. UV-vis absorption spectra of 4-CzIPN (15 µM in DME) in the presence of increasing amounts of dihydropyridine **R-1** [Q].

The Stern-Volmer plot (Figure 3.40), derived from the normalized emission intensity at 530 nm, shows a linear correlation between the amounts of **R-1** and the ratio I^0/I. Based on the following Equation 1, we Calculated the Stern-Volmer constant $K_{SV\,2}$[80] as 30.5 M^{-1}.

$$\frac{I^0}{I} = 1 + K_{SV}[Q] \cdots\cdots\cdots\cdots\cdots\cdots\cdots \boldsymbol{Eq.1}$$

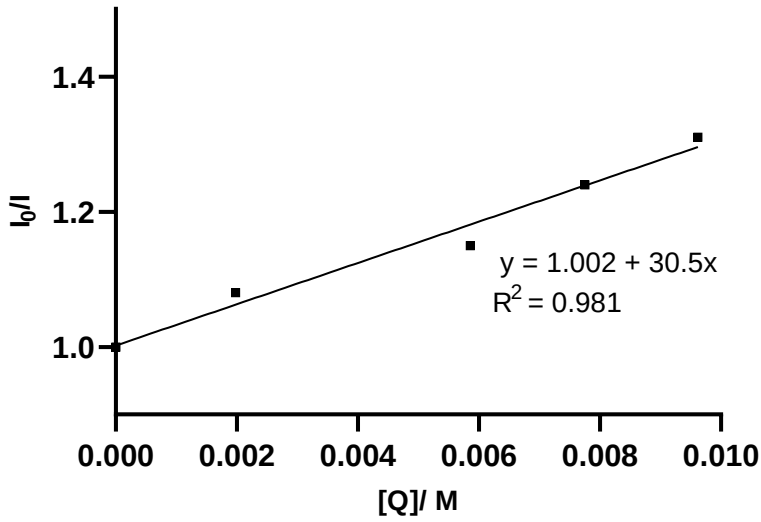

Figure 3.40. Stern-Volmer quenching plot using **R-1** as the quencher.

Stern-Volmer quenching studies with Acrylate

A 1.00 M solution of acrylate **7a** in DME was prepared, and 20 μL of this stock solution was added to the solution of photocatalyst 4-CzIPN, prepared as described above. The addition of acrylate solution was repeated three consecutive times. After each addition, the solution was sparged with argon for 20 s. An absorption spectrum and an emission spectrum of the solution were then recorded. The excitation wavelength was fixed at 460 nm (incident light slit regulated to 3 nm); the emission light was acquired from 470 nm to 650 nm (emission light slit regulated to 3 nm). A solvent blank was subtracted from all the measurements. The excitation wavelength was chosen in order to avoid saturation of the emission detector. The

[80] J. R. Lakowicz, Ed. *Principles of Fluorescence Spectroscopy*, Plenum Press, **1983**, 52–93.

results shown in Figure 3.41 indicate that acrylate does not quench the excited state of 4-CzIPN and its emission significantly. No change in the relevant region of absorption spectra were observed during the addition of acrylate (Figure 3.42).

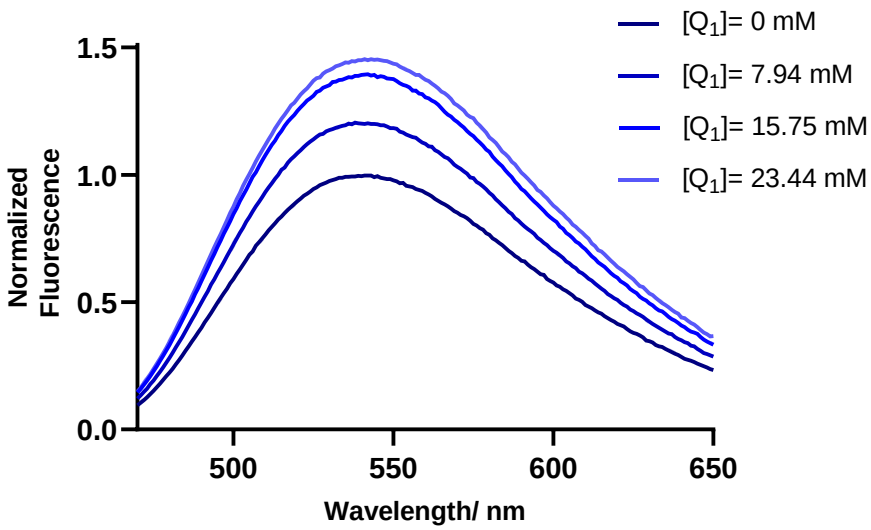

Figure 3.41. Emission of the photocatalyst 4-CzIPN (15 μM in DME) in the presence of increasing amounts of acrylate [Q_1].

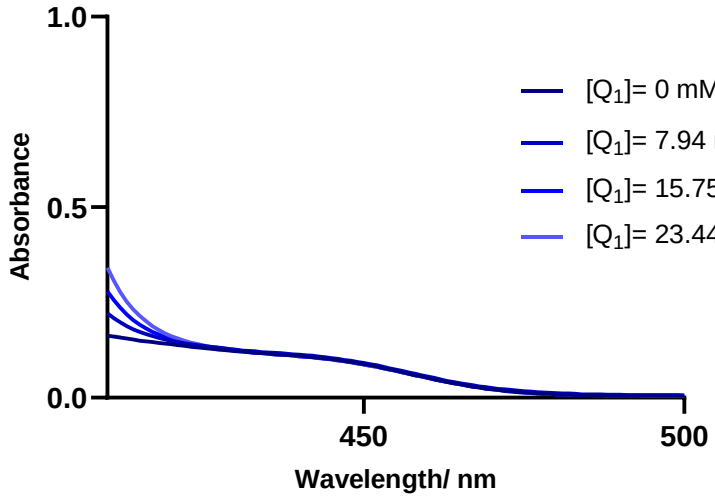

Figure 3.42. UV-Vis absorption spectra of 4-CzIPN (15 μM in DME) in the presence of increasing amounts of acrylate [Q_1].

The Stern-Volmer plot (Figure 3.43), derived from the normalized emission intensity at 530 nm, shows a linear correlation between the amounts of acrylate and the ratio I^0/I. Based on equation 1, we Calculated the Stern-Volmer constant K_{SV-1} as -13.5 M^{-1}.

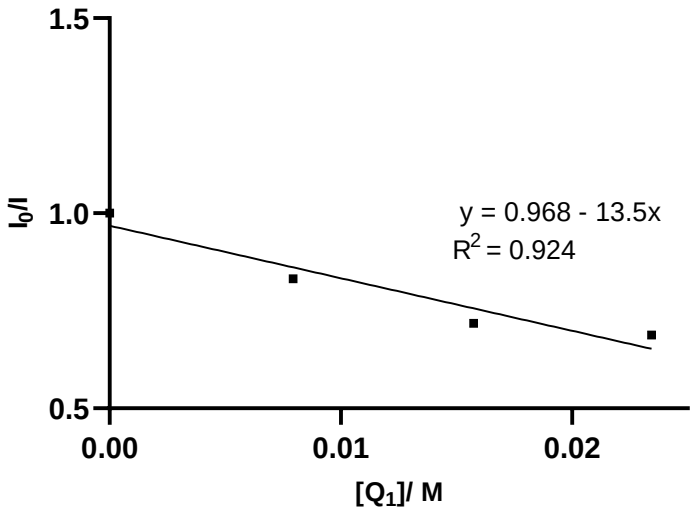

Figure 3.43. Stern-Volmer quenching plot using acrylate [Q_1] as the quencher.

Stern-Volmer quenching studies with TsCN

A 1.00 M solution of TsCN in DME was prepared, and 20 μL of this stock solution was added to the solution of photocatalyst 4-CzIPN, prepared as described above. The addition of TsCN solution was repeated three consecutive times. After each addition, the solution was sparged with argon for 20 s. An absorption spectrum and an emission spectrum of the solution were then recorded. The excitation wavelength was fixed at 460 nm (incident light slit regulated to 3 nm); the emission light was acquired from 470 nm to 650 nm (emission light slit regulated to 3 nm). A solvent blank was subtracted from all the measurements. The excitation wavelength was chosen in order to avoid saturation of the emission detector. The results shown in Figure 3.44 indicate that TsCN does not quench the excited state of 4-CzIPN and its emission significantly. No change in the relevant region of absorption spectra were observed during the addition of TsCN (Figure 3.45).

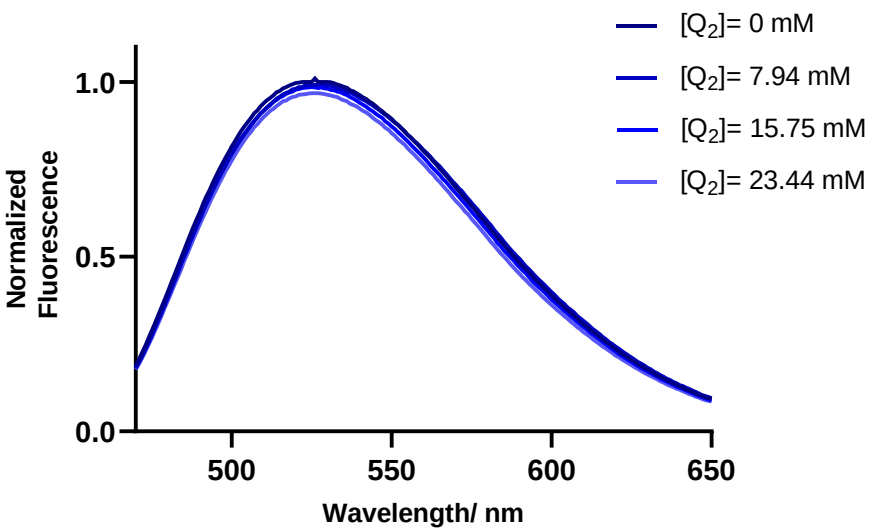

Figure 3.44. Emission of the photocatalyst 4-CzIPN (15 µM in DME) in the presence of increasing amounts of TsCN [Q_2].

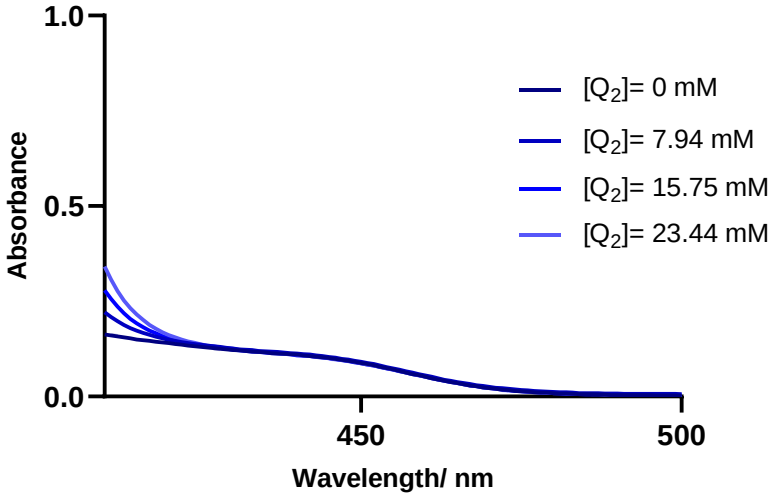

Figure 3.45. UV-Vis absorption spectra of 4-CzIPN (15 µM in DME) in the presence of increasing amounts of TsCN [Q_2].

The Stern-Volmer plot (Figure 3.46), derived from the normalized emission intensity at 530 nm, shows a linear correlation between the amounts of TsCN and the ratio I^0/I. Based on equation 1, we Calculated the Stern-Volmer constant K_{SV-2} as 1.7 M^{-1}.

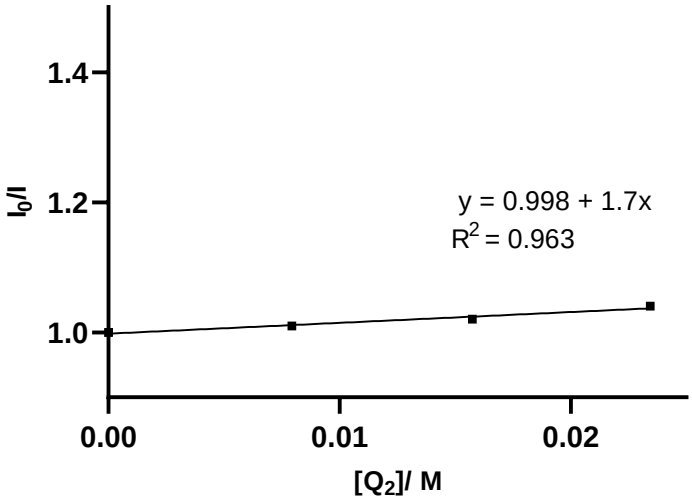

Figure 3.46. Stern-Volmer quenching plot using TsCN as the quencher.

3.6.9 Quantumn Yield Determination

In order to confirm the proposed reaction mechanism for the cross-electrophile coupling, a quantum yield measurement was conducted on the reaction of **1a** and **7b** (Figure 3.47).

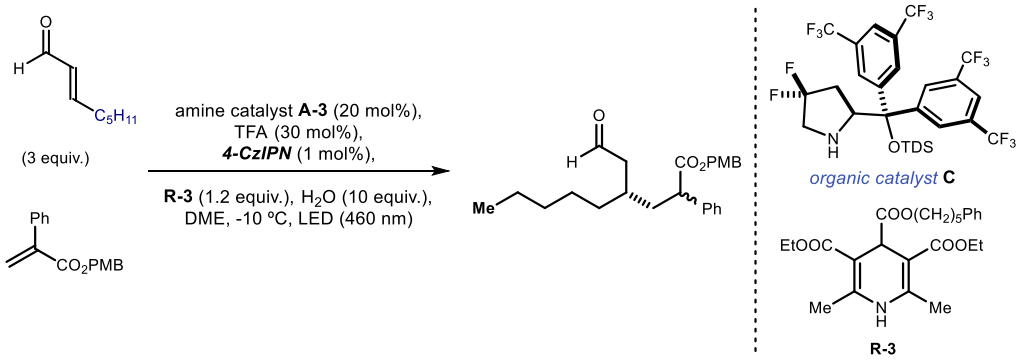

Figure 3.47. Conditions for the quantum yield determination of the cross electrophile coupling.

In this case, reductant **R-3** was used to guarantee homogeneity of the reaction mixture due to improved solubility.

A ferrioxalate actinometer solution was prepared by following the Hammond variation of the Hatchard and Parker procedure[81] outlined in the *Handbook of Photochemistry*.[82] Ferrioxalate actinometer solution measures the decomposition of Fe(III) to Fe(II) ions, which are complexed by 1,10-phenanthroline and monitored by UV/Vis absorbance at 510 nm. The number of moles of Fe(II)-phenanthroline complex formed are directly proportional to moles of photons absorbed. The values of the quantum yield of potassium ferrioxalate are related to concentration and wavelength.

The solutions were prepared and stored in the dark (wrapped with aluminium foil, red light environment):

0.012M Potassium ferrioxalate solution: 147.4 mg of potassium ferrioxalate (commercially available from Alfa Aesar) and 69.5 μL of sulfuric acid (96%) were added to a 25 mL volumetric flask, and filled to the mark with HPLC grade water.

Phenanthroline solution: 100 mg of 1,10-phenanthroline in a 50 mL volumetric flask, filled to the mark with HPLC grade water (0.2% by weight).

Buffer solution: to a 100 mL volumetric flask 4.94 g of NaOAc and 1.0 mL of sulfuric acid (96%) were added and filled to the mark with HPLC grade water.

Internal standard solution: 1.261 g of 1,3,5-trimethoxybenzene was added to a 5 mL volumetric flask which was filled up with HPLC grade acetonitrile (1.50 M).

Reaction setup.

Reaction solution: A Schlenk flask was charged with amine catalyst **C** (14.1 mg, 0.2 equiv., 20 μmol), DHP **R-3** (53.2 mg, 1.2 equiv., 120 μmol), *which was chosen for its improved solubility*, unsaturated ester **7b** (26.8 mg, 1.0 eq., 100 μmol), photocatalyst 4-CzIPN (0.8 mg, 1 mol%, 1.00 μmol), *(E)*-oct-2-enal **1a** (44.8 μL, 3.0 eq., 300 μmol) and water (18 μL, 10 equiv., 1.00 mmol). After four cycles of freeze-pump-thaw (with septum), TFA (2.2 μL, 30.0 μmol) in DME (0.4 mL) and were added and the tube was sealed with parafilm and put in the HP-LED 460 nm at 1 cm distance at -10 ºC with irradiance of 60 mW/cm^2. Three different

[81] Hatchard, C. G., Parker, C. A. "A new sensitive chemical actinometer II. Potassium ferrioxalate as a standard chemical actinometer." Proc. R. Soc. (London), **1956**, 235, 518.

[82] Montalti, M., Credi, A., Prodi, L., Gandolfi, M.T. *Handbook of photochemistry*, Taylor & Francis, **2006**, 601.

reactions were set up and irradiated for different times: 15 min, 30 min and 45 min. After each reaction was finished, internal standard solution (66 µL, 0.1 mmol) was added. This solution was diluted with 3 mL of acetone, from the solution was taken 1 mL to be analyzed by GC-FID.

Actinometer solutions: A Schlenk flask of the same dimensions as used for the reaction mixtures was loaded with 0.4 mL of actinometer solution and placed on the HP-LED the same light intensity as the reaction (without freeze-pump-thaw). Three different actinometer solutions were irradiated in sequence for 10 s, 25 s and 40 s. To irradiate the Schlenk tube, it was placed on the holder with the light off and the light was turned on for the desired time. After each irradiation the actinometer solutions were carefully transferred into a 10 mL volumetric flask, then 0.5 mL of phenanthroline solution and 2.0 mL of buffer solution were added and the flask was filled up with water. The mixture was then analyzed by UV-Vis absorption spectroscopy (Figure 3.48).

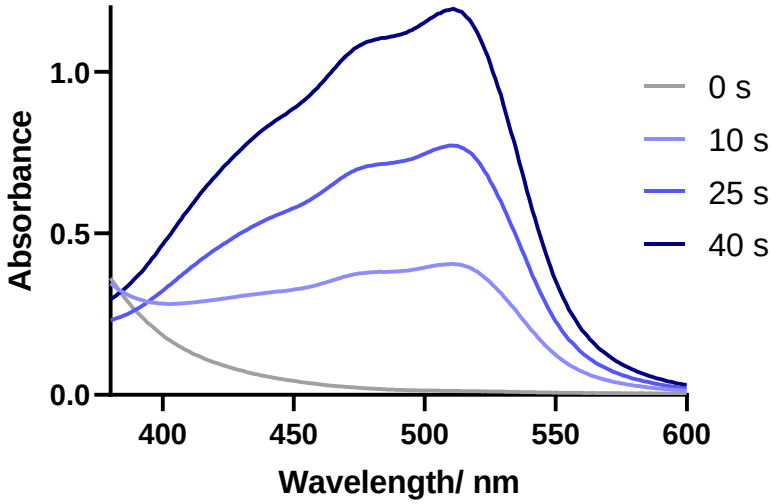

Figure 3.48. UV-Vis spectra of the actinometer solutions irradiated for different periods.

The moles of Fe(II) formed for each sample are determined using Beers' Law (Eq. 2):

$$Moles\ of\ Fe(II) = \frac{V_1 V_3 \cdot \Delta A\ (510\ nm)}{10^3 V_2 l \cdot \varepsilon(510\ nm)} \cdots\cdots\cdots\cdots\cdots\cdots \boldsymbol{Eq.2}$$

where V_1 is the irradiated volume (0.4 mL), V_2 is the aliquot of the irradiated solution taken for the quantification of the Fe(II) complex (0.4 mL), V_3 is the final volume after complexation with phenanthroline (10 mL), l is the optical path-length of the irradiation cell (1 cm), ΔA(510 nm) is the optical difference in absorbance between the irradiated solution and the one stored in the dark, $\varepsilon_{510\ nm}$ is the extinction coefficient the complex $[Fe(phen)_3]^{2+}$ at 510 nm (11100 L mol^{-1} cm^1).

The moles of Fe(II) formed (x) are plotted as a function of time (t) (Figure 3.46). The slope of this line was correlated to the moles of incident photons by unit of time ($q^0_{n,p}$) by the use of the following Equation 3:

$$\Phi(\lambda) = \frac{dx/dt}{q^0_{n,p}[1 - 10^{-A(\lambda)}]} \cdots\cdots\cdots\cdots\cdots\cdots \boldsymbol{Eq.3}$$

where the quantum yield (Φ) for formation of Fe(II) at 458 nm is 1.11[83], dx/dt is the rate of change of a measurable quantity (spectral or any other property), $[1\text{-}10^{-A(\lambda)}]$ is the ratio of absorbed photons by the solution, and A(λ) is the absorbance of the actinometer at the wavelength used to carry out the experiments (460 nm). The absorbance at 460 nm was 0.03.

[83] Holubov, C. A.; Langford, C. H. "Wavelength and Temperature Dependence in the Photolysis of the Chemical Actinometer, Potassium trisoxalatoferrate(III), at Longer Wavelengths." *Inorganica Chim. Acta* **1981**, 53,59.

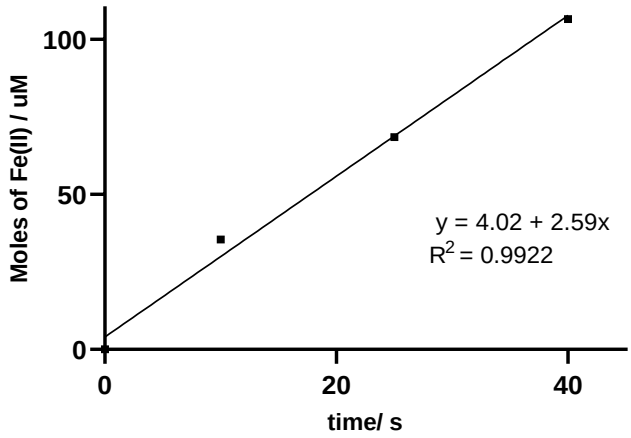

Figure 3.49. Plot of the moles of Fe(II) generated from the irradiation of the actinometer solutions against time.

The photon flux, which is $q^0_{n,p}$, was determined to *3.08 x 10^{-7} einstein s^{-1}*.

The moles of product **8b** per unit of time are plotted against the number of photons absorbed (Figure 3.50). The photons absorbed are correlated to the number of incident photons by the use of Equiv. 3. According to this, if we plot the moles of product (y-axis) versus the moles of incident photons ($q^0_{n,p}dt$, x-axis), the slope is equal to:

$$\text{slope} = \Phi[1 - 10^{-A(460\ nm)}] \ldots\ldots\ldots\ldots\ldots\ldots \boldsymbol{Eq.4}$$

where Φ is the quantum yield to be determined and $A_{460\ nm}$ is the absorption of the reaction under study. $A_{460\ nm}$ was measured to be of 0.12 for the model reaction mixture after 25-fold dilution.

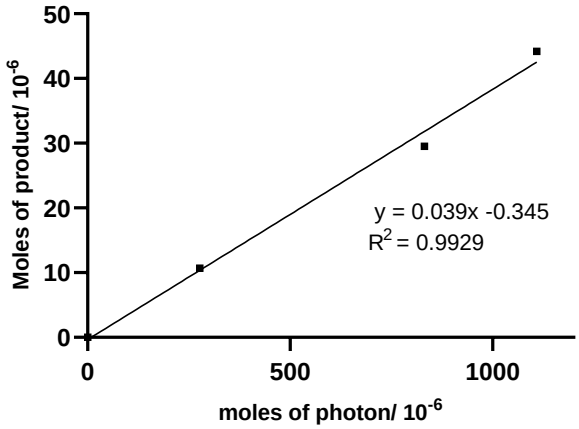

Figure 3.50. Plot of the moles of products **8b** generated from the irradiation of the reaction solutions, against the moles of photons absorbed.

The quantum yield of the cross electrophile coupling process was calculated to be 0.04.

3.6.10 Cyclic Voltammetry Studies

Cyclic voltammetry (CV) measurements were carried out on a Princeton Applied Research PARSTAT 2273 instrument with a glassy carbon disk electrode (diameter: 3 mm) as working electrode. A silver wire coated with AgCl immersed in a saturated aqueous solution of KCl and separated from the analyte by a fritted glass disk was employed as the reference electrode and a Pt wire auxiliary electrode completed the electrochemical setup. The scan rate was 100 mV/s. The substrates were measured in acetonitrile with 0.1M NBu_4PF_6 as electrolyte. Potentials are quoted with E_p^C (E_{Red}) refers to the cathodic peak potential, E_p^A (E_{Ox}) refers to the anodic peak potential.

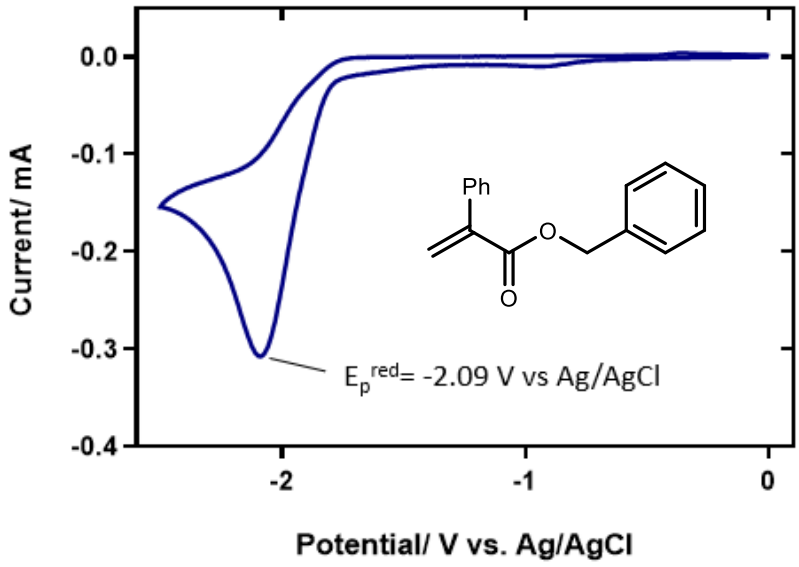

Figure 3.51. Cyclic voltammogram of 1mM **7a** in MeCN. Irreversible reduction. $E_p^c = E_p^{red}$ (**7a**/**7a**$^{\bullet-}$) = -2.09 V.

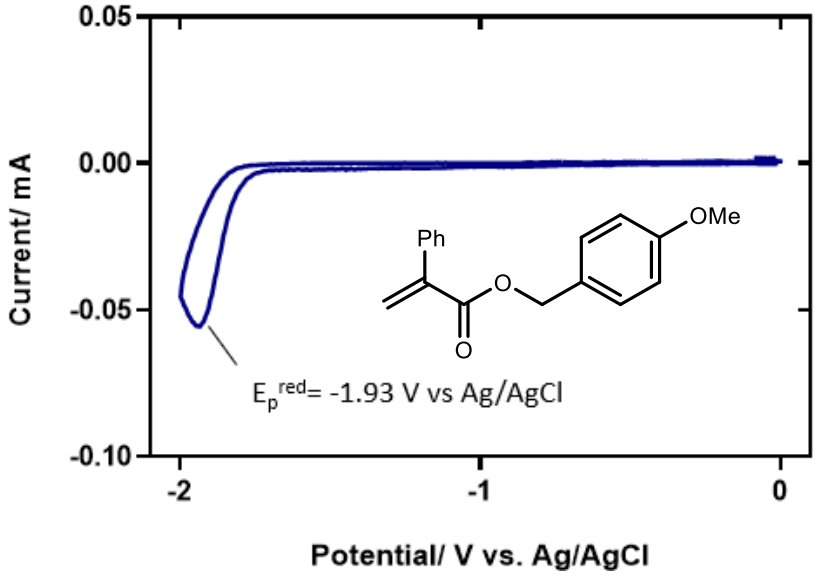

Figure 3.52. Cyclic voltammogram of 1mM **7b** in MeCN. Irreversible reduction. $E_p^c = E_p^{red}$ (**7b**/**7b**$^{\bullet-}$) = -1.93 V.

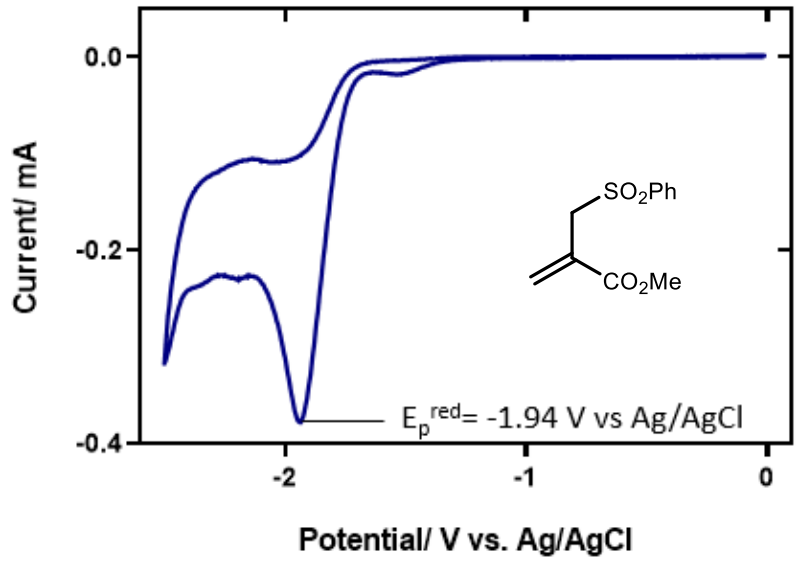

Figure 3.53. Cyclic voltammogram of 5 mM **[21]** in MeCN. Irreversible reduction. $E_p^C = E_p^{red}$ (**21**/**21**$^{\bullet-}$) = -1.94 V.

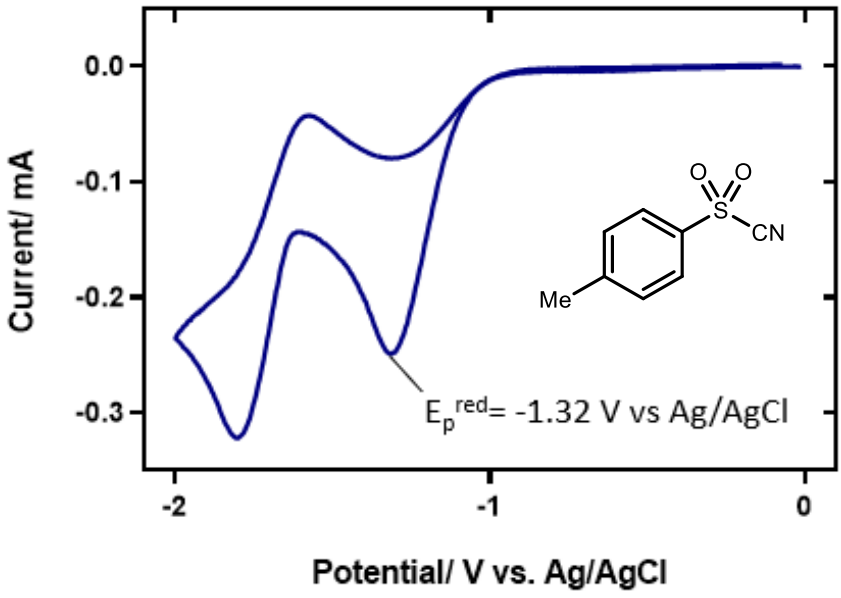

Figure 3.54. Cyclic voltammogram of 5mM **TsCN** in MeCN. Irreversible reduction. $E_p^C = E_p^{red}$ (TsCN/TsCN$^{\bullet-}$) = -1.32V.

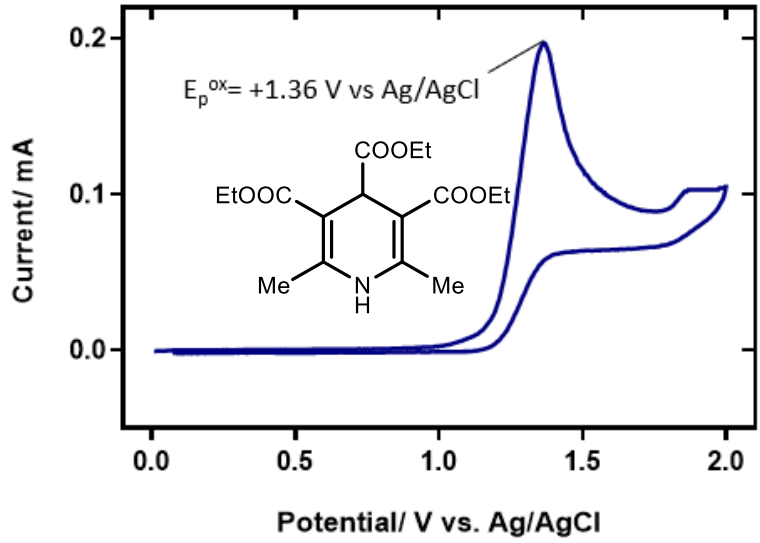

Figure 3.55. Cyclic voltammogram of 5mM **R-1** in MeCN. Irreversible oxidation. $E_p^A = E_p^{ox}$ (**R-1**$^{\bullet+}$/ **R-1**) = +1.36 V.

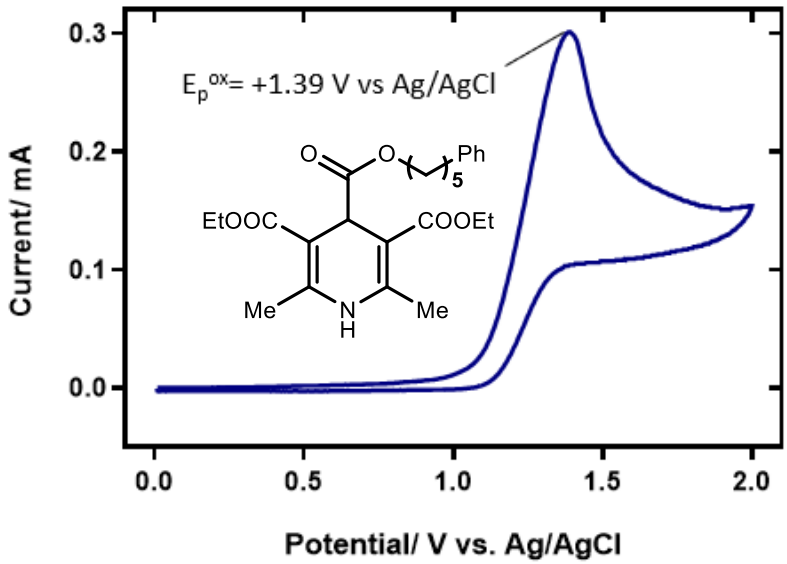

Figure 3.54. Cyclic voltammogram of 5 mM **R-3** in MeCN. Irreversible oxidation. $E_p^A = E_p^{ox}$(**R-3**$^{\bullet+}$/ **R-3**) = +1.39 V.

As described in section 2.6.8, the redox potentials *vs.* SCE in MeCN were calculated as below:

E_p^{red} (**7a**/**7a**$^{\bullet-}$) = -2.17 V *vs.* SCE; E_p^{red} (**7b**/**7b**$^{\bullet-}$) = -2.01 V *vs.* SCE; E_p^{red} (**21**/**21**$^{\bullet-}$) = -2.02 V *vs.* SCE; E_p^{red} (**TsCN**/**TsCN**$^{\bullet-}$) = -1.40 V *vs.* SCE.

E_p^{ox} (**R-1**$^{\bullet+}$/ **R-1**) = +1.28 V vs. SCE; E_p^{ox} (**R-3**$^{\bullet+}$/**R-3**) = +1.31 V vs. SCE.

3.6.11 Probing Reaction Intermediates

Radical Clock Experiment

4-Methoxybenzyl (*E*)-2-(3-oxoprop-1-en-1-yl)-1,4-diphenylcyclopentane-1-carboxylate (29).

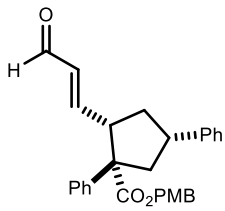

Following the general procedure **C** using acrylate **7b** (250 μmol, 67.0 mg) and enal **28** (750 μmol, 129 mg), purification of the crude product by flash column chromatography (SiO_2, 5-8% EtOAc in hexanes) afforded product **29** as a pale yellow oil (39.0 mg, 35% yield) in a 16.5:2.5:1:1 diastereomeric ratio.

NMR peaks of major diastereomer only:

^{1}H NMR (500 MHz, $CDCl_3$): δ = 9.28 (d, *J* = 7.9 Hz, 1H, H1), 7.40 – 7.19 (m, 10H, H9-H16), 7.16 – 7.08 (m, 2H, H20), 6.94 (dd, *J* = 15.6, 7.8 Hz, 1H, H3), 6.84 – 6.76 (m, 2H, H21), 6.05 (ddd, *J* = 15.6, 7.9, 1.2 Hz, 1H, H2), 5.06 (d, *J* = 11.9 Hz, 1H, H18a), 4.98 (d, *J* = 11.9 Hz, 1H, H18b), 3.80 (s, 3H, H23), 3.58 – 3.50 (m, 1H, H4), 3.31 – 3.19 (m, 1H, H7), 2.90 (dd, *J* = 13.9, 10.3 Hz, 1H, H6a), 2.70 (dd, *J* = 14.6, 8.8 Hz, 1H, H6b), 2.46 – 2.39 (m, 1H, H8a), 2.08 – 2.00 (m, 1H, H8b) ppm.

^{13}C{^{1}H} NMR (126 MHz, $CDCl_3$): δ = 193.9 (C1), 174.3 (C17), 159.9 (C22), 157.7 (C3), 143.8 (C9), 142.6 (C13), 133.0 (C2), 130.5 (C20), 128.8 (C_{arom}), 128.7(C_{arom}), 127.6(C_{arom}), 127.3(C_{arom}), 127.3(C_{arom}), 126.6(C_{arom}), 126.6(C_{arom}), 114.1 (C21), 66.9 (C18), 62.1 (C5), 55.4 (C23), 51.4 (C4), 45.3 (C6), 42.9 (C7), 39.7 (C8) ppm.

HRMS (ESI): Calculated for $C_{29}H_{28}O_4Na$ $[M+Na]^+$: 463.1880; found: 463.1877.

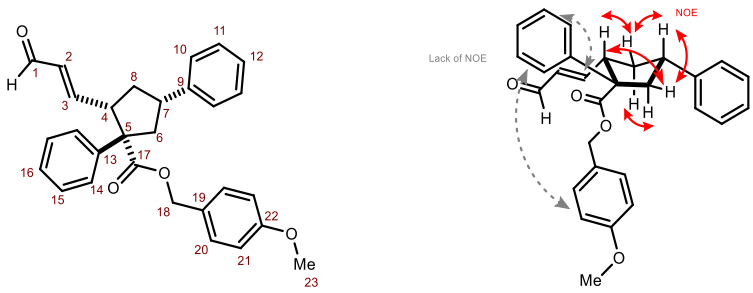

Figure 3.55. Atom numbering *(left)* and NOE correlations (*right)* within product **29**

Deuterium-labelling Experiments

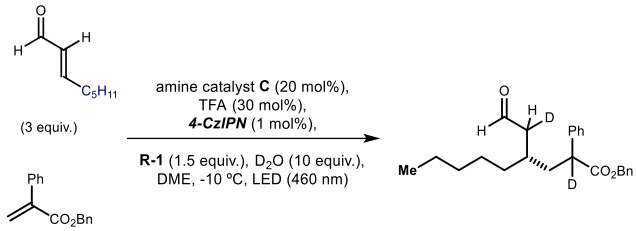

To a 8.0 mL argon-purged glass vial, containing the acrylate **7a** (20 µL, 1.0 equiv.), enal **1a** (45 µL, 3.0 equiv.), DHP **R-1** (48.8 mg, 1.5 equiv.), 4-CzIPN (0.8 mg, 1 mol%) and amine catalyst **C** (14.1 mg, 20 mol%), was added 20 µL of dimethoxyethane, D_2O (18 µL, 2.50 mmol, 10 equiv.) and CF_3COOH (5.5µL, 30 mol%). The vial was sealed with Parafilm, and then placed into a cooled aluminium support mounted on an aluminium block fitted with a 460 nm high-power single LED. This set-up secured a reliable irradiation while keeping a constant distance of 1 cm between the reaction vessel and the light source. The reaction was stirred under visible light irradiation at -10 °C internal temperature for 16 hours. The crude product was purified by flash column chromatography (silica, 10% Et_2O in n-hexanes) to obtain product **8a-d** as a colorless oil (28.9 mg, 78% yield) in a 1.2:1 diastereomeric ratio.

^{1}H NMR (500 MHz, $CDCl_3$):δ = 9.66 – 9.64 (m, 2H), 7.35 – 7.29 (m, 14H), 7.27 – 7.24 (m, 6H), 5.16 (d, J = 12.4 Hz, 2H), 5.08 (dd, J = 12.4, 2.4 Hz, 2H), 3.74 – 3.70 (*m, 1.1 H*), 2.36 – 2.33 (*m, 1.7H*), 2.22 – 2.16 (m, 2H), 2.13 – 2.02 (m, 1H), 1.86 – 1.73 (m, 1H), 1.50 – 1.13 (m, 18H), 0.91 – 0.87 (m, 6H) ppm.

^{2}H NMR (77 MHz, $CHCl_3$): δ = 3.68 (br, 0.9 d), 2.30 (br, 2.3 d) ppm.

3.6.12 X-Ray Crystallography

4-Nitrobenzoate derivative **25r** was obtained from an analytical sample prepared according to the general procedure as described in section 8 using diol **24r** obtained upon reduction of 1,6-dicarbonyl **8r**. Crystals of the compound **25r** were obtained by slow evaporation of a dichloromethane/hexane solution. *Data Collection*. Measurements were performed at 100 K on a Bruker Kappa Apex II DUO diffractometer equiped with a Cryostream 700 plus low temperature device, a microsource anode with Mo Kα (λ= 0.71073 Å).

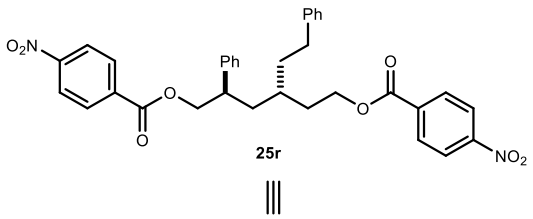

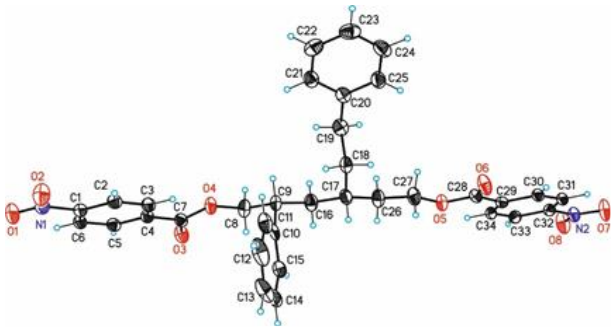

This chiral compound crystallizes in the space group P1 showing disorder in the group with the benzene ring (atoms C18 to C25) with a ratio of 75:25. Both disordered orientations show the same stereochemistry. The absolute structure could be determined reliable with a Flack value based on Parsons' quotients of -0.05(9)[84]. Flack X determined using 1202 quotients [(I+)-(I-)]/[(I+)+(I-)]). The Flack parameter value for the correct absolute structure

[84] (a) Flack, H. D. "On enantiomorph-polarity estimation." *Acta Cryst. A* **1983,** 39, 876; (b) Parsons, S. and Flack, H. D. "Precise absolute-structure determination in light-atom crystals." *Acta Cryst. A* **2004,** 60, 61; (c) Parsons, S., Flack, H. D. and Wagner, T. "Use of intensity quotients and differences in absolute structure refinement" *Acta Cryst. B* **2013,** 69, 249; (d) Escudero-Adán, E.C., Benet-Buchholz, J. & Ballester P. "The use of Mo Kα radiation in the assignment of the absolute configuration of light-atom molecules; the importance of high-resolution data." Acta Cryst. B **2014,** 70, 660-668.

determination should be 0; the inverted structure would give 1; always taking in account the standard deviation. The absolute configuration based on the absolute structure of the measured crystal was determined with S(C9), R(C17). The structure is of excellent quality (no A-alerts and ***one commented B-alerts related to the poor data to parameter ratio***, see CIF/checkCIF) and of publishable quality with a R1 value of 3.18%.

The B alert in the checkCIF file is due to formation of small chiral crystals of low symmetry (Space group P1) which were measured using CuKalfa radiation. Additionally, the structure showed disorder which enlarged the number of parameters. Maximum exposition time and intensity was used for the measurement.

Table 3.4. Crystal data and structure refinement for *CCDC 2197380*

Identification code	cu_YBA203D1-c_0m
Empirical formula	C34 H32 N2 O8
Formula weight	596.61
Temperature	100(2)K
Wavelength	1.54178 Å
Crystal system	triclinic
Space group	P 1
Unit cell dimensions	a = 6.9484(2)Å a= 82.727(2)°.
	b = 7.1418(2)Å b = 86.432(2)°.
	c = 15.8024(5)Å g = 75.4121(19)°.
Volume	752.42(4) $Å^3$
Z	1
Density (Calculated)	1.317 Mg/m^3
Absorption coefficient	0.778 mm^{-1}
F(000)	314
Crystal size	0.300 x 0.030 x 0.020 mm^3
Theta range for data collection	2.820 to 66.476°.
Index ranges	-8<=h<=8,-8<=k<=8,-16<=l<=18
Reflections collected	8999
Independent reflections	4737[R(int) = 0.0243]

Completeness to theta =66.476°	96.8%
Absorption correction	Multi-scan
Max. and min. transmission	0.75 and 0.52
Refinement method	Full-matrix least-squares on F^2
Data / restraints / parameters	4737/ 150/ 469
Goodness-of-fit on F^2	1.046
Final R indices [I>2sigma(I)]	R1 = 0.0318, wR2 = 0.0823
R indices (all data)	R1 = 0.0356, wR2 = 0.0848
Flack parameter	x =-0.05(9)
Largest diff. peak and hole	0.116 and -0.193 e.$Å^{-3}$

Table 3.5. Bond lengths [Å] and angles [°] for *CCDC 2197380*

Bond lengths----		
O1	N1	1.229(3)
O2	N1	1.223(3)
O3	C7	1.206(3)
O4	C7	1.333(3)
O4	C8	1.450(3)
O5	C28	1.330(3)
O5	C27	1.461(3)
O6	C28	1.201(3)
O7	N2	1.223(3)
O8	N2	1.219(3)
N1	C1	1.473(3)
N2	C32	1.469(3)
C1	C2	1.386(4)
C1	C6	1.386(3)
C2	C3	1.380(4)
C2	H2	0.9500
C3	C4	1.402(3)

C3	H3	0.9500
C4	C5	1.388(4)
C4	C7	1.494(4)
C5	C6	1.382(4)
C5	H5	0.9500
C6	H6	0.9500
C8	C9	1.523(4)
C8	H8A	0.9900
C8	H8B	0.9900
C9	C10	1.510(3)
C9	C16	1.528(3)
C9	H9	1.0000
C10	C15	1.385(4)
C10	C11	1.393(3)
C11	C12	1.390(5)
C11	H11	0.9500
C12	C13	1.377(6)
C12	H12	0.9500
C13	C14	1.371(5)
C13	H13	0.9500
C14	C15	1.384(4)
C14	H14	0.9500
C15	H15	0.9500
C16	C17	1.528(4)
C16	H16A	0.9900
C16	H16B	0.9900
C17	C26	1.531(3)
C17	C18	1.563(4)
C17	C18'	1.586(10)
C17	H17	1.0000
C17	H17'	1.0000
C26	C27	1.487(4)

C26	H26A	0.9900
C26	H26B	0.9900
C27	H27A	0.9900
C27	H27B	0.9900
C28	C29	1.496(3)
C29	C30	1.392(4)
C29	C34	1.393(3)
C30	C31	1.382(3)
C30	H30	0.9500
C31	C32	1.386(3)
C31	H31	0.9500
C32	C33	1.383(4)
C33	C34	1.382(4)
C33	H33	0.9500
C34	H34	0.9500
C18	C19	1.532(5)
C18	H18A	0.9900
C18	H18B	0.9900
C19	C20	1.508(5)
C19	H19A	0.9900
C19	H19B	0.9900
C20	C25	1.386(6)
C20	C21	1.391(6)
C21	C22	1.394(8)
C21	H21	0.9500
C22	C23	1.379(7)
C22	H22	0.9500
C23	C24	1.370(7)
C23	H23	0.9500
C24	C25	1.391(7)
C24	H24	0.9500
C25	H25	0.9500

C18'	C19'	1.541(10)
C18'	H18C	0.9900
C18'	H18D	0.9900
C19'	C20'	1.508(10)
C19'	H19C	0.9900
C19'	H19D	0.9900
C20'	C25'	1.379(11)
C20'	C21'	1.391(11)
C21'	C22'	1.397(13)
C21'	H21'	0.9500
C22'	C23'	1.377(12)
C22'	H22'	0.9500
C23'	C24'	1.369(12)
C23'	H23'	0.9500
C24'	C25'	1.393(12)
C24'	H24'	0.9500
C25'	H25'	0.9500

Angles

C7	O4	C8	117.3(2)
C28	O5	C27	114.90(19)
O2	N1	O1	123.8(2)
O2	N1	C1	118.4(2)
O1	N1	C1	117.8(2)
O8	N2	O7	123.6(2)
O8	N2	C32	118.7(2)
O7	N2	C32	117.8(2)
C2	C1	C6	122.9(2)
C2	C1	N1	118.8(2)
C6	C1	N1	118.4(2)
C3	C2	C1	118.2(2)
C3	C2	H2	120.9

C1	C2	H2	120.9
C2	C3	C4	120.0(2)
C2	C3	H3	120.0
C4	C3	H3	120.0
C5	C4	C3	120.4(2)
C5	C4	C7	117.9(2)
C3	C4	C7	121.8(2)
C6	C5	C4	120.1(2)
C6	C5	H5	119.9
C4	C5	H5	119.9
C5	C6	C1	118.3(2)
C5	C6	H6	120.8
C1	C6	H6	120.8
O3	C7	O4	124.0(2)
O3	C7	C4	124.2(2)
O4	C7	C4	111.8(2)
O4	C8	C9	106.59(19)
O4	C8	H8A	110.4
C9	C8	H8A	110.4
O4	C8	H8B	110.4
C9	C8	H8B	110.4
H8A	C8	H8B	108.6
C10	C9	C8	109.8(2)
C10	C9	C16	114.1(2)
C8	C9	C16	109.4(2)
C10	C9	H9	107.8
C8	C9	H9	107.8
C16	C9	H9	107.8
C15	C10	C11	117.6(2)
C15	C10	C9	121.4(2)
C11	C10	C9	120.9(2)
C12	C11	C10	120.7(3)

C12	C11	H11	119.6
C10	C11	H11	119.6
C13	C12	C11	120.5(3)
C13	C12	H12	119.8
C11	C12	H12	119.8
C14	C13	C12	119.4(3)
C14	C13	H13	120.3
C12	C13	H13	120.3
C13	C14	C15	120.3(3)
C13	C14	H14	119.9
C15	C14	H14	119.9
C14	C15	C10	121.5(2)
C14	C15	H15	119.3
C10	C15	H15	119.3
C17	C16	C9	114.4(2)
C17	C16	H16A	108.7
C9	C16	H16A	108.7
C17	C16	H16B	108.7
C9	C16	H16B	108.7
H16A	C16	H16B	107.6
C16	C17	C26	109.8(2)
C16	C17	C18	116.9(2)
C26	C17	C18	116.0(2)
C16	C17	C18'	99.0(4)
C26	C17	C18'	99.8(4)
C16	C17	H17	104.1
C26	C17	H17	104.1
C18	C17	H17	104.1
C16	C17	H17'	115.3
C26	C17	H17'	115.3
C18'	C17	H17'	115.3
C27	C26	C17	112.2(2)

C27	C26	H26A	109.2
C17	C26	H26A	109.2
C27	C26	H26B	109.2
C17	C26	H26B	109.2
H26A	C26	H26B	107.9
O5	C27	C26	108.65(19)
O5	C27	H27A	110.0
C26	C27	H27A	110.0
O5	C27	H27B	110.0
C26	C27	H27B	110.0
H27A	C27	H27B	108.3
O6	C28	O5	123.7(2)
O6	C28	C29	123.2(2)
O5	C28	C29	113.12(19)
C30	C29	C34	120.3(2)
C30	C29	C28	117.0(2)
C34	C29	C28	122.7(2)
C31	C30	C29	120.5(2)
C31	C30	H30	119.7
C29	C30	H30	119.7
C30	C31	C32	117.8(2)
C30	C31	H31	121.1
C32	C31	H31	121.1
C33	C32	C31	123.0(2)
C33	C32	N2	118.7(2)
C31	C32	N2	118.3(2)
C34	C33	C32	118.4(2)
C34	C33	H33	120.8
C32	C33	H33	120.8
C33	C34	C29	119.9(2)
C33	C34	H34	120.0
C29	C34	H34	120.0

C19	C18	C17	112.9(3)
C19	C18	H18A	109.0
C17	C18	H18A	109.0
C19	C18	H18B	109.0
C17	C18	H18B	109.0
H18A	C18	H18B	107.8
C20	C19	C18	112.0(3)
C20	C19	H19A	109.2
C18	C19	H19A	109.2
C20	C19	H19B	109.2
C18	C19	H19B	109.2
H19A	C19	H19B	107.9
C25	C20	C21	118.1(4)
C25	C20	C19	120.3(4)
C21	C20	C19	121.6(4)
C20	C21	C22	120.9(5)
C20	C21	H21	119.6
C22	C21	H21	119.6
C23	C22	C21	119.7(6)
C23	C22	H22	120.1
C21	C22	H22	120.1
C24	C23	C22	120.1(5)
C24	C23	H23	120.0
C22	C23	H23	120.0
C23	C24	C25	120.2(6)
C23	C24	H24	119.9
C25	C24	H24	119.9
C20	C25	C24	120.9(5)
C20	C25	H25	119.5
C24	C25	H25	119.5
C19'	C18'	C17	106.2(7)
C19'	C18'	H18C	110.5

C17	C18'	H18C	110.5
C19'	C18'	H18D	110.5
C17	C18'	H18D	110.5
H18C	C18'	H18D	108.7
C20'	C19'	C18'	112.9(8)
C20'	C19'	H19C	109.0
C18'	C19'	H19C	109.0
C20'	C19'	H19D	109.0
C18'	C19'	H19D	109.0
H19C	C19'	H19D	107.8
C25'	C20'	C21'	118.6(9)
C25'	C20'	C19'	120.7(9)
C21'	C20'	C19'	120.6(9)
C20'	C21'	C22'	120.9(11)
C20'	C21'	H21'	119.6
C22'	C21'	H21'	119.6
C23'	C22'	C21'	119.0(12)
C23'	C22'	H22'	120.5
C21'	C22'	H22'	120.5
C24'	C23'	C22'	120.7(11)
C24'	C23'	H23'	119.7
C22'	C23'	H23'	119.7
C23'	C24'	C25'	119.9(13)
C23'	C24'	H24'	120.1
C25'	C24'	H24'	120.1
C20'	C25'	C24'	120.7(11)
C20'	C25'	H25'	119.7
C24'	C25'	H25'	119.7

Table 3.6. Torsion angles [°] for *CCDC 2197380*

O2	N1	C1	C2	-0.5(3)
O1	N1	C1	C2	179.3(2)
O2	N1	C1	C6	-179.6(2)
O1	N1	C1	C6	0.2(3)
C6	C1	C2	C3	0.6(3)
N1	C1	C2	C3	-178.5(2)
C1	C2	C3	C4	0.0(4)
C2	C3	C4	C5	-0.7(4)
C2	C3	C4	C7	-179.6(2)
C3	C4	C5	C6	0.9(3)
C7	C4	C5	C6	179.8(2)
C4	C5	C6	C1	-0.3(3)
C2	C1	C6	C5	-0.4(3)
N1	C1	C6	C5	178.7(2)
C8	O4	C7	O3	-0.8(4)
C8	O4	C7	C4	178.87(19)
C5	C4	C7	O3	-10.5(4)
C3	C4	C7	O3	168.4(2)
C5	C4	C7	O4	169.8(2)
C3	C4	C7	O4	-11.3(3)
C7	O4	C8	C9	-159.8(2)
O4	C8	C9	C10	58.7(3)
O4	C8	C9	C16	-175.5(2)
C8	C9	C10	C15	65.6(3)
C16	C9	C10	C15	-57.6(3)
C8	C9	C10	C11	-109.8(3)
C16	C9	C10	C11	127.0(3)
C15	C10	C11	C12	-1.3(4)
C9	C10	C11	C12	174.3(3)
C10	C11	C12	C13	-0.8(5)

C11	C12	C13	C14	1.8(5)
C12	C13	C14	C15	-0.8(5)
C13	C14	C15	C10	-1.2(4)
C11	C10	C15	C14	2.3(4)
C9	C10	C15	C14	-173.2(2)
C10	C9	C16	C17	-57.1(3)
C8	C9	C16	C17	179.5(2)
C9	C16	C17	C26	177.9(2)
C9	C16	C17	C18	-47.3(3)
C9	C16	C17	C18'	-78.2(4)
C16	C17	C26	C27	-174.9(2)
C18	C17	C26	C27	49.8(3)
C18'	C17	C26	C27	81.7(4)
C28	O5	C27	C26	169.3(2)
C17	C26	C27	O5	172.3(2)
C27	O5	C28	O6	-0.2(4)
C27	O5	C28	C29	-178.8(2)
O6	C28	C29	C30	0.3(3)
O5	C28	C29	C30	179.0(2)
O6	C28	C29	C34	-178.1(2)
O5	C28	C29	C34	0.5(3)
C34	C29	C30	C31	0.6(3)
C28	C29	C30	C31	-177.9(2)
C29	C30	C31	C32	-0.6(3)
C30	C31	C32	C33	0.3(3)
C30	C31	C32	N2	-178.66(19)
O8	N2	C32	C33	2.5(3)
O7	N2	C32	C33	-176.2(2)
O8	N2	C32	C31	-178.5(2)
O7	N2	C32	C31	2.8(3)
C31	C32	C33	C34	0.0(4)
N2	C32	C33	C34	178.9(2)

C32	C33	C34	C29	0.1(3)
C30	C29	C34	C33	-0.4(3)
C28	C29	C34	C33	178.0(2)
C16	C17	C18	C19	-62.6(3)
C26	C17	C18	C19	69.5(3)
C17	C18	C19	C20	-176.2(3)
C18	C19	C20	C25	84.2(5)
C18	C19	C20	C21	-94.2(5)
C25	C20	C21	C22	1.3(9)
C19	C20	C21	C22	179.7(7)
C20	C21	C22	C23	0.1(14)
C21	C22	C23	C24	-2.0(14)
C22	C23	C24	C25	2.6(13)
C21	C20	C25	C24	-0.7(9)
C19	C20	C25	C24	-179.1(7)
C23	C24	C25	C20	-1.2(12)
C16	C17	C18'	C19'	129.9(6)
C26	C17	C18'	C19'	-118.0(6)
C17	C18'	C19'	C20'	175.7(7)
C18'	C19'	C20'	C25'	-92.9(14)
C18'	C19'	C20'	C21'	89.0(14)
C25'	C20'	C21'	C22'	1(3)
C19'	C20'	C21'	C22'	179(2)
C20'	C21'	C22'	C23'	-3(4)
C21'	C22'	C23'	C24'	5(4)
C22'	C23'	C24'	C25'	-6(4)
C21'	C20'	C25'	C24'	-2(3)
C19'	C20'	C25'	C24'	-179.8(19)
C23'	C24'	C25'	C20'	4(4)

Symetry operations

---

1 'x, y, z'

4-Nitrobenzoate derivative **35** was obtained from an analytical sample prepared according to the general procedure **E** as described using β-cyano alcohol **34d**. Crystals of the compound **35** were obtained by slow evaporation of a dichloromethane/hexane solution. *Data Collection*. Measurements were performed at 100 K on a Bruker Kappa Apex II DUO diffractometer equiped with a Cryostream 700 plus low temperature device, a microsource anode with Mo Kα (λ= 0.71073 Å).

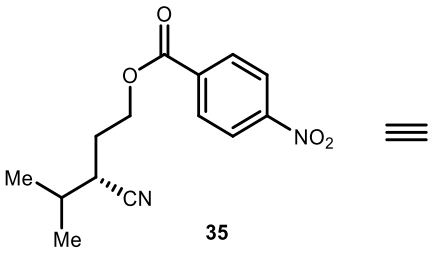

35

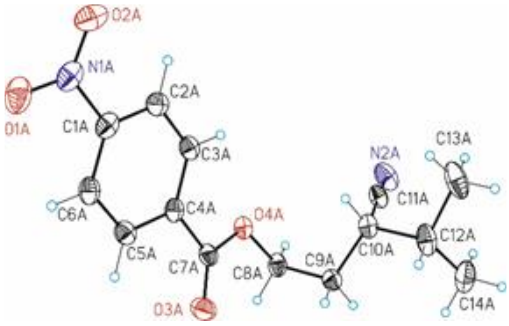

This chiral compound crystallizes in the space group P21 with two identical molecules (A and B) in the asymmetric unit. One of the molecules is disordered in two inverted orientations of the chiral center with a ratio 82:18. The absolute structure could be determined reliable with a Flack value based on Parsons' quotients of 0.02(8)[84] Flack X determined using 2186 quotients [(I+)-(I-)]/[(I+)+(I-)]). The Flack parameter value for the correct absolute structure determination should be 0; the inverted structure would give 1; always taking in account the standard deviation. For molecule A the absolute configuration was assigned with S(C10A). In molecule B the absolute configuration was assigned with 82% of configuration S(C10B) and 18% of configuration R(C10'). Adding the results, it was determined that the majoritarian part of the structure (91%) shows S configuration and a minoritarian part (9%) shows a R configuration in accordance with the e.r. value obtained in the preparation of the product. The structure is of excellent quality (no A- or B-alerts) and of publishable quality with a R1 value of 3.07%.

Table 3.7. Crystal data and structure refinement for *CCDC2197381*

Identification code	cu_MBE389_0m	
Empirical formula	C28 H32 N4 O8	
Formula weight	552.57	
Temperature	100(2)K	
Wavelength	1.54178 Å	
Crystal system	monoclinic	
Space group	P 21	
Unit cell dimensions	a = 7.2034(2)Å	a= 90°.
	b = 18.8414(6)Å	b = 91.8741(14)°.
	c = 10.3566(3)Å	g = 90°.
Volume	1404.87(7) $Å^3$	
Z	2	
Density (Calculated)	1.306 Mg/m^3	
Absorption coefficient	0.806 mm^{-1}	
F(000)	584	
Crystal size	0.200 x 0.200 x 0.010 mm^3	
Theta range for data collection	4.271 to 67.930°.	
Index ranges	-8<=h<=8,-22<=k<=21,-8<=l<=12	
Reflections collected	11462	
Independent reflections	4916[R(int) = 0.0278]	
Completeness to theta =67.930°	98.6%	
Absorption correction	Multi-scan	
Max. and min. transmission	0.75 and 0.65	
Refinement method	Full-matrix least-squares on F^2	
Data / restraints / parameters	4916/ 99/ 432	
Goodness-of-fit on F^2	1.058	
Final R indices [I>2sigma(I)]	R1 = 0.0307, wR2 = 0.0814	
R indices (all data)	R1 = 0.0315, wR2 = 0.0819	
Flack parameter	x =0.02(8)	

Largest diff. peak and hole 0.189 and -0.158 e.Å^{-3}

Table 3.8. Bond lengths [Å] and angles [°] for *CCDC2197381*

Bond lengths		
O1A	N1A	1.225(3)
O2A	N1A	1.229(3)
O3A	C7A	1.203(3)
O4A	C7A	1.340(3)
O4A	C8A	1.454(3)
N1A	C1A	1.475(3)
N2A	C11A	1.145(3)
C1A	C2A	1.382(4)
C1A	C6A	1.385(4)
C2A	C3A	1.388(3)
C2A	H2A	0.9500
C3A	C4A	1.389(3)
C3A	H3A	0.9500
C4A	C5A	1.391(4)
C4A	C7A	1.496(3)
C5A	C6A	1.385(3)
C5A	H5A	0.9500
C6A	H6A	0.9500
C8A	C9A	1.517(3)
C8A	H8AA	0.9900
C8A	H8AB	0.9900
C9A	C10A	1.533(3)
C9A	H9AA	0.9900
C9A	H9AB	0.9900
C10A	C11A	1.470(3)
C10A	C12A	1.547(3)
C10A	H10A	1.0000

C12A	C14A	1.522(4)
C12A	C13A	1.530(4)
C12A	H12A	1.0000
C13A	H13A	0.9800
C13A	H13B	0.9800
C13A	H13C	0.9800
C14A	H14A	0.9800
C14A	H14B	0.9800
C14A	H14C	0.9800
O1B	N1B	1.224(3)
O2B	N1B	1.228(3)
O3B	C7B	1.204(3)
O4B	C7B	1.338(3)
O4B	C8B	1.449(3)
N1B	C1B	1.472(3)
C1B	C6B	1.381(4)
C1B	C2B	1.385(3)
C2B	C3B	1.386(3)
C2B	H2B	0.9500
C3B	C4B	1.389(4)
C3B	H3B	0.9500
C4B	C5B	1.399(3)
C4B	C7B	1.494(3)
C5B	C6B	1.382(3)
C5B	H5B	0.9500
C6B	H6B	0.9500
C8B	C9'	1.322(17)
C8B	C9B	1.550(4)
C8B	H8BA	0.9900
C8B	H8BB	0.9900
C8B	H8BX	0.9900
C8B	H8BY	0.9900

N2B	C11B	1.145(4)
C9B	C10B	1.536(4)
C9B	H9BA	0.9900
C9B	H9BB	0.9900
C10B	C11B	1.470(4)
C10B	C12B	1.548(4)
C10B	H10B	1.0000
C12B	C13B	1.527(6)
C12B	C14B	1.534(5)
C12B	H12B	1.0000
C13B	H13D	0.9800
C13B	H13E	0.9800
C13B	H13F	0.9800
C14B	H14D	0.9800
C14B	H14E	0.9800
C14B	H14F	0.9800
N2'	C11'	1.11(2)
C9'	C10'	1.46(3)
C9'	H9BC	0.9900
C9'	H9BD	0.9900
C10'	C11'	1.52(2)
C10'	C12'	1.59(2)
C10'	H10'	1.0000
C12'	C13'	1.45(3)
C12'	C14'	1.52(3)
C12'	H12'	1.0000
C13'	H13G	0.9800
C13'	H13H	0.9800
C13'	H13I	0.9800
C14'	H14G	0.9800
C14'	H14H	0.9800
C14'	H14I	0.9800

Angles

C7A	O4A	C8A	116.25(18)
O1A	N1A	O2A	124.1(2)
O1A	N1A	C1A	118.0(2)
O2A	N1A	C1A	117.9(2)
C2A	C1A	C6A	123.0(2)
C2A	C1A	N1A	118.7(2)
C6A	C1A	N1A	118.2(2)
C1A	C2A	C3A	118.2(2)
C1A	C2A	H2A	120.9
C3A	C2A	H2A	120.9
C2A	C3A	C4A	119.7(2)
C2A	C3A	H3A	120.1
C4A	C3A	H3A	120.1
C3A	C4A	C5A	121.0(2)
C3A	C4A	C7A	121.6(2)
C5A	C4A	C7A	117.4(2)
C6A	C5A	C4A	119.8(2)
C6A	C5A	H5A	120.1
C4A	C5A	H5A	120.1
C5A	C6A	C1A	118.2(2)
C5A	C6A	H6A	120.9
C1A	C6A	H6A	120.9
O3A	C7A	O4A	124.4(2)
O3A	C7A	C4A	123.5(2)
O4A	C7A	C4A	112.08(19)
O4A	C8A	C9A	109.83(18)
O4A	C8A	H8AA	109.7
C9A	C8A	H8AA	109.7
O4A	C8A	H8AB	109.7
C9A	C8A	H8AB	109.7

H8AA	C8A	H8AB	108.2
C8A	C9A	C10A	113.50(19)
C8A	C9A	H9AA	108.9
C10A	C9A	H9AA	108.9
C8A	C9A	H9AB	108.9
C10A	C9A	H9AB	108.9
H9AA	C9A	H9AB	107.7
C11A	C10A	C9A	109.66(18)
C11A	C10A	C12A	110.26(19)
C9A	C10A	C12A	114.1(2)
C11A	C10A	H10A	107.5
C9A	C10A	H10A	107.5
C12A	C10A	H10A	107.5
N2A	C11A	C10A	177.8(3)
C14A	C12A	C13A	111.5(2)
C14A	C12A	C10A	112.4(2)
C13A	C12A	C10A	109.9(2)
C14A	C12A	H12A	107.6
C13A	C12A	H12A	107.6
C10A	C12A	H12A	107.6
C12A	C13A	H13A	109.5
C12A	C13A	H13B	109.5
H13A	C13A	H13B	109.5
C12A	C13A	H13C	109.5
H13A	C13A	H13C	109.5
H13B	C13A	H13C	109.5
C12A	C14A	H14A	109.5
C12A	C14A	H14B	109.5
H14A	C14A	H14B	109.5
C12A	C14A	H14C	109.5
H14A	C14A	H14C	109.5
H14B	C14A	H14C	109.5

C7B	O4B	C8B	118.02(19)
O1B	N1B	O2B	123.8(2)
O1B	N1B	C1B	118.3(2)
O2B	N1B	C1B	117.9(2)
C6B	C1B	C2B	122.9(2)
C6B	C1B	N1B	118.4(2)
C2B	C1B	N1B	118.7(2)
C1B	C2B	C3B	118.1(2)
C1B	C2B	H2B	120.9
C3B	C2B	H2B	120.9
C2B	C3B	C4B	120.2(2)
C2B	C3B	H3B	119.9
C4B	C3B	H3B	119.9
C3B	C4B	C5B	120.4(2)
C3B	C4B	C7B	118.4(2)
C5B	C4B	C7B	121.2(2)
C6B	C5B	C4B	119.8(2)
C6B	C5B	H5B	120.1
C4B	C5B	H5B	120.1
C1B	C6B	C5B	118.6(2)
C1B	C6B	H6B	120.7
C5B	C6B	H6B	120.7
O3B	C7B	O4B	125.0(2)
O3B	C7B	C4B	123.6(2)
O4B	C7B	C4B	111.3(2)
C9'	C8B	O4B	128.7(9)
O4B	C8B	C9B	104.0(2)
O4B	C8B	H8BA	111.0
C9B	C8B	H8BA	111.0
O4B	C8B	H8BB	111.0
C9B	C8B	H8BB	111.0
H8BA	C8B	H8BB	109.0

C9'	C8B	H8BX	105.1
O4B	C8B	H8BX	105.1
C9'	C8B	H8BY	105.1
O4B	C8B	H8BY	105.1
H8BX	C8B	H8BY	105.9
C10B	C9B	C8B	113.6(2)
C10B	C9B	H9BA	108.9
C8B	C9B	H9BA	108.9
C10B	C9B	H9BB	108.9
C8B	C9B	H9BB	108.9
H9BA	C9B	H9BB	107.7
C11B	C10B	C9B	109.9(2)
C11B	C10B	C12B	110.2(2)
C9B	C10B	C12B	112.0(3)
C11B	C10B	H10B	108.2
C9B	C10B	H10B	108.2
C12B	C10B	H10B	108.2
N2B	C11B	C10B	179.3(4)
C13B	C12B	C14B	111.0(3)
C13B	C12B	C10B	112.9(4)
C14B	C12B	C10B	111.0(3)
C13B	C12B	H12B	107.2
C14B	C12B	H12B	107.2
C10B	C12B	H12B	107.2
C12B	C13B	H13D	109.5
C12B	C13B	H13E	109.5
H13D	C13B	H13E	109.5
C12B	C13B	H13F	109.5
H13D	C13B	H13F	109.5
H13E	C13B	H13F	109.5
C12B	C14B	H14D	109.5
C12B	C14B	H14E	109.5

H14D	C14B	H14E	109.5
C12B	C14B	H14F	109.5
H14D	C14B	H14F	109.5
H14E	C14B	H14F	109.5
C8B	C9'	C10'	105.2(16)
C8B	C9'	H9BC	110.7
C10'	C9'	H9BC	110.7
C8B	C9'	H9BD	110.7
C10'	C9'	H9BD	110.7
H9BC	C9'	H9BD	108.8
C9'	C10'	C11'	108.6(12)
C9'	C10'	C12'	117.6(14)
C11'	C10'	C12'	107.1(14)
C9'	C10'	H10'	107.7
C11'	C10'	H10'	107.7
C12'	C10'	H10'	107.7
N2'	C11'	C10'	179(2)
C13'	C12'	C14'	113.8(17)
C13'	C12'	C10'	110.6(18)
C14'	C12'	C10'	112.8(15)
C13'	C12'	H12'	106.3
C14'	C12'	H12'	106.3
C10'	C12'	H12'	106.3
C12'	C13'	H13G	109.5
C12'	C13'	H13H	109.5
H13G	C13'	H13H	109.5
C12'	C13'	H13I	109.5
H13G	C13'	H13I	109.5
H13H	C13'	H13I	109.5
C12'	C14'	H14G	109.5
C12'	C14'	H14H	109.5
H14G	C14'	H14H	109.5

C12'	C14'	H14I	109.5
H14G	C14'	H14I	109.5
H14H	C14'	H14I	109.5

Table 3.9. Torsion angles [°] for *CCDC2197381*

O1A	N1A	C1A	C2A	175.8(2)
O2A	N1A	C1A	C2A	-6.0(3)
O1A	N1A	C1A	C6A	-6.6(3)
O2A	N1A	C1A	C6A	171.6(2)
C6A	C1A	C2A	C3A	-0.6(3)
N1A	C1A	C2A	C3A	176.77(18)
C1A	C2A	C3A	C4A	-0.9(3)
C2A	C3A	C4A	C5A	1.7(3)
C2A	C3A	C4A	C7A	-176.63(19)
C3A	C4A	C5A	C6A	-1.0(3)
C7A	C4A	C5A	C6A	177.41(18)
C4A	C5A	C6A	C1A	-0.5(3)
C2A	C1A	C6A	C5A	1.3(3)
N1A	C1A	C6A	C5A	-176.09(19)
C8A	O4A	C7A	O3A	-2.9(3)
C8A	O4A	C7A	C4A	175.97(16)
C3A	C4A	C7A	O3A	167.4(2)
C5A	C4A	C7A	O3A	-11.0(3)
C3A	C4A	C7A	O4A	-11.5(3)
C5A	C4A	C7A	O4A	170.11(18)
C7A	O4A	C8A	C9A	-85.8(2)
O4A	C8A	C9A	C10A	-59.7(3)
C8A	C9A	C10A	C11A	-59.9(3)
C8A	C9A	C10A	C12A	175.8(2)
C11A	C10A	C12A	C14A	-58.4(3)

C9A	C10A	C12A	C14A	65.5(3)
C11A	C10A	C12A	C13A	66.4(3)
C9A	C10A	C12A	C13A	-169.7(2)
O1B	N1B	C1B	C6B	-177.3(2)
O2B	N1B	C1B	C6B	3.3(3)
O1B	N1B	C1B	C2B	4.4(3)
O2B	N1B	C1B	C2B	-175.0(2)
C6B	C1B	C2B	C3B	-0.5(3)
N1B	C1B	C2B	C3B	177.75(18)
C1B	C2B	C3B	C4B	1.0(3)
C2B	C3B	C4B	C5B	-0.7(3)
C2B	C3B	C4B	C7B	-179.16(18)
C3B	C4B	C5B	C6B	-0.2(3)
C7B	C4B	C5B	C6B	178.18(18)
C2B	C1B	C6B	C5B	-0.4(3)
N1B	C1B	C6B	C5B	-178.67(18)
C4B	C5B	C6B	C1B	0.8(3)
C8B	O4B	C7B	O3B	13.7(3)
C8B	O4B	C7B	C4B	-165.90(17)
C3B	C4B	C7B	O3B	9.7(3)
C5B	C4B	C7B	O3B	-168.7(2)
C3B	C4B	C7B	O4B	-170.65(18)
C5B	C4B	C7B	O4B	10.9(3)
C7B	O4B	C8B	C9'	73.3(12)
C7B	O4B	C8B	C9B	93.9(3)
O4B	C8B	C9B	C10B	166.1(2)
C8B	C9B	C10B	C11B	-63.2(3)
C8B	C9B	C10B	C12B	174.0(3)
C11B	C10B	C12B	C13B	-66.3(4)
C9B	C10B	C12B	C13B	56.3(4)
C11B	C10B	C12B	C14B	59.1(4)
C9B	C10B	C12B	C14B	-178.3(3)

O4B	C8B	C9'	C10'	67.6(13)
C8B	C9'	C10'	C11'	65.3(16)
C8B	C9'	C10'	C12'	-173.0(12)
C9'	C10'	C12'	C13'	167.4(18)
C11'	C10'	C12'	C13'	-70(2)
C9'	C10'	C12'	C14'	-63.8(19)
C11'	C10'	C12'	C14'	58.7(19)

Symetry operations

---

1 'x, y, z'

2 '-x, y+1/2, -z'

Chapter IV

Photochemical Organocatalytic Synthesis of Thioethers from Aryl Chlorides and Alcohols

Target

To develop a metal- and thiol-free procedure for the synthesis of aryl alkyl thioethers from aryl chloride and aliphatic alcohols by combining photoredox catalyzed aryl chloride activation and thermal deoxythiolation.

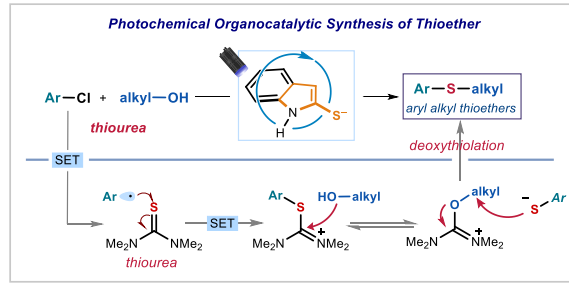

Tool

Use of a strongly reducing organic photocatalyst for the activation of the strong C(sp^2)-Cl bond in aryl chlorides towards radical formation. Identification of *N*-tetramethyl thiourea as a competent radical acceptor, which enables an ionic deoxythiolation path with alcohols to realize an overall radical-polar cascade to afford thioethers.[1]

[1] The project discussed in this chapter has been conducted in collaboration with Mr. Shuo Wu. I have contributed to the reaction development, the exploration of substrate scope, and the mechanistic investigations.

This study has been published: Wu, S.; Wong, T. H.-F.; Righi, P.; Melchiorre, P. "Photochemical Organocatalytic Synthesis of Thioethers from Aryl Chlorides and Alcohols". *J. Am. Chem. Soc.* **2024**, *146*, 2907.

4.1 Introduction

Thioethers are common motifs prevalent in natural products and pharmaceuticals with bioactivity against diseases like cancer, HIV, and Alzheimer's diseases.[2] Development of synthetic methods for their efficient preparation has therefore attracted substantial interest.

The preparation of seemingly simple thioethers **3** from aryl (pseudo)halides **1** (where X is commonly I, Br, Cl etc.) and thiols, by means of the the construction of a C(sp^2)-S bond, is not trivial through thermal, ionic chemistry (Figure 4.1a). Unlike nucleophilic substitution of alkyl halides at an sp^3 center, nucleophilic aromatic substitutions (S_NAr)[3] at an arene carbon involves population of the high energy σ*(C-X) orbital sterically protected by the aromatic system. Therefore, the thiolate nucleophile would have to engage the π* orbitals of arene, forming product through a dearomatized, anionic Meisenheimer intermediate. This reactivity would only occur at electronically deficient aryl fluorides under intense heating, while less activated aryl halides, such as affordable aryl chlorides with varied commercial assortment are incompatible.

---

[2] (a) Feng, M.; Tang, B.; Liang, S. H.; Jiang, X. "Sulfur Containing Scaffolds in Drugs: Synthesis and Application in Medicinal Chemistry." *Curr. Top. Med. Chem.* **2016**, *16*, 1200; (b) Scott, K. A.; Njardarson, J. T. "Analysis of US FDA-Approved Drugs Containing Sulfur Atoms." *Top. Curr. Chem.* **2018**, *376*, 5; (c) Ilardi, E. A.; Vitaku, E.; Njardarson, J. T. "Data-Mining for Sulfur and Fluorine: An Evaluation of Pharmaceuticals to Reveal Opportunities for Drug Design and Discovery." *J. Med. Chem.* **2014**, *57*, 2832; (d) Le Grand, B. L.; Pignier, C.; Letienne, R.; Cuisiat, F.; Rolland, F.; Mas, A.; Vacher, B. "Sodium Late Current Blockers in Ischemia Reperfusion: Is the Bullet Magic?" *J. Med. Chem.* **2008**, *51*, 3856; (e) Chaffman, M.; Brogden, R. N. "Diltiazem: a review of its pharmacological properties and therapeutic efficacy." *Drugs* **1985**, *29*, 387; (f) Robinson, S. E.; Berney, S.; Mishra, R. and Sulser, F. "The relative role of dopamine and norepinephrine receptor blockade in the action of antipsychotic drugs: Metoclopramide, thiethylperazine, and molindone as pharmacological tools." *Psychopharm.* **1979**, *64*, 141.

[3] (a) Bunnett, J. F.; Zahler, R. E. "Aromatic Nucleophilic Substitution Reactions." *Chem. Rev.* **1951**, *49*, 273; (b) Bunnett, J. F. "The Remarkable Reactivity of Aryl Halides with Nucleophiles." *J. Chem. Educ.* **1974**, *51*, 312; (c) Mortier,J. *Arene Chemistry: Reaction Mechanism and Methods for Aromatic Compounds*; John Wiley & Sons, Inc.: Hoboken, NJ, **2016**. (d) Rohrbach, S.; Smith, A. J.; Pang, J. H.; Poole, D. L.; Tuttle, T.; Chiba, S.; John A. Murphy, J. A. "Concerted Nucleophilic Aromatic Substitution Reactions." *Angew. Chem., Int. Ed.* **2019**, *58*, 16368.

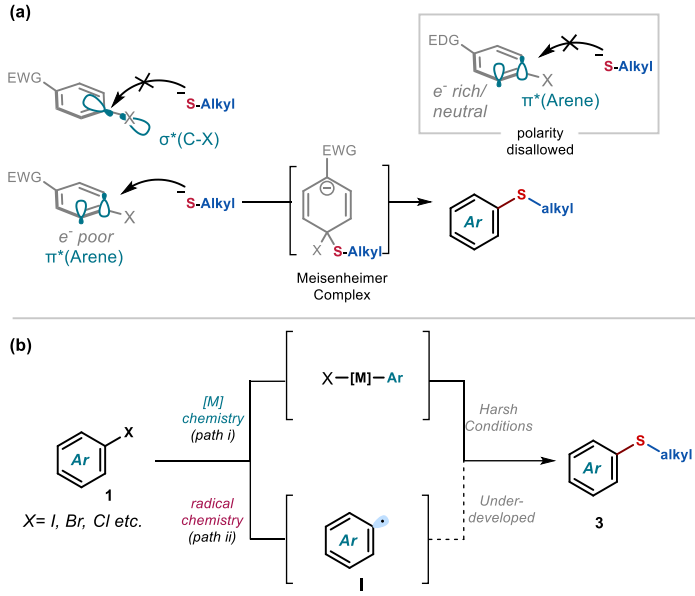

Figure 4.1. Strategy for aryl alkyl thioether synthesis. (**a**) Limitations of polar S_NAr reactions **(b)** State of the art of ary thioether syntheses by transition-metal catalysis and photoredox ctalysis. EWG: electron withdrawing groups, EDG: electron donating groups

A more general C(sp^2)-S cross coupling can be acheived by transition-metal catalysis,[4] where C-Cl bond can be cleaved through oxidative addition, providing a metal-aryl intermediate which can react with thiols (Figure 4.1b). However, there are practical drawbacks for the existing organometallic protocols, including high catalyst loading, specialized catalyst design, necessity of elevated temperature and strong base. These factors can be partly attributed to the mediocre capability of metal-based catalysts to break C(sp^2)-Cl bond in aryl chlorides, and prevent their general applications to substrates containing sensitive moieties. In addition, thiols are recognized as problematic starting materials, with undesirable traits like unpleasant odor, air instability, limited commercial diversity and the propensity to deactivate metal catalyst.

[4] (a) Norris, T.; Leeman, K. "Development of a New Variant of the Migita Reaction for Carbon−Sulfur Bond Formation Used in the Manufacture of Tetrahydro-4-[3-[4-(2-methyl-1H-imidazol-1-yl)-phenyl]thio]phenyl-2H-pyran-4-carboxamide." *Org. Process Res. Dev.* **2008**, 12, 869; (b) de Koning, P. D.; Murtagh, L.; Lawson, J. P.; Vonder Embse, R. A.; Kunda, S. A.; Kong, W. "Development an Efficient Route to the 5-Lipoxygenase Inhibitor PF-04191834." *Org. Process Res. Dev.* **2011**, 15, 1046.

Photoinduced single-electron transfer (SET) is a mild alternative for inert bond activation, which leads to the formation of a highly reactive aryl radicals **I**. Yet, photoredox catalytic approaches for thiol-free C-S bond formation has not been explored. In this chapter, we aim at realizing a photochemical, thiol-free organocatalytic method to synthesize aryl alkyl thioether from simple alkyl alcohols and unreactive aryl chlorides (Figure 4.2). The central target was to identify a suitable sulfur surogate able to intercept aryl radicals generated upon SET activation of aryl chlorides from a strongly reducing photoredox catalysis, thus leading to the formation of the desired Ar-S bond.

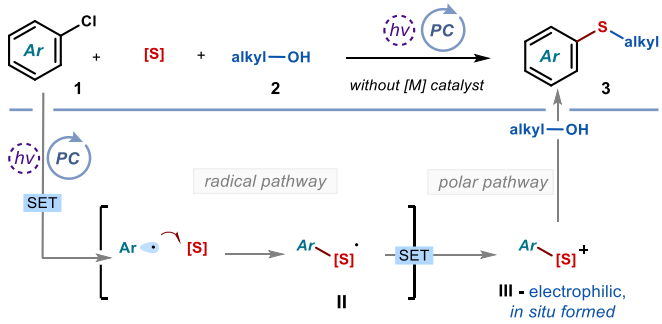

Figure 4.2. Proposed strategy for developing a metal and thiol-free synthesis of aryl alkyl thioethers, enabled by combining radical and polar reactivity in a single sequence. SET: single electron transfer, PC: photocatalyst.

The following sections will detail precedent methodologies to construct aryl-alkyl thioethers with transition-metal catalysis and/or photochemical activation, with particular focus on the more challenging formation of C(sp^2)-S bonds from C(sp^2)-Cl bonds.

4.2 Background

4.2.1 Transition-Metal Catalyzed Methods for the Construction of C(sp^2)-S Bond

The synthesis of thioethers is prevalently conducted by means of transition-metal catalyzed cross coupling. Exploration have begun in 1978, when Migita described the first C(sp^2)-S cross coupling catalyzed by a palladium catalyst (Figure 4.3).[5] It was proposed that Pd(0) catalyst could undergo oxidative addition with aryl iodide **4**, forming the Pd(II) aryl complex **IV**. Transmetallation with sodium thiolate, generated upon in situ deprotonation of thiols, provided Pd(II) sulfide species **V** to facilitate carbon-sulfur reductive elimination, delivering aryl alkyl thioether **3** as the product.

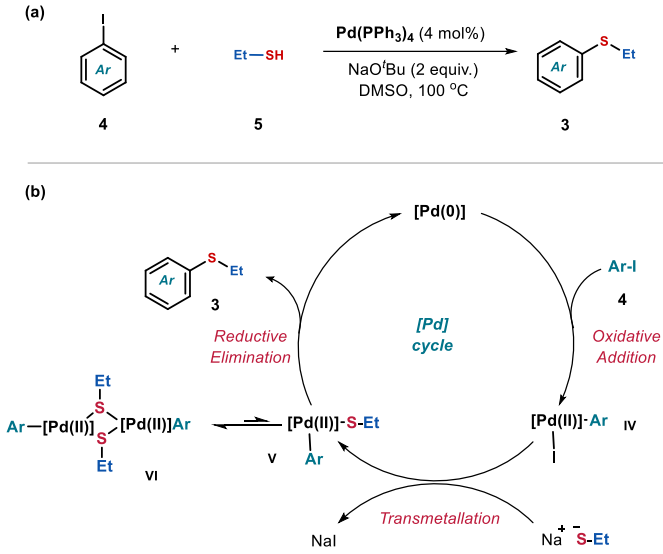

Figure 4.3. Palladium-catalyzed C-S cross coupling. **(a)** Standard reaction conditions, (**b**) Proposed catalytic cycle. Coordination of ligand to metal catalyst was not shown and was represented as brackets []. DMSO: dimethyl sulfoxide.

[5] (a) Kosugi, M.; Shimizu, T.; Migita, T. "Reactions of Aryl Halides with Thiolate Anions in Presence of Catalytic Amounts of Tetrakis(Triphenylphosphine)Palladium Preparation of Aryl Sulfides." *Chem. Lett.* **1978**, 13; (b) Migita, T.; Shimizu, T.; Asami, Y.; Shiobara, J.; Kato, Y.; Kosugi, M. "The Palladium Catalyzed Nucleophilic-Substitution of Aryl Halides by Thiolate Anions." *Bull. Chem. Soc. Jpn.* **1980**, *53*, 1385.

However, this approach was complicated by the tendency of thiolates to coordinate with transition-metal catalysts and form deactivated metal sulfide dimer **VI**.[6] The process also required activated aryl bromides and iodides as starting materials, elevated temperatures (> 90 ºC) and strong bases (NaO*t*-Bu). In addition to the irreversible formation of significant amounts of the disulfide by-product, the functional group tolerance and the structural diversity of the thioether products were limited. This seminal work was followed by reports on nickel[7] and copper[8] catalyzing the same transformation. Yet they required a higher catalyst loading (typically 5-10 mol%), while suffering from similar limitations as their palladium counterpart.

To overcome these limitations, DuPont introduced an uncommon phosphine oxide ligand for more effective C-S cross-coupling protocols.[9] Not only it was capable of activating aryl bromides and iodides, but also, for the first time, less activated yet more cost-effective and available aryl chloride[10] was reacted as a single entry. Subsequent work focused on designing specialized ligands for the activation of aryl chlorides.[11] Buchwald and co-workers[11a] reported the first general aryl alkyl thioether synthesis from aryl chlorides (Figure 4.4a). The bidentate ligand DiPPF secured the C(sp^2)-S cross coupling with reduced catalyst loading,

---

[6] (a) Hegedus, L. L.; McCabe, R. W. "Catalyst Poisoning." *Stud. Surf. Sci. Catal.* **1980,** *6*, 471; (b) Crabtree, R. H. *The Organometallic Chemistry of the Transition Metals*; John Wiley & Sons, Inc.: Hoboken, NJ, **2014**.

[7] (a) Cristau, H. J.; Chabaud, B.; Chene, A.; Christol, H. "Synthesis of Diaryl Sulfides by Nickel(II)-Catalyzed Arylation of Arenethiolates." *Synthesis* **1981**, *11*, 892; (b) Takagi, K. "Nickel(0)-catalyzed Synthesis of Diaryl Sulfides from Aryl Halides and Aromatic Thiols." *Chem. Lett.* **1987**, 2221.

[8] Bates, C. G.; Gujadhur, R. K. and Venkataraman, D. "A General Method for the Formation of Aryl−Sulfur Bonds Using Copper(I) Catalysts." *Org. Lett.* **2002**, *4*, 16, 2803; (d) Kwong, F. Y.; Buchwald, S. L. "A General, Efficient, and Inexpensive Catalyst System for the Coupling of Aryl Iodides and Thiols." *Org. Lett.* **2002**, *4*, 20, 3517.

[9] Li, G. Y. "The First Phosphine Oxide Ligand Precursors for Transition Metal Catalyzed Cross Coupling Reactions: C-C, C-N, and C-S Bond Formation on Unactivated Aryl Chlorides." *Angew. Chem., Int. Ed.* **2001**, *40*, 1513.

[10] Huang, L.; Ackerman, L. K. G.; Kang, K.; Parsons, A. M.; Weix, D. J. "LiCl-Accelerated Multimetallic Cross-Coupling of Aryl Chlorides with Aryl Triflates." *J. Am. Chem. Soc.* **2019**, *141*, 28, 10978.

[11] (a) Murata, M.; Buchwald, S. L. "A general and efficient method for the palladium-catalyzed cross-coupling of thiols and secondary phosphines." *Tetrahedron.* **2004**, *60*, 7397; (b) Fernandez-Rodriguez, M. A.; Shen, Q. L.; Hartwig, J. F. "A General and Long-Lived Catalyst for the Palladium-Catalyzed Coupling of Aryl Halides with Thiols." *J. Am. Chem. Soc.* **2006**, *128*, 2180.

using electron-rich and hindered aryl halides which were incompatible with earlier conditions. Independently, at the same time, Hartwig[11b] disclosed a similar system to activate aryl chlorides and couple them with alkyl thiols in excellent yields (Figure 4.4b). A highly active and robust catalyst was generated using bidentate Josiphos ligand in the presence of exceedingly low loading of palladium pre-catalyst (down to 0.01%). Apart from tackling the challenging oxidative addition, the higher potency of these catalyst systems was also attributed to the chelating ability of bidentate phosphine ligands, which protected the metal center from deactivation through ligand displacement and formation of bridging thiolate complexes.[12]

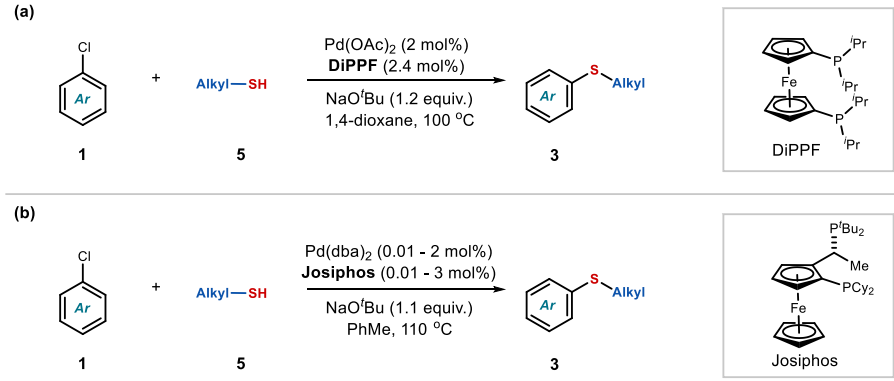

Figure 4.4. Palladium-catalyzed C-S cross coupling with specially designed ligands. **(a)** Use of the DiPPF ligand and **(b)** Josiphos ligand. Dba: dibenzylideneacetone.

Mechanistic investigations by Hartwig concluded that the rate limiting step was the slow dissociation of dibenzylideneacetone (dba) ligand to form on-cycle active Pd(0) catalyst.[13] Therefore, efforts to further improve conditions for thioether synthesis via organometallic strategies should be dedicated to more efficient catalyst activation. This

[12] Louie, J.; Hartwig, J. F. "Transmetalation, Involving Organotin Aryl, Thiolate, and Amide Compounds. An Unusual Type of Dissociative Ligand Substitution Reaction." *J. Am. Chem. Soc.* **1995**, *117*, 11598.

[13] Alvaro, E.; Hartwig, J. F. "Resting State and Elementary Steps of the Coupling of Aryl Halides with Thiols Catalyzed by Alkylbisphosphine Complexes of Palladium." *J. Am. Chem. Soc.* **2009**, *131*, 7858.

insight justified the later design of an air-stable, nickel-based oxidative addition complex for a mild cross coupling between aryl chlorides **1** and alkyl thiols **5** (Figure 4.5). [14] The reaction could readily occur at room temperature, providing thioethers in high yields. The proposed mechanism based on DFT computations (depicted in Figure 4.5b) suggested that the pre-catalyst **Ni** would undergo ligand substitution, providing an acetate complex **VII** with thiol as a neutral L-type ligand. Through an event similar to a concerted metalation-deprotonation, Ni(II) thiolate complex **VIII** could be formed, which underwent reductive elimination to release the active Ni(0) catalyst **IX** for cross coupling.

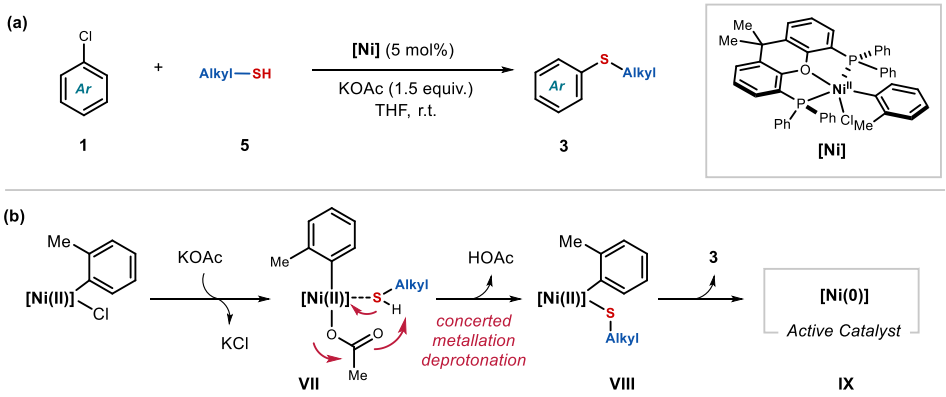

Figure 4.5. Palladium-catalyzed C-S cross coupling using **[Ni]** precatalyst. **(a)** Standard reaction conditions, **(b)** Proposed steps for catalyst activation. THF: tetrahydrofuran, r.t.: room temperature.

Despite these advances, the described cross-coupling strategies largely relied on thiols **5** characterized by undesirable traits such as unpleasant odor, air instability, and limited commercial variety. To alleviate these practical concerns, metal-catalyzed approaches were developed based on sulfur surrogate, in order to bypass the handling of thiols (Figure 4.6). [15]

[14] (a) Gehrtz, P. H.; Geiger, V.; Schmidt, T.; Sršan, L. and Fleischer, I. "Cross-Coupling of Chloro(hetero)arenes with Thiolates Employing a Ni(0)-Precatalyst." *Org. Lett.* **2019**, *21*, 1, 50. (b) Oechsner, R. M.; Wagner, J. P.; Fleischer, I. "Acetate Facilitated Nickel Catalyzed Coupling of Aryl Chlorides and Alkyl Thiols." *ACS Catal.* **2022**, *12*, 2233.

[15] For selected examples: (a) Qiao, Z.; Wei, J.; Jiang, X. "Direct Cross-Coupling Access to Diverse Aromatic Sulfide: Palladium Catalyzed Double C−S Bond Construction Using $Na_2S_2O_3$ as a Sulfurating

These reagents served as donors of a sulfur atom that reacted with an aliphatic electrophile in situ. This provided a masked thiol ready to participate in C(sp^2)-S bond formation through the action of a transition-metal catalyst. However, these systems required refluxing conditions. Further improvements are still pending to make these methods generally useful.

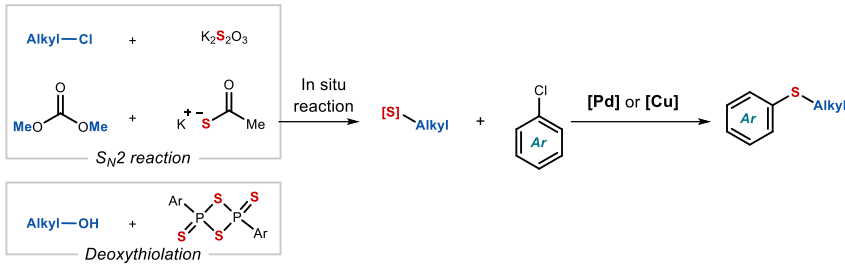

Figure 4.6. Metal-catalyzed C-S cross coupling using sulfur surrogate.

The preceding reports have underscored the challenges associated with constructing C(sp^2)-S bonds through thermal activation. A different approach to tackle this problem was based on photochemistry: single electron transfer (SET) events can modulate the oxidation state of metal catalysts, tailoring the electronic needs suited for different elementary steps in a catalytic cycle.

A pioneering study by Fu and Peters[16] (2013) reported a thioether synthesis based on the photochemistry of copper catalyst at 0 ºC (Figure 4.7). Specifically, photophysical studies demonstrated that a copper (I) thiolate cluster **X** can be directly excited by visible light (λ_{max}= 418 nm). Upon photoexcitation, this intermediate was proposed to reduce 4-chlorobenzonitrile **1** (E_{red} = -2.03 V vs SCE, standard calomel electrode) via an SET step, affording aryl radical **I** which reacted with the electrophilic Cu(II) thiolate complex **XI**. Through reductive elimination, thioether products would be formed while releasing the Cu(I)

Reagent." *Org. Lett.* **2014**, *16*, 1212; (b) Gholinejad, M. "One-Pot Copper-Catalysed Thioetherification of Aryl Halides Using Alcohols and Lawesson's Reagent in Diglyme." *Eur. J. Org. Chem.* **2015**, 4162. (c) Wang, M.; Qiao, Z.; Zhao, J.; Jiang, X. "Palladium-Catalyzed Thiomethylation via a Three-Component Cross-Coupling Strategy." *Org. Lett.* **2018**, *20*, 6193.

[16] Uyeda, C.; Tan, Y.; Fu, G. C.; Peters, J. C. "A New Family of Nucleophiles for Photoinduced, Copper-Catalyzed Cross-Couplings via Single-Electron Transfer: Reactions of Thiols with Aryl Halides Under Mild Conditions (0°C)." *J. Am. Chem. Soc.* **2013**, 135, 9548.

halide complex, restarting the catalytic cycle. This work showcased a complementary reactivity to two-electron oxidative addition, specifically how the strong C-Cl bond could be broken by electron transfer followed by mesolytic cleavage. A radical clock experiment (Figure 4.7c) with aryl iodide **6** provided a cyclic thioether **7** through one-electron cyclization pathway, consistent with the radical nature of the proposed intermediate. Nevertheless, the reduction potential of copper catalyst **X** at the excited state was not able to activate other aryl chlorides, significantly limited the scope of compatible substrates.

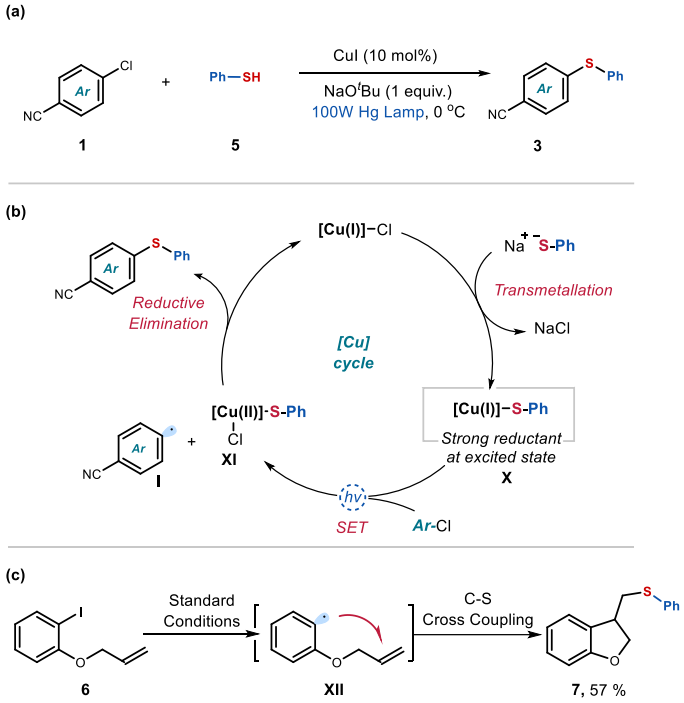

Figure 4.7. Photochemical copper-catalyzed C-S cross coupling. **(a)** Standard reaction conditions (**b**) Proposed catalytic cycle. **(c)** Radical clock experiment.

A more general method for cross coupling is to disentangle photoinduced electron transfer from metal-assisted bond breakage and formation, especially by including an external photocatalyst. This metallophotoredox[17] C-S cross coupling tactic was first published by

[17] (a) Chan, A. Y.; Perry, I. B.; Bissonnette, N. B.; Buksh, B. F.; Edwards, G. A.; Frye, L. I.; Garry, O. L.; Lavagnino, M. N.; Li, B. X.; Liang, Y.; Mao, E.; Millet, A.; Oakley, J. V.; Reed, N. L.; Sakai, H. A.; Seath, C. P.; MacMillan, D. W. C. "Metallaphotoredox: The Merger of Photoredox and Transition

Oderinde and Johannes. [18] In their procedure, 10% of nickel pre-catalyst was employed with external photocatalyst **PC-a** to enable C-S bond formation between aryl iodides **4** and thiols **5** at ambient temperature (Figure 4.8a).

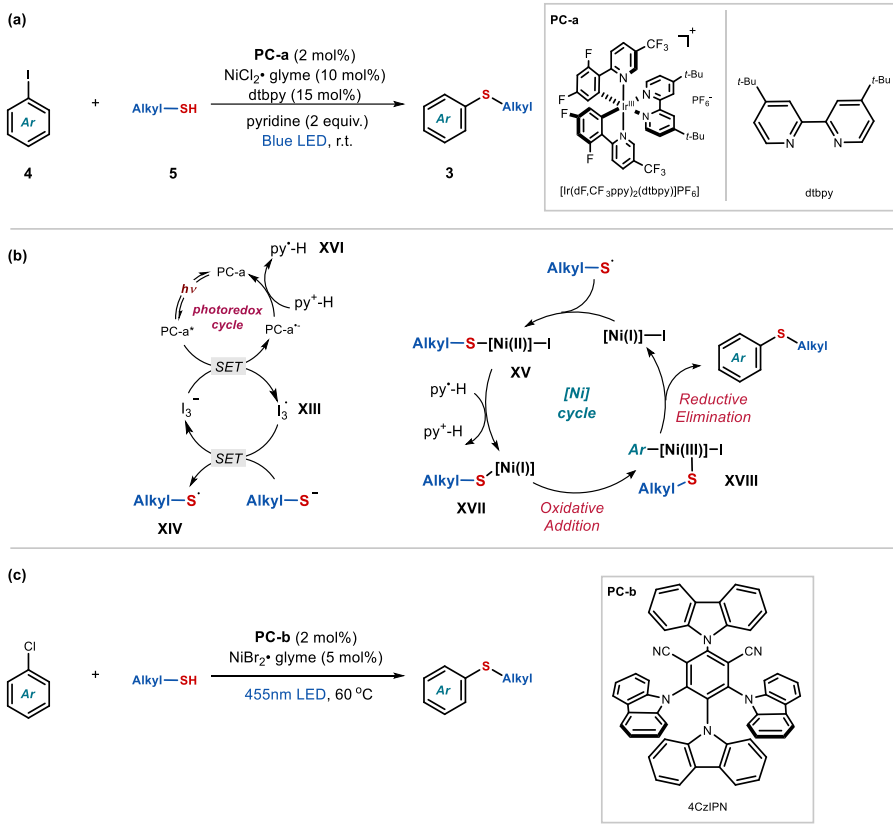

Figure 4.8. Metallophotoredox C-S cross coupling. **(a)** Standard reaction conditions, (**b**) Proposed catalytic cycle **(c)** Recently reported procedure for C-S cross coupling from aryl chloride. LED: light-emitting diode.

Metal Catalysis." *Chem. Rev.* **2022**, *122*, 1485; (b) Beletskaya, I. P.; Ananikov, V. P. "Transition-Metal-Catalyzed C−S, C−Se, and C−Te Bond Formations via Cross-Coupling and Atom-Economic Addition Reactions. Achievements and Challenges." *Chem. Rev.* **2022**, *122*, 16110.

[18] For selected examples, see: (a) Oderinde, M. S.; Frenette, M.; Robbins, D. W.; Aquila, B.; Johannes, J. W. "Photoredox Mediated Nickel Catalyzed Cross-Coupling of Thiols with Aryl and Heteroaryl Iodides via Theil Radicals." *J. Am. Chem. Soc.* **2016**, *138*, 1760; (b) Düker, J.; Ghosh, I.; Konig, B. "Sequential One-Pot (Het)arene Thioetherification and Amination with Nickel and Visible Light." *ACS Catal.* **2023**, *13*, 13618. (c) Ghosh, I.; Shlapakov, N.; Karl, T. A.; Düker, J.; Nikitin, M.; Burykina, J. V.; Ananikov, V. P.; König, B. "General cross-coupling reactions with adaptive dynamic homogeneous catalysis." *Nature* **2023**, *619*, 87.

An in-depth mechanistic investigation led by Nocera[19] suggested the following reaction mechanism (Figure 4.8b). Light irradiation facilitated a SET mediated by photocatalyst **PC-a** within pyridinium triiodide ion pair, generated during the reaction. The triiodide radical **XIII** furnished thiyl radicals **XIV** from alkyl sulfides that, upon capture by Ni(I) catalyst, became prone to reduction by pyridinyl radical **XVI**. This sequence provided the electron-rich Ni(I) sulfide intermediate **XVII** that readily underwent oxidative addition with aryl iodide. The ensuing electron-deficient Ni(III) intermediate **XVIII** then forged the C(sp^2)-S bond through reductive elimination, meanwhile regenerating the Ni(I) catalyst. Overall, the Ni(I)/Ni(III) cycle is self-perpetuating without the need of photonic input.

Despite these progresses, aryl chlorides had been incompatible with protocols based on the merger of photoredox catalysis and metal cross coupling. Only in 2023, the first general methodology based on aryl chlorides for metallophotoredox C(sp^2)-S-alkyl cross coupling was reported (Figure 4.8c).[18c]

4.2.2 Metal-free, Photochemical Methods for the Activation of Aryl (Pseudo)Halides and the Construction of C(sp^2)-S Bond

Activating aryl chlorides for thioether synthesis under mild conditions is difficult with metal catalysis. Alternative approaches to disconnect C(sp^2)-Cl bonds by radical chemistry, without relying on an organometallic intermediate for cross-coupling, was recently investigated.[20]

Traditionally, the activation of electronic neutral aryl chlorides (E_{red} < -2.5 V) by SET is challenging, and typically requires dissolved alkali metals as reductants.[21] Recent advances in photoredox catalysis offered effective solutions under mild conditions. A versatile

[19] Qin, Y.; Sun, R.; Gianoulis, N. P.; Nocera, D. G. "Photoredox Nickel-Catalyzed C−S Cross-Coupling: Mechanism, Kinetics, and Generalization." *J. Am. Chem. Soc.* **2021**, *143*, 2005.

[20] Kvasovs, N.; Gevorgyan, V. "Contemporary methods for generation of aryl radicals" *Chem. Soc. Rev.* **2021**, *50*, 2244.

[21] Yan, Y.; Kawamata, Y.; Baran, P. S. "Synthetic Organic Electrochemical Methods Since 2000: On the Verge of a Renaissance." *Chem. Rev.* **2017**, *117*, 13230.

approach utilized anionic organic catalysts[22] that, upon light excitation, could activate C(sp^2)-Cl bonds via SET reduction. These anionic catalysts have the distinct advantage of acquiring a high redox potential in the excited state (< -3 V vs SCE), along with a greater ability to absorb visible light. For example, our research group has recently reported a class of highly reducing thioamide photo-organocatalysts, which upon deprotonation, to form indole thiolates (Figure 4.9).[22c] The anionic structures are capable of absorbing purple light and exhibiting strong reducing power in their excited state (E* < -3.0 V) that served to activate, by SET reduction, strong bonds in aromatic substrates, including C(sp^2)-Cl bonds. These organic photoactive motifs are also readily accessible: **C2** is a bench-table solid that can be synthesized on a gram-scale in a single step by oxygen−sulfur exchange of commercially available oxindole (see section 4.6.1 for details). The strategy has been particularly successful in reacting C-Cl bond by engaging a broad array of radical acceptors, such as phosphorylation (by $P(OEt)_3$) and borylation (by B_2pin_2). It is important to note that to date, conditions to derive aryl radicals from aryl chlorides are not compatible with metal-free, photochemical synthesis of aryl alkyl thioethers.

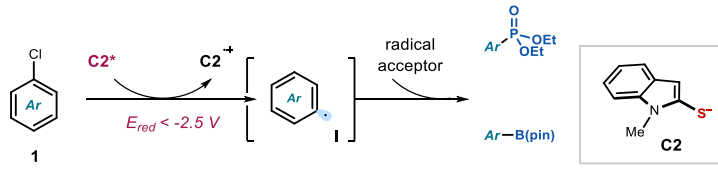

Figure 4.9. Photoredox activation of aryl chlorides, enabled by excitation of organic anion **C2**.

To prepare alkyl aryl thioethers, there are methods for the direct coupling between thiol and aryl moieties through radical pathways (Figure 4.10), without involving a metal catalyst. One

[22] For selected examples: (a) Liang, K.; Liu, Q.; Shen, L.; Li, X.; Wei, D.; Zheng, L. and Xia, C. "Intermolecular oxyarylation of olefins with aryl halides and TEMPOH catalyzed by the phenolate anion under visible light." *Chem. Sci.* **2020**, *11*, 6996; (b) Li, H.; Tang, X.; Pang, J. H.; Wu, X.; Yeow, E. K. L.; Wu, J. and Chiba, S. "Polysulfide Anions as Visible Light Photoredox Catalysts for Aryl Cross-Couplings." *J. Am. Chem. Soc.* **2021**, *143*, 481; (c) Wu, S.; Schiel, F.; Melchiorre, P. "A General Light-Driven Organocatalytic Platform for the Activation of Inert Substrates." *Angew. Chem., Int. Ed.* **2023**, *62*, No. e202306364. (d) Schmalzbauer, M.; Marcon, M. and König, B. "Excited State Anions in Organic Transformations." *Angew. Chem., Int. Ed.* **2021**, *60*, 6270; (e) Wang, W.; Wang, H. and König, B. "Light-Induced Single-Electron Transfer Processes involving Sulfur Anions as Catalysts." *J. Am. Chem. Soc.* **2021**, *143*, 15530.

of such approaches is the thiol-ene click reaction, rejuvenated by modern visible light photocatalysis (Figure 4.10a).[23] This reaction operates via thiyl radical addition to alkenes, followed by hydrogen atom transfer (HAT) from thiols to afford thioether product while propagating a radical chain. Although the system is operationally and mechanistically simple, the key C(sp^2)-S bond is already pre-installed in thiophenol substrate, where structural diversity is limited by commercial availability.

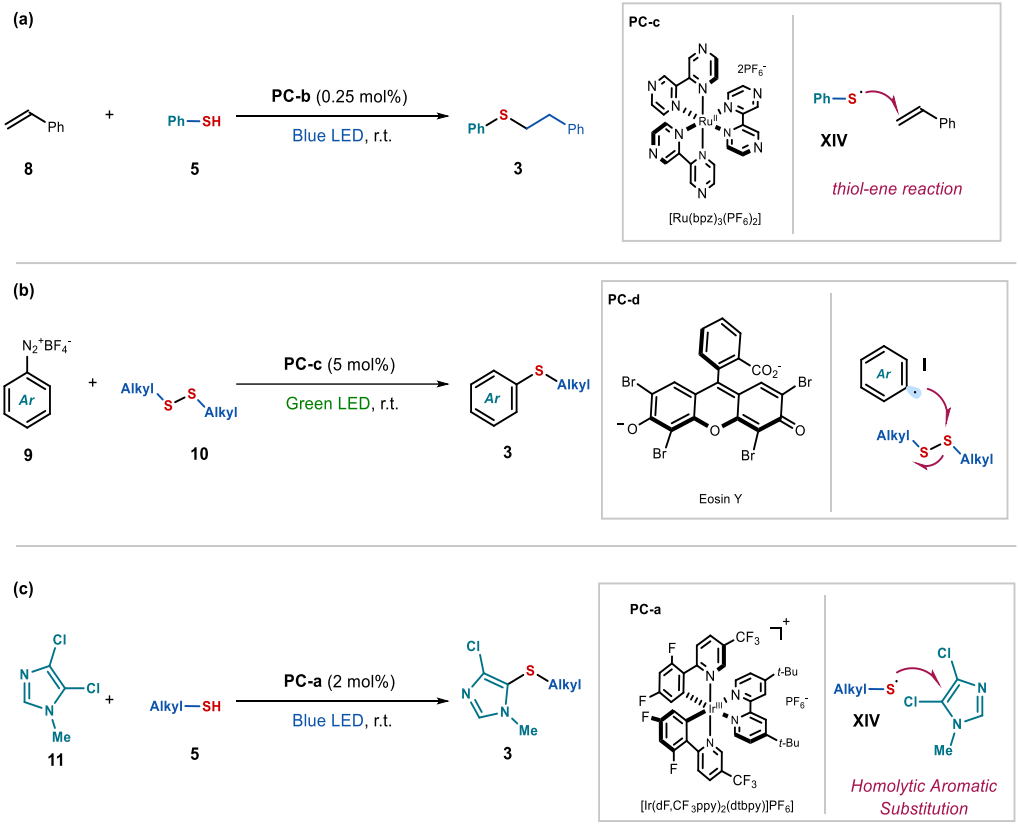

Figure 4.10. Metal-free photoredox C-S cross coupling. **(a)** Standard reaction conditions for thiol-ene reactions (**b**) A photoredox thioether synthesis via aryl radical **I** addition to disulfide **(c)** A photoredox thioether synthesis via thiyl radical **XIV** addition to halogenated heterocycles.

[23] (a) Tyson, E. L.; Ament, M. S.; Yoon, T. P. "Transition Metal Photoredox Catalysis of Radical Thiol-Ene Reactions." *J. Org. Chem.* **2013**, *78*, 2046; (b) Das, A. K.; Thomas, R. J. "Facile Thiol−Ene Click Protocol Using Benzil as Sensitizer and White LED as Light Source." *Eur. J. Org. Chem.* **2020**, *2020*, 7214; (c) Singh, M.; Yadav, A. K.; Yadav, L. D. S.; Singh, R. K. P. "Visible Light Photocatalysis with Benzophenone for Radical Thiol-Ene Reactions." *Tetrahedron Lett.* **2017**, *58*, 2206.

In an alternative method, aryl (pseudo)halides were used for metal-free thioether preparation. An example was reported to involve SET reduction of aryl diazonium salt **9** mediated by **PC-d** (Figure 4.10b).[24] The resulting electrophilic aryl radicals **I** were trapped by alkyl disulfide **10**, forming the key C(sp^2)-S bond to deliver alkyl aryl thioether products. The utility of this protocol was constrained by specialized starting materials.

Thiyl radical is also known to attack heterocyclic aryl chlorides,[25] providing product through site-selective homolytic aromatic substitution. (Figure 4.10c) Electron-rich (furan, pyrrole) and neutral (imidazole and thiazole) five-membered chlorinated heterocycles of type **11** were employed, while the sulfurating site is always the most electron-rich carbon on the heterocycle. Due to electrophilic nature of the thiyl radical, electron-deficient arenes were not suitable substrates. The use of thiol as reactant is also unavoidable.

[24] Majekz, M. and von Wangelin, A. J. "Organocatalytic visible light mediated synthesis of aryl sulfides." *Chem. Comm.*, **2013**, *49*, 5507.

[25] Sandfort, F.; Knecht, T.; Pinkert, T.; Daniliuc, C. G.; Glorius, F. "Site-Selective Thiolation of (Multi)halogenated Heteroarenes." *J. Am. Chem. Soc.* **2020**, *142*, 6913.

4.3 Design and Target of the Project

As discussed above, both transition-metal catalyzed and photochemical strategies for thioether synthesis has fallen short in practicality. Devising a metal- and thiol-free protocol that utilizes widely accessible, affordable, and bench-stable chemicals to construct C-S bonds, especially aryl C(sp^2)-S bonds, would be significant.

An available approach that matches the described criteria rests on the chemistry of thiourea. Specifically, alkyl-isothiouronium salts **III** are obtained via nucleophilic substitution reaction between tetramethylthiourea **A** and alkyl electrophiles (Figure 4.11a). [26] Subsequent nucleophilic addition of common alkyl alcohols to *pre-synthesized* **III** generates a hemithioacetal, which is in equilibrium with isouronium salt **XIX** upon extrusion of thiolate. Eventually, the transiently formed nucleophile re-attacks the intermediate **XIX** at the alcoholic carbon, following a *deoxythiolation polar* pathway that leads to the formation of the desired dialkyl thioethers. Although this method uses readily available substrates, its scope is limited to the formation of aliphatic products.

We envisioned to expand the chemistry of isothiouronium salts by designing a radical-polar cascade based on the ability of thiourea **A** to engage in radical pathways (Figure 4.11b). Specifically, we anticipated to combine the photochemical activation of aryl chlorides via SET and polar deoxythiolation step in a domino fashion. Although there has been a recent surge in versatile tactics to cleave C(sp^2)-Cl bonds photochemically, the formation of C-S(alkyl) bond from the arising aryl radical remained underdeveloped. Our reaction design relied on the ability of the electron-rich tetramethylthiourea **A** to intercept aryl radicals, generated upon SET reduction of aryl halides, thus constructing the key aryl C(sp^2)-S bond. Oxidation of the resulting radical intermediate **II** would afford the aryl isothiouronium salts **III** directly formed in situ, which would react with alcohols. Here, the pathway would

[26] (a) Fujisaki, S.; Fujiwara, I.; Norisue, Y.; Kajigaeshi, S. "A Facile One-pot Synthesis of Sulfides from Alkyl Halides and Alcohols Using Tetramethylthiourea." *Bull. Chem. Soc. Jpn.* **1985**, *58*, 2429; (b) Alan Aitken, R.; Ali, K.; Mesher, S. T. E. "Kinetic Resolution of Secondary Alcohols Using Proline-Derived Bicyclic Iminium Salts." *Tetrahedron Lett.* **1997**, *38*, 4179; (c) Merad, J.; Matyasovsky, J.; Stopka, T.; Brutiu, B. R.; Pinto, A.; Drescher, M.; Maulide, N. "Stable and Easily Available Sulfide Surrogates Allow a Stereoselective Activation of Alcohols." *Chem. Sci.* **2021**, *12*, 7770.

converge back to the established ionic deoxythiolation mechanism to yield the desired aryl-alkyl thioether product **3a**.

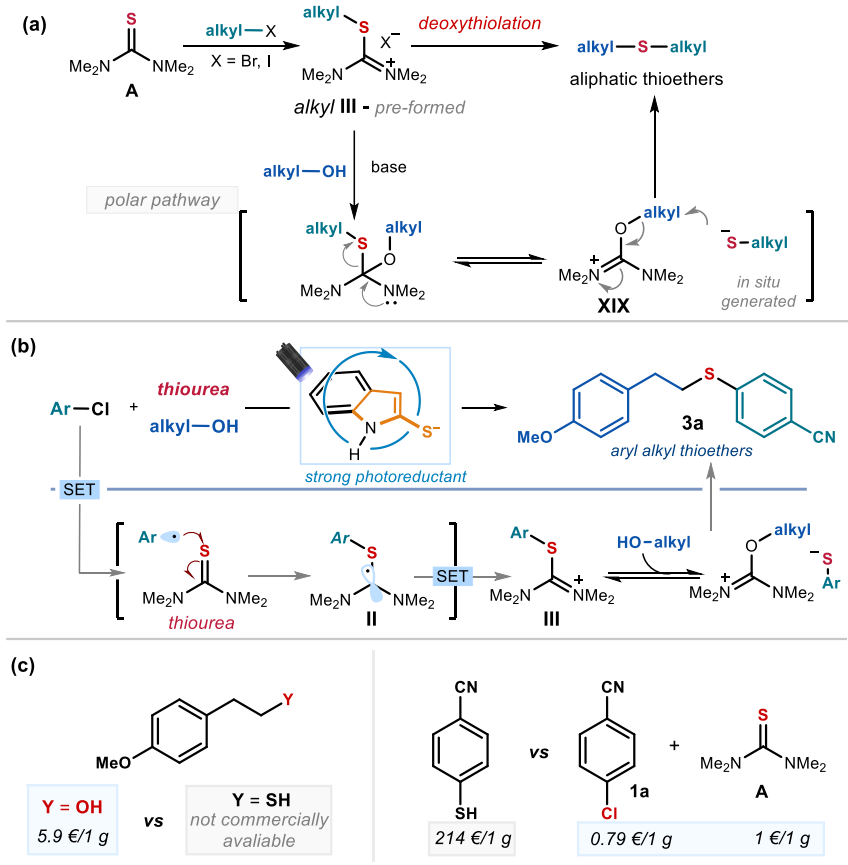

Figure 4.11. Ionic and Radical chemical properties of thiourea. **(a)** A dialkyl thioether synthesis through polar deoxythiolation, **(b)** The proposed strategy for combining photoredox activation of aryl chloride with polar deoxythiolation **(c)** Practical Considerations for thioether synthesis by price comparison of starting materials; data from Sigma-Aldrich, accessed in November 2023.

The practical benefits of our method for thioether preparation can be appreciated when evaluating the commercial supply of precursors to access thioether **3a** (Figure 4.11c): while current methods necessitate costly or commercially unavailable thiols for the one-step

synthesis of the target product **3a**, our approach instead would capitalize on the affordability of a wide commercial assortment of aliphatic alcohols[27] and aryl chlorides.[28]

In the sections below, the development and implementation of this simple method for synthesizing aryl-alkyl thioethers is discussed. The protocol requires a low temperature (40 °C), purple light irradiation (405 nm), and inexpensive, widely available substrates such as aryl chlorides **1** and aliphatic alcohols **2**.

4.4 Results and Discussion

4.4.1 Optimization of Reaction Conditions and Substrate Scope

We started our investigations by using 1,1,3,3-tetramethylthiourea **A** as the sulfur source and radical trap, 4-chlorobenzonitrile **1a** as the radical precursor [$E(\mathbf{1a}/\mathbf{1a}^{\bullet-})$ = -2.2 V vs Ag/AgCl], and 4-methoxyphenethyl alcohol **2a** as the nucleophile (Table 4.1). The experiments were performed in acetonitrile (CH_3CN) as the solvent under irradiation by a purple light-emitting-diode (LED, *evoluchem*, λ_{max} = 405 nm).

Initially, we tested the highly reducing cyclic thioamide catalysts **C1** and **C2**, which we recently developed to activate C(sp^2)-Cl bonds.[22c] Performing the model reaction using 10 mol% of photocatalysts **C1** and **C2**, in the presence of Cs_2CO_3 (3 equiv.), afforded the target product **3a** in 80% and 50% yield, respectively (Table 4.1, entries 1 and 2). We also tested catalyst **C3**, a newly synthesized photoreductant, which displayed significantly reduced reactivity (entry 3). Control experiments established that the presence of photocatalyst **C1** and light was essential for product formation (entries 4-5). When adding the radical scavenger TEMPO (2 equiv.) to the reaction mixture (entry 6), the reactivity was completely inhibited, which was congruent with a radical path being operative.

---

[27] Dong, Z.; MacMillan, D. W. C. "Metallaphotoredox-enabled deoxygenative arylation of alcohols." *Nature* **2021,** *598*, 451.

[28] In the current study, 35 different products were synthesized from corresponding aryl chlorides/bromides substrates, all procured directly from a chemical supplier. On the other hand, only 10 of the corresponding thiophenols are purchasable, based on information accessed from Sigma Aldrich in February 2024. For a more general analyses of organic chloride availability, see ref 10.

Table 4.1. Optimization of the reaction conditions with electrophilic aryl chloride 1a.[a]

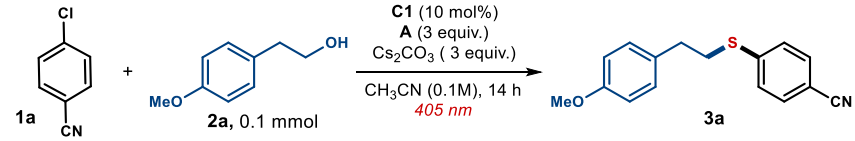

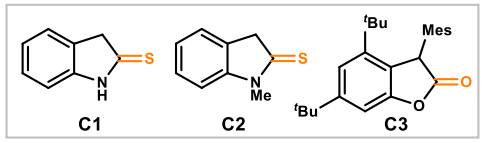

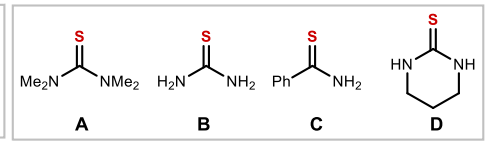

entry	deviation	yield [%][a]
1	none	**80**
2	**C2** (10%)	50
3	**C3** (10%)	30
4	no light or no base	0
5	dark, 70 °C	0

entry	deviation	yield [%][a]
6	TEMPO (2 equiv.)	0
7	**B-D**	0
8	K_2CO_3	50
9	DMSO or DMF or DCM	0
10	PhCl insetad of **1a**	5

[a] Reactions performed on a 0.1 mmol scale for 14 h using 3 equiv. of **1a**, 1 equiv. of **2a**, 10 mol% of **C1** photocatalyst, 3 equiv. of **A** and cesium carbonate, in 0.2 mL of MeCN under illumination by a purple LED (*EvoluChem*) at 405 nm, ambient temperature. [a] Yield inferred by NMR analysis of the crude mixture using 1,3,5-trimethoxybenzene as an internal standard. Mes: mesityl.

Exploration of other sulfur sources, exemplified by reagents **B-D**, had deleterious effects on product yield. A possible explanation (Figure 4.12) can be ascribed to the presence of acidic protons in substrates **B-D**, which may be deprotonated to afford nucleophilic thiolates, significantly complicating the reaction. **B-D** are also less electron-rich than **A**, potentially making them less reactive towards intercepting electrophilic aryl radicals. Additionally, aryl-isothiouronium salts from tetramethylthiourea **A** are more electrophilic than the neutral adducts from **B-D**, making them more efficient in the deoxythiolation step with alcohols. Additional screening of bases and solvents resulted in inferior results (entries 8-9). Using simpler chlorobenzene as reaction partner led to negligible reactivity (entry 10).

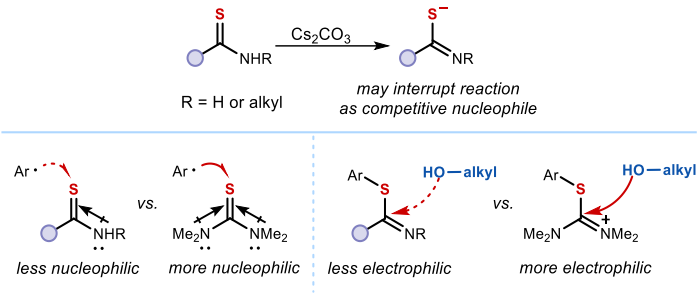

Figure 4.12. Rationalization of the poor performance of sulfur surrogate **B-D**

Using the conditions in entry 1 of Table 4.1, we investigated the scope of the photochemical thioetherification strategy. In these studies, aryl bromides were used when the corresponding chlorides were not commercially available.

We initially explored the reactivity of diverse aryl chlorides **1** as radical precursors, using 4-methoxyphenethyl alcohol **2a** as the nucleophile (Figure 4.13). First, we demonstrated that the process was equally efficient on a 5 mmol scale, yielding 1.0 g of product **3a** (75% yield). Compound **3a** could be synthesized not only by SET activation of chloride **1a** but also upon reduction of the corresponding fluoride, bromide, and iodide. Aryl chlorides with diverse substituents at various positions on the phenyl ring were well tolerated, yielding products **3b**−**3h** in a high yield. It is noteworthy that when multiple halides are present, only the weakest C-X bond was activated, and less reactive yet reducible halide(s) (**3g** and **3h**) could be retained.

The reaction was proven to be compatible with substrates containing polycyclic aromatic structures (adducts **3i**−**3k**) and valuable *N*-heterocyclic frameworks, encompassing pyridines, pyrimidines, and quinolines (products **3l**−**3q**). Notably, late-stage modifications of chlorine-containing drug molecules, such as selective COX-2 inhibitor *Etoricoxib* (product **3r**) and antidepressant *Moclobemide* (**3s**), were achieved, albeit in moderate yields. Functional groups such as ketone (**3c**), sulfone (**3d**, **3r**), secondary amide and amine (**3s**) were tolerated, showcasing the chemoselectivity of the transformation.

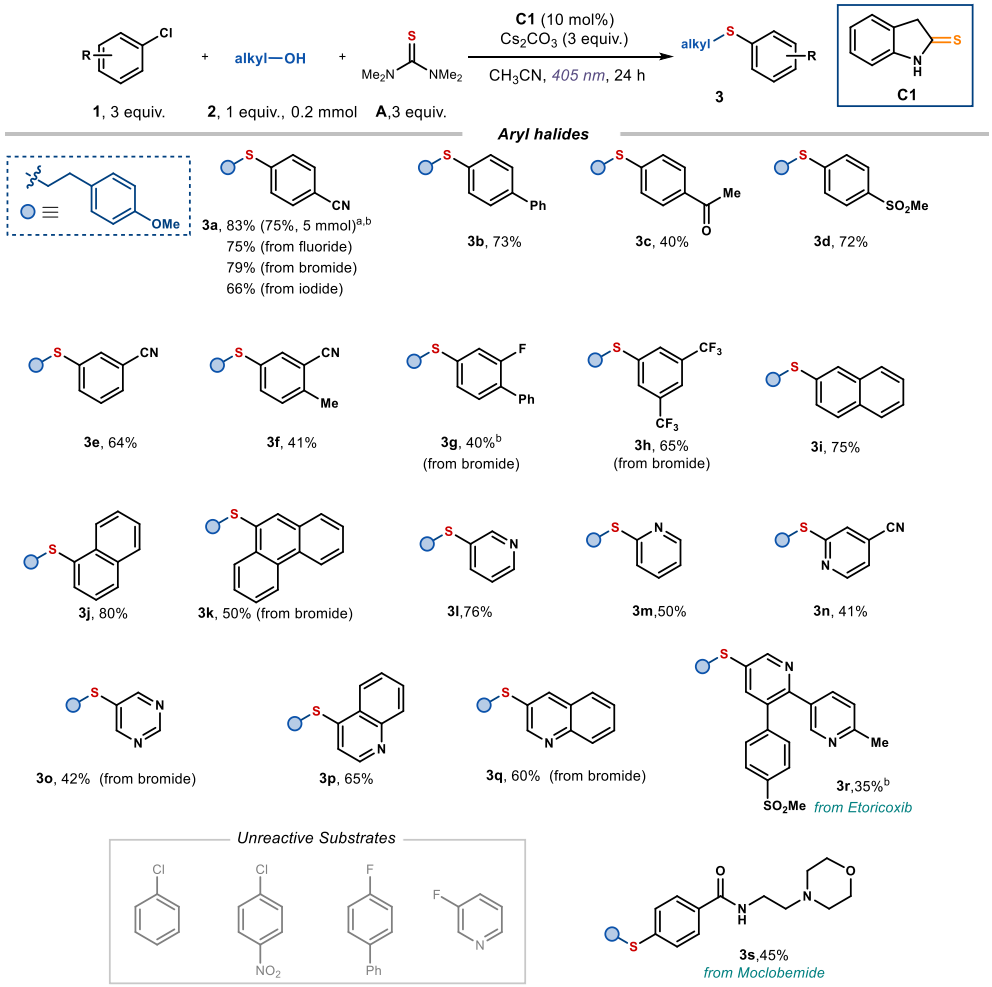

Figure 4.13. Substrate scope for aryl halide in the photochemical organocatalytic synthesis of thioethers from aryl chlorides and alcohols. Reactions performed on a 0.2 mmol scale at 40 °C using photocatalyst **C1** (10 mol %), 3 equiv of **1** and 3 equiv of thiourea **A** under illumination by a purple LED (*EvoluChem*) at 405 nm. Yields refer to isolated products **3** after purification. Aryl chlorides were used as radical precursors unless otherwise stated. [a]5 mmol scale reaction. [b]48 h reaction time. Boc: tert-butyloxycarbonyl.

A major restriction concerned the lack of reactivity observed in electronic neutral or electron-rich aryl chlorides, such as chlorobenzene. Activation of strong C-F bond was also unsuccessful with some substrates, and nitro groups were not tolerated under this set of conditions (Figure 4.13, grey box).

We next examined the spectrum of alcohols compatible with this photochemical organocatalytic method (Figure 4.14). Primary alcohols **2**, bearing potentially reactive aromatic systems such as phenol, thiophene, and halogen substituents, underwent smooth reactions, producing thioethers **3t–3w**. A diverse array of functional groups was well-tolerated, including an ether (adduct **3aa**), tertiary amine (**3ab**), carbamate (**3ac**), and thioether **(3ad**). Sensitive functional moieties were preserved effectively, including trimethylsilane (**3ae**), silyl ether (**3af**), acrylate (**3ag**), and oxetane (**3ah**). Alkenes and alkynes, susceptible to radical additions, showed compatibility (**3ai–3an**). Straightforward thioetherification of feedstock methanol, ethanol and benzyl alcohol was also achieved (**3ao–3aq**). Complex substrates such as natural products *myrtenol* (adduct **3aj**), *geraniol* (**3ak**), *perillol* (**3al**), *Lithocholic acid* derivative (**3ar**), and pharmaceutical agent *Perphenazine* (**3as**) were efficiently functionalized.

Interestingly, diols exhibited selective thioetherification of only one hydroxyl group, while the other alcohol moiety was converted into a carbamate (products **3at**–**3au**). This path likely arises from the hydrolysis of isouronium intermediates. As a limitation of the protocol, secondary alcohols, such as 1-phenylethanol, provided thioethers in moderate yield (**3av**), while phenol, multi-fluorinated and tertiary alcohols remained completely unreactive, mainly reasoned to their inability to undergo the substitution step.

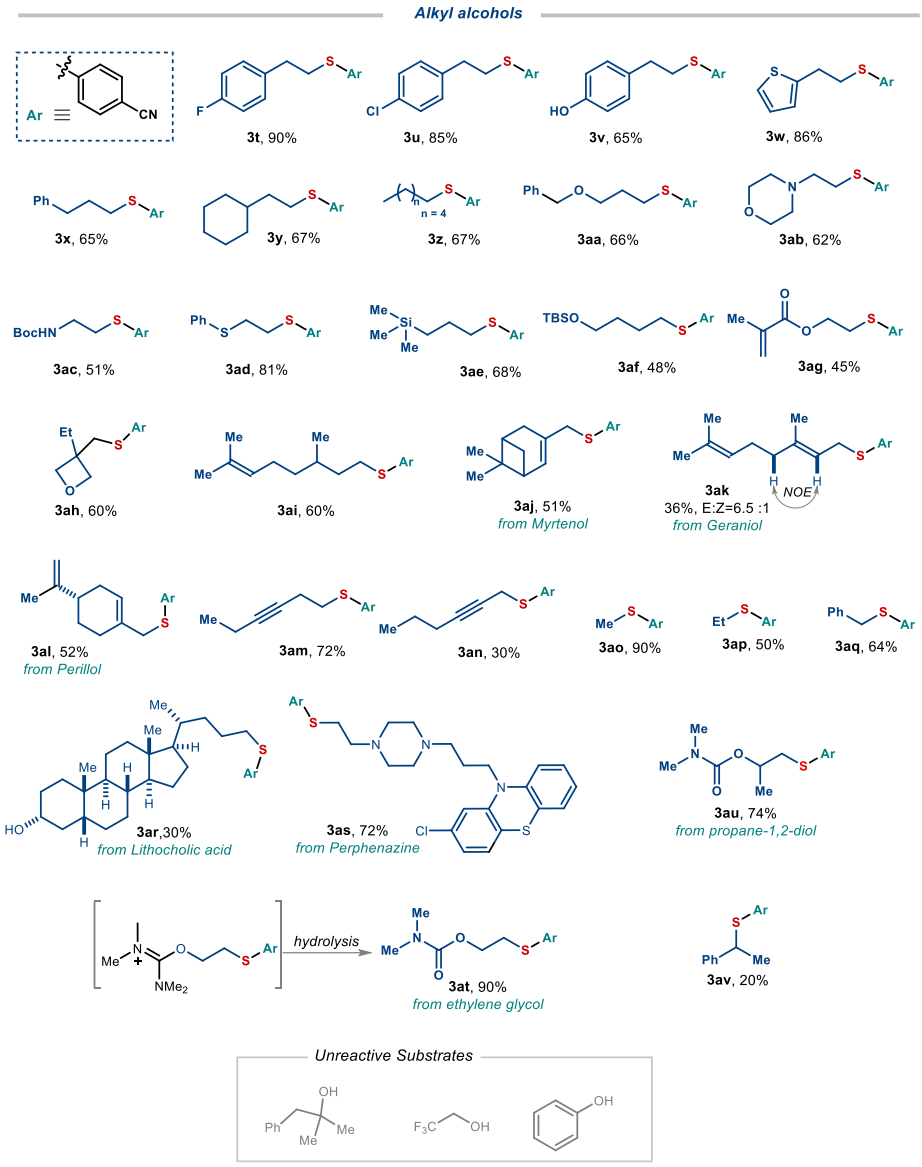

Figure 4.14. Substrate scope for alcohols in the photochemical organocatalytic synthesis of thioethers from aryl chlorides and alcohols. Reactions performed on a 0.2 mmol scale at 40 °C using photocatalyst **C1** (10 mol %), 3 equiv of **1** and 3 equiv of thiourea **A** under illumination by a purple LED (*EvoluChem*) at 405 nm. Yields refer to isolated products **3** after purification. TBS: butyl(dimethyl)silyl.

4.4.2 Expanding the Scope to Electron Neutral and Rich Aryl Halides

The inability of photocatalyst **C1** to provide thioether products from the corresponding electron-neutral and rich aryl chlorides was out of expectation, as these substrates were activated by the same catalyst in a previous study from our research group for proto-dehalogenation.[22c] To tackle this challenge, we found that the newly prepared dioxindole-based organocatalyst **C3** could act, upon deprotonation and excitation, as an effective photoreductant (E* ~ −3.35 V vs. SCE) to activate these substrates (optimization detailed in Table 4.3 in the experimental section). Consequently, we significantly broadened the range of aryl chlorides amenable to thioetherification (Figure 4.15). However, the protocol required the use of 40 mol % of **C3** along with 5 equiv. of aryl halides **1**.

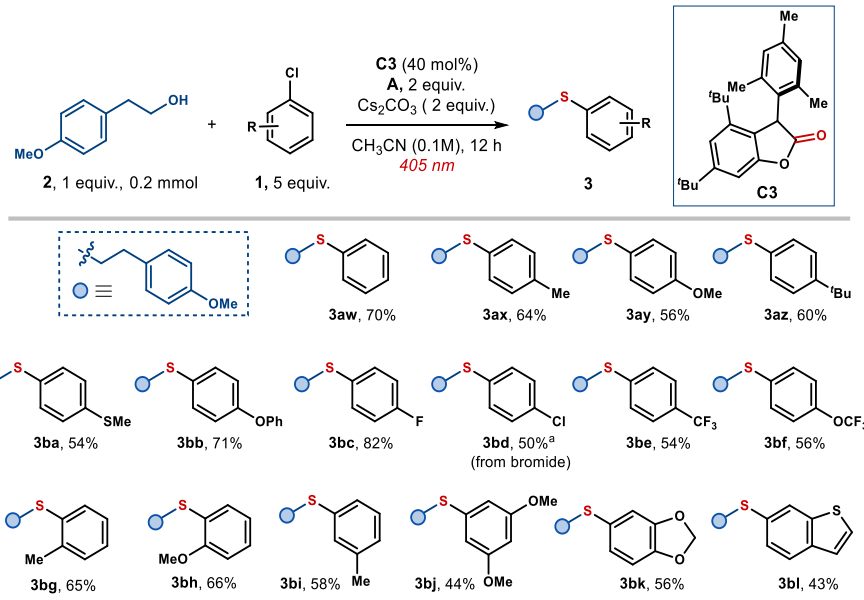

Figure 4.15. Thioetherification of electron-neutral or electron-rich aryl chlorides **1** with alcohol **2a**. Reactions performed on a 0.2 mmol scale at 40 °C using 5 equiv of **1** and 2 equiv of **A** under illumination by a purple LED at 405nm. Yields refer to isolated products **3** after purification.

Electron-neutral chlorobenzene (product **3aw**) and those substituted with electron-donating groups (**3ax**–**3bb**, **3bj**) underwent successful transformations. Substitution pattern on the arene appeared to have insignificant effects, as *para*- (**3ax**), *meta*- (**3bg**) and *ortho*-tolyl (**3bi**) chlorides were converted to a similar extent. Additionally, other substituents, including less

active halides (**3bc** and **3bd**), trifluoromethyl group (**3be–3bf**), benzodioxole (**3bk**) and thiophene (**3bl**), were well-tolerated (see Figure 4.25 for a comprehensive list of moderately reactive or unreactive substrates).

Based on the redox potentials of the excited catalysts **C1-3** (see section 4.4.3), the catalysts have comparable photoproperties and redox potentials. Therefore, the difference in efficiency should not depend on their ability to activate aryl chlorides via SET reduction. All of them could be capable of reducing the substrates, generating aryl radicals and oxidized catalyst **XX** or **XXI** (Figure 4.16).

We reasoned that the polarity mismatch between the generated electron-rich aryl radicals and the electron-rich tetramethylthiourea **A** may impede an efficient radical trap (*step I* in Figure 4.16), slowing down the formation of the radical intermediate **II**. Under these conditions, the SET reduction of sulfur radical **XX** by **II**, which secures the regeneration of the catalyst (*step II*), might become problematic. This could lead to the deactivation of the catalyst since the reactive intermediate **XX** could engage in different pathways. We hypothesize that the lactone catalyst **C3**, which lacks the reactive sulfur atom and features the bulkier mesitylene group, may have effectively circumvented this issue. The presence of the mesitylene group could potentially stabilize the radical formed in the corresponding intermediate **XXI**, making it long-lived. To validate our speculations, further comprehensive investigations would be required.

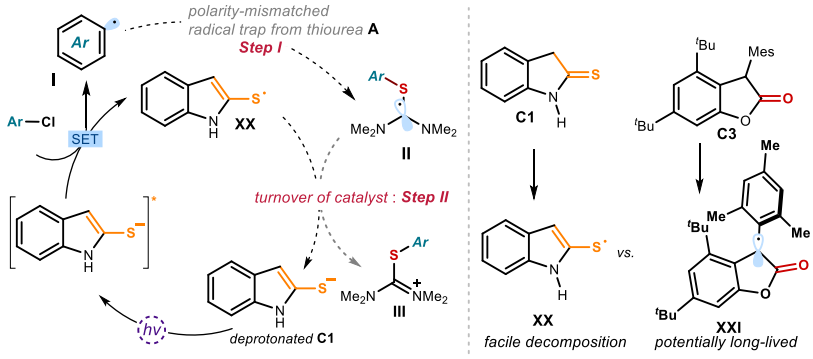

Figure 4.16. Rationale for the higher reactivity of catalyst **C3** in activating electron-rich aryl chlorides.

4.4.3 Mechanistic Investigations

To better understand the radical generation processes in our system for thioether synthesis, a series of mechanistic experiments were conducted.

Photochemical Activation of C(sp^2)-Cl bond by catalysts C1 and C3

To elucidate their mechanism of action, photocatalysts **C1-C3** underwent thorough characterization, detailed in Section 4.6.6 and 4.6.7. NMR studies and absorption spectroscopic investigations established that the thiolate anions, generated upon catalyst deprotonation can absorb visible light to access an electronically excited state (Figure 4.17a).

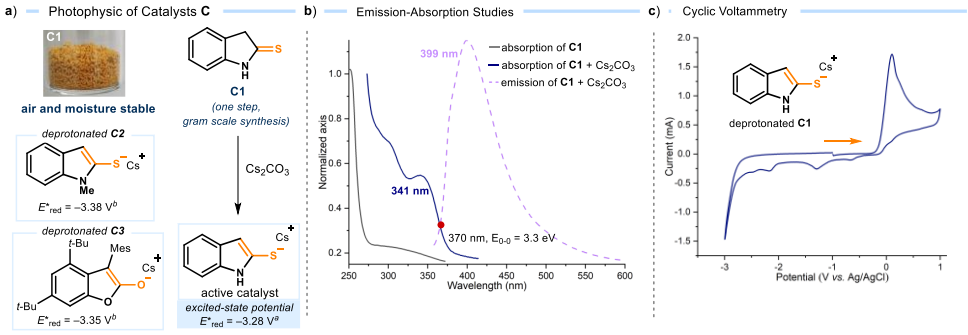

Figure 4.17. Photophysical and electrochemical properties of the photocatalysts. (**a**) Deprotonation of **C1** and the estimated redox potential of the excited thiolates derived from catalysts **C1**−**C3**. **(b)** Emission of the excited thiolate (formed in situ treating **C1** with Cs_2CO_3) in CH_3CN upon irradiation at 350 nm and its intercept with the absorption spectrum at 373 nm, with a 0−0 transition energy ($E_{0,0}$) of 3.3 eV. **(c)** Cyclic voltammetry measurements of deprotonated catalyst C1 carried out in CH3CN vs. Ag/AgCl. [a]Estimated redox potential vs. SCE in CH_3CN.

Spectroscopic studies and cyclic voltammetry (Figure 4.17b and c) were used to estimate the redox potential of the excited thiolates (with E* ranging from −3.28 to −3.38 V vs SCE in CH_3CN for deprotonated **C1**−**C3**), applying the Rehm−Weller formalism.[29] This confirmed that the anions of catalysts **C1**−**C3** acquire a strongly reducing power upon excitation. Stern−Volmer quenching studies showed that the fluorescence of deprotonated photocatalyst

[29] Farid, S.; Dinnocenzo, J. P.; Merkel, P. B.; Young, R. H.; Shukla, D.; Guirado, G. "Reexamination of the Rehm-Weller Data Set Reveals Electron Transfer Quenching that Follows a Sandros-Boltzmann Dependence on Free Energy." *J. Am. Chem. Soc.* **2011**, *133*, 11580.

C1, excited by a laser at 350 nm, was effectively quenched by 4-chlorobenzonitrile **1a** (see section 4.6.6).

These observations are consonant with the following photocatalytic cycle (Figure 4.18a): The reaction starts upon excitation of deprotonated catalyst **C1** (E* ~ −3.2 V vs. Ag/AgCl), which activates substrate **1a** (E_{red} = −2.2 V vs. Ag/AgCl) through SET reduction. Mesolytic cleavage of the C-Cl bond affords in the aryl radical, which is trapped by tetramethylthiourea **A**. This affords radical **II** (E(**III/II**) ~ −1.6 V vs Ag/AgCl) with the appropriate redox potential to reduce the sulfur-centered radical **XX** (E (**XX/C1**$^{-}$) ~ +0.1 V vs Ag/AgCl) via SET, thus turning over catalyst **C1**. An equivalent catalytic cycle can also be proposed for the action of **C3**, as supported by photophysical studies, Stern-Volmer quenching and quantum yield determination detailed in section 4.6.6.

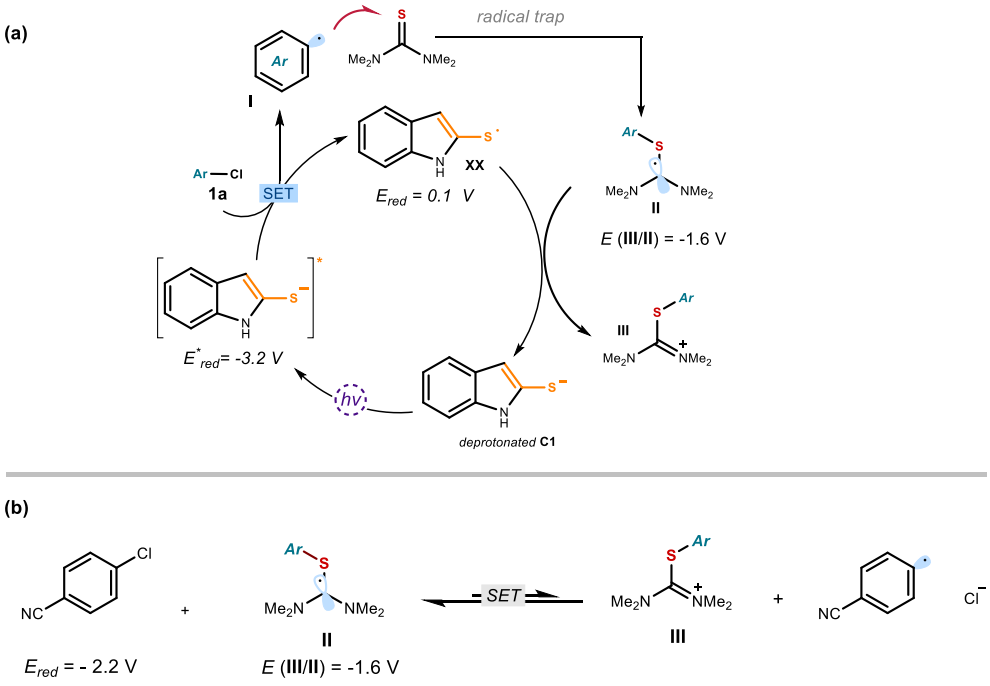

Figure 4.18. (**a**) Proposed Photoredox catalytic cycle. **(b)** a hypothetical radical propagation step leading to a light-independent chain mechanism found implausible.

In an alternative scenario, the light-driven SET mastered by the excited catalyst **C1** may just serve as an initiating event of a chain propagation mechanism. For instance, radical **II** (E(**III**/**II**) ~ -1.6 V) might hypothetically reduce another equivalent of aryl halide **1** (E_{red} = -2.2V), providing a propagation step to sustain a light-independent radical chain (Figure 4.18b). Electrochemical measurement suggested that this step is endergonic. We also determined the quantum yield (Φ) of the model reaction between **1a** and **2a**, which stood at a low value of 0.017. This is consistent with the proposed closed photoredox cycle, and suggests that a radical chain pathway has limited contribution to the conversion of starting materials, if any.

Polar Deoxythiolation Steps

In our initial design plan, we envisaged that the photochemical activation of aryl chlorides would form isothiouronium ions in situ. At this juncture, the pathway would converge back to the ionic deoxythiolation. The involvement of this polar reactivity was evaluated through an experiment using pre-formed isothiouronium ion **III** (Figure 4.19a). Under dark conditions and in the presence of Cs_2CO_3, stirring **III** with alcohol **2a** resulted in the formation of product **3aw**, albeit in low yield. This is in agreement with our proposal that **III** is an intermediate in the reaction, and light is not necessary for forming C(sp^3)-S bond within the thioether product. It is noteworthy that an elevated temperature led to a significant amount of diphenyl disulfide as side product, potentially hindering the progression of polar reaction.

In an additional experiment, we subjected the enantioenriched chiral alcohol **2av** (97% e.e.) and chlorobenzene **6** to the standard reaction conditions, which led to the corresponding chiral thioether product **12** with the same enantiopurity (Figure 4.19b). Analysis of the absolute configuration via optical rotation established that the process proceeded with complete stereoinversion,[30] a signature of a stereospecific S_N2 ionic pathway. This is congruent with the proposed mechanism where thiophenolate would attack the isouronium intermediate, displacing urea as a leaving group.

[30] Li, F.; Wang, D.; Chen, H.; He, Z.; Zhou, L.; Zeng, Q. "Transition Metal-Free Coupling Reactions of Benzylic Trimethylammonium Salts with Di(hetero)aryl Disulfides and Diselenides." *Chem. Commun.* **2020**, *56*, 13029.

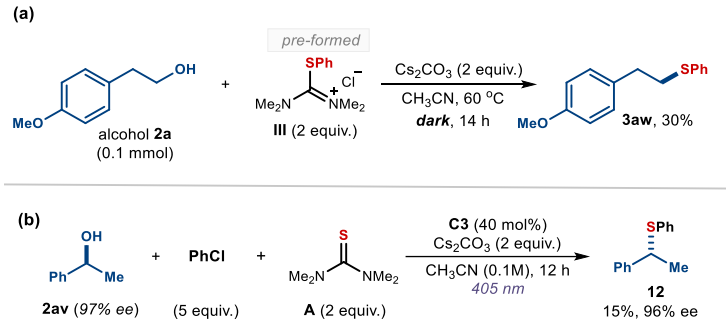

Figure 4.19. Mechanistic experiments to probe the polar pathway in the photochemical organocatalytic thioether synthesis. (**a**) Reaction between alcohol **2a** and pre-formed **III (b)** Thioether synthesis from an enantioenriched chiral alcohol

By-product Formation

We wondered why a large excess (5 equivalent) of aryl chlorides and 40 mol% of catalyst **C3** were needed in processes involving electron-neutral and rich precursors, such as chlorobenzene. To interrogate undesirable processes responsible for this lack of efficiency, GC-MS analyses of the reaction mixture using **C3** photoreductant were conducted (Figure 4.20a). In addition to the expected tetramethylurea arising from the deoxythiolation sequence, traces of diphenyl disulfide were also observed. A pertinent finding was the detection of species **13**, assignable to **C3** modification with a phenyl group. Its formation can be justified by the coupling between the generated phenyl radical **I** and radical **XXI**. This explained the relative instability of **C3** under the reaction conditions, and the necessity to employ a large excess of aryl chloride.

Regarding the reaction involving **C1**, a biaryl thioether side product **14** was also found in the reaction mixture (Figure 4.20b). This structure might have arisen from the radical coupling between aryl radical **I** and thiyl radical (from oxidation of thiophenolate). While this observation confirmed the intermediacies of phenyl radicals and thiophenol in the system, it has also accounted for the mass balance of excess aryl chloride.

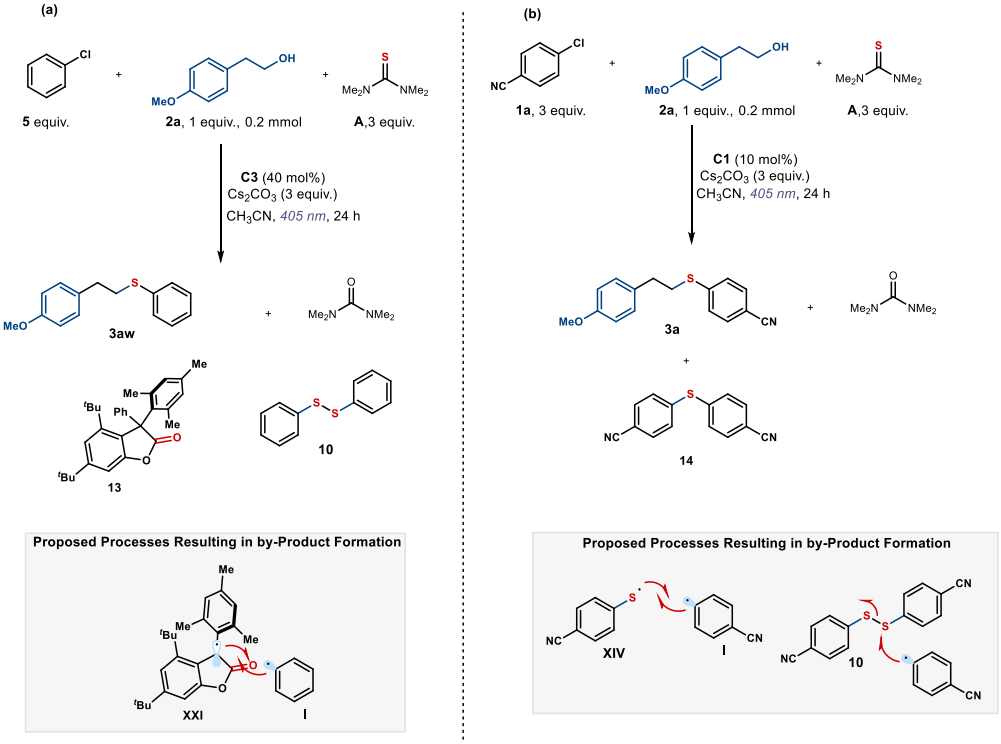

Figure 4.20. Detection of undesirable products in photochemical organocatalytic reaction. (**a**) GC-MS analyses of reaction mixture of thioether synthesis catalyzed by **C3 (b)** GC-MS analyses of reaction mixture of thioether synthesis catalyzed by **C1**.

4.5 Conclusions

In summary, we reported a photochemical catalytic protocol for the efficient preparation of a wide range of alkyl aryl thioethers, preventing the need for thiols or transition metals. The method operates under mild conditions using easily accessible substrates and catalysts, and is compatible with precursors of different electronic demands, or decorated with various functionalities. Benefiting from the abundance of commercial substrates and remarkable tolerance for functional groups, our protocol allows for broad synthetic utilities, from transformation of simple feedstock chemicals to late-stage modifications of biorelevant compounds. Mechanistically, the aryl C(sp^2)-S bond is forged by an unusual interception of aryl radicals by thiourea, without the aid of metal-based catalyst.

4.6 Experimental Section

General Information. The ^{1}H NMR, $^{19}F\{^{1}H\}$ NMR, $^{13}C\{^{1}H\}$ NMR spectra are available in the literature[1] and are not reported in the present dissertation.

The NMR spectra were recorded at 400 MHz and 500 MHz for ^{1}H, 101 or 126 MHz for $^{13}C\{^{1}H\}$ and 376 MHz for $^{19}F\{^{1}H\}$. The chemical shift (δ) for ^{1}H and $^{13}C\{^{1}H\}$ are given in ppm relative to residual signals of the solvents ($CHCl_3$ at 7.26 ppm for ^{1}H NMR and 77.16 ppm for $^{13}C\{^{1}H\}$ NMR). Coupling constants are given in Hertz. The following abbreviations are used to indicate the multiplicity: s, singlet; d, doublet; q, quartet; m, multiplet; br, broad signal

High resolution mass spectra (HRMS) were obtained from the ICIQ HRMS unit on MicroTOF Focus and Maxis Impact (Bruker Daltonics) with electrospray ionization (ESI) and Atmospheric-pressure chemical ionization (APCI). Optical rotations were measured on a Polarimeter Jasco P-1030 and are reported as follows: $[\alpha]_D$ ambient temperature (c in g per 100 mL, solvent). Cyclic voltammetry studies were carried out on a Princeton Applied Research PARSTAT 2273 potentiostat, offering compliance voltage up to ± 100 V (available at the counter electrode), ± 10 V scan range and ±2 A current range.

Yields refer to isolated materials of >95% purity as determined by ^{1}H NMR analysis.

General Procedures. All reactions were set up under an argon atmosphere in oven-dried glassware. Synthesis grade solvents were used as purchased, anhydrous solvents were taken from a commercial SPS solvent dispenser. Chromatographic purification of products was accomplished using forced-flow chromatography (FC) on silica gel (230-400 mesh). For thin layer chromatography (TLC) analysis throughout this work, Merck pre-coated TLC plates (silica gel 60 GF_{254}, 0.25 mm) were employed, using UV light as the visualizing agent and an acidic mixture of vanillin or basic aqueous potassium permanganate ($KMnO_4$) stain solutions, and heat as developing agents. Organic solutions were concentrated under reduced pressure on a Büchi rotatory evaporator.

Materials. Commercial grade reagents and solvents were purchased at the highest quality from commercial suppliers and used as received, unless otherwise stated.

4.6.1 Synthesis of the Substrates and Catalysts

Substrate Synthesis

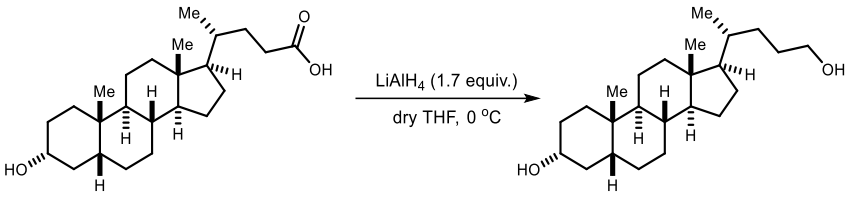

An oven-dried 25 mL round-bottom flask equipped with magnetic stirring bar was charged with lithocholic acid (5 mmol, 1.0 equiv.). The flask was sealed, evacuated and refilled with nitrogen (3 times). Anhydrous THF (15 mL) was added and the resulting clear solution was cooled to 0 °C and stirred for 5 min at the same temperature. $LiAlH_4$ (8.5 mmol, 1.7 equiv.) was then added in small portions at 0 °C. After stirring at 0 °C for 1 hour, the mixture was allowed to stir at room temperature for additional 16 hours. The reaction was quenched by adding H_2O (1.4 mL) dropwise over 10 min. Then 15% w/w NaOH (1.4 mL) was added and the reaction was allowed to stirred at room temperature for 20 minutes. Then the resulting suspension was diluted with H_2O (15 mL) followed by extraction with ethyl acetate (3 ×20 mL). The combined organic layers were dried over anhydrous Na_2SO_4, filtered, and evaporated to dryness under reduced pressure. The crude residue was purified by column chromatography on silica gel (petroleum ether/ethyl acetate = 10: 1) to afford product as white solid (1.1g, 65% yield).

^{1}H NMR (400 MHz, CD_3OD): δ= 3.68 – 3.47 (m, 3H), 2.15 – 2.06 (m, 1H), 2.05 – 1.80 (m, 4H), 1.76 – 1.63 (m, 3H), 1.60 – 1.31 (m, 14H), 1.29 – 1.12 (m, 6H), 1.06 – 0.98 (m, 6H), 0.78 (s, 3H) ppm.

^{13}C{^{1}H} NMR (101 MHz, CD_3OD): δ= 71.1, 62.2, 56.6, 56.4, 42.5, 42.2, 40.6, 40.2, 35.9, 35.9, 35.6, 35.2, 34.4, 31.9, 29.9, 29.0, 28.0, 27.0, 26.3, 24.0, 22.6, 20.6, 17.9, 11.2 ppm.

HRMS (ESI): calculated for $C_{24}H_{42}NaO_2$ [M+Na^+]: 385.3077, found 385.3086.

Catalysts Synthesis

Indoline-2-thione (catalyst **C1):**

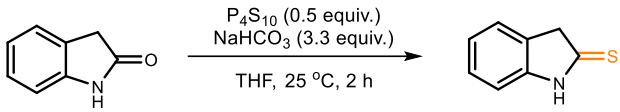

To a solution of 2-oxindole (5 mmol, 1.0 equiv.) in 15 mL of anhydrous THF, $NaHCO_3$ (10 mmol, 2.0 equiv.) was added and the reaction was stirred at room temperature for 10 minutes. P_4S_{10} (3 mmol, 0.6 equiv.) was then added portion wise and the resulting mixture was stirred at room temperature for 3 hours. On completion of the reaction, as indicated by TLC, the mixture was concentrated in vacuo to one fourth of its volume. Ice-cold water (10 mL) was then added in small portions to the oily residue with vigorous stirring, which resulted in precipitate formation. The mixture was left to stand in the ice-cold water for 15 minutes before vacuum filtration. The precipitates collected were washed with water followed by hexanes and air dried to yield product (597 mg, 80% yield). The purity was confirmed by ^{1}H NMR.

^{1}H NMR (400 MHz, $CDCl_3$): δ= 7.30 – 7.23 (m, 2H), 7.15 – 7.09 (m, 1H), 7.06 – 6.99 (m, 1H), 4.08 (s, 2H) ppm

.**^{13}C{^{1}H} NMR (101 MHz, $CDCl_3$):** δ= 203.5, 144.4, 130.5, 128.1, 124.2, 124.2, 110.2, 49.3 ppm. Matching reported literature data.[31]

1-Methylindoline-2-thione (catalyst **C2):**

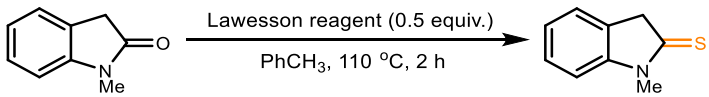

An oven dried flask was charged with 1-methylindolin-2-one (736.0 mg, 5.0 mmol, 1.0 equiv.), the Lawesson reagent (2.5 mmol, 0.5 equiv.) and toluene (20 mL). The flask was

[31] Rhodes, S.; Short, S.; Sharma, S.; Kaur, R.; Jha, M. "One-Pot Mild and Efficient Synthesis of [1,3]thiazino[3,2-a]indol-4-ones and Their Anti-Proliferative Activity." *Org. Biomol. Chem.* **2019**, *17*, 3914.

placed in an oil-bath preheated to 110 ºC. After 2 hours stirring, the solution was concentrated in vacuo and the crude mixture was purified by flash column chromatography on silica gel (1% ethyl acetate in hexanes as eluent) to afford the catalyst as light yellow solid (620.5 mg, 76% yield).

^{1}H NMR (400 MHz, $CDCl_3$): δ= 7.37 – 7.28 (m, 2H), 7.19 – 7.14 (m, 1H), 6.97 (d, *J* = 8.0 Hz, 1H), 4.11 (s, 2H), 3.63 (s, 3H) ppm.

^{13}C{^{1}H} NMR (101 MHz, $CDCl_3$): δ= 201.2, 146.6, 129.2, 128.0, 124.4, 124.0, 109.6, 49.1, 31.3 ppm.

Matching reported literature data[22c]

1-Methyl-3,4-dihydroquinoline-2(1H)-thione (catalyst **C3):**

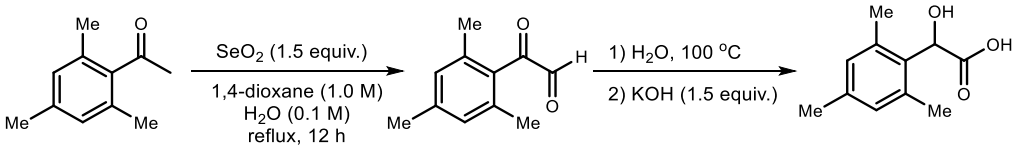

Based on a procedure reported in the literature [32] : a solution containing 2,4,6-trimethylacetophenone (10.0 mmol), SeO_2 (15.0 mol) and water (1 mL) in 1,4-dioxane (10 mL) was heated at reflux for 12 h. During the reaction, black selenium precipitated and was broken up to aid stirring. The solution was carefully decanted to separate free selenium. Removal of the solvent in vacuo gave a yellow oil which was used for the next step without further purification. Glyoxal was then added to water (20 mL) and heated until the yellow colour disappeared. White needle-like crystals of 2,4,6-trimethylphenylgloxal hydrate precipitated from water and were collected by filtration. Crude gloxal hydrate was heated with aqueous potassium hydroxide (10 mL, 1.5 M) at 100°C for 1 h and then cooled down to ambient temperature. The solution was filtered and acidified with conc. HCl to reach pH 1-3, when precipitation occurred. The solid was collected, carefully washed with water, air

[32] Allen, B. M.; Hegarty, A. F.; O'Neill, P.; Nguyen, M. T. "Hydration of Bis(pentamethylpheny1)- and Bismesityl-ketenes leading to Ene-1, 1 -diols (Enols of Carboxylic Acids)." *J. Chem. Soc., Perkin Trans* 2 **1992**, 927.

dried and recrystallised from ethanol to afford white crystalline 2,4,6-trimethylmandelic acid (1.77g, 91% yield).

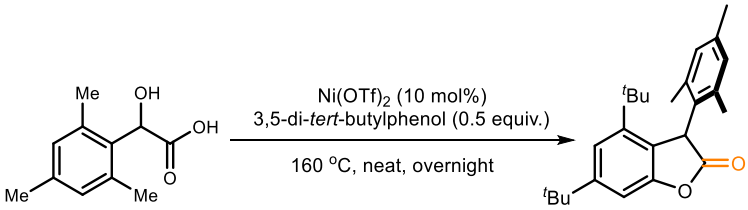

Based on a literature procedure[33]: 2-hydroxy-2-mesitylacetic acid (2.0 mmol), 3,5-di-*tert*-butylphenol (1.0 mmol, 0.5 equiv.), and $Ni(OTf)_2$ (0.1 mmol, 10 mol%) were added to an oven-dried 25 mL Schlenk tube equipped with a magnetic stirring bar. The mixture was vigorously stirred at 160 °C for 12 hours under argon conditions before being cooled to ambient temperature. Then 15 mL of water was added, and the resulting mixture was extracted with EtOAc (15 mL × 3). The combined organic phases were dried over anhydrous Na_2SO_4, filtered and concentrated in vacuo. Further purification by flash column chromatography on silica gel (eluting with petroleum ether/ethyl acetate = 150: 1) provided catalyst **C3** as a white solid (310 mg, 85%).

^{1}H NMR (400 MHz, $CDCl_3$): δ= 7.23 (d, *J* = 1.9 Hz, 1H), 7.05 (d, *J* = 1.9 Hz, 1H), 6.97 (s, 1H), 6.69 (s, 1H), 5.38 (s, 1H), 2.55 (s, 3H), 2.25 (s, 3H), 1.59 (s, 3H), 1.34 (s, 9H), 1.08 (s, 9H) ppm.

^{13}C{^{1}H} NMR (101 MHz, $CDCl_3$): δ= 175.8, 154.7, 152.6, 147.9, 137.5, 137.2, 137.2, 131.3, 130.9, 130.0, 121.6, 119.5, 106.3, 46.5, 35.8, 35.2, 31.4, 30.5, 21.1, 20.9, 19.6 ppm.

HRMS (ESI): calculated for $C_{24}H_{42}NaO_2$ [M+Na^+]: 387.2295, found 387.2302.

[33] Tang, Z.; Tong, Z.; Xu, Z.; Au, C.-T.; Qiu, R.; Yin, S.-F. "Recyclable Nickel-Catalyzed C–H/O–H Dual Functionalization of Phenols with Mandelic Acids for The Synthesis of 3-aryl benzofuran-2(3H)-ones Under Solvent-Free Conditions." *Green Chem*. **2019**, *21*, 2015.

4.6.2 Preparation of Thioethers from alcohols and electron-deficient aryl halides

Optimization Studies

Table 4.2. Optimization of the model reaction using **C1** as catalyst

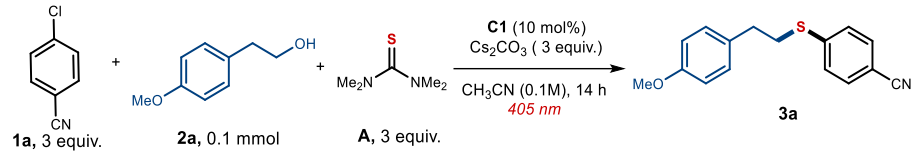

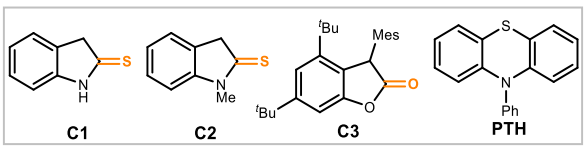

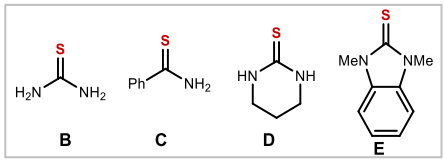

Entry	Deviations	Yield of 3a
1	none	80%
2	No light	0%
3	No base	0%
4	No **C1**	20%
5	No **C1** and light, 50 or 70 ^{o}C	0%
6	2 equiv. **1a**, **A** and Cs_2CO_3	60%
7	5 mol% **C1**	44%
8	**C2** (10 mol%)	50%
9	**C3** (10 mol%)	30%
10	PTH (10 mol%), 456 nm	57%
11	Ir-(ppy)$_3$ (3 mol%), 456 nm	45%
12	**B-D** or elemental S_8	0%
13	**E**	60%
14	DMSO, DMF, THF, DCM as solvent	0
15	Acetone as solvent	59%
16	$KHCO_3$, K_2CO_3, K_3PO_4, TMG as base	30-60%
17	PhCl as radical precursor	5%

18	With TEMPO	0%
19	0.2 mmol scale, 14 h	63% [a]
20	0.2 mmol scale, 24 h	85% (83%) [a]

All reactions were performed on a 0.1 mmol scale; yield of **3a** determined by ^{1}H NMR analysis of the crude reaction mixture by comparison with 1,3,5-trimethoxybenzene as internal standard. [a] Yield of isolated **3a**. Mes: mesityl.

General Procedure A for electron-deficient aryl halides

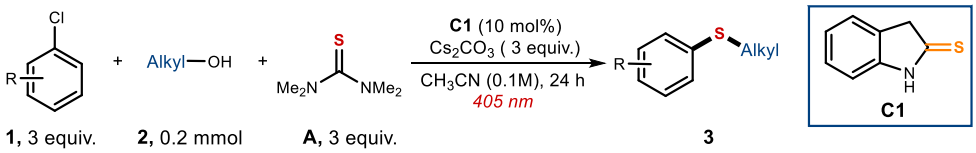

To a 7 mL glass vial, catalyst **C1** (3 mg, 0.02 mmol, 0.1 equiv.), cesium carbonate (196 mg, 0.6 mmol, 3.0 equiv.), 1,1,3,3-tetramethylthiourea (79.3 mg, 0.6 mmol, 3.0 equiv.), alcohols **2** (if solid, 0.2 mmol, 1 equiv.) and aryl chlorides **1** (if solid, 0.6 mmol, 3 equiv.) were sequentially added. The vial was sealed with a screw-top cap with septum and then vacuumed and backfilled with argon for 3 times. Afterwards, aryl chlorides **1** (if liquid, 0.6 mmol, 3.0 equiv.) and alcohols (if liquid, 0.2 mmol, 1 equiv.) followed by argon-sparged acetonitrile (0.1 M, 2.0 mL) were added *via* syringe. The vial was sealed with Parafilm and then stirred under 405 nm for 24 hours using ***Set-up 1*** detailed in Figure 4.21. After reaction was completed, the crude mixture was concentrated and purified by column chromatography to afford the corresponding products with the reported yields (>95% purity according to ^{1}H NMR analysis).

Experimental Setup

Set-up 1 *405 nm EvoluChem setup* (**Figure 4.21**)

The reactions were performed using an *EvoluChem* P303-30-1 lamp (18 W, λ_{max}= 405 nm, 2-3 cm away), and a fan to cool down the vials (under these conditions, the reaction temperature within the reaction vessel was measured to be between 40 - 42 ºC).

Figure 4.21. Reaction setup using *EvoluChem* lamps emitting at 405 nm

Set-up 2 Gram scale experiment (**Figure 4.22**)

The gram scale reaction was performed under illumination by two EvoluChem P303-30-1 lamps (18 W, λ_{max}= 405 nm, 2-3 cm away from the reaction vessel) and using a fan to cool the flask.

Figure 4.22. Setup for the gram-scale experiment using two *EvoluChem* lamps emitting at 405 nm.

4.6.3 Characterization of Products from electron-deficient aryl halides

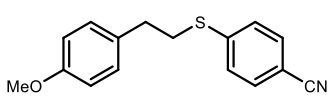

4-(4-Methoxyphenethyl)thio)benzonitrile (3a): Synthesized according to the General Procedure **A** using 2-(4-methoxyphenyl)ethan-1-ol (30.5 mg, 0.2 mmol, 1.0 equiv.), 1,1,3,3-tetramethylthiourea (79.5 mg, 0.6 mmol, 3.0 equiv.) and 4-fluorobenzonitrile (72.5 mg, 0.6 mmol, 3.0 equiv.) or 4-chlorobenzonitrile (82.5 mg, 0.6 mmol, 3.0 equiv.) or 4-bromobenzonitrile (109.0 mg, 0.6 mmol, 3.0 equiv.) or 4-iodobenzonitrile (137.5 mg, 0.6 mmol, 3.0 equiv.). The crude mixture was purified by flash column chromatography on silica gel (Hexane: EtOAc = 30: 1 as eluent) to afford **3a** (40.5 mg, 75% yield with 4-fluorobenzonitrile; 44.7 mg, 83% yield with 4-chlorobenzonitrile; 42.5 mg, 79% yield with 4-bromobenzonitrile; 35.5 mg, 66% yield with 4-iodobenzonitrile and 1.0g, 75% yield was obtained from 5 mmol scale) as a pale yellow liquid.

^{1}H NMR (400 MHz, $CDCl_3$) δ= 7.55 – 7.48 (m, 2H), 7.33 – 7.27 (m, 2H), 7.16 – 7.10 (m, 2H), 6.89 – 6.82 (m, 2H), 3.80 (s, 3H), 3.24 – 3.17 (m, 2H), 2.92 (t, *J* = 7.7 Hz, 2H) ppm.

^{13}C{^{1}H} NMR (101 MHz, $CDCl_3$): δ= 158.5, 144.8, 132.3, 131.5, 129.5, 126.90, 118.9, 114.1, 108.2, 55.3, 34.1, 33.7 ppm.

HRMS (ESI): calculated for $C_{16}H_{15}NNaOS$ [M+Na^+]: 292.0767, found 292.0763.

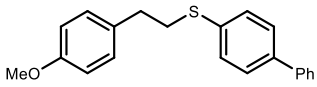

[1,1'-Biphenyl]-4-yl(4-methoxyphenethyl)sulfane (3b): Synthesized according to the General Procedure **A** using 2-(4-methoxyphenyl)ethan-1-ol (30.5 mg, 0.2 mmol, 1.0 equiv.), 1,1,3,3-tetramethylthiourea (79.5 mg, 0.6 mmol, 3.0 equiv.) and 4-chloro-1,1'-biphenyl (113.0 mg, 0.6 mmol, 3.0 equiv.). The crude mixture was purified by flash column chromatography on silica gel (hexane:EtOAc = 500: 1 as eluent) to afford **3b** (47.0 mg, 73% yield) as a white solid.

^{1}H NMR (400 MHz, $CDCl_3$): δ= 7.61 – 7.56 (m, 2H), 7.55 – 7.51 (m, 2H), 7.47 – 7.39 (m, 4H), 7.37 – 7.31 (m, 1H), 7.17 – 7.11 (m, 2H), 6.89 – 6.82 (m, 2H), 3.80 (s, 3H), 3.22 – 3.15 (m, 2H), 2.95 – 2.88 (m, 2H) ppm.

$^{13}C\{^{1}H\}$ NMR (101 MHz, $CDCl_3$): δ= 158.3, 140.5, 138.9, 135.6, 132.3, 129.5, 129.4, 128.8, 127.6, 127.3, 126.9, 114.0, 55.3, 35.4, 34.8 ppm.

HRMS (ESI): calculated for $C_{21}H_{21}OS$ $[M+H^+]$: 321.1308, found 321.1293.

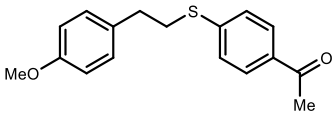

1-(4-((4-Methoxyphenethyl)thio)phenyl)ethan-1-one (3c): Synthesized according to the General Procedure **A** using 2-(4-methoxyphenyl)ethan-1-ol (30.5 mg, 0.2 mmol, 1.0 equiv.), 1,1,3,3-tetramethylthiourea (79.5 mg, 0.6 mmol, 3.0 equiv.) and 1-(4-chlorophenyl)ethan-1-one (93.0 mg, 0.6 mmol, 3.0 equiv.). The crude mixture was purified by flash column chromatography on silica gel (Hexane: EtOAc = 30: 1 as eluent) to afford **3c** (23.0 mg, 40% yield) as a pale yellow liquid.

^{1}H NMR (400 MHz, $CDCl_3$): δ= 7.89 – 7.83 (m, 2H), 7.35 – 7.29 (m, 2H), 7.17 – 7.11 (m, 2H), 6.89 – 6.82 (m, 2H), 3.80 (s, 3H), 3.24 – 3.18 (m, 2H), 2.96 – 2.89 (m, 2H), 2.57 (s, 3H) ppm.

^{13}C NMR (101 MHz, $CDCl_3$): δ= 197.2, 158.4, 144.4, 134.0, 131.8, 129.5, 128.8, 126.5, 114.0, 55.3, 34.3, 33.8, 26.4 ppm.

HRMS (ESI): calculated for $C_{17}H_{18}NaO_2S$ $[M+Na^+]$: 309.0920, found 309.0930.

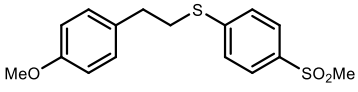

(4-Methoxyphenethyl)(4-(methylsulfonyl)phenyl)sulfane (3d): Synthesized according to the General Procedure **A** using 2-(4-methoxyphenyl)ethan-1-ol (30.5 mg, 0.2 mmol, 1.0 equiv.), 1,1,3,3-tetramethylthiourea (79.5 mg, 0.6 mmol, 3.0 equiv.) and 1-chloro-4-(methylsulfonyl)benzene (114.5 mg, 0.6 mmol, 3.0 equiv.). The crude mixture was purified by flash column chromatography on silica gel (Hexane: DCM = 1:1 as eluent) to afford **3d** (46.5 mg, 72% yield) as a yellow solid.

^{1}H NMR (400 MHz, $CDCl_3$): δ= 7.82 – 7.77 (m, 2H), 7.41 – 7.34 (m, 2H), 7.16 – 7.10 (m, 2H), 6.88 – 6.82 (m, 2H), 3.79 (s, 3H), 3.25 – 3.19 (m, 2H), 2.96 – 2.90 (m, 2H), 3.03 (s, 3H) ppm.

$^{13}C\{^{1}H\}$ NMR (101 MHz, $CDCl_3$): δ= 158.5, 145.8, 136.7, 131.5, 129.5, 127.7, 126.9, 114.1, 55.3, 44.7, 34.2, 33.8 ppm.

HRMS (ESI): calculated for $C_{16}H_{18}NaO_3S_2$ [M+Na^+]: 345.0590, found 345.0592.

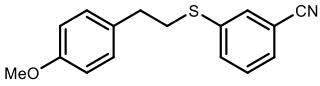

3-((4-Methoxyphenethyl)thio)benzonitrile (3e): Synthesized according to the General Procedure **A** using 2-(4-methoxyphenyl)ethan-1-ol (30.5 mg, 0.2 mmol, 1.0 equiv.), 1,1,3,3-tetramethylthiourea (79.5 mg, 0.6 mmol, 3.0 equiv.) and 3-chlorobenzonitrile (82.5 mg, 0.6 mmol, 3.0 equiv.). The crude mixture was purified by flash column chromatography on silica gel (Hexane: EtOAc = 30: 1 as eluent) to afford **3e** (34.5 mg, 64% yield) as a pale yellow liquid.

^{1}H NMR (400 MHz, $CDCl_3$): δ= 7.53 – 7.48 (m, 2H), 7.45 – 7.40 (m, 1H), 7.39 – 7.32 (m, 1H), 7.15 – 7.09 (m, 2H), 6.88 – 6.81 (m, 2H), 3.80 (s, 3H), 3.21 – 3.14 (m, 2H), 2.93 – 2.86 (m, 2H) ppm.

$^{13}C\{^{1}H\}$ NMR (101 MHz, $CDCl_3$): δ= 158.5, 139.3, 132.5, 131.5, 131.1, 129.5, 129.4, 129.0, 118.4, 114.1, 113.2, 55.3, 34.9, 34.4 ppm.

HRMS (ESI): calculated for $C_{16}H_{16}NOS$ [M+H^+]: 270.0947, found 270.0943.

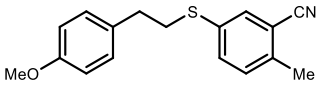

5-((4-Methoxyphenethyl)thio)-2-methylbenzonitrile (3f): Synthesized according to the General Procedure **A** using 2-(4-methoxyphenyl)ethan-1-ol (30.5 mg, 0.2 mmol, 1.0 equiv.), 1,1,3,3-tetramethylthiourea (79.5 mg, 0.6 mmol, 3.0 equiv.) and 5-chloro-2-methylbenzonitrile (91.0 mg, 0.6 mmol, 3.0 equiv.). The crude mixture was purified by flash column chromatography on silica gel (Hexane: EtOAc = 30: 1 as eluent) to afford **3f** (23.5 mg, 41% yield) as a pale yellow liquid.

^{1}H NMR (400 MHz, $CDCl_3$): δ= 7.50 (d, *J* = 2.1 Hz, 1H), 7.42 (dd, *J* = 8.1, 2.1 Hz, 1H). 7.24 – 7.19 (m, 1H), 7.12 – 7.07 (m, 2H), 6.87 – 6.81 (m, 2H), 3.79 (s, 3H), 3.16 – 3.10 (m, 2H), 2.89 – 2.83 (m, 2H), 2.51 (s, 3H) ppm.

$^{13}C\{^{1}H\}$ NMR (101 MHz, $CDCl_3$): δ= 158.4, 139.4, 135.3, 133.5, 132.4, 131.7, 130.7, 129.5, 117.7, 114.0, 113.6, 55.3, 35.5, 34.6, 20.0 ppm.

HRMS (ESI): calculated for $C_{17}H_{17}NNaOS$ [M+Na^+]: 306.0923, found 306.0928.

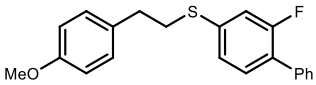

(2-Fluoro-[1,1'-biphenyl]-4-yl)(4-methoxyphenethyl)sulfane (3g): Synthesized according to the General Procedure **A** using 2-(4-methoxyphenyl)ethan-1-ol (30.5 mg, 0.2 mmol, 1.0 equiv.), 1,1,3,3-tetramethylthiourea (79.5 mg, 0.6 mmol, 3.0 equiv.) and 4-bromo-2-fluoro-1,1'-biphenyl (151.0 mg, 0.6 mmol, 3.0 equiv.). The crude mixture was purified by flash column chromatography on silica gel (Hexane:EtOAc = 200: 1 as eluent) to afford **3g** (27.0 mg, 40% yield) as a pale yellow liquid.

^{1}H NMR (400 MHz, $CDCl_3$): δ= 7.57 – 7.53 (m, 2H), 7.49 – 7.42 (m, 3H), 7.39 – 7.34 (m, 2H), 7.17 – 7.13 (m, 3H), 6.89 – 6.84 (m, 2H), 3.80 (s, 3H), 3.22 – 3.16 (m, 2H), 2.97 – 2.90 (m, 2H) ppm.

^{13}C{^{1}H} NMR (101 MHz, $CDCl_3$): δ= 161.0, 158.4, 138.1 (d, *J* = 8.3 Hz), 135.4 (d, *J* = 8.3 Hz), 132.0, 130.9 (d, *J* = 4.3 Hz), 129.5, 128.9 (d, *J* = 3.1 Hz), 128.5, 127.7, 126.4 (d, *J* = 13.9 Hz), 124.4 (d, *J* = 3.4 Hz), 115.8 (d, *J* = 25.1 Hz), 114.0, 55.3, 35.0, 34.6 ppm.

^{19}F{^{1}H} NMR (376 MHz, $CDCl_3$): δ= -117.3 ppm.

HRMS (ESI): calculated for $C_{21}H_{19}FNaOS$ [M+Na^+]: 361.1033, found 361.1033.

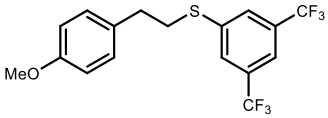

(3,5-Bis(trifluoromethyl)phenyl)(4-methoxyphenethyl)sulfane (3h): Synthesized according to the General Procedure **A** using 2-(4-methoxyphenyl)ethan-1-ol (30.5 mg, 0.2 mmol, 1.0 equiv.), 1,1,3,3-tetramethylthiourea (79.5 mg, 0.6 mmol, 3.0 equiv.) and 1-bromo-3,5-bis(trifluoromethyl)benzene (175.5 mg, 0.6 mmol, 3.0 equiv.). The crude mixture was purified by flash column chromatography on silica gel (Hexane: EtOAc = 500: 1 as eluent) to afford **3h** (49.5 mg, 65% yield) as a pale yellow liquid.

^{1}H NMR (400 MHz, $CDCl_3$): δ= 7.68 – 7.63 (m, 2H), 7.64 – 7.60 (m, 1H), 7.17 – 7.10 (m, 2H), 6.89 – 6.83 (m, 2H), 3.80 (s, 3H), 3.28 – 3.22 (m, 2H), 2.97 – 2.90 (m, 2H).

$^{13}C\{^{1}H\}$ NMR (101 MHz, $CDCl_3$): δ= 158.5, 140.9, 132.1 (q, *J* = 33.3 Hz), 131.2 129.5, 127.6 – 127.3 (m, 1C), 124.5(q, *J* = 273.7 Hz), 119.1 – 118.8 (m, 1C), 114.1, 55.2, 34.8, 34.3 ppm.

$^{19}F\{^{1}H\}$ NMR (376 MHz, $CDCl_3$): δ= -63.2 ppm.

HRMS (ESI): calculated for $C_{17}H_{13}F_6OS$ [M^+]: 379.0586, found 379.0588.

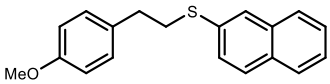

(4-Methoxyphenethyl)(naphthalen-2-yl)sulfane (3i): Synthesized according to the General Procedure **A** using 2-(4-methoxyphenyl)ethan-1-ol (30.5 mg, 0.2 mmol, 1.0 equiv.), 1,1,3,3-tetramethylthiourea (79.5 mg, 0.6 mmol, 3.0 equiv.) and 2-chloronaphthalene (97.5 mg, 0.6 mmol, 3.0 equiv.). The crude mixture was purified by flash column chromatography on silica gel (Hexane: EtOAc = 300: 1 as eluent) to afford **3i** (44.5 mg, 75% yield) as a white solid.

^{1}H NMR (400 MHz, $CDCl_3$): δ= 7.83 – 7.73 (m, 4H), 7.52 – 7.42 (m, 3H), 7.18 – 7.13 (m, 2H), 6.90 – 6.83 (m, 2H), 3.80 (s, 3H), 3.29 – 3.23 (m, 2H), 2.97 – 2.91 (m, 2H) ppm.

$^{13}C\{^{1}H\}$ NMR (101 MHz, $CDCl_3$): δ= 158.3, 134.1, 133.8, 132.3, 131.8, 129.5, 128.4, 127.6, 127.4, 127.1, 126.8, 126.6, 125.6, 114.0, 55.3, 35.3, 34.7 ppm.

HRMS (ESI): calculated for $C_{19}H_{19}OS$ [$M+H^+$]: 295.1151, found 295.1138.

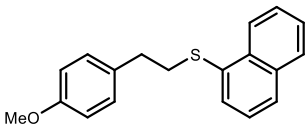

(4-Methoxyphenethyl)(naphthalen-1-yl)sulfane (3j): Synthesized according to the General Procedure **A** using 2-(4-methoxyphenyl)ethan-1-ol (30.5 mg, 0.2 mmol, 1.0 equiv.), 1,1,3,3-tetramethylthiourea (79.5 mg, 0.6 mmol, 3.0 equiv.) and 1-chloronaphthalene (97.5 mg, 0.6 mmol, 3.0 equiv.). The crude mixture was purified by flash column chromatography on silica gel (Hexane: EtOAc = 300: 1 as eluent) to afford **3j** (47.0 mg, 80% yield) as a yellow liquid.

^{1}H NMR (400 MHz, $CDCl_3$): δ= 8.44 – 8.40 (m, 1H), 7.89 – 7.85 (m, 1H), 7.77 – 7.74 (m, 1H), 7.63 – 7.60 (m, 1H), 7.59 – 7.51 (m, 2H), 7.45 – 7.41 (m, 1H), 7.14 – 7.10 (m, 2H), 6.86 – 6.82 (m, 2H), 3.80 (s, 3H), 3.24 – 3.19 (m, 2H), 2.94 – 2.89 (m, 2H) ppm.

$^{13}C\{^{1}H\}$ NMR (101 MHz, $CDCl_3$): δ= 158.2, 134.0, 133.7, 133.1, 132.4, 129.5, 128.6, 128.1, 127.2, 126.4, 126.2, 125.6, 125.1, 113.9, 55.3, 36.0, 34.8 ppm.

HRMS (ESI): calculated for $C_{19}H_{19}OS$ $[M+H^+]$: 295.1151, found 295.1137.

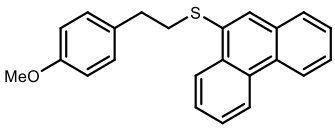

(4-Methoxyphenethyl)(phenanthren-9-yl)sulfane (3k): Synthesized according to the General Procedure **A** using 2-(4-methoxyphenyl)ethan-1-ol (30.5 mg, 0.2 mmol, 1.0 equiv.), 1,1,3,3-tetramethylthiourea (79.5 mg, 0.6 mmol, 3.0 equiv.) and 9-bromophenanthrene (154.5 mg, 0.6 mmol, 3.0 equiv.). The crude mixture was purified by flash column chromatography on silica gel (Hexane: EtOAc = 300: 1 as eluent) to afford **3k** (34.5 mg, 50% yield) as a yellow solid.

^{1}H NMR (400 MHz, $CDCl_3$): δ= 8.74 – 8.70 (m, 1H), 8.67 – 8.63 (m, 1H), 8.51 – 8.47 (m, 1H), 7.84 – 7.80 (m, 2H), 7.72 – 7.67 (m, 2H), 7.65 – 7.58 (m, 2H), 7.17 – 7.12 (m, 2H), 6.87 – 6.82 (m, 2H), 3.79 (s, 3H), 3.31 – 3.26 (m, 2H), 3.00 – 2.94 (m, 2H) ppm.

$^{13}C\{^{1}H\}$ NMR (101 MHz, $CDCl_3$): δ= 158.3, 134.1, 133.8, 132.3, 131.6, 129.5, 128.4, 127.8, 127.4, 127.1, 126.8, 126.6, 125.6, 114.0, 55.3, 35.3, 34.7 ppm.

HRMS (ESI): calculated for $C_{23}H_{21}OS$ $[M+H^+]$: 345.1308, found 345.1294.

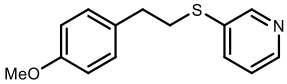

3-((4-Methoxyphenethyl)thio)pyridine (3l): Synthesized according to the General Procedure **A** using 2-(4-methoxyphenyl)ethan-1-ol (30.5 mg, 0.2 mmol, 1.0 equiv.), 1,1,3,3-tetramethylthiourea (79.5 mg, 0.6 mmol, 3.0 equiv.) and 3-chloropyridine (68.0 mg, 0.6 mmol, 3.0 equiv.). The crude mixture was purified by flash column chromatography on silica gel (DCM as eluent) to afford **3l** (37.5 mg, 76% yield) as a yellow liquid.

^{1}H NMR (400 MHz, $CDCl_3$): δ= 8.58 (d, *J* = 1.6 Hz, 1H), 8.42 (dd, *J* = 4.8, 1.6 Hz, 1H), 7.63 (ddd, *J* = 8.0, 2.4, 1.5 Hz, 1H), 7.20 (ddd, *J* = 8.0, 4.8, 0.8 Hz, 1H). 7.12 – 7.07 (m, 2H), 6.86 – 6.82 (m, 2H), 3.78 (s, 3H), 3.17 – 3.12 (m, 2H), 2.89 – 2.85 (m, 2H) ppm.

$^{13}C\{^{1}H\}$ NMR (101 MHz, $CDCl_3$): δ= 158.4, 150.3, 147.2, 136.9, 133.6, 131.7, 129.5, 123.6, 114.0, 55.3, 35.5, 34.7 ppm.

HRMS (ESI): calculated for $C_{14}H_{16}NOS$ [M+H$^+$]: 246.0947, found 246.0956.

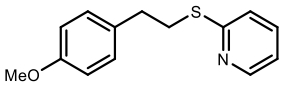

2-((4-Methoxyphenethyl)thio)pyridine (3m): Synthesized according to the General Procedure **A** using 2-(4-methoxyphenyl)ethan-1-ol (30.5 mg, 0.2 mmol, 1.0 equiv.), 1,1,3,3-tetramethylthiourea (79.5 mg, 0.6 mmol, 3.0 equiv.) and 2-chloropyridine (80.0 mg, 0.6 mmol, 3.0 equiv.). The crude mixture was purified by flash column chromatography on silica gel (Hexane: EtOAc = 100: 1 as eluent) to afford **3m** (24.5 mg, 50% yield) as a yellow liquid.

^{1}H NMR (400 MHz, CDCl$_3$): δ= 8.47 – 8.42 (m, 1H), 7.50 – 7.43 (m, 1H), 7.22 – 7.14 (m, 3H), 7.01 – 6.94 (m, 1H), 6.88 – 6.82 (m, 2H), 3.80 (s, 3H), 3.43 – 3.36 (m, 2H), 3.00 – 2.92 (m, 2H) ppm.

^{13}C{^{1}H} NMR (101 MHz, CDCl$_3$): δ= 159.1, 158.2, 149.5, 135.8, 132.7, 129.6, 122.4, 119.3, 113.9, 55.3, 34.9, 31.7 ppm.

HRMS (ESI): calculated for $C_{14}H_{16}NOS$ [M+H$^+$]: 246.0947, found 246.0957.

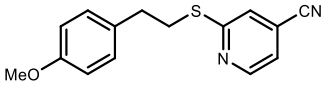

2-((4-Methoxyphenethyl)thio)isonicotinonitrile (3n): Synthesized according to the General Procedure **A** using 2-(4-methoxyphenyl)ethan-1-ol (30.5 mg, 0.2 mmol, 1.0 equiv.), 1,1,3,3-tetramethylthiourea (79.5 mg, 0.6 mmol, 3.0 equiv.) and 2-chloroisonicotinonitrile (83.0 mg, 0.6 mmol, 3.0 equiv.). The crude mixture was purified by flash column chromatography on silica gel (Hexane: EtOAc = 50: 1 as eluent) to afford **3n** (22.0 mg, 41% yield) as a yellow liquid.

^{1}H NMR (400 MHz, CDCl$_3$): δ= 8.57 (dd, *J* = 5.1, 1.0 Hz, 1H), 7.37 – 7.33 (m, 1H), 7.19 – 7.13 (m, 3H), 6.87 – 6.83 (m, 2H), 3.80 (s, 3H), 3.43 – 3.38 (m, 2H), 2.97 – 2.93 (m, 2H) ppm.

^{13}C{^{1}H} NMR (101 MHz, CDCl$_3$): δ= 161.6, 158.3, 150.2, 132.1, 129.6, 124.0, 120.2, 119. 9, 116.3, 113.9, 55.3, 34.7, 31.8 ppm.

HRMS (ESI): calculated for $C_{15}H_{15}N_2OS$ [M+H$^+$]: 271.0900, found 271.0897.

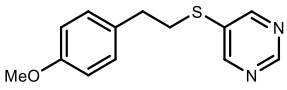

5-((4-Methoxyphenethyl)thio)pyrimidine (3o): Synthesized according to the General Procedure **A** using 2-(4-methoxyphenyl)ethan-1-ol (30.5 mg, 0.2 mmol, 1.0 equiv.), 1,1,3,3-tetramethylthiourea (79.5 mg, 0.6 mmol, 3.0 equiv.) and 5-bromopyrimidine (95.5 mg, 0.6 mmol, 3.0 equiv.). The crude mixture was purified by flash column chromatography on silica gel (DCM: EtOAc = 50: 1 as eluent) to afford **3o** (20.5 mg, 42% yield) as a yellow liquid.

^{1}H NMR (400 MHz, $CDCl_3$): δ= 9.02 (s, 1H), 8.66 (s, 2H), 7.13 – 7.07 (m, 2H), 6.87 – 6.81 (m, 2H), 3.79 (s, 3H), 3.22 – 3.15 (m, 2H), 2.93 – 2.87 (m, 2H) ppm.

^{13}C{^{1}H} NMR (101 MHz, $CDCl_3$): δ= 158.5, 156.9, 155.9, 133.1, 131.1, 129.5, 114.1, 55.3, 35.3, 34.7 ppm.

HRMS (ESI): calculated for $C_{13}H_{15}N_2OS$ [M+H$^+$]: 247.0900, found 247.0896.

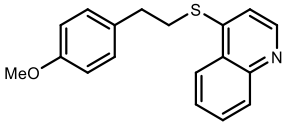

4-((4-Methoxyphenethyl)thio)quinoline (3p): Synthesized according to the General Procedure **A** using 2-(4-methoxyphenyl)ethan-1-ol (30.5 mg, 0.2 mmol, 1.0 equiv.), 1,1,3,3-tetramethylthiourea (79.5 mg, 0.6 mmol, 3.0 equiv.) and 4-chloroquinoline (98.5 mg, 0.6 mmol, 3.0 equiv.). The crude mixture was purified by flash column chromatography on silica gel (Hexane: EtOAc = 3: 1 as eluent) to afford **3p** (38.5 mg, 65% yield) as a yellow liquid.

^{1}H NMR (400 MHz, $CDCl_3$): δ= 8.71 (d, *J* = 4.8 Hz, 1H), 8.15 – 8.10 (m, 1H), 8.10 – 8.05 (m, 1H), 7.74 – 7.68 (m, 1H), 7.57 – 7.50 (m, 1H), 7.21 – 7.14 (m, 3H), 6.90 – 6.84 (m, 2H), 3.80 (s, 3H), 3.35 – 3.28 (m, 2H), 3.06 – 3.00 (m, 2H) ppm.

^{13}C{^{1}H} NMR (101 MHz, $CDCl_3$): δ= 158.5, 149.2, 147.6, 147.4, 131.6, 130.0, 129. 8, 129.5, 126.6, 126.3, 123.7, 115.9, 114.1, 55.3, 33. 8, 32.9 ppm.

HRMS (ESI): calculated for $C_{18}H_{18}NOS$ [M+H$^+$]: 296.1104, found 296.1115.

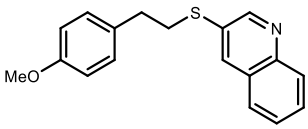

3-((4-Methoxyphenethyl)thio)quinoline (3q): Synthesized according to the General Procedure **A** using 2-(4-methoxyphenyl)ethan-1-ol (30.5 mg, 0.2 mmol, 1.0 equiv.),

1,1,3,3-tetramethylthiourea (79.5 mg, 0.6 mmol, 3.0 equiv.) and 3-bromoquinoline (124.5 mg, 0.6 mmol, 3.0 equiv.). The crude mixture was purified by flash column chromatography on silica gel (Hexane: EtOAc = 20: 1 as eluent) to afford **3q** (35.5 mg, 60% yield) as a yellow liquid.

^{1}H NMR (400 MHz, $CDCl_3$): δ= 8.85 (d, *J* = 2.3 Hz, 1H), 8.09 – 8.05 (m, 1H), 8.03 – 8.00 (m, 1H), 7.74 – 7.69 (m, 1H), 7.69 – 7.64 (m, 1H), 7.56 – 7.51 (m, 1H), 7.14 – 7.10 (m, 2H), 6.85 – 6.81 (m, 2H), 3.77 (s, 3H), 3.27 – 3.22 (m, 2H), 2.96 – 2.90 (m, 2H) ppm.

^{13}C{^{1}H} NMR (101 MHz, $CDCl_3$): δ=158.4, 151.6, 146.3, 135.1, 131.7, 130.6, 129.6, 129.3, 129.1, 128.2, 127.2, 127.0, 114.0, 55.3, 35.7, 34.8 ppm.

HRMS (ESI): calculated for $C_{18}H_{18}NOS$ [M+H$^+$]: 296.1104, found 296.1115.

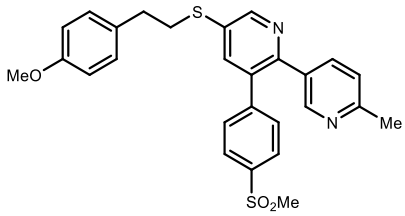

5-((4-Methoxyphenethyl)thio)-6'-methyl-3-(4-(methylsulfonyl)phenyl)-2,3'-bipyridine (3r): Synthesized according to the General Procedure b using 2-(4-methoxyphenyl)ethan-1-ol (30.5 mg, 0.2 mmol, 1.0 equiv.), 1,1,3,3-tetramethylthiourea (79.5 mg, 0.6 mmol, 3.0 equiv.) and 5-chloro-6'-methyl-3-(4-(methylsulfonyl)phenyl)-2,3'-bipyridine (215.5 mg, 0.6 mmol, 3.0 equiv.). The crude mixture was purified by flash column chromatography on silica gel (Hexane: Acetone= 3: 1 as eluent) to afford **3r** (34.5 mg, 35% yield) as a yellow solid.

^{1}H NMR (400 MHz, $CDCl_3$): δ= 8.66 (d, *J* = 2.2 Hz, 1H), 8.37 (s, 1H), 7.92 – 7.85 (m, 2H), 7.60 – 7.53 (m, 2H), 7.39 – 7.33 (m, 2H), 7.15 – 7.04 (m, 3H), 6.84 – 6.78 (m, 2H), 3.76 (s, 3H), 3.26 – 3.20 (m, 2H), 3.08 (s, 3H), 2.95 (t, *J* = 7.5 Hz, 2H), 2.52 (s, 3H) ppm.

^{13}C{^{1}H} NMR (101 MHz, $CDCl_3$): δ= 158.4, 158.1, 151.2, 149.8, 149.2, 144.7, 139.9, 138.4, 137.4, 134.3, 133.4, 131.8, 131.4, 130.5 , 129.6, 127.8, 122.8, 114.0, 55.3, 44.5, 35.3, 34.9, 24.2 ppm.

HRMS (ESI): calculated for $C_{27}H_{27}N_2O_3S_2$ [M+H$^+$]: 491.1458, found 491.1472 ppm.

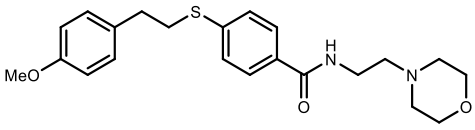

4-((4-Methoxyphenethyl)thio)-N-(2-morpholinoethyl)benzamide (3s): Synthesized according to the General Procedure **A** using 2-(4-methoxyphenyl)ethan-1-ol (30.5 mg, 0.2 mmol, 1.0 equiv.), 1,1,3,3-tetramethylthiourea (79.5 mg, 0.6 mmol, 3.0 equiv.) and 4-chloro-N-(2-morpholinoethyl)benzamide (161.5 mg, 0.6 mmol, 3.0 equiv.). The crude mixture was purified by flash column chromatography on silica gel (EtOAc: MeOH= 50: 1 as eluent) to afford **3s** (36.0 mg, 45% yield) as a white solid.

^{1}H NMR (400 MHz, $CDCl_3$): δ= 8.12 – 8.06 (m, 2H), 7.77 – 7.70 (m, 2H), 7.55 – 7.50 (m, 2H), 7.28 – 7.23 (m, 2H), 7.18 (br, 1H), 4.19 (s, 3H), 4.14 (t, *J* = 4.7 Hz, 4H), 3.99 – 3.93 (m, 2H), 3.63 – 3.55 (m, 2H), 3.34 – 3.27 (m, 2H), 3.03 (t, *J* = 6.0 Hz, 2H), 2.94 (t, *J* = 4.0 Hz, 4H) ppm.

^{13}C{^{1}H} NMR (101 MHz, $CDCl_3$): δ= 166.9, 158.4, 141.7, 131.9, 131.4, 129.5, 127.4, 127.4, 114.0, 66.9, 56.96, 56.0, 53.3, 36.0, 34.4, 34.3 ppm.

HRMS (ESI): calculated for $C_{22}H_{29}N_2O_3S$ [M+H$^+$]: 401.1893, found 401.1891.

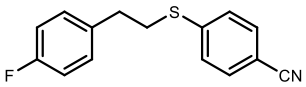

4-((4-Fluorophenethyl)thio)benzonitrile (3t): Synthesized according to the General Procedure **A** using 2-(4-fluorophenyl)ethan-1-ol (28.0 mg, 0.2 mmol, 1.0 equiv.), 1,1,3,3-tetramethylthiourea (79.5 mg, 0.6 mmol, 3.0 equiv.) and 4-chlorobenzonitrile (82.5 mg, 0.6 mmol, 3.0 equiv.). The crude mixture was purified by flash column chromatography on silica gel (Hexane: EtOAc = 30: 1 as eluent) to afford **3t** (49.5 mg, 90% yield) as a pale yellow liquid.

^{1}H NMR (400 MHz, $CDCl_3$): δ= 7.56 – 7.50 (m, 2H), 7.33 – 7.28 (m, 2H), 7.20 – 7.14 (m, 2H), 7.04 – 6.96 (m, 2H), 3.24 – 3.18 (m, 2H), 2.95 (t, *J* = 7.6 Hz, 2H) ppm.

^{13}C{^{1}H} NMR (101 MHz, $CDCl_3$): δ= 161.8 (d, *J* = 246.1 Hz), 144.4, 135.05 (d, *J* = 3.3 Hz), 132.3, 130.0 (d, *J* = 8.0 Hz), 127.0, 118.8, 115.5 (d, *J* = 21.3 Hz), 108.4, 34.2, 33.57 (d, *J* = 1.4 Hz) ppm.

^{19}F{^{1}H} NMR (376 MHz, $CDCl_3$): δ= -116.1 ppm.

HRMS (ESI): calculated for $C_{15}H_{12}FNNaS$ [M+Na$^+$]: 280.0567, found 280.0571.

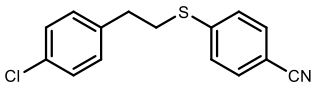

4-((4-Chlorophenethyl)thio)benzonitrile (3u): Synthesized according to the General Procedure **A** using 2-(4-chlorophenyl)ethan-1-ol (31.5 mg, 0.2 mmol, 1.0 equiv.), 1,1,3,3-tetramethylthiourea (54.0 mg, 0.4 mmol, 2.0 equiv.) and 4-chlorobenzonitrile (82.5 mg, 0.6 mmol, 3.0 equiv.). The crude mixture was purified by flash column chromatography on silica gel (Hexane: EtOAc = 30: 1 as eluent) to afford **3u** (46.5 mg, 85% yield) as a pale yellow liquid.

^{1}H NMR (400 MHz, $CDCl_3$): δ= 7.55 – 7.49 (m, 2H), 7.33 – 7.25 (m, 4H), 7.16 – 7.11 (m, 2H), 3.24 – 3.18 (m, 2H), 2.95 (t, *J* = 7.6 Hz, 2H) ppm.

^{13}C{^{1}H} NMR (101 MHz, $CDCl_3$): δ= 144.3, 137.8, 132.3, 129.9, 128.8, 127.1, 118.8, 108.4, 34.3, 33.3.

HRMS (ESI): calculated for $C_{15}H_{12}ClNNaS$ [M+Na^+]: 296.0271, found 296.0276.

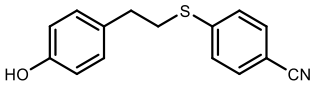

4-((4-Hydroxyphenethyl)thio)benzonitrile (3v): Synthesized according to the General Procedure **A** using 4-(2-hydroxyethyl)phenol (27.5 mg, 0.2 mmol, 1.0 equiv.), 1,1,3,3-tetramethylthiourea (79.5 mg, 0.6 mmol, 3.0 equiv.) and 4-chlorobenzonitrile (82.5 mg, 0.6 mmol, 3.0 equiv.). The crude mixture was purified by flash column chromatography on silica gel (Hexane: EtOAc = 300: 1 as eluent) to afford **3v** (33.5 mg, 65% yield) as a yellow liquid.

^{1}H NMR (400 MHz, $CDCl_3$): δ= 7.56 – 7.49 (m, 2H), 7.34 – 7.27 (m, 2H), 7.11 – 7.05 (m, 2H), 6.83 – 6.76 (m, 2H), 5.00 (br, 1H), 3.22 – 3.16 (m, 2H), 2.91 (t, *J* = 7.7 Hz, 2H) ppm.

^{13}C{^{1}H} NMR (101 MHz, $CDCl_3$): δ= 154.5, 144.8, 132.3, 131.6, 129.7, 126.9, 118.9, 115.5, 108.1, 34.1, 33.7 ppm.

HRMS (ESI): calculated for $C_{15}H_{13}NNaOS$ [M+Na^+]: 278.0610, found 278.0607.

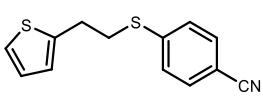

4-((2-(Thiophen-2-yl)ethyl)thio)benzonitrile (3w): Synthesized according to the General Procedure **A** using 2-(thiophen-2-yl)ethan-1-ol (25.5 mg, 0.2 mmol, 1.0 equiv.), 1,1,3,3-tetramethylthiourea (79.5 mg, 0.6 mmol, 3.0 equiv.) and 4-chlorobenzonitrile (82.5 mg, 0.6 mmol, 3.0 equiv.). The crude mixture was purified by flash column chromatography

on silica gel (Hexane: EtOAc = 150: 1 as eluent) to afford **3w** (40.5 mg, 86% yield) as a yellow liquid.

^{1}H NMR (400 MHz, $CDCl_3$): δ= 7.56 – 7.50 (m, 2H), 7.34 – 7.29 (m, 2H), 7.18 (dd, *J* = 5.1, 1.2 Hz, 1H), 6.97 – 6.93 (m, 1H), 6.89 – 6.85 (m, 1H), 3.31 – 3.24 (m, 2H), 3.23 – 3.16 (m, 2H) ppm.

^{13}C{^{1}H} NMR (101 MHz, $CDCl_3$): δ= 144.2, 141.7, 132.4, 127.1, 127.0, 125.4, 124.1, 118.8, 108.5, 33.7, 29.4 ppm.

HRMS (ESI): calculated for $C_{13}H_{12}NS_2$ [M+H$^+$]: 246.0406, found 246.0405.

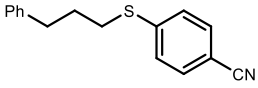

4-((3-Phenylpropyl)thio)benzonitrile (3x): Synthesized according to the General Procedure **A** using 3-phenylpropan-1-ol (27.2 mg, 0.2 mmol, 1.0 equiv.), 1,1,3,3-tetramethylthiourea (79.5 mg, 0.6 mmol, 3.0 equiv.) and 4-chlorobenzonitrile (82.5 mg, 0.6 mmol, 3.0 equiv.). The crude mixture was purified by flash column chromatography on silica gel (Hexane: EtOAc = 200: 1 as eluent) to afford **3x** (33.0 mg, 65% yield) as a pale yellow liquid.

^{1}H NMR (400 MHz, $CDCl_3$): δ= 7.53 – 7.46 (m, 2H), 7.34 – 7.28 (m, 2H), 7.26 – 7.21 (m, 3H), 7.21 – 7.17 (m, 2H), 2.97 (t, *J* = 7.4 Hz, 2H), 2.78 (t, *J* = 7.4 Hz, 2H), 2.02 – 1.97 (m, 2H) ppm.

^{13}C{^{1}H} NMR (101 MHz, $CDCl_3$): δ= 144.8, 140.7, 132.2, 128.6, 128.5, 126.8, 126.3, 118.9, 108.1, 34.7, 31.0, 30.1 ppm.

HRMS (ESI): calculated for $C_{16}H_{15}NNaS$ [M+Na$^+$]: 276.0817, found 276.0824.

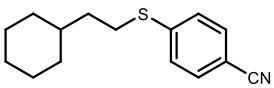

4-((2-Cyclohexylethyl)thio)benzonitrile (3y): Synthesized according to the General Procedure **A** using 2-cyclohexylethan-1-ol (25.6 mg, 0.2 mmol, 1.0 equiv.), 1,1,3,3-tetramethylthiourea (79.5 mg, 0.6 mmol, 3.0 equiv.) and 4-chlorobenzonitrile (82.5 mg, 0.6 mmol, 3.0 equiv.). The crude mixture was purified by flash column chromatography on silica gel (Hexane: EtOAc = 300: 1 as eluent) to afford **3y** (33.0 mg, 67% yield) as a pale yellow liquid.

^{1}H NMR (400 MHz, $CDCl_3$): δ= 7.54 – 7.49 (m, 2H), 7.30 – 7.26 (m, 2H), 3.01 – 2.95 (m, 2H), 1.78 – 1.64 (m, 5H), 1.60 – 1.56 (m, 2H), 1.45 – 1.37 (m, 1H), 1.26 – 1.14 (m, 3H), 0.98 – 0.90 (m, 2H) ppm.

^{113}C{^{1}H} NMR (101 MHz, $CDCl_3$): δ= 145.4, 132.2, 126.6, 119.0, 107.8, 37.0, 36.0, 33.0, 29.5, 26.5, 26.2 ppm.

HRMS (ESI): calculated for $C_{15}H_{19}NNaS$ [M+Na^+]: 268.1130, found 268.1131.

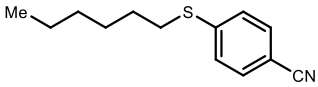

4-(Hexylthio)benzonitrile (3z): Synthesized according to the General Procedure **A** using hexan-1-ol (20.4 mg, 0.2 mmol, 1.0 equiv.), 1,1,3,3-tetramethylthiourea (79.5 mg, 0.6 mmol, 3.0 equiv.) and 4-chlorobenzonitrile (82.5 mg, 0.6 mmol, 3.0 equiv.). The crude mixture was purified by flash column chromatography on silica gel (Hexane: EtOAc = 300: 1 as eluent) to afford **3z** (28.5 mg, 65% yield) as a pale yellow liquid.

^{1}H NMR (400 MHz, $CDCl_3$): δ 7.54 – 7.49 (m, 2H), 7.31 – 7.27 (m, 2H), 2.97 (t, *J* = 8.0 Hz, 2H),

1.72 – 1.66 (m, 2H), 1.48 – 1.41 (m, 2H), 1.33 – 1.28 (m, 4H), 0.91 – 0.87 (m, 3H) ppm.

^{13}C{^{1}H} NMR (101 MHz, $CDCl_3$): δ= 145.3, 132.2, 126.7, 119.0, 107.9, 31.9, 31.3, 28.6, 28.5, 22.5, 14.0 ppm.

HRMS (ESI): calculated for $C_{13}H_{17}NNaS$ [M+Na^+]: 242.0974, found 242.0977.

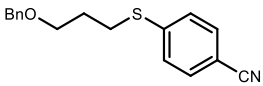

4-((3-(Benzyloxy)propyl)thio)benzonitrile (3aa): Synthesized according to the General Procedure A using 3-(benzyloxy)propan-1-ol (33.2 mg, 0.2 mmol, 1.0 equiv.), 1,1,3,3-tetramethylthiourea (79.5 mg, 0.6 mmol, 3.0 equiv.) and 4-chlorobenzonitrile (82.5 mg, 0.6 mmol, 3.0 equiv.). The crude mixture was purified by flash column chromatography on silica gel (Hexane: EtOAc = 30: 1 as eluent) to afford **3aa** (37.4 mg, 66% yield) as a pale yellow liquid.

^{1}H NMR (400 MHz, $CDCl_3$): δ= 7.53 – 7.47 (m, 2H), 7.39 – 7.27 (m, 7H), 4.51 (s, 2H), 3.60 (t, *J* = 5.8 Hz, 2H), 3.12 (t, *J* = 5.8 Hz, 2H), 2.03 – 1.94 (m, 2H) ppm.

$^{13}C\{^{1}H\}$ NMR (101 MHz, $CDCl_3$): δ= 144.9, 138.2, 132.2, 128.5, 127.7, 127.6, 126.8, 119.0, 108.0, 73.1, 68.2, 29.1, 28.7 ppm.

HRMS (ESI): calculated for $C_{17}H_{17}NNaOS$ [M+Na^+]: 306.0923, found 306.0924.

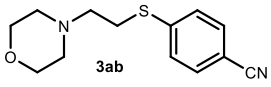

3ab

4-((2-Morpholinoethyl)thio)benzonitrile (3ab): Synthesized according to the General Procedure **A** using 2-morpholinoethan-1-ol (26.2 mg, 0.2 mmol, 1.0 equiv.), 1,1,3,3-tetramethylthiourea (79.5 mg, 0.6 mmol, 3.0 equiv.) and 4-chlorobenzonitrile (82.5 mg, 0.6 mmol, 3.0 equiv.). The crude mixture was purified by flash column chromatography on silica gel (Hexane: EtOAc = 1: 1 as eluent) to afford **3ab**) (31.0 mg, 62% yield) as a pale yellow liquid.

^{1}H NMR (400 MHz, $CDCl_3$): δ= 7.54 – 7.48 (m, 2H), 7.34 – 7.28 (m, 2H), 3.74 – 3.68 (m, 4H), 3.15 – 3.08 (m, 2H), 2.70 – 2.64 (m, 2H), 2.54 – 2.44 (m, 4H) ppm.

$^{13}C\{^{1}H\}$ NMR (101 MHz, $CDCl_3$): δ= 144.7, 132.3, 126.9, 118.8, 108.3, 66.8, 57.2, 53.5, 29.3 ppm.

HRMS (ESI): calculated for $C_{13}H_{17}N_2OS$ [M+H^+]: 249.1056, found 249.1063.

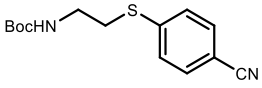

Tert-butyl (2-((4-cyanophenyl)thio)ethyl)carbamate (3ac): Synthesized according to the General Procedure **A** using tert-butyl (2-hydroxyethyl)carbamate (32.0 mg, 0.2 mmol, 1.0 equiv.), 1,1,3,3-tetramethylthiourea (79.5 mg, 0.6 mmol, 3.0 equiv.) and 4-chlorobenzonitrile (82.5 mg, 0.6 mmol, 3.0 equiv.). The crude mixture was purified by flash column chromatography on silica gel (Hexane: EtOAc = 10: 1 as eluent) to afford **3ac** (28.5 mg, 51% yield) as a yellow liquid.

^{1}H NMR (400 MHz, $CDCl_3$): δ= 7.57 – 7.49 (m, 2H), 7.40 – 7.34 (m, 2H), 4.89 (br, 1H), 3.38 (q, *J* = 6.6 Hz, 2H), 3.13 (t, *J* = 6.8 Hz, 2H), 1.44 (s, 9H) ppm.

$^{13}C\{^{1}H\}$ NMR (101 MHz, $CDCl_3$): δ= 155.7, 143.6, 132.4, 127.2, 118.8, 108.6, 79.8, 39.6, 32.0, 28.4 ppm.

HRMS (ESI): calculated for $C_{14}H_{18}N_2NaO_2S$ [M+Na^+]: 301.0981, found 301.0982.

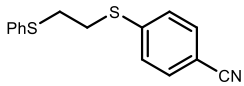

4-((2-(Phenylthio)ethyl)thio)benzonitrile (3ad): Synthesized according to the General Procedure **A** using 2-(phenylthio)ethan-1-ol (30.8 mg, 0.2 mmol, 1.0 equiv.), 1,1,3,3-tetramethylthiourea (79.5 mg, 0.6 mmol, 3.0 equiv.) and 4-chlorobenzonitrile (82.5 mg, 0.6 mmol, 3.0 equiv.). The crude mixture was purified by flash column chromatography on silica gel (Hexane: EtOAc = 150: 1 as eluent) to afford **3ad** (44.5 mg, 81% yield) as a pale yellow liquid.

^{1}H NMR (400 MHz, $CDCl_3$): δ= 7.50 – 7.45 (m, 2H), 7.42 – 7.37 (m, 2H), 7.36 – 7.30 (m, 2H), 7.30 – 7.24 (m, 1H), 7.22 – 7.15 (m, 2H), 3.18– 3.13(m, 2H), 3.13 – 3.07 (m, 2H) ppm.

^{13}C{^{1}H} NMR (101 MHz, $CDCl_3$): δ= 143.4, 134.4, 132.4, 131.1, 129.2, 127.3, 127.3, 118.7, 108.7, 33.5, 31.5 ppm.

HRMS (ESI): calculated for $C_{15}H_{13}NNaS_2$ [M+Na^+]: 294.0382, found 294.0387.

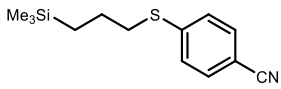

4-((3-(Trimethylsilyl)propyl)thio)benzonitrile (3ae): Synthesized according to the General Procedure **A** using 3-(trimethylsilyl)propan-1-ol (26.5 mg, 0.2 mmol, 1.0 equiv.), 1,1,3,3-tetramethylthiourea (79.5 mg, 0.6 mmol, 3.0 equiv.) and 4-chlorobenzonitrile (82.5 mg, 0.6 mmol, 3.0 equiv.). The crude mixture was purified by flash column chromatography on silica gel (Hexane: EtOAc = 300: 1 as eluent) to afford **3ae** (34.0 mg, 68% yield) as a pale yellow liquid.

^{1}H NMR (400 MHz, $CDCl_3$): δ= 7.54 – 7.48 (m, 2H), 7.31 – 7.26 (m, 2H), 3.01 – 2.94 (m, 2H), 1.72 – 1.64 (m, 2H), 0.69 – 0.61 (m, 2H), 0.01 (s, 9H) ppm.

^{13}C{^{1}H} NMR (101 MHz, $CDCl_3$): δ= 145.3, 132.2, 126.7, 119.0, 107.9, 35.5, 23.5, 16.5, -1.8.

HRMS (ESI): calculated for $C_{13}H_{20}NSSi$ [M+H^+]: 250.1080, found 250.1076.

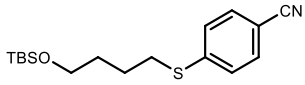

4-((4-((Tert-butyldimethylsilyl)oxy)butyl)thio)benzonitrile (3af): Synthesized according to the General Procedure **A** using 4-((tert-butyldimethylsilyl)oxy)butan-1-ol (41.0 mg, 0.2 mmol, 1.0 equiv.), 1,1,3,3-tetramethylthiourea (79.5 mg, 0.6 mmol, 3.0 equiv.) and 4-chlorobenzonitrile (82.5 mg, 0.6

mmol, 3.0 equiv.). The crude mixture was purified by flash column chromatography on silica gel (Hexane: EtOAc = 150: 1 as eluent) to afford **3af** (31.0 mg, 48% yield) as a pale yellow liquid.

^{1}H NMR (400 MHz, $CDCl_3$): δ= 7.54 – 7.47 (m, 2H), 7.32– 7.27 (m, 2H), 3.64 (t, *J* = 6.0 Hz, 2H), 3.00 (t, *J* = 6.0 Hz, 2H),1.82 – 1.73 (m, 2H), 1.69 – 1.63(m, 2H), 0.87 (s, 9H), 0.03 (s, 6H) ppm.

^{13}C{^{1}H} NMR (101 MHz, $CDCl_3$): δ= 145.1, 132.2, 126.8, 119.0, 108.0, 62.4, 31.8, 31.8, 25.9, 25.3, 18.3, -5.3 ppm.

HRMS (ESI): calculated for $C_{17}H_{27}NNaOSSi$ [M+Na$^+$]: 344.1475, found 344.1482.

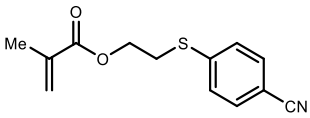

2-((4-Cyanophenyl)thio)ethyl methacrylate (3ag): Synthesized according to the General Procedure **A** using 2-hydroxyethyl methacrylate (26.0 mg, 0.2 mmol, 1.0 equiv.), 1,1,3,3-tetramethylthiourea (79.5 mg, 0.6 mmol, 3.0 equiv.) and 4-chlorobenzonitrile (82.5 mg, 0.6 mmol, 3.0 equiv.). The crude mixture was purified by flash column chromatography on silica gel (Hexane: EtOAc = 20: 1 as eluent) to afford **3ag** (22.5 mg, 45% yield) as a yellow liquid.

^{1}H NMR (400 MHz, $CDCl_3$): δ= 7.58 – 7.51 (m, 2H), 7.44 – 7.37 (m, 2H), 6.09 – 6.05 (m, 1H), 5.61 – 5.55 (m, 1H), 4.36 (t, *J* = 6.9 Hz, 2H), 3.27 (t, *J* = 6.9 Hz, 2H), 1.94 – 1.89 (m, 3H) ppm.

^{13}C{^{1}H} NMR (101 MHz, $CDCl_3$): δ= 167.1, 143.3, 135.8, 132.4, 127.3, 126.3, 118.7, 108.9, 62.6, 30.5, 18.2 ppm.

HRMS (ESI): calculated for $C_{13}H_{13}NNaO_2S$ [M+Na$^+$]: 270.0559, found 270.0558.

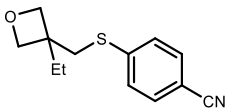

4-(((3-Ethyloxetan-3-yl)methyl)thio)benzonitrile (3ah): Synthesized according to the General Procedure **A** using (3-ethyloxetan-3-yl)methanol (23.2 mg, 0.2 mmol, 1.0 equiv.), 1,1,3,3-tetramethylthiourea (79.5 mg, 0.6 mmol, 3.0 equiv.) and 4-chlorobenzonitrile (82.5 mg, 0.6

mmol, 3.0 equiv.). The crude mixture was purified by flash column chromatography on silica gel (Hexane: EtOAc = 30: 1 as eluent) to afford **3ah** (28.0 mg, 60% yield) as a yellow liquid.

^{1}H NMR (400 MHz, $CDCl_3$): δ= 7.58 – 7.51 (m, 2H), 7.39 – 7.33 (m, 2H), 4.48 – 4.41 (m, 4H),

3.35 (s, 2H), 1.83 (q, *J* = 7.4 Hz, 2H), 0.92 (t, *J* = 7.4 Hz, 3H) ppm.

^{13}C{^{1}H} NMR (101 MHz, $CDCl_3$): δ= 144.6, 132.3, 127.5, 118.7, 108.7, 80.0, 43.3, 38.6, 28.3, 8.2 ppm.

HRMS (ESI): calculated for $C_{13}H_{15}NNaOS$ [M+Na^+]: 256.0767, found 256.0764.

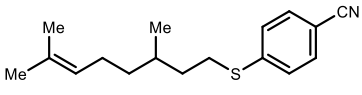

4-((3,7-Dimethyloct-6-en-1-yl)thio)benzonitrile (3ai): Synthesized according to the General Procedure **A** using 3,7-dimethyloct-6-en-1-ol (31.3 mg, 0.2 mmol, 1.0 equiv.), 1,1,3,3-tetramethylthiourea (79.5 mg, 0.6 mmol, 3.0 equiv.) and 4-chlorobenzonitrile (82.5 mg, 0.6 mmol, 3.0 equiv.). The crude mixture was purified by flash column chromatography on silica gel (Hexane: EtOAc = 300: 1 as eluent) to afford **3ai** (33.0 mg, 60% yield) as a pale yellow liquid.

^{1}H NMR (400 MHz, $CDCl_3$): δ= 7.54 – 7.49 (m, 2H), 7.31– 7.26 (m, 2H), 5.11 – 5.04 (m, 1H), 3.05 – 2.89 (m, 2H), 2.05 – 1.90 (m, 2H), 1.76 – 1.68 (m, 4H), 1.60 – 1.48 (m, 5H), 1.40 – 1.32 (m, 1H), 1.24 – 1.16 (m, 1H), 0.94 (d, *J* = 6.4 Hz, 3H) ppm.

^{13}C{^{1}H} NMR (101 MHz, $CDCl_3$): δ= 145.3, 132.2, 131.6, 126.7, 124.4, 119.0, 107.9, 36.7, 35.6, 32.0, 29.8, 25.7, 25.4, 19.2, 17.7 ppm.

HRMS (ESI): calculated for $C_{17}H_{23}NNaS$ [M+Na^+]: 296.1443, found 296.1452.

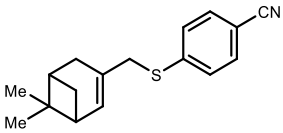

4-(((6,6-Dimethylbicyclo[3.1.1]hept-2-en-3-yl)methyl)thio)benzonitrile (3aj): Synthesized according to the General Procedure **A** using (6,6-dimethylbicyclo[3.1.1]hept-2-en-3-yl)methanol (30.5 mg, 0.2 mmol, 1.0 equiv.), 1,1,3,3-tetramethylthiourea (79.5 mg, 0.6 mmol, 3.0 equiv.) and 4-chlorobenzonitrile (82.5 mg, 0.6

mmol, 3.0 equiv.). The crude mixture was purified by flash column chromatography on silica gel (Hexane: EtOAc = 150: 1 as eluent) to afford **3aj** (27.5 mg, 51% yield) as a yellow liquid.

^{1}H NMR (400 MHz, $CDCl_3$): δ= 7.52 – 7.47 (m, 2H), 7.33 – 7.28 (m, 2H), 5.56 – 5.51 (m, 1H), 3.60 – 3.56 (m, 2H), 2.41 – 2.35 (m, 1H), 2.29 – 2.16 (m, 3H), 2.11 – 2.05 (m, 1H), 1.28 (s, 3H), 1.05 (d, *J* = 8.7 Hz, 1H), 0.73 (s, 3H) ppm.

^{13}C{^{1}H} NMR (101 MHz, $CDCl_3$): δ= 145.1, 141.7, 132.0, 127.3, 121.7, 119.0, 108.1, 45.2, 40.4, 38.6, 38.2, 31.6, 31.3, 26.1, 21.1 ppm.

HRMS (ESI): calculated for $C_{17}H_{20}NS$ [M+H$^+$]: 270.1311, found 270.1307.

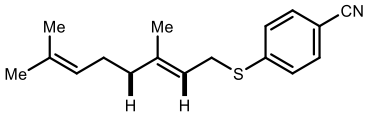

(E)-4-((3,7-Dimethylocta-2,6-dien-1-yl)thio)benzonitrile *(E: Z= 6.5 :1) (major isomer)* (3ak): Synthesized according to the General Procedure **A** using (E)-3,7-dimethylocta-2,6-dien-1-ol (31.0 mg, 0.2 mmol, 1.0 equiv.), 1,1,3,3-tetramethylthiourea (79.5 mg, 0.6 mmol, 3.0 equiv.) and 4-chlorobenzonitrile (82.5 mg, 0.6 mmol, 3.0 equiv.). The crude mixture was purified by flash column chromatography on silica gel (Hexane: EtOAc = 300: 1 as eluent) to afford **3ak** (19.5 mg, 36% yield) as a yellow liquid.

^{1}H NMR (400 MHz, $CDCl_3$): δ= 7.54 – 7.49 (m, 2H), 7.32– 7.27(m, 2H), 5.32 – 5.25 (m, 1H), 5.07 – 4.99 (m, 1H), 3.64 – 3.59 (m, 2H), 2.12 – 1.98 (m, 4H), 1.69 (s, 3H), 1.66 (s, 3H), 1.59 (s, 3H) ppm.

^{13}C{^{1}H} NMR (101 MHz, $CDCl_3$): δ= 145.3, 141.4, 132.1, 131.9, 127.2, 123.6, 119.0, 117.8, 108.1, 39.5, 30.5, 26.3, 25.7, 17.7, 16.3 ppm.

HRMS (ESI): calculated for $C_{17}H_{21}NNaS$ [M+Na$^+$]: 294.1287, found 294.1290.

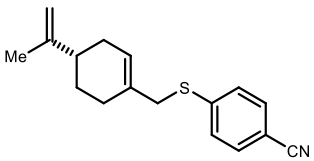

(S)-4-(((4-(Prop-1-en-2-yl)cyclohex-1-en-1-yl)methyl)thio)benzonitrile (3al): Synthesized according to the General Procedure **A** using (S)-(4-(prop-1-en-2-yl)cyclohex-1-en-1-yl)methanol (30.5 mg, 0.2 mmol, 1.0 equiv.), 1,1,3,3-tetramethylthiourea (79.5 mg, 0.6 mmol, 3.0 equiv.) and 4-chlorobenzonitrile (82.5 mg, 0.6 mmol, 3.0 equiv.). The crude mixture was purified by

flash column chromatography on silica gel (Hexane: EtOAc = 300: 1 as eluent) to afford **3al** (28.0 mg, 52% yield) as a yellow liquid.

^{1}H NMR (400 MHz, $CDCl_3$): δ= 7.53 – 7.49 (m, 2H), 7.33 – 7.29 (m, 2H), 5.74 – 5.70 (m, 1H), 4.74 – 4.70 (m, 1H), 4.69 – 4.66(m, 1H), 3.57 (s, 2H), 2.19 – 2.06 (m, 4H), 2.00 – 1.88 (m, 1H), 1.88 – 1.80 (m, 1H), 1.73 – 1.71 (m, 3H), 1.53 – 1.42 (m, 1H) ppm.

^{13}C{^{1}H} NMR (101 MHz, $CDCl_3$): δ= 149.3, 145.1, 132.1, 131.7, 127.6, 126.0, 119.0, 108.9, 108.3, 40.6, 39.9, 30.7, 27.8, 27.5, 20.8 ppm.

HRMS (ESI): calculated for $C_{17}H_{19}NNaS$ [M+Na^+]: 292.1130, found 292.1137.

4-(Hex-3-yn-1-ylthio)benzonitrile (3am): Synthesized according to the General Procedure

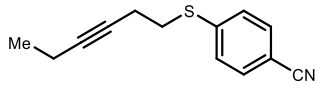

A using hex-3-yn-1-ol (19.6 mg, 0.2 mmol, 1.0 equiv.), 1,1,3,3-tetramethylthiourea (79.5 mg, 0.6 mmol, 3.0 equiv.) and 4-chlorobenzonitrile (82.5 mg, 0.6 mmol, 3.0 equiv.). The crude mixture was purified by flash column chromatography on silica gel (Hexane: EtOAc = 200: 1 as eluent) to afford **3am** (31.0 mg, 72% yield) as a yellow liquid.

^{1}H NMR (400 MHz, $CDCl_3$): δ= 7.55 – 7.49 (m, 2H), 7.35 – 7.29 (m, 2H), 3.11 (t, *J* = 7.5 Hz, 2H), 2.55 – 2.48 (m, 2H), 2.19 – 2.10 (m, 2H), 1.09 (t, *J* = 7.5 Hz, 3H) ppm.

^{13}C{^{1}H} NMR (101 MHz, $CDCl_3$): δ= 144.2, 132.3, 127.2, 118.8, 108.5, 84.0, 76.5, 31.5, 19.4, 14.0, 12.4 ppm.

HRMS (ESI): calculated for $C_{13}H_{13}NNaS$ [M+Na^+]: 238.0661, found 238.0655.

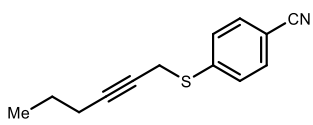

4-(Hex-2-yn-1-ylthio)benzonitrile (3an): Synthesized according to the General Procedure **A** using hex-2-yn-1-ol (19.6 mg, 0.2 mmol, 1.0 equiv.), 1,1,3,3-tetramethylthiourea (79.5 mg, 0.6 mmol, 3.0 equiv.) and 4-chlorobenzonitrile (82.5 mg, 0.6 mmol, 3.0 equiv.). The crude mixture was purified by flash column chromatography on silica gel (Hexane: EtOAc = 300: 1 as eluent) to afford **3an** (13.0 mg, 30% yield) as a yellow liquid.

^{1}H NMR (400 MHz, $CDCl_3$): δ= 7.58 – 7.53 (m, 2H), 7.44 – 7.39 (m, 2H), 3.70 (t, *J* = 2.4 Hz, 2H), 2.16 – 2.11 (m, 2H), 1.52 – 1.42 (m, 2H), 0.91 (t, *J* = 7.4 Hz, 3H) ppm.

^{13}C{^{1}H} NMR (101 MHz, $CDCl_3$): δ= 143.6, 132.2, 127.3, 118.7, 108.7, 84.8, 74.3, 22.0, 21.3, 20.7, 13.4 ppm.

HRMS (ESI): calculated for $C_{13}H_{13}NNaS$ [M+Na^+]: 238.0661, found 238.0653.

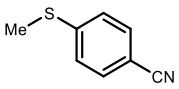

4-(Methylthio)benzonitrile (3ao): Synthesized according to the General Procedure **A** using methanol (6.5 mg, 0.2 mmol, 1.0 equiv.), 1,1,3,3-tetramethylthiourea (79.5 mg, 0.6 mmol, 3.0 equiv.) and 4-chlorobenzonitrile (82.5 mg, 0.6 mmol, 3.0 equiv.). The crude mixture was purified by flash column chromatography on silica gel (Hexane: EtOAc = 150: 1 as eluent) to afford **3ao** (27.0 mg, 90% yield) as a pale yellow liquid.

^{1}H NMR (400 MHz, $CDCl_3$): δ =7.54 – 7.49 (m, 2H), 7.27 – 7.23 (m, 2H), 2.50 (s, 3H) ppm.

^{13}C{^{1}H} NMR (101 MHz, $CDCl_3$): δ 146.1, 132.2, 125.5, 119.0, 107.7, 14.7 ppm. Matching reported literature data[34].

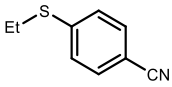

4-(Methylthio)benzonitrile (3ap): Synthesized according to the General Procedure **A** using ethanol (9.2 mg, 0.2 mmol, 1.0 equiv.), 1,1,3,3-tetramethylthiourea (79.5 mg, 0.6 mmol, 3.0 equiv.) and 4-chlorobenzonitrile (82.5 mg, 0.6 mmol, 3.0 equiv.). The crude mixture was purified by flash column chromatography on silica gel (Hexane: EtOAc = 150: 1 as eluent) to afford **3ap** (16.5 mg, 50% yield) as a yellow liquid.

^{1}H NMR (400 MHz, $CDCl_3$): δ= 7.55 – 7.49 (m, 2H), 7.31 – 7.27 (m, 2H), 3.01 (q, *J* = 7.4 Hz, 2H), 1.37 (t, *J* = 7.4 Hz, 3H) ppm.

^{13}C{^{1}H} NMR (101 MHz, $CDCl_3$): δ= 145.0, 132.2, 126.7, 119.0, 108.0, 26.0, 13.8 ppm. Matching reported literature data[35].

---

[34] Zhang, G.; Zhang, C.; Tian, Y.; Chen, F. "Fe-Catalyzed Direct Synthesis of Nitriles from Carboxylic Acids with Electron-Deficient *N*-Cyano-*N*-aryl–arylsulfonamide." *Org. Lett.* **2023**, 25, *6*, 917.

[35] Scattolin, T.; Senol, E.; Yin, G.; Guo, Q.; Schoenebeck, F. "Site-Selective C−S Bond Formation at C−Br over C−OTf and C−Cl Enabled by an Air-Stable, Easily Recoverable, and Recyclable Palladium(I) Catalyst." *Angew. Chem., Int. Ed*. **2018**, *57*, 12425 –12429.

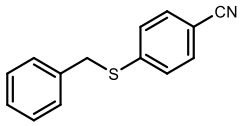

4-(Benzylthio)benzonitrile (3aq): Synthesized according to the General Procedure **A** using phenylmethanol (21.6 mg, 0.2 mmol, 1.0 equiv.), 1,1,3,3-tetramethylthiourea (79.5 mg, 0.6 mmol, 3.0 equiv.) and 4-chlorobenzonitrile (82.5 mg, 0.6 mmol, 3.0 equiv.). The crude mixture was purified by flash column chromatography on silica gel (Hexane: EtOAc = 100: 1 as eluent) to afford **3aq** (29.0 mg, 64% yield) as a yellow liquid.

^{1}H NMR (400 MHz, $CDCl_3$): δ= 7.52 – 7.47 (m, 2H), 7.39– 7.26 (m, 7H), 4.2 (s, 2H) ppm.

^{13}C{^{1}H} NMR (101 MHz, $CDCl_3$): δ= 144.5, 135.8, 132.2, 128.8, 128.7, 127.7, 127.4, 118.8, 108.6, 37.1 ppm.

HRMS (ESI): calculated for $C_{14}H_{11}NNaS$ [M+Na^+]: 248.0504, found 248.0509.

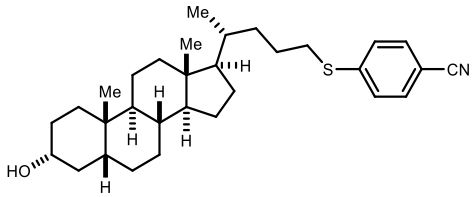

4-(((4R)-4-((3R,5R,8R,9S,10S,13R)-3-Hydroxy-10,13-dimethylhexadecahydro-1H-cyclopenta[a]phenanthren-17-yl)pentyl)thio)benzonitrile (3ar): Synthesized according to the General Procedure **A** using (3R,5R,8R,9S,10S,13R)-17-((R)-5-hydroxypentan-2-yl)-10,13-dimethylhexadecahydro-1H-cyclopenta[a]phenanthren-3-ol (72.5 mg, 0.2 mmol, 1.0 equiv.), 1,1,3,3-tetramethylthiourea (79.5 mg, 0.6 mmol, 3.0 equiv.) and 4-chlorobenzonitrile (82.5 mg, 0.6 mmol, 3.0 equiv.). The crude mixture was purified by flash column chromatography on silica gel (DCM as eluent) to afford **3ar** (28.0 mg, 30% yield) as a yellow liquid.

^{1}H NMR (400 MHz, $CDCl_3$): δ= 7.55 – 7.49 (m, 2H), 7.30 – 7.27 (m, 2H), 3.66 – 3.58 (m, 1H), 3.01 – 2.86 (m, 2H), 1.98 – 1.92 (m, 1H), 1.88 – 1.72 (m, 5H), 1.60 – 1.52 (m, 6H), 1.43 – 1.35 (m, 6H), 1.30 – 1.15 (m, 5H), 1.12 – 1.02 (m, 4H), 1.00 – 0.86 (m, 1H), 0.94 – 0.89 (m, 6H), 0.64 (s, 3H) ppm.

^{13}C{^{1}H} NMR (101 MHz, $CDCl_3$): δ= 145.4, 132.2, 126.7, 119.0, 107.9, 71.9, 56.5, 56.1, 42.7, 42.1, 40.5, 40.2, 36.5, 35.9, 35.5, 35.4, 35.2, 34.6, 32.4, 30.6, 28.3, 27.2, 26.4, 25.3, 24.2, 23.4, 20.8, 18.6, 12.1 ppm.

HRMS (ESI): calculated for $C_{31}H_{45}NNaOS$ [M+Na^+]: 502.3114, found 502.3127.

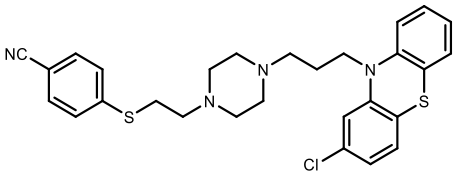

4-((2-(4-(3-(2-Chloro-10H-phenothiazin-10-yl)propyl)piperazin-1-yl)ethyl)thio)benzonitrile (3as): Synthesized according to the General Procedure **A** using 2-(4-(3-(2-chloro-10H-phenothiazin-10-yl)propyl)piperazin-1-yl)ethan-1-ol (81.0 mg, 0.2 mmol, 1.0 equiv.), 1,1,3,3-tetramethylthiourea (79.5 mg, 0.6 mmol, 3.0 equiv.) and 4-chlorobenzonitrile (82.5 mg, 0.6 mmol, 3.0 equiv.). The crude mixture was purified by flash column chromatography on silica gel (EtOAc as eluent) to afford **3as** (73.0 mg, 72% yield) as a yellow liquid.

^{1}H NMR (400 MHz, $CDCl_3$): δ= 7.54 – 7.48 (m, 2H), 7.32 – 7.28 (m, 2H), 7.18 – 7.09 (m, 2H), 7.03 – 6.99 (m, 1H), 6.98 – 6.82 (m, 4H), 3.90 (t, *J* = 6.7 Hz, 2H), 3.13 – 3.05 (m, 2H), 2.70 – 2.63 (m, 2H), 2.62 – 2.28 (m, 10H), 2.00 – 1.87 (m, 2H) ppm.

^{13}C{^{1}H} NMR (101 MHz, $CDCl_3$): δ= 146.5, 144.7, 144.5, 133.2, 132.3, 127.9, 127.5, 127.4, 126.9, 124.9, 123.6, 123.0, 122.3, 118.9, 115.9, 115.9, 108.3, 56.7, 55.4, 53.1, 52.8, 45.2, 29.4, 24.0 ppm.

HRMS (ESI): calculated for $C_{28}H_{30}ClN_4S_2$ [M+H$^+$]: 521.1595, found 521.1600.

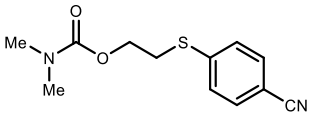

2-((4-Cyanophenyl)thio)ethyl dimethylcarbamate (3at): Synthesized according to the General Procedure **A** using ethane-1,2-diol (12.5 mg, 0.2 mmol, 1.0 equiv.), 1,1,3,3-tetramethylthiourea (79.5 mg, 0.6 mmol, 3.0 equiv.) and 4-chlorobenzonitrile (82.5 mg, 0.6 mmol, 3.0 equiv.). The crude mixture was purified by flash column chromatography on silica gel (Hexane: EtOAc = 20: 1 as eluent) to afford **3at** (40.5 mg, 90% yield) as a yellow solid.

^{1}H NMR (400 MHz, $CDCl_3$): δ= 7.56 – 7.50 (m, 2H), 7.42 – 7.36 (m, 2H), 4.26 (t, *J* = 6.9 Hz, 2H), 3.23 (t, *J* = 6.9 Hz, 2H), 2.89 (s, 3H), 2.82 (s, 3H) ppm.

^{13}C{^{1}H} NMR (101 MHz, $CDCl_3$): δ= 156.1, 143.7, 132.4, 127.1, 118.8, 108.6, 63.2, 36.5, 35.9, 30.8 ppm.

HRMS (ESI): calculated for $C_{12}H_{14}N_2NaO_2S$ [M+Na$^+$]: 273.0668, found 273.0662.

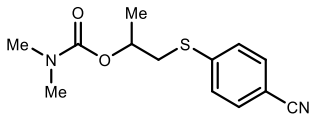

1-((4-Cyanophenyl)thio)propan-2-yl dimethylcarbamate (3au): Synthesized according to the General Procedure **A** using propane-1,2-diol (15.2 mg, 0.2 mmol, 1.0 equiv.), 1,1,3,3-tetramethylthiourea (79.5 mg, 0.6 mmol, 3.0 equiv.) and 4-chlorobenzonitrile (82.5 mg, 0.6 mmol, 3.0 equiv.). The crude mixture was purified by flash column chromatography on silica gel (Hexane: EtOAc = 20: 1 as eluent) to afford **3au** (39.0 mg, 74% yield) as a yellow solid.

^{1}H NMR (400 MHz, $CDCl_3$): δ= 7.55 – 7.48 (m, 2H), 7.44 – 7.39 (m, 2H), 5.01 – 4.91 (m, 1H), 3.31 (dd, *J* = 13.7, 5.3 Hz, 1H), 3.02 (dd, *J* = 13.8, 6.9 Hz, 1H), 2.88 (s, 3H), 2.79 (s, 3H), 1.36 (d, *J* = 6.3 Hz, 3H) ppm.

^{13}C{^{1}H} NMR (101 MHz, $CDCl_3$): δ= 155.8, 144.2, 132.3, 127.1, 118.8, 108.4, 69.8, 37.3, 36.4, 35.8, 19.4 ppm.

HRMS (ESI): calculated for $C_{13}H_{16}N_2NaO_2S$ [M+Na^+]: 287.0825, found 287.0824.

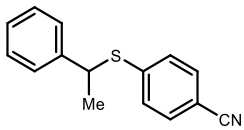

4-((1-Phenylethyl)thio)benzonitrile (3av): Synthesized according to the General Procedure **A** using 1-phenylethan-1-ol (24.4 mg, 0.2 mmol, 1.0 equiv.), 1,1,3,3-tetramethylthiourea (79.5 mg, 0.6 mmol, 3.0 equiv.) and 4-chlorobenzonitrile (82.5 mg, 0.6 mmol, 3.0 equiv.). The crude mixture was purified by flash column chromatography on silica gel (Hexane: EtOAc = 100: 1 as eluent) to afford **3av** (9.6 mg, 20% yield) as a yellow liquid.

^{1}H NMR (400 MHz, $CDCl_3$): δ= 7.47 – 7.42 (m, 2H), 7.39 – 7.34 (m, 2H), 7.33 – 7.27 (m, 3H), 7.28 – 7.21 (m, 2H), 4.50 (q, *J* = 7.0 Hz, 1H), 1.67 (d, *J* = 7.0 Hz, 3H) ppm.

^{13}C{^{1}H} NMR (101 MHz, $CDCl_3$): δ= 143.5, 142.2, 132.1, 129.4, 128.8, 127.6, 127.1, 118.8, 109.1, 46.6, 22.8 ppm.

HRMS (ESI): calculated for $C_{15}H_{13}NNaS$ [M+Na^+]: 262.0661, found 262.0668.

Unsuccessful Substrates

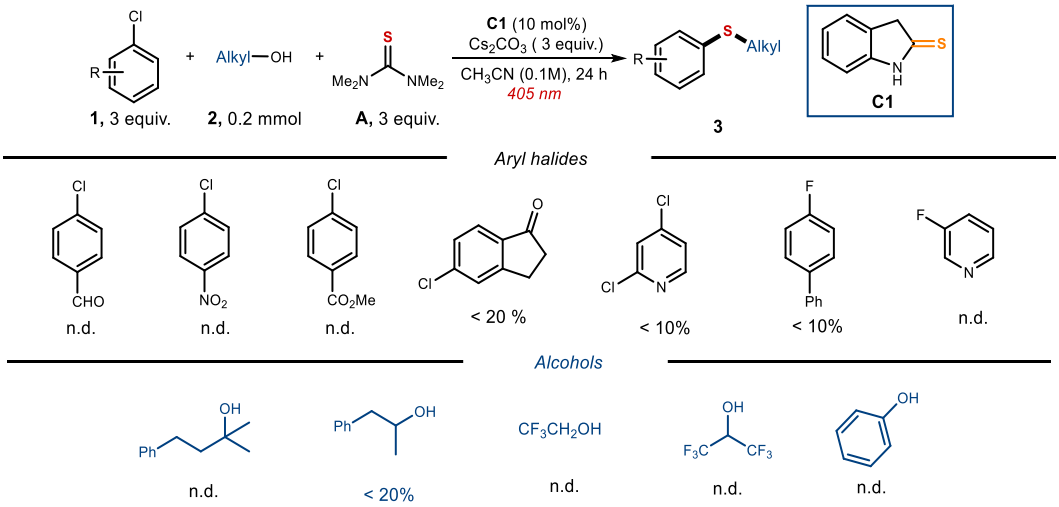

Figure 4.23. Unsuccessful aryl halides and alcohols, n.d. = product not detected

Other aryl halides as precursors

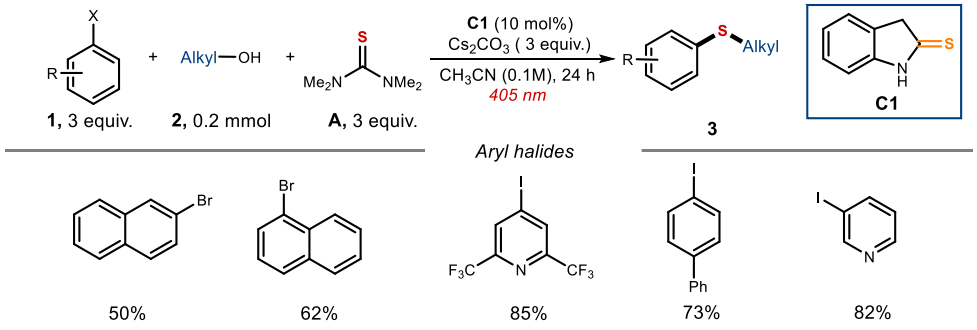

Figure 4.24. Reactivity of aryl bromides and iodides

4.6.4 Characterization of Products from electron-rich Aryl Halides

Optimization Studies

Table 4.3. Optimization of the thioetherification using **C3** as photoreductant

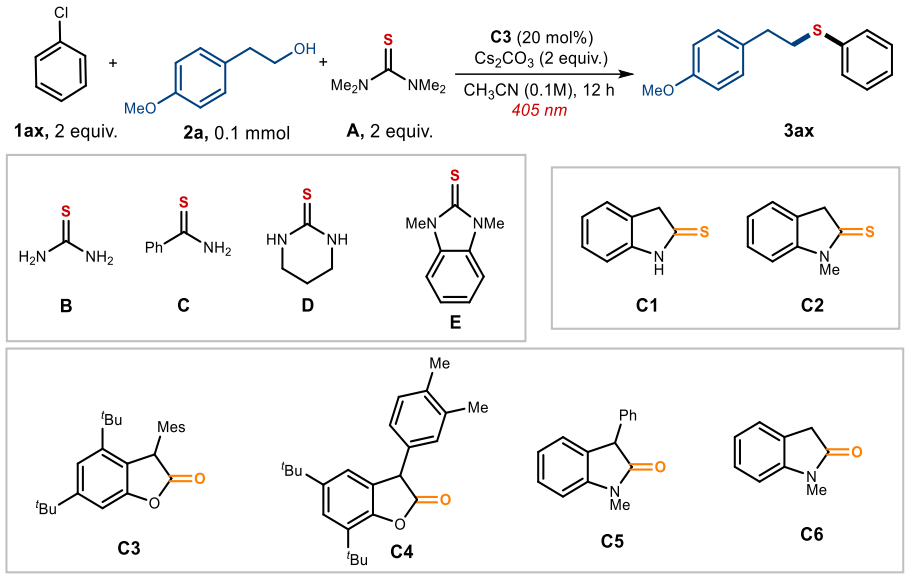

Entry	Deviations	Yield of 3ax
1	none	35%
2	No light or No base or No **C3**	0%
3	**E**	5%
4	**B-D**	0%
5	DMSO, DMF, Acetone as solvent	0%
6	$KHCO_3$, K_2CO_3, K_3PO_4, TMG as base	0%
7	**C1** or **C2** (5 mol%) as photocatalyst	5%
8	With TEMPO	0%
9	**C2** (10 mol%) as photocatalyst	5%
10	**C6** (10 mol%) as photocatalyst	0%
11	**C5** (10 mol%) as photocatalyst	10%

12	**C4** (10 mol%), 3 equiv. PhCl	15%
13	**C3** (10 mol%), 3 equiv. PhCl	20%
14	**C3** (20 mol%), 3 equiv. PhCl	45%
15	**C3** (40 mol%), 3 equiv. PhCl	60%
16	**C3** (40 mol%), 5 equiv. PhCl	70% [a]

All reactions were performed on a 0.1 mmol scale; yield of **3az** determined by ^{1}H NMR analysis of the crude reaction mixture by comparison with 1,3,5-trimethoxybenzene as internal standard. [a] isolated yield. Mes: mesityl.

General Procedure B for neutral and electron-rich aryl halides

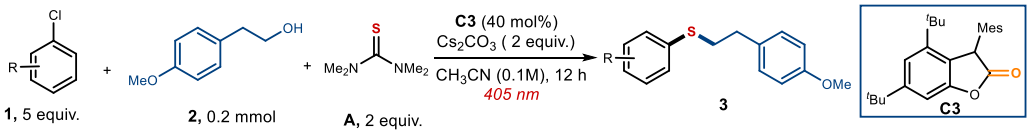

To a 7 mL glass vial, **C3** (29.5 mg, 0.08 mmol, 0.4 equiv.), cesium carbonate (130.0 mg, 0.4 mmol, 2 equiv.), 1,1,3,3-tetramethylthiourea **A** (53.0 mg, 0.4 mmol, 2.0 equiv.), alcohol **2** (30.5 mg, 0.2 mmol, 1 equiv.) and aryl chlorides **1** (if solid, 0.6 mmol, 5 equiv.) were sequentially added. The vial was sealed with a screw-top cap with septum and then vacuumed and backfilled with argon for 3 times. Afterwards, aryl chlorides **1** (if liquid, 0.6 mmol, 5 equiv.) followed by argon-sparged acetonitrile (0.1 M, 2.0 mL) were added *via* syringe. The vial was sealed with Parafilm and then stirred under 405 nm for 24 hours using ***Set-up 1*** detailed in Figure 4.21. After completion of the reaction, column chromatography purification afforded the corresponding products **3** with the reported yields

4.6.5 Characterization of Products from electron-neutral and rich aryl halides

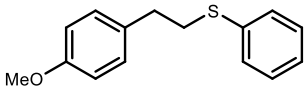

(4-Methoxyphenethyl)(phenyl)sulfane (3aw): Synthesized according to the General Procedure **B** using 2-(4-methoxyphenyl)ethan-1-ol (30.5 mg, 0.2 mmol, 1.0 equiv.), 1,1,3,3-tetramethylthiourea

(54.0 mg, 0.4 mmol, 2.0 equiv.) and chlorobenzene (112.5 mg, 1.0 mmol, 5.0 equiv.) or bromobenzene (157.0 mg, 1.0 mmol, 5.0 equiv.). The crude mixture was purified by flash column chromatography on silica gel (Hexane: EtOAc = 300: 1 as eluent) to afford **3aw** (34.0 mg, 70% yield with chlorobenzene and 33.2 mg, 68% yield with bromobenzene) as a yellow liquid.

^{1}H NMR (400 MHz, $CDCl_3$): δ= 7.39 – 7.34 (m, 2H), 7.33 – 7.27 (m, 2H), 7.22 – 7.17 (m, 1H), 7.15 – 7.10 (m, 2H), 6.88 – 6.83 (m, 2H), 3.80 (s, 3H), 3.18 – 3.11 (m, 2H), 2.91 – 2.85 (m, 2H) ppm.

^{13}C{^{1}H} NMR (101 MHz, $CDCl_3$): δ= 158.3, 136.5, 132.3, 129.5, 129.2, 128.9, 125.9, 114.0, 55.3, 35.4, 34.8 ppm.

Matching reported literature data[36].

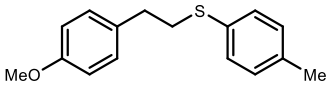

(4-Methoxyphenethyl)(p-tolyl)sulfane (3ax): Synthesized according to the General Procedure **B** using 2-(4-methoxyphenyl)ethan-1-ol (30.5 mg, 0.2 mmol, 1.0 equiv.), 1,1,3,3-tetramethylthiourea (54.0 mg, 0.4 mmol, 2.0 equiv.) and 1-chloro-4-methylbenzene (126.6 mg, 1.0 mmol, 5.0 equiv.). The crude mixture was purified by flash column chromatography on silica gel (Hexane: EtOAc = 300: 1 as eluent) to afford **3ax** (33.2 mg, 64% yield) as a yellow liquid.

^{1}H NMR (400 MHz, $CDCl_3$): δ= 7.31 – 7.27 (m, 2H), 7.15 – 7.08 (m, 4H), 6.87 – 6.82 (m, 2H), 3.80 (s, 3H), 3.13 – 3.08 (m, 2H), 2.88 – 2.82 (m, 2H), 2.34 (s, 3H) ppm.

^{13}C{^{1}H} NMR (101 MHz, $CDCl_3$): δ= 158.2, 136.2, 132.6, 132.5, 130.1, 129.7, 129.5, 113.9, 55.3, 36.1, 34.9, 21.0 ppm.

Matching reported literature data[37].

[36] Yang, Y.-Z.; Li, Y.; Lv, G.-F.; He, D.-L.; Li, J.-H. "Nickel-Catalyzed C-S Reductive Cross-Coupling of Alkyl Halides with Arylthiosilanes toward Alkyl Aryl Thioethers." *Org. Lett.* **2022**, *24*, 5115−5119.

[37] Huang, Y.; Xin, Z.; Yao, W.; Hu, Q.; Li, Z.; Xiao, L.; Yang, B.; Zhang, J. A Recyclable Self-Assembled Composite Catalyst Consisting of Fe_3O_4-Rose bengal-Layered Double Hydroxides for Highly Efficient Visible Light Photocatalysis in Water. *Chem. Commun.* **2018**, *54*, 13587–13590.

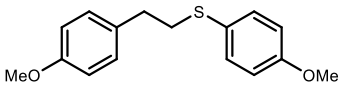

(4-Methoxyphenethyl)(4-methoxyphenyl)sulfane (3ay): Synthesized according to the General Procedure **B** using 2-(4-methoxyphenyl)ethan-1-ol (30.5 mg, 0.2 mmol, 1.0 equiv.), 1,1,3,3-tetramethylthiourea (54.0 mg, 0.4 mmol, 2.0 equiv.) and 1-chloro-4-methoxybenzene (142.5 mg, 1.0 mmol, 5.0 equiv.). The crude mixture was purified by flash column chromatography on silica gel (Hexane: EtOAc = 100: 1 as eluent) to afford **3ay** (31.0 mg, 56% yield) as a yellow liquid.

^{1}H NMR (400 MHz, $CDCl_3$): δ= 7.39 – 7.34 (m, 2H), 7.11 – 7.06 (m, 2H), 6.89 – 6.80 (m, 4H), 3.81 (s, 3H), 3.79 (s, 3H), 3.13 – 3.08 (m, 2H), 2.85 – 2.78 (m, 2H) ppm.

^{13}C{^{1}H} NMR (101 MHz, $CDCl_3$): δ= 158.9, 158.2, 133.2, 132.5, 129.5, 126.4, 114.6, 113.9, 55.4, 55.3, 37.5, 35.0 ppm.

HRMS(APCI): calculated for $C_{16}H_{18}O_2S$ [M^+]: 274.1022, found 274.1021.

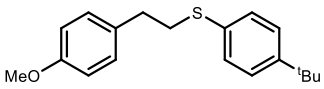

(4-(Tert-butyl)phenyl)(4-methoxyphenethyl)sulfane (3az): Synthesized according to the General Procedure B using 2-(4-methoxyphenyl)ethan-1-ol (30.5 mg, 0.2 mmol, 1.0 equiv.), 1,1,3,3-tetramethylthiourea (54.0 mg, 0.4 mmol, 2.0 equiv.) and 1-(tert-butyl)-4-chlorobenzene (168.5 mg, 1.0 mmol, 5.0 equiv.). The crude mixture was purified by flash column chromatography on silica gel (Hexane: EtOAc = 300: 1 as eluent) to afford **3az** (36.5 mg, 60% yield) as a yellow liquid.

^{1}H NMR (400 MHz, $CDCl_3$): δ= 7.35 – 7.28 (m, 4H), 7.15 – 7.10 (m, 2H), 6.87 – 6.82 (m, 2H), 3.80 (s, 3H), 3.79 (s, 3H), 3.15 – 3.09 (m, 2H), 2.90 – 2.84 (m, 2H), 1.32 (s, 9H) ppm.

^{13}C{^{1}H} NMR (101 MHz, $CDCl_3$): δ= 158.2, 149.3, 132.8, 132.5, 129.5, 129.4, 126.0, 113.9, 55.3, 35.8, 34.9, 34.5, 31.3 ppm.

HRMS (ESI): calculated for $C_{19}H_{24}NaOS$ [M+Na^+]: 323.1440, found 323.1445.

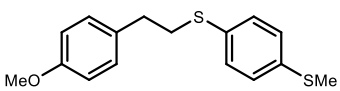

(4-Methoxyphenethyl)(4-(methylthio)phenyl)sulfane (3ba): Synthesized according to the General Procedure **B** using 2-(4-methoxyphenyl)ethan-1-ol (30.5 mg, 0.2

mmol, 1.0 equiv.), 1,1,3,3-tetramethylthiourea (54.0 mg, 0.4 mmol, 2.0 equiv.) and (4-chlorophenyl)(methyl)sulfane (158.5 mg, 1.0 mmol, 5.0 equiv.). The crude mixture was purified by flash column chromatography on silica gel (Hexane: EtOAc = 300: 1 as eluent) to afford **3bb** (31.4 mg, 54% yield) as a yellow liquid.

^{1}H NMR (400 MHz, $CDCl_3$): δ= 7.31 – 7.27 (m, 2H), 7.22 – 7.17 (m, 2H), 7.13 – 7.08 (m, 2H), 6.86 – 6.81 (m, 2H), 3.79 (s, 3H), 3.13 – 3.07 (m, 2H), 2.88 – 2.82 (m, 2H), 2.48 (s, 3H).

^{13}C NMR (101 MHz, $CDCl_3$) δ 158.2, 136.5, 132.8, 132.3, 130.5, 129.5, 127.3, 113.9, 55.3, 36.0, 34.8, 16.1.

HRMS(APCI): calculated for $C_{16}H_{18}OS_2$ [M^+]: 290.0794, found 290.0791.

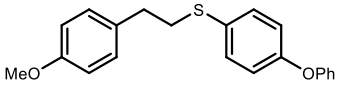

(4-Methoxyphenethyl)(4-phenoxyphenyl)sulfane (3bb): Synthesized according to the General Procedure **B** using 2-(4-methoxyphenyl)ethan-1-ol (30.5 mg, 0.2 mmol, 1.0 equiv.), 1,1,3,3-tetramethylthiourea (54.0 mg, 0.4 mmol, 2.0 equiv.) and 1-chloro-4-phenoxybenzene (204.5 mg, 1.0 mmol, 5.0 equiv.). The crude mixture was purified by flash column chromatography on silica gel (Hexane: EtOAc = 200: 1 as eluent) to afford **3bb** (48.0 mg, 71% yield) as a pale yellow liquid.

^{1}H NMR (400 MHz, $CDCl_3$): δ= 7.39 – 7.32 (m, 4H), 7.16 – 7.09 (m, 3H), 7.05 – 7.01 (m, 2H), 6.99 – 6.94 (m, 2H), 6.88 – 6.82 (m, 2H), 3.80 (s, 3H), 3.13 – 3.07 (m, 2H), 2.90 – 2.84 (m, 2H) ppm.

^{13}C NMR (101 MHz, $CDCl_3$): δ= 158.2, 157.0, 156.3, 132.3, 132.2, 130.0, 129.8, 129.5, 123.5, 119.4, 119.0, 113.9, 55.3, 36.8, 34.9 ppm.

HRMS (ESI): calculated for $C_{21}H_{20}NaO_2S$ [M+Na^+]: 359.1076, found 359.1074.

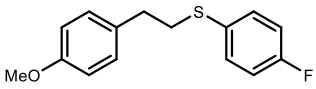

(4-Fluorophenyl)(4-methoxyphenethyl)sulfane (3bc): Synthesized according to the General Procedure **B** using 2-(4-methoxyphenyl)ethan-1-ol (30.5 mg, 0.2 mmol, 1.0 equiv.), 1,1,3,3-tetramethylthiourea (54.0 mg, 0.4 mmol, 2.0 equiv.) and 1-chloro-4-fluorobenzene (130.5 mg, 1.0 mmol, 5.0

equiv.). The crude mixture was purified by flash column chromatography on silica gel (Hexane: EtOAc = 300: 1 as eluent) to afford **3bc** (43.0 mg, 82% yield) as a pale yellow liquid.

^{1}H NMR (400 MHz, $CDCl_3$): δ= 7.39 – 7.33 (m, 2H), 7.12 – 7.07 (m, 2H), 7.05 – 6.97 (m, 2H), 6.87 – 6.81 (m, 2H), 3.79 (s, 3H), 3.12 – 3.06 (m, 2H), 2.88 – 2.81 (m, 2H) ppm.

^{13}C{^{1}H} NMR (101 MHz, $CDCl_3$): δ= 161.8 (d, *J* = 246.1 Hz), 158.3, 132.3(d, *J* = 8.1 Hz), 132.2, 131.2(d, *J* = 4.0 Hz), 129.5, 116.0 (d, *J* = 22.2 Hz), 113.9, 55.3, 36.8, 34.8 ppm.

^{19}F{^{1}H} NMR (376 MHz, $CDCl_3$): δ= -115.8 ppm.

HRMS(APCI): calculated for $C_{15}H_{15}FOS$ [M^+]: 262.0822, found 262.0826.

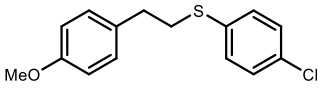

(4-Chlorophenyl)(4-methoxyphenethyl)sulfane (3bd): Synthesized according to the General Procedure **B** using 2-(4-methoxyphenyl)ethan-1-ol (30.5 mg, 0.2 mmol, 1.0 equiv.), 1,1,3,3-tetramethylthiourea (54.0 mg, 0.4 mmol, 2.0 equiv.) and 1-bromo-4-chlorobenzene (191.5 mg, 1.0 mmol, 5.0 equiv.). The crude mixture was purified by flash column chromatography on silica gel (Hexane: EtOAc = 200: 1 as eluent) to afford **3bd** (27.9 mg, 50% yield) as a yellow liquid.

^{1}H NMR (400 MHz, $CDCl_3$): δ= 7.29 – 7.24 (m, 4H), 7.13 – 7.08 (m, 2H), 6.87 – 6.82 (m, 2H), 3.79 (s, 3H), 3.14 – 3.09 (m, 2H), 2.89 – 2.83 (m, 2H) ppm.

^{13}C{^{1}H} NMR (101 MHz, $CDCl_3$): δ= 158.3, 135.0, 132.0, 131.9, 130.5, 129.5, 129.0, 114.0, 55.3, 35.7, 34.6 ppm.

HRMS (ESI): calculated for $C_{15}H_{15}ClNaO_2S$ [$M+Na^+$]: 317.0373, found 317.0365.

Note: The product may have oxidized upon storage, as only the mono-oxidized form of the product by HRMS. When freshly prepared product was analyzed, the molecule peak can be detected by GC-MS (calculated: 278.0, found 277.9).

(4-Methoxyphenethyl)(4-(trifluoromethyl)phenyl)sulfane (3be): Synthesized according to the General Procedure **B** using 2-(4-methoxyphenyl)ethan-1-ol (30.5 mg, 0.2 mmol, 1.0 equiv.), 1,1,3,3-tetramethylthiourea (54.0 mg, 0.4 mmol, 2.0 equiv.) and 1-chloro-4-

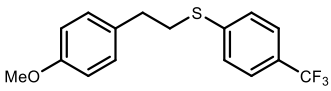

(trifluoromethyl)benzene (180.5 mg, 1.0 mmol, 5.0 equiv.). The crude mixture was purified by flash column chromatography on silica gel (Hexane: EtOAc = 200: 1 as eluent) to afford **3be** (34.0 mg, 54% yield) as a pale yellow liquid.

^{1}H NMR (400 MHz, $CDCl_3$): δ= 7.54 – 7.49 (m, 2H), 7.39 – 7.34 (m, 2H), 7.16 – 7.11 (m, 2H), 6.88 – 6.53 (m, 2H), 3.80 (s, 3H), 3.23 – 3.17 (m, 2H), 2.95 – 2.89 (m, 2H) ppm.

^{13}C{^{1}H} NMR (101 MHz, $CDCl_3$): δ= 158.4, 142.2, 131.8, 129.5, 127.5, 125.7 (q, *J* = 3.9 Hz). 124.2 (q, *J* = 273.7 Hz), 114.0, 55.3, 34.4, 34.3 ppm.

^{19}F{^{1}H} NMR (376 MHz, $CDCl_3$): δ= -62.5 ppm.

HRMS (ESI): calculated for $C_{16}H_{16}F_3OS$ [M+H$^+$]: 313.0868, found 313.0855.

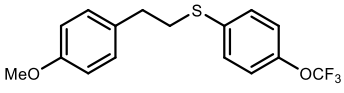

(4-Methoxyphenethyl)(4-(trifluoromethoxy)phenyl)sulfane (3bf): Synthesized according to the General Procedure **B** using 2-(4-methoxyphenyl)ethan-1-ol (30.5 mg, 0.2 mmol, 1.0 equiv.), 1,1,3,3-tetramethylthiourea (54.0 mg, 0.4 mmol, 2.0 equiv.) and 1-chloro-4-(trifluoromethoxy)benzene (196.5 mg, 1.0 mmol, 5.0 equiv.). The crude mixture was purified by flash column chromatography on silica gel (Hexane: EtOAc = 200: 1 as eluent) to afford **3bf** (37.0 mg, 56% yield) as a pale yellow liquid.

^{1}H NMR (400 MHz, $CDCl_3$): δ= 7.37 – 7.33 (m, 2H), 7.17 – 7.09 (m, 4H), 6.87 – 6.82 (m, 2H), 3.79 (s, 3H), 3.17 – 3.11 (m, 2H), 2.91 – 2.84 (m, 2H) ppm.

^{13}C{^{1}H} NMR (101 MHz, $CDCl_3$): δ= 158.3, 147.47 (q, *J* = 1.9 Hz), 135.4, 132.0, 130.5, 129.5, 121.6, 120.5 (q, *J* = 258.6 Hz), 114.0, 55.3, 36.7, 34.7 ppm.

^{19}F{^{1}H} NMR (376 MHz, $CDCl_3$): δ= -58.1 ppm.

HRMS (ESI): calculated for $C_{16}H_{16}F_3O_2S$ [M+H$^+$]: 329.0818, found 329.0804.

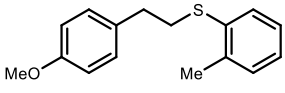

(4-Methoxyphenethyl)(p-tolyl)sulfane (3bg): Synthesized according to the General Procedure **B** using 2-(4-methoxyphenyl)ethan-1-ol (30.5 mg, 0.2 mmol, 1.0 equiv.), 1,1,3,3-tetramethylthiourea

(54.0 mg, 0.4 mmol, 2.0 equiv.) and 1-chloro-2-methylbenzene (126.5 mg, 1.0 mmol, 5.0 equiv.). The crude mixture was purified by flash column chromatography on silica gel (Hexane: EtOAc = 300: 1 as eluent) to afford **3bg** (33.5 mg, 65% yield) as a yellow liquid.

^{1}H NMR (400 MHz, $CDCl_3$): δ= 7.33 – 7.28 (m, 1H), 7.20 – 7.08 (m, 5H), 6.88 – 6.83 (m, 2H), 3.80 (s, 3H), 3.15 – 3.09 (m, 2H), 2.93 – 2.87 (m, 2H), 2.38 (s, 3H) ppm.

^{13}C{^{1}H} NMR (101 MHz, $CDCl_3$): δ= 158.2, 137.6, 135.8, 132.4, 130.1, 129.5, 127.8, 126.4, 125.6, 113.9, 55.3, 34.6, 20.4 ppm.

HRMS(APCI): calculated for $C_{16}H_{18}OS$ [M^+]: 258.1073, found 258.1076.

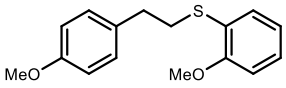

(4-Methoxyphenethyl)(2-methoxyphenyl)sulfane (3bh): Synthesized according to the General Procedure **B** using 2-(4-methoxyphenyl)ethan-1-ol (30.5 mg, 0.2 mmol, 1.0 equiv.), 1,1,3,3-tetramethylthiourea (54.0 mg, 0.4 mmol, 2.0 equiv.) and 1-chloro-2-methoxybenzene (142.6 mg, 1.0 mmol, 5.0 equiv.). The crude mixture was purified by flash column chromatography on silica gel (Hexane: EtOAc = 100: 1 as eluent) to afford **3bh** (36.5 mg, 66% yield) as a yellow liquid.

^{1}H NMR (400 MHz, $CDCl_3$): δ= 7.31 (dd, *J* = 7.7, 1.7 Hz, 1H), 7.23 – 7.17 (m, 1H), 7.16 – 7.11 (m, 2H), 6.97 – 6.91 (m, 1H), 6.88 – 6.82 (m, 3H), 3.90 (s, 3H), 3.79 (s, 3H), 3.15 – 3.08 (m, 2H), 2.91 – 2.85 (m, 2H) ppm.

^{13}C{^{1}H} NMR (101 MHz, $CDCl_3$): δ= 158.2, 157.4, 132.6, 129.5, 129.5, 127.2, 124.5, 121.1, 113.9, 110.5, 55.8, 55.3, 34.7, 33.8 ppm.

HRMS (ESI): calculated for $C_{16}H_{18}NaO_2S$ [M+Na^+]: 297.0920, found 297.0922.

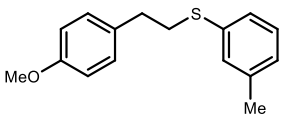

(4-Methoxyphenethyl)(p-tolyl)sulfane (3bi): Synthesized according to the General Procedure **B** using 2-(4-methoxyphenyl)ethan-1-ol (30.5 mg, 0.2 mmol, 1.0 equiv.), 1,1,3,3-tetramethylthiourea (54.0 mg, 0.4 mmol, 2.0 equiv.) and 1-chloro-3-methylbenzene (126.5 mg, 1.0 mmol, 5.0 equiv.). The crude mixture was purified by flash column chromatography on silica gel (Hexane: EtOAc = 300: 1 as eluent) to afford **3bi** (30.0 mg, 58% yield) as a yellow liquid.

^{1}H NMR (400 MHz, $CDCl_3$): δ= 7.22 – 7.10 (m, 5H), 7.02 – 6.98 (m, 1H), 6.87 – 6.82 (m, 2H), 3.80 (s, 3H), 3.16 – 3.11 (m, 2H), 2.91 – 2.84 (m, 2H), 2.33 (s, 3H) ppm.

^{13}C{^{1}H} NMR (101 MHz, $CDCl_3$): δ= 158.2, 138.7, 136.2, 132.4, 129.8, 129.5, 128.8, 126.8, 126.1, 113.9, 55.3, 35.4, 34.8, 21.4 ppm.

HRMS (APCI): calculated for $C_{16}H_{18}OS$ [M^+]: 258.1073, found 258.1079.

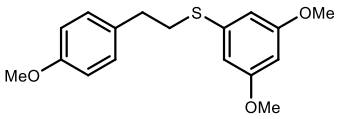

(3,5-Dimethoxyphenyl)(4-methoxyphenethyl)sulfane (3bj): Synthesized according to the General Procedure **B** using 2-(4-methoxyphenyl)ethan-1-ol (30.5 mg, 0.2 mmol, 1.0 equiv.), 1,1,3,3-tetramethylthiourea (54.0 mg, 0.4 mmol, 2.0 equiv.) and 1-chloro-3,5-dimethoxybenzene (172.5 mg, 1.0 mmol, 5.0 equiv.). The crude mixture was purified by flash column chromatography on silica gel (Hexane: EtOAc = 100: 1 as eluent) to afford **3bj** (26.8 mg, 44% yield) as a yellow liquid.

^{1}H NMR (400 MHz, $CDCl_3$): δ= 7.16 – 7.11 (m, 2H), 6.88 – 6.82 (m, 2H), 6.50 (d, *J* = 2.2 Hz, 2H), 6.29 (t, *J* = 2.2 Hz, 1H), 3.79 (s, 3H), 3.78 (s, 6H), 3.17 – 3.11 (m, 2H), 2.92 – 2.87 (m, 2H) ppm.

^{13}C{^{1}H} NMR (101 MHz, $CDCl_3$): δ= 161.0, 158.3, 138.6, 132.3, 129.5, 113.9, 106.5, 98.3, 55.4, 55.3, 35.0, 34.7 ppm.

HRMS (ESI): calculated for $C_{17}H_{21}O_3S$ [$M+H^+$]: 305.1206, found 305.1194.

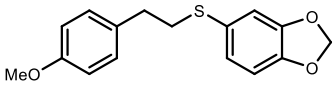

5-((4-Methoxyphenethyl)thio)benzo[d][1,3]dioxole (3bk): Synthesized according to the General Procedure **B** using 2-(4-methoxyphenyl)ethan-1-ol (30.5 mg, 0.2 mmol, 1.0 equiv.), 1,1,3,3-tetramethylthiourea (54.0 mg, 0.4 mmol, 2.0 equiv.) and 5-chlorobenzo[d][1,3]dioxole (156.5 mg, 1.0 mmol, 5.0 equiv.). The crude mixture was purified by flash column chromatography on silica gel (Hexane: EtOAc = 100: 1 as eluent) to afford **3bk** (32.5 mg, 56% yield) as a pale yellow liquid.

^{1}H NMR (400 MHz, $CDCl_3$): δ= 7.11 – 7.06 (m, 1H), 6.94 – 6.90 (m, 2H), 6.86 – 6.81 (m, 2H), 6.78 – 6.74 (m, 2H), 5.97 (s, 2H), 3.79 (s, 3H), 3.07 – 3.01(m, 2H), 2.86 – 2.79 (m, 2H)

ppm. **$^{13}C\{^{1}H\}$ NMR (101 MHz, $CDCl_3$)**: δ= 158.2, 148.0, 147.0, 132.3, 129.5, 128.1, 125.3, 113.9, 112.0, 108.7, 101.3, 55.3, 37.5, 34.9 ppm.

HRMS(APCI): calculated for $C_{16}H_{16}O_3S$ [M^+]: 288.0815, found 288.0816.

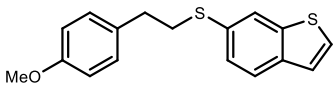

6-((4-Methoxyphenethyl)thio)benzo[b]thiophene (3bl): Synthesized according to the General Procedure **B** using 2-(4-methoxyphenyl)ethan-1-ol (30.5 mg, 0.2 mmol, 1.0 equiv.), 1,1,3,3-tetramethylthiourea (54.0 mg, 0.4 mmol, 2.0 equiv.) and 6-chlorobenzo[b]thiophene (168.5 mg, 1.0 mmol, 5.0 equiv.). The crude mixture was purified by flash column chromatography on silica gel (Hexane: EtOAc = 100: 1 as eluent) to afford **3bl** (26.0 mg, 43% yield) as a yellow liquid.

^{1}H NMR (400 MHz, $CDCl_3$): δ= 7.84 (d, *J* = 1.9 Hz, 1H), 7.82 – 7.78 (m, 1H), 7.46 (dd, J = 5.4, 0.5 Hz, 1H), 7.40 – 7.35 (m, 1H), 7.28 (dd, *J* = 5.5, 0.8 Hz, 1H), 7.14 – 7.09 (m, 2H), 6.86 – 6.81 (m, 2H), 3.79 (s, 3H), 3.21 – 3.15 (m, 2H), 2.91 – 2.85 (m, 2H) ppm.

$^{13}C\{^{1}H\}$ NMR (101 MHz, $CDCl_3$): δ= 158.2, 140.4, 138.0, 132.4, 131.9, 129.5, 127.4, 126.7, 125.2, 123.4, 122.8, 113.9, 55.3, 36.6, 34.9 ppm.

HRMS (ESI): calculated for $C_{17}H_{17}OS_2$ [M+H^+]: 301.0715, found 301.0706.

Unsuccessful Substrates

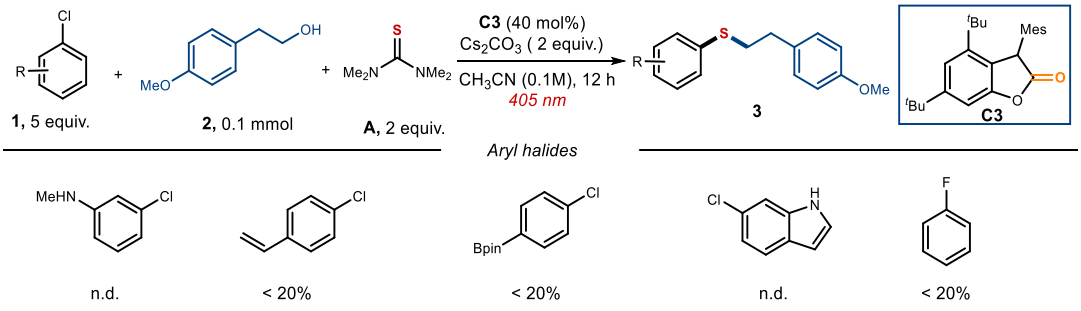

Figure 4.25. Unsuccessful aryl halides; n.d. = product not detected.

4.6.6 Reactivity Study of C1 and C3

Deprotonation Experiments for C1 and C3

- *Deprotonation of catalyst **C1**:*

To a 7 mL glass vial, catalyst **C1** (0.1 mmol, 1 equiv.) and cesium carbonate (0.3 mmol, 3 equiv.) were added. The vial was sealed with a screw-top cap with septum, then vacuumed and backfilled with argon for 3 times and CD_3CN (0.1 M) was added *via* syringe. The solution was stirred at ambient temperature for 10 min, transferred into an argon filled NMR tube *via* syringe and then the ^1H NMR spectrum was recorded (Figure 4.26).

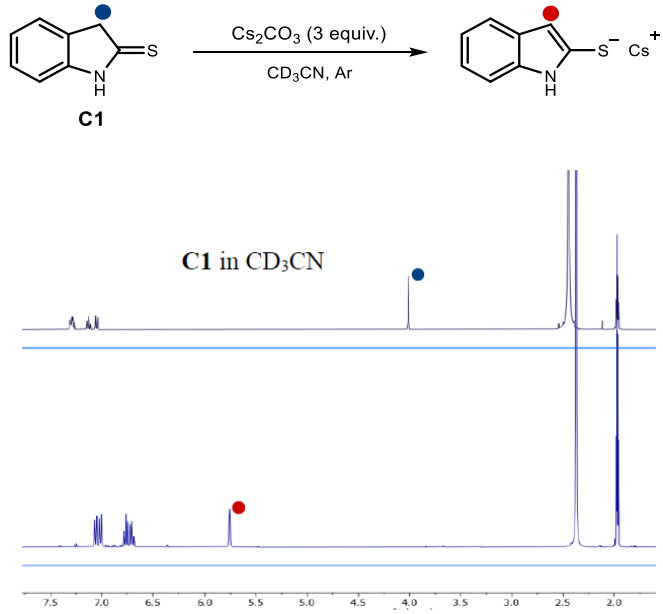

Figure 4.26. ^1H NMR analysis of catalyst **C1** before (*top*) and after (*bottom*) treatment with Cs_2CO_3.

*- Deprotonation of catalyst **C3**:*

To a 7 mL glass vial, catalyst **C3** (0.1 mmol, 1 equiv.) and cesium carbonate (0.3 mmol, 3 equiv.) or potassium *tert*-butoxide were added. The vial was sealed with a screw-top cap with septum, then vacuumed and backfilled with argon for 3 times and CD_3CN (0.1 M) were added *via* syringe. The solution was stirred at room temperature for 15 min or 1 h, transferred into an argon filled NMR tube *via* syringe and then the ^1H NMR spectrum was recorded (Figure 4.27 and 4.28).

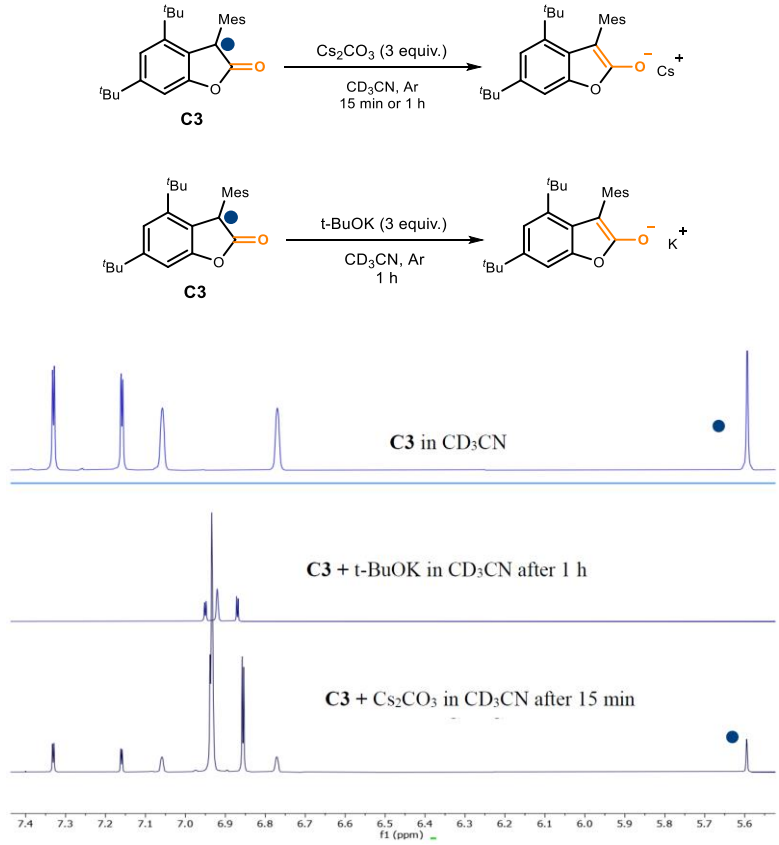

Figure 4.27. ^1H NMR analysis of catalyst **C1** before (*top*), after (*middle*) treatment with t-BuOK in 1 hour and after (*bottom*) treatment with Cs_2CO_3 in 15 min.

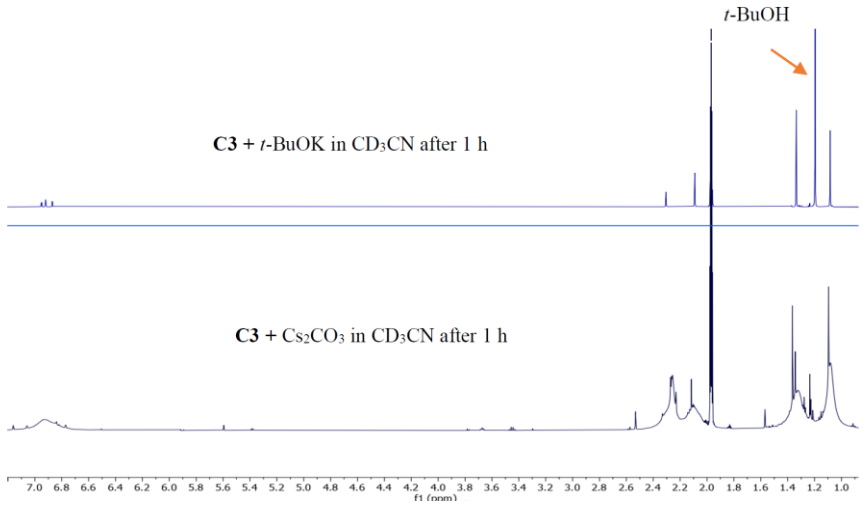

Figure 4.28. ^{1}H NMR analysis of catalyst **C1** after treatment with t-BuOK (*top*) and Cs_2CO_3 (*bottom*) in 1 hour.

Hydrodechlorination of Aryl Halides Catalyzed by C1 and C3

The reactivity of photocatalysts **C1** and **C3** in the hydrodechlorination of aryl halides were examined. [22c] The results in Figure 4.30 demonstrated the necessity of Cs_2CO_3 to deprotonate **C1** and **C3**, providing the active photoreductants.

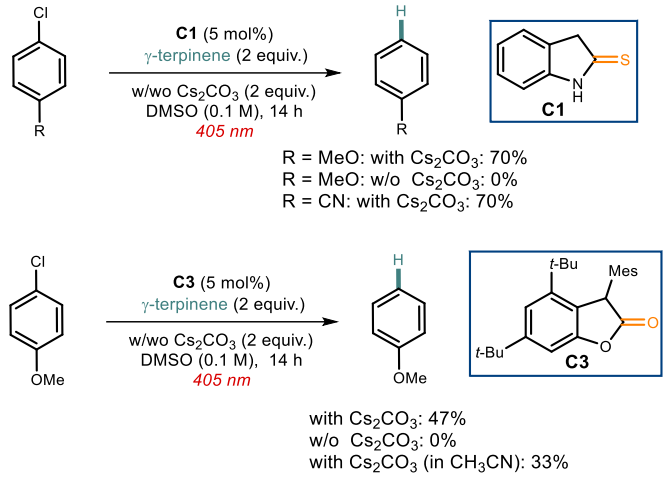

Figure 4.29. Effect of the base on the reactivity of catalysts **C1** and **C3** in the hydrodechlorination of aryl halides

4.6.7 Photophysical Studies

The photophysical properties of C2 have been presented in our previous reports[22c].

Sample Preparation:

- Neutral catalysts **C1** and **C3**

A 25 mL glass vial containing catalysts **C1** or **C3** (0.01 mmol) was sealed with a septum, vacuumed and backfilled with argon for 3 times, then degassed acetonitrile (5 mL, HPLC grade) was added via syringe to provide a 2 mM stock solution of catalyst. 20 µL of the stock solution were taken and diluted further with acetonitrile (4 mL) to obtain a 10 µM solution (200 µL were taken for a 0.1 mM solution). 2.5 mL of the solution was transferred into an argon filled quartz cuvette (10 x 10 mm light path) equipped with a septum.

- Deprotonated **C1** and **C3**

A 25 mL glass vial containing Cs_2CO_3 (130 mg) was sealed with a septum, vacuumed and backfilled with argon for 3 times, then degassed acetonitrile (8 mL, HPLC grade) was added via syringe. Addition of 40 µL of freshly prepared neutral **C1** or **C3** solution (2 mM) gave a

10 µM solution (400 µL were taken for a 0.1 mM solution). The vial was sealed with Parafilm and stirred at room temperature for 1 hour. 2.5 mL of the solution was transferred into an argon filled quartz cuvette (10 x 10 mm light path) equipped with a septum.

UV-visible Absorption Spectra

UV-Vis measurements were carried out on an Agilent Cary 60 UV-Vis spectrophotometer equipped with two silicon diode detectors, double beam optics and Xenon pulse light (Figure 4.30).

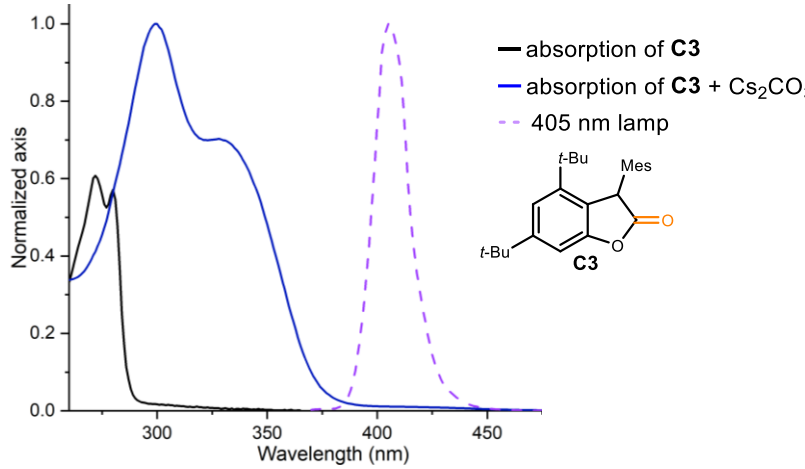

Figure 4.30. Normalized absorption spectra recorded for catalyst **C3** in CH_3CN, in absence (black line) or in presence (blue line) of Cs_2CO_3 in a 0.1 mM solution and 405 nm lamp spectrum (purple line).

Emission Spectra

Fluorescence measurements were carried out on an Fluorolog Horiba Jobin Yvon spectrofluorimeter equipped with a photomultiplier detector, a double monochromator, and a 450W xenon light source. The emission spectrum of the deprotonated **C1** and **C3** (formed in situ upon addition of Cs_2CO_3 in degassed CH_3CN) was recorded from 340 nm to 550 nm and 370 nm to 600 nm after excitation with 350 nm and 360 nm lasers respectively (Figure 4.31).

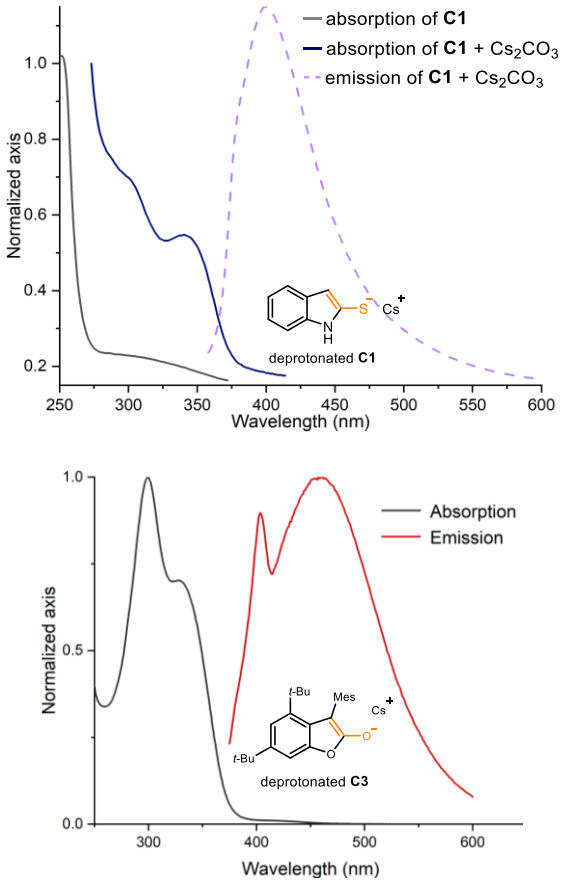

Figure 4.31. *left*) Normalized absorption of catalyst **C1**, absorption and emission spectra of the deprotonated **C1** (formed upon deprotonation with Cs_2CO_3) in CH_3CN in a 10 µM solution; *right*) Normalized absorption and emission spectra of the deprotonated catalyst **C3** (formed upon deprotonation with Cs_2CO_3 (3 equiv.)) in CH_3CN in a 0.1 mM solution.

Stern-Volmer Quenching Studies

Fluorescence measurements were carried out on an Fluorolog Horiba Jobin Yvon spectrofluorimeter equipped with a photomultiplier detector, a double monochromator, and a 450W xenon light source. A 1.0 M solution of the quencher substrate in degassed MeCN (HPLC grade) was prepared and 20 µL of this stock solution were added to the solution of the deprotonated catalyst. The addition of the substrate solution (the quencher) was repeated for four/five times. After each addition, the solution was mixed and the emission spectra of

the excited catalyst was acquired from 365 nm to 500 nm (the excitation wavelength was fixed at 350 nm, slit width = 5 nm). A solvent blank was subtracted from all the measurements. The excitation wavelength was chosen in order to avoid saturation of the emission detector.

The results shown in Figure 4.32 indicates that 4-chlorobenzonitrile quenched the excited state emission of the deprotonated catalyst **C1**. The Stern-Volmer plot shows a linear correlation between the amounts of substrates and the ratio I_0/I, following the relationship: $I_0/I = 1 + K_{SV}[Q]$ (Q = Quencher).

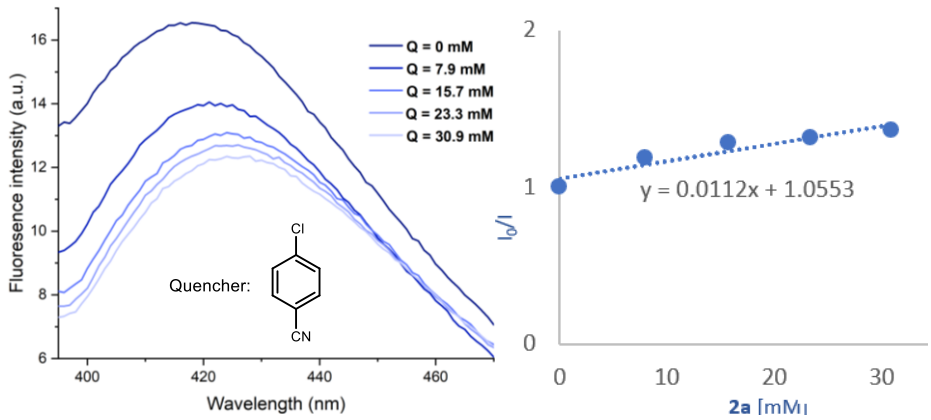

Figure 4.32. Stern-Volmer quenching studies with 4-chlorobenzonitrile (**1a**).

Quantum Yield Determination

-Experimental Setup

The experiments for the quantum yield determination were conducted under illumination by a 405 nm high-power single LED (setup depicted in Figure 4. 33), using an aluminum block on a 3D-printed holder, fitted with a 405 nm high-power single LED. The irradiance was fixed at 60±2 mW/cm^2, as controlled by an external power supply and measured using a photodiode light detector at the start of each reaction. This setup secured a reliable irradiation while keeping a distance of 1 cm between the reaction vessel and the light source.

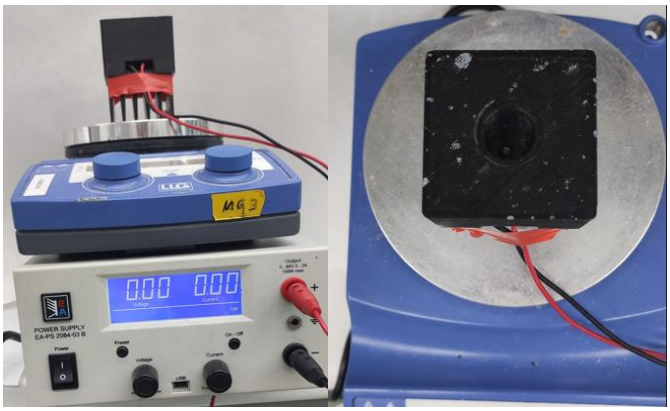

Figure 4.33. High-power single LED setup

-General Procedure for photon Flux (F) determination[38]

$$\Phi = \frac{\mathrm{M}}{\mathrm{F} \times \mathrm{t}[1 - 10^{A(\lambda)}]} \ldots\ldots\ldots\ldots\ldots\ldots\ldots \boldsymbol{Eq.5}$$

M is the moles of product formed (mol), **F** is the number of photons emitted per second (einstein s^{-1}), **t** is the time (s) and **A(λ)** is the measured absorbance at 405 nm.The number of photons emitted per second was determined using azobenzene as actinometer[39].

Using the reaction setup depicted in Figure 4.34, a glass vial was filled with a solution of *trans*-azobenzene (0.1 mmol) in CD_3OD (0.1M) and irradiated with a 405 nm light. The *trans-cis* isomerization was followed in time in ^{1}H-NMR using 1,3,5-trimethoxybenzene as internal standard.

[38] Cismesia, M. A.; Yoon, T. P. "Characterizing Chain Processes in Visible Light Photoredox Catalysis." *Chem. Sci.* **2015**, *6*, 5426.

[39] (a) Leeuwen, T. v.; Buzzetti, L.; Perego, L. A.; Melchiorre, P. "A Redox-Active Nickel Complex that Acts as an Electron Mediator in Photochemical Giese Reactions." *Angew. Chem.,Int. Ed.* **2019**, *58*, 4953, (b) Ladányi, V.; Dvořák, P.; Anshori, J. A.; Vetráková, Ľ.; Wirz, J.; Heger, D. "The Absorption Spectrum of Cis-azobenzene." *Photochem. Photobiol. Sci.* **2017**, *16*, 17

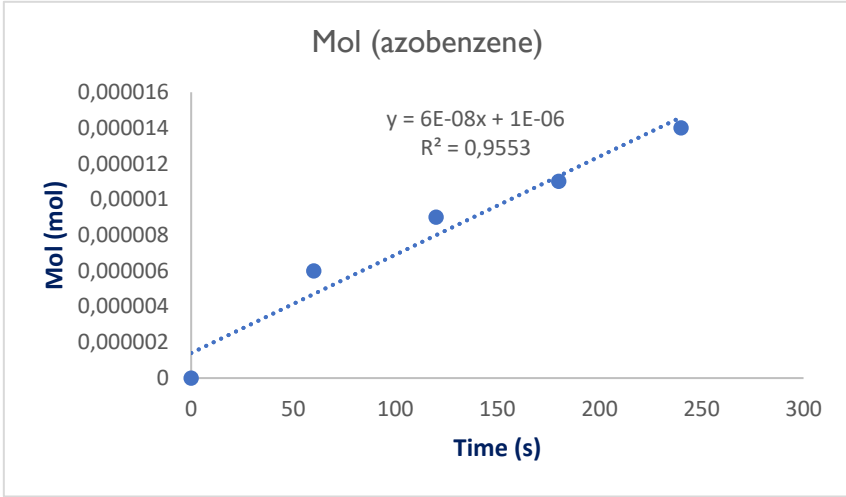

Figure 4.34. Plot of moles of *cis*-azobenzene formed vs irradiation time

The actinometer solution was irradiated for 0 min, 1 min, 2 min, 3 min and 4 min. According to the eq. 1-2 and reported quantum yield of trans-cis isomerization process ($\Phi = 0.288$) [39b], the number of photons emitted per time unit (**F**) was determined (3.0×10^{-7} mol s^{-1}).

*-Quantum Yield Determination Using **C1** as Photocatalyst*

Following the general procedure A, five model thioetherification reactions between **1a** and **2a** were performed separately using catalyst **C1**. Each reaction mixture was irradiated for 0 min, 30 min, 60 min, 90 min and 120 min. After irradiation, the amount of product **3a** formed was determined by ^{1}H NMR analysis using 1,3,5-trimethoxybenzene as the internal standard. An absorbance of 0.216 was determined for the model reaction mixture (1:4 dilution). The moles of the formed product **3a** are plotted against the number of incident photons (Figure 4.35).

The quantum yield (Φ) was calculated to be Φ = 0.017 based on the slope and Eq. 5.

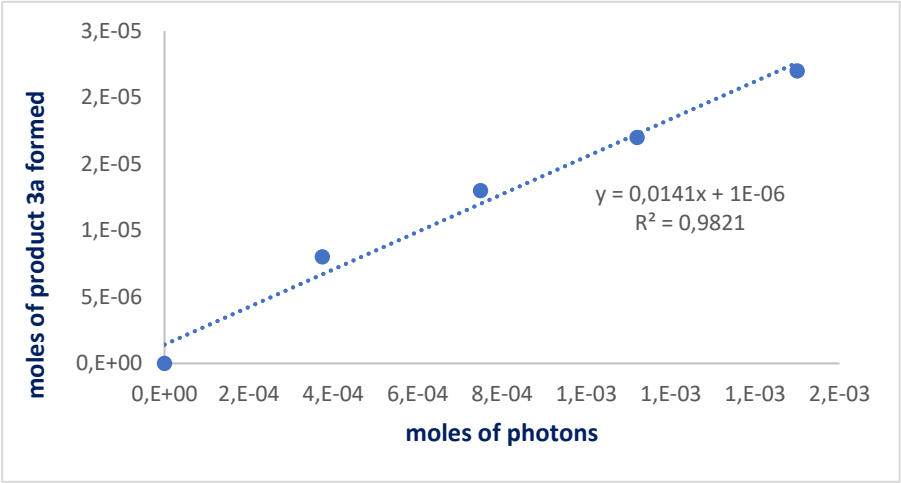

Figure 4.35. Plot of moles of incident photons vs moles of product **3a** formed

*-Quantum Yield Determination Using **C3** as Photoreductant*

Following the general procedure B, five model thioetherification reactions between **1aw** and **2a** were performed separately under **C3** catalysis. Each reaction mixture was irradiated for 0 min, 30 min, 60 min, 90 min and 120 min. After irradiation, the amount of product **3aw** formed was determined by ^{1}H NMR measurement using 1,3,5-trimethoxybenzene as the internal standard. An absorbance of 0.084 was determined for the model reaction mixture (1:4 dilution). The moles of the formed product are plotted against the number of incident photons (Figure 4.36).

The quantum yield (Φ) was calculated to be Φ = 0.052 based on the slope and Eq. 5.

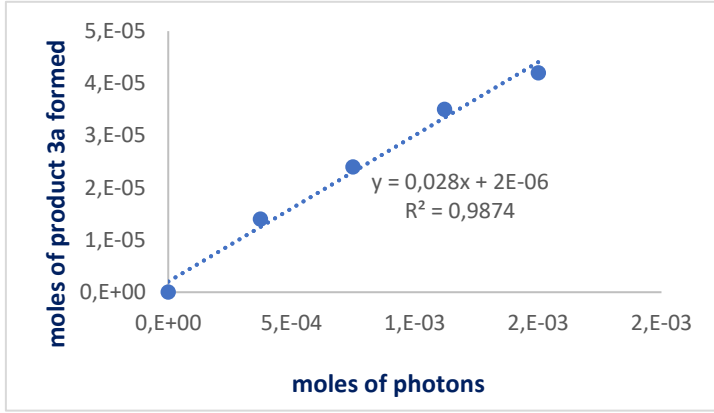

Figure 4.36. Plot of moles of incident photons vs moles of product **3aw** formed

Light On-off Experiment

Experiments with successive intervals of irradiation and dark periods were performed following general procedure **A**, using alcohol **2a** as model substrate in the presence of aryl halide **1a**, photocatalyst **C1**, thiourea **A1** and Cs_2CO_3 ([**2a**] = 0.1 M in CH_3CN). Formation of product **3a** was determined by means of ^1H NMR analysis from aliquots taken under nitrogen atmosphere from the reaction mixture.

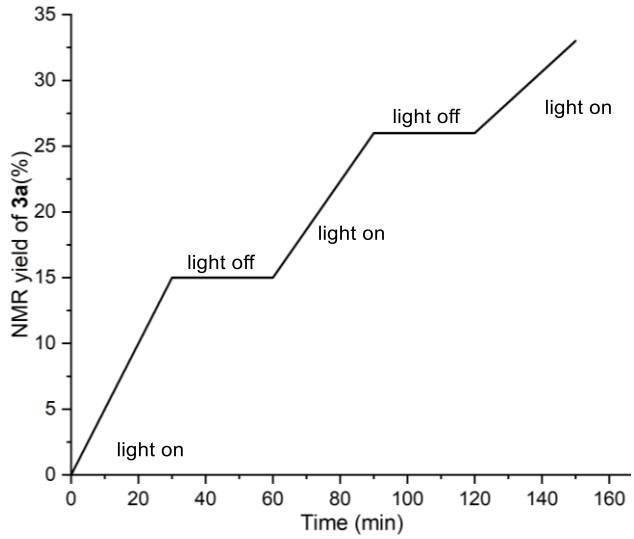

Figure 4.37. Light on-off experiment according to formation of **3a**

4.6.8 Electrochemical Studies

Cyclic voltammetry (CV) measurements were carried out on a Princeton Applied Research PARSTAT 2273 instrument with a glassy carbon disk electrode (diameter: 3 mm) as working electrode. A silver wire coated with AgCl immersed in a 3.0 M aqueous solution of NaCl and separated from the analyte by a fritted glass disk was employed as the reference electrode and a Pt wire counter-electrode completed the electrochemical setup. The scan rate was 100 mV/s unless otherwise stated. The substrates were measured at concentration of 0.02 M in acetonitrile with NBu_4PF_6 (0.1 M) as electrolyte. The preparation of the deprotonated catalyst solutions was carried out as described in the photophysical studies section 4.6.6, at a concentration of 0.02 M.

Potentials are quoted with the following notation: E_p^C (E_{Red}) refers to the cathodic peak potential, E_p^A (E_{Ox}) refers to the anodic peak potential.

Cyclic Voltammetry Measurements of the Model Substrates

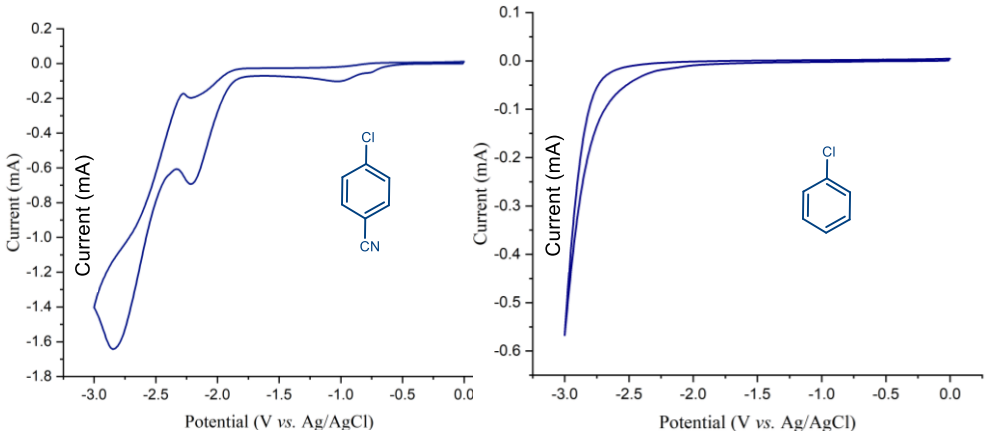

Figure 4.38. *(left)* CV of 0.02M 4-chlorobenzonitrile **1a** in 0.1 M [NBu_4PF_6] in CH_3CN. irreversible reductions E_p = -2.2 V, E_p = -2.8 V. (*right*) CV of 0.02M chlorobenzene **1aw** in 0.1 M [NBu_4PF_6] in CH_3CN. reduction was not observed in the registered potential window.

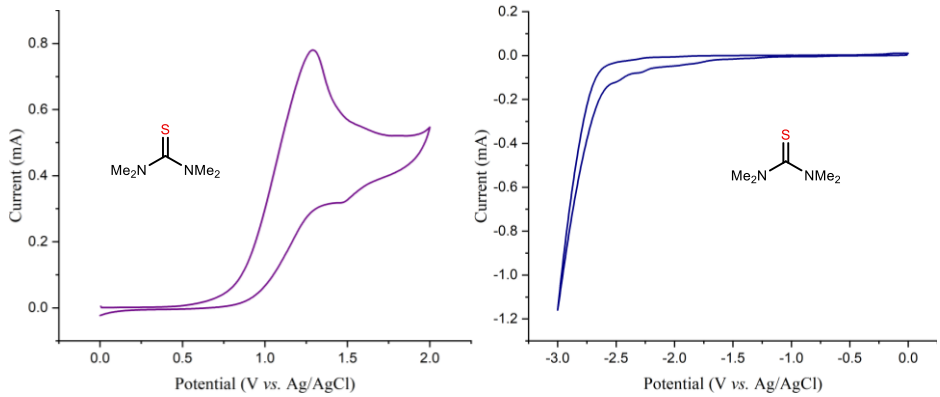

Figure 4.39. CV of 0.02M 1,1,3,3-tetramethylthiourea in 0.1 M [NBu_4PF_6] in CH_3CN, (*left*) measurement between 0 to +3.0 V. irreversible oxidation, E_p = +1.29 V. (*right*) Measurement between 0 to -3.0 V. reduction was not observed in the registered potential window.

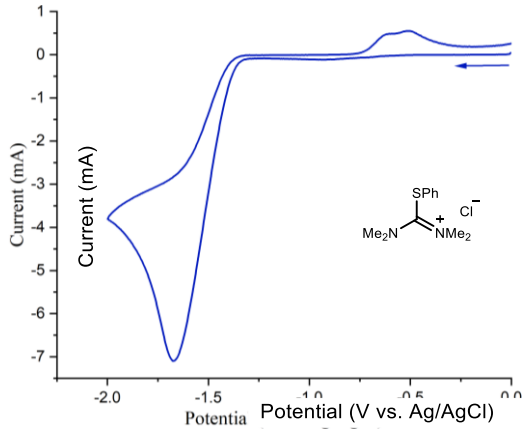

Figure 4.40. CV of 0.02M 1,1,3,3-tetramethyl-2-phenylisothiouronium chloride in 0.1 M [NBu_4PF_6] in CH_3CN., irreversible reduction E_p = -1.68 V.

Cyclic Voltammetry of Pre-catalysts and Catalytic Active Species

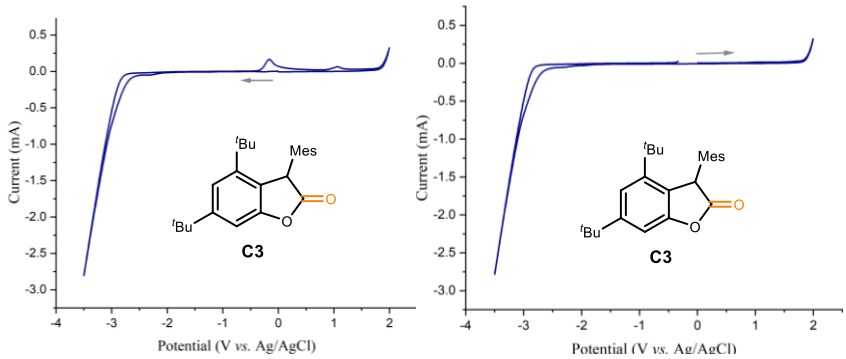

Figure 4.41. *(left)* CV of 0.02M [**C1**] in 0.1 M [NBu_4PF_6] in CH_3CN, irreversible oxidation E_p^A = -0.16 V; (*right*) *(left)* CV of 0.02M [deprotonated **C1**] in 0.1 M [NBu_4PF_6] in CH_3CN, oxidation was not observed.

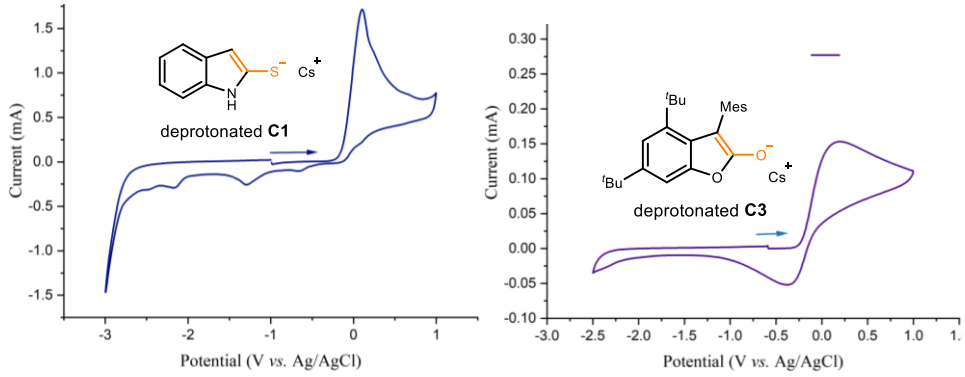

Figure 4.42. *(left)* CV of 0.02M [deprotonated **C1**] in 0.1 M [NBu_4PF_6] in CH_3CN, irreversible oxidation E_p^A = +0.1 V *(right*) CV of 0.02M [deprotonated **C3**] in 0.1 M [NBu_4PF_6] in CH_3CN, irreversible oxidation E_p^A = +0.17 V.

As described in section 2.6.8, the redox potentials *vs.* SCE in MeCN were calculated as below:

*For deprotonated **C1:***

$$E_p^A = -0.36 \text{ V } \textit{vs.}\ Fc/Fc^+;\ E_p^A = +0.02 \text{ V } \textit{vs.}\ SCE$$

*For deprotonated **C3:***

$$E_p^A = -0.29 \text{ V } \textit{vs.}\ Fc/Fc^+;\ E_p^A = +0.09 \text{ V } \textit{vs.}\ SCE$$

Evaluation of the Excited-State Potential of the Deprotonated Catalyst C1 and C3

Using the data collected from the CV studies (Figure 4.42) and from the absorption and emission spectra (Figure 4.17 and 4.31) of the deprotonated **C1** and **C3**, we could estimate the redox potential of the excited state with the following Equation[40]:

$$E(PC^{\bullet}/PC^{-*}) = E(PC^{\bullet}/PC^{-}) - E_{0-0}(PC^{-*}/PC^{-}) \cdots\cdots\cdots\cdots\cdots\cdots \boldsymbol{Eq.6}$$

Since the electrochemical oxidation of deprotonated **C1** and **C3** is irreversible (Figure 4.42), the irreversible peak potential E_p anode was used for $E(Pc^{\bullet}/Pc^{-})$. The oxidation potential was calculated to be +0.02 V *vs.* SCE (in MeCN) and +0.09 V *vs.* SCE (in MeCN) respectively. $E_{0\text{-}0}(PC^{-*})/(PC^{-})$ was approximately determined spectroscopically from the intersection of the normalized absorbance and emission spectra (roughly at 373 nm for deprotonated **C1** and 360 nm for deprotonated **C3**) to have values of 3.3 eV and 3.44 eV.

The oxidation potential of the excited deprotonated catalyst **C1**:

$$E(PC^{\bullet}/PC^{-*}) = 0.1 - 3.3 = \textbf{\textit{-3.2 V vs. Ag/AgCl}}$$

$$E(PC^{\bullet}/PC^{-*}) = 0.02 - 3.3 = \textbf{\textit{-3.28 V vs. SCE}}$$

The oxidation potential of excited deprotonated catalyst **C3**:

$$E(Pc^{\bullet}/Pc^{-*}) = 0.17 - 3.44 = \textbf{\textit{-3.27 V vs. Ag/AgCl}}$$

$$E(Pc^{\bullet}/Pc^{-*}) = 0.09 - 3.44 = \textbf{\textit{-3.35 V vs. SCE}}$$

[40] Buzzetti, L.; Crisenza, G. E. M.; Melchiorre, P. "Mechanistic Studies in Photocatalysis." *Angew. Chem., Int. Ed.* **2019**, *58*, 3730.

4.6.9 Mechanistic Experiments for Probing ionic deoxythiolation

Reactions Between Prepared Aryl Isothiourea Salts and Alcohols

-Preparation of Aryl Isothiouronium salts[41]:

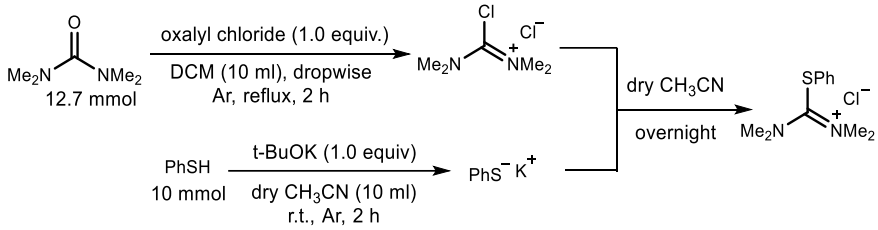

All manipulations were performed in anhydrous conditions under argon. Oxalyl chloride (1.1 mL, 1.0 equiv.) was added dropwise via syringe to a stirred solution of tetramethylurea (15.25 mL, 12.7 mmol) in DCM (10 mL). The reaction was refluxed for 2 hours, cooled to room temperature, and anhydrous ether (30 mL) was added. The tightly stoppered flask was refrigerated for 2 hours, then the precipitated intermediate was isolated by filtration under argon, and washed 3 times with anhydrous ether. In a separate flask, thiophenol (1.05 mL, 10 mmol) in dry acetonitrile (10 mL) was stirred vigorously and treated with potassium *tert*-butoxide (1.2 g). After 2 hours, the deprotonation reaction of thiophenol was evaporated to dryness in vacuo, and dried for a further 2 hours.

The filtered chloro-uronium salt without further drying, was mixed with newly obtained thiolate and washed in with 10 mL dry acetonitrile, and stirred vigorously. An exothermic reaction started immediately. The reaction was stirred overnight and resulting mixture was filtered (to remove precipitated KCl), and the residue washed 3 x with 5 mL dry acetonitrile. The filtrates were evaporated, anhydrous ether (~20 mL) added to the oily residue, and then refrigerated. After 2 hours, the crude product was isolated and washed with dry ether. The

[41] Biancalana, S.; Hudson, D.; Songster, M. F.; Thompson, S. A. "Fmoc Chemistry Compatible Thio-Ligation Assembly of Proteins." *Letters in Peptide Science*. **2001**, 7, 291.

material was suspended in acetone (15 mL), sonicated and vortexed, which effectively extracted a yellow impurity from the product. The mixture was refrigerated, and the product isolated by filtration was washed with cold acetone and dried. The isothiourea salt was obtained as white solid in 82% yield (*which is sensitive to moisture, and therefore should be stored carefully under dry condition*).

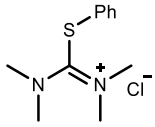

1,1,3,3-tetramethyl-2-phenylisothiouronium chloride (III):

^{1}H NMR (400 MHz, $CDCl_3$): δ= 7.49 – 7.42 (m, 2H), 7.42 – 7.32 (m, 3H), 3.30 (s, 12H) ppm. **^{13}C{^{1}H} NMR (101 MHz, $CDCl_3$)**: δ= 174.1, 131.7, 130.6, 130.0, 127.8, 44.8 ppm. Matching reported literature data[41].

- *Thioetherification from preformed phenyl isothiouronium salt **III** and alcohol **2a***:

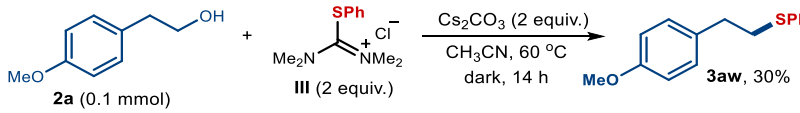

Figure 4.43. Thioetherification from pre-formed aryl Isothiouronium salts and alcohols

As shown above, primary alcohol **2a** can be converted into corresponding thioether **3aw** by reacting with isothiouronium salt **III** under dark conditions, while accompanying with 1,1,3,3-tetramethylurea as by-products.

Stereospecific Displacement: Configuration Inversion

To verify the occurrence of *S_N2 substitution* process in the photochemical thioetherification, we subjected an enantioenriched alcohol to the standard condition and observed inversion of configuration (96% ee), which is consistent with an S_N2 polar manifold being operative. The optical rotation was in good agreement with the value reported in the literature[30].

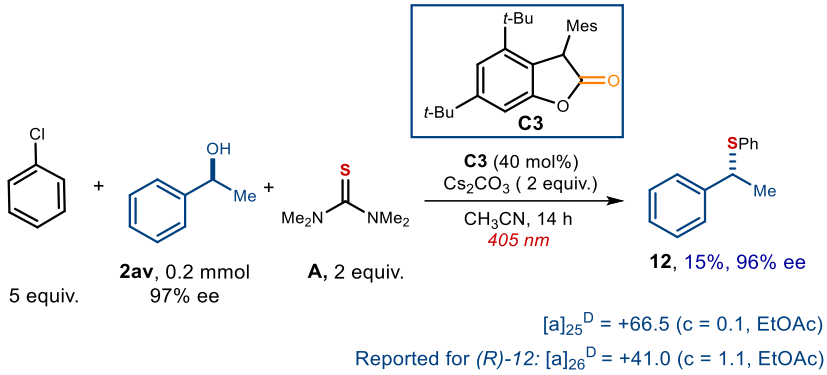

Figure 4.43. Stereospecific displacement of enantiopure alcohol **2av**

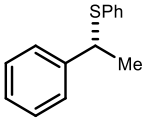

(*R*)-Phenyl(1-phenylethyl)sulfane (12): Synthesized according to the General Procedure using (*S*)-1-phenylethan-1-ol (*S*)-**5** (24.5 mg, 0.2 mmol, 1.0 equiv.), 1,1,3,3-tetramethylthiourea **A** (79.5 mg, 0.6 mmol, 3.0 equiv.) and chlorobenzene **6** (112.6 mg, 1.0 mmol, 5.0 equiv.). The crude mixture was purified by flash column chromatography on silica gel (Hexane: EtOAc = 300: 1 as eluent) to afford (*R*)-**12** (6.5 mg, 15% yield) as a yellow liquid.

^{1}H NMR (500 MHz, $CDCl_3$): δ= 7.36 – 7.28 (m, 6H), 7.27 – 7.20 (m, 4H), 4.37 (qd, J = 7.0, 1.8 Hz, 1H), 1.66 (dd, J = 7.0, 1.8 Hz, 3H) ppm.

^{13}C{^{1}H} NMR (126 MHz, $CDCl_3$): δ= 143.3, 135.2, 132.5, 128.7, 128.4, 127.3, 127.2, 127.2, 48.0, 22.4 ppm. Matching reported literature data[30].

The enantiomeric excess of the corresponding product was determined to be 96% by Agilient 1200 series HPLC, using Daicel Chiralpak IB-3 column (eluent: *n*-hexane; flow rate 1.0 mL/min; λ = 215 nm: t_R(major) = 9.98 min, t_R(minor) = 9.19 min)

$[\alpha]_D^{25}$ = +66.5 (c = 0.1, EtOAc), reported:[10] $[\alpha]_D^{26}$ = +41 (c = 1.1, EtOAc)

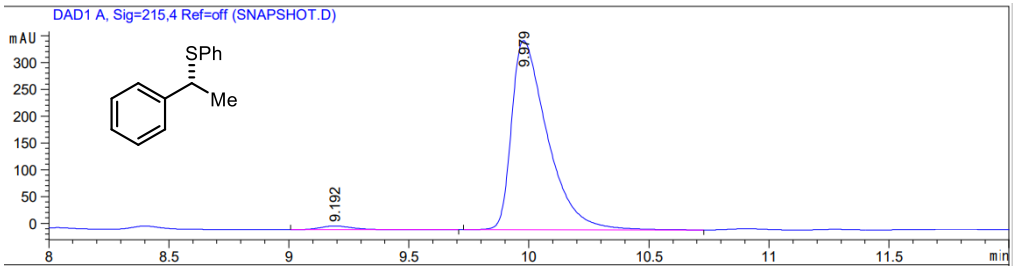

Peak #	RetTime [min]	Type	Width [min]	Area [mAU*s]	Height [mAU]	Area %
1	9.192	BB	0.1485	66.13474	6.85553	1.7704
2	9.979	BB	0.1562	3669.54980	353.21246	98.2296

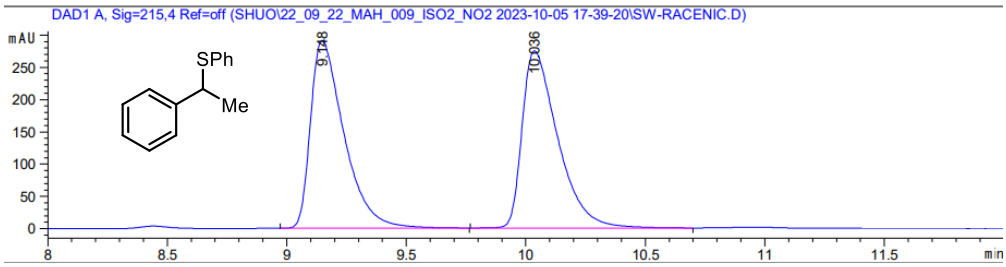

Peak #	RetTime [min]	Type	Width [min]	Area [mAU*s]	Height [mAU]	Area %
1	9.148	BB	0.1454	2829.27246	291.16721	49.8440
2	10.036	BB	0.1569	2846.97754	274.71118	50.1560

4.7.9 Detection and analyses of Side products

GC-MS Analyses of Reaction mixtures

Reaction between aryl chloride **1a** and alcohol **2a** was conducted according to general procedure **A**. After completion of reaction, the reaction mixture was diluted and injected into GC-MS. 1,1,3,3-tetramethylurea was confirmed as common co-byproduct of both conditions, as predicted side-product from deoxythiolation step. In addition, 4,4'-thiodibenzonitrile **14** can be detected as undesired product in the reaction using **C1** catalyst.

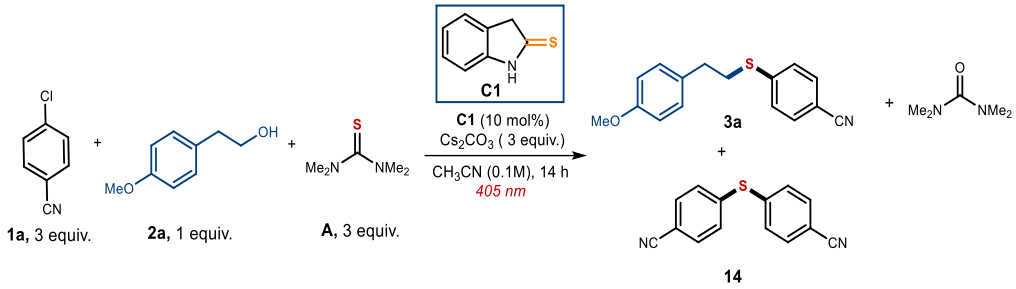

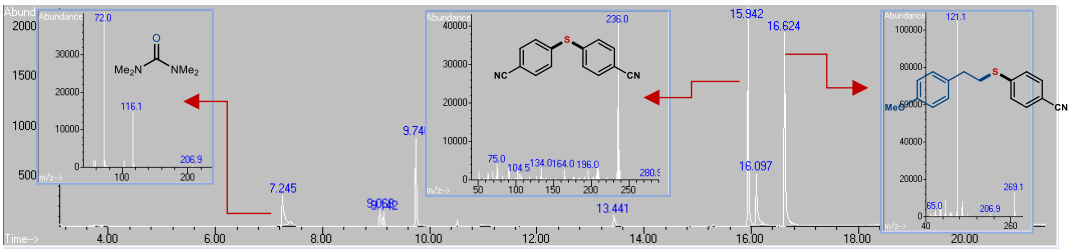

Figure 4.44. Assignment of species in reaction mixture by GC-MS analyses

Reaction between chlorobenzene and alcohol **2a** was conducted according to general procedure **B**. After completion of reaction, the reaction mixture was diluted and injected into GC-MS. In addition to 1,1,4,4-tetramethylurea, diphenyl disulfide can be detected. Pertinently, a species with m/z= 440.3 can be detected, which can be assignable to **C3** modified by a phenyl group. Its formation can be justified by the coupling between phenyl radical and **C3** radical within the reaction mixture, accounting for its decomposition.

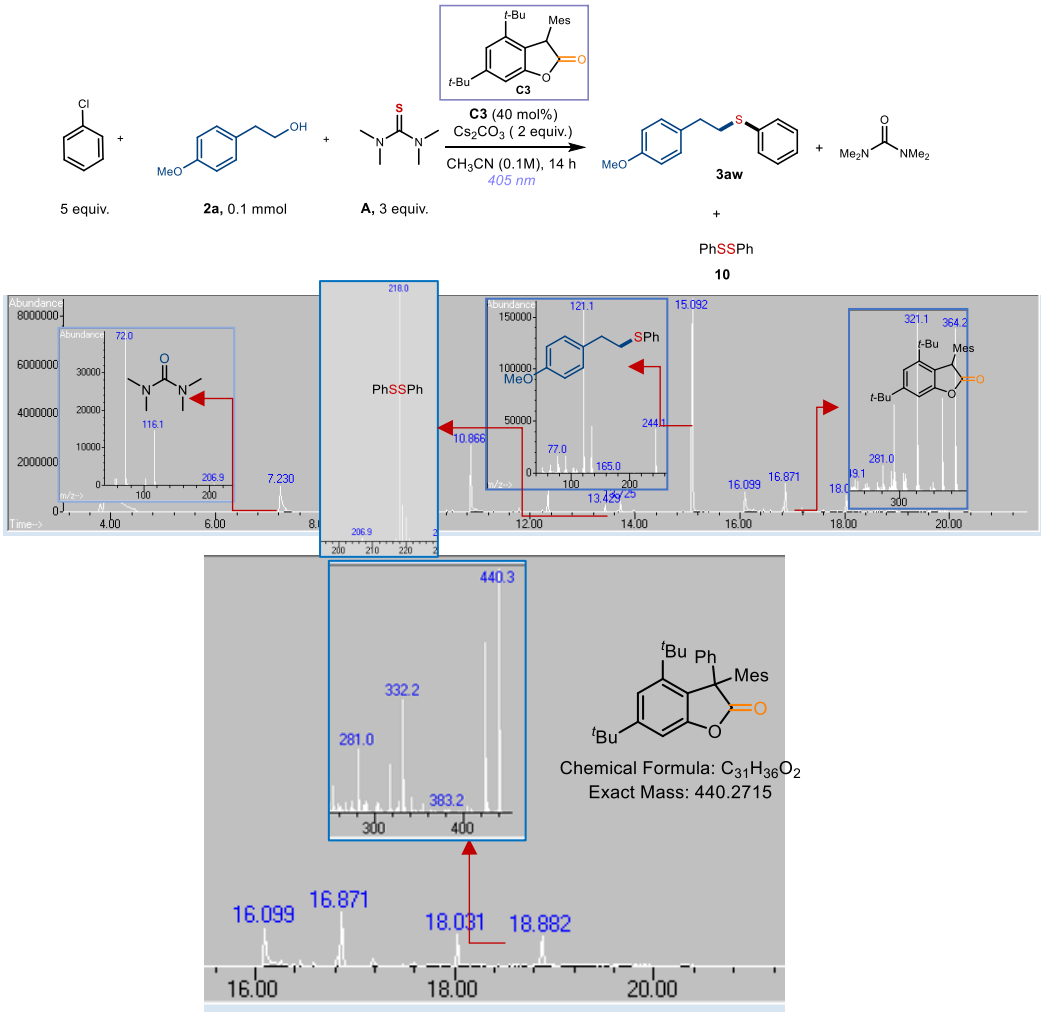

Figure 4.45. Assignment of species in reaction mixture by GC-MS analyses observation of coupling product in GC-MS

To confirm the identity of the decomposition product, a stoichiometric reaction between **C3** and aryl chloride **1ay** (Figure 4.46)**:** To a 7 mL glass vial, **C3** (36.9 mg, 0.1 mmol, 1.0 equiv.), cesium carbonate (65.0 mg, 0.2 mmol, 2 equiv.) were added. The vial was sealed with a screw-top cap with septum and then vacuumed and backfilled with argon for 3 times. Afterwards, aryl chlorides **1ay** (0.2 mmol, 2 equiv.) followed by argon-sparged acetonitrile (0.1 M, 2.0 mL) were added *via* syringe. The vial was sealed with Parafilm and then stirred

under 405 nm for 14 hours using ***Set-up 1***. After completion of the reaction, purification by preparative TLC afforded the predicted arylation product.

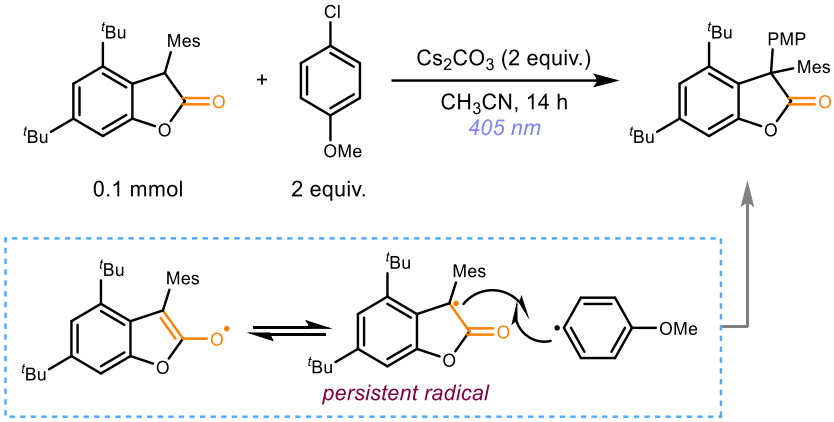

Figure 4.46. Stoichiometric Reaction for characterization of decomposition product of **C3**

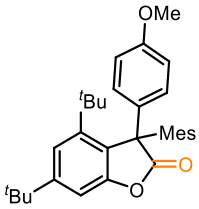

4,6-di-tert-butyl-3-mesityl-3-(4-methoxyphenyl)benzofuran-2(3H)-one:

^{1}H NMR (500 MHz, CDCl$_3$): δ= 7.92 (dd, *J* = 9.0, 2.5 Hz, 1H), 7.37 (d, *J* = 2.0 Hz, 1H), 7.02 (d, *J* = 2.0 Hz, 1H), 6.87 (dd, *J* = 9.0, 2.6 Hz, 1H), 6.79 – 6.83 (m, 2H), 6.63 – 6.70 (m, 2H), 3.77 (s, 3H), 2.24 (s, 3H), 1.84 (s, 3H), 1.72 (s, 3H), 1.35 (s, 9H), 1.03 (s, 9H) ppm.

^{13}C{^{1}H} NMR (126 MHz, CDCl$_3$): δ =178.7, 159.6, 153.7, 152.4, 149.2, 139.4, 138.3, 137.0, 134.1, 133.2, 131.7, 130.5, 130.4, 120.4, 114.0, 112.4, 107.3, 64.3, 55.2, 36.6, 35.1, 31.7, 31.3, 25.3, 21.6, 20.6 ppm.

HRMS (ESI): calculated for $C_{32}H_{38}NaO_3$ [M+Na$^+$]: 493.2713, found 493.2718.

Chapter V

General Conclusions

The work carried out in this doctoral thesis has demonstrated how intermediates with established polar chemistry can be repurposed for radical reactivity to solve otherwise challenging synthetic problems. Through the judicious selection of photocatalysts and radical precursors, these classical intermediates could be involved in novel radical chemistry. This opened up new opportunities for selective C-C and C-S bond formations, yielding diverse scaffolds with potential bioactivity.

Iminium ions exhibit a rich chemistry in the polar domain. In Chapter II, it was demonstrated that iminium ion catalysis is also effective in radical pathways, ensuring the interception of nucleophilic primary radicals for conjugate addition with high stereocontrol. Employing a strongly oxidizing acridinium organic photocatalyst, the non-stabilized primary radicals were generated upon oxidative ring opening of cyclobutanols. The chiral iminium intermediates were effective in overcoming racemic background processes while trapping short-lived open-shell species, ensuring good enantioselectivity in 1,7-dicarbonyl scaffold formation. The resulting products offered a straightforward access to analogs of natural products and pharmaceuticals with new stereocenters through simple transformations.

Chapter III detailed the development of a radical *umpolung* strategy for chiral iminium ions. Leveraging their electrophilicity, the SET reduction of chiral iminium ions switched the electrophilic β-position to nucleophilic within the resultant chiral 5π-electron radical. This polarity-inversion permitted the cross-electrophile coupling between two unsaturated carbonyl compounds to take place, affording chiral 1,6-dicarbonyl compounds as a single regioisomer with excellent enantioselectivity. Building on this photoredox organocatalytic approach, the first example of asymmetric conjugate cynation of enals was also disclosed. The preparation of β-cyanoaldehyde with good enantioselectivity and exclusive chemoselectivity permitted a short synthetic route to unnatural chiral amino acids.

Isothiouronium ions is another class of polar intermediate that was utilized for metal and thiol-free synthesis of thioethers. Chapter IV described an extension to its chemistry through a radical-polar sequence. Using a strongly reducing thioxindole organic photocatalyst, unreactive C(sp^2)-Cl bond can be cleaved to form aryl radicals, which in turn engage in aryl C-S bond formation with thiourea. This resultant aryl isothiouronium intermediate can then intersect with established ionic pathways, reacting with alkyl alcohols in a single cascade to deliver aryl alkyl thioether. Benefiting from the abundance of commercial substrates and remarkable tolerance for functional groups, our protocol allowed the preparation of diverse thioether products that were previously inaccessible and facilitated late-stage modifications of biorelevant compounds.

UNIVERSITAT
ROVIRA i VIRGILI